



Palladium Nanoparticles: Plant Aided Biosynthesis, Characterization, Applications

Satish B. Manjare¹ · Priyanka D. Pendhari¹ · Sushil M. Badade² · Shankar R. Thopate³

Received: 1 June 2021 / Accepted: 24 September 2021 / Published online: 11 October 2021
© The Tunisian Chemical Society and Springer Nature Switzerland AG 2021

Abstract

Among diverse metal nanoparticles, palladium nanoparticles (PdNPs) have captured the special attention of researchers because of their unique applications. However, the synthesis of PdNPs by conventional procedures incorporates harmful solvents, reducing agents, and produces toxic pollutants and by-products. The plant part extract-assisted green synthesis of palladium nanoparticles has been known as the best solution to minimize the limitations of conventional methods. Bio synthesized nanoparticles have good selectivity and catalytic properties. Thus, they have been investigated as nanocatalysts in numerous catalyst based reactions. In this review article, we have explored the various plant parts responsible for the bioreduction of palladium ions, characterization of PdNPs and heterogeneous catalytic activity of PdNPs in the C–C coupling reaction. In addition, we reviewed a plausible mechanist approach for the fabrication of PdNPs.

Keywords Green synthesis · Plant part extracts · Palladium nanoparticles · Catalysis

Abbreviations

PdNPs	Palladium nanoparticles
Pd	Palladium metal
XRD	Palladium nanoparticles
FTIR	Fourier transforms infrared spectroscopy
TEM	Transmission electron microscopy
SEM	Scanning electron microscopy
EDS	Energy-dispersive X-ray spectroscopy
FE-SEM	Field emission SEM
HRTEM	High-resolution TEM
SAED	Selected area electron diffraction
XPS	X-ray photoelectron spectroscopy
TON	Turnover number
TOF	Turnover frequency
PEG	Polyethylene glycol

ICP-AES	Inductively coupled plasma atomic emission spectroscopy
WEPBA	Water extract of papaya bark ash
EDX	Energy dispersive X-ray analysis
SALE	<i>Syzygium aqueum</i> Leaves extract

1 Introduction

There are several conventional methods for the synthesis of metal nanoparticles. These approaches for the synthesis of metal nanoparticles include chemical and photochemical reduction, microwave-assisted, sol–gel, thermal decomposition & aerosol methods [1]. But these conventional methods have various disadvantages such as the utilisation of toxic solvents and hazardous reducing or stabilising agents such as hydrazine, sodium citrate, hydroxylamine etc. These limitations have increased the necessity to develop safe, eco-friendly and non-toxic alternatives for the synthesis of metal nanoparticles. The greener pathway avoids the incorporation of toxic solvent, reducing agent and reduces the formation of toxic by-products. The eco-friendly methods for the preparation of nanoparticles can be achieved by using naturally occurring biomolecules or metabolites such as vitamins, sugar, polyols, terpenoids, microorganism and biodegradable polymers etc. as reducing and stabilising agents. The green synthesis of metal nanoparticles is designed in such a way

✉ Satish B. Manjare
satish.manjare@rediffmail.com

¹ Department of Chemistry, Ratnagiri Sub-campus, University of Mumbai, P-61, MIDC Mirjole, Ratnagiri, Maharashtra 413639, India

² Department of Chemistry, Prof. John Barnabas School for Biological Studies, Ahmednagar College, Station Road, Ahmednagar, Maharashtra 414001, India

³ Department of Chemistry, S.S.G.M College, Kopergaon, Ahmednagar, Maharashtra 423601, India

that solvent, reducing agents or stabilising agent employed in synthesis follows the twelve principles of green chemistry [2–5].

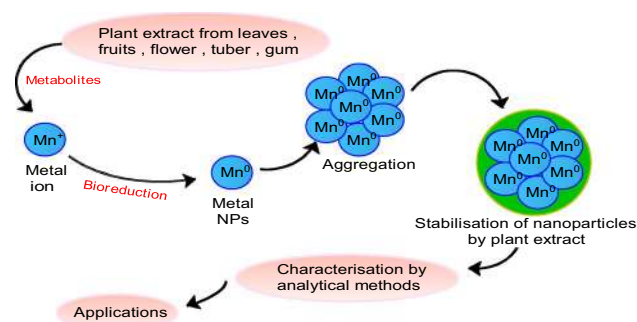
In 2018, Mpungose et al. have taken a review on the heterogenous PdNPs as a catalyst for the Heck and Suzuki coupling reaction [6]. Some of the systems include the PdNPs supported on the various supports such as carbonaceous, metal oxide, magnetic, polymer and hybrids inorganic–organic material. Heterogeneous PdNPs are prepared by using organic solvents & chemical reducing agents which may render the method expensive.

In another study, Fahmy et al. in 2020 have taken a review on the synthesis of PdNPs using microorganisms and plant part extracts [7]. The highlight of the study was the biosynthesis of nanoparticles, factors affecting biosynthesis and their potential biomedical applications as anticancerous activity. However, the review article as unable to discuss the mechanism of bioreduction and its function as an effective catalyst in the cross-coupling reaction.

In this review, we discussed the synthesis of PdNPs using various plant part extracts, economical supports and their application in the field of catalysis.

2 Plant Assisted Synthesis of Metal Nanoparticles

Over the decades, it was found that plant parts can biologically reduce metal ions. Because of these captivating features, plants have been considered as a potential and environment-friendly path for the synthesis of metal nanoparticles. Plant extract comprises bioactive polyphenols, proteins, alkaloids, sugars, phenolic acids and terpenoids which are believed to be responsible for the reduction [8]. Importantly, the biosynthesis of metal nanoparticles when compared with conventional methods, relatively takes place at room temperature. The plant extract also plays a crucial role in stabilising the nanoparticles. It was found that the concentration of extract, concentration of salt, pH of the solution, time of reaction affect the quality, size, shape and morphology of nanoparticles [9–11]. Phytochemicals in plant extract reduces metal ion M^{n+} to zero-valent metal nanoparticles [12, 13]. Characterization and conformation studies have been done by X-ray Diffraction (XRD), Fourier Transforms Infrared Spectroscopy (FTIR), Transmission Electron Microscopy (TEM), Scanning Electron Microscopy (SEM), Energy-Dispersive X-ray Spectroscopy (EDS), Field Emission Scanning Electron Microscopy (FE-SEM) and other analytical techniques [14–16].



Scheme 1 General scheme for the green synthesis of Pd nanoparticles

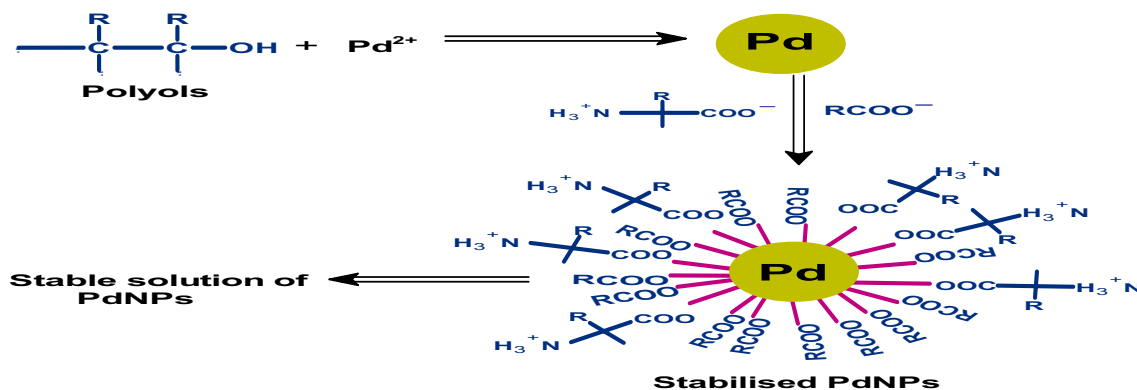
2.1 Biosynthesis of Pd Nanoparticles Using Plant Extract

In recent years, PdNPs have been the center of attraction due to their unique applications such as catalyst, supercapacitor, sensors, lithium-ion batteries and organic synthesis [17]. The plant-mediated synthesis of nanoparticles especially the palladium nanoparticles depends on the reducing properties of phytochemicals present in the plant extract. Biomolecules play an important role as reducing/capping and stabilizing agents for PdNPs. The general scheme for the synthesis of PdNPs is shown in Scheme 1.

In this review, we have explored the recent developments in the eco-friendly, non-hazardous, non-toxic, simple and green methods for the synthesis of palladium nanocatalyst by reducing Pd^{2+} ion using plant extract and their characterization using UV–Vis, FTIR, EDS, SEM, TEM, and XRD. In addition, we have discussed the applications of PdNPs in the field of catalysis.

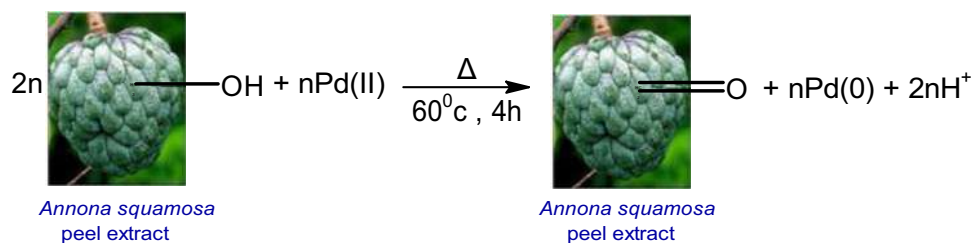
Green synthesis of palladium nanoparticles from *Cinnamomum camphora* leaf broth has been done by stirring the mixture of $PdCl_2$ and extract [18]. Based on HR-TEM, SAED, XPS, and XRD, it was believed that the Pd(II) ion and the hydroxyl (-OH) group of polyols in *Cinnamomum camphora* leaf broth undergo a redox reaction. The decrease in the pH of the solution further confirmed the production of H^+ ions in the redox reaction. The TEM analysis concluded that higher the Pd(II) ion concentration, the smaller is the size of Pd nanoparticles.

In 2012, Shen et al. reported the biogenic synthesis of palladium nanoparticles using *Anacardium occidentale* leaves extract [19]. The biosynthesised nanoparticles were characterized by UV–Vis, FTIR and XRD. The TEM images of nanoparticles showed that the particle size ranges between 2 and 5 nm in diameter with a face centered cubic (FCC) structure. FTIR spectrum revealed polyalcohol in *Anacardium occidentale* extract to be responsible for the bioreduction of Pd(II) ion and carboxylate

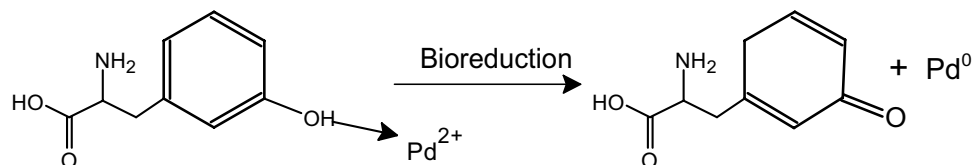


Scheme 2 Mechanism of reduction of palladium ion by polyols [19]

Scheme 3 The reaction of *Annona squamosa* peel extract and Pd(II) ion [20]



Scheme 4 Plausible mechanism for reduction of palladium ion Pd^{2+} to Pd^0 nanoparticles by tyrosine in *Glycine max* leaf extract [21]



ions along with protein molecules that act as a stabilizing agent. The mechanism for the formation of PdNPs is as shown in Scheme 2.

In 2012, Roopan et al. reported a green method for the synthesis of palladium nanoparticles using *Annona squamosa* fruit extract [20]. The TEM showed PdNPs in spherical shape with particle size in range of 80 ± 5 nm. The study depicted that the *Annona squamosa* peel extract contains aldehyde and the hydroxyl groups. The reaction between the *Annona squamosa* extract and the Pd(II) ion which might be occurring during the bioreduction depicted in Scheme 3.

In 2012, Petla et al. synthesized palladium nanoparticles using protein-rich *Glycine max* or soybean leaf extract [21]. The reduction of palladium ions to the Pd(0) nanoparticles was investigated by UV–Vis spectroscopy. The predicted reduction reaction of palladium ion by tyrosine in *Glycine max* broth is shown in Scheme 4.

Green synthesis of PdNPs using *Catharanthus roseus* leaf extract has been reported by Kalaiselvi et al. [22]. The PdNPs were formed when an aqueous solution of palladium

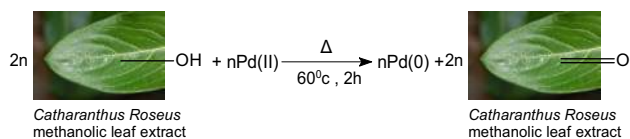


Scheme 5 The reduction of palladium acetate in presence of plant extract [22]

acetate [Pd(OAc)_2] was stirred with *C. roseus* leaf extract at 60°C for 1 h. The general reaction is depicted in Scheme 5.

The morphological study indicated that particles are spherical with an average size range of 38 ± 2 nm. The study also revealed that a higher yield of nanoparticles was achieved at 2 h of stirring. These used the optimized palladium nanoparticle for catalytic degradation of phenol red dye by varying the pH of the solution. At optimum pH of 6, the surface plasmon resonance band associated with dye disappeared and indicated the complete degradation of dye. That study could be considered as an efficient approach towards industrial effluent treatment. Scheme 6

Palladium metal supported on the carbon played a major role in the removal of carbon monoxide from the environment. Palliyarayil et al. reported a novel method for



Scheme 6 The reaction of *Catharanthus roseus* leaf extract and Pd(II) ion [22]

Scheme 7 A mechanistic approach for the formation of PdNPs using catechin as a reducing agent [23]

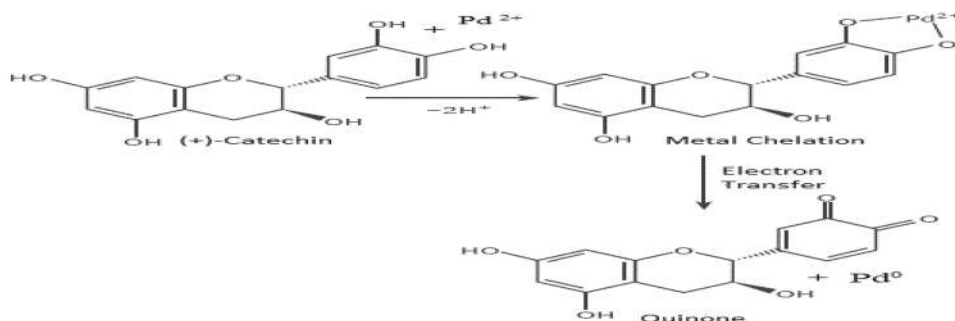


Table 1 Pd nanoparticle synthesized using plant part extracts

Plant extract	Metal salt	Size in nm	Morphology of PdNPs	References
<i>Cinnamomum camphora</i> leaf	PdCl ₂	3–6	Spherical	[18]
<i>Anacardium occidentale</i>	PdCl ₂	2.5–4.5	Spherical	[19]
<i>Annona squamosa</i>	Pd(OAc) ₂	80 ± 5	Spherical	[20]
<i>Glycine max</i>	PdCl ₂	15–15	Spherical	[21]
<i>Catharanthus roseus</i>	Pd(OAc) ₂	38 ± 2	Spherical	[22]
Green tea	Pd/C	13–23	Spherical	[23]
Gardenia Jasminoides Ellis	PdCl ₂	3–5	Spherical	[24]
Tea and coffee	PdCl ₂	20–60	Spherical	[25]
Red Grape Pomace	PdCl ₂	5–10	Spherical	[26]
<i>Curcuma longa</i> Tuber	PdCl ₂	15–25	Spherical	[27]
Banana peel	PdCl ₂	50	Crystalline	[28]
Mushroom extract	PdCl ₂	–	Spherical	[29]
<i>Astraglmanna</i>	PdCl ₂	20–25	Spherical	[30]
Beet juice	–	5	Spherical	[31]
<i>Piper betle</i>	PdCl ₂	4 ± 1	Spherical	[32]
Watermelon rind	PdCl ₂	96	Spherical	[33]
Xanthan gum	PdCl ₂	10	Spherical	[34]
<i>Antigonon leptopus</i>	PdCl ₂	5–70	Spherical	[35]
<i>Moringa oleifera</i>	Pd(OAc) ₂	27 ± 2	Spherical	[36]
<i>Chlorella Vulgaris</i>	PdCl ₂	15	Spherical	[37]
<i>Filicium decipiens</i>	PdCl ₂	2–22	Spherical	[38]
<i>Spirulina platenis</i>	PdCl ₂	10–20	Spherical	[39]
<i>Saccharomyces cerevisiae</i>	PdCl ₂	–	Hexagonal	[40]
<i>Moringa oleifera</i>	Pd(OAc) ₂	10–50	Spherical	[41]
Black Pepper	PdCl ₂	7	Spherical	[42]
Onion extract	PdCl ₂	19	Spherical	[43]
<i>Lagenaria siceraria</i>	Pd(OAc) ₂	16–73	Spherical	[44]
<i>Ananas comosus</i>	PdCl ₂	4.46 ± 2.44	Spherical	[45]

3 Catalytic Applications of Biosynthesized PdNPs

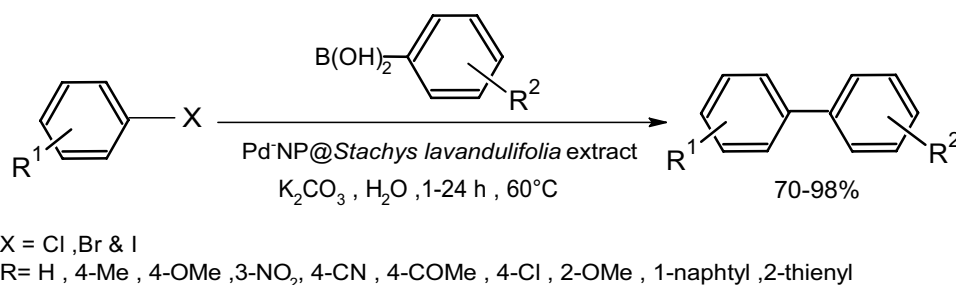
The Pd nanoparticles are utilized as homogenous and heterogeneous catalysts in coupling reactions due to their high surface area and high surface–volume ratio [46]. The PdNPs fabricated by plant extract have been studied for their heterogeneous catalytic activity in coupling reactions like Suzuki–Miyaura coupling, Sonogashira cross-coupling, Heck coupling reaction, Hiyama cross-coupling reactions. The Pd(0) provides a surface for the adsorption of molecules and the C–C coupling reaction proceeds via metal–carbon bonds. The arylation has become the important step for structural modification of the lead to generate a new potential pharmaceutical intermediate. Therefore, in recent years the palladium catalysed coupling reactions have become an important tool for the synthesis of biologically active compounds.

In 2014, Veisi et al. designed a green route for the biosynthesis of palladium nanoparticles using naturally occurring *Stachys lavandulifolia* (herbal tea) extract [47]. The synthesized palladium nanoparticles were studied as

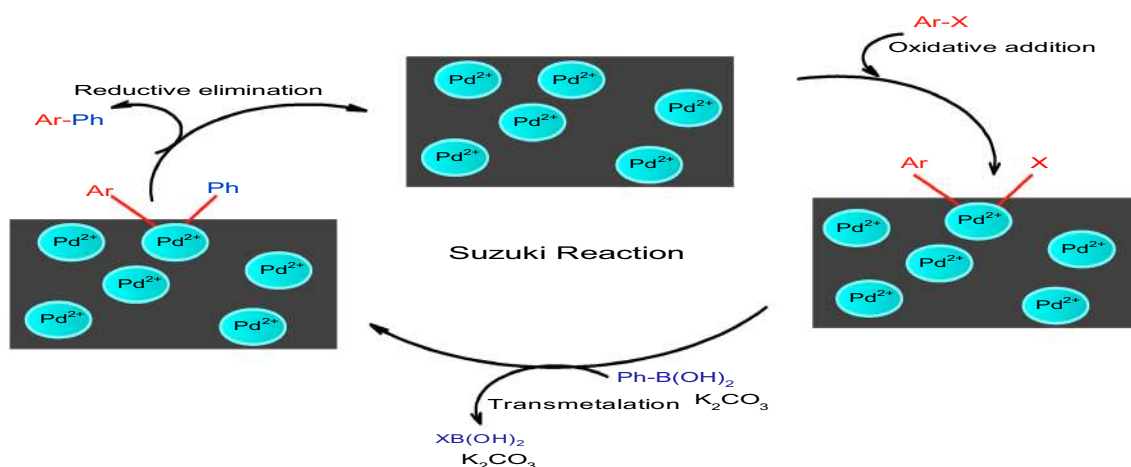
a stable and efficient heterogeneous catalyst for Suzuki–coupling reactions, Scheme 8. The reaction has advantages such as zero leachings, easy recovery of nanocatalyst, easy workup and the excellent yield of coupled products. They reported that the Pd nanocatalyst remained on the support even at elevated temperatures, Scheme 9. Palladium nanoparticles exhibited good reusability and recyclability up to the eight-run without remarkable loss of activity.

In 2014, Nasrollahzadeh et al. reported a green path for the synthesis of PdNPs using *Hippophae rhamnoides* Linn leaves extract [48]. It was found that the Pd ion was reduced to nanoparticles with the help of flavonoid (FIOH) metabolites in the plant which acts as a green option over commonly utilized hydride containing reducing agents. They used biosynthesized nanocatalyst in coupling reactions, Scheme 10. The Pd catalyzed coupling reaction showed some features such as excellent yields of coupling product, no utilization of toxic ligands, easy operation, workup, good reusability and recyclability of green nanocatalyst.

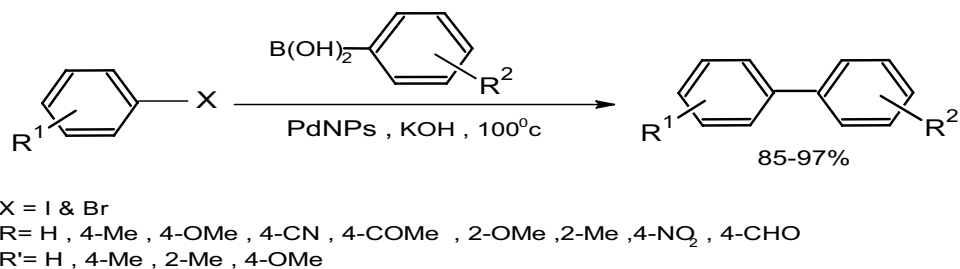
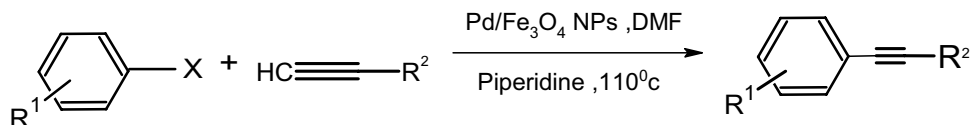
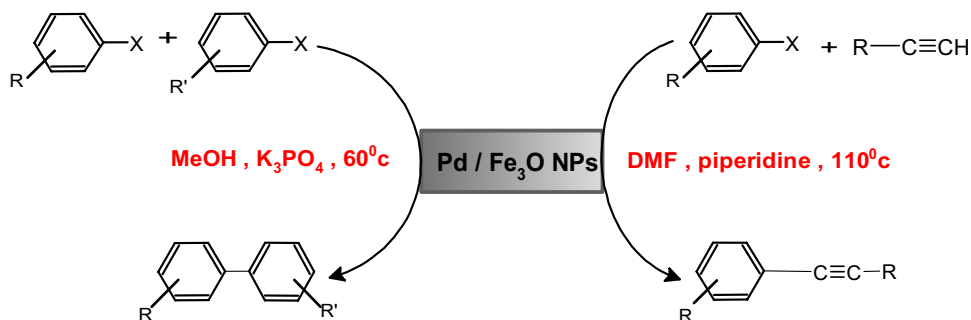
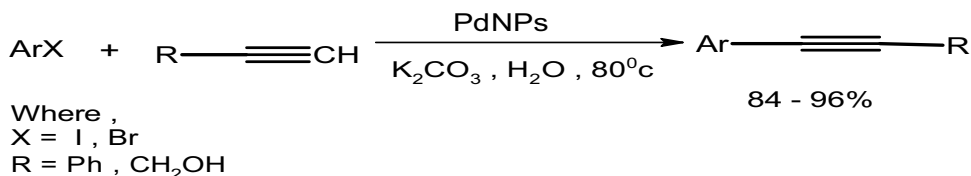
In another study, Nasrollahzadeh et al. proposed a green pathway for the synthesis of palladium supported on Fe_3O_4 nanoparticles by *Euphorbia condylocarpa* M.bied root extract [49]. The catalytic activity of Pd/ Fe_3O_4 was



Scheme 8 PdNPs@*lavandulifolia* catalyzed biaryl synthesis [47]



Scheme 9 The possible mechanism of the Suzuki coupling reaction proposed by Veisi et al. [47]

Scheme 10 PdNPs catalyzed biaryl synthesis [48]**Scheme 11** PdNPs catalyzed biaryl synthesis (Sonogashira coupling reaction) [49]**Scheme 12** Sonogashira and Suzuki reaction catalyzed by Pd/Fe₃O₄ nanocomposite [49]**Scheme 13** Sonogashira coupling reaction catalyzed by PdNPs [50]

examined in Suzuki and Sonogashira reactions. Schemes 11 and 12. Some of the attractive features of the reaction were fast and clean route, elimination of toxic ligands, a wide spectrum of substrates, excellent yield, higher turnover time (TON=6) and since Pd/Fe₃O₄ has magnetic properties, it can be separated by simple treatment of external magnets.

In 2015, the Nasrollahzadeh group developed a green method for the fabrication of PdNPs via bioreduction of Pd²⁺ ion to Pd nanoparticle by the *piper longum* fruit extract [50]. The characterized PdNPs were examined in Sonogashira coupling reactions, Scheme 13. The prepared catalyst was recycled five times in the coupling reaction.

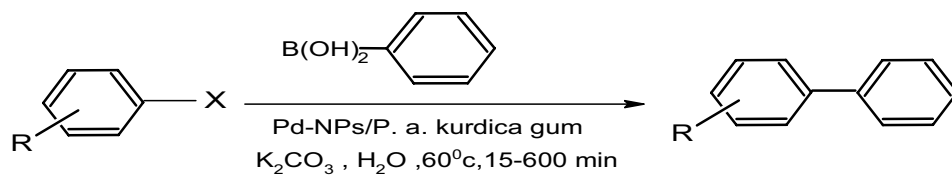
In 2015, Veisi et al. developed a one-pot green method for the fabrication of PdNPs supported on *Pistacia Atlantica kurdica* gum [51]. The nanoparticles were employed as the heterogeneous nanocatalyst for Suzuki–Miyaura and Mizoroki–Heck cross-coupling reaction. Schemes 14 and 15. The reaction resulted in 98% of the product

yield, without any evidence of alteration of performance, leaching. The catalyst could be reused at least eight times without loss of efficiency.

In the same year, Nasrollahzadeh et al. fabricated a Pd/CuO NPs by *Theobroma cacao* L. seed extract [52]. The palladium supported on CuO (Pd/CuO) was studied in the degradation of 4-Nitrophenol and Heck coupling reaction. The catalyst generated the corresponding cross-coupled product in excellent yield. The catalyst was also examined for reduction of 4-nitrophenol and it has a good reusability up to sixth cycle. The general reaction scheme for Heck reaction is as shown in Scheme 16.

A green and convenient protocol for the generation of PdNPs supported on polyethylene glycol i.e. (PdNPs@PEG) by the *Colocasia esculenta* leaf extract was studied by Borah et al. in 2015 [53]. The supported PdNPs showed high catalytic capacity towards Suzuki–Miyaura cross-coupling reaction in isopropanol:water (1:1). The

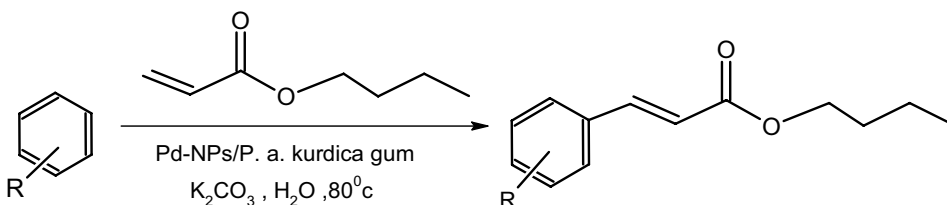
Scheme 14 Suzuki coupling reaction catalyzed by PdNPs/*Pistacia Atlantica kurdica* gum [51]



X = I, Br, Cl

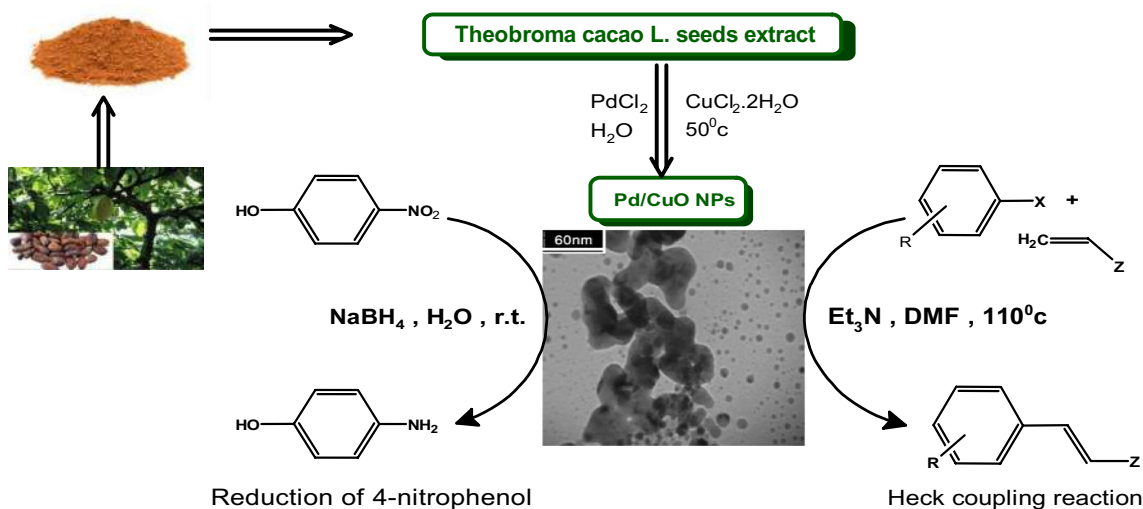
R = H, 4-Me, 2-Me, 4-CHO, 3-NO₂, 4-COMe, 1-naphthyl, 2-thienyl

Scheme 15 Mizoroki–Heck coupling reaction catalyzed by PdNPs/*Pistacia Atlantica kurdica* gum [51]



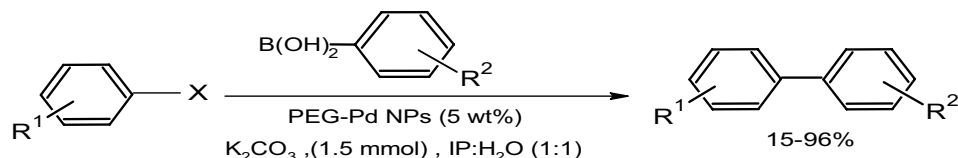
X = I, Br, Cl

R = H, 4-Me, 2-Me, 4-OMe, 4-NO₂, 1-naphthyl



Scheme 16 Green synthesis of PdNPs supported on CuO and their catalytic activity [52]

Scheme 17 Suzuki coupling reaction catalyzed by PdNPs supported on PEG [53]



X = I, Br, Cl

R¹ = H, 4-NO₂, 4-OMe

R² = H, 4-OMe, 2-OMe, 2-Me, 3-Me, 4-tert-butyl, 2-CHO, 2-NH₂

PdNPs nanocomposite showed reusability up to the fifth cycle, Scheme 17.

A green approach for the fabrication of PdNPs using *Euphorbia granulata* leaf extract was reported by Sajadi et al. in 2016 [54]. The biosynthesized nanoparticles were employed as a heterogeneous catalyst in the Suzuki–Miyaura coupling reaction. The nanoparticles exhibited good catalytic power in the coupling reaction of biaryls at room temperature, Scheme 18.

In the same year, Nasrollahzadeh and Sajadi proposed a green method for the fabrication of Pd nanoparticles by *Euphorbia thymifolia* leaves extract [55]. The catalytic activity of PdNPs was examined for cyanation of aryl iodides in presence of $K_4Fe(CN)_6$. The TEM images showed that the average particle size was in the range of 30–35 nm in diameter and reusability even after the fifth cycle. The advantages include the high yield of nitrile product, reusability, and low amount for loading, Scheme 19.

In 2016, Veisi et al. reported a biosynthesis of PdNPs using oak gum [56]. They examined the catalytic capability of PdNPs@Oak Gum in the reduction of nitroarenes and Suzuki coupling reactions. Scheme 20. The reduction of nitroarenes was achieved by catalyst and sodium borohydride in EtOH:Water (1:2) mixture, Scheme 21.

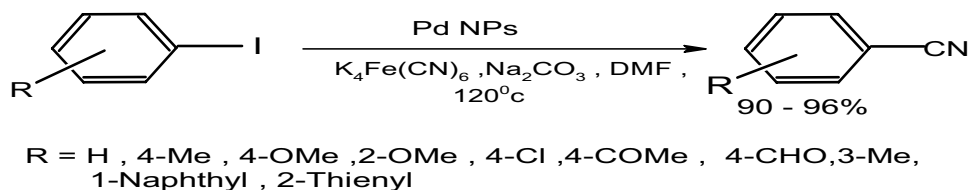
In the same year, Liu and colleagues designed a green route for the synthesis of PdNPs by the Poplar leaves extract [57]. The synthesized PdNPs were characterized and confirmed by XRD, SEM, TEM, XPS, EDS, ICP-AES and FTIR. The Pd nanocomposite was employed as a heterogeneous catalyst for the Suzuki reaction Scheme 22.

In 2017, Liu et al. developed a simple method for the generation of PdNPs by pine needle extract [58]. The Pd/pine needle extract exhibited high catalytic activity in the fabrication of biaryl, Scheme 23. The reaction of phenylboronic acid with 4-bromotoluene catalyzed by Pd/

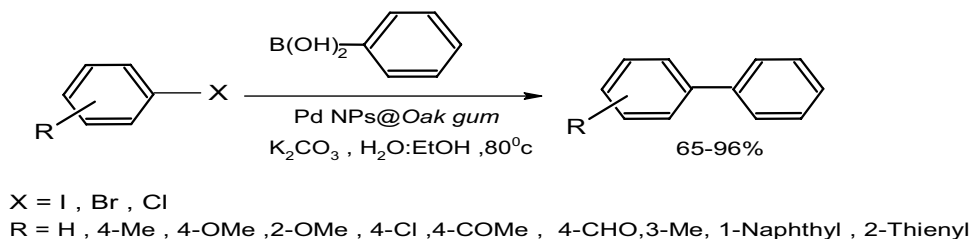


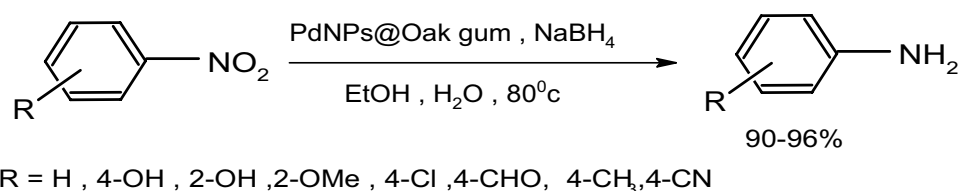
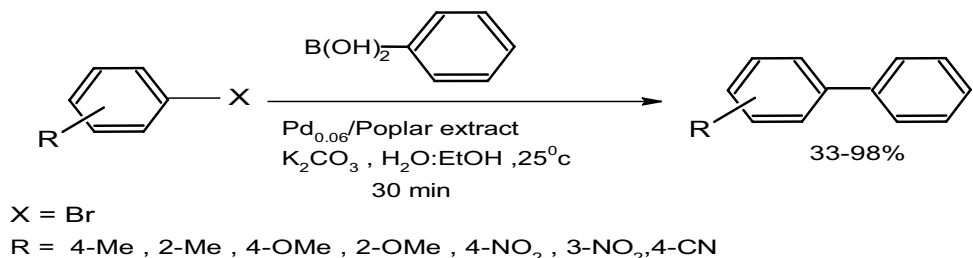
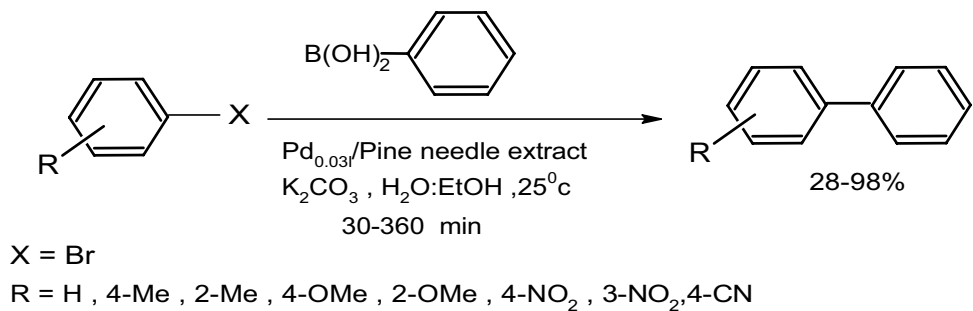
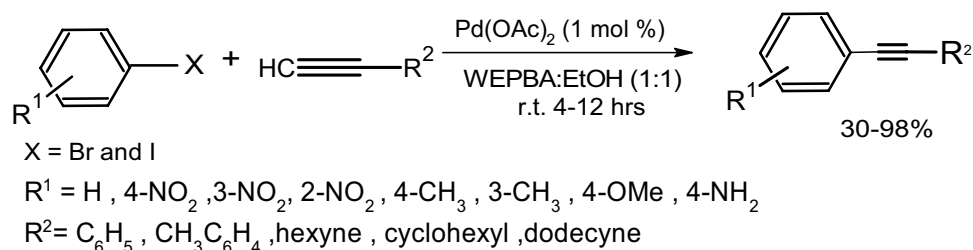
Scheme 18 Phosphine free Suzuki–Miyaura coupling reaction catalyzed by PdNPs [54]

Scheme 19 Synthesis of nitriles from aryl iodides (cyanation) reaction catalyzed by PdNPs [55]



Scheme 20 Suzuki coupling reaction catalyzed by PdNPs@Oak gum [56]



Scheme 21 Nitroarenes reduction reaction by PdNPs@Oak gum [56]**Scheme 22** Suzuki coupling reaction catalyzed by PdNPs@Poplar extract [57]**Scheme 23** Suzuki coupling reaction catalyzed by PdNPs@Pine needle extract [58]**Scheme 24** Sonogashira cross-coupling reaction by Pd(OAc)₂ and WEPBA and EtOH [59]

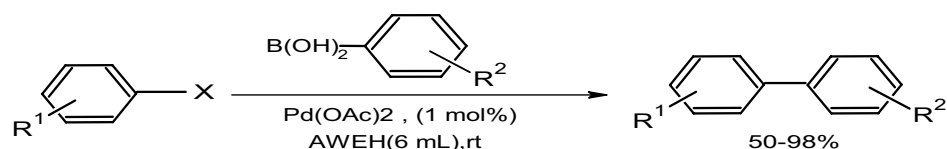
pine needle extract yielded 90% of the product and good reusability up to six cycles.

Agricultural waste (agro-waste) and by-products have been reported as the highest potential green materials for catalyst preparation in past decades. Agricultural waste like peel extract is rich in cellulose and hemicellulose nanofibers. Dewan et al. reported a green method for the fabrication of palladium nanoparticles using extract of waste papaya bark ash (WEPBA) and Pd(OAc)₂ solution [59]. The catalytic activity of the resulted catalyst was investigated in the Sonogashira cross-coupling reaction. The catalyst was found to be highly selective and active in copper, amine and ligand-free cross-coupling reaction in presence of 1 mol% palladium acetate in WEPBA:EtOH (1:1) solvent at room temperature, Scheme 24.

In 2017, Sarmah et al. reported a green synthesis of palladium nanoparticles using waterborne species *Eichhornia crassipes* (common name: water Hyacinth) and incorporated it as a nanocatalyst in the Suzuki–Miyaura coupling reaction [60]. The ash extract contains metal oxide and hydroxide. Because of these, the basic medium provided by water extract resulted in excellent catalytic activity in the Pd-catalysed coupling reaction. One can say that reaction does not require an external base as the extract assists the coupling reactions, Scheme 25.

In 2018, Dewan et al. developed a biogenic approach for the synthesis of PdNPs by papaya peel extract [61]. The bio-reducing biomolecules present in the papaya peel reduced the Pd²⁺ ion of Pd(OAc)₂ to the Pd nanoparticles in water. The TEM micrographs showed that prepared nanoparticles

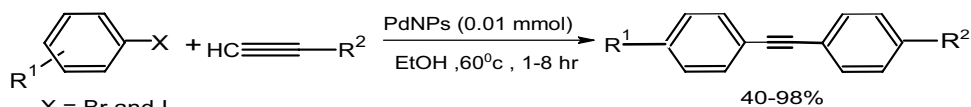
Scheme 25 Suzuki–Miyaura coupling reaction of aryl halide and aryl boronic acid in aqueous extract of water hyacinth [60]



X = Br, I and Cl

R¹ = 4-OMe, 4-NO₂, 4-CHO, 4-OH, 4-Me, 4-COMe, 3-OMe, 2-Me, 2-OH, Ph
R² = H, 4-Cl, 4-C₂H₅, 4-COMe, 4-CN, 3-CH₃

Scheme 26 Sonogashira cross-coupling reaction of an aryl halide with terminal alkynes catalyzed by PdNPs prepared by papaya peel extract [61]

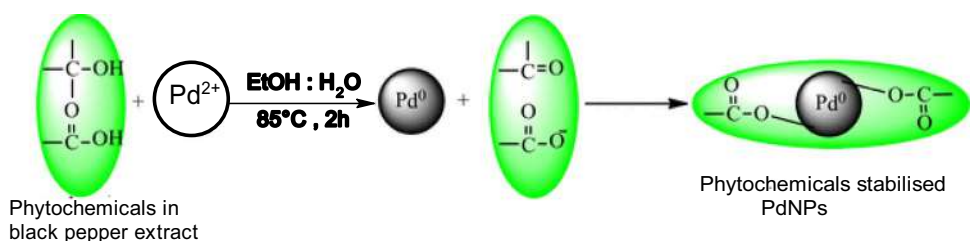


X = Br and I

R¹ = H, 4-NO₂, 3-NO₂, 4-Me, 3-Me, 4-OMe, 4-OH, 4-NH₂

R² = C₆H₅, dodecyl, hexyl, cyclohexyl, 4-Me.C₆H₅

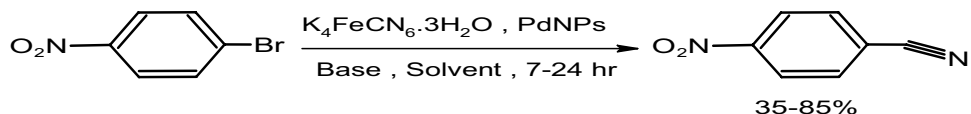
Scheme 27 A probable mechanism of PdNPs formation using black pepper extract [62]



Phytochemicals in black pepper extract

Phytochemicals stabilised PdNPs

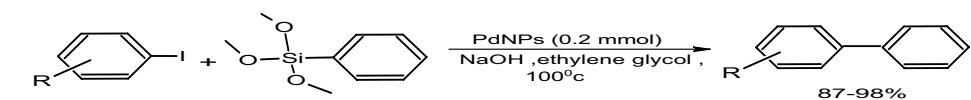
Scheme 28 Palladium nanoparticle catalyzed Suzuki coupling reaction via different methods [62]



Base : K₂CO₃, Na₂CO₃, NaOH, KOH

Solvent : DMF, DMF:H₂O(1:1), ACN, EtOH

Scheme 29 Palladium nanoparticle catalyzed Hiyama cross-coupling reaction [62]



X = Br, Cl and I

R = H, 4-Me, 4-OMe, 4-OH, 4-CN, 4-NO₂, 4-NH₂, 4-CHO, 2-CHO, 4-COOH, 3-COOH, 2-COOH, 4-F, 4-t-bu

were highly crystalline in the range of 1–5 nm. The EDS analysis indicated the presence of Pd and O that confirmed the generation of Pd/PdO (i.e. palladium oxide). The prepared PdNPs showed good catalytic activity in Suzuki–Miyaura and Cu, amine and ligand-free Sonogashira reactions with good yields (see Scheme 26).

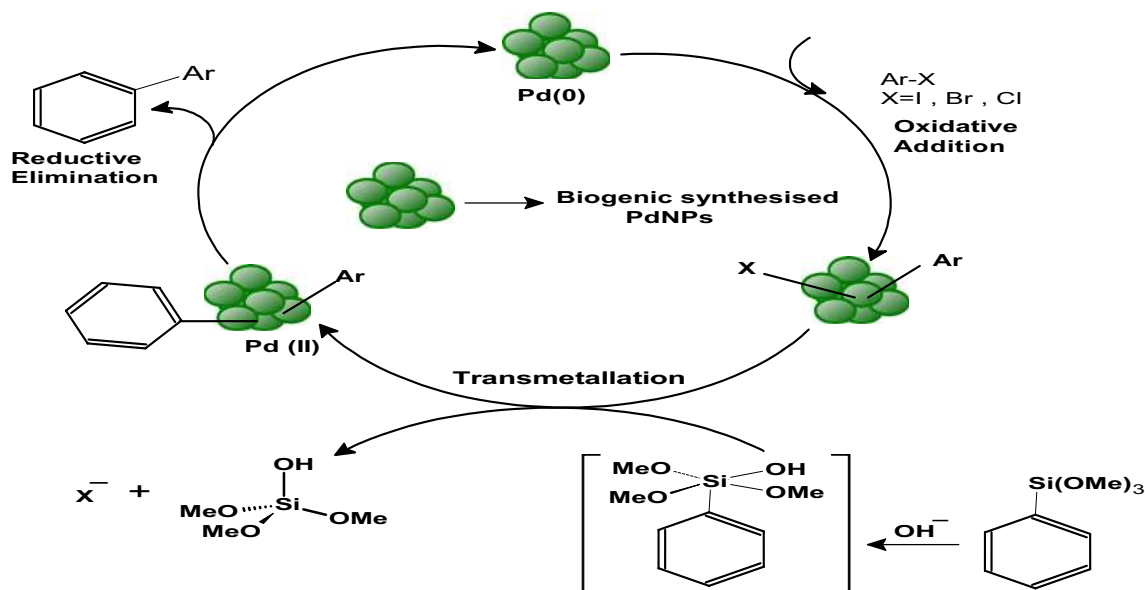
Another green and facile method for the synthesis of Pd nanocatalyst has been reported by Kandathil et al. in 2018 [62]. They synthesized biogenic PdNPs using an aqueous extract of *Piper nigrum* commonly known as black pepper. The probable mechanism for the synthesis is shown in Scheme 27. It was believed that the reduction of Pd²⁺ ions is achieved by the phytochemical in the piper nigrum like piperine, pellitorine, N-isobutyl-tetradeca-2, 4-dienamide and ethyl piperonyl cyanoacetate. The biosynthesized

PdNPs (0.5 mol%) were utilized in the cyanation reaction of aryl halides by using potassium hexacyanoferrate(II) trihydrate K₄Fe(CN)₆·3H₂O. Here K₄Fe(CN)₆·3H₂O acts as a non-toxic and low-cost cyanide source and sodium carbonate as a base to produce corresponding nitriles in good yields. The reaction of the cyanation of aryl halide by PdNPs is shown in Scheme 28. Along with that, they studied the catalytic activity of Pd nanocatalyst (0.2 mol%) in the Hiyama cross-coupling reaction of an aryl halide with trimethoxyphenyl silane in NaOH at 100 °C, Scheme 29. The possible catalytic cycle for the Hiyama cross-coupling reaction is shown in Scheme 30. The PdNPs have reusability up to five runs in aryl halide cyanation and ten times in Hiyama cross-coupling without notable loss in their catalytic activity.

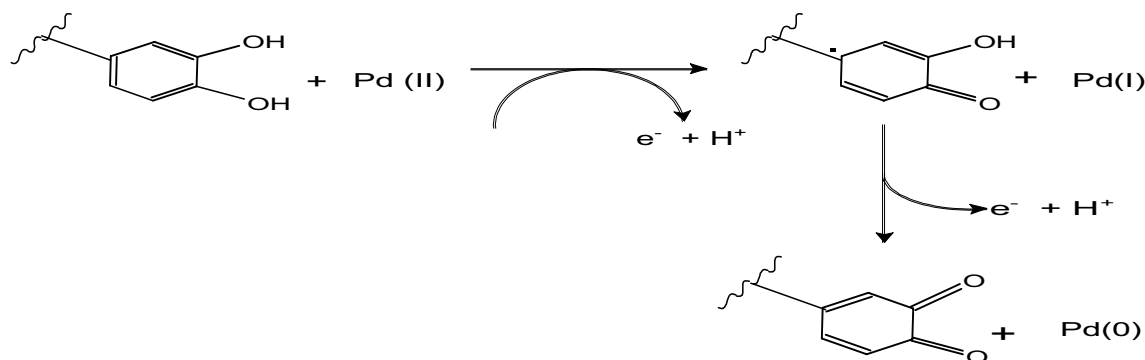
In 2019, Nasrollahzadeh et al. reported a simple and green method for the fabrication of Pd nanoparticles using an aqueous extract of *Cucurbita pepo* leaves as a stabilising agent and coral reef as a green support [63]. It was believed that the polar hydroxyl groups in the extract carry out the bioreduction of Pd(II) to Pd(0). The plausible mechanism is described in Scheme 31. The catalytic activity of

nanocomposite was investigated in the cyanation of aryl halide in presence of a non-toxic nucleophilic cyanide ion source, potassium ferrocyanide, Scheme 32. The nanocomposite displayed good reusability up to the fifth cycle.

In 2019, Hemmati et al. synthesized palladium nanoparticles using strawberry fruit extract immobilized on Fe₃O₄ nanoparticles [64]. The catalytic activity of the strawberry/

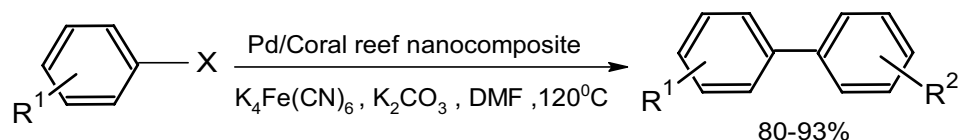


Scheme 30 A probable mechanism for the Hiyama cross-coupling reaction [62]



Scheme 31 A plausible mechanism of bioreduction of Pd(II) ion by *Cucurbita pepo* leaves extract [63]

Scheme 32 Pd/Coral reef catalyzed cyanation of aryl halides reaction in presence of K₄Fe(CN)₆ [63]



X = Br, I, Cl

R¹ = H, 4-Me, 4-OMe, 4-OH, 2-CN, 3-CN, 4-CN, 4-I, 4-Cl, 3-Cl, 4-OMe, 4-Br, 3-Br

Pd coated on magnetic Fe_3O_4 nanocatalyst was investigated for the Suzuki–Miyaura C–C coupling reaction Scheme 33. The unique feature of synthesized nanoparticles was their recyclability and their separation from the reaction mixture by an external magnetic field without significant leaching and modification of performance.

In 2020, Manjare and Chaudhari designed a green synthesis method for the synthesis of Pd nanoparticles supported on Bentonite clay with the help of *Syzygium aqueum* (or water apple) leaves extract (named as SALE) [65]. A powdered Bentonite clay and PdCl_2 mixture were allowed to react with SALE at 100 °C for 10 h to produce PdNP@AT-Bentonite. PdNPs@AT-Bentonite showed good catalytic activity in the Suzuki–Miyaura C–C coupling reaction with greater than 90% yield, Scheme 34. Prepared heterogeneous catalyst PdNPs @AT-Bentonite has good reusability up to the tenth run without a notable loss in its catalytic activity. It was believed that palladium nanoparticles supported on Bentonite clay are a better alternative than reported catalysts.

In 2020, Manjare and Chaudhari reported an eco-friendly and effective method for the synthesis of palladium nanoparticles supported on Zeolite Type-Y (Na form) using *Anacardium occidentale* shell (commonly known as Cashew apple) extract as the reducing agent [66]. The supported nanocatalyst PdNP@Zeolite Type-Y (Na-form) was examined for the

Suzuki–Miyaura C–C coupling reaction, Scheme 35. The catalyst was recycled up to the tenth cycle without remarkable loss of catalytic activity.

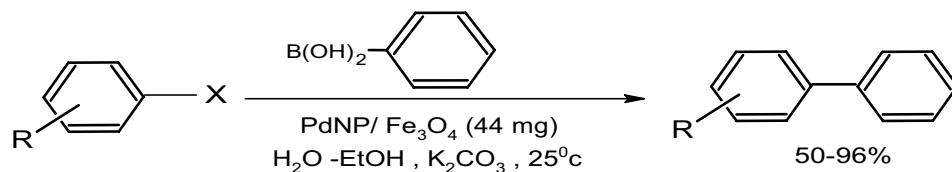
Over a decade PdNPs have gained attention as a nanocatalyst in coupling reactions and have also been employed in other reactions such as oxidation, degradation, and reduction reactions. A few more applications of biosynthesized palladium nanoparticles in coupling reactions are summarised in Table 2.

4 Conclusion

In this review article, we focused on the biogenic synthesis of palladium nanoparticles using various plant parts (i.e. leaves, fruits, tuber, flowers) and implementation of PdNPs in numerous reactions to study its catalytic activity. Due to the large surface area and surface-volume ratio, minimum utilisation of Pd metal salts, and good reusability in catalytic cycles make Pd nanoparticles an inexpensive catalyst compared to Pd metal salts catalysts.

Researchers have developed several green methods to obtain PdNPs as discussed in this review. These synthesized PdNPs were explored as nanocatalyst in a C–C coupling reaction with no significant loss of catalytic activity.

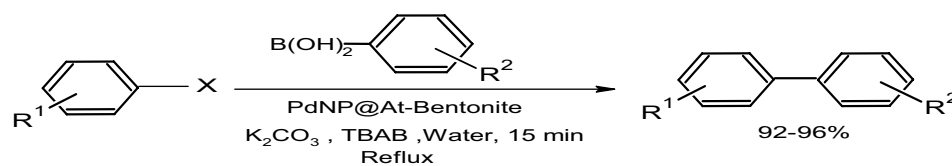
Scheme 33 Magnetic PdNPs/ Fe_3O_4 catalyzed Suzuki–Miyaura coupling reaction [64]



X = Br, I

R = H, 4-CH₃, 4-COMe, 4-NO₂, 4-F

Scheme 34 PdNPs@AT-Bentonite catalyzed Suzuki–Miyaura C–C coupling reaction [65]

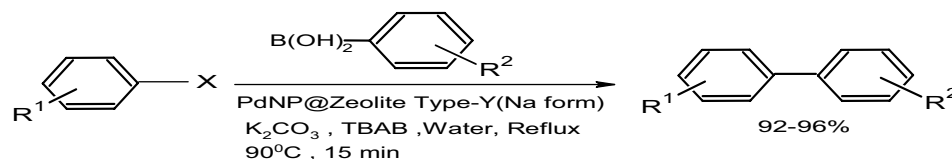


X = Br, I

R¹ = 4-OMe

R² = H, 4-Cl, 4-tert butyl, 3-OMe, 3-CH₃, 2-OMe, Naphtyl, 4-F

Scheme 35 PdNP@Zeolite Type-Y (Na-form) catalyzed Suzuki–Miyaura C–C coupling reaction [66]



X = Br, I

R¹ = 4-OMe

R² = H, 2-CH₃, 4-Cl, 4-tert butyl, 3-OMe, 3-CH₃, 2-OMe, Naphtyl

Table 2 Application of biosynthesized palladium nanoparticles

Plant Extract	Size (nm)	Application of PdNPs	References
<i>Pulicaria glutinosa</i>	20–25	Suzuki Coupling reaction	[67]
<i>Myrtus communis L</i>	17–25	Suzuki coupling reaction	[68]
<i>Artocarpus lakoocha Roxb</i>	10–30	Suzuki and Heck coupling reaction	[69]
<i>Camellia sinensis</i>	7	Suzuki coupling reaction	[70]
<i>Origanum vulgare</i>	–	Reduction of organic dyes & coupling reaction	[71]
<i>Ficus carica fruit</i>	–	Suzuki coupling reaction	[72]
<i>Lolium multiflorum</i>	–	Suzuki, Mizoroki, Heck coupling reaction	[73]
<i>Anogeissus latifolia</i>	4.8 ± 1.6	Antioxidant and catalytic activity	[74]
<i>Andean blackberry leaf</i>	55–60	Photocatalytic and antioxidant activity	[75]
Green tea	7–10	Suzuki–Miyaura coupling reaction	[76]
<i>Miswak</i>	~ 2.2 to 15	Suzuki coupling reaction	[77]
<i>Chrysophyllum Cainito</i>	59	Heck coupling reaction	[78]
<i>Rosmarinus officinalis</i>	15–90	Mizoroki–Heck reaction and biological activities	[79]
Nicotinamide (Tobacco)	50	Hydrogen Peroxide Electro reduction	[80]
<i>Sapindus mukorossi seed</i>	3–5	Suzuki coupling reaction	[81]
<i>Rosa canina</i>	10 ± 3	Suzuki–Miyaura coupling reaction	[82]
<i>GarciniapedunculataRoxb</i>	1.5	Suzuki coupling reaction & antimicrobial activity	[83]
<i>Salvia hydrangea</i>	10	Reduction of organic dyes	[84]
Fenugreek Seeds	20–50	Reduction of NP & Suzuki coupling reaction	[85]
<i>Hibiscus sabdariffa L</i>	5–8	Suzuki–Miyaura coupling reaction	[86]

We believe that as a next step, the mechanistic approach for the bioreduction of metal ions M^{n+} to zero-valent Mn^0 should get clearer with an explicit explanation. These nanoparticles have numerous applications in the future which can be summarised as follows;

(1) Biologically more stable PdNPs can be synthesized from a variety of plants that are growing in developing countries. African countries are rich in various vegetation. These plant species could be utilized for the biogenic synthesis of more stable and efficient PdNPs.

(2) Pd nanoparticles provide a shorter route for the C–C bond formation. As a result, the finding of this review article could be useful in the synthesis of pharmaceutical lead compounds and will help to reduce the cost of the drug by catalytic reactions.

It can be taken into note that, the improvement in the performance and application of biosynthesized Pd nanoparticles is a growing field. It opens up a whole new research area for the preparation of plant-based PdNPs from various plants which are specifically growing in developing countries. The progress in the development of catalysts will provide reliable industrial and commercial opportunities. The coupled product of Pd catalyzed reactions could be useful in the synthesis of the pharmaceutical drug via coupling reactions.

Acknowledgements The authors are grateful to Dr. Prafulla B. Sawant, Ratnagiri, Maharashtra, India for his kind help.

Declarations

Conflict of interest The corresponding author states that there is no conflict of interest.

References

1. Irvani S (2011) Green synthesis of metal nanoparticles using plants. *Green Chem* 13:2638–2650. <https://doi.org/10.1039/C1GC15386B>
2. Vajtai R (2013) Springer handbook of nanomaterials. Springer, Berlin. <https://doi.org/10.1007/978-3-642-20595-8>
3. Couvreur P (2013) Nanoparticles in drug delivery: past, present and future. *Adv Drug Deliv Rev* 65(1):21–23. <https://doi.org/10.1016/j.addr.2012.04.010>
4. Raveendran P, Fu J, Wallen SL (2003) Completely “Green” synthesis and stabilization of metal nanoparticles. *J Am Chem Soc* 125(46):13940–13941. <https://doi.org/10.1021/ja029267j>
5. Chandra H, Kumari P, Bontempi E, Yadav S (2020) Medicinal plants: treasure trove for green synthesis of metallic nanoparticles and their biomedical applications. *Biocatal Agric Biotechnol* 24:101518. <https://doi.org/10.1016/j.bcab.2020.101518>
6. Mpungose PP, Vundla ZP, Maguire GEM, Friedrich HB (2018) The current status of heterogeneous palladium catalysed Heck and Suzuki cross-coupling reactions. *Molecules* 23(7):1–24. <https://doi.org/10.3390/molecules23071676>
7. Fahmy SA, Preis E, Bakowsky U, El-Said Azzazy H (2020) Palladium nanoparticles fabricated by green chemistry: promising chemotherapeutic. *Antioxid Antimicrob Agents Mater* 13:3661. <https://doi.org/10.3390/ma13173661>

8. Qazi F, Hussain Z, Tahir MN (2016) Advances in biogenic synthesis of palladium nanoparticles. *RSC Adv* 6:60277–60286. <https://doi.org/10.1039/C6RA11695G>
9. Gowramma B, Keerthi U, Rafi M, Muralidhara Rao D (2015) Biogenic silver nanoparticles production and characterization from native strain of *Corynebacterium* species and its antimicrobial activity. *Biotech* 5(2):195–201. <https://doi.org/10.1007/s13205-014-0210-4>
10. Nasrollahzadeh M, Sajjadi M, Dadashi J, Ghafuri H (2020) Pd-based nanoparticles: Plant-assisted biosynthesis, characterization, mechanism, stability, catalytic and antimicrobial activities. *Adv Coll Interface Sci* 276:1–34. <https://doi.org/10.1016/j.cis.2020.102103>
11. Mittal AK, Chisti Y, Banerjee UC (2013) Synthesis of metallic nanoparticles using plant extracts. *Biotechnol Adv* 31(2):346–356. <https://doi.org/10.1016/j.biotechadv.2013.01.003>
12. Kavitha K, Baker S, Rakshith D, Kavitha H, Harini BP, Satish S (2013) Plants as green source towards synthesis of nanoparticles. *Int Res J Biological Sci* 2(6):66–76
13. Kharissova OV, Dias HVR, Kharisov BI, Perez BO (2013) The greener synthesis of nanoparticles. *Trends Biotechnol* 31(4):240–248. <https://doi.org/10.1016/j.tibtech.2013.01.003>
14. Shah M, Fawcett D, Sharma S, Tripathy SK, Poinern GEJ (2015) Green synthesis of metallic nanoparticles via biological entities. *Materials (Basel)* 8(11):7278–7308. <https://doi.org/10.3390/ma8115377>
15. Kulkarni N, Muddapur U (2014) Biosynthesis of metal nanoparticles: a review. *J Nanotechnol*. <https://doi.org/10.1155/2014/510246>
16. Mohamad NAN, Arham NA, Jai J, Hadi A (2013) Plant extract as reducing agent in synthesis of metallic nanoparticles: a review. *Adv Mater Res* 832:350–355. <https://doi.org/10.4028/www.scientific.net/amr.832.350>
17. Vishnukumar P, Vivekanandhan S, Muthuramkumar S (2017) Plant-mediated biogenic synthesis of palladium nanoparticles: recent trends and emerging opportunities. *Chem Biol Eng Rev* 4(1):18–36. <https://doi.org/10.1002/cben.201600017>
18. Yang X, Li Q, Wang H, Huang J, Lin L, Wang W, Sun D, Su Y, Opiyo JB, Hong L, Wang Y, He N, Jia L (2010) Green synthesis of palladium nanoparticles using broth of *Cinnamomum camphora* leaf. *J Nanopart Res* 12(5):1589–1598. <https://doi.org/10.1007/s11051-009-9675-1>
19. Sheny DS, Philip D, Mathew J (2012) Rapid green synthesis of palladium nanoparticles using the dried leaf of *Anacardium occidentale*. *Spectrochim Acta Part A Mol Biomol Spectrosc* 91:35–38. <https://doi.org/10.1016/j.saa.2012.01.063>
20. Roopan SM, Bharathi A, Kumar R, Khanna VG, Prabhakarn A (2012) Acaricidal, insecticidal, and larvicidal efficacy of aqueous extract of *Annona squamosa L* peel as biomaterial for the reduction of palladium salts into nanoparticles. *Colloids Surf B Biointerfaces* 92:209–212. <https://doi.org/10.1016/j.colsurfb.2011.11.044>
21. Petla RM, Vivekanandhan S, Misra M, Mohanty A, Satyanarayana N (2012) Soybean (*glycine max*) leaf extract based green synthesis of palladium nanoparticles. *J Biomater Nanobiotechnol* 3(1):14–19. <https://doi.org/10.4236/jbnb.2012.31003>
22. Kalaiselvi A, Roopan SM, Madhumitha G, Ramalingam C, Elango G (2015) Synthesis and characterization of palladium nanoparticles using *Catharanthus roseus* leaf extract and its application in the photo-catalytic degradation. *Spectrochim Acta Part A Mol Biomol Spectrosc* 135:116–119. <https://doi.org/10.1016/j.saa.2014.07.010>
23. Palliyarayil A, Jayakumar KK, Sil S, Kumar NS (2018) A facile green tea assisted synthesis of palladium nanoparticles using recovered palladium from spent palladium impregnated carbon. *Johns Matthey Technol Rev* 62(1):60–73. <https://doi.org/10.1595/205651317X696252>
24. Jia L, Zhang Q, Li Q, Song H (2009) The biosynthesis of palladium nanoparticles by antioxidants in *Gardenia jasminoides Ellis*: Long lifetime nanocatalysts for p-nitrotoluene hydrogenation. *Nanotechnology* 20(38):1–10. <https://doi.org/10.1088/0957-4484/20/38/385601>
25. Nadagouda MN, Varma RS (2008) Green synthesis of silver and palladium nanoparticles at room temperature using coffee and tea extract. *Green Chem* 10(8):859–886. <https://doi.org/10.1039/B804703K>
26. Baruwati B, Varma RS (2009) High value products from waste: Grape pomace extract—a three-in-one package for the synthesis of metal nanoparticles. *Chemoschem* 2(11):1041–1044. <https://doi.org/10.1002/cssc.200900220>
27. Sathishkumar M, Sneha K, Yun Y (2009) Palladium nanocrystal synthesis using *Curcuma longa Tuber* extract. *Int J Mater Sci* 4(1):11–17
28. Bankar A, Joshi B, Kumar AR, Zinjarde S (2010) Banana peel extract mediated novel route for the synthesis of palladium nanoparticles. *Mater Lett* 64(18):1951–1953. <https://doi.org/10.1016/j.matlet.2010.06.021>
29. Mallikarjuns K, Sushma NJ, Narasimha G, Venkateswara RK, Manoj L, Raju BDP (2011) Synthesis and spectroscopic characterization of palladium nanoparticles by using broth of edible mushroom extract. *Proc Int Conf Nanosci Eng Technol ICONSET 2011*:612–615. <https://doi.org/10.1109/ICONSET.2011.6168045>
30. Farhadi K, Pourhossein A, Forough M, Molaei R, Abdi A, Siyamic A (2013) Biosynthesis of highly dispersed palladium nanoparticles using *Astragalmanna* aqueous extract. *J Chinese Chem Soc* 60(9):1144–1149. <https://doi.org/10.1002/jccs.201300006>
31. Kou J, Varma RS (2012) Beet juice utilization: expeditious green synthesis of noble metal nanoparticles (Ag, Au, Pt, and Pd) using microwaves. *RSC Adv* 2(27):10283–10290. <https://doi.org/10.1039/C2RA21908E>
32. Mallikarjuna K, Sushma NJ, Reddy BVS, Narasimha G, Raju BDP (2013) Palladium nanoparticles: Single-step plant-mediated green chemical procedure using *Piper betle* leaves broth and their antifungal studies. *Int J Chem Anal Sci* 4(1):14–18. <https://doi.org/10.1016/j.ijcas.2013.03.006>
33. Lakshmiopathy R, Reddy BP, Sarada NC, Chidambaram K, Pasha SKK (2015) Watermelon rind-mediated green synthesis of noble palladium nanoparticles: catalytic application. *Appl Nanosci* 5(2):223–228. <https://doi.org/10.1007/s13204-014-0309-2>
34. Santoshi kumari A, Venkatesham M, Ayodhya D, Veerabhadram G (2015) Green synthesis, characterization and catalytic activity of palladium nanoparticles by xanthan gum. *Appl Nanosci* 5(3):315–320. <https://doi.org/10.1007/s13204-014-0320-7>
35. Ganaie SU, Abbasi T, Abbasi SA (2016) Low-cost, environment-friendly synthesis of palladium nanoparticles by utilizing a terrestrial weed *Antigonon leptopus*. *Part Sci Technol* 34(2):201–208. <https://doi.org/10.1080/02726351.2015.1058874>
36. Surendra TV, Roopan SM, Arasu MV, Al-Dhabi NA, Rayalu GM (2016) RSM optimized *Moringa oleifera* peel extract for green synthesis of *M. oleifera* capped palladium nanoparticles with antibacterial and hemolytic property. *J Photochem Photobiol B Biol* 162:550–557. <https://doi.org/10.1016/j.jphotobiol.2016.07.032>
37. Arsiya F, Sayadi MH, Sobhani S (2017) Green synthesis of palladium nanoparticles using *Chlorella vulgaris*. *Mater Lett* 186:113–115. <https://doi.org/10.1016/j.matlet.2016.09.101>
38. Sharmila G, Farzana MF, Haries S, Geetha S, Manoj Kumar N, Muthukumaran C (2017) Green synthesis, characterization and antibacterial efficacy of palladium nanoparticles synthesized using *Filicium decipiens* leaf extract. *J Mol Struct* 1138:35–40. <https://doi.org/10.1016/j.molstruc.2017.02.097>

39. Sayadi MH, Salmani N, Heidari A, Rezaei MR (2018) Bio-synthesis of palladium nanoparticle using *Spirulina platensis* alga extract and its application as adsorbent. Surf Interfaces 10:136–143. <https://doi.org/10.1016/j.surfin.2018.01.002>
40. Sriramulu M, Sumathi S (2018) Biosynthesis of palladium nanoparticles using *Saccharomyces cerevisiae* extract and its photocatalytic degradation behaviour. Adv Nat Sci Nanosci Nanotechnol 9(2):1–6. <https://doi.org/10.1088/2043-6254/aac506>
41. Anand K, Tiloke C, Phulukdaree A, Ranjan B, Chuturgoon A, Singh S, Gengan RM (2016) Biosynthesis of palladium nanoparticles by using *Moringa oleifera* flower extract and their catalytic and biological properties. J Photochem Photobiol B Biol 165:87–95. <https://doi.org/10.1016/j.jphotobiol.2016.09.039>
42. Kandathil V, Dateer RB, Sasidhar BS, Patil SA, Patil SA (2018) Green synthesis of palladium nanoparticles: applications in aryl halide cyanation and Hiyama cross-coupling reaction under ligand free conditions. Catal Lett 148:1562–1578. <https://doi.org/10.1007/s10562-018-2369-5>
43. Liu D, Wu F (2017) Biosynthesis of pd nanoparticle using onion extract for electrochemical determination of carbendazim. Int J Electrochem Sci 12(3):2125–2134. <https://doi.org/10.20964/2017.03.70>
44. Kalpana VN, Rajeswari VD (2018) Synthesis of palladium nanoparticles via a green route using *Lagenaria siceraria*: assessment of their innate antidandruff, insecticidal and degradation activities. Mater Res Express 5(11):1154066
45. Olajire AA, Mohammed AA (2019) Green synthesis of palladium nanoparticles using *Ananas comosus* leaf extract for solid-phase photocatalytic degradation of low density polyethylene film. J Environ Chem Eng 7(4):103270. <https://doi.org/10.1016/j.jece.2019.103270>
46. Søjberg LS, Gauthier D, Lindhardt AT, Bunge M, Finster K, Meyer RL, Skrydstrup T (2009) Bio-supported palladium nanoparticles as a catalyst for Suzuki-Miyaura and Mizoroki-Heck reactions. Green Chem 11(12):2041–2046. <https://doi.org/10.1039/B918351P>
47. Veisi H, Ghorbani-Vaghei R, Hemmati S, Haji Aliani M, Ozturk T (2015) Green and effective route for the synthesis of monodispersed palladium nanoparticles using herbal tea extract (*Stachys lavandulifolia*) as reductant, stabilizer and capping agent, and their application as homogeneous and reusable catalyst in Suzuki coupling reactions in water. Appl Organomet Chem 29(1):26–32. <https://doi.org/10.1002/aoc.3243>
48. Nasrollahzadeh M, Sajadi SM, Maham M (2015) Green synthesis of palladium nanoparticles using *Hippophae rhamnoides* Linn leaf extract and their catalytic activity for the Suzuki-Miyaura coupling in water. J Mol Catal A Chem 396:297–303. <https://doi.org/10.1016/j.molcata.2014.10.019>
49. Nasrollahzadeh M, Mohammad Sajadi S, Rostami-Vartooni A, Khalaj M (2015) Green synthesis of Pd/Fe₃O₄ nanoparticles using *Euphorbia condylocarpa* M. bieb root extract and their catalytic applications as magnetically recoverable and stable recyclable catalysts for the phosphine-free Sonogashira and Suzuki coupling reactions. J Mol Catal A Chem 396:31–39. <https://doi.org/10.1016/j.molcata.2014.09.029>
50. Nasrollahzadeh M, Sajadi SM, Maham M, Ehsani A (2014) Facile and surfactant-free synthesis of Pd nanoparticles by the extract of the fruits of *Piper longum* and their catalytic performance for the Sonogashira coupling reaction in water under ligand and copper-free conditions. RSC Adv 3:2562–2567. <https://doi.org/10.1039/C4RA12875C>
51. Veisi H, Faraji AR, Hemmati S, Gil A (2015) Green synthesis of palladium nanoparticles using *Pistacia atlantica kurdica* gum and their catalytic performance in Mizoroki-Heck and Suzuki-Miyaura coupling reactions in aqueous solutions. Appl Organomet Chem 29(8):517–523. <https://doi.org/10.1002/aoc.3325>
52. Nasrollahzadeh M, Sajadi SM, Rostami-Vartooni A, Bagherzadeh M (2015) Green synthesis of Pd/CuO nanoparticles by *Theobroma cacao* L. seeds extract and their catalytic performance for the reduction of 4-nitrophenol and phosphine-free Heck coupling reaction under aerobic conditions. J Colloid Interface Sci 448:106–113. <https://doi.org/10.1016/j.jcis.2015.02.009>
53. Borah RK, Saikia HJ, Mahanta A, Das VK, Bora U, Thakur AJ (2015) Biosynthesis of poly(ethylene glycol)-supported palladium nanoparticles using *Colocasia esculenta* leaf extract and their catalytic activity for Suzuki-Miyaura cross-coupling reactions. RSC Adv 5(89):72453–72457. <https://doi.org/10.1039/C5RA12657F>
54. Nasrollahzadeh M, Mohammad Sajadi S (2016) Pd nanoparticles synthesized in situ with the use of *Euphorbia granulate* leaf extract: catalytic properties of the resulting particles. J Colloid Interface Sci 462:243–251. <https://doi.org/10.1016/j.jcis.2015.09.065>
55. Nasrollahzadeh M, Sajadi SM (2016) Green synthesis of Pd nanoparticles mediated by *Euphorbia thymifolia* L. leaf extract: catalytic activity for cyanation of aryl iodides under ligand-free conditions. J Colloid Interface Sci 469:191–195. <https://doi.org/10.1016/j.jcis.2016.02.024>
56. Veisi H, Nasrabadi NH, Mohammadi P (2016) Biosynthesis of palladium nanoparticles as a heterogeneous and reusable nanocatalyst for reduction of nitroarenes and Suzuki coupling reactions. Appl Organomet Chem 30(11):890–896. <https://doi.org/10.1002/aoc.3517>
57. Liu G, Bai X, Lv H (2017) Biosynthesis of supported Pd nanoparticles using poplar leaf as a reducing agent and carrier: a green route to highly efficient and reusable Suzuki coupling reaction catalyst. Inorg Nano-Metal Chem 47(8):1226–1233. <https://doi.org/10.1080/24701556.2017.1284114>
58. Liu G, Bai X, Lv H (2017) Green synthesis of supported palladium nanoparticles employing pine needles as reducing agent and carrier: new reusable heterogeneous catalyst in the Suzuki coupling reaction. Appl Organomet Chem 31(4):1–7. <https://doi.org/10.1002/aoc.3587>
59. Sarmah M, Dewan A, Mondal M, Thakur AJ, Bora U (2016) Analysis of the water extract of waste papaya bark ash and its implications as an in situ base in the ligand-free recyclable Suzuki-Miyaura coupling reaction. RSC Adv 6(34):28981–28985. <https://doi.org/10.1039/C6RA00454G>
60. Sarmah M, Dewan A, Thakur AJ, Bora U (2017) Extraction of base from *Eichhornia crassipes* and its implication in palladium-catalyzed Suzuki cross-coupling reaction. Chem Sel 2(24):7091–7095. <https://doi.org/10.1002/slct.201701057>
61. Dewan A, Sarmah M, Thakur AJ, Bharali P, Bora U (2018) Greener biogenic approach for the synthesis of palladium nanoparticles using papaya peel: an eco-friendly catalyst for C-C coupling reaction. ACS Omega 3(5):5327–5335. <https://doi.org/10.1021/acsomega.8b00039>
62. Kandathil V, Dateer RB, Sasidhar BS, Patil SA, Patil SA (2018) Green synthesis of palladium nanoparticles: applications in aryl halide cyanation and Hiyama cross-coupling reaction under ligand free conditions. Catal Lett 148(6):1562–1578. <https://doi.org/10.1007/s10562-018-2369-5>
63. Nasrollahzadeh M, Ghorbannezhad F, Sajadi SM, Varma RS (2019) Pd nanocatalyst adorning coral reef nanocomposite for the synthesis of nitriles: Utility of *cucurbita pepo* leaf extract as a stabilizing and reducing agent. Nanomaterials 9(4):565. <https://doi.org/10.3390/nano9040565>
64. Hemmati S, Yousefi M, Salehi MH, Amiri M, Hekmati M (2020) Palladium nanoparticles immobilized over Strawberry fruit extract coated Fe₃O₄ NPs: A magnetic reusable nanocatalyst for Suzuki-Miyaura coupling reactions. Appl Organomet Chem 34(8):1–8. <https://doi.org/10.1002/aoc.5653>

65. Manjare SB, Chaudhari RA (2020) Palladium nanoparticle-bentonite hybrid using leaves of *Syzygium aqueum* plant from India: design and assessment in the catalysis of -C-C- coupling reaction. *Chem Afr* 3(2):329–341. <https://doi.org/10.1007/s42250-020-00139-2>
66. Manjare SB, Chaudhari RA (2020) Environment-friendly synthesis of palladium nanoparticles loaded on Zeolite Type-Y (Na-form) using *Anacardium occidentale* shell extract (Cashew nut shell extract), characterization and application in -C-C- coupling reaction. *J Environ Chem Eng* 8(5):104213. <https://doi.org/10.1016/j.jece.2020.104213>
67. Khan M, Khan M, Kuniyil M, Adil SF, Al-Warthan A, Alkathlan HZ, Tremel W, Tahir MN, Siddiqui MRH (2014) Biogenic synthesis of palladium nanoparticles using *Pulicaria glutinosa* extract and their catalytic activity towards the Suzuki coupling reaction. *Dalt Trans* 43(24):9026–9031. <https://doi.org/10.1039/C3DT53554A>
68. Nasrollahzadeh M, Mohammad Sajadi S (2016) Green synthesis, characterization and catalytic activity of the Pd/TiO₂ nanoparticles for the ligand-free Suzuki-Miyaura coupling reaction. *J Colloid Interface Sci* 465:121–127. <https://doi.org/10.1016/j.jcis.2015.11.038>
69. Baruah D, Das RN, Hazarika S, Konwar D (2015) Biogenic synthesis of cellulose supported Pd(0) nanoparticles using hearth wood extract of *Artocarpus lakoocha Roxb*—a green, efficient and versatile catalyst for Suzuki and Heck coupling in water under microwave heating. *Catal Commun* 72:73–80. <https://doi.org/10.1016/j.catcom.2015.09.011>
70. Lebaschi S, Hekmati M, Veisi H (2017) Green synthesis of palladium nanoparticles mediated by black tea leaves (*Camellia sinensis*) extract: Catalytic activity in the reduction of 4-nitrophenol and Suzuki-Miyaura coupling reaction under ligand-free conditions. *J Colloid Interface Sci* 485:223–231. <https://doi.org/10.1016/j.jcis.2016.09.027>
71. Seyedi N, Saidi K, Sheibani H (2018) Green synthesis of Pd nanoparticles supported on magnetic graphene oxide by *Origanum vulgare* leaf plant extract: catalytic activity in the reduction of organic dyes and Suzuki-Miyaura cross-coupling reaction. *Catal Lett* 148(1):277–288. <https://doi.org/10.1007/s10562-017-2220-4>
72. Kannaiyan P, Raiza AJ, Ramya R, Devi S (2015) Biogenic synthesis of palladium nanoparticles modified graphene using *Ficus carica* fruit extract and study its catalytic activity in organic synthesis. *Int J Chem Tech Res* 7(3):1247–1252
73. Garel C, Renard BL, Escande V, Galtayries A, Hesemann P, Grison C (2015) C-C bond formation strategy through ecocatalysis: Insights from structural studies and synthetic potential. *Appl Catal A Gen* 504:272–286. <https://doi.org/10.1016/j.apcata.2015.01.021>
74. Kora AJ, Rastogi L (2018) Green synthesis of palladium nanoparticles using gum ghatti (*Anogeissus latifolia*) and its application as an antioxidant and catalyst. *Arab J Chem* 11(7):1097–1106. <https://doi.org/10.1016/j.arabj.2015.06.024>
75. Kumar B, Smita K, Cumbal L, Debut A (2015) Ultrasound agitated phytofabrication of palladium nanoparticles using *Andean blackberry leaf* and its photocatalytic activity. *J Saudi Chem Soc* 19(5):574–580. <https://doi.org/10.1016/j.jscs.2015.05.008>
76. Veisi H, Rostami A, Shirinbayan M (2016) Greener approach for synthesis of monodispersed palladium nanoparticles using aqueous extract of green tea and their catalytic activity for Suzuki-Miyaura coupling reaction and the reduction of nitroarenes. *Appl Organomet Chem* 31(6):1–9. <https://doi.org/10.1002/aoc.3609>
77. Khan M, Albalawi GH, Shaik MR, Khan M, Adil SF, Kuniyil M, Alkathlan HZ, Al-Warthan A, Siddiqui MRH (2016) Miswak mediated green synthesized palladium nanoparticles as effective catalyst for Suzuki coupling reactions in aqueous media. *J Saudi Chem Soc* 21(4):450–457. <https://doi.org/10.1016/j.jscs.2016.03.008>
78. Majumdar R, Tantayanon S, Bag BP (2017) Synthesis of palladium nanoparticles with leaf extract of *Chrysophyllum cainito* (Star apple) and their applications as efficient catalyst for C-C coupling and reduction reactions. *Int Nano Lett* 7:267–274. <https://doi.org/10.1007/s40089-017-0220-4>
79. Rabiee N, Bagherzadeh M, Kiani M, Ghadiri AM (2020) *Rosmarinus officinalis* directed palladium nanoparticle synthesis: investigation of potential anti-bacterial, anti-fungal and Mizoroki-Heck catalytic activities. *Adv Power Technol Technol* 31:1–10. <https://doi.org/10.1016/j.appt.2020.01.024>
80. Yang F, Cao B, Tao Y, Cao D, Zhang Y (2016) Nicotinamide-assisted fabrication of high-stability gold-palladium nanoparticles on carbon fiber cloth for hydrogen peroxide electroreduction. *Electrochim Acta* 210:199–205. <https://doi.org/10.1016/j.electacta.2016.05.152>
81. Borah RK, Mahanta A, Dutta A, Bora U, Thakur AJ (2017) A green synthesis of palladium nanoparticles by *Sapindus mukorossi* seed extract and use in efficient room temperature Suzuki-Miyaura cross-coupling reaction. *Appl Organomet Chem* 31(11):1–9. <https://doi.org/10.1002/aoc.3784>
82. Veisi H, Rashtiani A, Barjasteh V (2016) Biosynthesis of palladium nanoparticles using *Rosa canina* fruit extract and their use as a heterogeneous and recyclable catalyst for Suzuki-Miyaura coupling reactions in water. *Appl Organomet Chem* 30:231–235. <https://doi.org/10.1002/aoc.3421>
83. Hazarika M, Borah D, Bora P, Silva AR, Das P (2017) Biogenic synthesis of palladium nanoparticles and their applications as catalyst and antimicrobial agent. *PLoS ONE* 12(9):1–19. <https://doi.org/10.1371/journal.pone.0184936>
84. Khodadadi B, Bordbar M, Nasrollahzadeh M (2017) Green synthesis of Pd nanoparticles at Apricot kernel shell substrate using *Salvia hydrangea* extract: catalytic activity for reduction of organic dyes. *J Colloid Interface Sci* 490:1–10. <https://doi.org/10.1016/j.jcis.2016.11.032>
85. Mallikarjuna K, Bathula C, Buruga K, Shrestha NK, Noh YY, Kim H (2017) Green synthesis of palladium nanoparticles using fenugreek tea and their catalytic applications in organic reactions. *Mater Lett* 205:138–141. <https://doi.org/10.1016/j.matlet.2017.06.081>
86. Hekmati M, Bonyasi F, Javaheri H, Hemmati S (2016) Green synthesis of palladium nanoparticles using *Hibiscus sabdariffa* L. flower extract: heterogenous and reusable nanocatalyst in Suzuki coupling reaction. *Appl Organomet Chem* 31(11):1–7. <https://doi.org/10.1002/aoc.3757>



Design and synthesis of novel conformationally constrained 7,12-dihydro-dibenzo[b,h][1,6] naphthyridine and 7H-Chromeno[3,2-c] quinoline derivatives as topoisomerase I inhibitors: *In vitro* screening, molecular docking and ADME predictions

Ramakant A. Kardile^a, Aniket P. Sarkate^b, Avinash S. Borude^a, Rajendra S. Mane^c, Deepak K. Lokwani^d, Shailee V. Tiwari^e, Rajaram Azad^f, Prasad V.L.S. Burra^g, Shankar R. Thopate^{h,*}

^a Department of Chemistry, Ahmednagar College, Ahmednagar 414001, Maharashtra, India

^b Department of Chemical Technology, Dr. Babasaheb Ambedkar Marathwada University, Aurangabad 431004, Maharashtra, India

^c Department of Chemistry, Dr. S. D. D. Arts College and Commerce and Science College, Wada 421303, Maharashtra, India

^d Department of Pharmaceutical Chemistry, R. C. Patel Institute of Pharmaceutical Education & Research, Shirpur 425405, Maharashtra, India

^e Department of Pharmaceutical Chemistry, Durgamata Institute of Pharmacy, Dharmapuri, Parbhani 431401, Maharashtra, India

^f Department of Animal Biology, University of Hyderabad, Hyderabad 500046, India

^g Department of Biotechnology, KLEF University, Vaddeswaram 522502, Andhra Pradesh, India

^h Department of Chemistry, S. S. G. M. College, Kopargaon 423601, Maharashtra, India

ARTICLE INFO

Keywords:

Anticancer agents
Topoisomerase I inhibitors
Non-Camptothecin Topo I inhibitors
Dibenzo[b,h][1,6] naphthyridines
Chromeno[3,2-c] quinolones
Molecular docking
ADME study

ABSTRACT

Novel non-camptothecin (non-CPT) class of conformationally constrained, hitherto unknown 7,12-dihydro-dibenzo[b,h][1,6] naphthyridine and 7H-Chromeno[3,2-c] quinoline derivatives have been designed, synthesized and evaluated for anti-cancer activity. *In vitro* anti-proliferation evaluation against human cancer cell lines (A549 and MCF-7) exhibited significant cytotoxicity. Among the derivatives (8–24), **8** (IC₅₀ 0.44 μM and IC₅₀ 0.62 μM) and **12** (IC₅₀ 0.69 μM and IC₅₀ 0.54 μM) were identified as the most promising candidate against A-549 and MCF-7 cancer cell lines respectively. Topo I inhibitory activity of **8** and **12** suggested that, they may be developed as potential anti-cancer molecules in future and rationalized by docking analysis with effective binding modes. Further, *in silico* ADME prediction studies of all derivatives were found promising, signifying the drug like properties. In precise, the present investigation displays a new strategy to synthesize and emphasis on anticancer activities of conformationally constrained dibenzo[b,h][1,6] naphthyridine derivatives and Chromeno[3,2-c] quinoline derivatives in the context of cancer drug development and refinement.

1. Introduction

As a ubiquitous and essential enzyme, DNA Topoisomerases I (Topo I) plays a crucial role in relaxing the topological constraints and achieving infinite replicative potential by cancer cells during DNA replication [1]. The biological function and significances of fluctuation in the activity of Topo I have been broadly distinguished [2]. Camptothecin (CPT) (Fig. 1) and its several structurally modified derivatives such as topotecan, belotecan and irinotecan are contemporary anticancer chemotherapeutic agents for treatment of various cancers in an effort to overcome numerous limitations [3]. Several limitations include

metabolic instability due to the ring E opening, subsequent resistance, toxicity, solubility and side effects [4]. Due to these inadequacies, there is a great interest in an understanding and developing the structural features essential for binding in the active site. Many alterations have been attained to develop suitable inhibitor to overcome the drawback of CPTs and discovery of non-CPT Topo I inhibitors has emerged as a favorable field to find improved chemotherapeutic agents [5].

Discovery of indenoisoquinoline analogues (Fig. 1) (LMP400, LMP776 and LMP744) as an attractive scaffold has entered phase I clinical trials for treatment in adults with solid tumours and lymphomas [6]. In an attempt to find dual inhibitors of Topo I and Topo II, SAR

* Corresponding author at: Address: Department of Chemistry, S. S. G. M. College, Kopargaon 423601, Maharashtra, India.
E-mail address: srthopate@gmail.com (S.R. Thopate).

<https://doi.org/10.1016/j.bioorg.2021.105174>

Received 11 May 2021; Received in revised form 8 July 2021; Accepted 11 July 2021

Available online 16 July 2021

0045-2068/© 2021 Elsevier Inc. All rights reserved.

studies revealed that structural features in TAS-103: indeno[2,1-c]-quinoline derivative and indeno[1,2-c]quinoline derivatives are crucial for the selectivity [5b, 7]. Through a scaffold modification from the indeno isoquinolines, LaVoie's group discovered dibenzo[c,h][1,6]naphthyridinone derivative ARC-111, as a highly potent Topo I inhibitor [8]. Genz-644282, has emerged as a promising candidate for antitumor agents and has entered into phase I clinical trial [9]. 8-substituted imidazoquinoline based, Panulisib P-7170 and analogues drugs (Dactolisib and LY-3023414) are currently under clinical trials as anticancer therapeutics that are targeted against the PI3Ks, which are important regulators of cell growth and transformation, which are downward to the receptor kinases [10]. Apart from all beyond Topo I inhibitors, the novel 7-(ethoxycarbonyl)-8-(arylamino)-[1,3]dioxolo[4,5-g] quinolin-5-ium iodide have identified significant antitumor and antibacterial activity [11].

Focussing on the therapeutic potential of quinoline skeleton, in the process of drug developing and designing valuable therapeutic alternatives, one of the most crucial aspect is fine tuning of both pharmacodynamic and pharmacokinetics profiles. It does not depend on the number of oxygen and nitrogen atoms, but rationally match their overall distribution and optimization. In this context, quinoline nucleus always has been conjugated with quite a few other pharmacophores to obtain compounds with improved potency

Conformational control of molecular scaffolds offers pharmacological efficiency in anticancer compounds. With this rationale, in search of novel non-Camptothecin scaffold, we articulate that if the structural correspondence were indeed responsible for the anticancer activity, then an analogous compounds might be synthesized by making a compound having a structural similarity that would more closely resembles with an indenoisoquinoline, indeno[2,1-c]-quinoline, indeno[1,2-c]quinoline,

dibenzo[c,h][1,6]naphthyridinone, Genz-644282, 8-substituted imidazoquinoline and quinolone derivatives. In search of a potent Topo I inhibitor endowed with improved physicochemical and pharmacokinetic profiles, owing to the drug-like properties and therapeutic potential of novel non-Camptothecin scaffold, conformationally constrained 7,12-dihydrodibenzo[b,h][1,6] naphthyridine and 7H-Chromeno[3,2-c] quinoline derivatives, we believe that both scaffolds have a number of features that make it attractive as a potential lead compound for the development of Topo I inhibitors that may overcome some of the limitations of CPTs. Imidazole is a privileged fragment in modern medicinal chemistry considering its broad spectrum and affinity towards various biological targets. The applications of imidazole derivatives in medicinal chemistry have achieved great progress. The imidazole ring forms the core of many pharmacological important molecules having a wide array of activities like anti-inflammatory, antimicrobial, antiulcer and antioxidant. It has been revealed that introduction of imidazole moiety in anticancer drugs embrace considerable potential. The imidazole derivatives are also found naturally in the amino acid like histidine, in vitamin B12 and a component of the DNA base structure [12].

With this inspiration, we herein report the efficient synthetic procedures for the preparation of a hitherto unknown conformationally constrained 7,12-dihydrodibenzo[b,h][1,6] naphthyridine and 7H-Chromeno[3,2-c] quinoline backbone and *in vitro* screening, molecular docking and ADME predictions in order to develop some potential anticancer structures leads which could be compared to parent molecules in cancer chemotherapy.

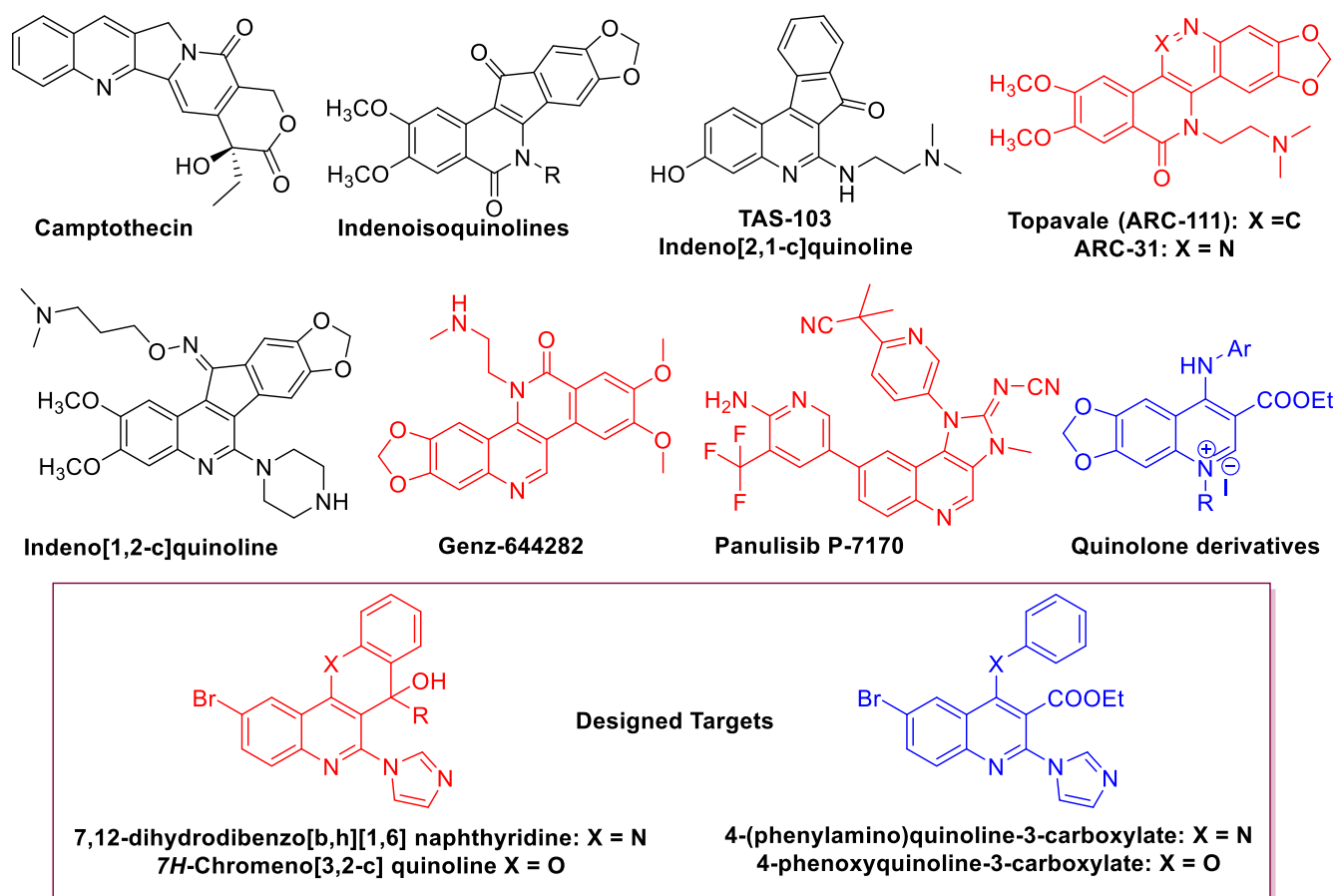


Fig. 1. Topo I inhibitors, Quinolone derivatives and designed targets.

2. Results and discussion

2.1. Chemistry

The synthesis of 4-(phenylamino)quinoline-3-carboxylates (**6** and **7**) and 7,12-dihydrodibenzo[*b,h*][1,6] naphthyridines (**8–15**) were depicted in [Scheme 1](#).

2.1.1. Synthesis of quinoline derivatives (**8–15**)

4-Bromoaniline **1** and malonic acid **2** were converted to the known 6-bromo-2,4-dichloroquinoline derivative **3** having well defined chloro substituents [\[13\]](#). Selective substitution in **3** was achieved with freshly prepared LDA in anhydrous THF at $-78\text{ }^{\circ}\text{C}$ and subsequent addition of ethyl chloroformate to afford requisite ethyl-3-carboxylate derivative **4** [\[14\]](#) with moderate 67 % yield. To achieve synthesis of 2-(1H-imidazol-1-yl) quinolone derivative **5**, various conditions were employed. Substitution of both chloro groups in **4** with imidazole was observed to get di-substituted imidazole derivative. Mono-substitution in **4** at position-2 was succeeded with imidazole (1.01 eq) and K_2CO_3 (2 eq) in dry DMF at rt for 12 h, which afforded compound **5** [\[15\]](#).

In general, introduction of 4-phenylamino and 4-phenoxy at C-4 of the quinoline skeleton is difficult; however, we utilized 4-chloro substituent of the common intermediate 2-(1H-imidazol-1-yl) quinolone **5** to get the required substituents while building the 4-(phenylamino) quinoline derivative **6** and 4-phenoxyquinoline-3-carboxylate **16** ([Scheme 2](#)).

The synthesis of 4-(phenylamino)quinoline derivative **6**, under diverse conditions resulted in substitution of both imidazole and chloro substituents at position-2 and 4 respectively with aniline to get di-aniline substituted derivative affording desired product formation in less yields. Under reviewed conditions, derivative **6** with substitution only at position 4 was achieved with distilled aniline (1.01 eq.) in catalytic *p*-toluenesulfonic acid in dry toluene in 76% yield as yellow solid

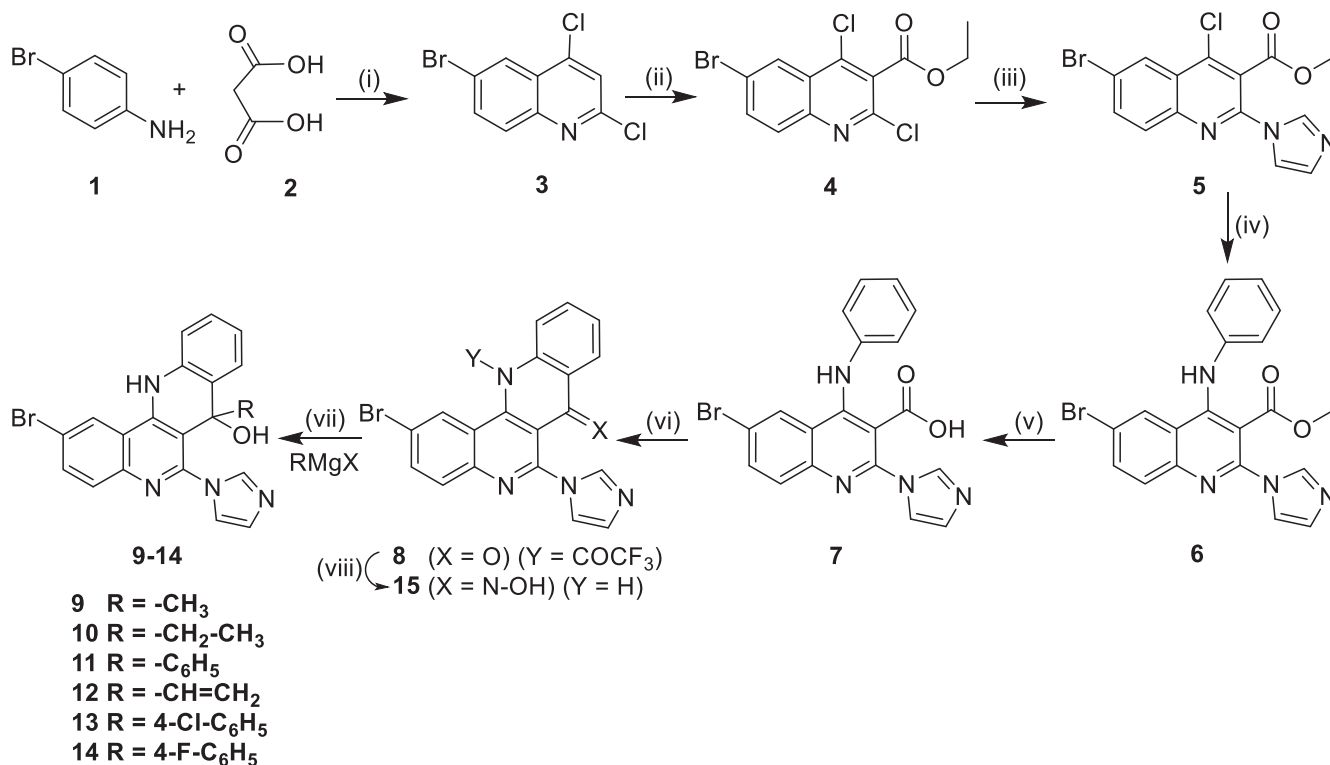
[\[16\]](#).

The compound **6** was hydrolyzed with 10 % aq. NaOH in THF: H_2O (1:1, v/v) then the reaction mass was acidified with acetic acid to afford acid **7** with good yield (93 %). The compound **7** was treated with trifluoro acetic anhydride (20 eq.) in THF: DCM (1:1, v/v) at $0\text{ }^{\circ}\text{C}$ to rt for 4–5 h afforded cyclized compound **8** [\[17\]](#) with moderate yield 87%. The compounds **9–14** [\[18\]](#) were prepared by treating compound **8** with different Grignard reagent in molar solution in THF or diethyl ether (R-Mg-X) (2 eq.) in dry THF with moderate yield 62–35 %. The oxime **15** was obtained with treatment of **8** with hydroxylamine hydrochloride (1.5 eq.) and NaHCO_3 (1.5 eq.) in EtOH: THF (4:5) [\[17a\]](#).

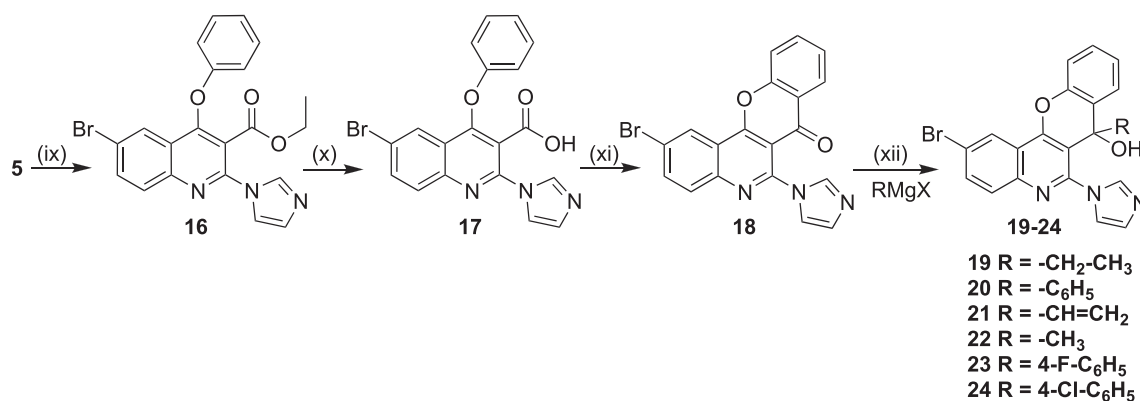
2.1.2. Synthesis of quinoline derivatives (**18–24**):

While targeting the synthesis of 4-phenoxyquinoline-3-carboxylates (**16** and **17**) and 7H-Chromeno[3,2-*c*] quinoline (**18–24**) ([Scheme 2](#)), the common intermediate 2-(1H-imidazol-1-yl) quinolone derivative **5** was treated with phenol (1.1 eq.) and K_2CO_3 (1.1 eq.) dry DMF at $100\text{ }^{\circ}\text{C}$ for 16 h to afford 4-phenoxyquinoline-3-carboxylates **16** [\[19\]](#).

Hydrolysis of carboxylate **16** under numerous acidic and basic conditions [\[20\]](#) using HCl, H_2SO_4 and aq. NaOH, LiOH, and KOH respectively was occurred without desired product. Alternatively, potassium trimethylsilylionate (3 eq.) in THF at $0\text{ }^{\circ}\text{C}$ to rt for 12 h afforded desired potassium salt of compound **17** [\[21\]](#). The salt of compound **17** was treated with trifluoroacetic anhydride (20 eq.) in THF: DCM (1:1, v/v) at $0\text{ }^{\circ}\text{C}$ to rt for 3 h afforded cyclized compound **18** with moderate yield 81.3 %. The compounds **19–24** [\[18\]](#) were prepared by treating **18** with different Grignard reagent in molar solution in THF or diethyl ether (R-Mg-X) (2 eq.) in dry THF at $0\text{ }^{\circ}\text{C}$ to rt for 2 h, which afforded compounds **19–24** with moderate yield 23–80%.



Scheme 1. Reagents and conditions: (i) POCl_3 , $100\text{ }^{\circ}\text{C}$, 6 h; 48.4%; (ii) Ethyl chloroformate (1.2 eq.), *n*-BuLi (1.2 eq.), DIPA (1.3 eq.), $-78\text{ }^{\circ}\text{C}$, 2 h; 67%; (iii) Dry DMF, K_2CO_3 (2 eq.), imidazole (1.01 eq), rt, 12 h; 55%; (iv) Aniline (1.01 eq.), cat. PTSA, dry toluene, $100\text{ }^{\circ}\text{C}$, 16 h; 76.5%; (v) 10% NaOH, THF: EtOH (4:4, v/v), $0\text{ }^{\circ}\text{C}$ -rt, 1 h, 93%; (vi) DCM: THF (1:1, v/v), TF_2O (20 eq.), $0\text{ }^{\circ}\text{C}$ -rt, 3 h; 81.3%; (vii) dry THF, R-Mg-X (2 eq.), $0\text{ }^{\circ}\text{C}$ -rt, 3 h; (viii) aq. NaHCO_3 (1.5 eq.), $\text{NH}_2\text{OH}\cdot\text{HCl}$ (1.5 eq.), EtOH: THF (4:5, v/v), $0\text{ }^{\circ}\text{C}$ -rt, 1 h, 58%.



Scheme 2. Reagents and conditions:(ix) Phenol (1.1 eq.), K₂CO₃ (1.1 eq.), DMF, 100 °C, 16 h, 75%; (x) Potassium trimethylsilanolate (3 eq.), 0 °C-rt, THF, 12 h, crude; (xi) DCM: THF (1:1, v/v), Tf₂O (20 eq.), 0 °C-rt, 3 h, 81.3%; (xii) Dry THF, R-Mg-X (2 eq.), 0 °C-rt, 3 h.

2.2. Biological evaluation

2.2.1. *In vitro* anticancer activity against A-549, MCF-7 and MCF-10A cancer cell lines

In order to evaluate the *in vitro* anticancer activity, the A549 (lung cancer) and MCF-7 (breast cancer) were treated with the synthesized compounds; the IC₅₀ values were determined using MTT assay. *In vitro* anticancer activity results in comparison to the positive control Camptothecin are expressed in IC₅₀ values and are reported in Table 1. Most of the synthesized compounds exhibited considerable cytotoxicity values against the selected cancer cell lines. Compounds **8**, **9**, **10**, **12**, **13**, **14**, **15** and **18** had showed good activity with their IC₅₀ values < 5 μM for the selected cancer cell lines. Among the synthesized compounds **8** and **12** were found to be more potent anticancer agents than that of standard drug Camptothecin as per the MTT assay results. The compound **8** was one of the most active compounds among the synthesized derivatives with IC₅₀ 0.44 μM and IC₅₀ 0.62 μM against A-549 and MCF-7 cancer cell lines respectively. The compound **12** has shown IC₅₀ 0.69 μM and IC₅₀ 0.54 μM against A-549 and MCF-7 cancer cell lines respectively. The compound **10** has interestingly shown almost equipotent activity to that of standard drug camptothecin.

From the activity data details obtained we have tried to put forth the SAR of our synthesized derivatives. The combination of different heterocycles was used to synthesise the novel derivatives. The various combi hetero-cycles used are quinoline-imidazole, quinoline-imidazole-naphthridine and the quinoline-imidazole-chromone. The results have

Table 1

IC₅₀ (μM) values of the synthesized compounds.

Compound	A-549	MCF-7	MCF-10A
5	40.11 ± 0.12	40.96 ± 0.78	ND
6	29.43 ± 0.11	32.11 ± 0.82	ND
7	34.92 ± 0.14	40.69 ± 0.92	ND
8	0.44 ± 0.08	0.62 ± 0.28	>50
9	1.42 ± 0.22	0.99 ± 1.12	ND
10	0.98 ± 0.32	0.99 ± 1.02	ND
12	0.69 ± 0.09	0.54 ± 0.04	>50
13	2.77 ± 0.12	2.60 ± 0.82	ND
14	2.94 ± 0.32	3.02 ± 0.99	ND
15	1.57 ± 0.11	1.03 ± 0.02	ND
16	42.44 ± 0.09	43.12 ± 0.45	ND
18	2.07 ± 0.08	2.28 ± 0.86	ND
20	8.12 ± 0.92	8.19 ± 0.55	ND
21	5.19 ± 0.24	7.41 ± 0.12	ND
23	9.99 ± 0.21	9.82 ± 1.02	ND
24	12.55 ± 0.82	11.23 ± 0.66	ND
Camptothecin	0.92 ± 0.29	0.80 ± 0.02	ND

A549: lung cancer cell line; MCF-7: breast cancer cell line; MCF-10A: normal breast cell line; Each data represents mean ± S.D. from three different experiments performed in triplicate.

shown that the quinoline-imidazole-naphthridine and the quinoline-imidazole-chromone rings are essential for the good anticancer activity in these derivatives. The derivatives containing quinoline-imidazole-naphthridine rings (**8**, **9**, **10**, **12**, **13**, **14**, **15** and **18**) were found to be more active than that of derivatives containing quinoline-imidazole-chromone rings (**20**, **21**, **23** and **24**). The 2-Bromo-6-(1H-imidazol-1-yl)-12-(2,2,2-trifluoroacetyl) dibenzo [b, h] [1,6] naphthridine-7 (12H)-one (**8**) was found to be most active synthesized derivative among the synthesized one.

This gives an emphasis on SAR that the quinoline-imidazole-naphthridine hybrid scaffolds can act as good anticancer agents and can be developed as a lead molecule in coming days. Among the quinoline-imidazole-naphthridine derivatives it was observed that the derivatives with the phenyl ring substitution at the 7th position of the naphthridine ring (**13** and **14**) were found to be less active than that of oxygen or hydroxy or the alkyl substitution at the 7th position of the naphthridine ring (**8**, **9**, **10** and **12**). Similar observation was also observed for the quinoline-imidazole-chromone hybrid scaffolds (**20**, **21**, **23** and **24**). The quinoline ring coupling with the naphthridine or the chromone ring is essential for the anticancer activity which can be said depending upon the activity data reported in the Table 1. The compounds **5**, **6**, **7** and **16** have shown less activity than that of other derivatives containing the quinoline ring coupling with the naphthridine or the chromone ring.

The good activity results shown by our synthesized compounds took our interest towards its mechanistic study. Depending upon the literature survey [22], we decided to carry out the mechanistic study using Topo I enzyme. The key safety feature of cancer chemotherapy is specific killing of cancer cells without affecting normal cell growth. In this connection, compounds **8** and **12** were screened for their possible cytotoxicity in normal cell line MCF-10A by using MTT assay. The assay results suggested that these compounds did not significantly affect the growth of normal cells (as these compounds showed IC₅₀ values > 50), suggesting that these molecules selectively inhibited the growth of cancer cells.

2.2.2. Topoisomerase I (Topo I) inhibition study:

Topo I is considered as one of the potential targets for scores of clinically used anticancer drugs. It is involved in the replication and proliferation process. Topo I is expressed much higher in tumour cells than in normal cells [22–26]. Inhibition against relaxation activity of Topo I was measured by detecting the conversion of supercoiled pBR322 DNA to its relaxed form in the presence of synthesized compounds **8** and **12**. Inhibitory activities were evaluated both at 100 μM. Camptothecin was used as positive control. The most active synthesized compounds, **8** and **12** were tested for their Topo I inhibitory activity. The compound **8** has shown the 72.4 % inhibition at 100 μM (Table 2).

Interestingly, the synthesized compound **12** have shown Topo I

Table 2
Topo I inhibitory activity of the synthesized compounds:

Compound	Topo I (% Inhibition)
8	72.4
12	60.6
Camptothecin	61.4

Camptothecin: positive control for Topo I.

inhibition at 100 μ M concentration like Camptothecin (Fig. 2). Since these compounds were found to be good in Topo I inhibition, they may be developed as potential anti-cancer molecules in future.

2.2.3. Molecular docking

The activity of synthesized compounds was further rationalized by predicting its binding pattern at the DNA cleavage site of Topo I. The docking analysis was first reviewed by overlaying the docked pose and the co-crystallized bound structure of camptothecin at the binding site of the enzyme and RMSD was found to be 0.377 Å. The analysis of the human Topo I crystal structure complexed with DNA and camptothecin (PDB code 1T8I) has shown that it is equipped with three chains, A, B and C, where chain A defines entire protein and chain B and C indicates the bound DNA. The camptothecin was found to be located perpendicular to the main axis of the DNA, parallel to the bases, and projected away from the main groove. It was shown from docking study that camptothecin is integrated between the base pair of DNA and formed hydrogen bonds with amino acid residues arg 364, Asp 533 and hydrophobic interactions with the DNA fragment DT10, TGP11 (5'-Thio-2'-Deoxy-Guanosine Phosphonic Acid, a modified fragment of DG in DNA), DC112, and DT113 (Fig. 3b). Likewise, all the synthesized compounds acquired flat-planar polycyclic geometry at the binding site of Topo I by pointing out one ring (bromine substituted ring) towards the backbone of the non-scissile DNA strand with another ring end pointed away from the main grooves (Fig. 3). Therefore, the polycyclic ring skeleton of all compounds is found to be intercalated between the base pairs, allowing p-interactions between all compound rings and base pairs. It was found that compound **12** forms the hydrogen bond with DNA fragment DT10 and pi-pi stacking interactions with DT10, TGP11 DC112, and DT113 DNA fragments (Fig. 4d). Likewise, it was revealed in most synthesized compounds that the hydroxyl group formed a hydrogen bond with the DT10 DNA fragment. In addition, bromine atom substituted on quinolone ring support most of compounds by forming the weak halogen bond with amino acid residue Arg 364. Exceptionally, compound **8** due to the presence of bulkier trifluoroacetyl group, causes it to form a pose at the active site of Topo I, where the bromine-substituted ring was positioned away from the main grooves (Fig. 4a). Although all polycyclic ring skeleton compounds were able to form pi-pi interaction with DT10, TGP11 DC112, and DT113 DNA fragments. Docking findings showed that all synthesized compounds also have identical binding patterns at the binding site of the DNA Topo I protein.

2.2.4. In-silico ADME prediction

It is well known that several drug candidates have failed in clinical

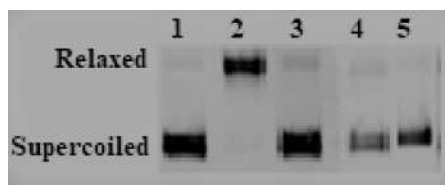
trials due to their poor pharmacokinetic profiles and therefore often fail to reach the market. The inclusion of the *in silico* ADME predictions at earlier stages of the drug discovery program has become extremely popular as this method consumes a relatively lower cost and time factor compared to traditional experimental ADME profiling approaches. The results of ADME prediction are shown in Table 3.

The drug-likeness evaluation of all compounds was conducted by predicting the Lipinski's rule of five which includes Molecular weights (MW), lipophilicity (log P), number of hydrogen bond acceptors (HBA) and number of hydrogen bond donors (HBD) were used to determine the "drug-likeness" of all synthetic compounds. It was observed that twelve compounds, out of eighteen synthesized compounds showed no violations of Lipinski's rule and remaining six compounds showed ≤ 2 violations. It is also stated that if compounds comply with Jorgensen's rule of three (QPlogS > -5.7, QPPCaco > 22 nm/s, # Primary Metabolites < 7) with fewer violations, then they are more likely to be available orally. The seven compounds were found to comply with Jorgensen's rule of three, with the remaining compounds showing an infringement of the rule for one property only. Absorption also relies on the solubility and permeability of the drug, as well as interactions of drug with transporters and metabolic enzymes in the gut wall. It was also shown that most of the compounds showed high value for predicted qualitative human oral absorption and 100% for predicted human oral absorption.

It is notable that binding of drugs to plasma substantially decreases the amount of the drug in the blood circulation and, therefore, the less bound a drug is, the more effective it can traverse or diffuse cell membranes. Almost all compounds are found in the recommended range of -1.5 to 1.5 of QPlogKhsa (prediction of binding to human serum albumin). This means that most of the compounds are likely to circulate freely inside the blood stream and therefore have access to the target site. The findings of ADME showed that almost all drugs have drug-like properties.

2.3. Conclusion

In conclusion, we have adroitly designed, synthesized and exploited the common intermediate 2-(1H-imidazol-1-yl) quinolone **5** to get the required substituents while building the 4-(phenylamino)quinoline derivative **6** and 4-phenoxyquinoline-3-carboxylate **16** to introduce novel non-Camptothecin scaffold- conformationally constrained 7,12-dihydrodibenzo[b,h][1,6] naphthyridine (**8-15**) and 7H-Chromeno[3,2-c]quinoline (**18-24**) derivatives respectively. Compounds were evaluated for *in vitro* cytotoxic potential against A-549 and MCF-7 cancer cell lines. Compound **8** (IC₅₀ 0.44 μ M and IC₅₀ 0.62 μ M) and **12** (IC₅₀ 0.69 μ M and IC₅₀ 0.54 μ M) displayed potent cytotoxicity. Topo I inhibitory activity studies of compounds **8** and **12** showed 72.4% and 60.6% inhibition respectively as comparatively to camptothecin (61.4%). Molecular docking studies showed that, the synthesized compounds have identical binding patterns and interactions at binding site of the DNA Topo I protein. Findings of *in silico* ADME prediction studies of all derivatives are found promising and signifying the drug like properties. Advance synthetic studies on this promising scaffold with further altered modifications could be a very useful approach for targeting various



Lane 1: pBR322 only, Lane 2: pBR322 + Topo I, Lane 3: pBR322 + Topo I + Camptothecin, Lane 4: pBR322 + Topo I + compound **8**, Lane 5: pBR322 + Topo I + compound **12**.

Fig. 2. Human DNA Topo I inhibitory activity of the synthesized compounds.

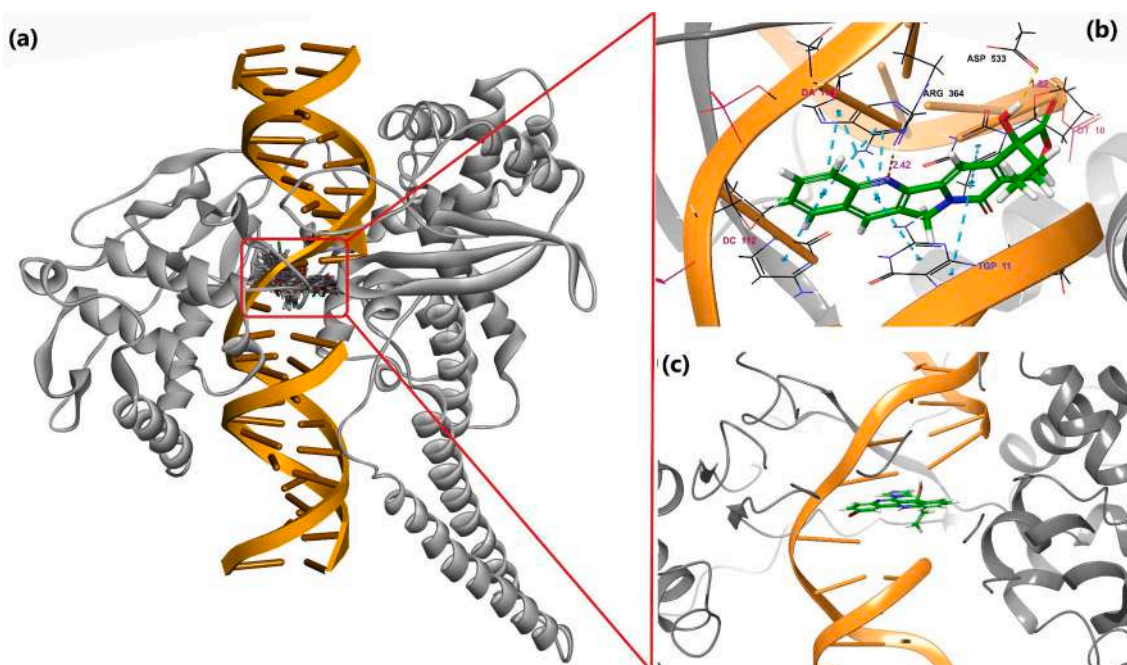


Fig. 3. (a) Pictorial representation of the human Topoisomerase I enzyme complexes with DNA showing superimposition of all synthesized compounds at the DNA cleavage site (b) The interaction pose of Camptothecin at active site of Topo I enzyme. Yellow coloured dotted lines indicate H-bond interaction and light blue coloured dotted lines indicated pi-pi interactions (c) The binding mode of compound 12 at active site of Topo I enzyme. (For interpretation of the references to colour in this figure legend, the reader is referred to the web version of this article.)

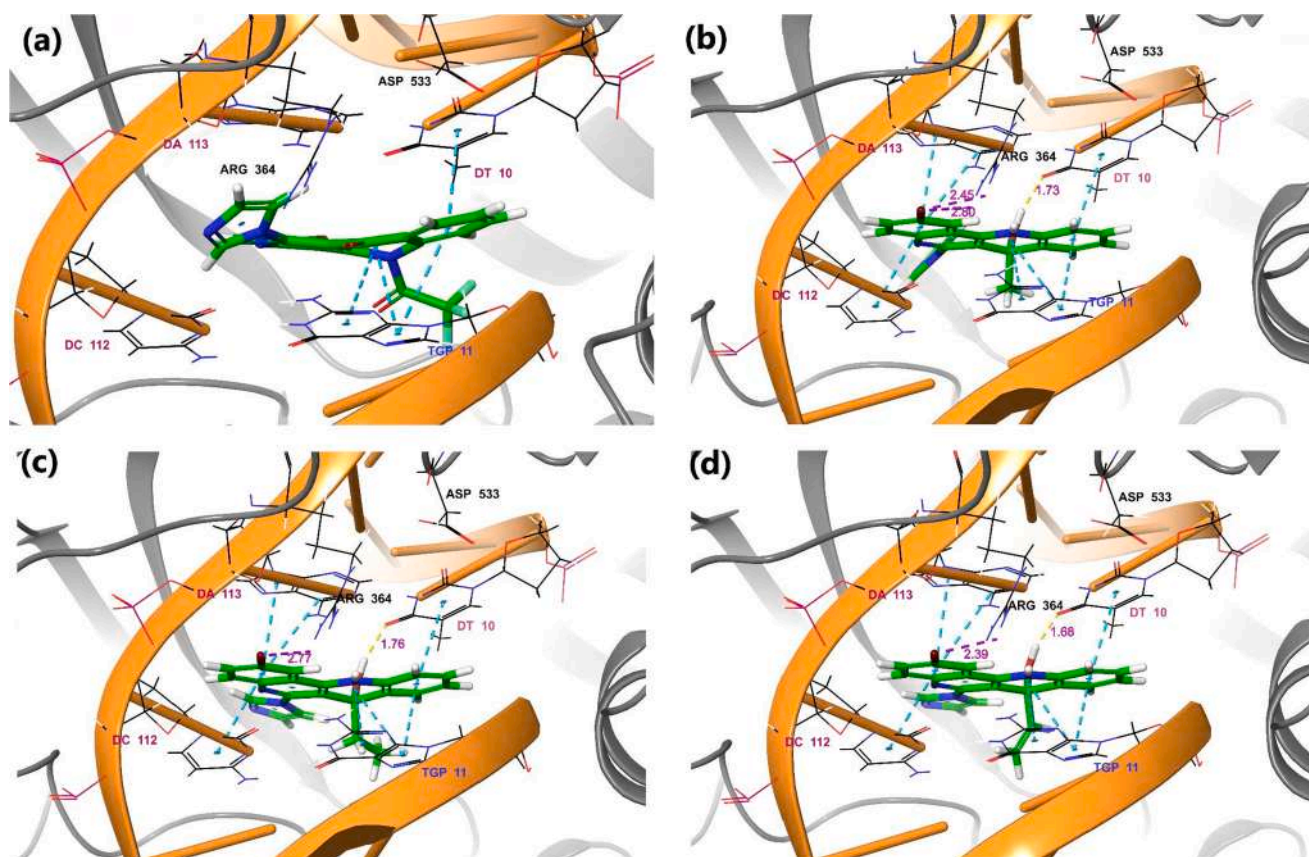


Fig. 4. The interaction pose of (a) Compound 8, (b) Compound 9, (c) Compound 10 and (d) Compound 12 at the DNA cleavage site of Topo I enzyme. Yellow coloured dotted lines indicate H-bond interaction, light blue coloured dotted lines indicated pi-pi interactions and purple coloured dotted lines denotes halogen bonds. (For interpretation of the references to colour in this figure legend, the reader is referred to the web version of this article.)

Table 3
In silico ADME properties of the synthesized compounds (5–24).

Compound	MW	Donor HB	Acceptor HB	QPlog Po/w	QPlogS	QPPCaco	metab	QPlog Khsa	Human Oral Absorption	Percent Human Oral Absorption	Rule of Five	Rule of Three
5	380.628	0	4.5	3.73	-4.776	1857.858	0	0.171	3	100	0	0
6	437.295	0	4	5.384	-6.426	2224.694	2	0.821	1	100	1	1
7	409.241	1	4	4.711	-5.671	175.302	2	0.449	3	94.687	0	0
8	487.235	0	7.5	3.45	-5	1128.353	1	-0.073	3	100	0	0
9	407.269	2	3.75	4.455	-5.498	2687.638	4	0.642	3	100	0	0
9	407.269	2	3.75	4.455	-5.498	2687.226	4	0.642	3	100	0	0
10	421.295	2	3.75	4.704	-5.709	2423.257	4	0.725	3	100	0	1
12	419.28	2	3.75	4.657	-5.888	2098.01	4	0.702	3	100	0	1
13	487.33	2	3.75	5.756	-7.124	2454.492	4	1.088	1	100	1	1
14	503.785	2	3.75	6.012	-7.489	2463.683	4	1.161	1	96.935	2	1
15	406.241	2	5.7	3.421	-4.915	1378.178	1	0.231	3	100	0	0
16	438.28	0	5	4.881	-5.977	2066.098	0	0.56	3	100	0	1
18	392.211	0	5	3.72	-4.897	2134.064	0	0.194	3	100	0	0
20	470.324	1	3.75	5.733	-6.821	2823.038	3	1.116	1	100	1	1
21	420.264	1	3.75	4.883	-5.998	2483.982	2	0.767	3	100	0	1
21	420.264	1	3.75	4.887	-5.986	2488.612	2	0.769	3	100	0	1
23	488.315	1	3.75	5.968	-7.187	2821.921	2	1.159	1	100	1	1
24	504.769	1	3.75	6.226	-7.555	2837.127	2	1.234	1	100	2	1

diseases in general and cancer in particular.

3. Experimental section

All chemicals and reagents used were of reagent grade. Purification and drying of reagents and solvents was carried out according to literature procedure. Thin layer chromatographic analyses were performed on E-Merck 60 F²⁵⁴ precoated aluminum thin layer chromatographic plates. All air-sensitive reactions were carried out under nitrogen atmosphere. Melting points were determined on a Büchi melting point B-540 instrument and are uncorrected. ¹H and ¹³C NMR spectra were recorded on a Bruker Biospin 400 MHz spectrometer in the indicated solvents (TMS as an internal standard). The values of chemical shifts are expressed in ppm and the coupling constants (*J*) in hertz (Hz). Mass spectra were recorded in API 2000 LC/MS/MS system spectrometer and the IR spectra were recorded on Perkin Elmer FT-IR spectrometer.

6-bromo-2,4-dichloroquinoline (3): A mixture of *p*-bromoaniline (10 g, 1.0 eq, 58.13 mmol) and malonic acid (12.09 g, 2.0 eq, 116.25 mmol) in POCl₃ (80 mL) was heated to 100 °C for 6 h. After completion of reaction, the volatiles were evaporated in vacuum and the residual black oil was poured onto crushed ice with stirring. The resulting mixture was extracted with dichloromethane (300 mL × 3). The combined organic layers were washed with a saturated aqueous solution of sodium bicarbonate until the water phase was pH 7–8, then washed with brine (300 mL), dried over sodium sulfate filtered and concentrated in vacuo. The residue was purified by flash column chromatography (silica gel 100–200 mesh, eluent: 3–4% ethyl acetate in *n*-hexane) to afford **3** (7.8 g, 48.4%) as an off-white solid; mp: 133–134 °C. ¹H NMR (400 MHz, CDCl₃): δ 7.52 (s, 1H, Ar-H), 7.83–7.90 (m, 2H, Ar-H), 8.34 (d, *J* = 1.96 Hz, 1H, Ar-H). ESI-MS *m/z* of 277.50 [M + H]⁺ was obtained for a calculated mass of 276.94.

Ethyl 6-bromo-2,4-dichloroquinoline-3-carboxylate (4): To the cooled solution (-20 °C) of LDA (DIPA, 6.6 mL, 1.3 eq, 49 mmol; *n*-BuLi, 27.07 mL, 1.2 eq, 43 mmol) in dry THF (40 mL) the compound 6-Bromo-2,4-dichloro quinoline (10 g, 1.0 eq, 36.10 mmol) in dry THF (200 mL) was added dropwise, changing reaction colour to reddish brown and stirred at -78 °C for 40 min. After the anion formation ethyl chloroformate (4.14 mL, 1.2 eq, 43.32 mmol) was added. Reaction was stirred at -78 °C for 2 h and quenched by ice cold water. Reaction mixture was concentrated on rotatory evaporator, and extracted with ethyl acetate (200 mL × 3 times). The combined organic layer was washed with brine. The crude product was purified by column chromatography (silica gel 100–200 mesh, 2–3% ethyl acetate in *n*-hexane) to get 6-Bromo-2,4-dichloro-quinoline-3-carboxylic acid ethyl ester **4** (8.5 g, 67%) as an off white solid; mp: 120–121 °C. ¹H NMR (CDCl₃, 400 MHz): δ 1.45 (t, *J*

= 7 Hz, 3H, -CH₂CH₃), 4.52 (q, *J* = 7 Hz, 2H, -CH₂CH₃), 7.90 (d, *J* = 1.2 Hz, 2H, Ar-H), 8.37 (s, 1H, Ar-H). ¹³C NMR (100.6 MHz, CDCl₃): δ 13.99 (-CH₂CH₃), 63.03 (-CH₂CH₃), 123.03 (Ar-C), 125.68 (Ar-C), 126.83 (Ar-C), 128.07 (Ar-C), 128.74 (Ar-C), 130.53 (Ar-C), 130.83 (Ar-C), 135.78 (Ar-C), 140.13 (Ar-C), 145.86 (Ar-C), 146.05 (Ar-C), 163.34 (-CH₂CH₂C=O). ESI-MS *m/z* of 348.00 [M + H]⁺ was obtained for a calculated mass of 346.91.

Ethyl 6-bromo-4-chloro-2-(1H-imidazol-1-yl) quinoline-3-carboxylate (5): To this solution of compound **4** (10 g, 1.0 eq, 28.4 mmol) in dry DMF (150 mL) were added Imidazole (1.96 g, 1.01 eq, 28.8 mmol) and K₂CO₃ (7.90 g, 2.0 eq, 56.8 mmol) and stirred for RT for 12 h. After completion of reaction was quenched with ice-water to get solid ppt was filter, wash with excess water and solid was purified by column chromatography (silica gel 100–200 mesh, eluent: 20–25% ethyl acetate in *n*-hexane) to afford **5** (6.0 g, 55%) as off white solid; mp: 134–136 °C. ¹H NMR (400 MHz, CDCl₃): δ 1.19 (t, *J* = 7.2 Hz, 3H, -CH₂CH₃), 4.26 (q, *J* = 7.2 Hz, 2H, -CH₂CH₃), 7.20–7.25 (m, 1H, Ar-H), 7.34 (s, 1H, Ar-H), 7.64 (d, *J* = 2 Hz, 1H, Ar-H), 7.71 (s, 1H, Ar-H), 7.93 (dd, *J* = 2.0 Hz and 9.2 Hz, 1H, Ar-H), 8.00 (d, *J* = 8.8 Hz, 1H, Ar-H). ¹³C NMR (100.6 MHz, DMSO-*d*₆): δ 13.76 (-CH₂CH₃), 63.20 (-CH₂CH₃), 121.22 (Ar-C), 123.73 (Ar-C), 124.38 (Ar-C), 125.17 (Ar-C), 126.28 (Ar-C), 130.62 (Ar-C), 130.69 (Ar-C), 136.21 (Ar-C), 137.95 (Ar-C), 140.18 (Ar-C), 146.56 (Ar-C), 146.64 (Ar-C), 162.89 (-CH₃CH₂C=O). ESI-MS *m/z* of 379.90 [M + H]⁺ was obtained for a calculated mass of 378.97.

Ethyl 6-bromo-2-(1H-imidazol-1-yl)-4-(phenylamino)quinoline-3-carboxylate (6): A mixture of **5** (5 g, 1.0 eq, 13.19 mmol), Aniline (distilled) (1.24 g, 1.01 eq, 13.33 mmol) and *p*-toluene sulfonic acid (0.020 g, cat.) in dry toluene (100 mL) was heated at 100 °C for 16 h. Yellow precipitate formed in reaction mixture, which was filtered and washed with toluene and hexane to afford **6** (4.4 g, 76.5%) as a Yellow solid; mp: 187–188 °C. ¹H NMR (400 MHz, CDCl₃): δ 1.03 (t, *J* = 7.16 Hz, 3H, -CH₂CH₃), 4.12 (q, *J* = 7.12 Hz, 2H, -CH₂CH₃), 7.07–7.14 (m, 1H, Ar-H), 7.16–7.18 (m, 1H, Ar-H), 7.32 (s, 1H, Ar-H), 7.36–7.44 (m, 3H, Ar-H), 7.66 (s, 1H, Ar-H), 7.67–7.74 (m, 1H, Ar-H), 7.77–7.84 (m, 2H, Ar-H), 9.07 (s, 1H, -NH, D₂O exchangeable). ¹³C NMR (100.6 MHz, DMSO-*d*₆): δ 13.35 (-CH₃CH₂), 62.30 (-CH₃CH₂), 115.35 (Ar-C), 116.88 (Ar-C), 121.02 (Ar-C), 121.56 (Ar-C), 122.12 (Ar-C), 123.12 (Ar-C), 124.87 (Ar-C), 124.87 (Ar-C), 128.62 (Ar-C), 128.86 (Ar-C), 129.23 (Ar-C), 135.06 (Ar-C), 138.59 (Ar-C), 139.59 (Ar-C), 141.40 (Ar-C), 146.44 (Ar-C), 150.54 (Ar-C), 164.11, (-CH₃CH₂C=O). ESI-MS *m/z* of 439.00 [M + H]⁺ was obtained for a calculated mass of 436.05.

6-Bromo-2-(1H-imidazol-1-yl)-4-(phenylamino)quinoline-3-carboxylic acid (7): Compound **6** (2.3 g, 1.0 eq, 5.26 mmol) was

hydrolyzed by dissolving it in THF:EtOH (1:1, v/v, 100 mL) mixture in presence of 10% aqueous sodium hydroxide (10 mL) at 0 °C and stirred for 1 h. After completion of reaction, the volatiles were evaporated in vacuo and the residue obtained was acidified with 10% acetic acid. The off-white solid obtained was filtered and dried under vacuum to afford acid **7** (2 g, 93 %) as a off white solid; mp: 224–226 °C. ¹H NMR (400 MHz, DMSO-*d*₆): δ 7.04 (t, *J* = 7.2 Hz, 1H, Ar–H), 7.15 (d, *J* = 1.48 Hz, 1H, Ar–H), 7.30–7.46 (m, 3H, Ar–H), 7.63–7.73 (m, 2H, Ar–H), 7.80 (dd, *t*, *J* = 1.84 Hz and 9.02 Hz, 1H, Ar–H), 7.88 (d, *J* = 8.24 Hz, 2H, Ar–H), 8.39 (s, 1H, Ar–H), 10.58 (s, 1H, –COOH, D₂O exchangeable). ¹³C NMR (100.6 MHz, DMSO-*d*₆): δ 116.49 (Ar–C), 118.30 (Ar–C), 120.07 (Ar–C), 121.71 (Ar–C), 122.53 (Ar–C), 123.01 (Ar–C), 124.63 (Ar–C), 125.31 (Ar–C), 128.76 (Ar–C), 134.36 (Ar–C), 138.36 (Ar–C), 139.20 (Ar–C), 139.96 (Ar–C), 145.83 (Ar–C), 151.89 (Ar–C), 165.18 (–COOH). ESI-MS *m/z* of 409.30 [M + H]⁺ was obtained for a calculated mass of 408.02.

2-Bromo-6-(1H-imidazol-1-yl)-12-(2,2,2-trifluoroacetyl) dibenzo [b,h] [1,6] naphthyridine-7(12H)-one (8): To a mixture of **7** (5 g, 1.0 eq, 13.3 mmol) in THF:DCM (1:1, v/v, 300 mL), trifluoroacetic anhydride (55.9 g, 20.0 eq, 266 mmol) was added drop wise at 0 °C. The reaction was stirred at room temperature for 4–5 h. After completion of reaction the volatiles were evaporated in vacuo. The obtained residue was neutralized with cold sodium bicarbonate solution to obtain yellow precipitate. The yellow precipitate obtained was filtered and washed with methanol, hexane, and dried under vacuum to afford cyclized compound **8** (5.6 g, 87 %) as a pale-yellow solid; mp: 226–230 °C. ¹H NMR (400 MHz, DMSO-*d*₆): δ 7.42–7.62 (m, 6H, Ar–H), 7.88 (d, *J* = 9.12 Hz, 1H, Ar–H), 8.10 (d, *J* = 9.04 Hz, 1H, Ar–H), 8.68–8.78 (m, 2H, Ar–H). ¹³C NMR (100.6 MHz, DMSO-*d*₆): δ 113.68 (Ar–C), 114.42 (Ar–C), 116.45 (Ar–C), 117.29 (Ar–C), 120.88 (Ar–C), 122.92 (Ar–C), 125.33 (Ar–C), 128.49 (Ar–C), 129.42 (Ar–C), 131.43 (Ar–C), 137.31 (Ar–C), 137.88 (Ar–C), 138.14 (Ar–C), 145.52 (Ar–C), 146.48 (Ar–C), 146.51 (Ar–C), 149.64 (Ar–C), 149.73 (Ar–C), 150.12 (Ar–C), 156.23 (Ar–C), 156.59 (Ar–C), 156.95 (Ar–C), 156.96 (Ar–C), 174.69 (C=O). ESI-MS *m/z* of 487.50 [M + H]⁺ was obtained for a calculated mass of 485.99.

Representative procedure for synthesis of 9 to 14: (Procedure A):

To a mixture of **8** (1.0 eq) was dissolved in dry THF (15 mL) were added molar solution of R-Mg-X in THF/diethyl ether (2.0 eq) was added in one portion at 0 °C under nitrogen atmosphere. The reaction was stirred for 2 h and then quenched by ice. Reaction mixture was concentrated under reduced pressure and extracted with ethyl acetate (3 × 50 mL). Combined organic layer was washed with water (50 mL), brine and dried over anhydrous sodium sulfate. Organic layer was filtered and concentrated under reduced pressure to obtain crude product. Crude product was purified by column chromatography (silica gel 100–200 mesh, eluent: 25% ethyl acetate in *n*-hexane) to afford **9** to **14**.

2-Bromo-6-(1H-imidazol-1-yl)-7-methyl-7,12-dihydrodibenzo [b, h] [1,6] naphthyridin-7-ol (9): Procedure A, (R-Mg-X = 3.0 M Methyl magnesium bromide in diethyl ether) Yield: 62.4 %. Brown solid; mp 246–248 °C. ¹H NMR (400 MHz, CDCl₃): δ 1.92 (s, 3H, –CH₃), 7.10 (t, *J* = 7.4 Hz, 1H, Ar–H), 7.20 (d, *J* = 1.32 Hz, 1H, Ar–H), 7.32 (s, 1H, –OH, D₂O exchangeable), 7.40 (t, *J* = 7.56 Hz, 2H, Ar–H), 7.49 (d, *J* = 1.36 Hz, 1H, Ar–H), 7.62 (dd, *J* = 2 Hz and 9 Hz, 1H, Ar–H), 7.67 (d, *J* = 9.04 Hz, 1H, Ar–H), 7.71 (s, 1H, –NH, D₂O exchangeable), 7.83 (d, *J* = 7.68 Hz, 2H, Ar–H), 7.90 (d, *J* = 1.96 Hz, 1H, Ar–H). ¹³C NMR (100.6 MHz, CDCl₃): δ 23.65 (–CH₃), 71.35 (–C-OH), 113.43 (Ar–C), 114.46 (Ar–C), 116.29 (Ar–C), 119.16 (Ar–C), 120.44 (Ar–C), 122.16 (Ar–C), 123.39 (Ar–C), 128.62 (Ar–C), 129.45 (Ar–C), 133.19 (Ar–C), 133.67 (Ar–C), 139.02 (Ar–C), 139.60 (Ar–C), 147.27 (Ar–C), 150.29 (Ar–C), 158.75 (Ar–C). ESI-MS *m/z* of 407.10 [M + H]⁺ was obtained for a calculated mass of 406.04.

2-Bromo-6-(1H-imidazol-1-yl)-7-ethyl –7,12-dihydrodibenzo [b,h] [1,6] naphthyridin-7-ol (10): Procedure A, (R-Mg-X = 3.0 M

Ethyl magnesium bromide in diethyl ether) Yield: 59 %. Off white solid; mp 255–257 °C. ¹H NMR (400 MHz, DMSO-*d*₆): δ 0.56 (t, *J* = 7.6 Hz, 3H, –CH₃), 2.19–2.24 (m, 1H, –CH₂), 2.32–2.40 (m, 1H, –CH₂), 6.79 (s, 1H, –OH, D₂O exchangeable), 7.04 (t, *J* = 7.6 Hz, 1H, Ar–H), 7.36 (t, *J* = 7.6 Hz, 2H, Ar–H), 7.72 (d, *J* = 8.8 Hz, 1H, Ar–H), 7.81 (dd, *J* = 1.2 Hz and 8.8 Hz, 1H, Ar–H), 7.85 (s, 1H, –NH, D₂O exchangeable), 7.91 (d, *J* = 8.0 Hz, 2H, Ar–H), 8.42–8.44 (m, 2H, Ar–H). ¹³C NMR (100.6 MHz, DMSO-*d*₆): δ 7.55 (–CH₃), 29.43 (–CH₂CH₃), 74.84 (–C-OH), 114.17 (Ar–C), 114.88 (Ar–C), 116.28 (Ar–C), 119.22 (Ar–C), 119.70 (Ar–C), 122.29 (Ar–C), 123.84 (Ar–C), 128.71 (Ar–C), 129.44 (Ar–C), 133.69 (Ar–C), 133.73 (Ar–C), 139.77 (Ar–C), 139.99 (Ar–C), 147.06 (Ar–C), 150.31 (Ar–C), 157.35 (Ar–C). ESI-MS *m/z* of 421.10 [M + H]⁺ was obtained for a calculated mass of 420.06.

2-Bromo-6-(1H-imidazol-1-yl)-7-phenyl –7,12-dihydrodibenzo [b,h] [1,6] naphthyridin-7-ol (11): Procedure A, (R-Mg-X = 2.0 M Phenyl magnesium chloride in THF) Yield: 35 %. Off white solid; mp 176–178 °C. ¹H NMR (400 MHz, DMSO-*d*₆): δ 6.98 (t, *J* = 7.2 Hz, 1H, Ar–H), 7.25–7.36 (m, 6H, Ar–H and 1H, –OH, D₂O exchangeable), 7.42–7.44 (m, 1H, Ar–H), 7.51 (s, 1H, –NH, D₂O exchangeable), 7.71–7.78 (m, 3H, Ar–H), 7.86 (dd, *J* = 2 Hz and 8.8 Hz, 1H, Ar–H), 8.53 (m, 2H, Ar–H). ¹³C NMR (100.6 MHz, DMSO-*d*₆): δ 74.36 (–C-OH), 114.29 (Ar–C), 115.32 (Ar–C), 116.52 (Ar–C), 118.73 (Ar–C), 121.04 (Ar–C), 122.24 (Ar–C), 124.18 (Ar–C), 125.09 (Ar–C), 128.27 (Ar–C), 128.75 (Ar–C), 128.87 (Ar–C), 129.51 (Ar–C), 134.02 (Ar–C), 134.06 (Ar–C), 138.78 (Ar–C), 139.48 (Ar–C), 140.34 (Ar–C), 147.39 (Ar–C), 149.61 (Ar–C), 158.67 (Ar–C). ESI-MS *m/z* of 471.15 [M + H]⁺ was obtained for a calculated mass of 468.06.

2-Bromo-6-(1H-imidazol-1-yl)-7-vinyl –7,12-dihydrodibenzo [b,h] [1,6] naphthyridin-7-ol (12): Procedure A, (R-Mg-X = 1.0 M Vinyl magnesium chloride in THF) Yield: 62.2 %. Brown solid; mp 236–238 °C. ¹H NMR (400 MHz, DMSO-*d*₆): δ 5.44 (d, *J* = 10.4 Hz, 1H, –CHCH₂), 5.75 (d, *J* = 16.4 Hz, 1H, –CHCH₂), 6.05 (dd, *J* = 10.4 Hz and 16.4 Hz, 1H, –CHCH₂), 7.04 (t, *J* = 7.6 Hz, 1H, Ar–H), 7.16 (s, 1H, –OH, D₂O exchangeable), 7.29 (d, *J* = 1.2 Hz, 1H, Ar–H), 7.37 (t, *J* = 7.6 Hz, 2H, Ar–H), 7.53 (s, 1H, –NH, D₂O exchangeable), 7.75–7.78 (m, 1H, Ar–H), 7.82–7.89 (m, 3H, Ar–H), 8.43–8.50 (m, 2H, Ar–H). ¹³C NMR (100.6 MHz, DMSO-*d*₆): δ 73.59 (–C-OH), 114.25 (–CH-CH₂), 115.35 (–CH-CH₂), 116.38 (Ar–C), 116.55 (Ar–C), 118.57 (Ar–C), 118.97 (Ar–C), 122.26 (Ar–C), 123.97 (Ar–C), 128.89 (Ar–C), 129.48 (Ar–C), 133.94 (Ar–C), 135.42 (Ar–C), 139.69 (Ar–C), 140.02 (Ar–C), 147.31 (Ar–C), 150.00 (Ar–C), 156.61 (Ar–C). ESI-MS *m/z* of 421.10 [M + H]⁺ was obtained for a calculated mass of 418.04.

2-Bromo-6-(1H-imidazol-1-yl)-7-4-fluorophenyl-7-12-dihydrodibenzo [b,h] [1,6] naphthyridin-7-ol (13): Procedure A, (R-Mg-X = 1.0 M 4-fluorophenyl magnesium bromide in THF) Yield: 57 %. Off white solid; mp 170–172 °C. ¹H NMR (400 MHz, DMSO-*d*₆): δ 7.00 (t, *J* = 7.2 Hz, 1H, Ar–H), 7.14–7.18 (m, 2H, Ar–H), 7.26–7.32 (m, 3H, Ar–H and 1H, –OH, D₂O exchangeable), 7.47–7.50 (m, 2H, Ar–H), 7.57 (s, 1H, –NH, D₂O exchangeable), 7.72–7.79 (m, 3H, Ar–H), 7.86 (dd, *J* = 2 Hz and 9.2 Hz, 1H, Ar–H), 8.51–8.54 (m, 2H, Ar–H). ¹³C NMR (100.6 MHz, DMSO-*d*₆): δ 74.02 (–C-OH), 114.29 (Ar–C), 115.37 (Ar–C), 115.44 (Ar–C), 115.66 (Ar–C), 116.52 (Ar–C), 118.90 (Ar–C), 120.60 (Ar–C), 122.30 (Ar–C), 124.19 (Ar–C), 127.38 (Ar–C), 127.46 (Ar–C), 128.83 (Ar–C), 129.50 (Ar–C), 134.05 (Ar–C), 134.91 (Ar–C), 134.94 (Ar–C), 139.44 (Ar–C), 140.44 (Ar–C), 147.42 (Ar–C), 149.61 (Ar–C), 158.39 (Ar–C), 160.65 (Ar–C), 163.09 (Ar–C). ESI-MS *m/z* of 487.15 [M + H]⁺ was obtained for a calculated mass of 486.05.

2-Bromo-6-(1H-imidazol-1-yl)-7-4-chlorophenyl-7-12-dihydrodibenzo [b,h] [1,6] naphthyridin-7-ol (14): Procedure A, (R-Mg-X = 1.0 M 4-chlorophenyl magnesium bromide in THF) Yield: 45 %. Brown solid; mp 177–179 °C. ¹H NMR (400 MHz, DMSO-*d*₆): δ 6.97 (td, *J* = 7.2 Hz, 1H, Ar–H), 7.23–7.29 (m, 3H, Ar–H and 1H, –OH, D₂O

exchangeable), 7.35–7.37 (m, 2H, Ar–H), 7.42–7.44 (m, 2H, Ar–H), 7.58 (s, 1H, —NH, D₂O exchangeable), 7.70–7.75 (m, 3H, Ar–H), 7.82–7.84 (m, 1H, Ar–H), 8.48–8.51 (m, 2H, Ar–H). ¹³C NMR (100.6 MHz, DMSO-*d*₆): δ 74.02 (—C—OH), 114.28 (Ar—C), 115.48 (Ar—C), 116.57 (Ar—C), 118.94 (Ar—C), 120.44 (Ar—C), 122.34 (Ar—C), 124.22 (Ar—C), 127.18 (Ar—C), 128.73 (Ar—C), 128.85 (Ar—C), 129.52 (Ar—C), 132.90 (Ar—C), 134.12 (Ar—C), 137.92 (Ar—C), 139.43 (Ar—C), 140.52 (Ar—C), 147.46 (Ar—C), 149.58 (Ar—C), 158.19 (Ar—C). **ESI-MS** *m/z* of 505.00 [M + H]⁺ was obtained for a calculated mass of 502.02.

2-Bromo-6-(1H-imidazol-1-yl)dibenzo [b,h] [1,6] naphthyridin-7(12H)-one oxime (15): Sodium bicarbonate (0.22 g, 2.7 mmol) in water (1 mL) was added to a mixture of **8** (0.913 g, 1.8 mmol), hydroxylamine hydrochloride (0.186 g, 2.7 mmol) in Ethanol:THF (4:5, v/v, 90 mL) at 0 °C and stirred at room temperature for 1 h. Reaction mixture was concentrated under vacuum and residue obtained was dissolved in ethyl acetate (300 mL) and passed through celite. The organic layer was washed with brine, dried over anhydrous sodium sulfate, filtered and concentrated under vacuum to get crude compound. This compound was purified by MeOH and hexane wash to afford pure oxime **15** (0.43 g, 58 %) as a yellow solid. mp: 296–297 °C. IR_{max} (KBr, cm⁻¹) 1565.06, 3179.88; ¹H NMR (400 MHz, DMSO-*d*₆): δ 7.09 (t, *J* = 7.2 Hz, 1H, Ar–H), 7.41 (t, *J* = 2.0 Hz, 8.8 Hz, 1H, Ar–H), 7.56 (d, *J* = 8.7 Hz, 1H, Ar–H), 7.65 (s, 1H, Ar–H), 7.72–7.76 (m, 2H, Ar–H), 8.15–8.20 (m, 3H, Ar–H), 12.97 (s, 1H, —NH, D₂O exchangeable), 14.21 (s, 1H, =N—OH, D₂O exchangeable). ¹³C NMR (100.6 MHz, DMSO-*d*₆): δ 103.69 (Ar—C), 113.37 (Ar—C), 113.69 (Ar—C), 113.99 (Ar—C), 115.27 (Ar—C), 116.36 (Ar—C), 119.02 (Ar—C), 119.21 (Ar—C), 119.54 (Ar—C), 121.71 (Ar—C), 121.95 (Ar—C), 122.22 (Ar—C), 122.75 (Ar—C), 124.87 (Ar—C), 125.14 (Ar—C), 128.88 (Ar—C), 129.00 (Ar—C), 130.44 (Ar—C), 134.62 (Ar—C), 135.43 (Ar—C), 140.38 (Ar—C), 146.01 (Ar—C), 147.07 (Ar—C), 156.36 (Ar—C), 156.78 (Ar—C), 180.42 (Ar—C), 187.83 (Ar—C). **ESI-MS** *m/z* of 406.20 [M + H]⁺ was obtained for a calculated mass of 405.02.

Ethyl 6-bromo-2-(1H-imidazol-1-yl)-4-phenoxyquinoline-3-carboxylate (16): A mixture of **4** (2.0 g, 1.0 eq, 5.2 mmol), phenol (0.56 g, 1.1 eq, 5.78 mmol) and potassium carbonate (0.79 g, 1.1 eq, 5.78 mmol) was dissolved in dry DMF (15 mL) and heated to 100 °C for 16 h. Reaction was quenched with ice and extracted with ethyl acetate (3 × 100 mL). The combined organic layer was washed with water, brine and dried over anhydrous sodium sulphate. Organic layer was filtered and concentrated to get crude product. Crude compound was purified by column chromatography (silica gel 100–200 mesh, eluent: 10–15 % ethyl acetate in *n*-hexane) to afford **16** (1.7 g, 75 %) as a off white solid. mp: 168–170 °C. ¹H NMR (400 MHz, CDCl₃): δ 1.18 (t, *J* = 7.12 Hz, 3H, —CH₃), 4.26 (q, *J* = 7.12 Hz, 2H, —CH₂CH₃), 7.23–7.32 (m, 4H, Ar–H), 7.34 (s, 1H, Ar–H), 7.42–7.48 (m, 2H, Ar–H), 7.56 (d, *J* = 2.12 Hz, 1H, Ar–H), 7.65–7.69 (m, 1H, Ar–H), 7.74–7.78 (m, 1H, Ar–H). ¹³C NMR (100.6 MHz, CDCl₃): δ 13.87 (—CH₂CH₃), 62.73 (—CH₂CH₃), 118.16 (Ar—C), 120.55 (Ar—C), 121.19 (Ar—C), 121.74 (Ar—C), 123.05 (Ar—C), 125.02 (Ar—C), 125.55 (Ar—C), 129.48 (Ar—C), 129.85 (Ar—C), 130.43 (Ar—C), 135.23 (Ar—C), 137.97 (Ar—C), 140.94 (Ar—C), 145.36 (Ar—C), 152.63 (Ar—C), 157.78 (Ar—C), 163.12 (—C=O CH₂CH₃). **ESI-MS** *m/z* of 438.00 [M + H]⁺ was obtained for a calculated mass of 437.04.

6-bromo-2-(1H-imidazol-1-yl)-4-phenoxyquinoline-3-carboxylic acid (17): Compound **16** (1.0 g, 1 eq, 2.28 mmol) was hydrolyzed by dissolving it in THF (100 mL) were added Potassium trimethylsilanolate (0.88 g, 3 eq, 6.86 mmol) at 0 °C and stirred at rt for 12 h. The reaction mixture was filter and solid was washed with diethyl ether and hexane to afford **17** as a potassium salt (0.75 g, crude, potassium salt) as a off white solid, The crude potassium salt used for next step without purification.

2-Bromo-6-(1H-imidazol-1-yl)-7H-chromeno[3,2-c] quinoline-7-one (18):

To a mixture of **17** (0.5 g, 1.0 eq, 1.11 mmol) in THF, DCM (1:1, v/v,

25 mL), trifluoroacetic anhydride (4.68 g, 3.14 mL, 20.0 eq, 22.28 mmol) was added drop wise at 0 °C. The reaction was stirred at room temperature for 3 h and then solvent was evaporated on rotatory evaporator. The obtained residue was neutralized with cold sodium bicarbonate solution to obtain brown precipitate. The precipitate obtained was filtered and washed with methanol, hexane, and dried under vacuum to afford **18** (0.35 g, 81.3 %) as a yellow solid. mp: 331–333 °C. IR_{max} (KBr, cm⁻¹) 1672.100; ¹H NMR (400 MHz, DMSO-*d*₆): δ 7.30 (s, 1H, Ar–H), 7.47–7.53 (m, 2H, Ar–H), 7.72 (d, *J* = 8.14 Hz, 1H, Ar–H), 7.92–7.96 (m, 2H, Ar–H), 8.03 (dd, *J* = 1.5 Hz and 7.8 Hz, 1H, Ar–H), 8.06 (d, *J* = 9.04 Hz, 1H, Ar–H), 8.17 (dd, *J* = 2.0 Hz and 9.0 Hz, 1H, Ar–H). ¹³C NMR (100.6 MHz, DMSO-*d*₆): δ 112.80 (Ar—C), 117.93 (Ar—C), 120.73 (Ar—C), 121.28 (Ar—C), 121.52 (Ar—C), 124.90 (Ar—C), 125.31 (Ar—C), 125.91 (Ar—C), 126.41 (Ar—C), 129.21 (Ar—C), 129.98 (Ar—C), 136.59 (Ar—C), 137.07 (Ar—C), 138.29 (Ar—C), 146.90 (Ar—C), 154.50 (Ar—C), 175.83 (—C=O). **ESI-MS** *m/z* of 392.00 [M + H]⁺ was obtained for a calculated mass of 391.00.

Representative procedure for synthesis of 19 to 24: (Procedure B):

To a mixture of **18** (1.0 eq) was dissolved in dry THF (15 mL) were added molar solution of R-Mg-X in THF/diethyl ether (2.0 eq) was added in one portion at 0 °C under nitrogen atmosphere. The reaction was stirred for 2 h and then quenched by ice. Reaction mixture was concentrated under reduced pressure and extracted with ethyl acetate (3 × 50 mL). Combined organic layer was washed with water (50 mL), brine and dried over anhydrous sodium sulfate. Organic layer was filtered and concentrated under reduced pressure to obtain crude product. Crude product was purified by column chromatography (silica gel 100–200 mesh, eluent: 15–20% ethyl acetate in *n*-hexane) to afford **19 to 24**.

2-bromo-7-ethyl-6-(1H-imidazol-1-yl)-7H-chromeno [3,2-c]

quinolin-7-ol (19): Procedure B, (R-Mg-X = 3.0 M Ethyl magnesium bromide in diethyl ether), Yield: 28 %. Off white solid; mp 235–237 °C. ¹H NMR (400 MHz, DMSO-*d*₆): δ 0.69 (t, *J* = 7.6 Hz, 3H, —CH₂CH₃), 2.27–2.32 (m, 1H, —CH₃CH₂), 2.40–2.50 (m, 1H, —CH₃CH₂), 6.24 (s, 1H, —OH, D₂O exchangeable), 7.24–7.30 (m, 4H, Ar–H), 7.47 (t, *J* = 8 Hz, 2H, Ar–H), 7.62 (d, *J* = 8.8 Hz, 1H, Ar–H), 7.85 (dd, *J* = 2.0 Hz and 9.2 Hz, 1H, Ar–H), 8.48 (s, 1H, Ar–H), 8.59 (d, *J* = 2 Hz, 1H, Ar–H). ¹³C NMR (100.6 MHz, DMSO-*d*₆): δ 7.55 (—CH₃CH₂), 29.43 (—CH₃CH₂), 74.84 (—C—OH), 114.17 (Ar—C), 114.88 (Ar—C), 116.28 (Ar—C), 119.22 (Ar—C), 119.70 (Ar—C), 122.29 (Ar—C), 123.84 (Ar—C), 128.71 (Ar—C), 129.44 (Ar—C), 133.69 (Ar—C), 133.73 (Ar—C), 139.77 (Ar—C), 139.99 (Ar—C), 147.06 (Ar—C), 150.31 (Ar—C), 157.35 (Ar—C). **ESI-MS** *m/z* of 424.05 [M + H]⁺ was obtained for a calculated mass of 421.04.

2-bromo-6-(1H-imidazol-1-yl)-7-phenyl-7H-chromeno [3,2-c]

quinolin-7-ol (20): Procedure B, (R-Mg-X = 2.0 M Phenyl magnesium chloride in THF) Yield: 65 %. Off white solid; mp 244–246 °C. ¹H NMR (400 MHz, DMSO-*d*₆): δ 6.93–6.96 (m, 2H, Ar–H) and 1H, —NH, D₂O exchangeable), 7.20 (t, *J* = 7.2 Hz, 1H, Ar–H), 7.29–7.43 (m, 8H, Ar–H), 7.61 (d, *J* = 9.2 Hz, 1H, Ar–H), 7.87 (d, *J* = 8 Hz, 1H, Ar–H), 8.55 (s, 1H, Ar–H), 8.66 (s, 1H, Ar–H). ¹³C NMR (100.6 MHz, DMSO-*d*₆): δ 74.60 (—C—OH), 115.16 (Ar—C), 115.71 (Ar—C), 118.72 (Ar—C), 121.44 (Ar—C), 122.75 (Ar—C), 124.42 (Ar—C), 124.90 (Ar—C), 125.65 (Ar—C), 127.72 (Ar—C), 127.98 (Ar—C), 129.46 (Ar—C), 129.93 (Ar—C), 134.43 (Ar—C), 139.52 (Ar—C), 143.13 (Ar—C), 146.17 (Ar—C), 152.92 (Ar—C), 157.65 (Ar—C), 159.54 (Ar—C). **ESI-MS** *m/z* of 471.95 [M + H]⁺ was obtained for a calculated mass of 469.04.

2-bromo-6-(1H-imidazol-1-yl)-7-vinyl-7H-chromeno [3,2-c]

quinolin-7-ol (21): Procedure B, (R-Mg-X = 1.0 M Vinyl magnesium chloride in THF) Yield: 24 %. Off white solid; mp 171–173 °C. ¹H NMR (400 MHz, DMSO-*d*₆): δ 5.29 (d, *J* = 10.8 Hz, 1H, —CHCH₂), 5.44 (d, *J* = 17.2 Hz, 1H, —CHCH₂), 6.36 (q, *J* = 10.8 Hz and 17.2 Hz, 1H, —CHCH₂), 6.59 (s, 1H, —OH, D₂O exchangeable), 7.23–7.29 (m, 3H, Ar–H), 7.34 (s, 1H, Ar–H), 7.46 (t, *J* = 7.6 Hz, 2H, Ar–H), 7.62 (d, *J* = 8.8 Hz, 1H, Ar–H), 7.85 (d, *J* = 8.8 Hz, 1H, Ar–H), 8.52–8.60 (m, 2H,

Ar—H). ^{13}C NMR (100.6 MHz, DMSO- d_6): δ 73.82 (—C—OH), 115.19 (—CHCH $_2$), 115.60 (—CHCH $_2$), 116.32 (Ar—C), 118.65 (Ar—C), 121.00 (Ar—C), 121.56 (Ar—C), 124.22 (Ar—C), 124.91 (Ar—C), 129.54 (Ar—C), 129.91 (Ar—C), 134.33 (Ar—C), 134.35 (Ar—C), 135.27 (Ar—C), 142.69 (Ar—C), 146.01 (Ar—C), 153.12 (Ar—C), 157.33 (Ar—C), 157.82 (Ar—C). **ESI-MS** m/z of 420.10 [M + H] $^+$ was obtained for a calculated mass of 419.03.

2-bromo-6-(1H-imidazol-1-yl)-7-methyl-7H-chromeno [3,2-c] quinolin-7-ol (22): Procedure B, (R-Mg-X = 3.0 M Methyl magnesium bromide in diethyl ether) Yield: 23 %. Pale yellow solid; mp: 248–250 °C. ^1H NMR (400 MHz, DMSO- d_6): δ 1.48–1.52 (m, 3H, —CH $_3$), 6.27–6.42 (m, 1H, —OH, D $_2$ O exchangeable), 6.73–6.83 (m, 1H, Ar—H), 7.21–7.29 (m, 3H, Ar—H), 7.39–7.42 (m, 1H, Ar—H), 7.62–7.65 (m, 1H, Ar—H), 7.84 (s, 1H, Ar—H), 7.89–7.91 (m, 1H, Ar—H), 7.95–7.98 (m, 1H, Ar—H), 8.07–8.31 (m, 1H, Ar—H). ^{13}C NMR (100.6 MHz, DMSO- d_6): δ 22.23 (—CH $_3$), 77.70 (—C—OH), 120.03 (Ar—C), 120.74 (Ar—C), 120.99 (Ar—C), 123.66 (Ar—C), 124.20 (Ar—C), 125.57 (Ar—C), 128.23 (Ar—C), 128.89 (Ar—C), 130.27 (Ar—C), 130.94 (Ar—C), 133.44 (Ar—C), 134.36 (Ar—C), 134.63 (Ar—C), 137.76 (Ar—C), 145.52 (Ar—C), 145.74 (Ar—C), 152.02 (Ar—C). **ESI-MS** m/z of 408.00 [M + H] $^+$ was obtained for a calculated mass of 407.03.

2-bromo-7-(4-fluorophenyl)-6-(1H-imidazol-1-yl)-7H-chromeno [3,2-c] quinolin-7-ol (23): Procedure B, (R-Mg-X = 1.0 M 4-fluorophenyl magnesium bromide in THF) Yield: 58%. Pale yellow solid; mp 241–243 °C. ^1H NMR (400 MHz, DMSO- d_6): δ 6.95 (d, J = 8 Hz, 2H, Ar—H), 7.11–7.13 (m, 2H, Ar—H and 1H, —OH, D $_2$ O exchangeable), 7.21 (t, J = 7.2 Hz, 1H, Ar—H), 7.30–7.40 (m, 5H, Ar—H), 7.62 (d, J = 9.6 Hz, 1H, Ar—H), 7.87 (dd, J = 2.0 Hz and 9.2 Hz, 1H, Ar—H), 8.57 (s, 1H, Ar—H), 8.66 (d, J = 1.2 Hz, 1H, Ar—H). ^{13}C NMR (100.6 MHz, DMSO- d_6): δ 74.06 (—C—OH), 112.78 (Ar—C), 113.01 (Ar—C), 114.48 (Ar—C), 114.69 (Ar—C), 115.41 (Ar—C), 115.78 (Ar—C), 118.74 (Ar—C), 121.30 (Ar—C), 121.52 (Ar—C), 121.54 (Ar—C), 121.65 (Ar—C), 122.22 (Ar—C), 124.51 (Ar—C), 124.92 (Ar—C), 125.38 (Ar—C), 129.50 (Ar—C), 129.67 (Ar—C), 129.93 (Ar—C), 129.97 (Ar—C), 130.05 (Ar—C), 134.47 (Ar—C), 134.50 (Ar—C), 142.55 (Ar—C), 142.62 (Ar—C), 143.36 (Ar—C), 146.27 (Ar—C), 152.88 (Ar—C), 157.48 (Ar—C), 158.96 (Ar—C), 160.78 (Ar—C), 163.19 (Ar—C). **ESI-MS** m/z of 488.00 [M + H] $^+$ was obtained for a calculated mass of 487.03.

2-bromo-7-(4-chlorophenyl)-6-(1H-imidazol-1-yl)-7H-chromeno [3,2-c] quinolin-7-ol (24): Procedure B, (R-Mg-X = 1.0 M 4-chlorophenyl magnesium bromide in THF) Yield: 80 %. Off white solid; mp 157–159 °C. ^1H NMR (400 MHz, DMSO- d_6): δ 6.97 (d, J = 7.6 Hz, 2H, Ar—H), 7.07 (s, 1H, —OH, D $_2$ O exchangeable), 7.21 (t, J = 7.6 Hz, 1H, Ar—H), 7.30 (s, 1H, Ar—H), 7.36–7.46 (m, 6H, Ar—H), 7.62 (d, J = 9.2 Hz, 1H, Ar—H), 7.87 (dd, J = 2.0 Hz and 9.2 Hz, 1H, Ar—H), 8.57 (s, 1H, Ar—H), 8.66 (d, J = 1.6 Hz, 1H, Ar—H). ^{13}C NMR (100.6 MHz, DMSO- d_6): δ 74.12 (—C—OH), 115.34 (Ar—C), 115.72 (Ar—C), 118.77 (Ar—C), 121.37 (Ar—C), 122.21 (Ar—C), 124.45 (Ar—C), 124.94 (Ar—C), 127.67 (Ar—C), 128.00 (Ar—C), 129.51 (Ar—C), 129.93 (Ar—C), 132.34 (Ar—C), 134.51 (Ar—C), 138.62 (Ar—C), 143.27 (Ar—C), 146.25 (Ar—C), 152.87 (Ar—C), 157.52 (Ar—C), 159.08 (Ar—C). **ESI-MS** m/z of 506.00 [M + H] $^+$ was obtained for a calculated mass of 503.00.

3.1. *In vitro* anticancer screening

All the synthesized compounds were evaluated for their *in vitro* anticancer activity against human breast cancer cell line (MCF-7) and human lung cancer cell line (A-549) by MTT assay. The two cell lines MCF-7 and A-549 were grown in DMEM medium containing 10 % foetal bovine serum (Life technologies (Gibco)) and 0.7 % antibiotics. Cells were seeded into 96 well microtiter plates in 100 μL of media at plating density of 5000 cells/well. Seeded cells were incubated at 37 °C, 5 % CO $_2$, 95 % air and 100 % humidity for 24 h. At 24 h, old media was changed with fresh media followed by treatment with each compound at

10 μM , 1 μM , and 0.1 μM . After 24 h treatment, cell viability was assessed by 3-(4,5-dimethylthiazol)-2,5-diphenyltetrazolium bromide (MTT), cell were incubated with 20 μL of MTT (5 mg/mL) in PBS for 4 h at 37 °C. The medium was removed and formazan crystal was dissolved in DMSO. MTT reduction was quantified by measurement of absorbance at 570 nm using a multimode reader, Synergy Mx of BioTek [27].

3.2. Topoisomerase I (Topo I) inhibition assay

Assay for DNA topoisomerase I inhibition *in vitro* DNA Topo I inhibition assay was determined following the previously reported method, with minor modifications [28]. The test compounds were dissolved in DMSO at 20 mM as stock solutions. The activity of DNA Topo I was determined by assessing the relaxation of supercoiled DNA pBR322. The mixture of 100 ng of plasmid pBR322 DNA and 1 unit of recombinant human DNA topoisomerase I (Topo GEN INC., USA) was incubated without and with the prepared compounds at 37 °C for 30 min in the relaxation buffer (10 mM TrisHCl (pH 7.9), 150 mM NaCl, 0.1% bovine serum albumin, 1 mM spermidine, 5% glycerol). L of the stop μL was terminated by adding 2.5 μL . The reaction in the final volume of 10 solution containing 5% sarcosyl, 0.0025% bromophenol blue and 25% glycerol. DNA samples were then electrophoresed on a 1% agarose gel at 15 V for 7 h with a running buffer of TAE. Gels were stained for 30 min in an aqueous solution of ethidium bromide (0.5 $\mu\text{g}/\text{mL}$). DNA bands were visualized by transillumination with UV light and were quantitated using Alphamager.

3.3. Computational Study (Methodology)

The molecular docking studies were performed using Glide XP, docking mode (Schrodinger, 2020–1, LLC, New York, NY, USA). All compounds were built using Maestro build panel and optimized to lower energy conformers using Ligprep v3.5.9 (Schrodinger, LLC). The crystal structure of Topo I enzyme complexes with DNA were taken from RCSB Protein Data Bank (PDB code 1T8I) and prepared for docking using ‘protein preparation wizard’ in Maestro. The bond orders and formal charges were added for hetero groups and hydrogens were added to all atoms in the structure. The termini were capped by adding *N*-acetyl (ACE) and *N*-methyl amide (NMA) residue. After preparation, the hydrogen bond network in enzyme structure was optimized using OPLS force field. Minimization was terminated when the energy converged or root mean square deviation (RMSD) reached a maximum cut off of 0.30 Å. Grids were then defined by centering on ligand using default box size. Final docking studies for all synthesized compounds were performed using extra-precision (XP) docking mode on generated grid of protein structure.

A set of ADME-related properties were calculated by using the QikProp program running in normal mode. QikProp generates physically relevant descriptors, and uses them to perform ADME predictions [29–35].

Declaration of Competing Interest

The authors declare that they have no known competing financial interests or personal relationships that could have appeared to influence the work reported in this paper.

Acknowledgement

R.S.M. is thankful to SERB, New Delhi (Project No. EEQ/2017/000802) for providing financial support. P.V.L.S.B. is thankful to Indian Council of Medical Research (ICMR) [ISRM/12(07)/2019] and DST-SERB [CRG/2018/003276] for providing financial support. Authors are also thankful to The Head, Department of Biotechnology, KLEF University, Vaddeswaram for the computational support.

Appendix A. Supplementary material

Supplementary data includes $^1\text{H-NMR}$, $^{13}\text{C-NMR}$, DEPT, LCMS and HPLC for all new compounds in supplementary information.

Supplementary data to this article can be found online at <https://doi.org/10.1016/j.bioorg.2021.105174>.

References

- (a) Y. Pommier, DNA topoisomerase I inhibitors: chemistry, biology, and interfacial inhibition, *Chem. Rev.* 109 (2009) 2894–2902, <https://doi.org/10.1021/cr900097c>;
- (b) A.T. Baviskar, C. Madaan, R. Preet, P. Mohapatra, V. Jain, A. Agarwal, S. K. Guchhait, C.N. Kundu, U.C. Banerjee, P.V. Bharatam, N-fused imidazoles as novel anticancer agents that inhibit catalytic activity of topoisomerase II α and induce apoptosis in G1/S phase, *J. Med. Chem.* 54 (2011) 5013–5030;
- (c) C.A. Austin, K.L. Marsh, Eukaryotic DNA topoisomerase II β , *BioEssays.* 20 (1998) 215–226;
- (d) Y. Pommier, Topoisomerase I inhibitors: camptothecins and beyond, *Nat. Rev. Cancer.* 6 (10) (2006) 789;
- (e) Y. Pommier, E. Leo, H. Zhang, C. Marchand, DNA topoisomerases and their poisoning by anticancer and antibacterial drugs, *Chem. Biol.* 17 (5) (2010) 421–433;
- (f) K. Drlica, R.J. Franco, Inhibitors of DNA topoisomerases, *Biochem.* 27 (7) (1988) 2253–2259.
- (a) M.A. Bjornsti, S.H. Kaufmann, F1000 Res. Faculty Rev. 8 (2019) 1704, <https://doi.org/10.12688/f1000research.20201.1>;
- (b) S. Basili, S. Moro, *Expert Opin. Ther. Patents.* 19 (5) (2009) 555–574;
- (c) Y. Pommier, *A.C.S. Chem. Biol.* 8 (2013) 82–95;
- (d) K.E. Hevenern, T.A. Verstak, K.E. Lutat, D.L. Riggsbee, J.W. Mooney, Recent developments in topoisomerase-targeted cancer chemotherapy, *Acta Pharmaceutica Sinica B.* 8 (6) (2018), <https://doi.org/10.1016/j.apbs.2018.07.008>.
- (a) B.A. Hanson, R.L. Schowen, V.J. Stella, *Pharm. Res.* 20 (7) (2003) 1031–1038.
- (b) J. Fassberg, V.J. Stella, *Pharm. Sci.* 81 (7) (1992) 676–684.
- (c) R.P. Verma, C. Hansch, *Chem. Rev.* 109 (2009) 213–235.
- (d) A. Thomas and Y. Pommier, Targeting Topoisomerase I in the Era of Precision Medicine. DOI: 10.1158/1078-0432.CCR-19-1089.
- (a) M.C. Sheridan, M. Reddy, P.V. Morrell, A. Cobb, B. T. Marchand, C. A gama, K. Chergui, A. Renaud, A. G. Bindu, L. K. Pommier, Y. M. Cushman, Synthesis and biological evaluation of indenoisoquinolines that inhibit both tyrosyl-DNA phosphodiesterase I (Tdp1) and topoisomerase I (Top1), *J. Med. Chem.* 56 (2013) 182–200.
- (b) L. Zhu, C. Zhuang, N. Lei, Z. Guo, C. Sheng, G. Dong, S. Wang, Y. Zhang, J. Yao, Z. Miao, W. Zhang, Synthesis and preliminary bio-evaluation of novel E-ring modified acetal analog of camptothecin as cytotoxic agents, *Eur J Med Chem.* 56 (2012) 1–9;
- (c) T.X. Nguyen, A. Morrell, C.M. Sheridan, C. Marchand, K. Agama, A. Bermingham, A.G. Stephen, A. Chergui, A. Naumova, R. Fisher, B.R. O'Keefe, Y. Pommier, M. Cushman, Synthesis and biological evaluation of the first dual tyrosyl-DNA phosphodiesterase I (Tdp1)-topoisomerase I (Top1) inhibitors, *J. Med. Chem.* 55 (2012) 4457–4478;
- (d) J.X. Duan, X. Cai, F. Meng, J.D. Sun, Q. Liu, D. Jung, H. Jiao, J. Matteucci, B. Jung, D. Bhupathi, D. Ahluwalia, H. Huang, C.P. Hart, M. Matteucci, 14-Aminocamptothecins: their synthesis, preclinical activity, and potential use for cancer treatment, *J. Med. Chem.* 54 (2011) 1715–1723;
- (e) C. Samori, A. Guerrini, G. Varchi, G. Fontana, E. Bombardelli, S. Tinelli, G. L. Beretta, S. Basili, S. Moro, F. Zunino, A. Battaglia, Semi-synthesis, biological activity, and molecular modeling studies of C-ring-modified camptothecins, *J. Med. Chem.* 52 (2009) 1029–1039;
- (f) Q.D. You, Z.Y. Li, C.H. Huang, Q. Yang, X.J. Wang, Q.L. Guo, X.G. Chen, X. G. He, T.K. Li, J.W. Chern, Discovery of a Novel Series of Quinolone and Naphthyridine Derivatives as Potential Topoisomerase I Inhibitors by Scaffold Modification, *J. Med. Chem.* 52 (2009) 5649–5661;
- (g) C. Samori, A. Guerrini, G. Varchi, F. Zunino, G.L. Beretta, C. Femoni, E. Bombardelli, G. Fontana, A. Battaglia, Thio camptothecin, *J. Med. Chem.* 51 (2008) 3040–3044.
- (a) M. Ling-Hua, L. Zhi-Yong, Y. Pommier, Non-Camptothecin DNA Topoisomerase I Inhibitors in Cancer Therapy, *Curr. Topics Med. Chem.* 3 (2003) 305–320;
- (b) C. Sheng, Z. Miao, W. Zhang, New Strategies in the Discovery of Novel Non-Camptothecin Topoisomerase I Inhibitors, *Curr. Med. Chem.* 18 (2011) 4389–4409;
- (c) M.K. Kathiravan, A.N. Kale, S. Nilewar, Discovery and Development of Topoisomerase Inhibitors as Anticancer Agents, *Mini-Rev. Med. Chem.* 16 (2016) 1219–1229, <https://doi.org/10.2174/1389557516666160822110819>;
- (d) G. Kohlhagen, K.D. Paull, M. Cushman, P. Nagafuji, Y. Pommier, Protein-linked DNA strand breaks induced by NSC 314622, a novel noncamptothecin topoisomerase I poison, *Mol. Pharmacol.* 54 (1998) 50–58, <https://doi.org/10.1124/mol.54.1.50>;
- (e) Y. Pommier, M. Cushman, *Mol. Cancer Ther.* 8 (2009) 1008–1014;
- (f) S. Kummur, A. Chen, M. Gutierrez, D. Allen, J.M. Covey, L. Rubinstein, J. Collins, J. Tomaszewski, J.H. Doroshow, T.D. Pfister, L. Wang, W. Yutzy, Y. Zhang, R.J. Kinders, J. Ji, R. Parchment, C. Redon, W.M. Bonner, Y. Pommier, J. L. Eiseman, J.L. Holleran, J.H. Beumer, *Cancer Chemother. Pharmacol.* 78 (2016) 73–81;
- (g) M.A. Shah, R.H. Xu, Y.J. Bang, P.M. Hoff, T. Liu, L.A. Herr'aez-Baranda, F. Xia, A. Garg, M. Shing, J. Taberner, J. Clin. Oncol. 35 (2017) 2558–2573;
- (h) J.M. Yuan, N.Y. Chen, H.R. Liao, G.H. Zhang, X.J. Li, Z.Y. Gu, C.X. Pan, D. L. Mo, G.F. Su, *New J. Chem.* 44 (2020) 11203–11214, <https://doi.org/10.1039/C9NJ05846j>;
- (i) B. Kundu, S.K. Das, S.P. Chowdhuri, S. Pal, D. Sarkar, A. Ghosh, A. Mukherjee, D. Bhattacharya, B.B. Das, A. Talukdar, *J. Med. Chem.* 62 (2019) 3428–3446, <https://doi.org/10.1021/acs.jmedchem.8b01938>;
- (j) G. Joshi, S. Kalra, U.P. Yadav, P. Sharma, P.K. Singh, S. Amrutkar, A.J. Ansari, S. Kumar, A. Sharon, S. Sharma, D.M. Sawant, U.C. Banerjee, S. Singh, R. Kumar, *Bioorganic Chemistry.* 94 (2019), <https://doi.org/10.1016/j.bioorg.2019.103409>;
- (k) M. Kadagathura, G. ParimalaDevib, P. Grewal, D.K. Sigalappalia, P. N. Makhala, U.C. Banerjee, N.B. Bathinib, N.D. Tangellamudia, *Bioorganic Chemistry* 99 (2020), <https://doi.org/10.1016/j.bioorg.2020.103629>;
- (l) W.Y. Huang, X.R. Zhanga, L. Lyub, S.Q. Wanga, X.T. Zhanga, Pyridazino[1,6-b]quinazolinones as new anticancer scaffold: Synthesis, DNA intercalation, topoisomerase I inhibition and antitumor evaluation in vitro and in vivo, *Bioorganic Chemistry.* 99 (2020), <https://doi.org/10.1016/j.bioorg.2020.103814>;
- (m) T.C. Chen, D.S. Yu, S.J. Chen, C.L. Chen, C.C. Lee, Y.Y. Hsieh, L.C. Chang, J. H. Guh, J.J. Lin, H.S. Huang, *Arabian Journal of Chemistry* 12 (2019) 4348–4364;
- (n) P. Cheng, L. Zhu, W. Guo, W. Liu, J. Yao, G. Dong, Y. Zhang, C. Zhuang, C. Sheng, Z. Miao, W. Zhang, *Journal of Enzyme Inhibition and Medicinal Chemistry.* 27 (3) (2012) 437–442.(o)C. Zhang, S. Li, L. Ji, S. Liu, Z. Li, S. Li, X. Meng. DOI: 10.1016/j.bmc.2015.06.042.
- (p) L. Marzi, K. Agama, J. Murai, S. Difilippantonio, A. James, C. J. Peer, W. D. Figg, D. Beck, M. A. Elsayed, M. Cushman, and Y. Pommier, *Mol Cancer Ther.* 17 (8) (2018) 1694–1704. DOI: 10.1158/1535-7163.MCT-18-0028.
- (q) W. J. Zhang, P. H. Li, M. C. Zhao, Y. H. Gu, C. Z. Dong, X. Chen, Z. Y. Du, *Bioorganic Chemistry* 88 (2019) 102899.
- (r) A. H. Halawa, W. E. Elgammal, S. M. Hassan, A. H. Hassan, H. S. Nassar, H. Y. Ebrahim, A. M. Mehany, A. M. El-Agrody, *Bioorganic Chemistry* 98 (2020) 10372.
- (s) K. R. A. Abdellatif, W. A. A. Fadaly, Y. A. Mostafa, D. M. Zaher, H. A. Omar, *Bioorganic Chemistry* 91 (2019). DOI: 10.1016/j.bioorg.2019.103132.
- (a) M. Cushman, M. Jayaraman, J.A. Vroman, A.K. Fukunaga, B.M. Fox, G. Kohlhagen, D. Strumberg, Y. Pommier, *J. Med. Chem.* 43 (2000) 3688–3698, <https://doi.org/10.1021/jm000029d>;
- (b) M.A. Cinelli, P.V.N. Reddy, P.C. Lv, J.H. Liang, L. Chen, K. Agama, Y. Pommier, R.B.V. Breemen, M. Cushman, *J. Med. Chem.* 55 (24) (2012) 10844–10862.
- (a) K. Ishida, T. Asao, Self-association and unique DNA binding properties of the anti-cancer agent TAS-103, a dual inhibitor of topoisomerases I and II, *Biochim. Biophys. Acta.* 18 (2–3) 1587–2002) 155–163.
- (b) K. Padgett, A. Stewart, P. Charlton, M. J. Tilby, C. Austin, An investigation into the formation of N-[2-(dimethylamino) ethyl] acridine-4- carboxamide (DACA) and 6-[2-(dimethylamino)ethylamino]- 3-hydroxy-7Hindeno[2, 1-C]quinolin-7-one dihydrochloride (TAS-103) stabilised DNA topoisomerase I and II cleavable complexes in human leukaemia cells, *Biochem. Pharmacol.* 60 (2000) 817–821.
- (c) C. H. Tseng, C. C. Tzeng, C. L. Yang, P. J. Lu, H. L. Chen, H. Y. Li, Y. C. Chuang, C. N. Yang, Y. L. Chen, Synthesis and antiproliferative evaluation of certain indeno[1,2-c] quinoline derivatives, *J. Med. Chem.* 53 (2010) 6164–6179.
- (a) T.K. Li, P.J. Houghton, S.D. Desai, P. Daroui, A.A. Liu, E.S. Hars, A. L. Ruchelman, E.J. LaVoie, L.F. Liu, Characterization of ARC-111 as a novel topoisomerase I-targeting anticancer drug, *Cancer Res.* 63 (2003) 8400–8407;
- (b) F. Meng, X.T. Nguyen, X. Cai, J. Duan, M. Matteucci, C.P. Hart, ARC-111 inhibits hypoxia-mediated hypoxia-inducible factor-1 α accumulation, *Anticancer Drugs* 18 (2007) 435–445.
- (a) L.S. Kurtzberg, S. Roth, R. Krumbholz, et al., Genz-644282, a novel noncamptothecin topoisomerase I inhibitor for cancer treatment, *Clin Cancer Res.* 17 (2011) 2777–2787;
- (b) P.J. Houghton, R. Lock, H. Carol, et al., Testing of the topoisomerase I inhibitor Genz-644282 by the pediatric preclinical testing program, *Pediatr Blood Cancer.* 58 (2012) 200–209;
- (c) R. Musiol, An overview of quinoline as a privileged scaffold in cancer drug discovery, *Expert Opin. Drug Discovery.* 12 (6) (2017) 583–597, <https://doi.org/10.1080/17460441.2017.1319357>.
- (a) V.A. Venkatesha, A. Joshi, M. Venkataraman, et al., P7170, a novel inhibitor of mTORC1/mTORC2 and Activin receptor-like Kinase 1 (ALK1) inhibits the growth of non-small cell lung cancer, *Mol. Cancer.* 13 (2014) 259–270;
- (b) M. Smith, M.M. Mader, J.A. Cook, et al., Characterization of LY3023414, a novel PI3K/Mtor dual inhibitor eliciting transient target modulation to impede tumor growth, *Mol. Cancer Ther.* 15 (15) (2016) 2344–2356.
- G. Jin, Z. Li, F. Xiao, X. Qi, X. Sun, Optimization of activity localization of quinoline derivatives: Design, synthesis and dual evaluation of biological activity for potential antitumor and antibacterial agents, *Bioorganic Chem.* 99 (2020), 103837, <https://doi.org/10.1016/j.bioorg.2020.103837>.
- (a) I. Ali, M.N. Lonea, H.Y. Aboul-Eneinb, Imidazoles as potential anticancer agents, *Med. Chem. Commun.* 8 (9) (2017) 1742–1773, <https://doi.org/10.1039/c7md00067g>;
- (b) S.V. Tiwari, A.P.G. Nikalje, D.K. Lokwani, A.P. Sarkate, K. Jamir, Synthesis, biological evaluation, molecular docking study and acute oral toxicity study of coupled Imidazolyl-Pyrimidine derivatives, *Lett. Drug Des. Discov.* 15 (2018) 475–487;
- (c) A.P.G. Nikalje, S.V. Tiwari, A.P. Sarkate, K.S. Karnik, Imidazole-thiazole coupled derivatives as novel lanosterol 14 α demethylase inhibitors: Ionic liquid

- mediated synthesis, biological evaluation and molecular docking study, *Med. Chem. Res.* 27 (2018) 592–606;
- (d) A.P. Sarkate, D.K. Lokwani, S.S. Bahekar, D.B. Shinde, Synthesis and docking studies of 2-(nitrooxy) ethyl-4-(2-(substitutedphenyl)-4-(substitutedphenyl)-1H-imidazol-1-yl) benzoate as anti-inflammatory, analgesic and nitric oxide releasing agents, *Int. J. Pharm. Pharm. Sci.* 7 (2015) 197–205;
- (e) L. Zhang, X.M. Peng, G.L.V. Damu, R.X. Geng, C.H. Zhou, *Comprehensive Review in Current Developments of Imidazole-Based Medicinal Chemistry*, *Med Res Rev.* 34 (2014) 340–437.
- [13] (a) R. Kancherla, et al., (Sharjah, United Arab Emirates), *Medicinal Chemistry*. 11 (8) (2015) 789–797. (b) K. Leonard, et al., *PCT Int. Appl.*, 2015057626, 23 Apr 2015. (c) L. Chen, et al., *PCT Int. Appl.*, 2013020993, 14 Feb 2013.
- [14] J. Chattopadhyaya, R. S. Upadhyaya, Quinoline, naphthalene and conformationally constrained quinoline or naphthalene derivatives as anti-mycobacterial agents. WO 2009091324.
- [15] S. L. Qiang, et al., U.S. Pat. Appl. Publ., 20140127156, 08 May 2014.
- [16] (a) J. Chattopadhyaya, R.S. Upadhyaya, Quinoline, naphthalene and conformationally constrained quinoline or naphthalene derivatives as anti-mycobacterial agents, US20110059948A1. (b) S.L. Qiang, J.W. Chang, J. Wang, S. A. Kang, C.C. Thoreen, A. Markhard, H. Wooyoung, J. Zhang, S. Taobo, D. M. Sabatini, N. S. Gray, *J. Med. Chem.* 53 (2010) 7146–7155. DOI: 10.1021/jm101144f.
- [17] (a) R.S. Upadhyaya, S.V. Lahore, A.Y. Sayyed, S.S. Dixit, P.D. Shinde, J. Chattopadhyaya, Conformationally-constrained indeno[2,1-c] quinolines – a new class of anti-mycobacterial agents, *Org. Biomol. Chem.* 8 (2010) 2180–2197; (b) J.B. Bongui, et al., *Chem. Pharmaceut. Bull.* 53 (12) (2005) 1540–1546.
- [18] R.S. Upadhyaya, P.D. Shinde, S.A. Kadam, A.N. Bawane, A.Y. Sayyed, R. A. Kardile, P.N. Gitay, S.V. Lahore, S.S. Dixit, A. Földesi, J. Chattopadhyaya, Synthesis and antimycobacterial activity of prodrugs of indeno[2,1-c] quinoline derivatives, *Eur. J. Med. Chem.* 46 (4) (2011) 1306–1324, <https://doi.org/10.1016/j.ejmech.2011.01.053>.
- [19] V. Litchfield, R.B. Smith, A.M. Franklin, J.H. Davis, Synthesis of Acridine-Quinone Systems-A Potential Electrochemical Fluorescent Switch, *Synthetic Commun.* 38 (20) (2008) 3447–3455, <https://doi.org/10.1080/00397910802154261>.
- [20] (a) K. Ahmed, et al., An Efficient Synthesis of Quinoline Derivatives: Bio-Active Studies, *Letters in Drug Design & Discovery*. 4(8) (2007) 580–586. DOI: 10.2174/157018007782794536. (b) M. Anzini, A. Cappelli, S. Vomero, M. Seeber, M. C. Menziani, T. Langer, B. Hagen, C. Manzoni, J. J. Bourguignon, Mapping and Fitting the Peripheral Benzodiazepine Receptor Binding Site by Carboxamide Derivatives. Comparison of Different Approaches to Quantitative Ligand–Receptor Interaction Modeling, *Journal of Med. Chem.* 44 (8) (2001) 1134–1150. DOI: 10.1021/jm0009742. (c) F. Aribi, et al., *European Journal of Organic Chemistry*. 27–28 (2018) 3792–3802. (d) S. Kühner, G. Bahrenberg, A. Kless, W. Schröder, Substituted quinoline-3-carboxamides as KCNQ2/3 modulators, *U.S. Pat. Appl. Publ.*, 20120053204, 01 Mar 2012.
- [21] M. Lovrić, I. Cepanec, M. Litvić, A. Bartolinić, V. Vinković, Scope and Limitations of Sodium and Potassium Trimethylsilylanolate as Reagents for Conversion of Esters to Carboxylic Acids. 80 (1) (2007) 109–115.
- [22] B. Kundu, et al., Discovery and Mechanistic Study of Tailor-Made Quinoline Derivatives as Topoisomerase 1 Poison with Potent Anticancer Activity, *J. Med. Chem.* 62 (2019) 3428–3446.
- [23] J.J. Champoux, DNA topoisomerases: structure, function and mechanism, *Annu. Rev. Biochem.* 70 (2001) 369–413, <https://doi.org/10.1146/annurev.biochem.70.1.369>.
- [24] J.C. Wang, DNA topoisomerases, *Annu. Rev. Biochem.* 65 (1996) 635–692.
- [25] Z. Topcu, DNA topoisomerase targets for anti-cancer drugs, *J. Clin. Pharma. Ther.* 26 (2001) 405–416.
- [26] J.C. Wang, Cellular role of DNA topoisomerases: A molecular perspective, *Nat. Rev. Mol. Cell Biol.* 3 (2002) 430–440.
- [27] V.S. Dofe, A.P. Sarkate, R. Azad, H.G. Charansingh, *Res. Chem. Interme.* 21 (2017) 484.
- [28] M. Fukuda, N. Kishio, F. Kanzawa, H. Ogasawara, T. Ishida, H. Arioka, K. Bonjanowski, M. Oka, N. Saijo, *Cancer Res.* 56 (1996) 789.
- [29] A.V. Chate, A.A. Redlawar, G.M. Bondle, A.P. Sarkate, S.V. Tiwari, D.K. Lokwani, A new efficient domino approach for the synthesis of coumarin-pyrazolines as antimicrobial agents targeting bacterial D-alanine-D-alanine ligase, *N. J. Chem.* 43 (2019) 9002–9011.
- [30] M.R. Bhosle, L.D. Khillare, J.R. Mali, A.P. Sarkate, D.K. Lokwani, S.V. Tiwari, DIPEAc promoted one-pot synthesis of dihydropyrido[2,3-d:6,5-d'] dipyrimidinetetraone and pyrimido[4,5-d]pyrimidine derivatives as potent tyrosinase inhibitors and anticancer agents: in vitro screening, Molecular docking and ADMET predictions, *N. J. Chem.* 42 (2018) 18621–18632.
- [31] S.V. Tiwari, J.A. Seijas, M.P. Vazquez-Tato, A.P. Sarkate, K.S. Karnik, A.P. G. Nikalje, Ionic Liquid Promoted Synthesis of Novel Chromone-Pyrimidine Coupled Derivatives, *Antimicrobial Analysis, Enzyme Assay, Docking Study and Toxicity Study*, *Molecules* 23 (2018) 440.
- [32] D.K. Lokwani, R. Azad, A.P. Sarkate, P. Reddanna, D. Shinde, Structure Based Library Design (SBLD) for new 1,4-dihydropyrimidine scaffold as simultaneous COX-1/COX-2 and 5-LOX inhibitors, *Bioorganic Medicinal Chem.* 23 (2015) 4533–4543, <https://doi.org/10.1016/j.bmc.2015.06.008>.
- [33] W. Doherty, N. Adler, A. Knox, D. Nolan, J. McGouran, A.P. Nikalje, D.K. Lokwani, A.P. Sarkate, P. Evans, Synthesis and Evaluation of 1,2,3-Triazole-Containing Vinyl and Allyl Sulfones as Anti-Trypanosomal Agents, *Eur J Org Chem.* 1 (2017) 175–185.
- [34] S.V. Tiwari, S. Siddiqui, J.A. Seijas, M.P. Vazquez-Tato, A.P. Sarkate, D.K. Lokwani, A.P.G. Nikalje, Microwave-assisted Facile Synthesis, Anticancer Evaluation and Docking study Of N-((5-(substituted methylene amino)-1,3,4-thiadiazol-2-yl) methyl) Benzamide Derivatives, *Molecules* 22 (2017) 995.
- [35] D.K. Lokwani, A.P. Sarkate, K.S. Karnik, A.P.G. Nikalje, J.A. Seijas, Structure-Based Site of Metabolism (SOM) Prediction of Ligand for CYP3A4 Enzyme: Comparison of Glide XP and Induced Fit Docking (IFD), *Molecules* 25 (7) (2020) 1622. DOI: 0.3390/molecules25071622.



N-Benzoylation of 6-aminoflavone by reductive amination and efficient access to some novel anticancer agents via topoisomerase II inhibition

Nitin M. Thorat^{1,2} · Aniket P. Sarkate³ · Deepak K. Lokwani⁴ · Shailee V. Tiwari⁵ · Rajaram Azad⁶ · Shankar R. Thopate^{1,7}

Received: 28 November 2019 / Accepted: 23 March 2020
© Springer Nature Switzerland AG 2020

Abstract

Series of novel *N*-benzyl derivatives of 6-aminoflavone (**9a–n**) were synthesized and evaluated for anticancer and topoisomerase II enzyme inhibition activity. All the synthesized compounds were screened for in vitro anticancer activity against human breast cancer cell line (MCF-7) and human lung cancer cell line (A-549). Among the synthesized compounds, **9f** and **9g** were found to be the most potent anticancer agents against human breast cancer cell line (MCF-7) with IC₅₀ values of 9.35 μM and 9.58 μM, respectively. Compounds **9b**, **9c** and **9n** exhibited promising anticancer activity against human lung cancer cell line (A-549) with 43.71%, 46.48% and 44.26% inhibition at the highest concentration of 10 μM, respectively. Compounds **9c**, **9f** and **9g** have ability to inhibit the topoisomerase II enzyme. Compound **9f** showed most potent topoisomerase II enzyme inhibition activity with IC₅₀ value of 12.11 μM. Further, these compounds have a high potential to be developed as a promising topoisomerase II inhibitors.

Keywords Aminoflavones · Buchwald coupling · Reductive amination · Anticancer agent · Topoisomerase II enzyme inhibitor · Malic acid

Introduction

Processes of cell growth viz. proliferation, migration, and angiogenesis are regulated by the various growth factors and mitogen-stimulated signaling networks. Any dysregulation of these factors can lead to cancer. Flavones are known to have anticancer activity through modulation of these factors

[1]. Scientific findings have shown that the flavones inhibit mitosis [2, 3], angiogenesis [4] and enzymes such as tyrosine kinase [5], topoisomerase [6–8], aromatase [9], epoxide hydrase [10], and tubulin polymerization [11–14]. Most of these compounds are either natural products or derivatives (Fig. 1). Aminoflavones are a class of compounds having nitrogen directly attached to aromatic *sp*² carbon, exhibits diverse biological activity. Substituted aminoflavones (Fig. 1) show anti-tubercular, cytotoxic and kinase inhibitory activity with anti-proliferative effects [15, 16]. Compound

Electronic supplementary material The online version of this article (<https://doi.org/10.1007/s11030-020-10079-1>) contains supplementary material, which is available to authorized users.

✉ Shankar R. Thopate
srthopate@gmail.com

¹ Department of Chemistry, Prof. John Barnabas Post Graduate School for Biological Studies, Ahmednagar College, Ahmednagar, Station Road, Ahmednagar, Maharashtra 414001, India

² Department of Chemistry, Maharaja Jivajirao Shinde Arts, Science, Commerce College, Shrigonda, Maharashtra 413701, India

³ Department of Chemical Technology, Dr. Babasaheb Ambedkar Marathwada University, Aurangabad, Maharashtra 431004, India

⁴ Department of Pharmaceutical Chemistry, R.C. Patel Institute of Pharmaceutical Education and Research, Shirpur, Maharashtra 425405, India

⁵ Department of Pharmaceutical Chemistry, Durgamata Institute of Pharmacy, Dharmapuri, Parbhani, Maharashtra 431401, India

⁶ Department of Animal Biology, University of Hyderabad, Hyderabad 500046, India

⁷ Department of Chemistry, Shri Sadguru Gangageer Maharaj Science, Gautam Arts and Sanjivani Commerce College, Kopargaon, Dist. Ahmednagar, Maharashtra 423 601, India

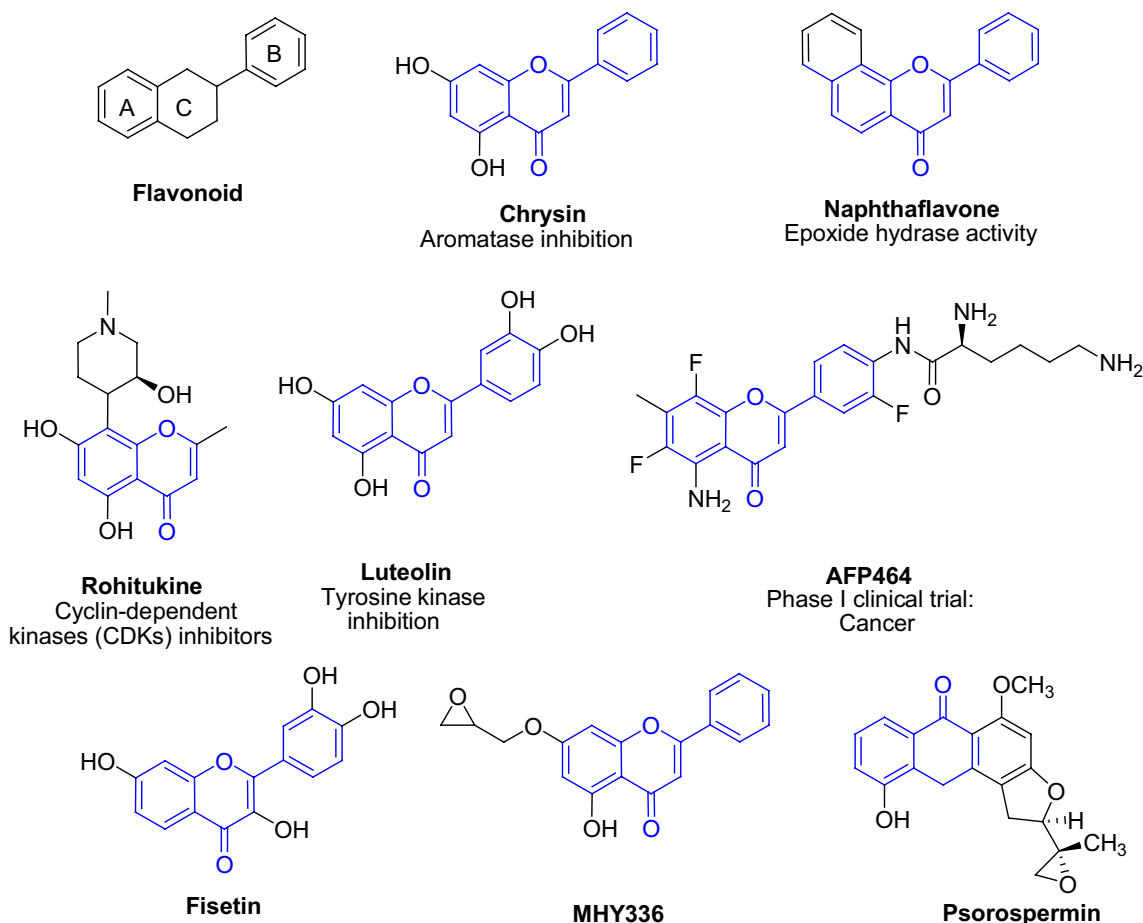


Fig. 1 Biologically active flavonoid structures

AFP646 is in phase-I clinical trial for cancer treatment [17]. A synthetic flavonoid MHY336 has ability to arrest the cell cycle in G2/M or S phase via Topo-II-dependent mechanism [18]. Dietary flavonoid fisetin acts as a dual inhibitor of Topo-I and Topo-II in cells [19]. Psorospermin, a natural antitumor antibiotic [20], intercalates DNA, and its alkylating potential is significantly increased in the presence of Topo-II [21, 22]. Unfortunate negligence of nature to aminoflavonoids as natural products might be attributed to intricacy in the synthesis of aminoflavones [15, 16], particularly those in which amino group is attached to A ring. This indeed limited structure activity relationship (SAR) studies of aminoflavones and related derivatives. Simon and co-workers have synthesized differently substituted 6-aminoflavones and shown that structural modifications particularly in B-ring would not have much impact on anticancer activity [23]. To improve inhibitory potency of 6-aminoflavone and to build SAR, a series of *N*-benzyl derivatives of 6-aminoflavones was designed as a novel anticancer agents. Herein, the present work reports the synthesis and anticancer activity of these novel flavones.

Results and discussion

Chemistry

Multistep synthetic protocol with synthesis of 1,3-diketone **5** from 4-bromophenol was initiated (**1**). 5-Bromo-2-hydroxyacetophenone (**3**) from **1** by methylation followed by Friedel–Craft acylation and in situ demethylation was prepared. To execute the Bekar–Venkataraman rearrangement, compound **3** was benzoylated by using benzoyl chloride and pyridine to get 5-bromo-2-benzoyloxy-acetophenone (**4**) which on further base catalyzed Bekar–Venkataraman rearrangement resulting in 1,3-diketone (**5**). Diketone **5** is then cyclized to 6-bromoflavone (**6**) employing malic acid under solvent free reaction condition [24]. The Buchwald coupling reaction of 6-bromoflavone (**6**) with benzophenone imine, Pd (II) catalyst and xantphos as ligand, Cs₂CO₃ as a base in dioxane at 90 °C delivered imine **7** in 72% yield. Hydrolysis of imine **7** with TFA in THF at room temperature gave 6-aminoflavone **8** in excellent yield. Kónya et al.

have reported direct amination of 6-bromoflavone; however, emphasized steric hindrance in the reacting amine is a limiting factor in this reaction [15]. α -Branching in reacting amine, hampers yield of the coupling reaction. However, to overcome this limitation, reductive amination protocol is used to synthesize novel 6-(1-arylmethanamino)-2-phenyl-4*H*-chromen-4-ones (**9a–n**). It improved the yields and efficacy of parallel synthetic protocol to intended target molecules. Various aldehydes were employed for synthesizing imines which were then reduced to corresponding arylmethanamino derivatives (**9a–n**) using $\text{NaBH}(\text{OAc})_3$ in one-pot reaction protocol to get excellent yield (Table 1).

Biology

Initially in vitro anti-proliferative efficacy of the synthesized N-benzyl derivatives of 6-aminoflavone (**9a–n**) was evaluated against human breast cancer cell line (MCF-7) and human lung cancer cell line (A-549) using MTT assay. Doxorubicin (standard antitumor drug) was used as a positive control. Cancer cells were treated with synthesized derivatives at various concentrations such as 0.1 μM , 1 μM and 10 μM to determine the % cancer cell inhibition and % cancer cell viability so as to predict the in vitro anticancer activity.

Table 2 shows that most of the synthesized compounds have shown good anticancer activity against human breast (MCF-7) and lung (A-549) cancer cell lines. **9f** was found to be the most potent anticancer compound among the synthesized derivatives against human breast cancer cell line (MCF-7) with 52.90% cancer cell line inhibition. **9g** was found to be the second most potent anticancer compound among the synthesized derivatives against human breast cancer cell line (MCF-7) with 52.17% cancer cell line inhibition. Other compounds such as **9a**, **9k** and **9n** showed good anticancer activity against human breast cancer cell line (MCF-7) with 42.03%, 30.67% and 44.76% cancer cell line inhibition, respectively.

New derivatives **9(a–n)** also displayed good anti-proliferative activity against human lung cancer cell line (A-549). Thus, compound **9c** exhibited 46.48% inhibition against human lung cancer cell line (A-549), while compounds **9n**, **9b** and **9j** showed 44.26%, 43.71% and 41.96% of human lung cancer cell line inhibition, respectively, at 10 μM concentration. Compounds **9f**, **9g** and **9n** were found to be more potent anticancer agent than that of standard drug Doxorubicin against MCF-7 cells. Compound **9a** was found to be equipotent to that of Doxorubicin against MCF-7 cells. Compounds **9b**, **9c**, and **9n** were found to be more potent anticancer agents than that of Doxorubicin against A-549 cells. Compound **9j** with *p*-methoxy group was found to be equipotent to that of Doxorubicin against A-549 cells.

From SAR (Table 2), it is confirmed that 2-phenyl-4*H*-chromen-4-one is essential for the anticancer activity. Various 6-(substituted benzyl amino)-2-phenyl-4*H*-chromen-4-one derivatives were synthesized to study the effect of substituent on benzyl amino ring. Compound **9f** i.e., 6-(4-Chlorobenzylamino)-2-phenyl-4*H*-chromen-4-one with 4-chloro substitution on the benzylamino group was found to be potent anticancer agent among all synthesized derivatives against human breast cancer cell line (MCF-7). Compound **9g** with 4-bromo substitution on the benzylamino group showed good anticancer activity against MCF-7 cell line. Substituents like *m*- NO_2 (**9a**), *p*-ethoxy (**9k**), 3, 4-dimethoxy (**9m**) and 3,4-dichloro (**9c**) on benzylamino group resulted in decrease in the activity.

Compound **9c** with 2,3-dichloro substituent on benzylamino group showed good (46.48%) inhibition against the human lung cancer cell line (A-549), while replacing 2,3-dichloro substituent either by nitrile (**9b**, 43.71%) or *p*-methoxy (**9j**, 41.96%) resulted in decrease in activity. Other substituents like 4-bromo (**9g**, 36.51), 5-Bromo-2-hydroxy (**9d**, 35.69%) and 3- NO_2 (**9a**, 21.08) exhibited lesser inhibition against human lung cancer cell line (A-549). Interestingly, when benzyl group was replaced by quinolin-2-ylmethyl group, compound **9n** showed good in vitro anticancer activity against both the selected cell lines. This means that the replacement of benzyl group by some other heterocyclic ring may result in good anticancer activity. In general, electron withdrawing groups such as chloro- and bromo substituents on benzyl group exhibit good anticancer activity against both cell lines. The benzyl substitution with dichloro group (**9c**) was found to be more potent than that of with *p*-chloro group (**9b**) against A-549 cell lines. The para-fluoro (**9e**) substituted derivatives were not found to be as good anticancer agents as that of para-chloro (**9b**) and para-bromo (**9g**) substituted derivatives.

Measurement of topoisomerase II activity

In order to shed light on core antitumor mechanism, the most active compounds (**9b**, **9c**, **9f**, **9g** and **9n**) were further evaluated to predict their ability to inhibit topoisomerase II enzyme. The catalytic activity of Topo II was evaluated according to the procedure reported by Patra et al. [18]. Doxorubicin was used as a standard drug in this assay. Doxorubicin inhibits the progression of topoisomerase II, enzyme which relaxes supercoils in DNA for transcription. Results of measurement of topoisomerase II activity are given in Table 3.

The synthesized compounds **9b**, **9c**, **9f**, **9g** and **9n** have an ability to inhibit topoisomerase II enzyme. Compounds **9f** and **9g** were found to be potent topoisomerase II enzyme inhibitor among tested synthesized compounds. Compounds **9f** and **9g** have shown IC_{50} value of 12.11 μM and 12.79 μM ,

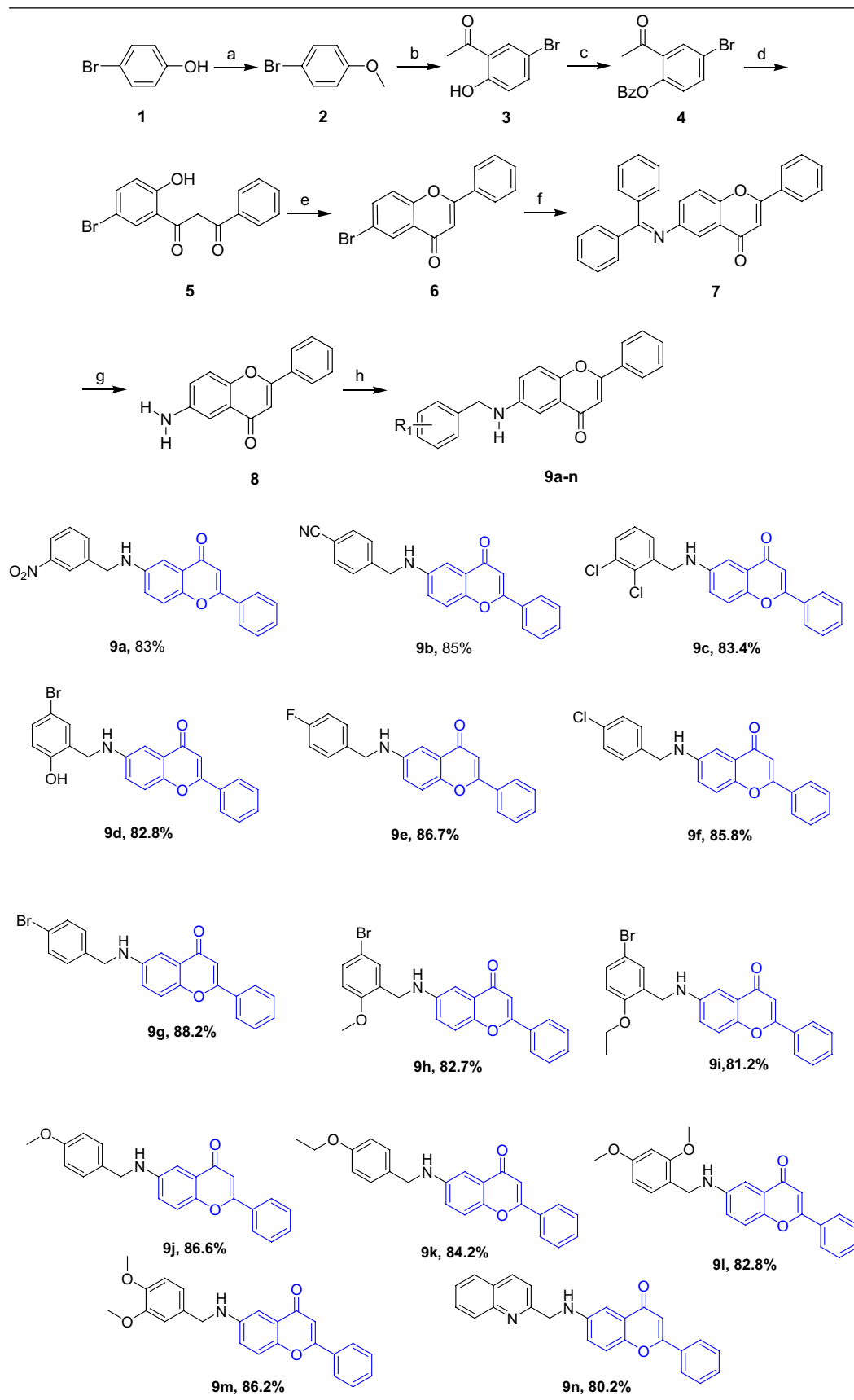
Table 1 Synthesis of novel *N*-benzyl derivatives of 6-aminoflavones

Table 1 (continued)

Reagents and Reaction Conditions: (a) K_2CO_3 , Methyl iodide, Acetonitrile, 50 °C, 6 h; (b) acetyl chloride, anhy. $AlCl_3$, 6 h, r.t.; (c) benzoyl chloride, C_5H_5N , 20 min, 3% HCl; (d) KOH, C_5H_5N , 15 min, 10% AcOH; (e) malic acid, oil bath preheated at 140 °C; (f) $Pd_2(dba)_3$, CS_2CO_3 , benzophenone imine, and xantphos, dioxane, 16 h, 90 °C; (g) TFA, THF, r.t. 2 h; (h) aldehyde, sodium triacetoxy borohydride, TFA, DCM, 0 °C to r.t. 45 min

Table 2 Anticancer activity of novel *N*-benzyl derivatives of 6-aminoflavones (at 10 μ M)

	MCF-7			A-549		
	% Viability	% Inhibition	SD	% Viability	% Inhibition	SD
Control	100	0	1.08	100	0	2.00
9a	57.96	42.03	4.27	78.91	21.08	3.26
9b	92.77	7.22	1.66	56.28	43.71	0.67
9c	78.93	21.06	1.13	53.51	46.48	0.03
9d	92.47	7.52	1.09	64.30	35.69	2.72
9e	91.72	8.27	0.21	83.83	16.16	0.70
9f	47.09	52.90	1.09	90.25	9.749	0.49
9g	47.82	52.17	1.02	63.48	36.51	0.45
9h	102.95	0	3.88	90.88	9.11	4.65
9i	102.754	0	0.88	94.37	5.62	1.23
9j	103.91	0	3.57	58.03	41.96	1.02
9k	69.32	30.67	0.60	83.38	16.61	3.14
9l	99.49	0.50	0.91	92.96	7.03	1.55
9m	75.87	24.12	2.15	85.33	14.66	4.45
9n	55.23	44.76	0.03	55.73	44.26	3.32
Doxorubicin	57.78	42.22	0.98	56.33	43.67	1.34

SD standard deviation; human breast cancer cell line: MCF-7 and human lung cancer cell line: A-549

Table 3 Topoisomerase II enzyme inhibition, docking score and MM GBSA binding free energy of selected compounds

Compound	IC ₅₀ μ M ^a	Docking score	MM GBSA Binding free energy
9b	35.46 \pm 0.05	-5.69	-23.25
9c	28.18 \pm 0.21	-6.69	-33.11
9f	12.11 \pm 0.15	-7.14	-28.25
9g	12.79 \pm 0.28	-6.63	-30.66
9n	30.92 \pm 0.16	-8.90	-56.61
Doxorubicin	0.94 \pm 0.05	-11.18	-42.33

^a Three independent experiments were performed for each concentration

respectively, as compared to the Doxorubicin (0.94 μ M). The synthesized compounds are not as strong topoisomerase II enzyme inhibitor as that of standard drug Doxorubicin.

Docking study

The activity of *N*-benzyl derivatives of 6-aminoflavone was justified by its predicted binding mode at the DNA cleavage site of topoisomerase II. Analysis of human Topo II co-crystal structure complexed with DNA and etoposide (PDB code 3QX3) showed that etoposide is incorporated between base

pairs of DNA and forms H bonds with amino acid residue Asp479 and DNA guanine fragment (DG13). Certainly, the molecular docking study showed that all docked compounds had been placed in between DNA base pair and had good contact with Topo II residues and DNA fragments. Analysis of interaction of docked compounds with Topo II-DNA complex revealed existence of H-bonding interaction with amino acid residue Gln778, and π - π stacking interactions with DG13, DC8, and DG12 DNA fragments. It was also revealed that in most of the compounds, carbonyl group of flavone moiety stabilizes ligand-protein complex by forming H-bond with amino acid residue Gln778. Similarly *N*-benzyl group support the complex by establishing π - π stacking interaction with various fragments of DNA. These results indicate that most of the compounds showed similar binding pattern with binding site amino acid residues as that of Doxorubicin (Figs. 2, 3).

Materials and methods

Chemistry

All reactions were performed in oven-dried glassware. All reagents and solvents were obtained from commercial

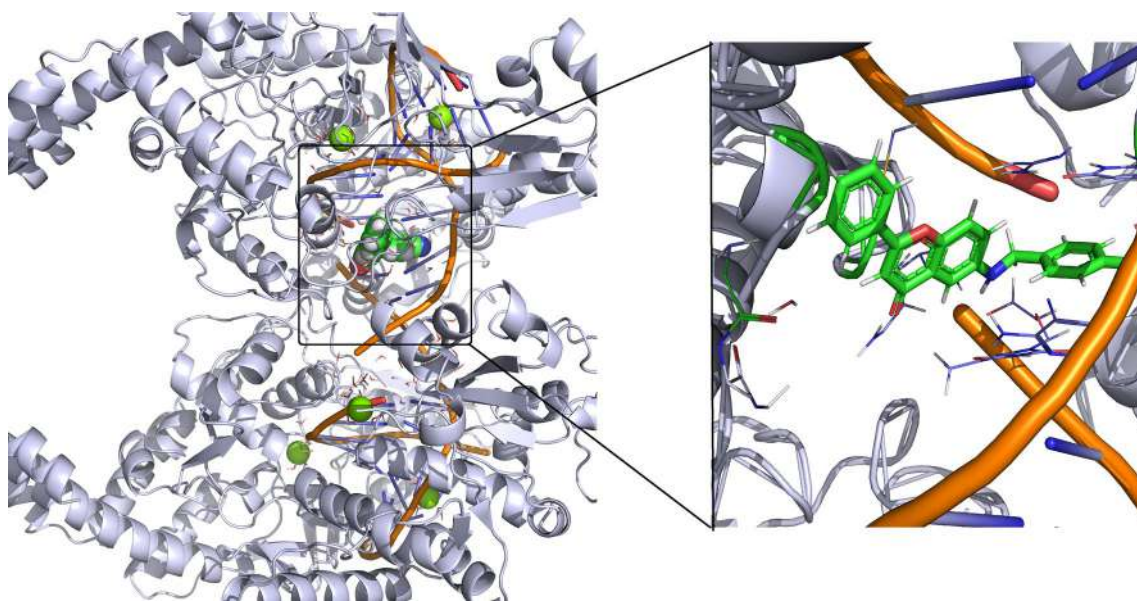


Fig. 2 Binding pose of *N*-benzyl derivative of 6-aminoflavone at DNA cleavage site of topoisomerase II

suppliers and used as received. Analytical thin-layer chromatography (TLC) was performed on precoated Merck silica gel plates (60F-254), visualized with a UV254 lamp and stained with KMnO_4 . Melting points are uncorrected and were determined in open capillary tubes using paraffin oil bath. ^1H and ^{13}C NMR spectra were obtained as solutions in deuterated solvents. Standard ^1H NMR (400 MHz) and ^{13}C NMR (100 MHz) were recorded on a Varian Mercury spectrometer in $\text{DMSO}-d_6$ and CDCl_3 solution and with tetramethylsilane as an internal standard. IR spectra were recorded on Perkin Elmer Model 1600 series FTIR instrument. Mass spectra were recorded on Agilent 1200SL-6100 LC/MS (ES-API) instrument. High-resolution mass spectra (HRMS) were performed with a QTOF Micromass Mass Spectrometer in electro spray ionization mode.

1-Bromo-4-methoxybenzene (2) Methyl iodide (1.31 g, 9.24 mmol) was added at RT to a stirred solution of 4-bromophenol (**1**, 1.0 g, 5.78 mmol) and K_2CO_3 (1.59 g, 11.56 mmol) in 10 mL acetonitrile. Reaction mixture was refluxed for 6 h at 50 °C. After completion of the reaction (TLC check), the mixture was cooled to room temperature, filtered through Celite bed and washed with ethyl acetate (3×20 mL). Organic layer was washed with water (3×40 mL), dried over anhydrous Na_2SO_4 concentrated on vacuo to get colorless oil (0.91 g, 84%); b.p. 223 °C; IR (KBr): 1657, 1339, 840, 670 cm^{-1} ; ^1H NMR (CDCl_3 , 400 MHz) δ 7.40 (d, $J=8$ Hz, 2H), 6.81 (d, $J=8$ Hz, 2H), 3.81 (s, 3H); ^{13}C NMR (CDCl_3 , 100 MHz) δ 158.1, 132.2, 115.7, 112.8, 55.4; LCMS (ES-API) m/z : 186.96 (M+H) $^+$.

5-Bromo-2-hydroxyacetophenone (3) To a stirred solution of 4-bromo anisole (**2**, 1.0 g, 5.37 mmol) in 10 mL dichloromethane, acetyl chloride (0.42 g, 5.37 mmol) was added at 0 °C. After 5 min of stirring anhydrous AlCl_3 (0.78 g, 5.91 mmol) was added portion wise, then reaction mixture was stirred for 6 h. After completion of the reaction (TLC check), the mixture was poured on crushed ice, product precipitates out. The precipitate thus obtained was filtered off, washed with diethyl ether and dried to get white solid. (0.9 g, 79%); m.p. 58–60 °C; IR (KBr): 3363, 1663, 845, 671 cm^{-1} ; ^1H NMR (CDCl_3 , 400 MHz) δ 12.70 (s, 1H), 7.84 (s, 1H), 7.55 (t, $J=8$ & 4 Hz, 1H), 6.90 (d, $J=8$ Hz, 1H), 2.64 (s, 3H); ^{13}C NMR (CDCl_3 , 100 MHz) δ 203.5, 161.3, 139.1, 132.9, 120.9, 120.5, 110.4, 26.7; LCMS (ES-API) m/z : 214.87 (M+H) $^+$.

5-Bromo-2-benzoyloxy-acetophenone (4) To a stirred solution of 5-bromo-2-hydroxyacetophenone (**3**, 1.0 g, 4.67 mmol) in 10 mL pyridine benzoyl chloride (0.78 g, 5.60 mmol) was added at 0 °C. After 20 min of stirring, reaction mixture was poured into ice cooled solution of 3% hydrochloric acid, product precipitates out. The crude product was filtered off washed with water and recrystallized from methanol to give yellow solid; m.p. 82–85 °C; IR (KBr): 3363, 1755, 1663, 845, 671 cm^{-1} ; ^1H NMR (CDCl_3 , 400 MHz) δ 8.20–8.18 (m, 2H), 7.96 (d, $J=2.4$ Hz, 1H), 7.69–7.64 (m, 2H), 7.55–7.51 (m, 2H), 7.13 (d, $J=8.8$ Hz, 1H), 2.53 (s, 3H); ^{13}C NMR (CDCl_3 , 100 MHz) δ 196.0, 164.8, 148.3, 136.1, 134.1, 132.9, 130.5, 130.3, 128.9, 125.8, 114.3, 29.7; LCMS (ES-API) m/z : 318.0 (M+H) $^+$.

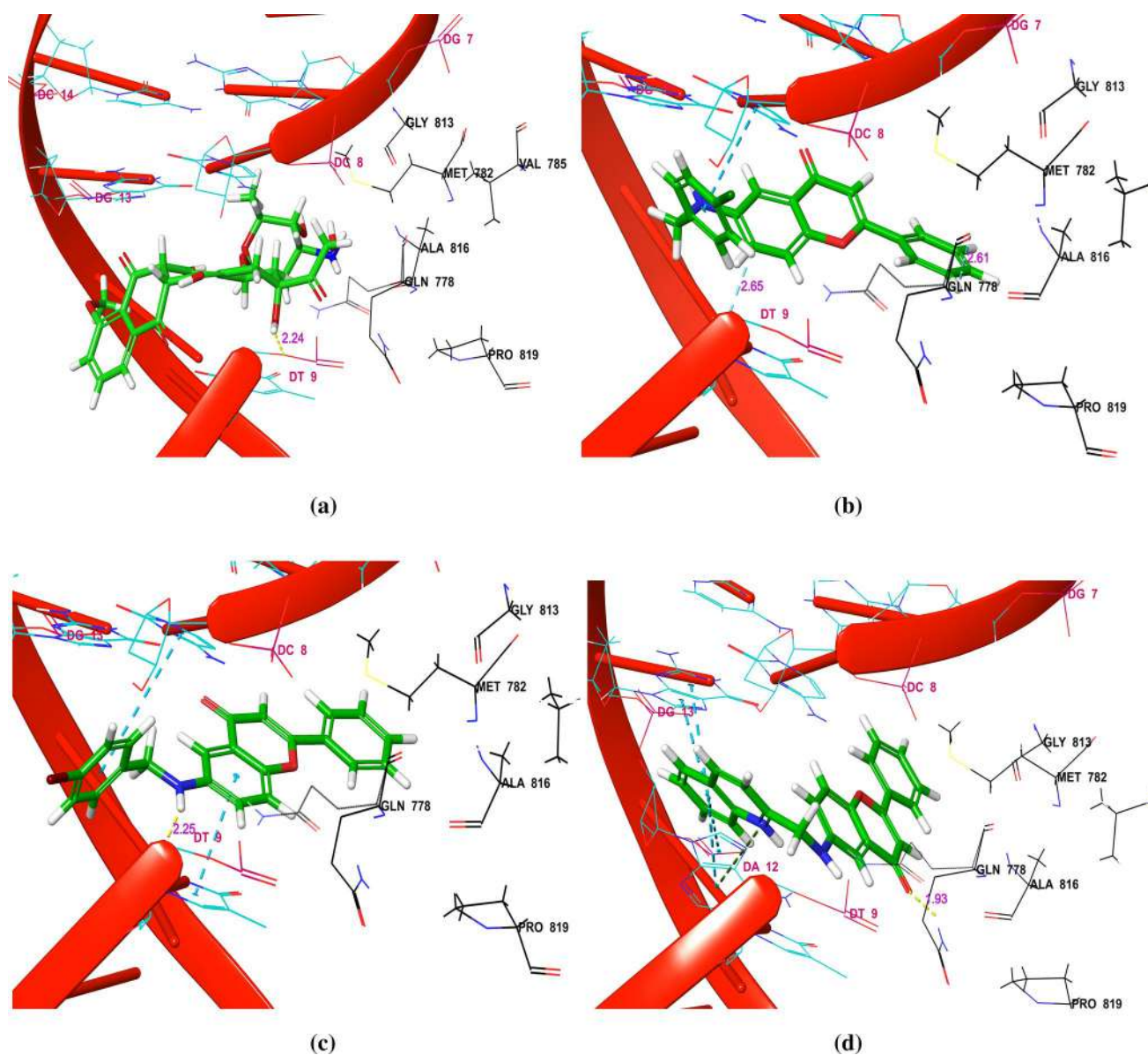


Fig. 3 Binding pose of compounds at DNA cleavage site of topoisomerase II. **a** Doxorubicin, **b** compound **9f**, **c** compound **9g** and **d** compound **9n**. Black colored wire representation of atoms indicates

amino acid residues, cyan colored wire representation of atoms are fragments of DNA, yellow colored dotted line indicates H-bonding and cyan colored dotted line indicates pi-pi stacking

1-(5-Bromo-2-hydroxyphenyl)-3-phenylpropane-1,3-dione (5) To a solution of 5-bromo-2-benzoyloxy-acetophenone (**4**, 1.0 g., 3.14 mmol) in 7.5 mL of pyridine, potassium hydroxide (0.26 g., 4.71 mmol) was added and reaction mixture was stirred at 50 °C for 15 min. After completion of the reaction (TLC check), the mixture was poured in ice cooled solution of 10% aq. acetic acid (50 mL) product precipitates out. The solid thus obtained was filtered off, washed with 10% aq. acetic acid and dried to get yellow solid (0.89 g, 80%), m.p. 108–109 °C; IR (KBr): 3363, 1663, 845, 671 cm^{-1} ; ^1H NMR (CDCl_3 , 400 MHz) δ 15.4 (bs, 1H), 12.05 (s, 1H), 7.97–7.95 (m, 2H), 7.86 (d, $J=2$ Hz,

1H), 7.60–7.49 (m, 4H), 6.91 (d, $J=8.8$ Hz, 1H), 6.76 (s, 1H); ^{13}C NMR ($\text{DMSO}-d_6$, 100 MHz) δ 186.5, 183.4, 172.7, 159.1, 138.4, 137.1, 135.1, 133.1, 131.7, 129.2, 128.9, 128.2, 127.5, 122.5, 121.0, 120.3, 110.8, 96.0; LCMS (ESI-API) m/z : 318.0 ($\text{M}+\text{H}$) $^+$.

6-Bromo-2-phenyl-4H-chromen-4-one (6) The mixture of 1-(2-hydroxyphenyl)-3-aryl-1,3-propanedione (**5**, 1.0 g., 3.14 mmol) and malic acid (0.42 g., 3.14 mmol) was heated in a preheated oil bath at 140 °C for 10 min. After completion of the reaction (TLC check), the mixture was allowed to cool at room temperature, water (10 mL) and ethyl acetate

(20 mL) were added. Organic layer was washed with aq. NaHCO_3 (3×40 mL) and dried over anhydrous Na_2SO_4 then concentrated in vacuo to get crude product. The crude product was purified by column chromatography on silica gel using hexane-ethylacetate (85:15) solvent system to give white solid (0.82 g, 87%); m.p. 194–196 °C; IR (KBr): 1645, 1604, 1568, 1130, 756 cm^{-1} ; ^1H NMR (CDCl_3 , 400 MHz) δ 8.20–8.10 (m, 3H), 8.01 (dd, $J = 10.8$ & 2.4 Hz, 1H), 7.83 (d, $J = 8.8$ Hz, 1H), 7.65–7.55 (m, 3H), 7.12 (s, 1H); ^{13}C NMR (CDCl_3 , 100 MHz) δ : 176.3, 163.4, 155.1, 137.3, 132.5, 131.3, 129.6, 127.3, 126.9, 125.3, 121.7, 118.3, 107.4; HRMS (ESI) m/z $[\text{M} + \text{H}]^+$: calcd for $\text{C}_{15}\text{H}_{10}\text{BrO}_2$: 300.9864, found: 300.9867.

6-(Benzhydrylidene-amino)-2-phenyl-chromen-4-one (7) The 6-bromo flavone (**6**, 1.0 g., 3.33 mmol), CS_2CO_3 (1.62 g., 5.65 mmol), benzophenone imine (0.6 g., 3.33 mmol) was dissolved in dioxane (10 mL). Then it was degassed by argon gas for 20 min, xantphos (50 mg., 0.10 mmol) and $\text{Pd}_2(\text{dba})_3$ (9 mg., 0.01 mmol) was added. The reaction mixture was stirred for 16 h at 90 °C. After completion of the reaction (TLC check), the mixture was cooled to room temperature, diluted with ethyl acetate and filtered through Celite bed. The filtrate was concentrated in vacuo. To this residue MeOH was added, the solid obtained was filtered and washed with diethyl ether. The crude product was purified by column chromatography on silica gel using hexane-ethylacetate (80:20) solvent system to give yellow solid (0.96 g, 72%); m.p. 248–249 °C; IR (KBr): 3442, 3063, 1637, 1616, 1455, 1361, 1290, 1025, 908, 775, 696 cm^{-1} ; ^1H NMR (CDCl_3 , 400 MHz) δ 7.89 (d, $J = 8$ Hz, 2H), 7.80–7.77 (m, 2H), 7.60–7.54 (m, 1H), 7.50–7.52 (m, 4H), 7.45 (t, $J = 8$ & 5 Hz, 2H), 7.40–7.38 (m, 1H), 7.28–7.29 (m, 1H), 7.17 (t, $J = 8$ & 4 Hz, 3H), 7.11 (t, $J = 8$ & 4 Hz, 2H), 6.76 (s, 1H); ^{13}C NMR (CDCl_3 , 100 MHz) δ 178.3, 169.9, 163.0, 152.6, 148.8, 139.7, 135.7, 131.9, 131.4, 129.4, 129.0, 128.3, 126.2, 124.1, 118.3, 116.0, 107.1; LCMS (ES-API) m/z : 402.14 ($\text{M} + \text{H}$) $^+$; HRMS (ESI) m/z $[\text{M} + \text{H}]^+$: calcd for $\text{C}_{28}\text{H}_{20}\text{NO}_2$: 402.1489, found: 402.1492.

6-Amino-2-phenyl-4H-chromen-4-one (8) To a solution of 6-(benzhydrylidene-amino)-2-phenyl-chromen-4-one (**7**, 1.0 g., 2.49 mmol) in 40 mL of THF, trifluoroacetic acid (0.28 g., 2.49 mmol) was added at 0 °C. The reaction mixture was stirred for 2 h at room temperature. After completion of the reaction (TLC check), the mixture was concentrated in vacuo. The residue was neutralized by addition of aq. NaHCO_3 solution and then extracted in ethyl acetate (2×10 mL). Combined organic extract was dried over anhydrous Na_2SO_4 and concentrated in vacuo. The crude product was purified by column chromatography on silica gel using hexane-ethylacetate (95:5) solvent system to give

yellow solid (1.37 g, 81%); m.p. 200–202 °C; IR (KBr): 3416, 3342, 1733, 1609, 1565, 768, 677 cm^{-1} ; ^1H NMR (CDCl_3 , 400 MHz) δ 8.10–8.01 (m, 2H), 7.55–7.58 (m, 3H), 7.54 (d, $J = 8.8$ Hz, 1H), 7.06–7.11 (m, 2H), 6.87 (s, 1H), 3.30 (s, 2H); ^{13}C NMR (CDCl_3 , 100 MHz) δ 178.4, 163.0, 150.0, 144.1, 132.1, 131.3, 128.9, 126.2, 124.7, 122.2, 119.0, 107.9, 106.7; LCMS (ES-API) m/z : 238.9 ($\text{M} + \text{H}$) $^+$; HRMS (ESI) m/z $[\text{M} + \text{H}]^+$: calcd for $\text{C}_{15}\text{H}_{12}\text{NO}_2$: 238.0868, found: 238.0874.

General procedure for the synthesis of 6-amino-2-phenyl-4H-chromen-4-ones (9a–9n) To a solution of 6-amino-2-phenyl-4H-chromen-4-one (**8**, 1 g., 4.21 mmol) and substituted aromatic aldehydes (4.21 mmol) in 1,2-dichloroethane (10 mL), sodium triacetoxy borohydride (1.34 g., 6.34 mmol) was added at 0 °C. Trifluoroacetic acid (0.96 g., 8.43 mmol) was added to the above solution and reaction mixture was stirred at 0 °C to RT for 45 min. After completion of the reaction (TLC check), the mixture was diluted by adding DCM, organic layer was first washed with aq. NH_4Cl and then with saturated solution of brine. Organic layer was dried over anhydrous Na_2SO_4 and concentrated in vacuo. The crude product was purified through column chromatography on silica gel using hexane-ethylacetate (85:15) solvent system to give the corresponding flavones derivatives in high yields.

6-(3-Nitrobenzylamino)-2-phenyl-4H-chromen-4-one (9a) Yellow solid, yield 82.6%, m.p. 157–160 °C; IR (KBr): 3280, 3062, 1762, 1222, 1188, 830, 504 cm^{-1} ; ^1H NMR ($\text{DMSO}-d_6$, 400 MHz) δ 8.25 (s, 1H), 8.12–8.10 (m, 1H), 8.05–8.03 (m, 2H), 7.87–7.85 (m, 1H), 7.67–7.63 (m, 1H), 7.59–7.57 (m, 4H), 7.23–7.20 (m, 1H), 6.98–6.96 (m, 1H), 6.91–6.90 (m, 1H), 6.88 (s, 1H), 4.54–4.52 (m, 2H); ^{13}C NMR ($\text{DMSO}-d_6$, 100 MHz) δ 177.3, 172.7, 159.2, 144.3, 134.0, 132.0, 130.0, 129.0, 128.4, 127.6, 126.2, 124.9, 121.2, 119.9, 118.0, 105.4, 103.1, 46.4; LCMS (ES-API) m/z : 372.0 ($\text{M} + \text{H}$) $^+$; HRMS (ESI) m/z $[\text{M} + \text{H}]^+$: calcd for $\text{C}_{22}\text{H}_{17}\text{N}_2\text{O}_4$: 373.1188, found: 373.1195.

6-(4-Cyanobenzylamino)-2-phenyl-4H-chromen-4-one (9b) Yellow solid, yield 85.2%, m.p. 167–168 °C; IR (KBr): 3287, 3043, 2222, 1613, 1497, 671, 543 cm^{-1} ; ^1H NMR ($\text{DMSO}-d_6$, 400 MHz) δ 8.05–8.03 (m, 2H), 7.81 (d, $J = 8.4$ Hz, 2H), 7.62–7.56 (m, 6H), 7.18 (dd, $J = 9.6$ & 3.2 Hz, 1H), 6.92 (d, $J = 2.8$ Hz, 1H), 6.88–6.86 (m, 2H), 4.48–4.47 (m, 2H); ^{13}C NMR ($\text{DMSO}-d_6$, 100 MHz) δ 178.5, 163.1, 149.9, 144.9, 144.4, 132.7, 132.1, 131.5, 129.1, 127.9, 126.3, 124.9, 121.2, 119.4, 118.9, 111.3, 106.8, 104.8, 48.0; LCMS (ES-API) m/z : 353.0 ($\text{M} + \text{H}$) $^+$; HRMS (ESI) m/z $[\text{M} + \text{H}]^+$: calcd for $\text{C}_{23}\text{H}_{17}\text{N}_2\text{O}_2$: 353.1290, found: 353.1286.

6-(2,3-Dichlorobenzylamino)-2-phenyl-4H-chromen-4-one (9c) Yellow solid, yield 83.4%, m.p. 168–171 °C; IR (KBr): 3299, 3068, 1685, 1288, 1096, 811, 770 cm^{-1} ; ^1H NMR (DMSO- d_6 , 400 MHz) δ 8.06–8.04 (m, 2H), 7.60–7.55 (m, 5H), 7.36–7.33 (m, 2H), 7.21–7.18 (m, 1H), 6.86–6.90 (m, 3H), 4.47–4.47 (m, 2H); ^{13}C NMR (DMSO- d_6 , 100 MHz) δ 178.3, 162.6, 149.3, 145.5, 138.6, 134.3, 132.9, 131.9, 131.3, 129.0, 128.9, 127.3, 126.7, 126.0, 124.5, 121.1, 119.0, 106.3, 103.5, 46.1; LCMS (ES-API) m/z : 396, 397.9, 400 (M + H) $^+$; HRMS (ESI) m/z [M + H] $^+$: calcd for $\text{C}_{22}\text{H}_{16}\text{Cl}_2\text{NO}_2$: 396.0558, found: 396.0552.

6-(5-Bromo-2-hydroxybenzylamino)-2-phenyl-4H-chromen-4-one (9d) Yellow solid, yield 82.8%, m.p. 188–191 °C; IR (KBr): 3287, 3105, 1719, 1643, 1413, 808, 548 cm^{-1} ; ^1H NMR (DMSO- d_6 , 400 MHz) δ 9.99 (s, 1H), 8.10–7.90 (m, 2H), 7.57–7.54 (m, 4H), 7.31–7.10 (m, 3H), 6.99–6.93 (m, 2H), 6.92 s, 1H), 6.61 (d, $J=6.4$ Hz, 1H), 4.27–4.27 (m, 2H); ^{13}C NMR (DMSO- d_6 , 100 MHz) δ 178.4, 162.6, 154.6, 149.4, 146.0, 131.9, 131.2, 131.1, 130.7, 128.9, 127.3, 126.0, 124.5, 121.7, 118.9, 117.2, 111.0, 106.3, 104.0, 43.51; LCMS (ES-API) m/z : 423.7 (M + H) $^+$; HRMS (ESI) m/z [M + H] $^+$: calcd for $\text{C}_{22}\text{H}_{17}\text{BrNO}_3$: 422.0392, found: 422.0398.

6-(4-Fluorobenzylamino)-2-phenyl-4H-chromen-4-one (9e) Yellow solid, yield 86.7%, m.p. 132–135 °C; IR (KBr): 3288, 3066, 1613, 1537, 1431, 842 cm^{-1} ; ^1H NMR (DMSO- d_6 , 400 MHz) δ 7.91 (s, 2H), 7.63–7.26 (m, 8H), 7.08–7.02 (m, 3H), 6.78 (s, 1H), 4.38 (s, 2H); ^{13}C NMR (DMSO- d_6 , 100 MHz) δ 178.6, 162.9, 149.8, 145.4, 137.7, 132.2, 131.9, 131.4, 129.3, 129.1, 126.3, 124.9, 121.4, 121.2, 119.2, 106.8, 104.6, 47.9; LCMS (ES-API) m/z : 346.2 (M + H) $^+$; HRMS (ESI) m/z [M + H] $^+$: calcd for $\text{C}_{22}\text{H}_{17}\text{FNO}_2$: 345.1165, found: 345.1172.

6-(4-Chlorobenzylamino)-2-phenyl-4H-chromen-4-one (9f) Yellow solid, yield 85.8%, m.p. 164–166 °C; IR (KBr): 3285, 3061, 1791, 1611, 1047, 999, 578 cm^{-1} ; ^1H NMR (DMSO- d_6 , 400 MHz) δ 7.94–7.92 (m, 2H), 7.55–7.54 (m, 4H), 7.53–7.43 (m, 1H), 7.34–7.29 (m, 5H), 7.04 (t, $J=8$ Hz, 1H), 6.81 (s, 1H), 4.41 (s, 2H); ^{13}C NMR (DMSO- d_6 , 100 MHz) δ 178.5, 162.9, 149.7, 145.4, 137.1, 132.1, 131.3, 129.0, 128.9, 128.8, 126.2, 124.8, 121.1, 119.1, 106.9, 104.4, 100.0, 47.7; LCMS (ES-API) m/z : 362.8 (M + H) $^+$; HRMS (ESI) m/z [M + H] $^+$: calcd for $\text{C}_{22}\text{H}_{17}\text{ClNO}_2$: 362.0869, found: 362.0873.

6-(4-Bromobenzylamino)-2-phenyl-4H-chromen-4-one (9g) White solid, yield 88.2%, m.p. 174–176 °C; IR (KBr): 3287, 3037, 1745, 1611, 1135, 793 cm^{-1} ; ^1H NMR (DMSO- d_6 , 400 MHz) δ 8.05–8.03 (m, 2H), 7.61–7.51 (m, 6H), 7.38 (s, 1H), 7.34 (s, 1H), 7.18 (dd, $J=8.8$ & 2.8 Hz, 1H), 6.94 (d,

$J=2.8$ Hz, 1H), 6.89 (s, 1H), 6.80–6.77 (m, 1 H), 4.35–4.33 (m, 2H); ^{13}C NMR (DMSO- d_6 , 100 MHz) δ 178.6, 162.9, 149.8, 145.4, 137.7, 132.2, 131.9, 131.4, 129.3, 129.1, 126.3, 124.9, 121.4, 121.2, 119.2, 106.8, 104.6, 47.9; LCMS (ES-API) m/z : 408.0 (M + H) $^+$; HRMS (ESI) m/z [M + H] $^+$: calcd for $\text{C}_{22}\text{H}_{17}\text{BrNO}_2$: 406.0442, found: 406.0446.

6-(5-Bromo-2-methoxybenzylamino)-2-phenyl-4H-chromen-4-one (9h) Yellow solid, yield 82.7%, m.p. 173–176 °C; IR (KBr): 3366, 3067, 1684, 1450, 1029, 708, 549 cm^{-1} ; ^1H NMR (DMSO- d_6 , 400 MHz) δ 8.05–8.03 (m, 2H), 7.58–7.56 (m, 4H), 7.42–7.32 (m, 2H), 7.18 (dd, $J=5.6$ & 3.2 Hz, 1H), 7.01 (d, $J=8$ Hz, 1H), 6.92–6.89 (m, 2H), 6.67–6.65 (m, 1H), 4.30–4.29 (m, 2H), 3.89 (s, 3H); ^{13}C NMR (DMSO- d_6 , 100 MHz) δ 178.6, 162.8, 156.5, 149.6, 145.6, 132.1, 131.2, 131.2, 131.0, 129.0, 128.9, 128.8, 126.2, 124.8, 121.2, 119.0, 110.9, 106.6, 104.6, 55.6, 43.2; LCMS (ES-API) m/z : 437.9 (M + H) $^+$; HRMS (ESI) m/z [M + H] $^+$: calcd for $\text{C}_{23}\text{H}_{19}\text{BrNO}_3$: 436.0558, found: 436.0548.

6-(5-Bromo-2-ethoxybenzylamino)-2-phenyl-4H-chromen-4-one (9i) Yellow solid, yield 81.2%, m.p. 180–184 °C; IR (KBr): 3374, 3038, 1618, 1506, 910, 753 cm^{-1} ; ^1H NMR (DMSO- d_6 , 400 MHz) δ 7.90 (s, 2H), 7.51–7.27 (m, 8H), 7.07–7.03 (m, 1H), 6.77 (s, 2H), 4.39 (s, 2H), 4.07 (d, $J=5.4$ Hz, 2H), 1.45 (m, 3H); ^{13}C NMR (DMSO- d_6 , 100 MHz) δ 178.6, 162.8, 155.9, 149.7, 145.7, 132.2, 131.3, 131.0, 129.2, 128.4, 128.9, 126.2, 124.9, 122.2, 121.2, 119.0, 112.9, 106.7, 104.7, 63.9, 43.3, 14.8; LCMS (ES-API) m/z : 450.1 (M + H) $^+$; HRMS (ESI) m/z [M + H] $^+$: calcd for $\text{C}_{24}\text{H}_{21}\text{BrNO}_3$: 450.0705, found: 450.0707.

6-(4-Methoxybenzylamino)-2-phenyl-4H-chromen-4-one (9j) Yellow solid, yield 86.6%, m.p. 134–136 °C; IR (KBr): 3296, 3107, 1613, 1484, 1177, 769 cm^{-1} ; ^1H NMR (DMSO- d_6 , 400 MHz) δ 8.06–8.03 (m, 2H), 7.60–7.52 (m, 4H), 7.30 (d, $J=8$ Hz, 2H), 7.18 (dd, $J=8.8$ & 2.8 Hz, 1H), 6.96 (d, $J=2.8$ Hz, 1H), 6.92–6.89 (m, 3H), 6.66–6.64 (m, 1 H), 4.28–4.26 (m, 2H), 3.66 (s, 3H); ^{13}C NMR (DMSO- d_6 , 100 MHz) δ 178.1, 162.2, 150.1, 146.1, 132.1, 131.8, 131.1, 130.7, 128.8, 128.6, 125.9, 124.4, 121.4, 118.7, 113.7, 106.1, 102.8, 55.1, 47.2; LCMS (ES-API) m/z : 358.0 (M + H) $^+$; HRMS (ESI) m/z [M + H] $^+$: calcd for $\text{C}_{23}\text{H}_{20}\text{NO}_3$: 358.1443, found: 358.1441.

6-(4-Ethoxybenzylamino)-2-phenyl-4H-chromen-4-one (9k) Yellow solid, yield 84.2%, m.p. 159–162 °C; IR (KBr): 3306, 3107, 1683, 1452, 1292, 767, 686 cm^{-1} ; ^1H NMR (DMSO- d_6 , 400 MHz) δ 8.08–8.01 (m, 2H), 7.60–7.51 (m, 4H), 7.28 (d, $J=8.4$ Hz, 2H), 7.17 (dd, $J=6.4$ & 2.4 Hz, 1H), 6.96 (d, $J=6.8$ Hz, 1H), 6.91–6.88 (m, 3H), 6.64 (d, $J=3.6$ Hz, 1H), 4.27–4.25 (d, $J=8$ Hz, 2H), 3.98 (q, $J=14$ & 6.8 Hz, 2H), 1.30 (t, $J=6.8$ Hz, 3H); ^{13}C NMR

(DMSO- d_6 , 100 MHz) δ 178.6, 162.7, 158.4, 149.5, 145.7, 132.2, 131.2, 130.4, 128.9, 128.1, 126.2, 124.8, 121.2, 118.9, 114.7, 106.6, 104.1, 63.4, 48.0, 14.8; LCMS (ES-API) m/z : 372.9 (M+H)⁺; HRMS (ESI) m/z [M+H]⁺: calcd for C₂₄H₂₁NO₃: 372.1599, found: 372.1599.

6-(2, 4-Dimethoxybenzylamino)-2-phenyl-4H-chromen-4-one (9l) Yellow solid, yield 82.8%, M.p. 126–129 °C; IR (KBr): 3359, 3038, 1613, 1523, 1274, 1120, 719 cm⁻¹; ¹H NMR (DMSO- d_6 , 400 MHz) δ 8.09–8.01 (m, 2H), 7.57–7.53 (m, 4H), 7.18–7.13 (m, 2H), 6.93 (d, J =2.8 Hz, 1H), 6.88 (s, 1H), 6.59 (d, J =2.4 Hz, 1H), 6.47–6.45 (m, 2H), 4.21–4.20 (m, 2H), 3.84 (s, 3H), 3.73 (s, 3H); ¹³C NMR (DMSO- d_6 , 100 MHz) δ 178.3, 162.4, 160.1, 158.3, 149.4, 146.2, 131.9, 131.1, 129.5, 126.9, 126.0, 124.5, 121.5, 118.9, 118.7, 106.2, 103.9, 103.5, 98.3, 55.3, 55.2, 42.8; LCMS (ES-API) m/z : 388.2 (M+H)⁺; HRMS (ESI) m/z [M+H]⁺: calcd for C₂₄H₂₂NO₄: 388.1549, found: 388.1544.

6-(3,4-dimethoxybenzylamino)-2-phenyl-4H-chromen-4-one (9m) Yellow solid, yield 86.2%, m.p. 138–141 °C; IR (KBr): 3288, 3106, 1613, 1484, 1152, 936, 541 cm⁻¹; ¹H NMR (DMSO- d_6 , 400 MHz) δ 8.08–8.01 (m, 2H), 7.57–7.53 (m, 4H), 7.18 (dd, J =8.8 & 2.8 Hz, 1H), 7.01–6.99 (d, J =2.8 Hz, 2H), 6.92–6.89 (m, 3H), 6.68–6.61 (m, 1 H), 4.27–4.25 (m, 2H), 3.74 (s, 3H), 3.71 (s, 3H); ¹³C NMR (DMSO- d_6 , 100 MHz) δ 178.6, 162.6, 160.4, 158.5, 149.4, 146.0, 132.2, 131.2, 129.9, 128.9, 126.1, 124.7, 121.4, 119.0, 118.8, 106.6, 104.5, 103.9, 98.7, 65.8, 55.4, 43.5; LCMS (ES-API) m/z : 388.2 (M+H)⁺; HRMS (ESI) m/z [M+H]⁺: calcd for C₂₄H₂₂NO₄: 388.1548, found: 388.1551.

6-((Quinolin-2-yl)methylamino)-2-phenyl-4H-chromen-4-one (9n) Brown solid, yield 80.3%, m.p. 146–149 °C; IR (KBr): 3347, 3037, 1696, 1198, 773 cm⁻¹; ¹H NMR (DMSO- d_6 , 400 MHz) δ 8.42 (d, J =8.6 Hz, 1H), 8.10–7.89 (m, 4H), 7.82–7.69 (m, 1H), 7.70–7.50 (m, 7H), 7.26–7.21 (m, 1H), 7.03–7.01 (m, 1H), 6.84 (s, 1H), 4.68–4.70 (m, 2H); ¹³C NMR (DMSO- d_6 , 100 MHz) δ 178.4, 162.0, 159.6, 153.3, 149.8, 145.3, 138.3, 132.2, 132.08, 130.6, 129.1, 126.3, 126.2, 124.9, 122.2, 119.3, 124.9, 122.2, 119.3, 118.7, 106.7, 103.7, 48.8; LCMS (ES-API) m/z : 379.0 (M+H)⁺; HRMS (ESI) m/z [M+H]⁺: calcd for C₂₅H₁₉N₂O₂: 379.1450, found: 379.1446.

Docking study

Molecular docking study was performed in Maestro 9.1 using Glide v. 6.8 (Schrodinger LLC). All compounds were built using Maestro build panel and optimized to lower energy conformers using Lig prep v3.5 (Schrodinger, Inc., New York, NY, USA). The X-ray crystallographic structure

of the human topoisomerase II beta (PDB ID: 3QX3), in which drugs simultaneously interact with both DNA and enzymes [25] was taken from RCSB Protein Data Bank. The protein was prepared by using protein preparation wizard for docking using ‘protein preparation wizard’ in Maestro v10.3. It contains two chains, a chain along with DNA and Mg²⁺ ion. The ligand within active site and all water molecules were removed, while magnesium ion was allowed to remain with the charge of + 2. The active site was defined to include all atoms within 6.5 Å radius of native ligand. The bond orders and formal charges were added to hetero-groups and hydrogen’s were added to all atoms in the structure. Side chains that are not close to the binding cavity and do not participate in salt bridges were neutralized and termini were capped by adding ACE and NMA residue. After preparation, structure was refined to optimize hydrogen bond network using OPLS_2005 force field. The minimization was terminated when the energy converged or the RMSD reached a maximum cut off of 0.30 Å. The extra precision (XP) docking mode for all compounds was performed on generated grid of protein structure [26]. Final evaluation of ligand–protein binding was done with Glide score [27–29].

Docked pose of ligands was further rescored using Prime MM-GBSA approach which is used to estimate free binding energy of enzyme–ligands complex. Energies of ligand–receptor complexes were calculated using Prime MM-GBSA with flexibility set for residue surrounding 5 Å region of ligand binding site. Binding energy of receptor and ligand is as calculated by Prime Energy, a Molecular Mechanics + Implicit Solvent Energy Function (kcal/mol).

The binding free energy ΔG_{bind} is estimated as

$$\Delta G_{\text{bind}} = G(C) - G(P) - G(L)$$

where ΔG_{bind} is total binding free energy, $G(C)$ is binding energy of protein ligand complex, $G(L)$ is binding energy of ligand and $G(P)$ is binding energy of protein.

Biological assay

In vitro anticancer screening

All newly synthesized compounds (9a–n) were evaluated for their in vitro anticancer activity against human breast cancer cell line (MCF-7) and human lung cancer cell line (A-549) by MTT assay. Two cell lines MCF-7 and A-549 (NCCS, Pune, India) were grown in DMEM medium containing 10% fetal bovine serum [Life technologies (Gibco)] and 0.7% antibiotics. Cells were seeded into 96 well microtiter plates in 100 μ L of media at plating density of 5000 cells/well. Seeded cells were incubated at 37 °C, 5% CO₂, 95% air and 100% humidity for 24 h. At 24 h, old media was changed with fresh media followed by treatment with each compound

at 10 μM , 1 μM , and 0.1 μM . After 24 h treatment, cell viability was assessed by 3-(4,5-dimethylthiazol)-2,5-diphenyltetrazolium bromide (MTT), cells were incubated with 20 μL of MTT (5 mg/mL) in PBS for 4 h at 37 $^{\circ}\text{C}$. The medium was removed and formazan crystals dissolved in DMSO. MTT reduction was quantified by measurement of absorbance at 570 nm using a multimode reader, Synergy Mx of BioTek [30]. Statistical employed methods were Sigma Plot 10.0 and Microsoft Excel 2010.

Measurement of topoisomerase II inhibitory activity

The most active anticancer agents from the synthesized series were further evaluated for prediction of their mode of action using Topo II drug screening kit (TopoGEN, Inc., Columbus) according to procedure reported by Patra et al. [18]. Doxorubicin was used as standard in this evaluation.

The reaction was started with incubation of a mixture consisted of human Topo II (2 μL), substrate super coiled pHot1 DNA (0.25 μg), 50 $\mu\text{g}/\text{mL}$ test compound (2 μL), and assay buffer (4 μL) in 37 $^{\circ}\text{C}$ for 30 min. In order to terminate reaction, 10% sodium dodecylsulphate (2 μL) and proteinase K (50 $\mu\text{g}/\text{mL}$) were added at 37 $^{\circ}\text{C}$ for 15 min. followed by incubation for 15 min at 37 $^{\circ}\text{C}$. Then, DNA was run on 1% agarose gel in Bio Rad gel electrophoresis system for 1–2 h followed by staining with GelRedTM stain for 2 h and destained for 15 min with TAE buffer. The gel was imaged via Bio Rad's Gel Doc TMEZ system. Both super coiled and linear strands DNA were incorporated in the gel as markers for DNA-Topo II intercalators. The results were reported as IC_{50} (50% inhibition concentration) values [31].

Conclusions

In conclusion, we have efficiently developed reductive amination protocol as an alternative route for the synthesis of novel *N*-benzyl derivatives of 6-aminoflavone which leads to increase in yield of the desired substituted aminoflavones. In vitro anti-proliferative activity against two human cancer cell lines (MCF-7 and A-549) and topoisomerase II inhibitory activity was performed. Among the synthesized derivatives, aminoflavones **9f** and **9g** were found to be most active anti-proliferative compounds against human breast cancer cell line (MCF-7) and aminoflavones **9c**, **9n**, **9b**, and **9j** demonstrated good anti-proliferative activity against human lung cancer cell line (A-549). However, compound **9n** has shown promising anti-proliferative activity against both cell lines. We found that compounds **9f** and **9g** exhibited robust inhibition of enzyme topoisomerase II with IC_{50} values 12.11 and 12.79 μM , respectively. The in silico docking studies of synthesized compounds showed that all compounds have good binding affinity toward topoisomerase II enzyme and have

placed in between DNA base pair at active site of enzyme. Consequently, these *N*-benzyl derivatives of 6-aminoflavone may serve as lead scaffold for development of novel anti-proliferative agents. Our efforts in this regard are underway.

Acknowledgements We thank Dr. D. K. Mhaske, Dr. L. R. Patil (Maharaja Jivajirao Shinde College, Shrigonda) and Dr. R. J. Barnabas (Ahmednagar College, Ahmednagar) for their constant support. NMT acknowledges the financial support by BCUD, SPPU, Pune (Grant No: 13SCI 000031).

Compliance with ethical standards

Conflict of interest There are no conflicts to declare.

References

1. Verma AK, Pratap R (2010) The biological potential of flavones. *Nat Prod Rep* 27:1571–1593. <https://doi.org/10.1039/C004698C>
2. Moon MJ, Lee SK, Lee JW et al (2006) Synthesis and structure–activity relationships of novel indirubin derivatives as potent anti-proliferative agents with CDK2 inhibitory activities. *Bioorg Med Chem* 14:237–246. <https://doi.org/10.1016/j.bmc.2005.08.008>
3. Zhai S, Senderowicz AM, Sausville EA, Figg WD (2002) Flavopiridol, a novel cyclin-dependent kinase inhibitor, in clinical development. *Ann Pharmacother* 36:905–911. <https://doi.org/10.1345/aph.1A162>
4. Panaro NJ, Popescu NC, Harris SR, Thorgeirsson UP (1999) Flavone acetic acid induces a G2/M cell cycle arrest in mammary carcinoma cells. *Br J Cancer* 80:1905–1911. <https://doi.org/10.1038/sj.bjc.6690619>
5. Alexandrakis M, Singh L, Boucher W, Letourneau R, Theoflopoulos P, Theoharides TC (1999) Differential effect of flavonoids on inhibition of secretion and accumulation of secretory granules in rat basophilic leukemia cells. *Int J Immunopharmacol* 21:379–390. [https://doi.org/10.1016/S0192-0561\(99\)00018-1](https://doi.org/10.1016/S0192-0561(99)00018-1)
6. Bernard FX, Sable S, Cameron B, Provost J, Desnottes JF, Crouzet J, Blanche F (1997) Glycosylated flavones as selective inhibitors of topoisomerase IV. *Antimicrob Agents Chemother* 41:992–998. <https://doi.org/10.1128/AAC.41.5.992>
7. Mittra B, Saha A, Roy Chowdhury A et al (2000) Luteolin, an abundant dietary component is a potent anti-leishmanial agent that acts by inducing topoisomerase II-mediated Kinetoplast DNA cleavage leading to apoptosis. *Mol Med* 6:527–541. <https://doi.org/10.1007/BF03401792>
8. Bhosle MR, Wahul DB, Bondle GM, Sarkate A, Tiwari SV (2018) An efficient multicomponent synthesis and in vitro anticancer activity of dihydropyranochromene and chromenopyrimidine-2,5-diones. *Syn Commun* 48:2046–2060. <https://doi.org/10.1080/00397911.2018.1480042>
9. Gobbi S, Cavalli A, Ram A et al (2006) Lead optimization providing a series of flavone derivatives as potent nonsteroidal inhibitors of the cytochrome P450 aromatase enzyme. *J Med Chem* 49:4777–4780. <https://doi.org/10.1021/jm060186y>
10. Alworth WL, Dang CC, Ching LM, Viswanathan T (1980) Stimulation of mammalian epoxide hydrase activity by flavones. *Xenobiotica* 10:395–400. <https://doi.org/10.3109/00498258009033774>
11. Beutler JA, Cardellina Ii JH, Lin CM, Hamel E, Craggand GM, Boyd MR (1993) Centaureidin, a cytotoxic flavone from *Polymnia fruticosa*, inhibits tubulin polymerization. *Bioorg Med Chem Lett* 3:581–584. [https://doi.org/10.1016/S0960-894X\(01\)81233-6](https://doi.org/10.1016/S0960-894X(01)81233-6)

12. Lichius JJ, Thoison O, Montagnac A et al (1994) Antimitotic and cytotoxic flavonols from *Zieridium pseudobtusifolium* and *Acronychia porter*. *J Nat Prod* 57:1012–1016. <https://doi.org/10.1021/np50109a024>
13. Lin CM, Singh SB, Chu PS et al (1988) Interactions of tubulin with potent natural and synthetic analogs of the antimitotic agent combretastatin: a structure–activity study. *Mol Pharmacol* 34:200–208
14. Singh M, Kaur M, Silakari O (2014) Flavones: an important scaffold for medicinal chemistry. *Eur J Med Chem* 84:206–239. <https://doi.org/10.1016/j.ejmech.2014.07.013>
15. Konya K, Pajtas D, Kiss-Szikszai A, Patonay T (2015) Buchwald–Hartwig reactions of monohalo-flavones. *Eur J Org Chem* 4:828–839. <https://doi.org/10.1002/ejoc.201403108>
16. Pajtas D, Patonay T, Konya K (2016) Synthesis of 8-bromoflavone and its Buchwald–Hartwig reaction with amines. *Synthesis* 48:97–102. <https://doi.org/10.1055/s-0035-1560325>
17. Wiegand R, Wu J, Sha X, LoRusso P, Heath E, Li J (2009) Validation and implementation of a liquid chromatography/tandem mass spectrometry assay to quantitate aminoflavone (NSC 686288) in human plasma. *J Chromatogr B Analyt Technol Biomed Life Sci* 877:1460–1464. <https://doi.org/10.1016/j.jchromb.2009.03.015>
18. Patra N, De U, Kang JA et al (2011) A novel epoxypropoxy flavonoid derivative and topoisomerase II inhibitor, MHY336, induces apoptosis in prostate cancer cells. *Eur J Pharmacol* 658:98–107. <https://doi.org/10.1016/j.ejphar.2011.02.015>
19. Lazaro ML, Willmore E, Austin CA (2010) The dietary flavonoids myricetin and fisetin act as dual inhibitors of DNA topoisomerases I and II in cells. *Mutat Res* 696:41–47. <https://doi.org/10.1016/j.mrgentox.2009.12.010>
20. Cassady JM, Baird WM, Chang CJ (1990) Natural products as a source of potential cancer chemotherapeutic and chemopreventive agents. *J Nat Prod* 53:23–41. <https://doi.org/10.1021/np50067a003>
21. Kim MY, Na Y, Vankayalapati H, Guzman MG, Hurley LH (2003) Design, synthesis, and evaluation of psorospermin/quinobenzoxazine hybrids as structurally novel antitumor agents. *J Med Chem* 46:2958–2972. <https://doi.org/10.1021/jm030096i>
22. Singh S, Baviskar AT, Jain V et al (2013) 3-Formylchromone based topoisomerase II α inhibitors: discovery of potent leads. *Med Chem Commun* 4:1257–1266. <https://doi.org/10.1039/C3MD00125C>
23. Simon L, Srinivasan KK, Mallikarjuna Rao C et al (2015) Synthesis and evaluation of anti-cancer activity of some 6-aminoflavones. *Int J Pharm Chem* 5:240–246. <https://doi.org/10.7439/ijpc.v5i7.2220>
24. Thorat NM, Kote SR, Thopate SR (2014) An efficient and green synthesis of flavones using natural organic acids as promoter under solvent-free condition. *Lett Org Chem* 11:601–605. <https://doi.org/10.2174/157017861108140613163214>
25. Wendorff TJ, Schmidt BH, Heslop P, Austin CA, Berger JM (2012) The structure of DNA-bound human topoisomerase II α : conformational mechanisms for coordinating inter-subunit interactions with DNA cleavage. *J Mol Biol* 424:109–124. <https://doi.org/10.1016/j.jmb.2012.07.014>
26. Friesner RA, Murphy RB, Repasky MP et al (2006) Extra precision glide: docking and scoring incorporating a model of hydrophobic enclosure for protein–ligand complexes. *J Med Chem* 49:6177–6196. <https://doi.org/10.1021/jm051256o>
27. Tiwari SV, Seijas JA, Vazquez-Tato MP, Sarkate AP, Lokwani DK, Nikalje AG (2016) Ultrasound mediated one-pot, three component synthesis, docking and ADME prediction of novel 5-amino-2-(4-chlorophenyl)-7-substituted phenyl-8,8a-dihydro-7h-(1,3,4)thiadiazolo(3,2- α)pyrimidine-6-carbonitrile derivatives as anti-cancer agents. *Molecules* 21:894. <https://doi.org/10.3390/molecules21080894>
28. Tiwari SV, Seijas JA, Vazquez-Tato MP, Sarkate AP, Karnik KS, Nikalje AG (2017) Facile synthesis of novel coumarin derivatives, antimicrobial analysis, enzyme assay, docking study, ADMET prediction and toxicity study. *Molecules* 22:1172. <https://doi.org/10.3390/molecules22071172>
29. Doherty W, Adler N, Knox A, Nolan D, McGouran J, Nikalje AP, Lokwani D, Sarkate A, Evans P (2017) Synthesis and evaluation of 1,2,3-triazole-containing vinyl and allyl sulfones as anti-trypanosomal agents. *Eur J Org Chem* 1:175–185. <https://doi.org/10.1002/ejoc.201601221>
30. Dofe VS, Sarkate AP, Azad R, Gill CH (2017) Novel quinoline-based oxadiazole derivatives induce G2/M arrest and apoptosis in human breast cancer MCF-7 cell line. *Res Chem Int* 43:7331–7345. <https://doi.org/10.1007/s11164-017-3078-1>
31. Ibrahim MK, Taghour MS, Metwaly AM et al (2018) Design, synthesis, molecular modeling and anti-proliferative evaluation of novel quinoxaline derivatives as potential DNA intercalators and topoisomerase II inhibitors. *Eur J Med Chem* 155:117–134. <https://doi.org/10.1016/j.ejmech.2018.06.004>

Publisher's Note Springer Nature remains neutral with regard to jurisdictional claims in published maps and institutional affiliations.



REGULAR ARTICLE

Pyruvic acid-catalyzed one-pot three-component green synthesis of isoxazoles in aqueous medium: a comparable study of conventional heating versus ultra-sonication

SANTOSH R DESHMUKH^{a,*} , ARCHANA S NALKAR and SHANKAR R THOPATE^b

^aProf. John Barnabas Post Graduate School for Biological Studies, Department of Chemistry, Ahmednagar College, Ahmednagar, Maharashtra 414001, India

^bDepartment of Chemistry, Shri Sadguru Gangageer Maharaj Science, Gautam Arts and Sanjivani Commerce College, Kopargaon, Maharashtra 423601, India

E-mail: sant.deshmukh@gmail.com

MS received 7 September 2021; revised 13 October 2021; accepted 23 October 2021

Abstract. A mild and efficient route for the one-pot synthesis of isoxazole derivatives has been developed using pyruvic acid as a catalyst under an aqueous medium. The reaction was carried out under conventional as well as ultrasonic conditions to afford the desired product in good yield. The features of this protocol are the use of environmental-friendly, commercially available, biodegradable catalyst, use of biologically safe solvent, simple experimental procedure and short reaction times. The given protocol can be a better alternative for the synthesis of 4*H*-isoxazol-5-one derivatives as compared to traditional methods.

Keywords. 4*H*-isoxazol-5-one; pyruvic acid; aldehyde; ultrasound irradiation; green chemistry; multicomponent reaction (MCR).

1. Introduction

A realization of the fundamental importance of nitrogen-containing heterocycles in pharmaceutical and medicinal chemistry captivated researchers across the world. These heterocycles are the core building block of several pharmaceutically active natural products. Furthermore, 59% of the approved small molecule drugs by the US FDA contain nitrogen heterocycles, which ranks them as the most privileged and momentous heterocycles by a medicinal chemist.¹ Among these, isoxazole and its derivatives are an important class of oxygen- and nitrogen-containing heterocycles with several applications in organic chemistry, medicinal chemistry and the pharmaceutical industry.^{2,3} Isoxazole derivatives are well-known for their widespread biological and pharmacological activities such as antifungal,⁴ analgesic,⁵ antitumor,⁶ antioxidant,⁷ antimicrobial,⁸ COX-2 inhibitor,⁹ anti-inflammatory,¹⁰ antiviral,¹¹ antimycobacterial,¹² anti-HIV,¹³ androgen antagonists,¹⁴ antibiotic,¹⁵

antihypertensive,¹⁶ antimalarial,¹⁷ antirheumatic,¹⁸ antianginal,¹⁹ anticonvulsant,²⁰ anti-obesity,²¹ anti-osteoporotic,²² nematicidal agents,²³ antiprotozoal,²⁴ hypoglycemic,²⁵ antituberculosis²⁶ and bronchodilating agent.²⁷ Furthermore, isoxazole derivatives have also been used for the design and manufacture of merocyanine dyes with applications in optical recording and nonlinear optical research,²⁸ liquid crystalline materials,²⁹ light-conversion molecular devices³⁰ and as a filter dye in photographic films.³¹ The isoxazole moiety is also a structural backbone of a variety of natural products like cycloserine,³² pantherine,³³ ibotenic acid and isoxazol-4-carboxylic acid.³² Some of the interesting compounds with isoxazole moiety are shown in Figure 1. Because of their diverse applications in multi-disciplinary fields, the development of new synthetic strategies for the synthesis of isoxazole derivatives has received great attention in organic synthesis.

In the literature, there are many methods to prepare this class of compounds. The most common method

*For correspondence

Supplementary Information: The online version contains supplementary material available at <https://doi.org/10.1007/s12039-021-02016-y>.

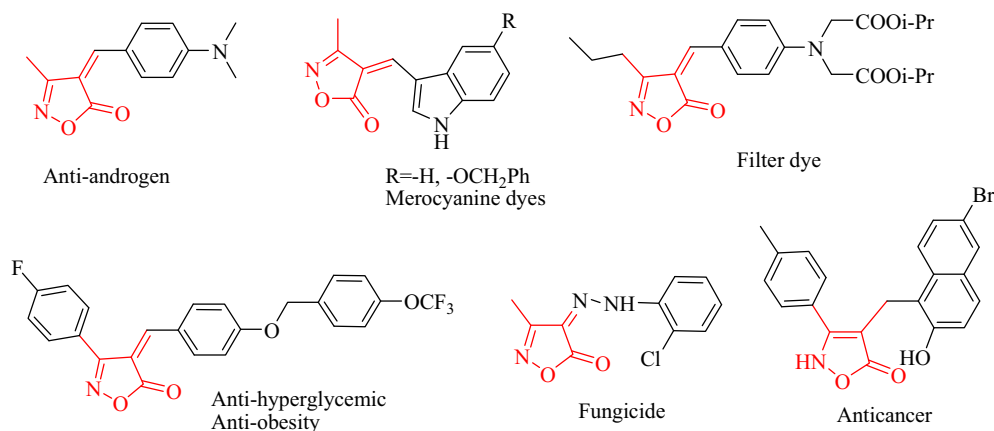


Figure 1. Isoxazole scaffold-containing interesting compounds.

for the synthesis of isoxazoles involves one-pot multicomponent reactions (MCRs) of aromatic aldehydes, ethyl acetoacetate and hydroxylamine hydrochloride using various catalysts.^{34–55} MCRs have been discovered to be a powerful synthetic tool for the synthesis of several natural products and biologically active compounds. MCRs have received significant advantages over conventional synthetic methodologies. This ensures good yields, high atom economy and low costs, reduction in reaction times, minimization of waste, energy, labour, operational simplicity and avoidance of tedious purification processes.^{56–58} A combination of MCR, green solvent like water and the use of non-conventional energy sources like ultrasound irradiation are important features of an ideal green synthesis.^{59–63}

The use of ultrasound irradiation to speed up the organic reactions has long been known in both academia and industry. The chemical and physical effects of ultrasound come from acoustic cavitations such as the formation, growth and implosive collapse of bubbles in a liquid. The cavitation collapse creates drastic conditions inside the medium for an extremely short time and temperatures of 2000–5000 K, as well as pressure up to 1800 atm inside the collapsing cavity, have been produced under ultrasonic conditions. The cavitation effect produces effective physical, chemical and biological transformations. Thus ultrasound irradiation has been employed in synthetic organic chemistry, medicinal chemistry and material sciences.^{64–68}

A number of catalysts have been used in one-pot MCRs for the synthesis of isoxazole scaffold including sodium acetate,³⁴ potassium hydrogen phthalate,³⁵ tetrabutylammonium perchlorate,³⁶ *N*-bromosuccinimide,³⁷ sodium benzoate,³⁸ boric acid,³⁹ pyridinium

p-toluenesulfonate,⁴⁰ 1,4-diazabicyclo[2.2.2]octane,⁴¹ 4-aminobenzene-1-sulfonic acid,⁴² cerium chloride heptahydrate,⁴³ antimony trichloride,⁴⁴ iodine,⁴⁵ 2-hydroxy-5-sulfobenzoic acid,⁴⁶ potassium phthalimide,⁴⁷ pyridine,⁴⁸ NaH₂PO₄,⁴⁹ Ag/SiO₂,⁵⁰ phosphotungstic acid,⁵¹ nano-MgO,⁵² itaconic acid,⁵³ sodium sulphide,⁵⁴ citric acid,⁵⁵ hydroxyapatite nanoparticles⁶⁹ and deep eutectic solvents.⁷⁰ The gold-catalyzed cyclization of *O*-propioloyl oxime *via* intermolecular arylidene group transfer,⁷¹ reaction of 1,3-dicarbonyl compounds with benzaldoximes derivatives,⁷² two-step condensation of 3-Phenylisoxazol-5-one with aryl halide in the presence of KF/alumina,⁷³ cycloadditions of ethyl benzoyl nitromethane or 2-nitroacetate with alkenes or terminal alkynes⁷⁴ were reported.

Although many of these protocols suffer from drawbacks and limitations such as strongly acidic or basic conditions, low yields, long reaction times, the use of toxic reagents, harsh reaction conditions, the use of expensive catalysts and tedious workup procedures that restricts their scope in practical applications. Moreover, compared to the commonly used organic solvents, water is the ideal green solvent for organic reactions, because of its cost-efficiency, abundance, easy handling, high stability, non-flammability, environmental compatibility and nontoxicity.⁷⁵

Considering the above points, there is still a need for novel and greener methodologies to fulfil the increasing demands of modern synthetic chemistry, which avoid harsh reaction conditions and allow an efficient route for the synthesis of isoxazole derivatives. Recently, we have reported pyruvic acid as a highly efficient catalyst for the synthesis of bis(indolyl)methanes.⁷⁶ This finding provoked us to evaluate the catalytic potential of pyruvic acid in the synthesis

of isoxazol-5(4*H*)-one derivative. Our literature survey revealed that there is no report on the use of pyruvic acid as a catalyst in the synthesis of isoxazol-5(4*H*)-one derivative; hence to explore its catalytic utility, herein we report the synthesis of isoxazol-5(4*H*)-one derivative *via* the one-pot, a three-component process catalyzed by pyruvic acid under conventional and ultrasound irradiation.

Apart from this Pyruvic acid is the most vital α -oxocarboxylic acid and plays a fundamental role in energy metabolism in living organisms. It effectively reduces cholesterol,⁷⁷ improves exercise endurance capacity,⁷⁸ serves as a potent antioxidant,⁷⁹ reduces anoxic injury and free radical formation.⁸⁰

2. Experimental

2.1 Materials

All the chemicals were purchased from commercial sources and used without further purification. Probe sonicator (Model ATP- 250 Athena Technology) was used for ultrasound irradiation. Thin-layer chromatography (TLC) was performed on silica gel 60F₂₅₄ (0.25 mm thickness) plates, which were visualized under short (254 nm) and long (365 nm) UV light. Column chromatography was performed using silica gel 100–200 mesh size. Melting points (Mp) were determined in open capillary tubes using paraffin oil bath and are uncorrected. ¹H and ¹³C NMR spectra were recorded on 500 and 125 MHz NMR spectrometer, respectively using CDCl₃ and DMSO-d₆ as solvent. Chemical shifts δ are reported in ppm relative to Me₄Si internal standard. The multiplicity of signals is designated by the following abbreviations: s (singlet), d (doublet), t (triplet), q (quartet), m (multiplet). FT-IR was recorded on the IR-Affinity1 Shimadzu DRS-8000A instrument. High-resolution mass spectra (HRMS) were obtained using micromass-Q-TOF machine operating in electrospray ionization (ESI) mode.

2.2 General procedure for the synthesis of 4a-i under ultrasound irradiation condition

A mixture of benzaldehyde (0.50 g, 4.71 mmol), hydroxylamine hydrochloride (0.33 g, 4.71 mmol), ethyl acetoacetate (0.61 g, 4.71 mmol) and pyruvic acid catalyst (0.02 g, 0.023 mmol) in water (10 mL) were sonicated at 50 °C for the indicated time. After the completion of the reaction (TLC check), the

reaction mixture was cooled to room temperature and extracted using ethyl acetate (2 X 5 mL). The organic layer was dried over anhydrous Na₂SO₄ and concentrated under reduced pressure to give the crude product, which was purified by column chromatography using ethyl acetate: *n*-hexane (20-40%) as the eluent to yield the pure product

2.2a (*Z*)-4-benzylidene-3-methylisoxazol-5(4*H*)-one (4a): Yellow solid; M.p.: 140-142 °C; IR (KBr): 3475, 3053, 2322, 1732, 1620, 1454, 1352, 1220, 1124, 879, 763, 689, 574 cm⁻¹; ¹H NMR (500 MHz, DMSO) δ 8.42 (d, *J* = 7.6 Hz, 2H), 7.97 (s, 1H), 7.68-7.65 (m, 1H), 7.59 (t, *J* = 7.6 Hz, 2H), 2.30 (s, 3H) ppm; ¹³C NMR (126 MHz, DMSO) δ 168.31, 162.71, 152.14, 134.39, 134.05, 132.92, 129.73, 129.36, 129.04, 119.33, 11.78 ppm; HRMS (ESI) *m/z*: calcd for C₁₁H₁₀NO₂ [M+H]⁺ 188.0706 found 188.0705.

2.2b (*Z*)-4-(4-hydroxybenzylidene)-3-methylisoxazol-5(4*H*)-one (4b): Yellow solid; M.p.: 212-214 °C; IR (KBr): 3261, 3037, 1728, 1552, 1301, 1232, 1132, 999, 894, 775, 561 cm⁻¹; ¹H NMR (500 MHz, DMSO) δ 11.06 (s, 1H), 8.46 (d, *J* = 8.8 Hz, 2H), 7.81 (s, 1H), 6.96 (d, *J* = 8.8 Hz, 2H), 2.26 (s, 3H) ppm; ¹³C NMR (125 MHz, DMSO) δ 169.32, 164.34, 162.78, 152.05, 138.03, 125.05, 116.64, 114.32, 11.78 ppm; HRMS (ESI) *m/z*: calcd for C₁₁H₁₀NO₃ [M+H]⁺ 204.0655 found 204.0645.

2.2c (*Z*)-3-methyl-4-(4-methylbenzylidene) isoxazol-5(4*H*)-one (4c): Light yellow solid; M.p.: 134-136 °C; IR (KBr): 3458, 3095, 2594, 1732, 1600, 1508, 1408, 1354, 1111, 879, 775, 588 cm⁻¹; ¹H NMR (500 MHz, CDCl₃) δ 8.29 (d, *J* = 8.2 Hz, 2H), 7.39 (s, 1H), 7.33 (d, *J* = 8.1 Hz, 2H), 2.45 (s, 3H), 2.30 (s, 3H) ppm; ¹³C NMR (125 MHz, CDCl₃) δ 168.22, 161.20, 149.93, 145.76, 134.16, 131.04, 129.93, 118.50, 22.11, 11.71 ppm; HRMS (ESI) *m/z*: calcd for C₁₂H₁₂NO₂ [M+H]⁺ 202.0862 found 202.0861.

2.2d (*Z*)-4-(2-hydroxybenzylidene)-3-methylisoxazol-5(4*H*)-one (4d): Yellow solid; M.p.: 198-200 °C; IR (KBr): 3192, 1955, 1753, 1602, 1458, 1267, 1095, 902, 773, 580 cm⁻¹; ¹H NMR (500 MHz, DMSO) δ 11.01 (s, 1H), 8.74 (dd, *J* = 8.0, 1.2 Hz, 1H), 8.09 (s, 1H), 7.51-7.48 (m, 1H), 7.02 (d, *J* = 8.0 Hz, 1H), 6.94 (m, 1H), 2.26 (s, 3H) ppm; ¹³C NMR (125 MHz, DMSO) δ 168.75, 162.63, 160.12, 145.49, 137.23, 132.78, 119.94, 119.57, 116.90, 116.61, 11.68 ppm; HRMS (ESI) *m/z*: calcd for C₁₁H₁₀NO₃ [M+H]⁺ 204.0655 found 204.0653.

2.2e (Z)-4-(3,4-dimethoxybenzylidene)-3-methylisoxazol-5(4H)-one (**4e**): Yellow solid; M.p.: 134–136 °C; IR (KBr): 3446, 3097, 2846, 1732, 1508, 1244, 1111, 995, 881, 777, 565 cm⁻¹; ¹H NMR (500 MHz, CDCl₃) δ 8.76 (d, *J* = 2.1 Hz, 1H), 7.60 (dd, *J* = 8.5, 2.1 Hz, 1H), 7.33 (s, 1H), 6.96 (d, *J* = 8.5 Hz, 1H), 4.01 (s, 3H), 3.99 (s, 3H), 2.29 (s, 3H) ppm; ¹³C NMR (125 MHz, CDCl₃) δ 169.02, 161.35, 154.58, 149.81, 149.09, 131.23, 126.38, 116.28, 115.06, 110.71, 56.23, 56.19, 11.68 ppm; HRMS (ESI) *m/z*: calcd for C₁₃H₁₄NO₄ [M+H]⁺ 248.0917 found 248.0916.

2.2f (Z)-4-(4-methoxybenzylidene)-3-methylisoxazol-5(4H)-one (**4f**): Yellow solid; M.p.: 174–176 °C; IR (KBr): 3448, 3034, 2833, 2357, 1732, 1514, 1435, 1269, 1176, 875, 775, 563 cm⁻¹; ¹H NMR (500 MHz, CDCl₃) δ 8.45 (d, *J* = 8.9 Hz, 2H), 7.35 (s, 1H), 7.02 (d, *J* = 9.0 Hz, 2H), 3.92 (s, 3H), 2.28 (s, 3H) ppm; ¹³C NMR (125 MHz, CDCl₃) δ 168.80, 164.62, 161.29, 149.35, 136.99, 125.84, 116.40, 114.69, 55.74, 11.71 ppm; HRMS (ESI) *m/z*: calcd for C₁₂H₁₂NO₃ [M+H]⁺ 218.0811 found 218.0810.

2.2g (Z)-4-(4-hydroxy-3-methoxybenzylidene)-3-methylisoxazol-5(4H)-one (**4g**): Yellow solid; M.p.: 214–216 °C; IR (KBr): 3273, 3005, 2140, 1936, 1732, 1558, 1313, 1284, 1184, 1001, 889, 756, 563 cm⁻¹; ¹H NMR (500 MHz, DMSO) δ 10.81 (bs, 1H), 8.53 (d, *J* = 1.9 Hz, 1H), 7.92 (dd, *J* = 8.4, 1.9 Hz, 1H), 7.80 (s, 1H), 6.97 (d, *J* = 8.4 Hz, 1H), 3.86 (s, 3H), 2.26 (s, 3H) ppm; ¹³C NMR (125 MHz, DMSO) δ 169.50, 162.78, 154.36, 152.38, 147.95, 132.09, 125.52, 117.14, 116.30, 114.14, 56.00, 11.78 ppm; HRMS (ESI) *m/z*: calcd for C₁₂H₁₂NO₄ [M+H]⁺ 234.0760 found 234.0759.

2.2h (Z)-4-(3-hydroxy-4-methoxybenzylidene)-3-methylisoxazol-5(4H)-one (**4h**): Orange solid; M.p.: 212–214 °C; IR (KBr): 3282, 3057, 2015, 1697, 1570, 1516, 1448, 1288, 1136, 1010, 881, 779, 569 cm⁻¹; ¹H NMR (500 MHz, CDCl₃) δ 8.11 (dd, *J* = 8.6, 2.1 Hz, 1H), 8.03 (d, *J* = 2.1 Hz, 1H), 7.30 (s, 1H), 6.98 (d, *J* = 8.6 Hz, 1H), 5.69 (s, 1H), 4.02 (s, 3H), 2.28 (s, 3H) ppm; ¹³C NMR (125 MHz, CDCl₃) δ 168.55, 161.24, 151.81, 149.59, 145.59, 129.09, 126.48, 119.54, 117.08, 110.60, 56.26, 11.70 ppm; HRMS (ESI) *m/z*: calcd for C₁₂H₁₂NO₄ [M+H]⁺ 234.0760 found 234.0763.

2.2i (Z)-4-((1H-indol-3-yl)methylene)-3-methylisoxazol-5(4H)-one (**4i**): Brown solid; M.p.: 240–242 °C; ¹H NMR (500 MHz, DMSO) δ 12.81 (s,

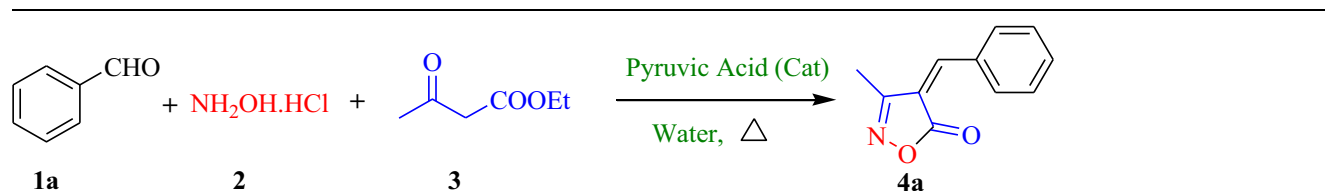
1H), 9.52 (s, 1H), 8.20–8.15 (m, 2H), 7.63–7.60 (m, 1H), 7.35–7.33 (m, 2H), 2.35 (s, 3H) ppm; ¹³C NMR (125 MHz, DMSO) δ 170.88, 162.20, 140.97, 139.00, 136.85, 128.45, 124.43, 123.05, 119.33, 113.62, 113.14, 109.29, 11.70 ppm; HRMS (ESI) *m/z*: calcd for C₁₃H₁₁N₂O₂ [M+H]⁺ 227.0815 found 227.0817.

2.3 General procedure for the synthesis of 4a-i under the conventional condition

A mixture of benzaldehyde (0.5 g, 4.71 mmol), hydroxylamine hydrochloride (0.327 g, 4.71 mmol), ethyl acetoacetate (0.613 g, 4.71 mmol) and pyruvic acid catalyst (0.02 g, 0.023 mmol) in water (10 mL) were refluxed for the indicated time. After the completion of the reaction (TLC check), the reaction mixture was cooled to room temperature and extracted using ethyl acetate (2 X 5 mL). The organic layer was dried over anhydrous Na₂SO₄ and concentrated under reduced pressure to give the crude product, which was purified by column chromatography using ethyl acetate: *n*-hexane (20–40%) as the eluent to yield the pure product.

3. Results and Discussion

In order to optimize the reaction conditions, the model reaction was performed using benzaldehyde (**1a**), hydroxylamine hydrochloride (**2**) and ethyl acetoacetate (**3**) in the presence of different amounts of catalyst in an aqueous medium and the results are summarized in Table 1. Firstly, the reaction conditions were optimized under conventional heating and the progress of the reaction was monitored by TLC analysis. When the reaction was conducted in water without pyruvic acid catalyst, the reaction did not proceed until 2 h (Table 1, entry 1). Performing the same reaction in the presence of 2 mol% pyruvic acid catalyst in an aqueous medium at R.T. and at 50 °C led to the formation of a trace amount of **4a** after 2 h (Table 1, entries 2, 3). In order to improve the results, the catalyst amount was increased to 5 mol% and the reaction mixture was stirred at 60 °C and 80 °C for 2 h. This showed a considerable impact on the yield (Table 1, entries 4, 5). Improvement in the reaction profile in terms of the yield was observed at higher temperatures (Table 1, entry 6). Finally, it was found that 5 mol% of pyruvic acid catalyst was sufficient to obtain the desired product **4a** in 86% yield after 2.5 h stirring at refluxed temperature (Table 1, entry 6). Increasing

Table 1. Optimization of the reaction condition under conventional heating^a.


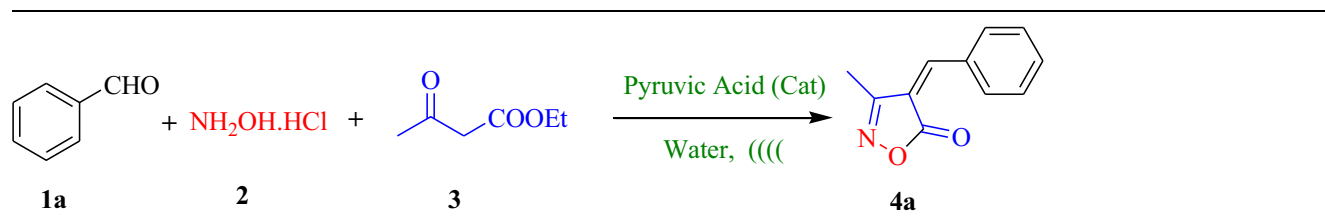
Entry	Catalyst (mol %)	Temp (°C)	Time (h)	% Yield ^b
1	0	R.T.	2	NR ^c
2	2	R.T.	2	Trace
3	2	50	2	Trace
4	5	60	2	40
5	5	80	2	73
6	5	100	2.5	86
7	10	100	2.5	86
8	5	100	3	85
9	5	100	3.5	86

^aThe reactions were carried out on 5.0 mmol scale; 1 equivalents of each benzaldehyde, hydroxylamine hydrochloride and ethyl acetoacetate were employed. ^bIsolated yield. ^cNo reaction.

the reaction time and catalyst load to 10 mol% did not show any great change in the reaction profile (Table 1, entries 7–9).

These results obtained at conventional conditions (Table 1) led us to explore an alternative procedure to prepare product **4a** in higher yield. In this sense, we choose ultrasound as an alternative energy source to provide a selective reaction. Thus, the same reaction condition was applied for the reaction under

ultrasound irradiation; however, product **4a** was not obtained in the absence of pyruvic acid catalyst at R.T. (Table 2, entry 1). By increasing the catalyst load to 2 and 5 mol% at 40 °C, the desired product **4a** was obtained in 25% and 71% yield, respectively (Table 2, entries 2, 3). To check the effect of temperature on reaction profile, we increased temperature to 50 °C, which resulted in the formation of the product in 90% yield in 15 min (Table 2, entry 4). No improvement

Table 2. Optimization of the reaction condition under ultrasonic irradiation^a.


Entry	Catalyst (mol %)	Temp (°C)	Time (min)	% Yield ^b
1	0	R.T.	10	NR ^c
2	2	40	15	25
3	5	40	15	71
4	5	50	15	90
5	10	50	20	90
6	5	60	20	89

^aThe reactions were carried out on 5.0 mmol scale; 1 equivalents of each benzaldehyde, hydroxylamine hydrochloride and ethyl acetoacetate were employed. ^bIsolated yield. ^cNo reaction.

was observed in the reaction profile by increasing the catalyst loading, temperature and time (Table 2, entries 5, 6). Thus, the optimum reaction condition for the reaction was found, when the benzaldehyde (**1a**) was sonicated in water at 50 °C with hydroxylamine hydrochloride (**2**) and ethyl acetoacetate (**3**) in the presence of 5 mol% pyruvic acid catalyst for 15 minutes which afforded isoxazole derivative **4a** in 90% yield (Table 2, entry 4).

The optimum reaction condition is applied to a variety of differently substituted aldehydes and the results obtained are summarized in Table 3. We notice that whatever the nature of the substituent and its position yields remain very good and vary between 73 to 90% (Table 3, entries 1–9). Moreover, it is observed that the mono, as well as di-substituted aldehydes, reacts smoothly to give corresponding 4*H*-isoxazol-5-ones derivatives in good yields. Phenolic aldehyde like vanillin and isovanillin also condensed efficiently to afford 4*H*-isoxazol-5-one derivative **4g** and **4h** in comparative yields (Table 3, entries 7, 8). In addition to benzaldehydes, indole-based aldehyde like Indole-3-carboxaldehyde also condensed efficiently to afford isoxazole derivative **4i** in good yield (Table 3, entry 9).

As shown in Table 3, the reactions were carried out under the ultrasound irradiation method happens comparatively at faster rates with higher yields

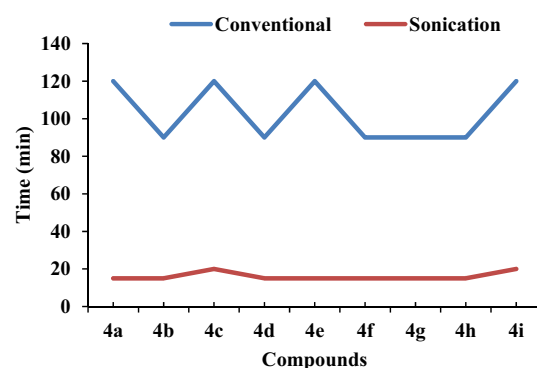


Figure 2. Time required for reaction under conventional and sonication method.

(Figure 2). While the same reactions were carried out under conventional heating, require a longer time and gave lower yields. Notably, a similar effect was seen in all reactions and it was evident that ultrasound irradiation can speed up the reaction considerably to reduce the reaction time with high yields. Thus, we found that ultrasonic irradiation was very effective and useful in our work, which was superior to the conventional method with respect to yields and reaction time. Moreover, although earlier reported methods are quite suitable with respect to reaction yield many of them were carried out at drastic conditions or require expensive catalysts. Furthermore, several previously

Table 3. Synthesis of 4*H*-isoxazol-5-one derivatives using pyruvic acid catalyst^a.

Entry	R	Compound	Conventional Heating (100 °C)		Ultrasonication (50 °C)	
			Time (h)	% Yield ^b	Time (min)	% Yield ^b
1 ^c	H	4a	2	85	15	90
2 ^c	4-OH	4b	1.5	80	15	85
3 ^c	4-Me	4c	2	88	20	92
4 ^c	2-OH	4d	1.5	85	15	90
5 ^c	3,4-di-OMe	4e	2	88	15	92
6 ^c	4-OMe	4f	1.5	81	15	88
7 ^c	3-OMe,4-OH	4g	1.5	83	15	85
8	3-OH,4-OMe	4h	1.5	85	15	90
9 ^c	Indole-3-carboxaldehyde	4i	2	73	20	78

^aThe reactions were carried out on 5.0 mmol scale; 1 equivalents of each aldehyde, hydroxylamine hydrochloride, ethyl acetoacetate and 5 mol% pyruvic acid catalyst were employed. ^bIsolated yield. ^cAll compounds are known and their spectroscopic and physical data is consistent with those of authenticating samples.^{34,39,40}

reported reactions are performed in volatile organic solvents, which are not environmentally friendly. Thereby, we propose the use of pyruvic acid as a catalyst and water as a biologically and environmentally safe solvent to provide an eco-friendly and economical procedure for the synthesis of 4*H*-isoxazol-5-one derivatives, which can be afforded in 15 to 20 min.

As described in Figure 3 we have proposed a plausible reaction mechanism for the pyruvic acid-catalyzed one-pot multicomponent reaction between aromatic aldehydes, ethyl acetoacetate and hydroxylamine hydrochloride in an aqueous medium. Initially, acidic proton of pyruvic acid interacts with the carbonyl oxygen of ethyl acetoacetate, which activates the carbonyl group to facilitate nucleophilic attack of the amino group of hydroxylamine followed by dehydration, resulting in the formation of oxime **A**. The keto-enol tautomerism of oxime **A** results in

the formation of intermediate **B**. The activated methylene carbon of intermediate **B** then shows nucleophilic attack on the carbonyl carbon of the aromatic aldehyde which is also activated by pyruvic acid under sonication followed by dehydration gives intermediate **C**. The formed intermediate **C** eventually undergoes cyclisation by the intramolecular attack of oxygen atom of hydroxyl group to ester carbonyl with the elimination of ethanol molecule to form intermediate **D**. Intermediate **D** on de-protonation results into desired product 3-methyl-4-arylmethylene isoxazole-5(4*H*)-one.

The reusability of catalyst was investigated through a series of sequential condensations of 4-hydroxybenzaldehyde, hydroxylamine hydrochloride and ethyl acetoacetate in the presence of pyruvic acid as a model reaction under ultra-sonication. After completion of the reaction, the reaction mixture was extracted using

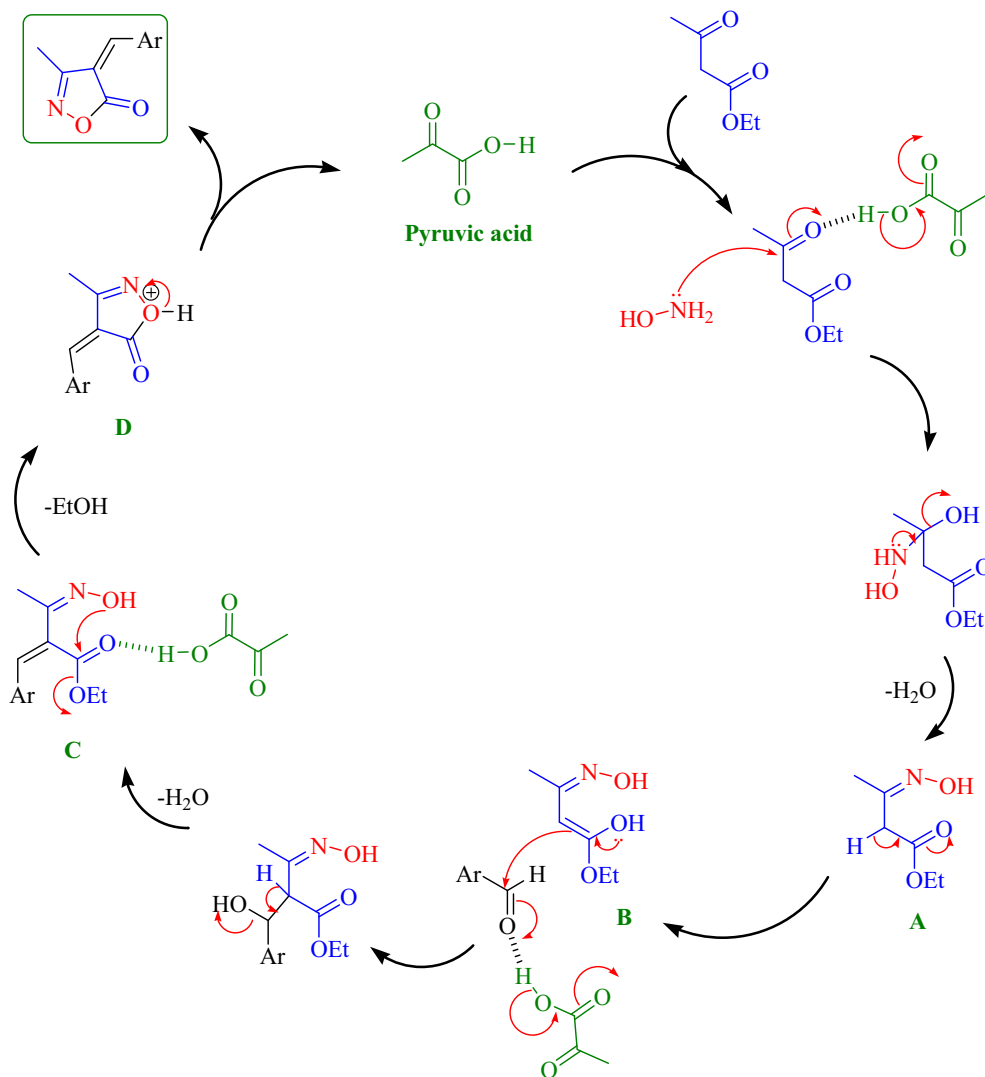


Figure 3. Plausible mechanism for the formation of isoxazoles using pyruvic acid catalyst.

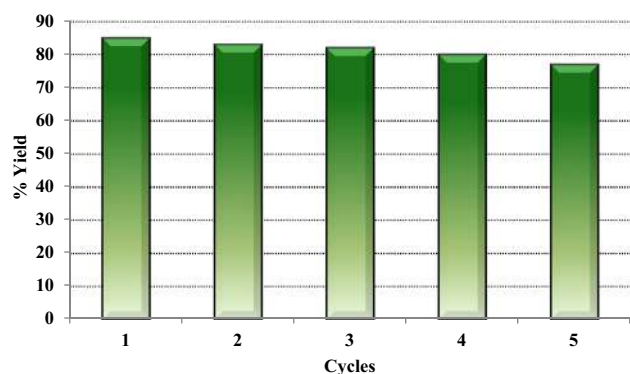


Figure 4. Reusability study of pyruvic acid catalyst under ultrasound irradiations.

ethyl acetate and an aqueous layer was used again for the model reaction without the addition of a catalyst. The obtained results revealed that the catalyst could be reused five consecutive cycles without any pre-treatment and with a negligible decrease in activity (Figure 4).

4. Conclusions

We describe here a new, efficient process for the synthesis of 3-methyl-4-arylmethylene isoxazole-5(4*H*)-ones by a one-pot multicomponent reaction between aromatic aldehydes, ethyl acetoacetate and hydroxylamine hydrochloride catalysed by pyruvic acid as a benign, commercially available, inexpensive catalyst. The essential advantages of this method are simplicity of use, good yields and short reaction times, use of non-toxic solvent and non-conventional energy source and eco-friendly method. We believe that the present protocol is a convenient and efficient alternative to the existing traditional methods.

Supplementary Information (SI)

The Supplementary Information contains all the ^1H NMR, ^{13}C NMR, IR and HRMS spectra's of synthesized compounds. Supplementary Information is available at www.ias.ac.in/chemsci.

Acknowledgements

We acknowledge financial support from ASPIRE Research Mentorship Grant (Project No: 18TEC000760) Savitribai Phule Pune University, Pune-411 007, MS, India. We are also thankful to Central Instrumentation Facility (CIF), Savitribai Phule Pune University for analytical support. We thank Dr R. J. Barnabas (Ahmednagar College, Ahmednagar) for his helpful discussion and suggestions.

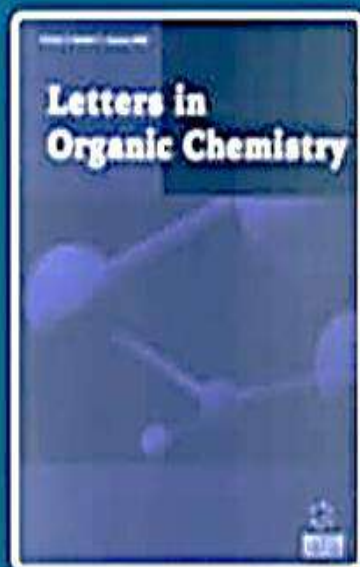
References

- Vitaku E, Smith D T and Njardarson J T 2014 Analysis of the structural diversity, substitution patterns, and frequency of nitrogen heterocycles among U.S. FDA approved pharmaceuticals *J. Med. Chem.* **57** 10257
- Vorobyeva D V, Karimova N M, Odinets I L, Röschenthaler G V and Osipov S N 2011 Click-chemistry approach to isoxazole-containing α -CF₃-substituted α -aminocarboxylates and α -aminophosphonates *Org. Biomol. Chem.* **9** 7335
- Wang L, Yu X, Feng X and Bao M 2012 Synthesis of 3,5-disubstituted isoxazoles via cope-type hydroamination of 1,3-dialkynes *Org. Lett.* **14** 2418
- Santos M M M, Faria N, Iley J, Coles S J, Hursthouse M B, Martins M L and Moreira R 2010 Reaction of naphthoquinones with substituted nitromethanes facile synthesis and antifungal activity of naphtho *Bioorg. Med. Chem. Lett.* **20** 193
- Kano H, Adachi I, Kido R and Hirose K 1967 Isoxazoles. XVIII. Synthesis and pharmacological properties of 5-aminoalkyl- and 3-aminoalkylisoxazoles and related derivatives *J. Med. Chem.* **10** 411
- Diana P, Carbone A, Barraja P, Kelter G, Fiebig H H and Cirrincione G 2010 Synthesis and antitumor activity of 2,5-bis(3'-indolyl)-furans and 3,5-bis(3'-indolyl)-isoxazoles, nortopsentin analogues *Med. Chem.* **18** 4524
- Padmaja A, Rajasekhar C, Muralikrishna A and Padmavathi V 2011 Synthesis and antioxidant activity of oxazolyl/thiazolylsulfonyl methyl pyrazoles and isoxazoles *J. Med. Chem.* **46** 5034
- Prashanthi Y, Kiranmai K, Subhashini N J P and Shivaraj, 2008 Synthesis, potentiometric and antimicrobial studies on metal complexes of isoxazole Schiff bases *Spectrochim. Acta A* **70** 5
- Talley J J, Brown D L, Carter J S, Graneto M J, Koboldt C M, Masferrer J L, et al. 2000 4-[5-Methyl-3-phenylisoxazol-4-yl] benzenesulfonamide, valdecoxib: a potent and selective inhibitor of COX-2 *J. Med. Chem.* **43** 775
- Karabasanagouda T, Adhikari A V and Girisha M 2009 Synthesis of some new pyrazolines and isoxazoles carrying 4-methylthiophenyl moiety as potential analgesic and anti-inflammatory agents *Indian J. Chem.* **48** 430
- Lee Y S, Park S M and Kim B H 2009 Synthesis of 5-isoxazol-5-yl-2'-deoxyuridines exhibiting antiviral activity against HSV and several RNA viruses *Bioorg. Med. Chem. Lett.* **19** 1126
- Changtam C, Hongmanee P and Suksamrarn A 2010 Isoxazole analogs of curcuminoids with highly potent multidrug-resistant antimycobacterial activity *Eur. J. Med. Chem.* **45** 4446
- Deng B L, Cullen M D, Zhou Z, Hartman T L, Buckheit R W, Pannecouque C, et al. 2006 Synthesis and anti-HIV activity of new alkenyl diaryl methane (ADAM) non-nucleoside reverse transcriptase inhibitors (NNRTIs) incorporating benzoxazolone and benzisoxazole rings *Bioorg. Med. Chem.* **14** 2366
- Ishioka T, Kubo A, Koiso Y, Nagasawa K, Itai A and Hashimoto Y 2002 Novel non-steroidal/non-anilide

- type androgen antagonists with an isoxazolone moiety *Bioorg. Med. Chem.* **10** 1555
15. Kusakabe Y, Nagatsu J, Shibuya M, Kawaguchi O, Hirose C and Shirato S 1972 Minimycin, a new antibiotic *J. Antibiot.* **25** 44
 16. Peglion J L, Vian J, Gourment B, Despau N, Audinot V and Millan M 1997 Tetracyclic analogues of [+-]S 14297: Synthesis and determination of affinity and selectivity at cloned human dopamine D₃ vs D₂ receptors *Bioorg. Med. Chem. Lett.* **7** 881
 17. Ren H, Grady S, Gamemara D, Heinzen H, Moyna P, Croft S, et al. 2001 Design, synthesis, and biological evaluation of a series of simple and novel potential antimalarial compounds *Bioorg. Med. Chem. Lett.* **11** 1851
 18. Matsuoka H, Ohi N, Mihara M, Suzuki H, Miyamoto K, Maruyama N, et al. 1997 Antirheumatic agents: novel methotrexate derivatives bearing a benzoxazine or benzothiazine moiety *J. Med. Chem.* **40** 105
 19. Benedini F, Bertolini G, Cereda R, Donia G, Gromo G, Levi S, et al. 1995 New antianginal nitro esters with reduced hypotensive activity. Synthesis and pharmacological evaluation of 3-[(nitrooxy)alkyl]-2H-1,3-benzoxazin-4(3H)-ones *J. Med. Chem.* **38** 130
 20. Frolund B, Jorgensen A T, Tagmose L, Stensbol T B, Vestergaard H T, Engblom C, et al. 2002 Novel class of potent 4-arylalkyl substituted 3-isoxazolol GABAA antagonists: synthesis, pharmacology, and molecular modeling *J. Med. Chem.* **45** 2454
 21. Kafle B, Aher N G, Khadka D, Park H and Cho H 2011 Isoxazol-5(4H)-one derivatives as PTP1B inhibitors showing an anti-obesity effect *Chem. Asian J.* **6** 2073
 22. Chen Y L, Tseng C H, Lo Y C, Lin R W, Chen C F, Wang G J, et al. 2013 Synthesis of aminoalkoxy substituted 4,5-diphenylisoxazole derivatives as potential anti-osteoporotic agents *Med. Chem.* **9** 748
 23. Srinivas A, Nagaraj A and Reddy C S 2010 Synthesis and in vitro study of methylene-bistetrahydro[1,3]thiazolo[4,5-c]isoxazoles as potential nematocidal agents *Eur. J. Med. Chem.* **45** 2353
 24. Patrick D A, Bakunov S A, Bakunova S M, Suresh Kumar E V K, Lobardy R J, Jones S K, et al. 2007 Synthesis and in vitro antiprotozoal activities of dicationic 3,5-diphenylisoxazoles *J. Med. Chem.* **50** 2468
 25. Kang Y K, Shin K J, Yo K H, Seo K J, Hong C Y, Lee C S, et al. 2000 Synthesis and antibacterial activity of new carbapenems containing isoxazole moiety *Bioorg. Med. Chem. Lett.* **10** 95
 26. Zhu J, Mo J, Lin H Z, Chen Y and Sun H P 2018 The recent progress of isoxazole in medicinal chemistry *Bioorg. Med. Chem.* **26** 3065
 27. Giustina A, Malerba M, Bresciani E, Desenzani P, Licini M, Zaltieri G and Grassi V 1995 Effect of two beta 2-agonist drugs, salbutamol and broxaterol, on the growth hormone response to exercise in adult patients with asthmatic bronchitis *J. Endocrin. Invest.* **18** 847
 28. Zhang X H, Zhan Y H, Chen D, Wang F and Wang L Y 2012 Merocyanine dyes containing an isoxazolone nucleus: synthesis, X-ray crystal structures, spectroscopic properties and DFT studies *Dyes Pigm.* **93** 1408
 29. Han J, Guo H, Wang X G, Pang M L and Meng J B 2007 Synthesis and liquid crystalline properties of 3-substituted pentane-2,4-dione, pyrazole and isoxazole derivatives *Chin. J. Chem.* **25** 129
 30. Biju S, Reddy M L P and Freire R O 2007 3-Phenyl-4-aryl-5-isoxazolone complexes of Tb³⁺ as promising light-conversion molecular devices *Inorg. Chem. Commun.* **10** 393
 31. Aret E, Meekes H, Vlieg E and Deroover G 2007 Polymorphic behavior of a yellow isoxazolone dye *Dyes Pigm.* **72** 339
 32. Stammer C H, Wilson A N, Spencer C F, Bachelor F W, Holly F W and Folkers K 1957 Synthesis of cycloserine and a methyl analog *J. Am. Chem. Soc.* **79** 3236
 33. Bowden K, Crank G and Ross W J 1968 The synthesis of pantherine and related compounds *J. Chem. Soc. C* 172
 34. Saikh F, Das J and Ghosh S 2013 Synthesis of 3-methyl-4-arylmethyleneisoxazole-5(4H)-ones by visible light in aqueous ethanol *Tetrahedron. Lett.* **54** 4679
 35. Kiyani H and Ghorbani F 2015 Efficient tandem synthesis of a variety of pyran-annulated heterocycles, 3,4-disubstituted isoxazol-5(4H)-ones, and α , β -unsaturated nitriles catalyzed by potassium hydrogen phthalate in water *Res. Chem. Intermed.* **41** 7847
 36. Kiyani H, Jabbari M and Mosallanezhad A 2014 Efficient three component synthesis of 3,4-disubstituted isoxazol-5(4H)-ones in green media *Jordan J. Chem.* **9** 279
 37. Kiyani H, Kanaani A, Ajloo D, Ghorbani F and Vakili M 2015 *N*-Bromosuccinimide (NBS)-promoted, three component synthesis of α , β -unsaturated isoxazol-5(4H)-ones, and spectroscopic investigation and computational study of 3-methyl-4-(thiophen-2-yl-methylene) isoxazol-5(4H)-one *Res. Chem. Intermed.* **41** 7739
 38. Liu Q and Zhang Y N 2011 One-pot synthesis of 3-methyl-4-arylmethylene-isoxazol-5(4H)-ones catalyzed by sodium benzoate in aqueous media: a green chemistry strategy *Bull. Korean Chem. Soc.* **32** 3559
 39. Kiyani H and Ghorbani F 2015 Boric acid-catalyzed multi-component reaction for efficient synthesis of 4H-isoxazol-5-ones in aqueous medium *Res. Chem. Intermed.* **41** 2653
 40. Laroum R and Debache A 2018 New eco-friendly procedure for the synthesis of 4-arylmethylene-isoxazol-5(4H)-ones catalyzed by pyridinium *p*-toluene sulfonate (PPTS) in aqueous medium *Synth. Commun.* **48** 1876
 41. Kim S J, Yang J, Lee S, Park C, Kang D, Akter J, et al. 2018 The tyrosinase inhibitory effects of isoxazolone derivatives with a (Z)- β -phenyl- α , β -unsaturated carbonyl scaffold *Bioorg. Med. Chem.* **26** 3882
 42. Kiyani H and Mosallanezhad A 2018 Sulfanilic acid-catalyzed synthesis of 4-arylidene-3-substituted isoxazole-5(4H)-ones *Curr. Org. Synth.* **15** 715
 43. Vaidya S P, Shridhar G, Ladage S and Ravishankar L 2016 A facile synthesis of isoxazolone derivatives catalyzed by cerium chloride heptahydrate in ethyl lactate as a solvent: a green methodology *Curr. Green Chem.* **3** 160
 44. Pourmousavi S A, Fattahi H R, Ghorbani F, Kanaani A and Ajloo D 2018 A green and efficient synthesis of

- isoxazol-5(4H)-one derivatives in water and a DFT study *J. Iran. Chem. Soc.* **15** 455
45. Nakkalwar S L, Patwari S B, Patel M M and Jadhav V B 2018 Iodine catalyzed highly efficient one pot three component synthesis of 4-arylidene-3-methylisoxazol-5(4H)-one in aqueous medium *Curr. Green Chem.* **5** 122
 46. Kiyani H, Darbandi H, Mosallanezhad A and Ghorbani F 2015 2-Hydroxy-5-sulfobenzoic acid: an efficient organo catalyst for the three-component synthesis of 1-amidoalkyl-2-naphthols and 3,4-disubstituted isoxazol-5(4H)-ones *Res. Chem. Intermed.* **41** 7561
 47. Kiyani H and Ghorbani F 2017 Potassium phthalimide as efficient basic organocatalyst for the synthesis of 3,4-disubstituted isoxazol-5(4H)-ones in aqueous medium *J. Saudi Chem. Soc.* **21** S112
 48. Ablajan K and Xiamuxi H 2012 Efficient one-pot synthesis of β -unsaturated isoxazol-5-ones and pyrazol-5-ones under ultrasonic irradiation *Synth. Commun.* **42** 1128
 49. Imène A K, Raouf B, Taous B, Boudjemaa B and Abdelmadjid D 2016 NaH_2PO_4 catalyzed a three-component 4-arylidene-3-methylisoxazol-5(4H)-ones synthesis in solvent-free conditions *Der. Pharma Chemica.* **8** 97
 50. Maddila S N, Maddila S, van Zyl W E and Jonnalagadda S B 2016 Ag/SiO_2 as a recyclable catalyst for the Facile green synthesis of 3-methyl-4(phenyl)methylene-isoxazole-5(4H)-ones *Res. Chem. Intermed.* **42** 2553
 51. Fozooni S, Hosseinzadeh N G, Hamidian H and Akhgar M R 2013 Nano Fe_2O_3 , clinoptilolite and $\text{H}_3\text{PW}_{12}\text{O}_{40}$ as efficient catalysts for solvent-free synthesis of 5(4H)-isoxazolone under microwave irradiation conditions *J. Braz. Chem. Soc.* **24** 1649
 52. Kiyani H and Ghorbani F 2016 Expeditious green synthesis of 3,4-disubstituted isoxazole-5(4H)-ones catalyzed by nano-MgO *Res. Chem. Intermed.* **42** 6831
 53. Kasar S B and Thopate S R 2019 Ultrasonically assisted efficient and green protocol for the synthesis of 4H-isoxazol-5-ones using itaconic acid as a homogeneous and reusable organocatalyst *Curr. Organocatal.* **6** 231
 54. Liu Q and Hou X 2012 One-pot three-component synthesis of 3-methyl-4-arylmethylene-isoxazol-5(4H)-ones catalyzed by sodium sulfide *Phosphor. Sulfur. Silicon Relat. Elem.* **187** 448
 55. Rikani A B and Setamdideh D 2016 One-pot and three-component synthesis of isoxazol-5(4H)-one derivatives in the presence of citric acid *Orient. J. Chem.* **32** 1433
 56. Gu Y 2012 Multicomponent reactions in unconventional solvents: state of the art *Green Chem.* **14** 2091
 57. Maleki B 2015 Solvent-free synthesis of 2,4,6-triarylpyridine derivatives promoted by 1,3-dibromo-5,5-dimethylhydantoin *Org. Prep. Proced. Int.* **47** 173
 58. Maleki B, Alinezhad H, Atharifar H, Tayebee R and Mofrad A V 2019 One-pot synthesis of polyhydroquinolines catalyzed by ZnCl_2 supported on nano $\text{Fe}_3\text{O}_4/\text{SiO}_2$ *Org. Prep. Proced. Int.* **51** 301
 59. Li C J 2005 Organic reactions in aqueous media with a focus on carbon-carbon bond formations: a decade update *Chem. Rev.* **105** 3095
 60. Pirrun M C 2006 Acceleration of organic reactions through aqueous solvent effects *Chem. Eur. J.* **12** 1312
 61. Knecht W and Löffler M 1998 Species-related inhibition of human and rat dihydroorotate dehydrogenase by immunosuppressive isoxazol and cinchoninic acid derivatives *Biochem. Pharmacol.* **56** 1259
 62. Wu T Y, Guo N, The C Y and Hay J X W 2013 Advances in ultrasound technology for environmental remediation (New York London: Springer Dordrecht Heidelberg)
 63. Srivastava R M, Filho R A W N, Silva C A and Bortoluzzi A J 2009 First ultrasound-one-pot synthesis of N-substituted amides *Ultrason. Sonochem.* **16** 737
 64. Ray S, Manna P and Mukhopadhyay C 2015 Simultaneous sonication assistance for the synthesis of pyrroloacridinones and its efficient catalyst HBF_4 supported on uniform spherical silica nanoparticles *Ultrason. Sonochem.* **22** 22
 65. Ashokkumar M 2011 The characterization of acoustic cavitation bubbles-an overview *Ultrason. Sonochem.* **18** 864
 66. Mason T J 1997 Ultrasound in synthetic organic chemistry *Chem. Soc. Rev.* **26** 443
 67. Wang S F, Guo C L, Cui K K, Zhu Y T, Ding Z X, Zou X Y and Li Y H 2015 Lactic acid as an invaluable green solvent for ultrasound-assisted scalable synthesis of pyrrole derivatives *Ultrason. Sonochem.* **26** 81
 68. Maleki B, Baghayeri M, Abadi S A J, Tayebee R and Khojastehnezhad A 2016 Ultrasound promoted facile one pot synthesis of highly substituted pyran derivatives catalyzed by silica-coated magnetic NiFe_2O_4 nanoparticle-supported $\text{H}_{14}[\text{NaP}_5\text{W}_{30}\text{O}_{110}]$ under mild conditions *RSC Adv.* **6** 96644
 69. Maleki B, Chahkandi M, Tayebee R, Kahrobaei S, Alinezhad H and Hemmati S 2019 Synthesis and characterization of nanocrystalline hydroxyapatite and its catalytic behavior towards synthesis of 3,4-disubstituted isoxazole-5(4H)-ones in water *Appl. Organomet. Chem.* **33** e5118
 70. Atharifar H, Keivanloo A and Maleki B 2020 Greener synthesis of 3,4-disubstituted isoxazole-5(4H)-ones in a deep eutectic solvent *Org. Prep. Proced. Int.* **52** 517
 71. Nakamura I, Okamoto M and Terada M 2010 Gold-catalyzed cyclization and subsequent arylidene group transfer of *o*-propioloyl oximes *Org. Lett.* **12** 2453
 72. Donleavy J J and Gilbert E E 1937 A synthesis of arylidene isoxazolones *J. Am. Chem. Soc.* **59** 1072
 73. Villemin D, Martin B and Garrigues B 1993 Potassium fluoride on alumina: dry condensation of 3-phenylisoxazol-5-one with aldehydes under microwave irradiation *Synth. Commun.* **23** 2251
 74. Chary G R, Reddy R G, Ganesh Y S S, Prasad K V, Raghunadh A, Krishna T, et al. 2014 Effect of aqueous polyethylene glycol on 1,3-dipolar cycloaddition of benzoylnitromethane/ethyl 2-nitroacetate with dipolarophiles: green synthesis of isoxazoles and isoxazolines *Adv. Synth. Catal.* **356** 160
 75. Kitanosono T, Masuda K, Xu P and Kobayashi S 2018 Catalytic organic reactions in water toward sustainable society *Chem. Rev.* **118** 679
 76. Deshmukh S R, Nalkar A S and Thopate S R 2021 Ultrasound-promoted pyruvic acid catalyzed green

- synthesis of biologically relevant bis(indolyl)methanes scaffold under aqueous condition *Polycycl. Compd. Aromat.* <https://doi.org/10.1080/10406638.2021.1984259>.
77. Stanko R T, Reynolds H R, Hoyson R, Janosky J E and Wolf R 1994 Pyruvate supplementation of a low-cholesterol, low-fat diet: effects on plasma lipid concentrations and body composition in hyperlipidemic patients *Am. J. Clin. Nutr.* **59** 423
78. Stanko R T, Robertson R J, Galbreath R W, Reilly J J, Greenawalt K D and Jr Goss F L 1990 Enhanced leg exercise endurance with a high-carbohydrate diet and dihydroxyacetone and pyruvate *J. Appl. Physiol.* **69** 1651
79. DeBoer L W, Bekx P A, Han L and Steinke L 1993 Pyruvate enhances recovery of rat hearts after ischemia and reperfusion by preventing free radical generation *J. Appl. Physiol.* **265** 1571
80. Borle A B and Stanko R T 1996 Pyruvate reduces anoxic injury and free radical formation in perfused rat hepatocytes *J. Appl. Physiol.* **270** 535



Letters in Organic Chemistry

[Editor-in-Chief >>](#)

ISSN (Print): 1570-1786

ISSN (Online): 1875-6255


[Back](#)

[Journal](#) ▼

[Subscribe](#)

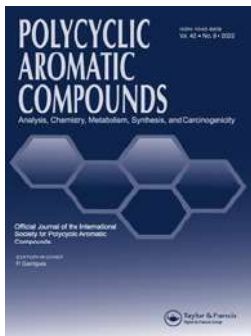
[Letter Article](#)

Water-Mediated Green Synthesis of Benzimidazoles Using Pyruvic Acid: A Comparable Study of Ultrasonication versus Conventional Heating

Author(s): Santosh Rangnath Deshmukh* , Archana

Subhash Nalkar and Shankar Ramchandra Thopate 

Volume 19 , Issue 7 , 2022 [REPLY](#)




Ultrasound-Promoted Pyruvic Acid Catalyzed Green Synthesis of Biologically Relevant Bis(Indolyl)Methanes Scaffold under Aqueous Condition

Santosh R. Deshmukh, Archana S. Nalkar & Shankar R. Thopate


To cite this article: Santosh R. Deshmukh, Archana S. Nalkar & Shankar R. Thopate (2022) Ultrasound-Promoted Pyruvic Acid Catalyzed Green Synthesis of Biologically Relevant Bis(Indolyl)Methanes Scaffold under Aqueous Condition, Polycyclic Aromatic Compounds, 42:9, 6501-6509, DOI: [10.1080/10406638.2021.1984259](https://doi.org/10.1080/10406638.2021.1984259)


To link to this article: <https://doi.org/10.1080/10406638.2021.1984259>

 View supplementary material 

 Published online: 28 Sep 2021.

 Submit your article to this journal 

 Article views: 142



 View related articles 

 View Crossmark data 

 Citing articles: 1 View citing articles 



Ultrasound-Promoted Pyruvic Acid Catalyzed Green Synthesis of Biologically Relevant Bis(Indolyl)Methanes Scaffold under Aqueous Condition

Santosh R. Deshmukh^a , Archana S. Nalkar^a, and Shankar R. Thopate^{a,b} 

^aProf. John Barnabas Post Graduate School for Biological Studies, Department of Chemistry, Ahmednagar College, Ahmednagar, Maharashtra, India; ^bDepartment of Chemistry, Shri Sadguru Gangageer Maharaj Science, Gautam Arts & Sanjivani Commerce College, Kopargaon, Maharashtra, India

ABSTRACT

An efficient and green protocol has been introduced for the synthesis of medicinally important bis(indolyl)methane derivatives using pyruvic acid catalyst in the presence of water. Pyruvic acid catalyzes the reaction of aldehyde with indole efficiently and products were obtained in good to excellent yields under sonication (50 °C) or under conventional heating (80 °C). The advantages of this synthetic methodology are use of environmental-friendly, commercially available, biodegradable catalyst, short reaction times, Lewis acid-free and metal-free mild reaction conditions with excellent yields and is compatible with a wide range of electronically diverse substrates. Pyruvic acid in water as a catalyst under ultrasound radiation can be a better alternative to synthesize bis(indolyl)methane derivatives than some of the traditional methods.

ARTICLE HISTORY

Received 26 May 2021

Accepted 16 September 2021

KEYWORDS


Aldehyde; bis(indolyl)methanes (BIMs); green chemistry; heterocyclic chemistry; pyruvic acid; ultrasound irradiation



Introduction

In nature, a large number of heterocyclic compounds are widely distributed due to their significance in various life processes. Among them, indole moiety is one of the most important heterocyclic compound having broad-spectrum biological and pharmacological activities. The bis(indolyl)methanes (BIMs) moiety is present in a range of natural products, agrochemicals and drug molecules^{1,2} (Figure 1). Researchers are employing BIMs to distinguish promising drugs and evade failures in the synthesis of potent drugs. Further, BIMs have proved to possess a great variety of applications in pharmaceutical industry.³ As previously reported, some of the BIMs exhibit excellent biological activities such as anticancer,⁴ antibacterial,⁵ antifungal,⁶ antihyperlipidemic,⁷

CONTACT Santosh R. Deshmukh  sant.deshmukh@gmail.com  Prof. John Barnabas Post Graduate School for Biological Studies, Department of Chemistry, Ahmednagar College, Ahmednagar, Maharashtra, 414001, India

 Supplemental data for this article can be accessed online at <https://doi.org/10.1080/10406638.2021.1984259>.

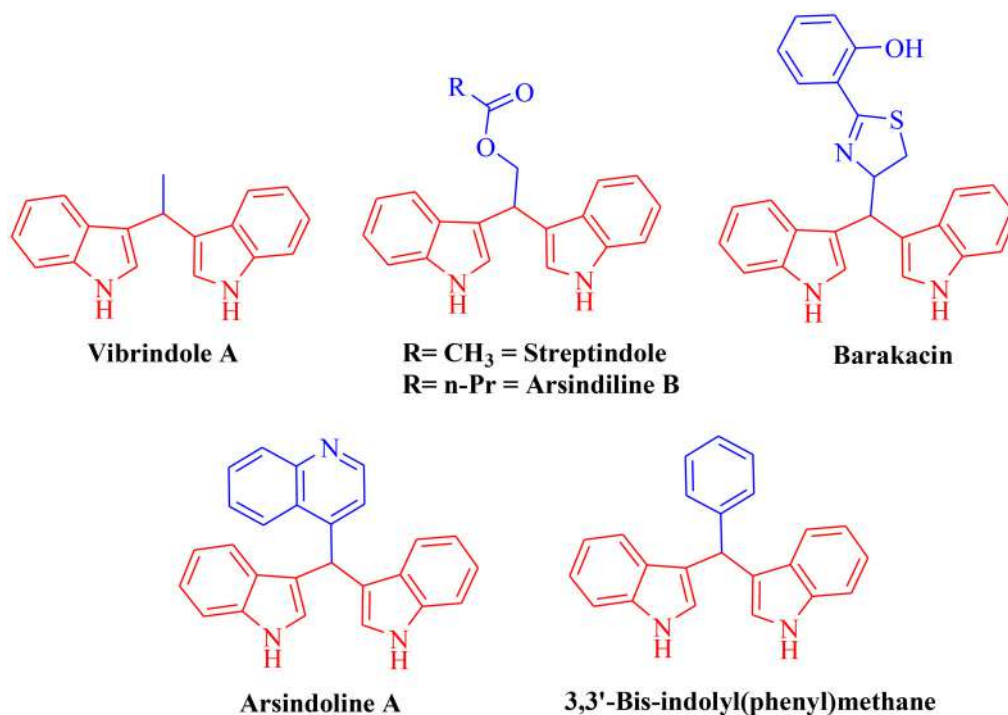
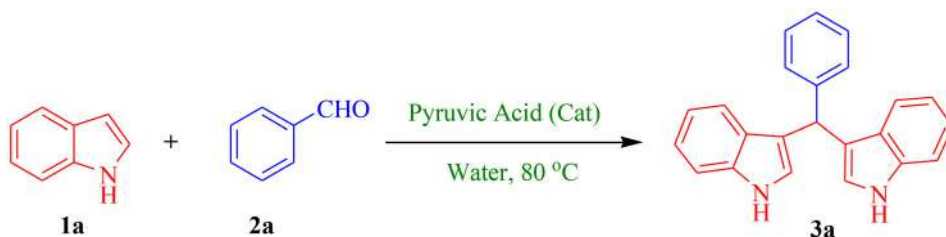


Figure 1. Representative biologically valued BIMs.

anti-inflammatory,⁸ topoisomerase II α inhibitory,⁹ DNA damaging,¹⁰ antileishmanial¹¹ and antibiotics.¹² In addition to these, heterocyclic compounds containing BIMs scaffold act as dietary supplements¹³ and colorimetric chemosensors.^{14–17} Because of their diverse applications in multi-disciplinary fields, the development of new synthetic strategies for the synthesis of BIMs has received great attention in organic synthesis.

In the literature, there are many methods reported for the synthesis of this class of compounds. Generally, the acid catalyzed electrophilic substitution of indoles with carbonyl compounds is the preferred method.^{18–23} A variety of acid catalysts, such as citric acid, sulfamic acid, boric acid, phosphoric acid, acetic acid, oxalic acid, lactic acid, itaconic acid, iridium, bisulfate, hexafluorophosphate salts of butyl methylimidazolium cation, tetrabutylammonium bromide, ammonium chloride, iodine, gallium trifluoromethanesulfonate, trifluoroethanol, protic solvent, TiCl₄/Zn, CuBr₂, α -chymotrypsin, nano-Ag, ammonium niobium oxalate, CeCl₃·7H₂O and amino-sulfonic acid have been reported.^{24–50} However, the drawback of these methods includes use of toxic reagents, volatile organic solvents, excess catalyst loading, longer reaction time, use of expensive catalysts, tedious workup and low product yields.

To overcome these problems, in recent years, researchers are striving to develop sophisticated green chemical methodologies to reduce costs, waste, hazards, pollution and energy expenditure by using eco-friendly reagents and economical reaction conditions to accomplish successful synthetic procedures. Hence, the synthesis of drugs and drug intermediates using environment friendly solvents and catalysts has become one of the most enthralling areas in academia and industry.^{51–53} Green chemistry is an evolving technology that provides access to novel techniques and robust catalysts, which permits enhancing conventional methodologies. Use of ultrasound irradiation to speed up the organic reactions has long been known in synthetic organic chemistry as well as in medicinal chemistry.⁵⁴

Table 1. Optimization of the reaction condition using indole and benzaldehyde under conventional heating^a.

Entry	Catalyst (mol%)	Temp (°C)	Time (h)	% Yield ^b
1	0	R.T.	2	NR ^c
2	1	R.T.	2	Trace
3	1	50	2	Trace
4	2	50	2	20
5	5	50	2	45
6	10	60	2	66
7	10	80	2.5	83
8	20	80	2.5	83

^aThe reactions were carried out on 2.0 mmol scale, 1 equivalents of benzaldehyde and 2 equivalents of indole were employed.

^bIsolated yield.

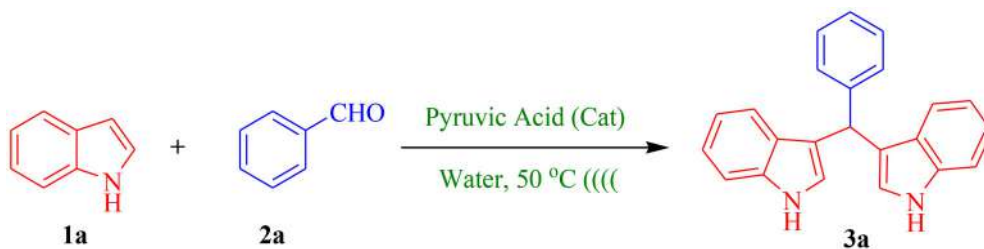
^cNo reaction.

In pursuit of the developing new synthetic methodologies, as well as designing the eco-friendly processes, herein we report, for the first time, use of naturally occurring, commercially cheap and biodegradable pyruvic acid as a catalyst in presence of water to catalyze electrophilic substitution reaction of indoles with carbonyl compounds to get library of BIMs.

Pyruvic acid, also known as α -ketopropionic acid, acetylformic acid or 2-oxopropanoic acid is the most vital α -oxocarboxylic acid and plays a fundamental role in energy metabolism in living organisms. It significantly increases fat and weight loss,⁵⁵ effectively reduces cholesterol,⁵⁶ improves exercise endurance capacity,⁵⁷ serves as a potent antioxidant,⁵⁸ and reduces anoxic injury and free radical formation.⁵⁹ On the contrary there is no report on its use as a catalyst in organic synthesis; hence to explore its catalytic utility, herein we report synthesis of BIMs using pyruvic acid as a catalyst under conventional as well as ultrasound irradiation condition.

Results and discussion

In order to evaluate the optimization of the reaction conditions, a model reaction was performed using indole (1a) and benzaldehyde (2a) at room temperature (R.T.) and the progress of the reaction was monitored by TLC analysis. The results are summarized in Table 1. It was found that when the reaction was conducted in water without pyruvic acid catalyst, the reaction did not proceed until 2 hours (Table 1, entry 1). Performing the same reaction in the presence of 1 mol% pyruvic acid catalyst in water at R.T. and at 50 °C led to the formation of a trace amount of 3a after 2 hours (Table 1, entries 2, 3). In order to improve the results, catalyst amount was increased and the reaction mixture was stirred at 50 °C for 2 hours. This showed considerable impact on the yield (Table 1, entries 4, 5). However, when 10 mol% catalyst and higher temperature was used then an improvement in the reaction profile in terms of the yield was observed (Table 1, entry 6). Finally, it was found that 10 mol% of pyruvic acid catalyst was sufficient to obtain the desired product 3a in 83% yield after 2.5 hours stirring at 80 °C temperature in water (Table 1, entry 7). Increasing the catalyst load to 20 mol% did not show any great change in the reaction profile (Table 1, entry 8).

Table 2. Optimization of the reaction condition using indole and benzaldehyde under ultrasound irradiation^a.

Entry	Catalyst (mol%)	Temp (°C)	Time (min)	% Yield ^b
1	0	R.T.	20	NR ^c
2	5	R.T.	20	Trace
3	10	R.T.	20	30
4	10	40	20	52
5	10	50	15	85
6	20	50	15	86
7	10	60	15	86

^aThe reactions were carried out on 2.0 mmol scale, 1 equivalents of benzaldehyde and 2 equivalents of indole were employed.

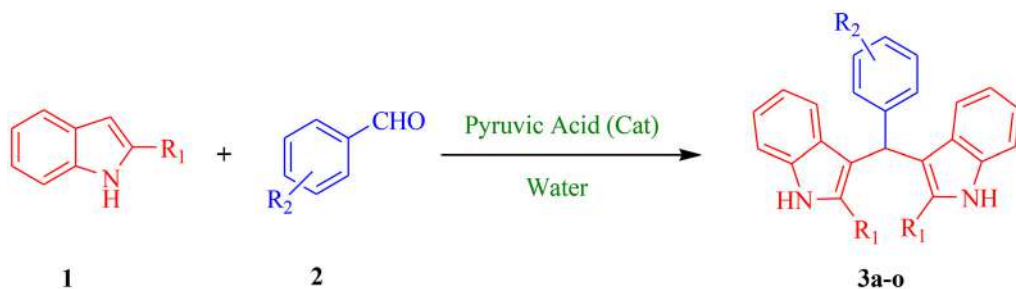
^bIsolated yield.

^cNo reaction.

In order to verify the effect of ultrasound irradiation on this reaction, the same model reaction was also carried out in the presence of ultrasound irradiation at different temperatures (Table 2). The passage of ultrasound irradiation through the reaction mixture without pyruvic acid catalyst at R.T. for 20 min did not lead to the desired product **3a** (Table 2, entry 1), while by increasing the catalyst load to 5 and 10 mol% at R.T. for 20 min the desired product **3a** was obtained in trace and 30% yield respectively (Table 2, entries 2, 3). In order to get better result temperature was increased to 40 °C and 50 °C, which delivered the **3a** product in 52% and 85% yield respectively. No improvement was observed in the yield of reaction by increasing the amount of the pyruvic acid catalyst and the temperature (Table 2, entries 6, 7). Thus, the use of 10 mol% pyruvic acid catalyst in water at 50 °C temperature under ultrasound irradiation was identified as the optimum condition for the above reaction (Table 2, entry 5). The reaction time can be reduced from hours to few minutes when ultrasound irradiation was used as an alternative energy source.

With the optimized reaction condition in hand, the scope and generality of the reaction was explored using various aromatic aldehydes and indoles under conventional as well as ultrasonic conditions in water to give a varied range of substituted BIMs in good to excellent yields (Table 3). Benzaldehyde bearing electron donating groups such as 4-Me, 4-OH and 3,4 di-OMe smoothly reacted with indole to give corresponding products **3b**, **3f** and **3l** respectively in good yields. This method was equally effective for the aldehydes bearing electron withdrawing groups in the aromatic ring like -NO₂ group at ortho (**3d**), meta (**3c**) and para (**3e**) positions and -CN group at para position (**3k**). Benzaldehyde with halogen substituents, such as -Cl at ortho (**3j**) and para (**3i**), -F (**3g**) and -Br (**3h**) at para position on benzene ring, was found to be compatible for this reaction. Our protocol also works well with substituted indoles to afford the corresponding BIMs (**3m**, **3n** and **3o**) in excellent yields.

As shown in Table 3, the reactions were carried out under conventional method, which happen comparatively in longer times with low yields. While the same reactions were carried out under the influence of ultrasonic irradiation giving high yields in short reaction times. Generally, a similar effect was seen in all reactions and it was evident that ultrasound irradiation can speed up the reaction considerably to reduce the reaction time with high yields. We found that ultrasonic irradiation was very effective and useful in our work, which was superior to the conventional method with respect to yields and reaction time. Particularly, considering the basic green

Table 3. Synthesis of BIMs derivatives using pyruvic acid catalyst^a.

Entry	R ₁	R ₂	Compd	Conventional Heating (80 °C)		Ultrasonication (50 °C)	
				Time (h)	% Yield ^b	Time (min)	% Yield ^b
1	H	H	3a	2.5	83	15	85
2	H	4-Me	3b	2	87	15	92
3	H	3-NO ₂	3c	1	80	15	86
4	H	2-NO ₂	3d	1.5	78	20	82
5	H	4-NO ₂	3e	1	85	15	90
6	H	4-OH	3f	2	82	15	90
7	H	4-F	3g	2	78	15	85
8	H	4-Br	3h	2	80	20	85
9	H	4-Cl	3i	2.5	78	15	83
10	H	2-Cl	3j	2	75	20	88
11	H	4-CN	3k	1.5	80	15	86
12	H	3,4-di-OMe	3l	2	77	20	88
13	Me	4-Cl	3m	2.5	89	20	95
14	Me	4-NO ₂	3n	1.5	88	15	92
15	Me	3,4-di-OMe	3o	2	77	20	85

^aThe reactions were carried out on 2.0 mmol scale, 1 equivalents of aldehyde, 2 equivalents of indole or 2-methyl indole and 10 mol% pyruvic acid catalyst were employed.

^bIsolated yield.

chemistry principles, which include use of non-conventional energy sources, use of green solvent, environmental friendly, biodegradable catalyst and metal and Lewis acid free synthesis. All these advantages make the proposed protocol superior to some of the traditional methods.

We proposed plausible reaction mechanism for the synthesis of bis(indolyl)methanes from aldehyde and indole using environmentally benign pyruvic acid catalyst in aqueous medium (Figure 2).

Experimental

General procedure for the synthesis of **3a-o** under ultrasound irradiation condition

A mixture of indole **1** (0.5 g, 4.27 mmol), aromatic aldehyde **2** (2.13 mmol) and pyruvic acid (10 mol%) in water (10 mL) were sonicated at 50 °C for 15–20 minutes. After the completion of the reaction (TLC check), the reaction mixture was cooled to room temperature and extracted using ethyl acetate (2 × 5 mL). The organic layer was dried over anhydrous Na₂SO₄ and concentrated under reduced pressure to give the crude product, which was purified by column chromatography using ethyl acetate: *n*-hexane (10-30%) as the eluent to yield the pure product.

3-((2-Chlorophenyl)(1H-indol-3-yl)methyl)-1H-indole (3j)⁶⁰

Pink solid; Mp: 72–74 °C; IR (KBr): 3412, 3057, 1624, 1456, 1419, 1338, 1037, 742 cm⁻¹; ¹H NMR (500 MHz, CDCl₃) δ 7.94 (bs, 2H), 7.42–7.35 (m, 5H), 7.24–7.08 (m, 5H), 7.03–7.0 (m, 2H), 6.66–

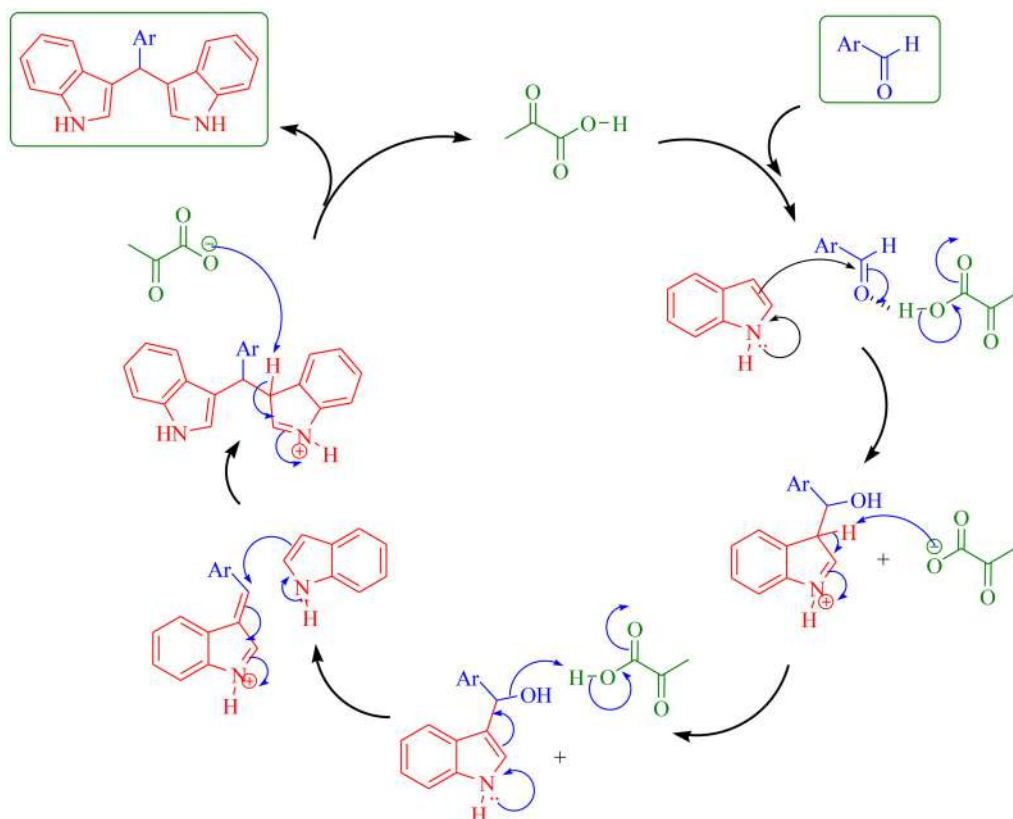


Figure 2. Plausible mechanism for formation of bis(indolyl)methanes catalyzed by pyruvic acid.

6.64 (m, 2H), 6.34 (s, 1H); ^{13}C NMR (126 MHz, CDCl_3) δ 141.28, 136.70, 133.96, 130.31, 129.49, 127.50, 126.98, 126.63, 123.75, 122.03, 119.86, 119.32, 118.38, 111.04, 36.62; HRMS (ESI) m/z : calcd for $\text{C}_{23}\text{H}_{16}\text{ClN}_2$ $[\text{M}-\text{H}]^+$ 355.10 found 355.1007.

The supporting material contains the spectral characterization data. This material can be found via the 'Supplementary Content' section of this article's webpage.

Conclusion

In conclusion, an efficient and green protocol has been introduced for the synthesis of BIMs derivatives using pyruvic acid as a catalyst in the presence of water. The advantage of this synthetic methodology is that it is green, eco-friendly, uses commercially available catalyst, has shorter reaction times, Lewis acid-free and transition metal-free mild reaction conditions and is compatible with a wide range of electronically diverse substrates. The reactions when carried out under ultrasonic conditions in short reaction durations produce the corresponding products from good to excellent yields. Therefore, pyruvic acid in water as a catalyst under ultrasound radiation can be a good alternative to synthesize BIMs than some of the traditional methods.

Acknowledgements

We acknowledge financial support from ASPIRE Research Mentorship Grant (Project No: 18TEC000760) Savitribai Phule Pune University, Pune-411 007, MS, India. We thank Dr R. J. Barnabas (Ahmednagar College, Ahmednagar) for his helpful discussion and suggestions.

Disclosure statement

The authors declare no conflict of interest, financial or otherwise.

ORCID

Santosh R. Deshmukh  <http://orcid.org/0000-0001-6095-8083>

Shankar R. Thopate  <http://orcid.org/0000-0001-5092-0196>

References

1. M. Shiri, M. A. Zolfigol, H. G. Kruger, and Z. Tanbakouchian, "Bis- and Trisindolylmethanes (BIMs and TIMs)," *Chemical Reviews* 110, no. 4 (2010): 2250–93.
2. P. P. Kaishap, and C. Dohutia, "Synthetic Approaches for Bis (Indolyl) Methanes," *International Journal of Pharmaceutical Sciences and Research* 4, no. 4 (2013): 1312–22. <http://citeseerx.ist.psu.edu/viewdoc/download?doi=10.1.1.301.5850&rep=rep1&type=pdf>.
3. (a) T. Fukuyama, and X. Chen, "Stereocontrolled Synthesis of (-)-Hapalindole G," *Journal of the American Chemical Society* 116, no. 7 (1994): 3125–3126. (b) A. O. Abdelhamid, S. M. Gomha, and S. M. Kandeel, "Synthesis of Certain New Thiazole and 1,3,4 Thiadiazole Derivatives via the Utility of 3-Acetylindole," *Journal of Heterocyclic Chemistry* 54, no. 2 (2017): 1529–1536. <https://doi.org/10.1002/jhet.2740>.
4. (a) M. Mari, A. Tassoni, S. Lucarini, M. Fanelli, G. Piersanti, and G. Spadoni, "Brønsted Acid Catalyzed Bisindolization of α -Amido Acetals: Synthesis and Anticancer Activity of Bis(indolyl)ethanamino Derivatives," *European Journal of Organic Chemistry* 2014, no. 18 (2014): 3822–3830. (b) A. O. Abdelhamid, S. M. Gomha, N. A. Abdelriheem, S. M. Kandeel, "Synthesis of New 3-Heteroarylindoles as Potential Anticancer Agents," *Molecules* 21, no. 7 (2016): 929. <https://doi.org/10.3390/molecules21070929>.
5. (a) S. Sarva, J. S. Harinath, S. P. Sthanikam, S. Ethiraj,; M. Vaithiyalingam,; S.R. Cirandur, "Synthesis Antibacterial and Anti-Inflammatory Activity of Bis(indolyl)methanes," *Chinese Chemical Letters* 27, no. 1 (2016), 16–20. (b) S. M. Gomha, S. M. Riyadh, "Synthesis under Microwave Irradiation of [1,2,4]Triazolo[3,4-b][1,3,4]thiadiazoles and Other Diazoles Bearing Indole Moieties and Their Antimicrobial Evaluation," *Molecules* 16, no. 10 (2011): 8244–8256. <https://doi.org/10.3390/molecules16108244>. (c) F. B. Essa, A. Bazbouz, S. Alhilal, S. A. Uof, S. M. Gomha, "Synthesis and Biological Evaluation of an Indole Core-Based Derivative with Potent Antimicrobial Activity," *Research on Chemical Intermediates* 44, no. 9 (2018): 5345–5356. <https://doi.org/10.1007/s11164-018-3426-9>. (d) I. M. Abbas, S. M. Riyadh, M. A. Abdallah, S. M. Gomha, "A novel Route to Tetracyclic Fused Tetrazines and Thiadiazines," *Journal of Heterocyclic Chemistry* 43, no. 4 (2006): 935–942. <https://doi.org/10.1002/jhet.5570430419>.
6. G. Sivaprasad, P. T. Perumal, V. R. Prabavathy, and N. Mathivanan, "Synthesis and anti-Microbial Activity of pyrazolylbisindoles-Promising anti-Fungal Compounds," *Bioorganic & Medicinal Chemistry Letters* 16, no. 24 (2006): 6302–5.
7. K. V. Sashidhara, A. Kumar, M. Kumar, A. Srivastava, and A. Puri, "Synthesis and Antihyperlipidemic Activity of Novel Coumarin Bisindole Derivatives," *Bioorganic & Medicinal Chemistry Letters* 20, no. 22 (2010): 6504–7.
8. K. Sujatha, P. T. Perumal, D. Muralidharan, and M. Rajendran, "Synthesis, Analgesic and Anti-Inflammatory Activities of Bis(Indolyl)methanes," *Indian Journal of Chemistry* 48B (2009): 267–72. <http://nopr.niscair.res.in/handle/123456789/3432>.
9. Y. Gong, G. L. Firestone, and L. F. Bjeldanes, "3,3'-Diindolylmethane is a Novel Topoisomerase II α Catalytic Inhibitor that Induces S-Phase Retardation and Mitotic Delay in Human Hepatoma HepG2 Cells," *Molecular Pharmacology* 69, no. 4 (2006): 1320–7.
10. T. Osawa, and M. Namiki, "Structure Elucidation of Streptindole, a Novel Genotoxic Metabolite Isolated from Intestinal Bacteria," *Tetrahedron Letters*. 24, no. 43 (1983): 4719–22.
11. S. B. Bharate, J. B. Bharate, S. I. Khan, B. L. Tekwani, M. R. Jacob, R. Mudududdla, R. R. Yadav, B. Singh, P. R. Sharma, S. Maity, et al. "Discovery of 3,3'-Diindolylmethanes as Potent Antileishmanial Agents," *European Journal of Medicinal Chemistry* 63 (2013): 435–43.
12. M. Kobayashi, S. Aoki, K. Gato, K. Matsunami, M. Kurosu, and I. Kitagawa, "Marine Natural Products XXXIV Trisindoline, a New Antibiotic Indole Trimer, Produced by a Bacterium of *Vibrio* sp. separated from the Marine Sponge *Hyrtios* Altum," *Chemical & Pharmaceutical Bulletin* 42, no. 12 (1994): 2449–51.
13. C. Bonnesen, I. M. Eggleston, and J. D. Hayes, "Dietary Indoles and Isothiocyanates That Are Generated from Cruciferous Vegetables Can Both Stimulate Apoptosis and Confer Protection against DNA Damage in Human Colon Cell Lines," *Cancer Research* 61, no. 16 (2001): 6120–30. <https://cancerres.aacrjournals.org/content/61/16/6120.short>.

14. R. Martinez, A. Espinosa, A. Tarraga, and P. Molina, "Bis(Indolyl)Methane Derivatives as Highly Selective Colourimetric and Ratiometric Fluorescent Molecular Chemosensors for Cu²⁺ Cations," *Tetrahedron* 64, no. 9 (2008): 2184–91.
15. R. Pegu, R. Mandal, A. K. Guha, and S. Pratihari, "A Selective Ratiometric Fluoride Ion Sensor with a (2,4-Dinitrophenyl) Hydrazine Derivative of Bis (Indolyl) Methane and Its Mode of Interaction," *New Journal of Chemistry* 39, no. 8 (2015): 5984–90.
16. X. He, S. Hu, K. Liu, Y. Guo, J. Xu, and S. Shao, "Oxidized Bis(Indolyl)Methane: A Simple and Efficient Chromogenic-Sensing Molecule Based on the Proton Transfer Signaling Mode," *Organic Letters* 8, no. 2 (2006): 333–6.
17. D. Sain, C. Kumari, A. Kumar, and S. Dey, "Indole-Based Distinctive Chemosensors for 'Naked-Eye' Detection of CN and HSO₄⁻, Associated with Hydrogen-Bonded Complex and Their DFT Study," *Supramolecular Chemistry* 28, no. 3–4 (2016): 239–48.
18. R. Nagarajan, and P. T. Perumal, "InCl₃ and in(OTf)₃ Catalyzed Reactions: synthesis of 3-Acetyl Indoles, Bis-Indolylmethane and Indolylquinoline Derivatives," *Tetrahedron* 58, no. 6 (2002): 1229–32.
19. J. Beltrá, M. C. Gimeno, and R. P. Herrera, "A New Approach for the Synthesis of Bisindoles through AgOTf as Catalyst," *Beilstein Journal of Organic Chemistry* 10 (2014): 2206–14.
20. D. Chen, L. Yu, and P. G. Wang, "Lewis Acid-Catalyzed Reactions in Protic Media. Lanthanide-Catalyzed Reactions of Indoles with Aldehydes or Ketones," *Tetrahedron Letters* 37, no. 26 (1996): 4467–70.
21. J. S. Yadav, B. V. S. Reddy, C. V. S. R. Murthy, G. M. Kumar, and C. Madan, "Lithium Perchlorate Catalyzed Reactions of Indoles: An Expedient Synthesis of Bis(Indolyl)Methanes," *Synthesis* 2001, no. 05 (2001): 0783–7.
22. G. Gupta, G. Chaudhari, P. Tomar, Y. Gaikwad, R. Azad, G. Pandya, G. Waghulde, and K. Patil, "Synthesis of Bis(Indolyl)Methanes Using Molten N-Butylpyridinium Bromide," *European Journal of Chemistry* 3, no. 4 (2012): 475–9.
23. H. Veisi, B. Maleki, F. H. Eshbala, H. Veisi, R. Masti, S. S. Ashrafi, and M. Baghayeri, "In Situ Generation of Iron(III) Dodecyl Sulfate as Lewis Acid-Surfactant Catalyst for Synthesis of Bis-Indolyl, Tris-Indolyl, Di(Bis-Indolyl), Tri(Bis-Indolyl), Tetra(Bis-Indolyl)Methanes and 3-Alkylated Indole Compounds in Water," *RSC Advances* 4, no. 58 (2014): 30683–8.
24. Z. K. Jaber, and L. Zarei, "Rapid Synthesis of 2-Substituted-2,3-Dihydro-4(1H)-Quinazolinones Using Boric Acid or Sodium Dihydrogen Phosphate under Solvent-Free Conditions," *South African Journal of Chemistry* 65 (2012): 36–8. <https://www.ajol.info/index.php/sajc/article/view/123758>.
25. X. Cheng, S. Vellalath, R. Goddard, and B. Lis, "Direct Catalytic Asymmetric Synthesis of Cyclic Aminals from Aldehydes," *Journal of the American Chemical Society* 130, no. 47 (2008): 15786–7.
26. A. G. Choghamarani, and T. Taghipour, "Green and One-Pot Three-Component Synthesis of 2,3-Dihydroquinazolin-4(1H)-Ones Promoted by Acetic Acid as Recoverable Catalyst in Water," *Letters in Organic Chemistry* 8, no. 7 (2011): 470–6.
27. R. A. Bunce, and B. Nammalwar, "New Conditions for Synthesis of (±)-2-Monosubstituted and (±)-2,2-Disubstituted 2,3-Dihydro-4(1H)-Quinazolinones from 2-Nitro- and 2-Aminobenzamide," *Journal of Heterocyclic Chemistry* 48, no. 5 (2011): 991–7.
28. A. Rostami, and A. Tavakoli, "Sulfamic Acid as a Reusable and Green Catalyst for Efficient and Simple Synthesis of 2-Substituted-2,3-Dihydroquinazolin-4(1H)-Ones in Water or Methanol," *Chinese Chemical Letters* 22, no. 11 (2011): 1317–20.
29. J. Zhou, and J. Fang, "One-Pot Synthesis of Quinazolinones via Iridium-Catalyzed Hydrogen Transfers," *The Journal of Organic Chemistry* 76, no. 19 (2011): 7730–6.
30. N. B. Darvatkar, S. V. Bhilare, A. R. Deorukhkar, D. G. Raut, and M. M. Salunkhe, "HSO₄: An Efficient and Reusable Catalyst for One-Pot Three-Component Synthesis of 2,3-Dihydro-4(1H)-Quinazolinones," *Green Chemistry Letters and Reviews* 3, no. 4 (2010): 301–6.
31. J. Chen, W. Su, H. Wu, M. Liu, and C. Jin, "Eco-Friendly Synthesis of 2,3-Dihydroquinazolin-4(1H)-Ones in Ionic Liquids or Ionic Liquid–Water without Additional Catalyst," *Green Chemistry* 9, no. 9 (2007): 972–5.
32. A. Shaabani, A. Maleki, and H. Mofakham, "Click Reaction: Highly Efficient Synthesis of 2,3-Dihydroquinazolin-4(1H)-Ones," *Synthetic Communications* 38, no. 21 (2008): 3751–9.
33. A. Davoodnia, S. Allameh, A. R. Fakhari, and T. Hoseini, "Highly Efficient Solvent-Free Synthesis of Quinazolin-4(3H)-Ones and 2,3-Dihydroquinazolin-4(1H)-Ones Using Tetrabutylammonium Bromide as Novel Ionic Liquid Catalyst," *Chinese Chemical Letters* 21, no. 5 (2010): 550–3.
34. L. Y. Zeng, and C. Cai, "Iodine: Selectively Promote the Synthesis of Mono Substituted Quinazolin-4(3H)-Ones and 2,3-Dihydroquinazolin-4(1H)-Ones in One-Pot," *Journal of Heterocyclic Chemistry* 47, no. 5 (2010): 1035–9.
35. J. Chen, D. Wu, F. He, M. Liu, H. Wu, J. Ding, and W. Su, "Gallium(III) Triflate-Catalyzed One-Pot Selective Synthesis of 2,3-Dihydroquinazolin-4(1H)-Ones and Quinazolin-4(3H)-Ones," *Tetrahedron Letters* 49, no. 23 (2008): 3814–8.
36. R. A. Qiao, B. L. Xu, and Y. H. Wang, "A Facile Synthesis of 2-Substituted-2,3-Dihydro-4(1H)-Quinazolinones in 2,2,2-Trifluoroethanol," *Chinese Chemical Letters* 18, no. 6 (2007): 656–8.

37. M. L. Deb, and P. J. Bhuyan, "An Efficient and Clean Synthesis of Bis(Indolyl)Methanes in a Protic Solvent at Room Temperature," *Tetrahedron Letters* 47, no. 9 (2006): 1441–3.
38. D. Shi, L. Rong, J. Wang, Q. Zhuang, X. Wang, and H. Hu, "Synthesis of Quinazolin-4(3H)-Ones and 1,2-Dihydroquinazolin-4(3H)-Ones with the Aid of a Low-Valent Titanium Reagent," *Tetrahedron Letters* 44, no. 15 (2003): 3199–201.
39. L.-P. Mo, Z.-C. Ma, and Z.-H. Zhang, "CuBr₂-Catalyzed Synthesis of Bis(Indolyl)Methanes," *Synthetic Communications* 35, no. 15 (2005): 1997–2004.
40. D. Sun, G. Jiang, Z. Xie, and Z. Le, "α-Chymotrypsin-Catalyzed Synthesis of Bis(Indolyl)Alkanes in Water," *Chinese Journal of Chemistry* 33, no. 4 (2015): 409–12.
41. B. Sadeghi, F. A. Tavasoli, and A. Hassanabadi, "Ag Nanoparticles: An Efficient and Versatile Reagent for Synthesis of Bis(Indolyl)Methanes," *Synthesis and Reactivity in Inorganic Metal* 45, no. 9 (2015): 1396–400.
42. S. R. Mendes, S. Thurow, F. Penteado, M. S. Da Silva, R. A. Gariani, G. Perin, and E. J. Lenardao, "Synthesis of Bis(Indolyl)Methanes Using Ammonium Niobium Oxalate (ANO) as an Efficient and Recyclable Catalyst," *Green Chemistry* 17, no. 8 (2015): 4334–9.
43. C. C. Silveira, S. R. Mendes, F. M. Líbero, E. J. Lenardao, and G. Perin, "Glycerin and CeCl₃·7H₂O: A New and Efficient Recyclable Medium for the Synthesis of Bis(Indolyl)Methanes," *Tetrahedron Letters* 50, no. 44 (2009): 6060–3.
44. J.-T. Li, H.-G. Dai, W.-Z. Xu, and T.-S. Li, "An Efficient and Practical Synthesis of Bis(Indolyl)Methanes Catalyzed by Aminosulfonic Acid under Ultrasound," *Ultrasonics Sonochemistry* 13, no. 1 (2006): 24–7.
45. S.-J. Ji, S.-Y. Wang, Y. Zhang, and T.-P. Loh, "Facile Synthesis of Bis(Indolyl)Methanes Using Catalytic Amount of Iodine at Room Temperature under Solvent-Free Conditions," *Tetrahedron* 60, no. 9 (2004): 2051–5.
46. M. Zahran, Y. Abdin, and H. Salama, "Eco-Friendly and Efficient Synthesis of Bis(Indolyl)Methanes under Microwave Irradiation," *Arkivoc* 2008, no. 11 (2008): 256–65.
47. N. Seyedi, and M. Kalantari, "An Efficient Green Procedure for the Synthesis of Bis (Indolyl) Methanes in Water," *Journal of Sciences, Islamic Republic Of Iran* 24, no. 3 (2013): 205–8.
48. L. Malkania, P. Bedi, and T. Pramanik, "Lactic Acid Catalyzed and Microwave-Assisted Green Synthesis of Pharmaceutically Important Bis(Indolyl) Methane Analogs in Aqueous Medium," *Drug Invention Today* 10, no. 9 (2018): 1740–1744.
49. N. D. Kokare, J. N. Sangshetti, and D. B. Shinde, "Oxalic Acid as a Catalyst for Efficient Synthesis of Bis(Indolyl)Methanes and 14-Aryl-14H-Dibenzo[a,j]Xanthenes in Water," *Chinese Chemical Letters* 19, no. 10 (2008): 1186–9.
50. S. B. Kasar, and S. R. Thopate, "Synthesis of Bis(Indolyl)Methanes Using Naturally Occurring, Biodegradable Itaconic Acid as a Green and Reusable Catalyst," *Current Organic Synthesis* 15, no. 1 (2018): 110–5.
51. J. Bayardon, J. Holz, B. Schaffner, V. Andrushko, S. Verevkin, A. Preetz, and A. Borner, "Propylene Carbonate as a Solvent for Asymmetric Hydrogenations," *Angewandte Chemie (International ed. in English)* 46, no. 31 (2007): 5971–4.
52. P. G. Jessop, "Searching for Green Solvents," *Green Chemistry* 13, no. 6 (2011): 1391–8.
53. Z. Zhang, J. Song, and B. Han, "Catalytic Transformation of Lignocellulose into Chemicals and Fuel Products in Ionic Liquids," *Chemical Reviews* 117, no. 10 (2017): 6834–80.
54. (a) S. M. Gomha, and K. D. Khalil, "A Convenient Ultrasound-Promoted Synthesis of Some New Thiazole Derivatives Bearing a Coumarin Nucleus and Their Cytotoxic Activity," *Molecules* 17, no. 8 (2012): 9335–9347. (b) F. S. Elsharabasy, S. M. Gomha, T. A. Farghaly, H. S. A. Elzahabi, "An Efficient Synthesis of Novel Bioactive Thiazolyl-Phthalazinediones under Ultrasound Irradiation," *Molecules* 22, no. 2 (2017) 319. <https://doi.org/10.3390/molecules22020319>.
55. R. T. Stanko, D. L. Tietze, and J. E. Arch, "Body Composition, Energy Utilization, and Nitrogen Metabolism with a 4.25-MJ/d low-energy diet supplemented with pyruvate," *The American Journal of Clinical Nutrition* 56, no. 4 (1992): 630–5.
56. R. T. Stanko, H. R. Reynolds, R. Hoyson, J. E. Janosky, and R. Wolf, "Pyruvate Supplementation of a Low-Cholesterol, Low-Fat Diet: effects on Plasma Lipid Concentrations and Body Composition in Hyperlipidemic Patients," *The American Journal of Clinical Nutrition* 59, no. 2 (1994): 423–7.
57. R. T. Stanko, R. J. Robertson, R. W. Galbreath, J. J. Reilly, K. D. Greenawalt, Jr, and F. L. Goss, "Enhanced Leg Exercise Endurance with a High-Carbohydrate Diet and Dihydroxyacetone and Pyruvate," *Journal of Applied Physiology (Bethesda, Md. : 1985)* 69, no. 5 (1990): 1651–6.
58. L. W. DeBoer, P. A. Bekx, L. Han, and L. Steinke, "Pyruvate Enhances Recovery of Rat Hearts after Ischemia and Reperfusion by Preventing Free Radical Generation," *The American Journal of Physiology* 265, no. 5 Pt 2 (1993): H1571–1576.
59. A. B. Borle, and R. T. Stanko, "Pyruvate Reduces Anoxic Injury and Free Radical Formation in Perfused Rat Hepatocytes," *The American Journal of Physiology* 270, no. 3 Pt 1 (1996): G535–540.
60. B. R. Nemallapudi, G. V. Zyryanov, B. Avula, M. R. Guda, and S. Gundala, "An Effective Green and Ecofriendly Catalyst for Synthesis of Bis(Indolyl)Methanes as Promising Antimicrobial Agents," *Journal of Heterocyclic Chemistry* 56, no. 12 (2019): 3324–32.



A Review on Synthesis, Characterization and Applications of Cadmium Ferrite and its Doped Variants

ARUN VIJAY BAGADE¹, PRATIK ARVIND NAGWADE², ARVIND VINAYAK NAGAWADE¹, SHANKAR RAMCHANDRA THOPATE³ and SANGITA NANASAHEB PUND^{1*}

¹Department of Chemistry, Ahmednagar College, Ahmednagar (MS), India.

²Department of Chemistry, Shri Anand College, Pathardi, Ahmednagar (MS), India.

³Department of Chemistry, SSGM, Kopargaon, Ahmednagar (MS), India.

*Corresponding author E-mail: sangitapund2@gmail.com

<http://dx.doi.org/10.13005/ojc/380101>

(Received: January 01, 2022; Accepted: February 02, 2022)

ABSTRACT

Ferrites have gained a lot of attention because of their diverse uses in domains including photocatalytic degradations, gas sensors, electronic devices, organic transformation catalysts, adsorption, and so on. This review focuses on cadmium ferrites and their numerous doped versions' production methodologies, characterization, and applications. The structural, electric, magnetic, and dielectric properties of cadmium ferrites are primarily influenced by the synthesis procedures and circumstances used during preparation. As a result, the main goal of this study was to provide the most often used synthesis processes, such as hydrothermal, co-precipitation, solvothermal, microwave-assisted, micro-emulsion, and solid state, as well as their benefits and drawbacks. Furthermore, the review focuses on the numerous characterization approaches used to investigate features such as optical, structural, magnetic, electric, and dielectric properties of cadmium ferrites. This analysis was further expanded to include applications in some of the most well-studied domains, such as photocatalysis and gas sensing.

Keywords: Cadmium ferrites, Synthesis, Characterization, Applications, Spinel.

INTRODUCTION

Alloy chemistry has gotten a lot of attention because they were first used in 2500 BC, much before the Bronze Age¹. Two or more elements, at least one of which is a metal, combine in varying amounts to generate a binary or ternary single intermetallic phase that is difficult to differentiate from the base metal used. Because of the lower cost and improved structural, electrical, and

magnetic qualities, as produced composites outperform their parent. The term ferrite refers to a category of iron oxide compounds that are ferromagnetic in nature and have high permeability and resistance². The oldest ferrite substance known to prehistoric humans was magnetite (Fe₃O₄). Because of their wide range of applications in numerous fields, ferrites are thoroughly explored. Drug administration, magnetic resonance imaging, gas sensing, magnetic fluids, catalysis, magnetic



recorders, transducers, and electromagnetic wave absorbers are just a few of the promising uses³. Ferrites are classified as spinel [General formula: MFe_2O_4], magnetoplumbite or hexaferrite [General formula: $MFe_{12}O_{19}$], and garnet [General formula: $M_3Fe_5O_{12}$] depending on crystal forms⁴⁻⁵.

Ferrites are chemical compounds that contain at least one iron(III) ion in their chemical formula. The chemical formula for spinel ferrites is $M^{II}Fe^{III}_2O_4$, where M and Fe represent divalent and trivalent metal ions, respectively. The oxygen ions (blue spheres) in the spinel structure are tightly packed in a face-centered cubic lattice, resulting in two types of interstitial voids for the metal ions, namely tetrahedral (A) (green spheres) and octahedral (B) (red spheres)⁶, as illustrated in reproduced Figure 1.

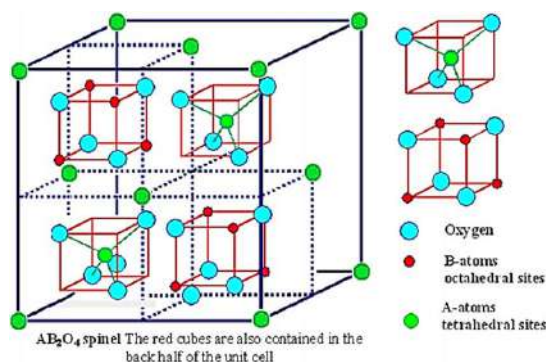


Fig. 1. Cubic cell of spinel structure showing tetrahedral & octahedral voids. (Copyright: License No. Open Access)⁶

The $M^{II}Fe^{III}_2O_4$ spinel ferrite includes 8 tetrahedral and 16 octahedral sites for the residence of divalent and trivalent metal ions⁷. According to the cation distribution (divalent and trivalent) across tetrahedral and octahedral sites, ferrites are classed as Normal, Inverse, or Mixed kinds. Consider the usual formula of ferrite as $(M_{1-x}^{2+})(Fe_x^{3+})[M_x^{2+}Fe_{2-x}^{3+}]O_4$ to shed light on this classification, where x denotes the degree of inversion and ions outside and within the square bracket occupy A and B sites, respectively. The ferrite is known as normal spinel when $x = 0$ in the preceding formula. The ferrite is known as inverse spinel when $x = 1$ in the preceding formula. Finally, when $0 < x < 1$ is present, the ferrite is known as mixed spinel⁸.

$ZnFe_2O_4$ is an example of normal spinel ferrite, whereas $NiFe_2O_4$ and Fe_3O_4 are inverse spinel ferrites. Mixed spinel ferrite $MnFe_2O_4$ ($Mn_{0.8}Fe_{0.2}[Mn_{0.2}Fe_{1.8}]O_4$) is an example⁹. The current study examined the benefits and drawbacks of the most regularly used cadmium ferrites production techniques. This review also discusses numerous characterization

strategies. Finally, the current research looks at the wide range of uses for cadmium ferrites.

Synthesis

Due to the wide range of uses, there is a lot of research going on in the subject of cadmium ferrite synthesis. Despite this, additional study is needed to synthesize cadmium ferrites that are high in purity, have a regulated size and morphology. There is no complete method for ferrite synthesis published, and most commonly used synthesis procedures have their own strengths and drawbacks. "Bottom-up" and "top-down" synthesis strategies are the two types of synthesis strategies. The atoms/ions/molecules are put together to manufacture nanoparticles in the "bottom-up" technique, whereas bulk solids are broken down to nano-sizes in the "top-down" approach, as shown in reproduced Fig. 2^{10,51}. Fig. 3 depicts a summary of the cadmium ferrites production methods used.

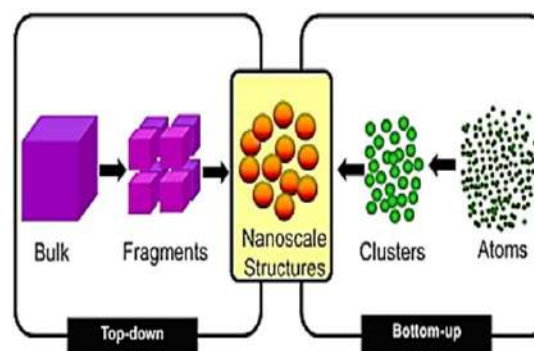


Fig. 2. "Bottom-up" and "Top-down" synthesis strategies. (Copyright: License No. 5052030388527)^{10,51}

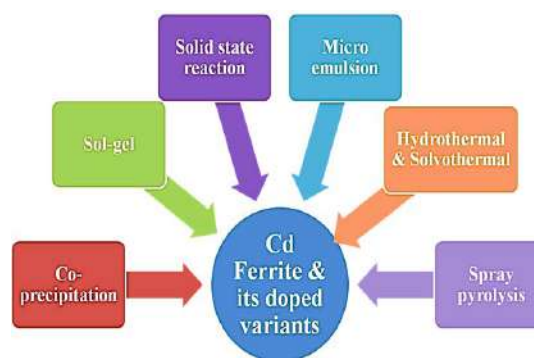


Fig. 3. Flow chart for various synthesis routes for cadmium ferrites

Co-precipitation

To synthesize uniform size ferrites, it is the most widely used convenient, inexpensive, efficient, and environmentally friendly approach¹¹. The aqueous solutions of divalent and trivalent metal ions are combined in a mole ratio of 1:2 in the co-precipitation process. Metal ions in the form

of nitrates, sulphates, chlorides, and tartrates, carbonates, oxalates, citrates, or hydroxides are co-precipitated from an aqueous medium as tartrates, carbonates, oxalates, citrates, or hydroxides using the appropriate precipitants. Using NaOH or ammonia solution, this procedure includes a precise and controlled pH change. Following that, the solution is vigorously agitated under inert conditions in the absence or presence of heat. The breakdown temperatures of the precipitate as obtained are lower than those used in solid-state processes. After drying, the precipitate is calcined to the required temperature to generate cadmium ferrite nanoparticles. Despite its advantages, co-precipitation has significant drawbacks, such as difficulty controlling pH. Fig. 4 shows a general schematic diagram for the manufacture of Cd ferrites and their doped variants.

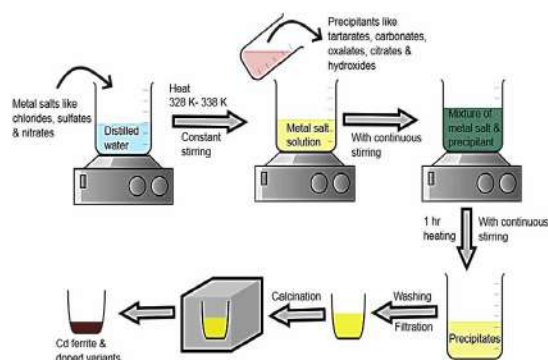


Fig. 4. General schematic diagram for Cd ferrites and its doped variant synthesis by co-precipitation

The selected examples of co-precipitations where CdFe_2O_4 and its doped variation are synthesized are shown in Table 1.

Table 1: Selected examples of co-precipitations

Entry No	Cd ferrite and its doped variants synthesized	Co-precipitant used	Method description	Reference
1	CdFe_2O_4	NaOH	Aqueous solutions of Cd chloride (0.1 mol/l) and iron (III) chloride (0.2 mol/l) mixed together and pH is adjusted to 13 by NaOH (3 mol/l). The reaction mixture boiled at 100°C for 0.5 hours. As obtained precipitate washed with DM water, dried at 60°C and finally annealed to get Cd ferrite nano-particles.	[12]
2	$\text{Co}_{0.5}\text{Ni}_{0.5}\text{Cd}_{1-2x}\text{Fe}_{2x}\text{O}_4$ (x=0.0, 0.1, 0.2, 0.3, 0.4 and 0.5)	Liquid ammonia	$\text{CdCl}_2 \cdot \text{H}_2\text{O}$, ZnCl_2 , $\text{FeCl}_3 \cdot 6\text{H}_2\text{O}$ and $\text{CoCl}_2 \cdot 6\text{H}_2\text{O}$ taken in stoichiometric ratio and dissolved in DM water. Liquid ammonia is added to get precipitate which later washed with DM water, dried for 5 h at 90°C. Lastly precipitate sintered at 800°C for 4 hours.	[13]
3	$\text{Cu}_x\text{Cd}_y\text{Fe}_2\text{O}_4$ (x=0, 0.2, 0.4, 0.6, 0.8 and 1)	NaOH	The 3.0 g PVP were dissolved in 100 mL DM water at 353K and this clear solution is added to 0.2 mmol of iron nitrate and 0.10 mmol of mixture of cadmium nitrate and copper nitrate (Cd, Fe:Cu = 1:2). The reaction is maintained for 2 h and later this homogeneous solution transferred to petri dish which is heated 24 hrs at 363K for water evaporation. The dried powder was ground and annealed at 773K for 9 h to get Cu-Cd ferrite.	[14]
4	$\text{Mg}_x\text{Cd}_y\text{Fe}_2\text{O}_4 + 5\% \text{Sm}^{3+}$ (x=0, 0.2, 0.4, 0.6, 0.8, 1.0)	Ammonium oxalate	The $\text{MgSO}_4 \cdot 7\text{H}_2\text{O}$, $\text{FeSO}_4 \cdot 7\text{H}_2\text{O}$ and samarium sulphate are dissolved in distilled water in desired stoichiometry. The pH of the solution is adjusted to 4.8 by conc. H_2SO_4 . The resulting solution was heated to 80°C for 1 h and then ammonium oxalate added under stirring till complete precipitation occurred. The precipitate was filtered and washed several times with water. The precipitate is dried and presintered at 700°C for 6 h and finally sintered at 1050°C for 5 hours.	[15]
5	$\text{Mg}_x\text{Cd}_y\text{Fe}_2\text{O}_4 + 5\% \text{Y}^{3+}$ (x=0, 0.2, 0.4, 0.6, 0.8, 1.0)	Ammonium oxalate	Same as in entry no. 4, only $\text{Y}(\text{SO}_4)_3 \cdot 38\text{H}_2\text{O}$ is used instead of samarium sulphate.	[16]
6	$\text{Cd}_{1-x}\text{Co}_x\text{Fe}_2\text{O}_4$ (x=0.0, 0.2, 0.4, 0.6, 0.8 and 1.0)	Sodium tartarate	The $\text{FeSO}_4 \cdot 7\text{H}_2\text{O}$ and $3\text{CdSO}_4 \cdot 8\text{H}_2\text{O}$ are dissolved in de-ionised water in molar ratio of 2:1. The pH of medium maintained below 6 so avoid hydroxide precipitate formation. Then sodium tartarate is added under vigorous stirring. Acetone was added in equal amounts to ensure high yield and fine-grained powders. The formed precipitate calcined at 700°C for 2 hours.	[17]

Sol-gel

During the silica synthesis in the mid-nineteenth century, chemist J. J. Ebelman first published the sol-gel method. It's a well-known bottom-up wet chemical approach¹⁸. This approach entails two main reactions: (1) hydrolysis of the precursor in an acidic or alkaline medium, and (2) subsequent polycondensation of the hydrolyzed product¹⁹. To make reactive monomers, partial hydrolysis of metal alkoxides or metal chlorides is used. Following that, through condensation, these monomers form colloid-like oligomers (sol formation). In addition, hydrolysis promotes polymerization, which leads to the production of a three-dimensional matrix (gel formation)²⁰. Fig. 5 depicts the primary reactions in the sol-gel technique: metal alkoxide hydrolysis and condensation.

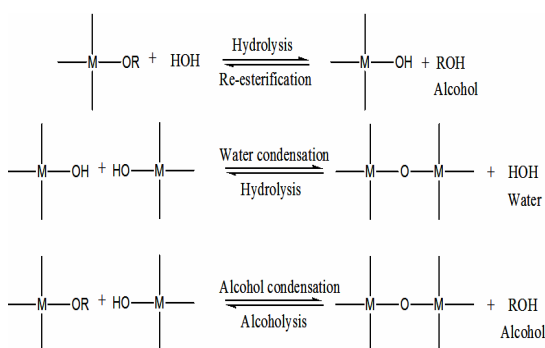


Fig. 5. Sol-gel reaction scheme

The sol-gel process is widely utilized because it is cost-effective, does not require specific equipment, and operates at a temperature range of 25-200°C, which is significantly lower than that of traditional solid-state reactions. The sol-gel process can be used to make ferrites with precise shapes such as microspheres, fibers, and flower-like structures with a limited size distribution. Aside from these appealing properties, key downsides of this technique include lower purity ferrites due to by-product degradation and the usage of organic solutions, which can be hazardous²¹. Fig. 6 depicts the flow chart for ferrite production using the sol-gel method.

The selected instances of the sol-gel approach where CdFe_2O_4 and its doped variation are made are included in Table 2.

Solid State Reactions

Solid-state reactions are commonly used to make polycrystalline solids from a mix of solid reactants. Because a mixture of solids does not react at room temperature for a long period of time, a high temperature is used to initiate the reaction (chemical breakdown of reactants). These reactions

are influenced by morphological and chemical features of the reactants, such as free energy change, surface area, and reactivity²⁹. These reactions aren't just for forming complex oxides; they're also used to create sophisticated materials like piezoelectrics. Physical mixing of simple oxides, hydroxide, nitrates, carbonate, oxalates, alkoxides, sulphate, or other metal salts is followed by high temperature treatment, usually between 1000 and 1500°C, to generate a new solid composition with gas evolution³⁰. Solid-state processes have several advantages, including the ability to create ferrite materials with minimum knowledge of material science, high yield, low pollution, and large-scale production³¹. However, as compared to the above-mentioned coprecipitation approach, the resulting powder has coarse grain size, strong agglomeration, and hence structures with comparatively large particle size, very low surface area, and low homogeneity, all of which are significant negatives. Because of the high temperatures required for solid state reactions, undesired phases develop from time to time, which can be difficult to regulate. Grinding, on the other hand, can introduce contaminants into the powder, causing crystal structural stresses and so affecting magnetic characteristics³².

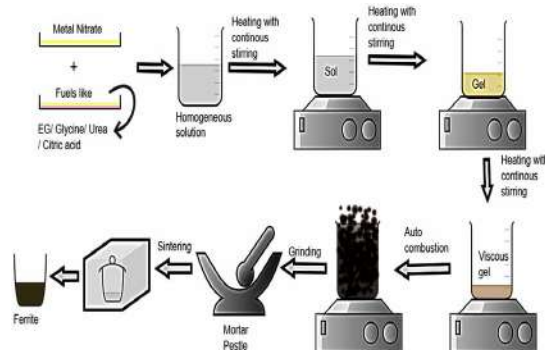


Fig. 6. Flow chart for ferrite synthesis via sol-gel method

The effect of ceria addition on the structural characteristics of Cd ferrite was investigated by Abbas K. Saadon³³. The Cd ferrites were made using the traditional ceramic process, which involved combining Fe_2O_3 and CdO in a 1:1 ratio with acetone. The blended powder was dried in a 500°C oven for 2 hours. The dried and cooled powder was then combined in a ball mill for 1 h before being sintered at 1000°C for 2 hours. By ball milling for 1 h with acetone, CeO_2 (0.5, 0.75, 1.0, 1.5, 2.0, and 2.5 wt percent) was blended with synthetic Cd ferrite. Finally, the powder is pressed with 5% PVA to produce a 20mm diameter pellet that is sintered for 3 h at 1200°C. XRD and SEM methods were used to characterize the produced composites.

Table 2: Selected examples of sol-gel method

Sr. No.	Cd ferrite and its doped variants	Chelating agent or fuel used	Chelating agent/ fuel to nitrate ratio	Method description	Structural properties		Reference
					Lattice constant (Å)	Crystallite size (nm)	
1	$Cd_{1-x}Ni_xFe_2O_4$ ($x=0.0$ & 0.5)	Urea	2.17 : 1	$Cd_{1-x}Ni_xFe_2O_4$ prepared by mixing of aqueous solutions Cd nitrate, Ferric nitrate & Ni nitrate stoichiometric quantities. This homogeneous solution is calcined at 400°C in muffle furnace. At the end, solution get ignited to form foamy ferrite powder.	$CdFe_2O_4=8.432$, $Cd_{0.9}Ni_{0.3}Fe_2O_4=8.417$	$CdFe_2O_4=24.73$, $Cd_{0.9}Ni_{0.3}Fe_2O_4=17.70$	[22]
2	$Cd_{1-x}Ni_xFe_2O_4$ ($x=0.4$ to 0.6)	Urea	Depends on reducing & oxidising element	$Cd_{1-x}Ni_xFe_2O_4$ prepared by mixing of aqueous solutions Cd nitrate, Ferric nitrate, Ni nitrate & urea stoichiometric quantities. This homogeneous solution is then heated for 2 h with stirring to form viscous gel. Then gel is fired in microwave, the burnt ferrite powder cooled and ground for 4 hours. Finally, powder is pressed to form pellet & annealed at 800°C for 4 hours.	$Cd_{0.6}Ni_{0.4}Fe_2O_4=8.612$, $Cd_{0.4}Ni_{0.6}Fe_2O_4=8.518$	$Cd_{0.6}Ni_{0.4}Fe_2O_4=19.48$, $Cd_{0.4}Ni_{0.6}Fe_2O_4=14.47$	[23]
3	$Cd_{0.2}Zn_{0.8-x}Fe_2O_4$ ($x=0.2$ & 0.8)	Urea	Depends on reducing & oxidising element	$Cd_{1-x}Ni_xFe_2O_4$ prepared by mixing of aqueous solutions Cd nitrate, Ferric nitrate, Zn nitrate & urea stoichiometric quantities. This homogeneous solution is then heated at 80°C for 4 h with stirring to form viscous gel. Then gel is fired in microwave in 3 min, the burnt ferrite powder cooled and ground. Finally, powder is pressed to form pellet & annealed at 800°C for 4 hours. CdFe ₂ O ₄ sol is synthesized by dropwise addition of an alcoholic mixture (IPA & Water) to the alcoholic mixture of Ferric nitrate & Cd nitrate (Mole ratio 2:1). The prepared sol is aged for 168 h then heated at 80°C for 48 hrs with stirring & calcined at 400°C for 1 h in air. The calcined powder is ground for 45 min then pressed to form pellet. The pellet is sintered at 600°C for 3 h in air.	$Cd_{0.2}Zn_{0.8}Fe_2O_4=8.51$, $Cd_{0.8}Zn_{0.2}Fe_2O_4=8.67$	$Cd_{0.2}Zn_{0.8}Fe_2O_4=19.48$, $Cd_{0.8}Zn_{0.2}Fe_2O_4=21.42$	[24]
4	$CdFe_2O_4$	Template-assisted sol-gel method	Alcoholic mixture of isopropyl alcohol (5mol) and distilled water (2mol)	The nitrates and citric acid are dissolved in distilled water to form the homogeneous solution. The pH is adjusted to 7.00 by liquid NH ₃ . This solution is then heated at 80°C for 4-5 h with stirring to form sol. Lastly, after auto-combustion ash converted into ferrite powder. The powder finally sintered at 400°C for 2 hours.	---	Average particle size 43 nm	[25]
5	$Mg_xCd_{1-x}Y_yFe_{2-x}O_4$ ($x=0.2, 0.4, 0.6$ and $y=0, 0.075$)	Citric acid	3.0 : 1.0	The nitrates and citric acid are dissolved in distilled water to form the homogeneous solution. The pH is adjusted to 7.00 by liquid NH ₃ . This solution is then heated at 80°C for 4-5 h with stirring to form sol. Lastly, after auto-combustion ash converted into ferrite powder. The powder finally sintered at 400°C for 2 hours.	8.3601 to 8.3658	24.2 to 17.79	[26]
6	$Ni_{0.9}Cd_{0.1}Gd_xFe_{2-x}O_4$ ($x=0, 0.1, 0.2$ and 0.3)	Ethylene glycol	---	The metal nitrates are dissolved in ethylene glycol. The sol is heated 60°C to obtain wet gel. Further wet gel is heated to 120°C for 6 h which is self-ignited to form Ni _{0.9} Cd _{0.1} Gd _x Fe _{2-x} O ₄ powder. Finally, powder is ground & annealed at 400°C for 2 hours.	$Ni_{0.9}Cd_{0.1}Fe_2O_4=0.8402$ nm	---	[27]
7	$Mn_xCd_{1-x}Fe_2O_4$ ($x=0.0, 0.2, 0.4, 0.6, 0.8$)	Citric acid	---	The metal nitrates & citric acid are dissolved in minimum quantity of DM water. The resulting solution is heated 65-70°C to obtain homogeneous form. The pH is adjusted to 7.00 by NH ₃ . Further mixture is heated to 90-95°C to evaporate residual water. The resulting viscous brown gel is self-ignited to form loose fluffy powder. Finally, powder is ground & annealed at 900°C for 5 hours.	8.508 to 8.643	31.214 to 41.856	[28]

Kaimin Shih *et al.*,³⁴ used a solid-state process to explore the formation of $\text{Cd}_x\text{Ni}_{1-x}\text{Fe}_2\text{O}_4$ by integrating Cd and Ni into haematite. Ball-milling was used to mix the precursors CdO, NiO, and $\alpha\text{-Fe}_2\text{O}_3$ for 1.0 hour. The mixed powders were baked in a vacuum oven at 105°C for 24 h before being homogenized in an agate mortar for 10 minutes. Under 250 MPa axial pressure, the dried mixes were crushed into 20mm diameter pellets. Finally, $\text{Cd}_x\text{Ni}_{1-x}\text{Fe}_2\text{O}_4$ particles ($x=0.0, 0.1, 0.3, 0.5, 0.7, 0.9$, and 1.0) were made by sintering formed pellets for 3 h at temperatures ranging from 700 to 950°C.

N. M. Deraz and M. M. Hessien³⁵ used a typical ceramic technique to make pure Cd ferrite and $\text{Al}_2\text{O}_3/\text{MgO}$ doped versions. To produce pure Cd ferrite, an equimolar combination of Cd nitrate and $\alpha\text{-Fe}_2\text{O}_3$ was impregnated, dried, and then thermally treated at 500-1200°C for 3 hours. Cd nitrate, $\alpha\text{-Fe}_2\text{O}_3$, and a calculated amount of aluminum and magnesium nitrate were also dissolved in minimal water, mixed, dried at 100°C, and then calcined for 3 h at 500-1200°C. XRD, DSC, FTIR, SEM, and VSM were used to characterize the pure Cd ferrite and composites formed.

P. B. Belavi *et al.*,³⁶ used the double sintering ceramic process to make $\text{Cd}_{1-x}\text{Ni}_x\text{Fe}_2\text{O}_4$ ($x=0.1, 0.2, 0.3$). As a starting material, CdO, NiO, and Fe_2O_3 were used. In an agate mortar, these precursors were thoroughly combined in the appropriate stoichiometry for several hours. The samples were then pre-sintered at 800°C for 8 h before being cooled to room temperature in the air. After cooling, the samples were milled for one hour. Using a hydraulic press, these homogenized samples were combined with 2-3 drops of PVA as a binder and pressed into a 13mm pellet. Finally, these pellets were sintered for 12 h at 1150°C and cooled to room temperature in the air. XRD, IR, SEM, EDX, and VSM were used to characterize the produced $\text{Cd}_{1-x}\text{Ni}_x\text{Fe}_2\text{O}_4$ particles. The electrical and dielectric characteristics of the material were also assessed.

Figure 7 shows a general schematic diagram for the production of Cd ferrites and their doped variants using a conventional solid-state process.

Microemulsion

Schulman *et al.*, were the first to coin the

term "microemulsion" in 1959. A colloidal suspension that is macroscopically homogeneous, isotropic, and thermodynamically stable is referred to as a microemulsion. With the help of a surfactant, two immiscible liquids exist in a single phase in this approach³⁷. Oil in water (O/W), Water in oil (W/O), and Water in supercritical CO_2 (W/sc- CO_2) are examples of microemulsions. When water (aqueous phase) is dispersed as microdroplets and covered by a monolayer of surfactant molecules in a hydrocarbon-based continuous phase, a Water in Oil (W/O) microemulsion is created (Oil). The Oil in Water (O/W) microemulsion, on the other hand, contains dispersed organic droplets in an aqueous continuous phase, which reduces the need of organic solvent and is thus environmentally friendly. In Fig. 8, the W/O and O/W microemulsions are summarized and reproduced with permission from Maqsood Malik *et al.*, work³⁸.

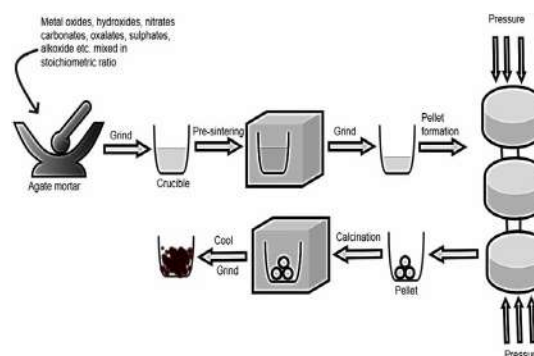


Fig. 7. General schematic diagram for Cd ferrites and its doped variant synthesis by solid-state reaction.

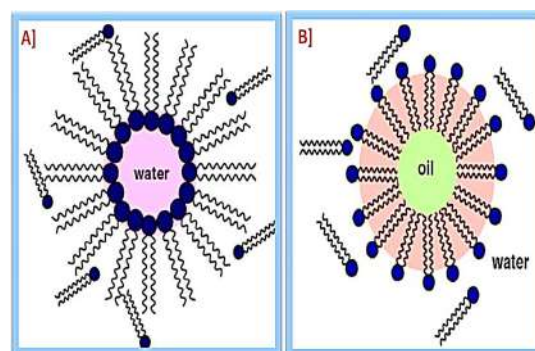


Fig.8 A) W/O microemulsion B) O/W microemulsion. (Copyright: License No. 501647850)³⁸

Zaheer Gilani *et al.*,³⁹ used this approach to make $\text{Co}_{0.5}\text{Cd}_{0.5}\text{Bi}_x\text{Fe}_{2-x}\text{O}_4$ using ($x=0.0, 0.05, 0.1, 0.15, 0.2$, and 0.25). The microemulsion process is straightforward and can create cadmium ferrite with a homogeneous size distribution and regulated

characteristics. Apart from these benefits, this approach has drawbacks such as high cost, limited yield, impurity in adsorbing surfactant on nanoparticle surfaces, and the need for a considerable amount of solvent⁴⁰.

Hydrothermal and Solvothermal method

Roderick Murchison, a British geologist, was the first to create the word "hydrothermal." Inorganic synthesis is dominated by the hydrothermal and solvothermal methods. Chemical reactions in hydrothermal synthesis take place in aqueous solutions above the boiling point of water, but in solvothermal synthesis, non-aqueous solvents are utilized and reactions take place at quite high temperatures. That is to say, hydrothermal and solvothermal procedures are named for the solvent used in the synthesis reaction⁴¹.

The solutions are subjected to high temperatures (almost 200°C) and pressures (usually greater than 125 atm) in high pressure reactors (autoclaves) in this approach⁴². The majority of trivalent transition metal and divalent metal salts are dissolved separately in solvent and then combined in a 2:1 ratio. To make a homogenous solution, solvents such as ethylene glycol or ethanol are added. In a high-pressure reactor, this reaction mixture is subjected to high pressure. The type, particle size, and morphology of ferrite particles are determined by the heating temperature, duration, and pressure⁴³. Low cost, low reaction temperature, ecologically friendly, exclusion from further calcination, narrow particle size distribution, product with excellent magnetic behavior, and practicality for large-scale manufacturing are all advantages of this approach⁴⁴. The slowness of the reaction is a major drawback of the hydrothermal approach. Fig. 9 depicts a general schematic diagram for the hydrothermal/solvothermal approach.

Hydrothermal and solvothermal method are successfully employed for synthesis of CdFe₂O₄ nano powder⁴⁵, CdFe₂O₄-rGO composite^{46,47}, Mn_{1-x}Cd_xFe₂O₄ (X=0.0, 0.1, 0.3 and 0.5) powder⁴⁸, Cd_xNi_{1-x}Al_yFe_{2-y}O₄⁴⁹, CoLi_xCd_xFe_{2-2x}O₄ (x=0.05, 0.1, 0.15, 0.2, 0.25)⁵⁰ and many more.

Spray pyrolysis

Spray pyrolysis is a method of forming a thin coating of cadmium ferrite and its doped variations by spraying a precursor solution over a

heated surface. At the deposition temperature, the reactants are chosen in such a way that by-products are volatile⁵¹. Spray pyrolysis method⁵² has three basic steps: precursor solution preparation, aerosol formation and deposition, and synthesis process. This process has several advantages, including cost effectiveness, equipment simplicity, efficiency, and the ability to generate thin films with a wide substrate surface area. Spray pyrolysis has a number of disadvantages, including vapour convection and poor thin film quality⁵³.

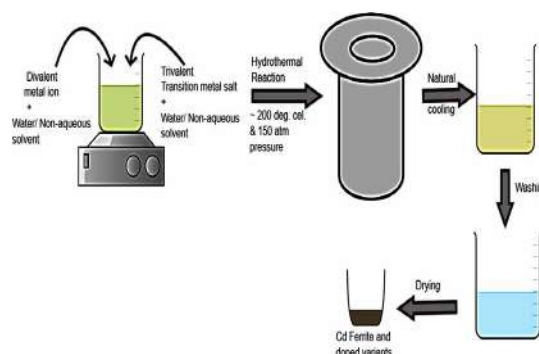


Fig. 9. General schematic diagram for Cd ferrites and its doped variant synthesis by hydrothermal method

The CdFe₂O₄ thin film was made by Veerappan Nagarajan and Arunachalam Thayumanavan and used for electro-resistive detection of formaldehyde and ethanol vapours⁵⁴ and benzene vapours⁵⁵. K. M. Jadhav *et al.*,⁵⁶ synthesized Ni_{1-x}Cd_xFe₂O₄ thin films (where x = 0.0-1.0 in steps of 0.2) by using the following experimental parameters: solution concentration 0.1 M, volumetric ratio 1:2, deposition temperature 360°C, annealing temperature 500°C for 4 hours, spray rate 2 mL/min, distance between substrate and nozzle 25 cm, and air pressure 0.30 MPa.

Characterization Techniques

To investigate the various physicochemical features of cadmium ferrite, various methodologies for characterization of nano ferrite are required. Thermogravimetry and Differential Thermal Analysis (TG-DTA), Fourier Transform Infrared Radiation spectroscopy (FT-IR), UV-Vis spectroscopy, Vibrating Sample Magnetometer (VSM), Dynamic Light Scattering (DLS), Brunauer-Emmett-Teller (BET), Transmission Electron Microscopy (TEM), and Scanning Electron Microscopy (SEM) are some of the techniques used.

X-ray Diffractometry

Max von Laue was the first to propose the XRD technique in 1912. The XRD technique can be used to analyse attributes such as crystalline grain size, crystalline phase presence, phase composition, XRD density, flaws and stresses present in the crystal, lattice parameter, and unit cell characterisation. This method uses constructive X-ray interference with a crystalline material. X-rays are generated using a cathode ray tube and then filtered to produce monochromatic X-rays in this process. The monochromatic X-ray beam produced is focused on the Cadmium ferrite sample. After that, the diffracted rays' scattering angles and intensities are recognised, processed, and shown as peaks in an XRD graph⁵⁷.

A well-known and simple expression called Debye-Scherrer equation is used to obtain the crystallite size as follows⁵⁸:

$$D = 0.9\lambda/\beta\cos\theta$$

Where, D=crystallite size (in nm), λ =X-ray wavelength ($\lambda=1.5406 \text{ \AA}$), θ =Bragg's angle (in radians), β =full width at half maximum of the peak (in radians).

The lattice parameter (a) is calculated by applying following formula⁵⁹:

$$d = \frac{a}{\sqrt{h^2 + k^2 + l^2}}$$

Where, d=interplanar distance, while, h, k and l are the miller indices.

By using lattice parameter value, true density (X-ray density) is calculated by following relation⁵⁹:

$$D_x = \frac{8M}{Na^3}$$

Where, M=Molecular weight of the sample, N=Avagadro number, a=lattice parameter.

Furthermore, the porosity (p) of the ferrite sample is can be calculated as follows⁵⁹:

$$p = 1 - \frac{D}{D_x}$$

Where, D=apparent density of the sample

which is calculated by Archimedes principle i.e. by weighing the ferrite sample and dividing by its apparent volume.

The reproduced Fig. 10 shows representative XRD of Ni-Zn ferrite synthesized by the ceramic method by P. S. Patil *et al.*,⁶⁰.

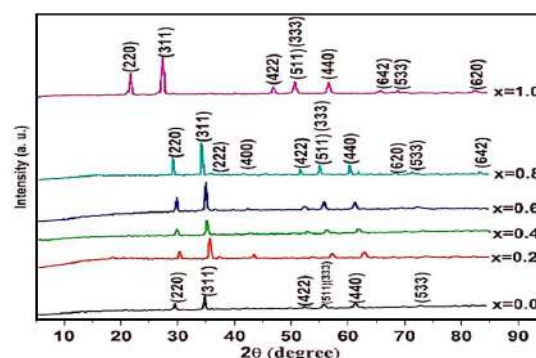


Fig. 10. XRD patterns of $Cd_xNi_{1-x}Fe_2O_4$ samples. (Copyright: License No. 5052631255642)⁶⁰

Fourier Transform Infrared Spectroscopy

It is the most widely used method for determining the functional groups of produced Cd ferrites. To do this, the sample is bombarded with IR between 400 and 4000 cm^{-1} , and the absorbance of these radiations by ferrite is measured to determine the molecular structure. It's worth noting that IR radiation rarely generates electrical excitation; instead, it induces vibration excitation, which means that the bond joining atoms or groups of atoms vibrates faster. The FT-IR spectrometer produces an IR spectrum by plotting the substance's absorbance of infrared light against its wavelength⁶¹. The reproduced Fig. 11 shows a sample FT-IR spectrum of yttrium substituted Cd ferrite prepared by Muhammad Imran Arshad *et al.*,⁶² using the co-precipitation method.

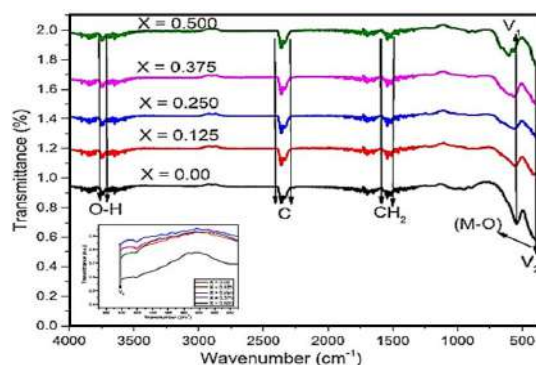


Fig. 11. FT-IR spectrum of $Cd_{1-x}Y_xFe_2O_4$ (X=0.00, 0.125, 0.250, 0.375, 0.500) (Copyright: License No. 5052681041074)⁶²

The lower and upper frequency bands (ν_2 and ν_1) in the ranges of 540.95 to 565.71 cm^{-1} and 419.31 to 417.02 cm^{-1} , respectively, are attributed to stretching vibrations caused by M-O interactions when metal ions are in tetrahedral and octahedral voids⁶³.

UV-Vis Diffuse Reflectance Spectroscopy

The optical band gap is determined using this method. Bonding or non-bonding electrons absorb energy from UV radiation and are stimulated to the anti-bonding orbital in UV spectroscopy. The band gap energy (direct or indirect bandgap, E_g) between the valence and conduction bands of cadmium ferrite is calculated using UV-Vis DRS. Tauc plot is the most commonly used approach for this purpose. The Tauc plot calculates the E_g using the following equation⁶⁴:

$$(\alpha h\nu)^n = K (h\nu - E_g)$$

Where, α =Absorption coefficient, $h\nu$ =Energy of incident photon, n =Constant which depends upon nature of transition i.e., 2 for direct allowed transition and $\frac{1}{2}$ for indirect allowed transition, K =Energy independent constant, E_g =Band gap energy.

The absorption coefficient (α) can be calculated by following formula:

$$\alpha = 2.303 \frac{\log(A)}{t}$$

Lastly, by plotting a graph of $(\alpha h\nu)^2$ verses $h\nu$ and extrapolating the linear part of the curve to $(\alpha h\nu)^2 = 0$ the direct bandgap (E_g) is determined.

Muhammad Imran Arshad *et al.*,⁶² prepared $\text{Cd}_{1-x}\text{Y}_x\text{Fe}_2\text{O}_4$ ($X=0.00, 0.125, 0.250, 0.375, 0.500$) samples and evaluated their bandgaps. Author found that bandgap decreases as Y doping increases. The reproduced Fig. 12 (with permission) shows that the band gap of $\text{Cd}_{1-x}\text{Y}_x\text{Fe}_2\text{O}_4$ decreases from 3.6011–2.8153 eV for $X=0.00$ – 0.500 .

Scanning Electron Microscopy

The morphological characteristics of the resulting nano-ferrite are examined using SEM. It creates images by scanning a ferrite surface with electrons of high energy⁶⁵. When these focused electrons collide with the ferrite surface, they interact with the various atoms in

the ferrite, producing secondary electrons, heat, backscattered electrons, visible light, distinctive X-ray, diffracted backscattered electrons, and other signals. Backscattered electrons are responsible for rapid phase discrimination and secondary electrons are responsible for showing topography and morphology of Cd ferrite⁶⁶. Secondary electrons are responsible for showing topography and morphology of Cd ferrite, a characteristic X-ray commonly used for elemental analysis.

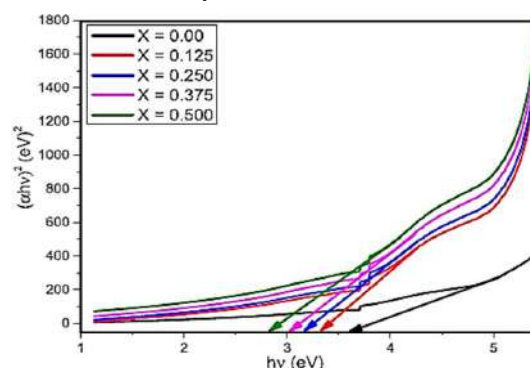


Fig. 12. UV-Vis with E_g for $\text{Cd}_{1-x}\text{Y}_x\text{Fe}_2\text{O}_4$. (Copyright: License No. 5053211164578)⁶²

M. Saravanan and T.C. Sabari Girisun⁶⁷ synthesized two CdFe_2O_4 samples using a simple combustion process and annealing at 500°C (sample a) and 800°C (sample b). With permission, SEM Fig. 13 demonstrates that sample (a) has a porous, spongy, and network-like structure, whereas sample (b) has a spherically homogenized structure.

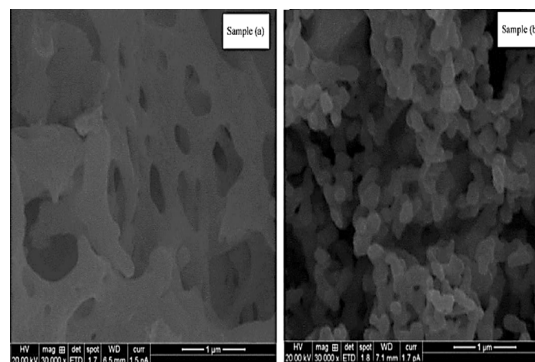


Fig. 13. SEM monographs of CdFe_2O_4 samples. (Copyright: License No. 5053251492395)⁶⁷

Similarly, A. K. Nandanwar *et al.*,⁶⁸ used the Sol-gel micro-oven approach to manufacture $\text{Cd}_{1-x}\text{Ni}_x\text{Fe}_2\text{O}_4$ samples ($x=0.4$ and 0.6) whose SEM image is reprinted with permission as Figure 14.

Transmission Electron Microscopy

Another essential approach for studying

the morphology and structure of cadmium ferrite is transmission electron microscopy. A high-voltage electron beam is sent through a ferrite sample to create a picture in this approach. Cadmium ferrite samples are typically analyzed as an ultrathin film (100nm) or as a suspension on a carbon-coated copper grid. In a TEM, electrons are created from a tungsten filament cathode and accelerated in the vacuum tube of the microscope. Later, an electromagnetic lens is used to focus electrons into a narrow beam that is conducted through ultrathin ferrite samples and then scatters or strikes the electron beam sensitive fluorescent screen at the microscope's bottom to form a picture⁶⁹.

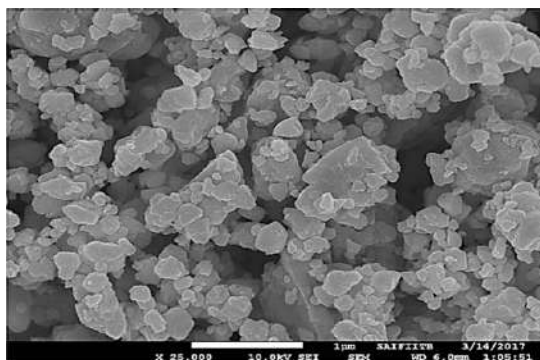


Fig. 14. SEM monographs of $Cd_{1-x}Ni_xFe_2O_4$ samples. (Copyright: License No. 5053440648513)⁶⁸

N. M. Deraz and M. M. Hessian³⁵ used a typical ceramic technique to make pure Cd ferrite. To synthesize pure Cd ferrite samples A, B, and C, an equimolar mixture of Cd nitrate and α -Fe₂O₃ was impregnated, dried, and then thermally treated at 900, 1100, and 1200°C for 3 hours. Agglomeration with particle sizes higher than 100nm can be seen in Cd ferrite calcined at 900°C (Fig. 15A). The authors also noticed variations in the size and form of ferrite particles as the calcination temperature increased. The quasi-spherical morphology of Cd ferrite calcined at 1100 and 1200°C (Fig. 15B and C) revealed reduced particle sizes. Fig. 15 is a representative Transmission Electron Microscopy image of Cd ferrite that has been reproduced with permission.

Thermogravimetry and Differential Thermal Analysis

Thermogravimetry is one of the most precise and quick methods for determining the thermal events that occur when cadmium ferrite is heated. Simultaneous thermal analysis (TG-DTA) is a technique for tracking sample mass versus

temperature and time in a controlled environment furnace⁷⁰. The TG indicates the temperatures at which reduction, decomposition, and oxidation take place, whereas the DTA determines whether decomposition is endothermic or exothermic. This technique offers several advantages, including the need for a small sample size, minimal cost, and the ability to perform qualitative or quantitative analysis. TGA is a destructive technique, which is one of its key drawbacks⁷¹.

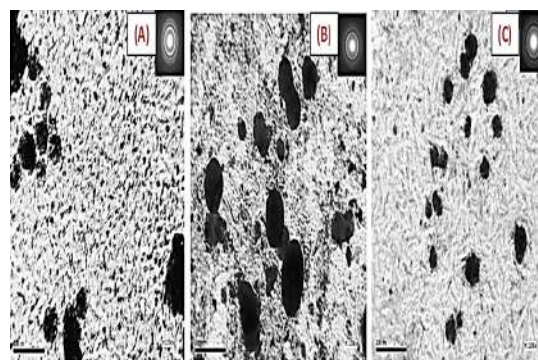


Fig. 15. TEM image of $CdFe_2O_4$ calcined at 900, 1100 and 1200°C. (Copyright: License No. 5053471351410)³⁵

S. V. Prabhakar Vattikuti *et al.*,⁷² used coprecipitation to make $Cd_{0.5}Co_{0.5}Fe_2O_4$ nanoparticles. Researchers investigated the temperature stability of manufactured nanoparticles, and the TG-DTA curve is reprinted with permission as Figure 16.

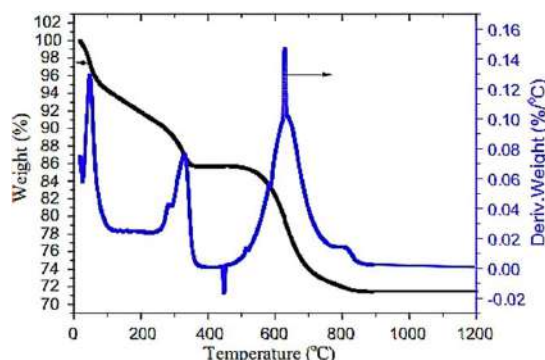


Fig. 16. TG-DTA curves of $Co_{0.5}Cd_{0.5}Fe_2O_4$ nanoparticles (Copyright: License No. 5053710166439)⁷²

Authors showed from Fig. 16 total weight loss observed about 28.62% and there is negligible weight loss after 790°C which ascribed to the stable phase formation of $Cd_{0.5}Co_{0.5}Fe_2O_4$ nanoparticles. In the DTA curve, the first exothermic peak is observed below 100°C which is attributed to evaporation of trapped solvent and absorbed water. Next major exothermic peak is observed at 335°C which is ascribed to decomposition of inorganic salts. The prominent weight loss is observed at 628°C.

Applications

Cadmium ferrites and their doped versions have piqued researchers' interest due to their unrivalled physicochemical features, including as electrical, magnetic, dielectric, and optical capabilities. Cadmium ferrites and their doped versions are used in a variety of fields.

Sensors

Cadmium ferrites, as well as their doped versions, are widely used in gas and electrochemical sensing. Surface character, particle size, lattice defects, and adsorbed oxygen all influence the gas response of a gas sensing material (Cd ferrite)⁷³. Table 3 summarizes some of the selected examples.

Table 3: Cadmium ferrites and its doped variants as sensors

Sr. No.	Cd ferrite and its doped variants synthesized	Synthesis method	Sensing property for	Method description	Reference
1	$Al_{0.5}Cd_{0.5}Fe_2O_4$	Co-precipitation	Relative Humidity	$Al_{0.5}Cd_{0.5}Fe_2O_4$ sensor response and sensor recovery time are 5.5 s and 8 s, respectively. The sensitivity value at 1 kHz in 15% RH and 90% RH is 0.83 and 0.48, respectively.	[74]
2	$Cu_{0.5}Cd_{0.5}La_xFe_{2-x}O_4$ (x=0, 0.05, 0.1, 0.15, 0.2)	Sol-gel auto-combustion	Ammonia	Sensing property measured at 10 ppm concentration. Excellent properties like response time 12 s, recovery time 60 s and moderate sensitivity observed for x=0.1	[75]
3	$CdFe_2O_4$	Sol-gel self-combustion	LPG, Ethanol, Acetone	Maximum selectivity observed at 350°C for gas concentration of 150 ppm.	[76]
4	$CdFe_2O_4$	Solid state reaction	Ethanol, Formaldehyde, Toluene, Benzene, Ammonia	Strongest response for formaldehyde is 14.71 at 260°C while for ethanol it is 12.51 at 300°C. For 1000 ppm ethanol, response time and recovery time are 2 s and 8 s, respectively. For 1000 ppm methanal, response time and recovery time are 5 s and 18 s, respectively.	[73]
5	$Cd_{1-x}Ni_xFe_2O_4$ (x=0.0, 0.5)	Sol-gel auto-combustion	Relative Humidity	Response time and recovery time are 123 s and 154 s when ferrite sample is moved from 25% RH to 95% RH and 95% to 25% RH, respectively at room temperature.	[77]
6	$CdFe_2O_4$	Spray Pyrolysis	Ethanol and Formaldehyde	For ethanol: Detection range- 15 75 ppm, Limit of detection 15 ppm, Response time 21 55 s, Recovery time 29 49 s, operating temperature- ambient. For methanal: Detection range- 15 75 ppm, Limit of detection 15 ppm, Response time 9 29 s, Recovery time 11 25 s, operating temperature- ambient.	[54]
7	$CdFe_2O_4$	Spray Pyrolysis	Benzene	Detection range- 15 75 ppm, Response time 15 47 s, Recovery time 11 45 s, operating temperature-ambient i.e. 300K.	[55]
8	5% Y^{3+} added $Mg_{1-x}Cd_xFe_2O_4$ (x=0, 0.2, 0.4, 0.6, 0.8 and 1)	Co-precipitation by oxalate	LPG, Cl_2 , Ethanol	Maximum sensitivity of 85% is observed at 218 & 197°C at x=0 & 0.2, respectively for LPG. Maximum sensitivity of 79% is observed at 218°C at x=0 for Cl_2 . Maximum sensitivity of 89% is observed at 325°C at x=1.0 for ethanol	[78]
9	5% Sm^{3+} added $Mg_{1-x}Cd_xFe_2O_4$ (x=0, 0.2, 0.4, 0.6, 0.8 and 1)	Co-precipitation by oxalate	LPG, Cl_2 , Ethanol	Response time and recovery time are 180 s and 225 s for LPG at x=1.0 and operating temperature 330°C. Response time and recovery time are 180 s and 225 s for Cl_2 at x=1.0 and operating temperature 330°C. Response time and recovery time are 210 s and 290 s for ethanol at x=1.0 and operating temperature 330°C.	[79]
10	$CdFe_2O_4$	Co-precipitation by NaOH	CO , H_2 , LPG, C_2H_5OH and C_2H_2	Best sensitivity for $CdFe_2O_4$ appears at 250°C for 2000 ppm LPG. $CdFe_2O_4$ is more sensitive to LPG, C_2H_5OH and C_2H_2 while less sensitive to H_2 and CO . Authors also studied relationship between sensitivity and concentration of gas (1000 to 6000 ppm).	[80]
11	$CdFe_2O_4$	Co-precipitation by Ammonium carbonate	Ethanol, CO , H_2 and $i-C_4H_{10}$.	The sensitivity is as high as 90 for 200 ppm to ethanol vapor, it reaches to 7.5, 4 and 5 to 1000 ppm CO , H_2 and $i-C_4H_{10}$.	[81]

Photocatalysis

Because photocatalysts may generate electron-holes, they are frequently used for water pollution treatment, bacterial control, water splitting, and other applications⁸²⁻⁸³. A photocatalyst with a narrow band gap allows solar energy to be converted and used for reduction and oxidation processes⁸⁴. Cadmium ferrites and their doped versions have proven to be outstanding photo-degradation candidates. Table 4 summarizes some of the selected examples.

Table 4: Cadmium ferrites and its doped variants as photocatalyst

Sr. No.	Catalyst	Synthesis method	Amount of catalyst (g/L)	Pollutant/ Dye	Pollutant/ Dye concentration (mg/L)	Irradiation source	Irradiation time (min)	Degradation (%)	Reference
1	CdFe ₂ O ₄ , Cd _{0.6} Mg _{0.4} Fe ₂ O ₄ , CdFe ₂ O ₄ @rGO & Cd _{0.8} Mg _{0.4} Fe ₂ O ₄ @rGO	Co-precipitation	0.1	Methylene Blue	5	Visible Light (200 W)	80	9.72, 20.10, 24.70 & 75.67	[85]
2	Ni _{1-x} Cd _x Ce _y Fe _{2-y} O ₄ /rGO (x,y=0.05) + H ₂ O ₂	Co-precipitation with ultrasonication	0.2	Methylene Blue	5	Visible Light (200 W)	120	98.24	[86]
3	Cd _x Zn _{1-x} Fe ₂ O ₄ (where x=0.0, 0.3, 0.7, 1.0)	Co-precipitation	--	Methyl Orange	10	Sun-light	240	--	[87]
4	Mn _{0.8} Cd _{0.2} Fe ₂ O ₄	Co-precipitation	0.05 to 0.1	Reduction of Cr (VI) to Cr (III)	15	UV irradiation	60	96	[88]
5	CdFe ₂ O ₄	Solid-state reaction	--	Degradation of acetic acid	--	Xenon lamp (300 W)	360	Amount of CO ₂ generated 148 μmol/g	[89]
6	Aluminium doped CdFe ₂ O ₄	Co-precipitation	--	Malachite Green	--	UV irradiation	80	Up-to 100	[90]

Other

Cadmium ferrites and their doped variations are used in a variety of fields in addition to the ones described above.

N. Rezalescu *et al.*,⁹¹ used a self-combustion process to make CdFe₂O₄. XRD, SEM-EDAX, and BET are used to characterize the generated ferrite material. The Cd ferrite powder was used to investigate the combustion reactions of diluted gasses such as methanol/air, acetone/air, and ethanol/air at temperatures ranging from 20 to 500 degrees Celsius. Acetone, methanol, and ethanol have combustion temperatures of about 425, 375, and 350 degrees Celsius, respectively.

S. R. Bhongale *et al.*,⁹² used the oxalate co-precipitation method to synthesise Mg_xCd_{1-x}Fe₂O₄ (x=0, 0.2, 0.4, 0.6, 0.8, and 1.0) and analysed it using XRD, SEM, VSM, and FT-IR techniques. Synthesized ferrites have grain sizes ranging from 2 to 6.5 μm. The authors found that as Mg²⁺ content increases, the real component of permittivity (ε') drops and the dielectric loss tangent increases up to x=0.6, then decreases. Mg_{0.4}Cd_{0.6}Fe₂O₄ sample has highest-10 dB bandwidth.

CONCLUSION

Synthesis, characterization, and performance evaluation of ferrite materials for various applications have been a growing study area for more than 50 years. This is due to exceptional physicochemical features such as electrical, magnetic, dielectric, and optical properties, among others. Co-precipitation, Sol-gel technique, Solid-state processes, Microemulsion, Hydrothermal and Solvothermal, Spray pyrolysis, and many more methods can be used to make CdFe₂O₄ and its doped versions; each method has its own set of advantages and disadvantages. The physical properties of synthesized ferrites are largely determined by the synthesis procedures and processing conditions used. As a result, new synthesis procedures are required at this time, with benefits such as efficiency, cost effectiveness, environmental friendliness, uniform and narrow size distribution with best magnetic behavior, large-scale production feasibility, and high yield, among others. XRD, FT-IR, UV-DRS, SEM, TEM, TG-DTA, VSM, and other techniques are used

to characterize the produced CdFe₂O₄ and its doped variations. Finally, the most well-studied application sectors, such as gas sensing and photocatalysis, are described.

ACKNOWLEDGEMENT

The authors would like to thank the CSIR and UGC for fellowships to this work.

REFERENCES

- Rickard, T. A. The use of meteoric iron, *J. R. Anthropol. Inst.*, **1941**, *71*, 55–66.
- Iqbal, M. A.; Islam, M. U.; Ali, I.; Khan, M. A.; Sadiq, I.; Ali, I. *J. Alloys Compd.*, **2014**, *586*, 404.
- Ngo, A. T.; Pileni, M. P. *J. Phys. Chem. B.*, **2001**, *105*(1), 53–58.
- Roess, E. *IEEE Trans. Magn.*, **1982**, *18*, 1529.
- Ozgüri, U.; Alivov, Y.; Morkoc, H. *J. Mater. Sci. Mater. Electron.*, **2009**, *20*, 789.
- Issa, B.; Obaidat, I. M.; Albiss, B. A.; Haik, Y. *Int. J. Mol. Sci.*, **2013**, *14*, 21266-21305.
- Sickafus, K. E.; Wills, J. M.; Grimes, N. W. *J. Am. Ceram. Soc.*, **1999**, *82*, 3279–3292.
- Gomes, J. A.; Sousa, M. H.; Tourinho, F. A.; Mestnik-Filho, J.; Itri R.; Depeyrot J. *J. Magn. Mater.*, **2005**, *289*, 184–187.
- Kefeni, K. K.; Msagati Titus, A. M.; Mamba, B. B. *Mater. Sci. Eng. B.*, **2017**, *215*, 37–55.
- Rawat, R. S. *Journal of Physics: Conference Series.*, **2015**, *591*, 012021.
- Amiri, S.; Shokrollahi, H. *J. Magn. Mater.*, **2013**, *345*, 18–23.
- Yokoyama, M.; Sato, T.; Ohta, E.; Sato, T. *J. Appl. Phys.*, **1996**, *80*(2).
- Kulkarni, A. B.; Hegde, N. D.; Shashidhara Gowda, H.; Mathad, S. N. *Macromol. Symp.*, **2020**, *393*, 1900213.
- Ghasemi, R.; Echeverría, J.; Pérez-Landazábal, J. I.; Beato-Lopez, J. J.; Naseri, M., Gómez-Polo, C. *J. Magn. Mater.*, **2019**, <https://doi.org/10.1016/j.jmmm.2019.166201>.
- Gadkari, A. B.; Shinde, T. J.; Vasambekar, P. N. *J. Magn. Mater.*, **2010**, *322*(3), 823–827.
- Gadkari, A. B.; Shinde, T. J.; Vasambekar, P. N. *Mater. Chem. Phys.*, **2009**, *114*, 505–510.
- Nikumbh, A. K.; Nagawade, A. V.; Tadke, V. B.; Bakare, P. P. *J. Mater. Sci.*, **2001**, *36*, 653–662.
- Aegerter, M. A.; Mennin, M. *Sol-Gel Technologies for Glass producers and Users*, *Kluwer Academic Publishers.*, ISBN 978-1-4419-5455-8.
- Pena-Pereira, F.; Duarte, Regina M.B.O.; Duarte, A. C. *Trends in Analytical Chemistry (TrAC)*, **2012**, *40*, 90-105.
- Brinker, C. J.; Scherer, G. W. *Sol-Gel Science: The Physics and Chemistry of Sol-Gel Processing-Academic Press.*, **1990**, ISBN 978-0-12-134970-7.
- Modan, E. M.; Plaiasu, A. G. The Annals Of “Dunarea De Jos” University of Galati Fascicle IX. *Metallurgy and Materials Science*, DOI:<https://doi.org/10.35219/mms.2020.1.08>
- Chethan, B.; Ravikiran, Y. T.; Vijayakumari, S. C.; Rajprakash, H. G.; Thomas, S. *Sens. Actuators A.*, **2018**, *280*, 466-474.
- Nandanwar, A. K.; Sarkar, N. N.; Sahu, D. K.; Choudhary, D. S.; Rewatkar, K. G. *Materials Today:Proceedings.*, **2018**, *5*, 22669–22674.
- Nandanwar, A. K.; Choudhary, D. L.; Kamde, S. N.; Choudhary, D. S.; Rewatkar, K. G. *Materials Today:Proceedings.*, **2020**, *29*(3), 951-955.
- Ismail, S. M.; Labib, Sh.; Attallah, S. S. *Journal of Ceramics.*, **2013**, *526-434*, 8.
- Bhise, R. B.; Rathod, S. M. *Int. Res. J. of Science & Engineering.*, **2018**, Special Issue A2, 49-54.
- Jacob, B. P.; Thankachan, S.; Xavier, S.; Mohammed, E. M. *Phys. Scr.*, **2011**, *84*, 045702.
- Dubey, H. K.; Lahiri, P. *Adv. Perform. Mater.*, **2021**, *36*(3), 131-144.
- Cho, S. J.; Uddin, M. J.; Alaboina, P. “Emerging Nanotechnologies in Rechargeable Energy Storage Systems”, **2017**, 83-129, doi:10.1016/b978-0-323-42977-1.00003-0.
- Buekenhoudt, A.; Kovalevsky, A.; Luyten, Ir J.; Snijkers, F. *Basic Aspects in Inorganic Membrane Preparation in “Comprehensive Membrane Science and Engineering”.*, **2010**, *1*, 217-252.
- Dao-hua, L.; Shao-fen, H.; Jie, C.; Cheng-yan, J.; Cheng Y. *IOP Conf. Ser.: Mater. Sci. Eng.*, **2017**, *242*, 012023.
- Yu, H. F.; Huang, K. C. *J. Mater. Res.*, **2002**, *17*, 199.
- Saadon, A. K. *Energy Procedia.*, **2019**, *157*, 561–567.
- Su, M.; Liao, C.; Chan, T.; Shih, K.; Xiao, T.; Chen, D.; Kong, L.; Song, G. *Environ. Sci. Technol.*, **2018**, *52*, 775–782.

35. Deraz, N. M.; Hessien, M. M. *J. Alloys Compd.*, **2009**, *475*, 832–839.
36. Chavan, G. N.; Belavi, P. B.; Naik, L. R.; Bammannavar, B. K.; Ramesh, K. P.; Kumar S. *International Journal of Scientific & Technology Research (IJSTR)*, **2013**, *2*(12), 82-89.
37. Santra, S.; Tapeç, R.; Theodoropoulou, N.; Dobson, J.; Hebard, A.; Tan W. *Langmuir*, **2001**, *17*, 2900–2906.
38. Malik, M. A.; Wani, M. Y.; Hashim, M. A. *Arab. J. Chem.*, **2012**, *5*(4), 397-417.
39. Sheikh, F. A.; Khalid, M.; Shifa, M. S.; Huda Khan Asghar, H M N. ul.; Aslam, S.; Perveen, A.; Rehman, J. ur.; Khan, M. A.; Gilani, Z. A. *Chin. Phys. B.*, **2019**, *28*(8), 088701.
40. Kaur, M.; Kaur, N.; Vibha Chapter 4 Ferrites: *Synthesis and Applications for Environmental Remediation*, **2016**, DOI: 10.1021/bk-2016-1238.
41. Feng, S.; Li, G. Chapter 4- Hydrothermal and solvothermal syntheses, *Modern Inorganic Chemistry*, **2011**, 63-95.
42. Sharifianjazi, F.; Moradi, M.; Parvin, N.; Nemati, A.; Rad, A. J.; Sheysi, N.; Abouchenari, A.; Mohammadi, A.; Karbasi, S.; Ahmadi, Z.; Esmaeilkhani, A.; Irani, M.; Pakseresht, A.; Sahman, S.; M. Shahedi *Asl Ceram. Int.*, **2020**, *46*, 18391–18412.
43. Pauline, S.; Amaliya, A. P. *Arch. Appl. Sci. Res.*, **2011**, *3*, 213–223.
44. Wongpratrat, U.; Maensiri, S.; Swatsitang, E. *Microelectron. Eng.*, **2015**, *146*, 68–75.
45. Shi, W.; Liu, X.; Zhang, T.; Wang, Q.; Zhang, L. *RSC Adv.*, **2015**, *5*, 51027.
46. Saravanan, M.; Sabari Girisan, T. C.; Vinitha G. *J. Mol. Liq.*, **2018**, *256*, 519–526.
47. Saravanan, M.; Sabari Girisan, T. C.; Venugopal Rao, S. *J. Mater. Chem. C.*, **2017**, *5*, 9929-9942.
48. Mostafa, N. Y.; Zaki, Z. I.; Heiba, Z. K. *J. Magn. Magn. Mater.*, **2013**, *329*, 71–76.
49. Wolska, E.; Wolski, W.; Kaczmarek, J.; Piszora, P. *Solid State Ion.*, **1997**, *101-103*, 1069-1074.
50. Rasheed, S.; Khan, R. A.; Shah, F.; Ismail, B.; Nisar, J.; Shah, S. M.; Rahim, A.; Khan, A. *R. J. magn. Magn. Mater.*, **2019**, *471*, 236-241.
51. Kafle, B. P. *Chemical Analysis and Material Characterization by Spectrophotometry*, **2020**, 147-198.
52. Falcony, C.; Angel Aguilar-Frutos, M.; García-Hipólito, M. *Micromachines*, **2018**, *9*, 414, 1-33.
53. Tahir, M. B.; Rafique, M.; Rafique, M. S.; Nawaz, T.; Rizwan, M.; Tanveer, M. *Nanotechnology and Photocatalysis for Environmental Applications, Micro and Nano Technologies*, **2020**, 119-138.
54. Nagarajan, V.; Thayumanavan, A., *Microchim Acta.*, **2018**, *185*, 319.
55. Nagarajan, V.; Thayumanavan, A., *Appl. Phys. A.*, **2018**, *124*, 155, 1-8.
56. Kardile, H. J.; Somvanshi, S. B.; Chavan, A. R.; Pandit, A. A.; Jadhav, K. M. *Optik*, **2020**, *207*, 164462.
57. Lamas, D. G.; Neto, M. de Oliveira.; Kellermann, G.; Craievich, A. F. *Nanocharacterization Techniques Micro and Nano Technologies*, **2017**, 111-182.
58. Kumar, C. G.; Pombala, S.; Poornachandra, Y.; Agarwal, S. V. *Nanobiomaterials in Antimicrobial Therapy, Applications of Nanobiomaterials*, **2016**, *6*, 103-152.
59. Nikumbh, A. K.; Nagawade, A. V.; Gugale, G. S.; Chaskar, M. G.; Bakare; P. P. *J. Mater. Sci.*, **2002**, *3*(7), 637–647.
60. Karanjkar, M. M.; Tarwal, N. L.; Vaigankar, A. S.; Patil, P. S. *Ceram. Int.*, **2013**, *39*, 1757-1764.
61. Silverstein, R.; Webster, F.; Kiemle, D., *Spectrometric Identification of Organic Compounds*, John Wiley and Sons Inc., New York., **2006**.
62. Amin, N.; Ul Hasan, M. S.; Majeed, Z.; Latif, Z.; un-Nabi, M. A.; Mahmood, K.; Ali, A.; Mehmood, K.; Fatima, M.; Akhtar, M.; Arshad, M. I.; Bibi, A.; Iqbal, M. Z.; Jabeen, F.; Bano, N., *Ceram. Int.*, **2020**, *46*(13), 20798-20809.
63. Ahmad, T.; Lone, I. H.; Ansari, S. G.; Ahmed, J.; Ahamad, T.; Alshehri, S. M. *Materials & Design*, **2017**, *126*, 331-338.
64. Tauc, J.; Grigorovici, R.; Vancu, A. *phys. stat. sol.*, **1966**, *15*, 627.
65. McMullan, D. *Scanning electron microscopy 1928-1965, Scanning*, **1995**, *17*, 175–185.
66. Baillot, R.; Deshayes, Y. *Tools and Analysis Methods of Encapsulated LEDs, Reliability Investigation of LED Devices for Public Light Applications*, **2017**, 43-106.
67. Saravanan, M.; Sabari Girisan, T. C., *Mater. Chem. Phys.*, **2015**, *160*, 413-419.
68. Nandanwar, A. K.; Sarkar, N. N.; Sahu, D. K.; Choudharya, D. S.; Rewatkar, K. G., *Materials Today: Proceedings*, **2018**, *5*, 22669–22674.

69. Senthil Kumar, P.; Grace Pavithra, K., Naushad, Mu. *Nanomaterials for Solar Cell Applications.*, **2019**, 97-124.
70. Tomoda, B. T.; Yassue-Cordeiro, P. H.; Vaz Ernesto, J.; Lopes, P. S.; Peres, L. O.; da Silva, C. F.; de Moraes, M. A. *Biopolymer Membranes and Films, Health, Food, Environment, and Energy Applications.*, **2020**, 67-95.
71. Dollimore, D., *Thermal analysis, Anal. Chem.*, **1994**, 66(12), 17–25.
72. Venkata Reddy Ch., Chan Byon; Narendra, B.; Baskar, D.; Srinivas, G.; Jaesool Shim.; Prabhakar Vattikuti, S. V. *Superlattices and Microstructures.*, **2015**, 82, 165-173.
73. Cao, Y.; Qin, H.; Niu, X.; Jia, D. *Ceram. Int.*, **2016**, 42(9), 10697-10703.
74. Sasmaz Kuru, T.; Sentürk, E. *Sensors and Actuators A.*, **2016**, 249, 62–67.
75. Tumberphale, U. B.; Jadhav, S. S.; Raut, S. D.; Shinde, P. V.; Sangle, S.; Shaikh, S. F.; Al-Enizi, A. M.; Ubaidullah, M.; Mane, R. S.; Gore, S. K. *Solid State Sciences.*, **2020**, 100, 106089.
76. Rezlescu, N.; Rezlescu, E.; Tudorache, F.; Popa, P. D. *Romanian Reports in Physics.*, **2009**, 61(2), 223-234.
77. Chethan, B.; Ravikiran, Y. T.; Vijayakumari, S. C.; Rajprakash, H. G.; Thomas, S. *Sens. Actuators A: Physical.*, **2018**, 280, 466-474.
78. Gadkari, A. B.; Shinde, T. J.; Vasambekar, P. N. *Sensors & Transducers Journal.*, **2012**, 146(11), 110-120.
79. Gadkari, A. B.; Shinde, T. J.; Vasambekar, P. N. *Sensors and Actuators B.*, **2013**, 178, 34– 39.
80. Chen, N. S.; Yang, X. J.; Liu, Er-Sheng.; *Ling Huang J. Sensors and Actuators B.*, **2000**, 66, 178–180.
81. Tianshu, Z.; Hing, P.; Jiancheng, Z.; Lingbing, K. *Materials Chemistry and Physics.*, **1999**, 61, 192-198.
82. Dutta, P. K.; Pehkonen, S. O.; Sharma, V. K.; Ray, A. K., *Environ. Sci. Technol.*, **2005**, 39, 1827–1834.
83. Hoffmann, M. R.; Martin, S. T.; Choi, W.; Bahnemann, D. W. *Chem. Rev.*, **1995**, 95, 69–96.
84. Casbeer, E.; Sharma, V. K.; Zhong, X. *Separation and Purification Technology*, **2012**, 87, 1–14.
85. Shahid, M. *Ceram. Int.*, **2020**, 46(8) Part A, 10861-10870.
86. Rahman, A.; Aadil, M.; Akhtar, M.; Warsi, M. F.; Jamil, A.; Shakir, I.; Shahid, M. *Ceram. Int.*, **2020**, 46, 13517–13526.
87. Harish, K. N.; Bhojya Naik, H. S.; Prashanth kumar, P. N.; Viswanath, R. *Catal. Sci. Technol.*, **2012**, 2, 1033–1039.
88. Ali, I. O.; Mostafa, A. G. *Mater. Sci. Semicond. Process.*, **2015**, 33, 89–198.
89. Tezuka, K.; Kogure, M.; Shan, Y. *J. Catal. Commun.*, **2014**, 48, 11–14.
90. Hegazy, E. Z.; Kosa, S. A.; Abd Elmaksod, I. H.; Mojamami, J. T. *Ceram. Int.*, **2019**, 45, 7318–7327.
91. Rezlescu, N.; Rezlescu, E.; Popa, P. D.; Popovici, E.; Doroftei, C.; Ignat, M. *Mater. Chem. Phys.*, **2013**, 137, 922-927.
92. Bhongale, S. R.; Ingawale, H. R.; Shinde, T. J.; Pubby, K.; Narang, S. B.; Vasambekar, P. N., *J. Magn. Magn. Mater.*, **2017**, 441, 475–481.



ORIGINAL ARTICLE

In silico exploration of binding potentials of anti SARS-CoV-1 phytochemicals against main protease of SARS-CoV-2



Abdullah G. Al-Sehemi ^{a,b}, Mehboobali Pannipara ^{a,b,*}, Rishikesh S. Parulekar ^c, Jaydeo T. Kilbile ^d, Prafulla B. Choudhari ^c, Mubarak H. Shaikh ^e

^a Research Center for Advanced Materials Science, King Khalid University, Abha, Saudi Arabia

^b Department of Chemistry, King Khalid University, Abha, Saudi Arabia

^c Department of Pharmaceutical Chemistry, Bharati Vidyapeeth College of Pharmacy, Kolhapur 416 013, India

^d Department of Basic and Applied Sciences, MGM University, Aurangabad 431 001, India

^e Department of Chemistry, Radhabai Kale Mahila Mahavidyalaya, Ahmednagar 414 001 India

Received 25 January 2022; revised 5 March 2022; accepted 6 March 2022

Available online 11 March 2022

KEYWORDS

SARS-CoV-1;
Phytochemicals;
SARS-CoV-2;
Main protease;
Molecular docking;
Molecular dynamics (MD)
simulation

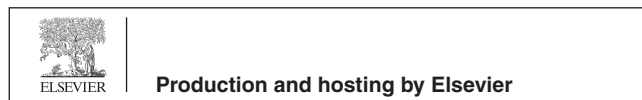
Abstract The phytochemicals can play complementary medicine compared to synthetic drugs considering their natural origin, safety, and low cost. Phytochemicals hold a key position for the expansion of drug development against corona viruses and need better consideration to the agents that have already been shown to display effective activity against various strains of corona viruses. In this study, we performed molecular docking studies on potential forty seven phytochemicals which are SARS-CoV-1 M^{Pro} inhibitors to identify potential candidate against the main proteins of SARS-CoV-2. *In Silico* Molecular docking studies revealed that phytochemicals **16** (Brousoflavan A), **22** (Dieckol), **31** (Hygromycin B), **45** (Sinigrin) and **46** (Theaflavin-3,3'-digallate) exhibited excellent SARS-CoV-2 M^{Pro} inhibitors. Furthermore, supported by Molecular dynamics (MD) simulation analysis such as Root Mean Square Deviation (RMSD), Root Mean Square Fluctuation (RMSF), Radius of gyration (R_g) and H-bond interaction analysis. We expect that our findings will provide designing principles for new corona virus strains and establish important frameworks for the future development of antiviral drugs.

© 2022 The Author(s). Published by Elsevier B.V. on behalf of King Saud University. This is an open access article under the CC BY license (<http://creativecommons.org/licenses/by/4.0/>).

* Corresponding author at: Department of Chemistry, King Khalid University, Abha, Saudi Arabia.

E-mail address: mpannipara@kku.edu.sa (M. Pannipara).

Peer review under responsibility of King Saud University.



1. Introduction

Current high outline, global outbreaks of viral diseases from the coronavirus family have been caused by enveloped viruses. Acute respiratory tract inflammation caused by SARS-CoV-2 is an infectious disease, often fatal, that is characterized by the rapid and unexpected spread. Worldwide, the COVID-19

pandemic has recorded, as of 1st March 2022, 437 million cases, 369 million recovered cases with 5.97 million deaths, and the numbers continue to increase progressively [1] (<https://covid19.who.int/>). Furthermore, patients with pre-existing kidney dysfunction, immune-compromised persons, pulmonary disease and diabetes are the most susceptible community with higher mortality rates from SARS-CoV-2 infection. Coronavirus families are able to cause a number of diseases, such as hepatitis, gastroenteritis, bronchitis, systemic diseases, and even death in birds, humans, and other animals [2]. The contagion effect of such epidemic could possibly bring key challenges to worldwide health systems and have far-reaching significances on the global economy if it is not controlled effectively.

The SARS coronavirus is the viable microorganism accountable for the worldwide outburst of a severe disease that caused several deaths [3]. To design the anti-SARS drug, the coronavirus main protease (M^{pro}), recognized as the utmost attractive target due to its crucial role in facilitating viral transcription and replication [4]. Near about 30,000 nucleotides comprised in the SARS-CoV-2 genome: the gene of SARS-CoV-2 namely, replicase encodes pp1a and pp1ab two overlapping polyproteins which are essential for viral replication and transcription [5]. Polyproteins excreted the functional polypeptides by extensive proteolytic processing, mostly by the 33.8-kDa M^{pro} (also known as 3C-like protease). Polyprotein digested by M^{pro} at least 11 conserved sites, initially the autolytic cleavage of this enzyme itself from pp1a and pp1ab [6]. In the viral life cycle M^{pro} plays functional importance, shared with the absence of closely associated homologues in humans, recognize M^{pro} as an attractive target for the design of antiviral drugs [7].

Herein we describe the *in silico* molecular docking results that intended quickly discovery of lead compounds for clinical use, by assimilation structure-assisted drug design, virtual drug screening. This *in silico* study focused on identifying drug leads that target main protease (M^{pro}) of SARS-CoV-2. Jin and co-worker identified a mechanism-based inhibitor by computer-aided drug design, and then determined the crystal structure of M^{pro} of SARS-CoV-2 [8]. We have screened 47 SARS-CoV-1 M^{pro} active phytochemicals for high binding affinity and interaction to the conserved residues of the substrate-binding pocket of SARS-CoV-2 M^{pro} using molecular docking-based virtual screening. Our results demonstrated the efficacy of our screening strategy, which can lead to the rapid discovery of drug leads with clinical potential in response to new infectious diseases for which no specific drugs or vaccines are available.

2. Results and discussion

2.1. Molecular docking analysis

Molecular docking study was performed to explore the binding potential of the selected phytochemicals against the M^{pro} of SARS-CoV-2. Structure of the M^{pro} of SARS-CoV-2 (PDB ID: 6W63) [9] was downloaded from the free protein database www.rcsb.org.

The phytochemical analyzed in this work are showed profound activity against SARS-CoV-1 and their possible mode of action is via inhibition of the main protease. SARS-CoV-2

is mutated form of the main protease of SARS-CoV-1 and has up to 96% similarity [10,11]. Table 1 shows structures of phytochemicals utilized in current study. In virtue of all these reports, we thought virtual analysis of the molecules with profound activity on the SARS-CoV-1 on main protease of SARS-CoV-2 will be an attractive strategy for identification and development of potent inhibitors against viruses. Thus, phytochemicals with reported activity against SARS-CoV-1 were selected for the docking analysis [12–14]. Grip based docking simulation was performed and best molecules were analyzed on the basis of docking score and binding interactions with M^{pro} of SARS-CoV-2.

Brousoflavan A (16) was found to be most active in docking simulation with showing docking score of -91.22 and hydrogen bond interaction with SER144(1.5 Å), CYS145(1.6 Å) and CYS166(2.5 Å), aromatic interaction with HIS41(1.5 Å) and hydrophobic interaction with HIS41, PHE140, LEU141, ASN142, SER144, CYS145, MET165, GLU166, LEU167, PRO168 as shown in Fig. 1.

Theaflavin-3,30-digallate (46) was found to be another active molecule in docking simulation with showing docking score of -76.85 and hydrogen bond interaction with THR26(1.6 Å), CYS44(2.3 Å), CYS145(2.1 Å) HIS164(2.0 Å), MET165(2.0 Å), GLU166(2.5 Å), ARG188(1.8 Å), aromatic interaction with HIS41(4.6 Å) and hydrophobic interaction with HIS41, HIS 46 as shown in Fig. 2.

Dieckol (22) was found to be showing docking score of -73.11 and hydrogen bond interaction with TYR54(2.3 Å), SER139(2.4 Å), GLU166(2.2 Å), ARG188(2.5 Å) aromatic interaction with HIS41(4.4 Å) as shown in Fig. 3.

4'-O-Methyl-di-placol (4) was found to be another phytochemical active in docking simulation with showing docking score of -68.78 and hydrogen bond interaction with HIS163(2.5 Å), aromatic interaction with HIS41(5.0 Å) and hydrophobic interaction with HIS41, ASN142, MET165, GLU166 as shown in Fig. 4.

Sinigrin (45) showing docking score of -65.08 and hydrogen bond interactions with CYS145(2.5 Å), GLU166(2.2 Å), THR190(2.5 Å), GLN192(2.6 Å) and hydrophobic interaction with MET165, GLU166, PRO168, GLN189, as shown in Fig. 5.

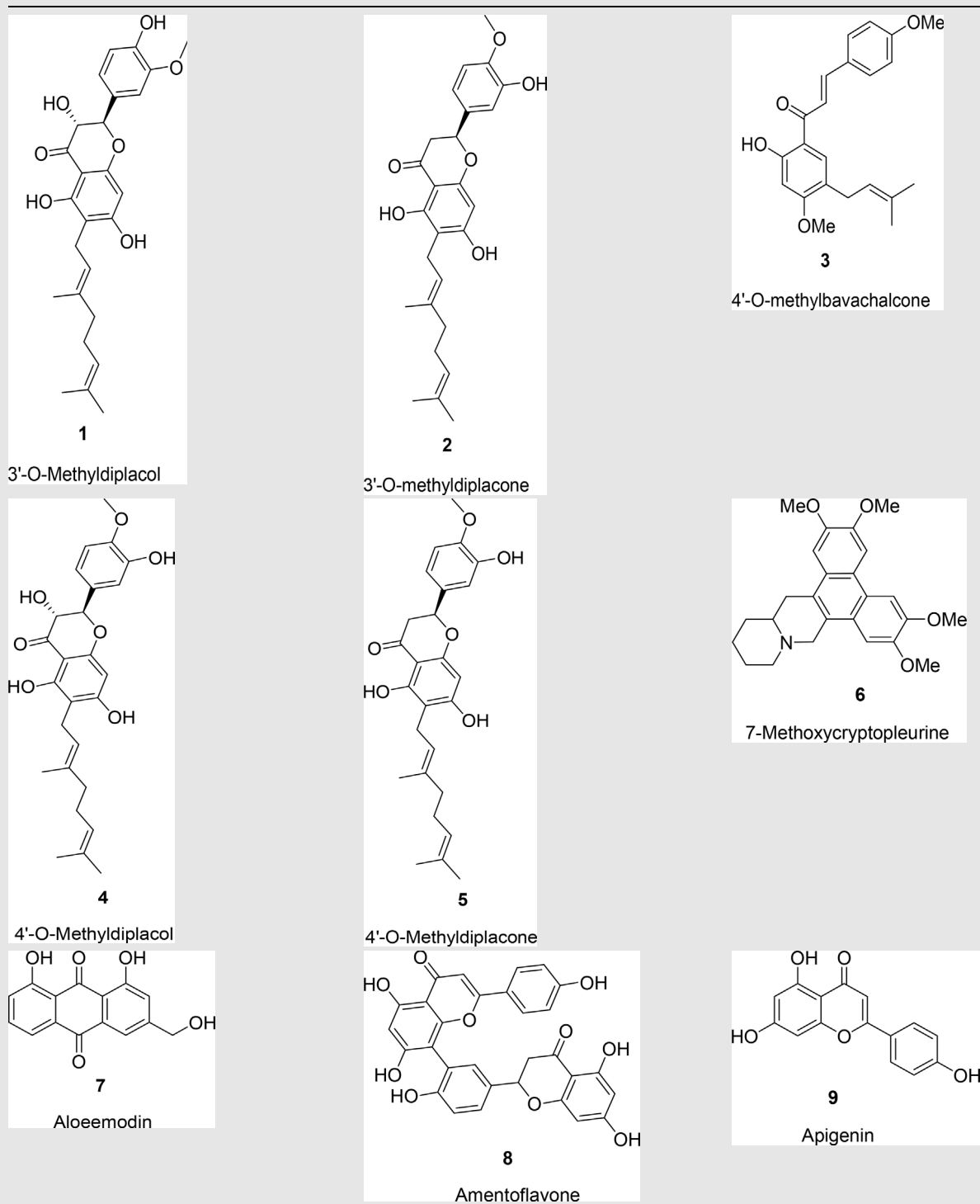
Hygromycin B (31) showing docking score of -62.48 and hydrogen bond interactions with HIS41(2.0 Å), TYR54(2.2 Å), PHE140(2.5 Å), SER144(2.0 Å), CYS145(1.5 Å), GLU166(2.2 Å) GLN189(2.5 Å), charge interaction with GLU166(2.4 Å) and hydrophobic interaction with THR25, HIS41, CYS44, THR45, MET49, PHE140, LEU141, ASN142, SER144, CYS145, MET165, GLU166, ARG188, GLN189 as shown in Fig. 6.

4'-O-Methyl-di-placone (5) showing docking score of -60.58 and hydrogen bond interactions with ASN142(2.5 Å), aromatic interaction with HIS41(5.2 Å) and hydrophobic interaction with THR25, HIS41, ASN142, MET165, GLU166 as shown in Fig. 7.

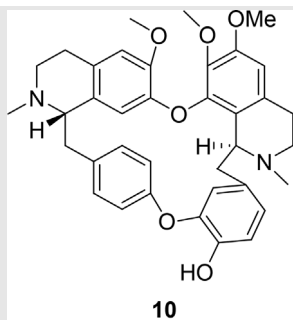
2.2. Molecular dynamics (MD) simulation analysis

The molecular docking study revealed the most promising phytochemical inhibitor molecules against SARS-CoV-2 M^{pro} protein and so these docked complexes were selected for simulations. MD simulations were performed with control

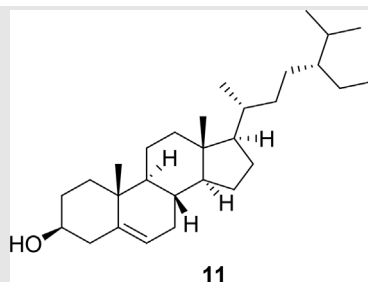
Table 1 The chemical structures of known phytochemical compounds acting against SARS-CoV-1.



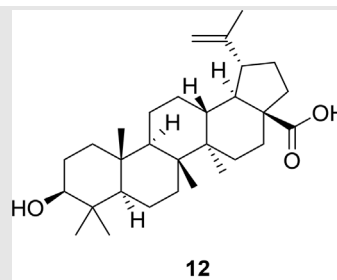
(continued on next page)



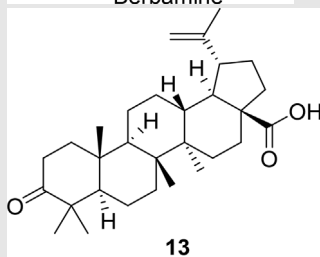
Berbamine



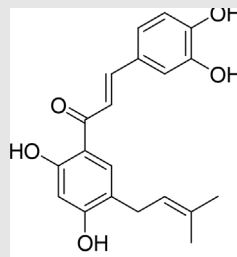
Beta-sitosterol



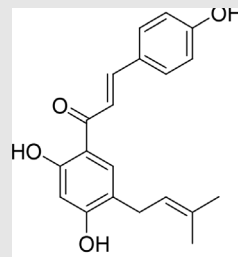
Betulinic acid



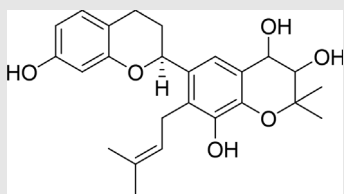
Betulonic acid



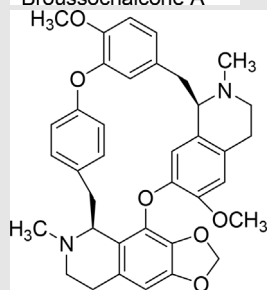
Brousochalcone A



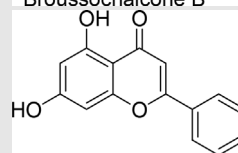
Brousochalcone B



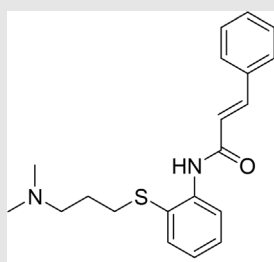
Brousoflavan A



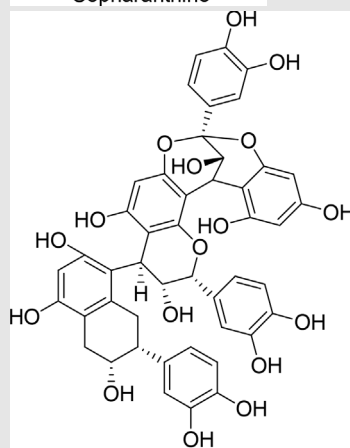
Cepharanthine



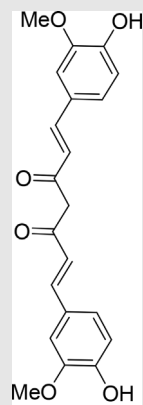
Chrysin



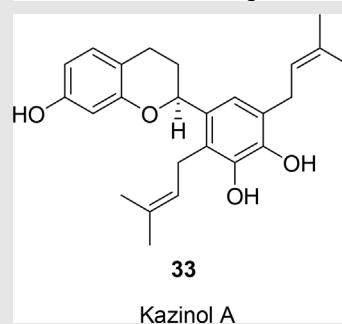
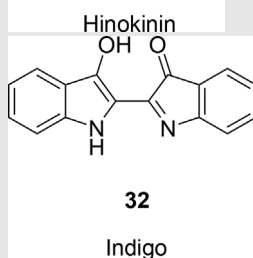
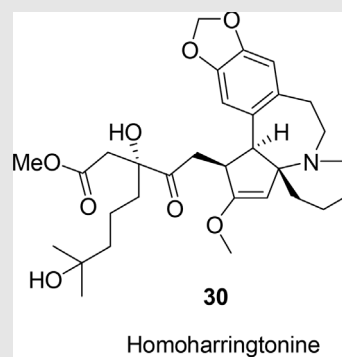
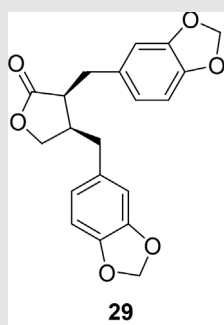
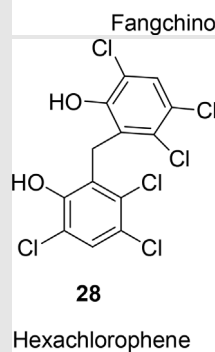
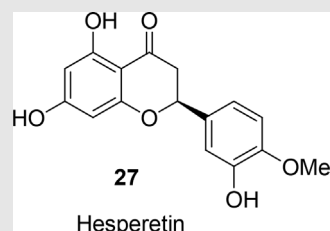
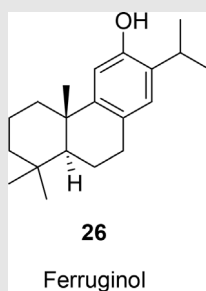
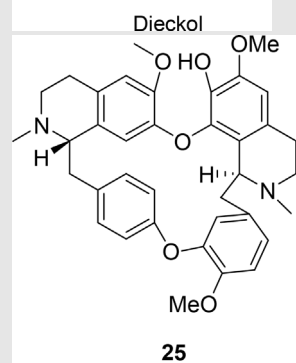
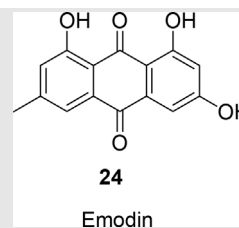
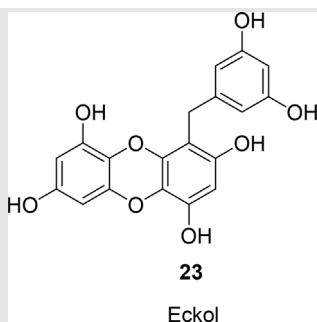
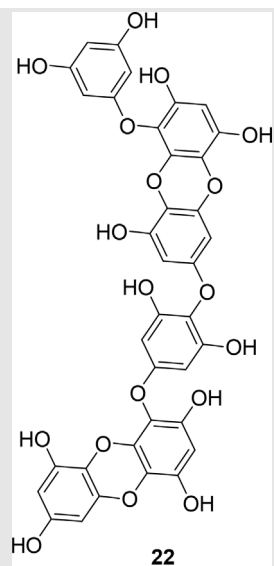
Cinanserin



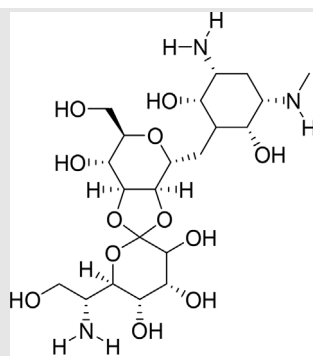
Cinnamtannin B1



Curcumin

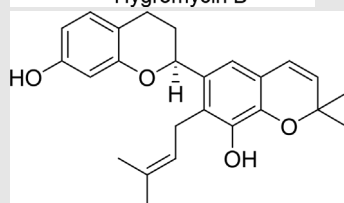


(continued on next page)



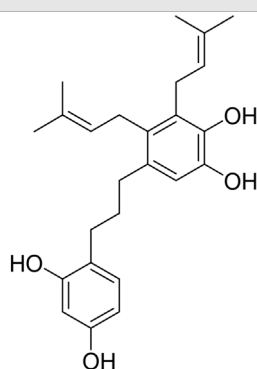
31

Hygromycin B



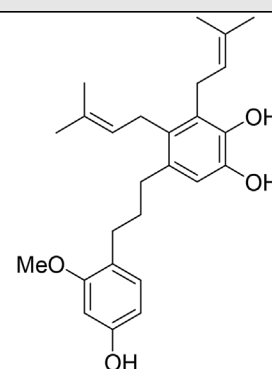
34

Kazinol B



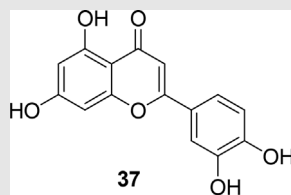
35

Kazinol F



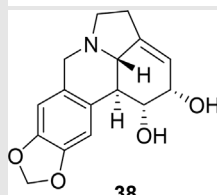
36

Kazinol J



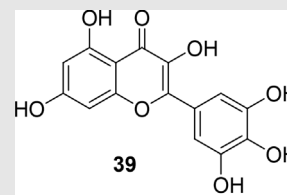
37

Luteolin



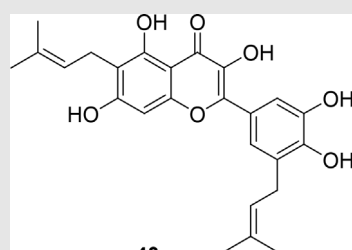
38

Lycorine



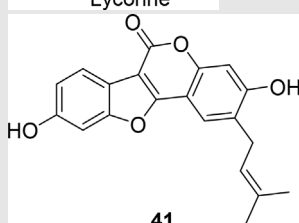
39

Myricetin



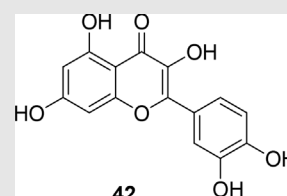
40

Papyriflavonol A



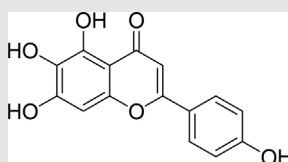
41

Psoralidin



42

Quercetin



44

Scutellarein

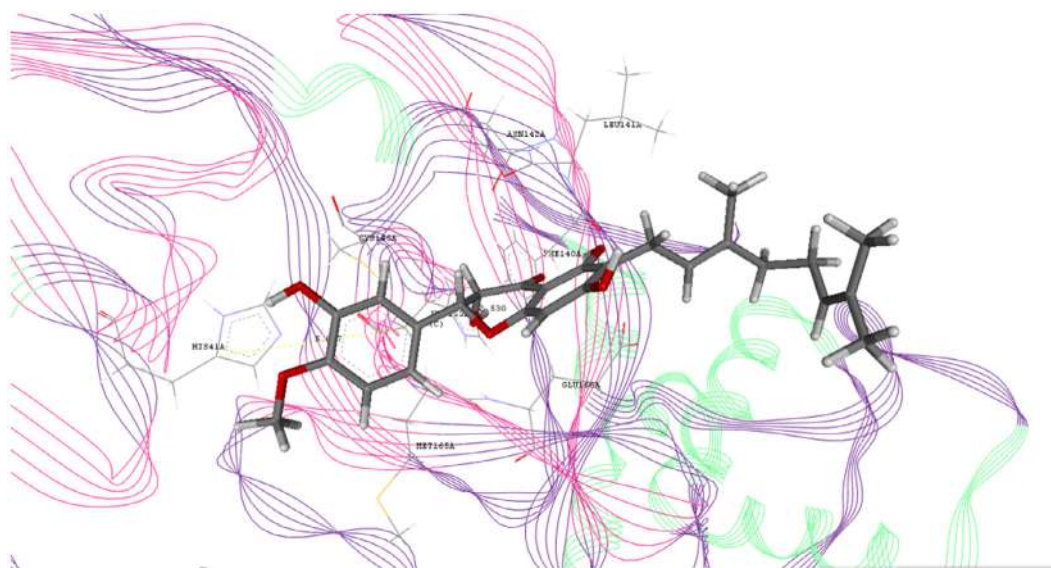


Fig. 4 Docking interaction of 4 (4'-O-Methyldiplacol).

mass weighted root mean square distance of a collection of atoms from their common center of mass. Therefore the overall conformation of the protein could be analyzed by calculating the Rg values. Fig. 8C indicates the Rg values of control and different M^{PRO}-inhibitor docked complexes over entire simulation period. The Rg values for control and different M^{PRO}-inhibitor complexes were found to be in the range of 2.2 nm to 2.26 nm (Fig. 8C). From this it is apparent that there is no change in the conformation of the M^{PRO} protein after binding of different phytochemical inhibitors and also the compactness of M^{PRO} structure was found to be similar in presence of experimental inhibitor X77 and computationally identified phytochemical inhibitors (Fig. 8C).

In order to have a stable protein-inhibitor interaction the formation of hydrogen bonds is of supreme importance. For this we have illustrated the number of hydrogen bonds formed

between SARS-CoV-2 M^{PRO} protein and different phytochemical inhibitor molecules *viz*; 4, 5, 16, 22, 31, 45, 46 and compared it with hydrogen bonding pattern observed in control (Fig. 9A-H). Thus, it can be clearly seen from Fig. 9B-H that significant hydrogen bonding pattern is observed in all M^{PRO}-inhibitor docked complexes in comparison to control (Fig. 9A). This is an indication of the fact that there is a strong interaction between SARS-CoV-2 M^{PRO} and phytochemical inhibitor molecules *viz*; 4, 5, 16, 22, 31, 45, 46. As seen from Fig. 9D-H, 3 hydrogen bonds are seen in M^{PRO}-16 complex, 4 hydrogen bonds are seen in M^{PRO}-22 complex, 5 hydrogen bonds are observed in M^{PRO}-31 complex, 4 hydrogen bonds are observed in M^{PRO}-45 complex and 6 hydrogen bonds are seen in M^{PRO}-46 complex. Thus, phytochemical inhibitors 16 (Brousoflavan A), 22 (Dieckol), 31 (Hygromycin B), 45 (Sinigrin) and 46 (Theaflavin-3,30-digallate) have

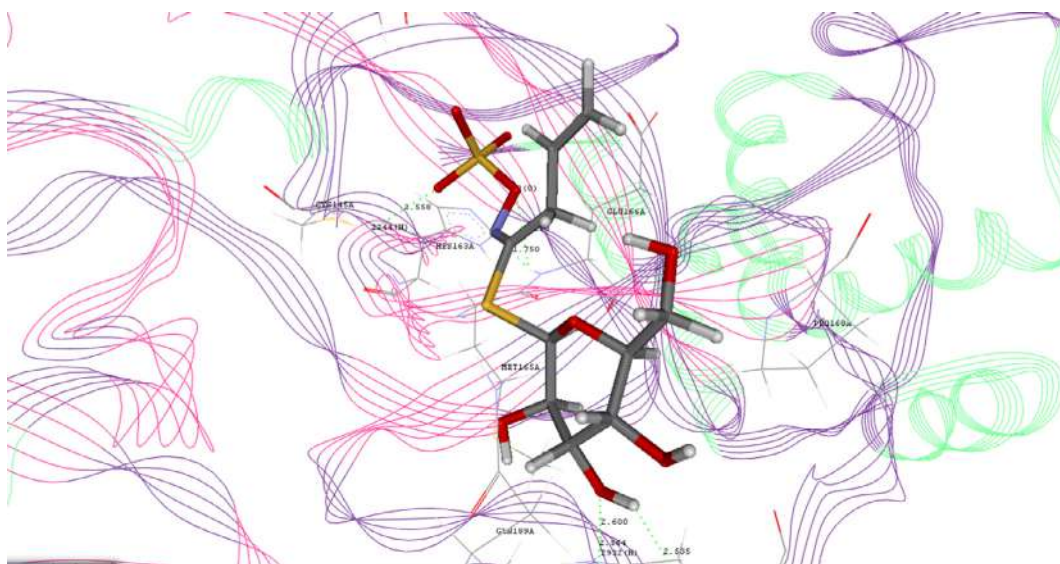


Fig. 5 Docking interaction of 45 (Sinigrin).

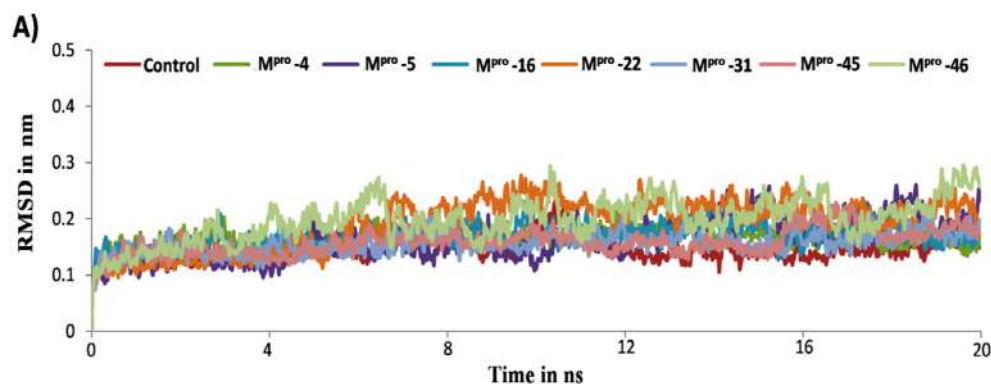


Fig. 8A Molecular dynamics (MD) simulation analysis for most stable docked complexes of SARS-CoV-2 M^{Pro} protein with different well-known phytochemicals (inhibitors) in comparison to control. A) Plot of backbone RMSD of SARS-CoV-2 M^{Pro}-phytochemical inhibitor complexes along with control during 20 ns simulation.

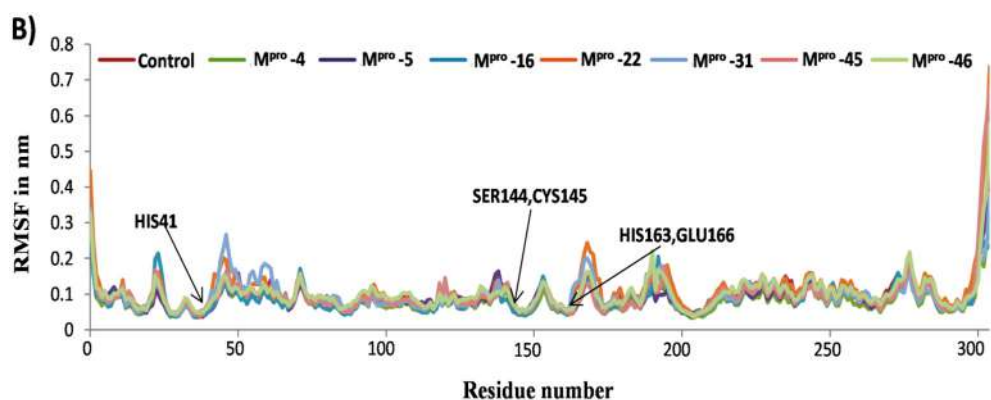


Fig. 8B Molecular dynamics (MD) simulation analysis for most stable docked complexes of SARS-CoV-2 M^{Pro} protein with different well-known phytochemicals (inhibitors) in comparison to control. B) RMSF plot of M^{Pro}-phytochemical inhibitor complexes along with control during simulation (arrows indicated key active sites of M^{Pro} involved in binding with phytochemical inhibitors).

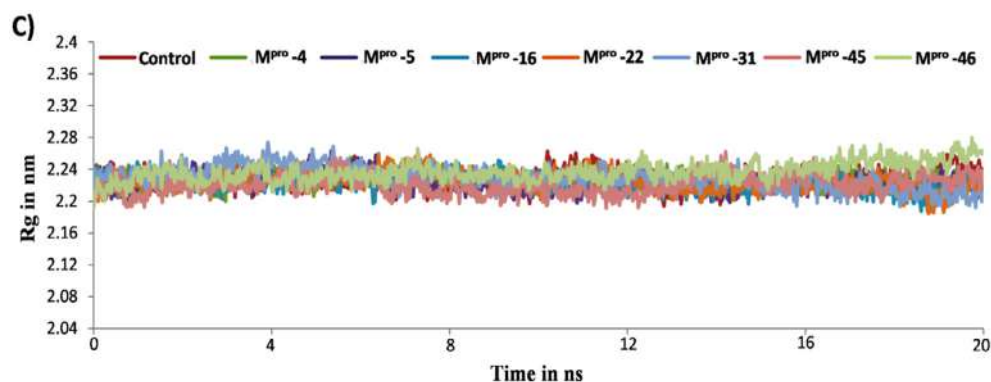


Fig. 8C Molecular dynamics (MD) simulation analysis for most stable docked complexes of SARS-CoV-2 M^{Pro} protein with different well-known phytochemicals (inhibitors) in comparison to control. C) Rg plot of SARS-CoV-2 M^{Pro}-phytochemical inhibitor complexes along with control during 20 ns simulation representing compactness of receptor M^{Pro}.

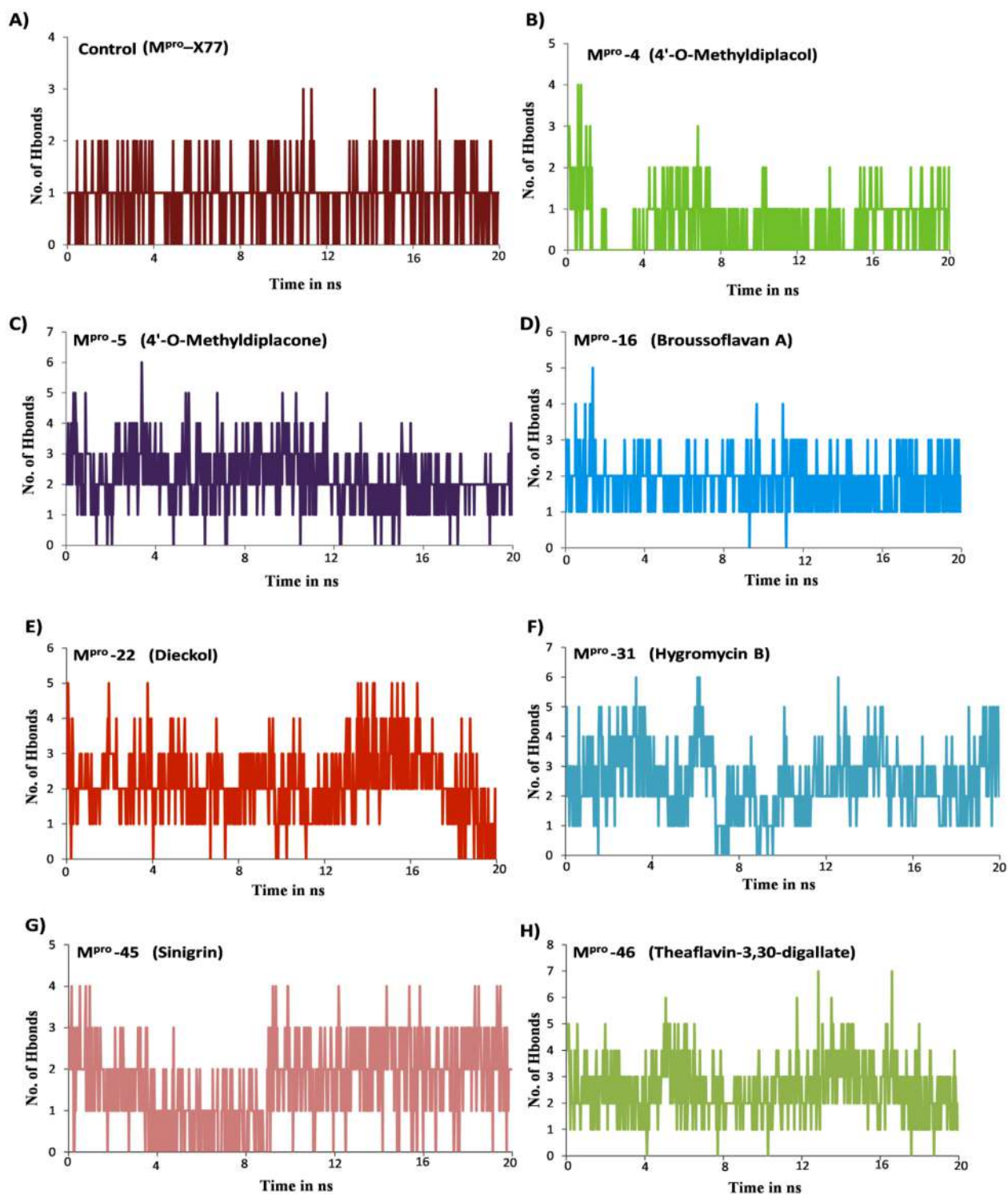


Fig. 9 Hydrogen bond analysis of different SARS-CoV-2 M^{PRO} -phytochemical inhibitor complexes in comparison with control for trajectories obtained from 20 ns MD simulations. A) Control (M^{PRO} -X77). B) M^{PRO} -4 (4'-O-Methyldiplacol). C) M^{PRO} -5(4'-O-Methyldiplacone). D) M^{PRO} -16 (Brousoflavan A). E) M^{PRO} -22 (Dieckol). F) M^{PRO} -31 (Hygromycin B). G) M^{PRO} -45 (Sinigrin). H) M^{PRO} -46 (Theaflavin-3,30-digallate).

3.3. Molecular docking study

The molecular docking study of the phytochemical compounds with receptor SARS-CoV-2 M^{PRO} protein was performed using

biopredicta module. Redocking was performed using native ligand X77 of SARS-CoV-2 M^{PRO} , to ascertain the docking protocol applied [15–17]. Grip based docking analysis was performed keeping ligand structures in the flexible conformation. For docking analysis the rotational angle was kept at 10° and

Table 2 *In silico* molecular docking interactions of phytochemical compounds with M^{Pro} of SARS-CoV-2.

Molecule no.	Name	Interactions				Docking Score
		H bond	Aromatic	Charge	Hydrophobic	
1	3'-O-Methylchalcone	LEU141(2.3)			MET49, LEU141, ASN142, GLU166	-63.72
2	3'-O-methylchalcone	LEU141(2.5)			HIS41, LEU141, ASN142, MET165, GLU166, ASP187, ARG188	-63.99
3	4'-O-methylchalcone	CYS145 (2.47)			MET165, GLU166	-65.25
4	4'-O-Methylchalcone	HIS163 (2.5)	HIS41 (5.07)		HIS41, ASN142, MET165, GLU166	-68.78
5	4'-O-Methylchalcone	ASN142 (2.5)	HIS41 (5.2)		HIS41, LEU141, MET165, GLU166, ASP187, ARG188	-60.58
6	7-Methoxycryptolepine	SER144 (2.3)	HIS41 (4.6)		THR25, LEU27, HIS41, CYS44, MET49, PHE140, LEU141, ASN142, SER144, CYS145, MET165, GLU166, LUE167, PRO168, GLN189	-56.43
7	Aloe emodin	GLU166 (2.3)	HIS41 (4.4)		ASN142, GLU166	-58.18
8	Amentoflavone	GLU166(1.7)	HIS41 (5.3)			-66.54
9	Apigenin	CYS44(2.5)				
10	Berberamine	LEU141 (1.88)	HIS41 (4.2)	HIS163 (3.1)	MET49, PHE140, LEU141, ASN142, GLY143, SER144, CYS145, MET165, GLU166, LEU167, PRO168, GLN189	-30.27
11	Beta-sitosterol	CYS44(1.3)			HIS41, CYS44, MET49, PR52, PRO140, LEU141, ASN142, CYS145, HIS164, MET165, GLU166, ASP187, ARG188, GLN189	-44.75
12	Betulonic acid	GLY143(1.9)		HIS41 (4.7)	THR25, ASN142, MET165, GLU166, LEU167, PRO168	-29.61
13	Betulonic acid	ASN143(2.3)			THR25, LEU27, MET49, ASN142, GLY143, CYC145, MET165, GLU166	-35.27
14	Brousochalcone A	GLN189(2.5)	HIS41 (3.7)		MET165, GLU166, ASP187, ARG188, GLN189	-77.70
15	Brousochalcone B	HIS163(1.8)	HIS41 (4.0), HIS (163) (4.6)		MET165, GLU166, ARG188, GLN189	-68.39
16	Brousoflavan A	HIS(163(2.2))	HIS41 (1.5)		HIS41, PHE140, LEU141, ASN142, SER144, CYS145, MET165, GLU166, LEU167, PRO168	-91.22
17	Cepharanthine	SER144(1.5), CYS145(1.6), CYS166(2.5)		HIS163 (3.3)	MET49, PHE140, LEU141, ASN142, GLY143, SER144, CYS145, MET165, GLU166, PRO168, GLN189	-24.89
18	Chrysin	GLY143 (1.4), GLU166 (1.99)	HIS41 (4.6)			-54.08
19	Cinanserin	GLY143 (2.2), GLU166(2.4)	HIS41 (4.6), HIS163 (5.4)		MET165, GLU166, LEU167, PRO168, GLN189	-38.67
20	Cinnamtannin B1	HIS41(1.9)	HIS41 (5.01)		HIS41, CYC44, MET49, ASN142, MET165	-59.98
21	Curcumin	PHE140(1.7), THR190(2.1)	HIS163 (4.67)		LEU141, ASN142, MET165, GLU166, LEU167, PRO168, THR190, GLN192	-66.52
22	Dieckol	TYR54(2.3), SER139(2.4), GLU166 (2.2), ARG188 (2.5)	HIS41 (4.4)			-73.11
23	Eckol	CYS145 (2.4), GLU166(2.5)	HIS41 (4.1)			-72.96

(continued on next page)

Table 2 (continued)

Molecule no.	Name	Interactions				Docking Score
		H bond	Aromatic	Charge	Hydrophobic	
24	Emodin	GLU166(2.2)			CYS145, MET165	-37.28
25	Fangchinoline	GLN 189 (2.4)			HIS41, MET49, HIS164, MET165, PRO168, ASP187, ARG188, GLN189, THR190	-48.40
26	Ferruginol	GLY143(2.3)			HIS41, MET49, PHE140, LEU141, ASN142, MET165, GLU166, GLN 189	-46.19
27	Hesperetin	SER144(1.6) CYS145(2.3) HIS163(2.4)	HIS163 (5.3)		GLU166	-52.42
28	Hexachlorophene	GLU166(2.3)			MET165, GLU166	-59.42
29	Hinokinin	SER144(2.5)			PHE140, LEU141, ASN142, MET165, GLU166, GLN189	-74.70
30	Homoharringtonine	ASN142(2.4)	HIS163 (5.3)		PHE140, LEU141, ASN142, SER144, MET165, GLU166, GLN189	-57.83
31	Hygromycin B	HIS41(2.0), TYR54(2.2), PHE140(2.5) SER144(2.0) CYS145(1.5) GLU166(2.2) GLN189(2.5)		GLU166 (2.4)	THR25, HIS41, CYS44, THR45, MET49, PHE140, LEU141, ASN142, SER144, CYS145, MET165, GLU166, ARG188, GLN189	-62.48
32	Indigo	HIS164(2.2)	HIS41 (4.1)			-74.37
33	Kazinol A	GLU166(2.4)	HIS41		THR25, LEU27, ASN142, GLY143, CYS145, MET165, GLU166, PRO168, ARG188, GLN189	-69.72
34	Kazinol B	GLN189(2.5)			ASN142, MET165, GLN189,	-31.72
35	Kazinol F	CYS145(2.5)			HIS41, MET49, ASN142, GLY143, CYS145, MET165, LEU167, PRO168, ASP187, ARG188, GLN189, GLN192	-58.43
36	Kazinol J	ASN142(2.4)			GLN189, LEU141, ASN142, MET165, GLU166, LEU167, PRO168, GLN189	-63.86
37	Luteolin	ASP187(2.5)	HIS163 (5.3), HIS41 (3.8)			-63.28
38	Lycorine	SER144(2.2)		GLU166 (2.4)	PHE140, LEU141, ASN142, GLU166	-39.07
39	Myricetin	GLU166(2.5)	HIS41 (1.9)			-63.71
40	Papyriflavonol A	GLU166(1.8)			LEU141, MET165, ASP187, ARG188, GLN189	-71.58
41	Psoralidin				MET165, GLU166	-62.19
42	Quercetin	ARG188 (2.5)	HIS41 (4.7)			-64.080
43	Savinin	SER144(2.2)	HIS41 (4.5)		HIS41, LEU141, ASN142, MET165, GLU166, GLN189	-71.08
44	Scutellarein		HIS163 (5.1), HIS41 (4.00)			-64.29
45	Sinigrin	CYS145(2.5) GLU166(2.2) THR190(2.5) GLN192(2.6)			MET165, GLU166, PRO168, GLN189	-65.08
46	Theaflavin-3,3'-digallate	THR26(1.6), CYS44(2.3), CYS145(2.1) HIS164(2.0) MET165 (2.0) GLU166(2.5) ARG188 (1.8)	HIS41 (4.6)		HIS41, MET165	-76.85
47	Tylophorine	CYS145(2.4)		GLU166 (3.4)	LUE141, ASN142, GLY143, SER144, CYS145, MET165, GLN189	-63.57

total number of rotation to 30. The best docking pose of used phytochemical compounds bound to SARS-CoV-2 M^{Pro} was selected on the basis of the docking score and type of interactions.

3.4. Molecular dynamics (MD) simulation

Molecular dynamics (MD) simulation was performed to study the dynamic behavior and assess the stability of SARS-CoV-2 M^{Pro} protein bound to different phytochemical compounds. The crystal structure of M^{Pro} protein of SARS-CoV-2 bound with non-covalent inhibitor X77 (PDB ID: 6 W63) [9] served as a control system in the MD simulation study. The reliability of the binding mode and conformation of predicted best docked phytochemical molecules were confirmed using molecular dynamic simulation of docked complexes by GROMACS 2018.3 (www.gromacs.org) software package [20]. Overall eight M^{Pro}-inhibitor complex conformations were considered for MD simulation study, viz; a) M^{Pro}-X77 complex which is control, b) M^{Pro}-4 complex consisting phytochemical inhibitor molecule 4'-O-Methyl-di-placol, c) M^{Pro}-5 complex with inhibitor 4'-O-Methyl-di-placone, d) M^{Pro}-16 complex comprising inhibitor Brousoflavan A, e) M^{Pro}-22 complex with inhibitor Dieckol, f) M^{Pro}-31 complex constituting inhibitor Hygromycin B, g) M^{Pro}-45 complex with Sinigrin as phytochemical inhibitor molecule and h) M^{Pro}-46 complex having Theaflavin-3,30-digallate as inhibitor. The topology of M^{Pro} receptor structure was built using pdb2gmx tool incorporating OPLS-AA/L (Optimized Potentials for Liquid-type Simulation) all atom force field [21], whereas topology files of all inhibitor molecules was generated using PRODRG server [22]. After generating topology of each complex, further each complex was centered in the system of cubic box by keeping periodic distance of 1 nm between complex and edge of the box. All complexes were then solvated with SPC216 water molecules to fill the defined box for each complex. The solvated systems were neutralized by addition of suitable number of Na⁺ ions to maintain electro-neutrality of the system. The Particle-Mesh-Ewald (PME) method [23] was used for calculation of long-range electrostatic interactions of all the systems. A 50,000-step energy minimization was performed with the steepest descent (SD) method at 300 K by applying periodic boundary conditions (PBC) in all directions. Berendsen thermostat temperature coupling and Parrinello-Rahman pressure coupling for each 500-ps run were used to keep all the systems in equilibrated environment 300 K and 1 bar, respectively. The leap-frog algorithm was used for integrating Newton's equation in molecular dynamics (MD) simulation of all the systems. All the bond lengths were constrained using the LINCS algorithm [24], and the time step was set to 0.002 ps. Finally, a 20-ns MD simulation was carried out for all eight systems. The simulation trajectories obtained after 20 ns MD simulations were analyzed using gm_x_rms, gm_x_rmsf, gm_x_gyrate and gm_x_hbond tools from the GROMACS 2018.3 package [20] and visualized using UCSF Chimera molecular visualizing software [25].

4. Conclusion

In the present study, we extensively analyzed the binding potential and mechanism of inhibition of phytochemical

towards the SARS-CoV-2 M^{Pro} having profound inhibition towards the SARS-CoV-1 M^{Pro}. Molecular docking analysis was used to find the number of hydrogen bonds formed between SARS-CoV-2 M^{Pro} protein and different inhibitor molecules. Molecular docking analysis along with molecular dynamics simulation analysis showed **16** (Brousoflavan A), **22** (Dieckol), **31** (Hygromycin B), **45** (Sinigrin) and **46** (Theaflavin-3,3'-digallate) have high binding affinity and interaction to the conserved residues of the substrate-binding pocket of SARS-CoV-2 M^{Pro}. Thus, these phytochemicals offer preventive and complementary medicine in the fight against viruses due to their natural origin, safety and low cost compared to synthetic drugs. This study provides foundation for the identification of SARS-CoV-2 M^{Pro} inhibitors by structural manipulation of active phytochemicals to develop antiviral drugs for future.

CRedit authorship contribution statement

Abdullah G. Al-Sehemi: Conceptualization. **Mehboobali Pannipara:** Writing – original draft. **Rishikesh S. Parulekar:** Software. **Jaydeo T. Kilbile:** Investigation. **Prafulla B. Choudhari:** Writing – review & editing. **Mubarak H. Shaikh:** Review.

Declaration of Competing Interest

The authors declare that they have no known competing financial interests or personal relationships that could have appeared to influence the work reported in this paper.

Acknowledgements

The authors are thankful to the Institute of research and consulting studies at King Khalid University for funding this research through grant number 3-N-20/21. Authors are also thankful to Dr. Yasinalli Tamboli for valuable suggestions during preparation of manuscript.

References

- [1] WHO Health Emergency Dashboard WHO (COVID-19) Homepage.
- [2] A. Chafekar, B. C. Fielding, MERS-CoV: Understanding the latest human coronavirus threat. *Viruses* 10 (2018) 93-114; 10.3390/v10020093.
- [3] J.S.M. Peiris, S.T. Lai, L.L.M. Poon, Y. Guan, L.Y.C. Yam, W. Lim, J. Nicholls, W.K.S. Yee, W.W. Yan, M.T. Cheung, V.C.C. Cheng, K.H. Chan, D.N.C. Tsang, R.W.H. Yung, T.K. Ng, K. Y. Yuen, SARS study group, Coronavirus as a possible cause of severe acute respiratory syndrome, *Lancet* 361 (9366) (2003) 1319-1325.
- [4] K. Anand, J. Ziebuhr, P. Wadhvani, J. R. Mesters, R. Hilgenfeld, Coronavirus main proteinase (3CLpro) structure: basis for design of anti-SARS drugs. *Science* 300 (2003) 1763-1767; 10.1126/science.1085658.
- [5] (a) P. Zhou, X. L. Yang, X. G. Wang, B. Hu, L. Zhang, W. Zhang, H. R. Si, Y. Zhu, B. Li, C. L. Huang, H. D. Chen, J. Chen, Y. Luo, H. Guo, R. D. Jiang, M. Q. Liu, Y. Chen, X. R. Shen, X. Wang, X. S. Zheng, K. Zhao, Q. J. Chen, F. Deng, L. L. Liu, B. Yan, F. X. Zhan, Y. Y. Wang, G. F. Xiao and Z. L. Shi, A pneumonia outbreak associated with a new coronavirus of probable bat origin. *Nature* 579 (2020) 270-273; 10.1038/s41586-020-2012-7; (b) F. Wu, S. Zhao, B. Yu, Y. M. Chen, W.

- Wang, Z. G. Song, Y. Hu, Z. W. Tao, J. H. Tian, Y. Y. Pei, M. L. Yuan, Y. L. Zhang, F. H. Dai, Y. Liu, Q. M. Wang, J. J. Zheng, L. Xu, E. C. Holmes and Y. Z. Zhang, A new coronavirus associated with human respiratory disease in China. *Nature* 579 (2020) 265-269. 10.1038/s41586-020-2008-3.
- [6] A. Hegyi, J. Ziebuhr, Conservation of substrate specificities among coronavirus main proteases. *J. Gen. Virol.* 83 (2002) 595-599; 10.1099/0022-1317-83-3-595.
- [7] T. Pillaiyar, M. Manickam, V. Namasivayam, Y. Hayashi and S. H. Jung, An Overview of Severe Acute Respiratory Syndrome-Coronavirus (SARS-CoV) 3CL Protease Inhibitors: Peptidomimetics and Small Molecule Chemotherapy. *J. Med. Chem.* 59 (2016) 6595-6628; 10.1021/acs.jmedchem.5b01461.
- [8] Z. Jin, X. Du, Y. Xu, Y. Deng, M. Liu, Y. Zhao, B. Zhang, X. Li, L. Zhang, C. Peng, Y. Duan, J. Yu, L. Wang, K. Yang, F. Liu, R. Jiang, X. Yang, T. You, X. Liu, X. Yang, F. Bai, H. Liu, X. Liu, L.W. Guddat, W. Xu, G. Xiao, C. Qin, Z. Shi, H. Jiang, Z. Rao, H. Yang, Structure of Mpro from SARS-CoV-2 and discovery of its inhibitors, *Nature* 582 (2020) 289-293. <https://www.nature.com/articles/s41586-020-2223-y>.
- [9] A. D. Mesecar, (2020); 10.2210/pdb6w63/pdb.
- [10] P.C. Woo, Y. Huang, S.K. Lau, K.Y. Yuen, Coronavirus genomics and bioinformatics analysis, *Viruses* 2 (2010) 1804-1820.
- [11] T. Zhang, Q. Wu, Z. Zhang, Probable pangolin origin of SARS-CoV-2 associated with the COVID-19 outbreak, *Curr. Biol.* 30 (2020) 1346-1351.e1342.
- [12] M. T. Islam, C. Sarkar, D. M. El-Kersh, S. Jamaddar, S. J. Uddin, J. A. Shilpi, M. S. Mubarak, Natural products and their derivatives against coronavirus: A review of the non-clinical and pre-clinical data. *Phytother. Res.* 34 (2020) 2471-2492; 10.1002/ptr.6700.
- [13] M. Tahir ul Qamar, S. M. Alqahtani, M. A. Alamri, L. L. Chen, Structural basis of SARS-CoV-2 3CLpro and anti-COVID-19 drug discovery from medicinal plants. *J. Pharm. Anal.* 10 (2020) 313-319; 10.1016/J.JPHA.2020.03.009.
- [14] S. Ben-Shabat, L. Yarmolinsky, D. Porat, A. Dahan, Antiviral effect of phytochemicals from medicinal plants: Applications and drug delivery strategies. *Drug. Deliv. Transl. Res.* 10 (2020) 354-367; 10.1007/s13346-019-00691-6.
- [15] A. G. Al-Sehemi, M. Pannipara, R. S. Parulekar, P. B. Choudhari, M. S. Bhatia, P. K. Zubaidha, Y. Tamboli, Potential of NO donor furoxan as SARS-CoV-2 main protease (M^{Pro}) inhibitors: *in silico* analysis, *J. Biol. Struct. Dyn.* 39 (2021) 5804-5818; 10.1080/07391102.2020.1790038.
- [16] G. M. Basha, R. S. Parulekar, A. G. Al-Sehemi, M. Pannipara, V. Siddaiah, S. Kumari, P. B. Choudhari, Y. Tamboli, Design and *in silico* investigation of novel Maraviroc analogues as dual inhibition of CCR-5/SARS-CoV-2 M^{Pro}, *J. Biol. Struct. Dyn.* (2021) 1-16; 10.1080/07391102.2021.1955742.
- [17] A. G. Al-Sehemi, R. S. Parulekar, M. Pannipara, M. A. PP, P. K. Zubaidha, M. S. Bhatia, T. K. Mohanta and A. Al-Harrasi, *In silico* evaluation of NO donor heterocyclic vasodilators as SARS-CoV-2 M^{Pro} protein inhibitor, *J. Biol. Struct. Dyn.* (2021) 1-18; 10.1080/07391102.2021.2005682.
- [18] R. S. Parulekar, K. D. Sonawane, Molecular modeling studies to explore the binding affinity of virtually screened inhibitor toward different aminoglycoside kinases from diverse MDR strains, *J. Cell. Biochem.* 119 (2018) 2679-2695; 10.1002/jcb.26435.
- [19] R. S. Parulekar and K. D. Sonawane, Insights into the antibiotic resistance and inhibition mechanism of aminoglycoside phosphotransferase from *Bacillus cereus*: *In silico* and *in vitro* perspective, *J. Cell. Biochem.* 119 (2018) 9444-9461; 10.1002/jcb.27261.
- [20] M. J. Abraham, T. Murtola, R. Schulz, S. Pall, J. C. Smith, B. Hess, E. Lindahl, GROMACS: High performance molecular simulations through multi-level parallelism from laptops to supercomputers, *SoftwareX* 1 (2015) 19-25; 10.1016/j.softx.2015.06.001.
- [21] G. A. Kaminski, R. A. Friesner, J. Tirado-Rives, W. L. Jorgensen, Evaluation and reparametrization of the OPLS-AA force field for proteins *via* comparison with accurate quantum chemical calculations on peptides. *J. Phys. Chem. B.* 105 (2001) 6474-6487; 10.1021/jp003919d.
- [22] D. M. Van Aalten, R. Bywater, J. B. Findlay, M. Hendlich, R. W. Hoof, G. Vriend, PRODRG, a program for generating molecular topologies and unique molecular descriptors from coordinates of small molecules. *J. Comp. Aided Mol. Des.* 10 (1996) 255-262; 10.1007/BF00355047.
- [23] U. Essmann, L. Perera, M.L. Berkowitz, T. Darden, H. Lee, L. G. Pedersen, A smooth particle mesh Ewald method, *J. Chem. Phys.* 103 (1995) 8577, <https://doi.org/10.1063/1.470117>.
- [24] B. Hess, H. Bekker, H.J. Berendsen, J.G. Fraaije, LINCS: A linear constraint solver for molecular simulations, *J. Comp. Chem.* 18 (1997) 1463-1472, [https://doi.org/10.1002/\(SICI\)1096-987X\(199709\)18:12<1463::AID-JCC4>3.0.CO;2-H](https://doi.org/10.1002/(SICI)1096-987X(199709)18:12<1463::AID-JCC4>3.0.CO;2-H).
- [25] E. F. Pettersen, T. D. Goddard, C. C. Huang, G. S. Couch, D. M. Greenblatt, E. C. Meng, T. E. Ferrin, UCSF chimera-A visualization system for exploratory research and analysis, *J. Comp. Chem.* 25 (2004) 1605-1612; 10.1002/jcc.20084.



SYNTHESIS, CHARACTERIZATION AND ANTIMICROBIAL EVALUATION OF SUBSTITUTED N2-((1R, 4R)-4-AMINOCYCLOHEXYL)-N6-(PHENYL)-9-CYCLOPENTYL-9H-PURIN-2,6-DIAMINE DERIVATIVES

Dhanraj Kamble¹, Anil Shankarwar¹, Radhakrishna Tigote², Yuvaraj Sarnikar³,
Mubarak Shaikh⁴, Pravin Chavan⁵, Balaji Madje*⁶

¹Department of Chemistry, S.B.E.S. College of Science, Aurangabad, Maharashtra, India

²Department of Chemistry Dr. B. A. M. University Sub campus, Osmanabad, Maharashtra, India

³Department of Chemistry Dayanand Science College, Latur, Dist. Latur, Maharashtra, India

⁴Department of Chemistry, Radhabai kale Mahila Mahavidyalaya, Ahemadnagar, Maharashtra, India

⁵Doshi Vakil Arts College and G.C.U.B. Science & Commerce College, Goregaon-Raigad, Maharashtra, India

⁶Department of Chemistry Vasantao Naik Mahavidyalaya, Aurangabad, Maharashtra, India

*Corresponding author: drmadjebr@gmail.com

ABSTRACT

In this study, we have synthesized N2-((1r,4r)-4-aminocyclohexyl)-N6-(substitutedphenyl)-9-cyclopentyl-9H-purin-2,6-diamine derivatives (**7a-j**) from N-(-substituted phenyl)-9-cyclopentyl-2-fluoro-9H-purin-6-amine, and cyclohexane-1,4-diamine under microwave irradiation condition and examined for their antibacterial activity against *Escherichia coli*, *Streptococcus aureus* and *Bacillus subtilis* strains. All compounds (**7a-j**) displayed moderate to good antibacterial activity in Minimum Inhibition Concentration (MIC).

Keywords: Purine, Purine fluoro-9H-purin-6-amine, N-9 Substituted-6-chloropurine, 9H-purin-2,6-diamine, Cyclohexane-1,4-diamine.

1. INTRODUCTION

The Purine antimetabolites have been used in the development of many potent medicinal agents, which exhibited antineoplastic, antileukemic, antiviral, antibacterial and antifungal activities [1, 2]. The purine nucleoside analogs are also used in the treatment of autoimmune diseases [3]. 6-Mercapto purine is used therapeutically as an immunosuppressive agent [4] and inhibits the growth of bacterial and mammalian cells [5]. Other 6-mercapto purine, mercapto-pyridine and mercapto-pyrimidine derivatives also exhibit antibacterial activity and have been studied as agents for targeting melanoma [6], reducing cholesterol and as vasodilators [7]. Purines and pyrimidines make up the two groups of nitrogenous bases, including the two groups of nucleotide bases. Two of the four deoxyribonucleotides and two of the four ribonucleotides, the respective building blocks of DNA and RNA, are purines. Purines are found in high concentration in meat and meat products, especially internal organs such as liver and kidney. Plant based diets are generally low in purines [8, 9]. Examples of high-purine sources include: sweetbreads, anchovies, sardines, liver, beef kidneys,

brains, meat extracts (e.g., Oxo, Bovril), herring, mackerel, scallops, game meats and gravy. A moderate amount of purine is also contained in beef, pork, poultry, fish and seafood, asparagus, cauliflower, spinach, mushrooms, green peas, lentils, dried peas, beans, oatmeal, wheat bran, wheat germ, and hawthorn. Virus-infected cells have an increased demand for purine nucleotides which are needed for viral RNA or DNA synthesis and this renders the enzyme, IMPDH, as a sensitive target for antiviral chemotherapy. Synthesized 2-functionalized purine nucleosides were tested as antiviral against vaccinia virus (*in vitro*) [9]. A series of dialkyl esters of purine N-[2-(phosphonomethoxy) ethyl] derivatives substituted at position 2, 6, or 8 of the purine bases have been evaluated for antiviral activity [10]. N-9 Substituted-6-chloropurine derivative was highly inhibitory of *in vitro* multiplication of American Leishmania and *T. rangeli* but had no effect on *T. cruzi* epimastigotes and on mice that were acutely infected with *T. cruzi* [11]. Purine derivatives of L-Ascorbic acid were evaluated for their antitumour activity against malignant tumor cell lines: pancreatic carcinoma (Mia PaCa2), breast carcinoma (MCF7), cervical carcinoma

(HeLa), laryngeal carcinoma (Hep2), murine leukemia (L1210/0), murine mammary carcinoma (FM3A), human T-lymphocytes (Molt4/C8 and CEM/0) [12].

2. EXPERIMENTAL

2.1. Material and Methods

From the commercial sources the reagents and solvent were purchased and have been used without further purification. The melting points were taken in open capillary tubes and are uncorrected. During the course of reaction, the formation of compounds was checked by TLC on silica- Gel plates of 0.5 mm thickness and checked the location of spots by iodine and UV light. By using suitable organic solvents, all the compounds were purified by recrystallization/silica gel (100-200 mesh) gravity column. The Mass spectra of the compound were carried out by using Shimadzu GC-MS-QP-2010 model using direct inlet probe technique. ¹H NMR, ¹³C NMR were recorded in CDCl₃ and DMSO-d₆ solution on a Bruker Ac 200 Or 400 MHz spectrometer.

2.1.1. Synthesis of N-(substituted phenyl)-9-cyclopentyl-2-fluoro-purin-6-amine (6)

N-(substituted phenyl)-9-cyclopentyl-2-fluoro-purin-6-amine (6) was synthesized by 6-chloro-9-cyclopentyl-2-fluoro-9H-purine (1.2 gm.), dry DMF (5 mL) and corresponding substituted amine Cpd -5, (1.2 eq.), 55% NaH (2 eq.) were added, under nitrogen, and the mixture was heated at 45°C for 8 hrs. The resultant reaction mixture was cooled to room temperature. The product was extracted with ethyl acetate (3 x 50 mL) and the combined organic fractions were washed with brine and dried over Na₂SO₄. After concentrating, the crude product was purified by column chromatography on silica (ethyl acetate: hexane =4:10) to yield N-(substituted phenyl)-9-cyclopentyl-2-fluoro-9H-purin-6-amine as a pale yellow or off white yellow solid compound (1.25 gm, yield 78 %).

2.1.2. General procedure for the synthesis of N2-((1r,4r)-4-aminocyclohexyl)-N6-(substituted phenyl)-9-cyclopentyl-9H-purin-2,6-diamine (7a-j)

In a sealed tube, N-(substituted phenyl)-9-cyclopentyl-2-fluoro-9H-purin-6-amine (0.7 gm.), and cyclohexane-1,4 diamine (3eq.) were added and the reaction was then carried out with microwave at 200°C for 40 to 80 min. The reaction mixture was cooled to the room temperature. The crude product was then purified by column chromatography on silica (methanol: DCM 3:10)

to yield compound (7a-j). ¹H NMR, ¹³C NMR, and ES-MS were used to confirm the product's production.

2.2. Spectral Data

2.2.1. N2-(4-aminocyclohexyl)-N6-(3-chloro-4-fluorophenyl)-9-cyclopentyl-9H-purine-2,6-diamine (7b):

¹H NMR 500 Hz, DMSO (D₆): δ ppm 9.70 (bs, 1H), 8.38 (s, 1H), 8.19 (s, 1H), 7.94(s, 2H), 7.35 (s, 1H), 6.63-6.65(d, 1H), 4.69 (s, 1H), 3.66 (s, 1H), 2.96 (m, 1H), 2.02-2.09 (m, 9H), 1.88 (m, 2H), 1.68 (m, 2H), 1.50-1.53 (m, 2H), 1.30-1.37 (m, 2H); ¹³C NMR 100 Hz, CDCl₃: δ ppm 152.2, 148.8, 144.8, 140.3, 138.3, 121.5, 118.3, 114.2, 66.6, 54.7, 50.7, 50.3, 34.3, 31.7, 28.8, 24.2; MS (ESI) m/e = 444 (M+H).

2.2.2. N2-(4-aminocyclohexyl)-N6-(3-chlorophenyl)-9-cyclopentyl-9H-purine-2,6-diamine (7i):

¹H NMR 400 Hz, CDCl₃: δ ppm 8.49 (bs, 2H), 8.15 (s, 1H), 7.79 (s, 1H), 7.58(s, 1H), 7.37-7.39 (m, 1H), 7.19-7.23 (m, 1H), 6.96-6.98 (m, 1H), 4.74-4.82 (m, 2H), 3.92-3.94 (m, 1H), 3.22-3.28 (t, 1H), 2.22-2.35 (m, 5H), 1.82-1.96 (m, 11H); ¹³C NMR 100 Hz, CDCl₃: δ ppm 181.7, 174.2, 158.2, 151.7, 147.8, 140.5, 136.1, 134.5, 129.8, 122.5, 119.5, 117.3, 92.4, 55.3, 50.5, 32.7, 30.9, 30.0, 24.1; MS (ESI) m/e = 426 (M+H).

2.3. Biological evaluation

All the N2-((1r,4r)-4-aminocyclohexyl)-N6-(substituted phenyl)-9-cyclopentyl-9H-purin-2,6-diamine (7a-j) derivatives were checked for *in vitro* antimicrobial activity against *E. coli*, *Bacillus subtilis* and *Streptococcus aureus* using time dose dependent growth inhibition assay. The results of antimicrobial activity of tested compounds (7a-j), using tetracycline as reference standard, are shown in table 2.

2.3.1. Procedure for Antibacterial activity

Clinical isolates were grown in Luria Bertini medium (pH 6.8) for 24 hours for activation of cultures. The colony forming units (CFUs) were calculated from the broth. A 100 uL (100x10² CFUs/mL) of the medium were inoculated into fresh Luria Bertini broth (5 ml) and kept for 16 hours to 18 hours for log phase culture. This log phase culture was used for the antimicrobial assay.

2.3.2. Preparation of compounds

The stock solution was prepared in DMSO and diluted further for antimicrobial action.

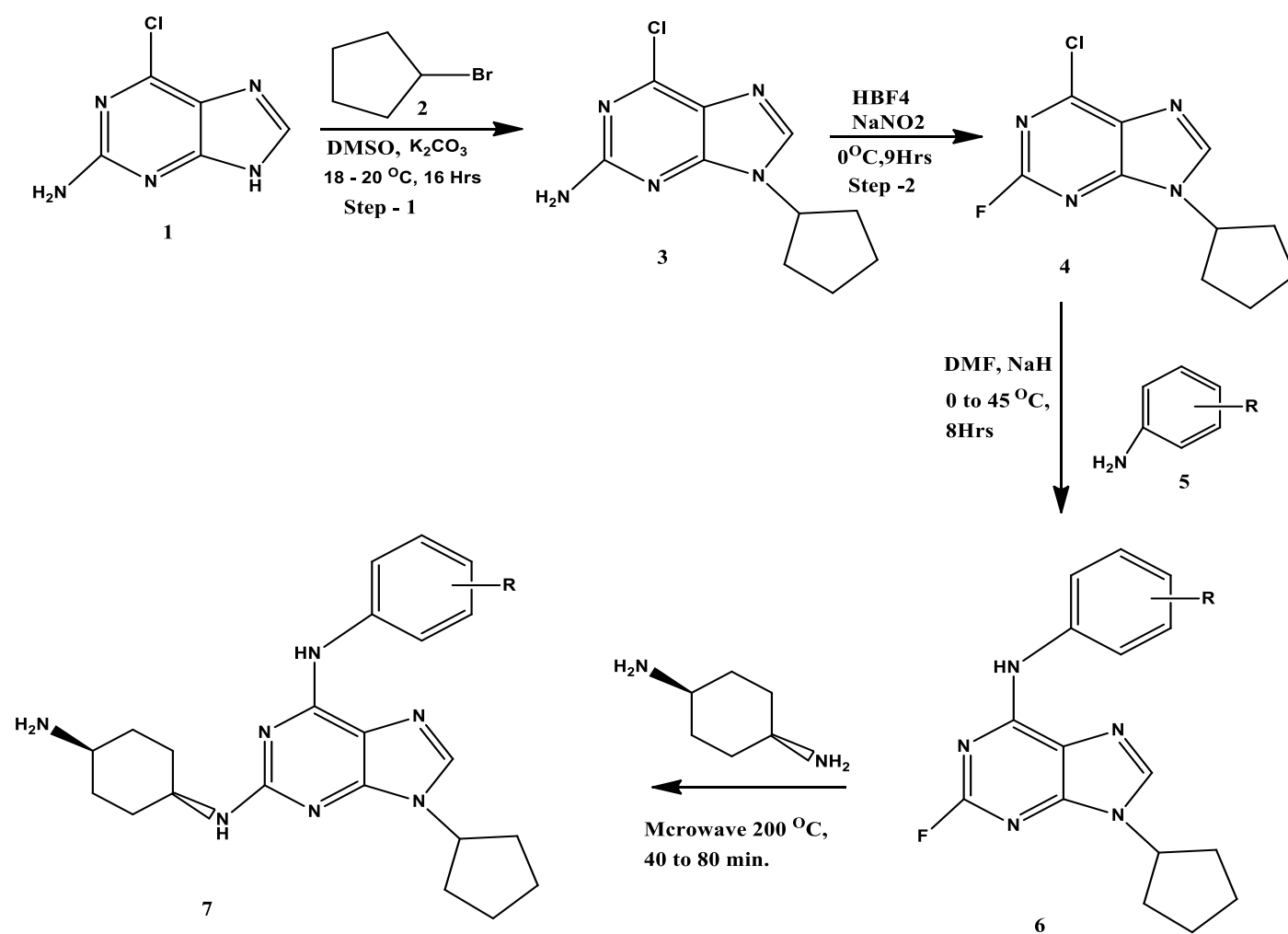
2.3.3. Time and dose dependent effect of compounds on the growth of the pathogenic microorganisms

The culture of MDR strain of *Escherichia coli*, *Streptococcus aureus* and *Bacillus subtilis* were inoculated separately into LB medium and incubated at 37°C for 16-18 hours. After 16 to 18 hours, the cultured tubes were exposed to the compounds at concentration of 10, 25 and 50 µg/mL. The O.D. was recorded at 660 nm after fixed interval of time. By using Graph pad prism 7, the time dependent growth of microorganism was analyzed.

3. RESULTS AND DISCUSSION

The following procedure was used for the synthesis of N2-((1*r*,4*r*)-4-aminocyclohexyl)-N6-(substitutedphenyl)-9-cyclopentyl-9H-purin-2,6-diamine (**7a-j**). The starting material (**1**) has been prepared by reaction with fluoboric acid, bromocyclopentane with commercially

available compound (**1**). The compound **4** (1.2 g) was reacted with corresponding substituted amine **5** (1.2 eq) in presence of dry DMF and 55% NaH (2 eq.) under nitrogen and reaction was heated at 45°C for 8 hrs. The resultant compound **6** was extracted with ethyl acetate and the combine organic fraction was washed with brine and dried over Na₂SO₄. After concentration, the crude product was purified by column chromatography to yield off white solid compound **6**. The compound (**7a-j**) was prepared by taking compound **6** in a sealed tube and cyclohexane 1, 4 diamine (3 eq) was added and the reaction was then carried out with microwave at 200°C for 40 to 80 min. The product was purified by column chromatography on silica (methanol: DCM 3:10) to yield compound (**7a-j**) in very good yield as shown in table 2. The formation of derivatives (**7a-j**) was justify by 1H NMR, 13C NMR and MS analysis.



Scheme 1: Synthesis of N2-((1*r*,4*r*)-4-aminocyclohexyl)-N6-(substitutedphenyl)-9-cyclopentyl-9H-purin-2,6-diamine (**7a-j**)

Table 1: Synthesis of N2-((1r,4r)-4-amino-cyclohexyl)-N6-(substitutedphenyl)-9-cyclopentyl-9H-purin-2,6-diamine (7a-j)

Entry	(R)	Product	Time (Hrs)	% Yield
1.	2-Me	(7a)	35	65
2.	3-Cl, 4-F	(7b)	45	65
3.	4-Br	(7c)	45	68
4.	2-Me, 4-Br	(7d)	50	75
5.	4-Me	(7e)	70	74
6.	4-Cl	(7f)	65	66
7.	2-F, 3-Cl	(7g)	65	73
8.	3-Br	(7h)	80	72
9.	3-Cl	(7i)	45	80
10.	4-OMe	(7j)	70	77

Reaction Condition: N-(substituted phenyl)-9-cyclopentyl-2-fluoro-9H-purin-6-amine (0.7 gm.), and cyclohexane-1,4 diamine (3eq.) were added and then the reaction was carried out with microwave at 200°C.

3.1. Antimicrobial effect of compounds (7a-j) on pathogenic microorganism by using Time Dose method

According to the time dose method, compound **7a** was found active at 25 and 50 µg/ml concentration at 10 hrs. The growth of *E. coli* was found at MIC 14.5 µg/ml. It was not found active against *Bacillus subtilis* and *S. aureus* at any concentration. The compound **7b** was found very active against all the three bacteria. The efficiency in controlling growth of pathogenic microorganism is carried out at very low concentration at 10 hrs. of exposure, the MIC was found at 6.3 µg/ml against *E. coli*, 7.8 µg/ml against *S. aureus* and 7.40 µg/ml against *Bacillus subtilis*. The compound **7c** was added to the 16 hrs. grown culture of the *E. coli*, the MIC was found at 12.4 µg/ml. The long phase *S. aureus* culture was used for determination of MIC of compound **7c**. A concentration of 0, 10, 25 and 50 µg/ml of compound was used against *S. aureus*, the MIC was found 10.6 µg/ml at 24 hrs. of incubation period. The compound **7c** was found more active against the *E. coli* than *S. aureus*. The compound **7d** was found active against *E. coli* and *Bacillus subtilis*. The growth of pathogenic *E. coli* and *Bacillus subtilis* was found at 10, 25 and 50 µg/ml at 10 hrs. of incubation, the MIC was found at 8.3 µg/ml against *E. coli* and 9.25 against *Bacillus subtilis*. The compound **7e** was found active against *E. coli* and inactive against *S. aureus* and *Bacillus subtilis* at 10 µL, 25 µL, 50 µL and 100 µL at 10, 16, 24

hrs. of incubation period. The compound **7f** showed activity at 10 µg/ml concentrations for 10 exposures with MIC 4.6 µg/ml against *E. coli* and 9.1 µg/ml against *S. aureus*. The compound **7g** was found active at 10 µg/ml concentration at 10 hrs. incubation with MIC 7.25 µg/ml against *E. coli* and MIC 6.8 µg/ml against *S. aureus*. The compound **7h** gives activity for 10 hrs. incubation at 10, 25, and 50 µg/ml concentration with MIC 16.1 µg/ml against *E. coli* and 12.6 µg/ml against *Bacillus subtilis*. The compound **7i** was found active against all the three pathogenic bacteria. It has effectively killed bacterial cell for 10 hrs. of incubation with MIC 5.80 µg/ml against *E. coli*, 8.4 µg/ml against *S. aureus* and 4.5 µg/ml against *Bacillus subtilis*. The compound **7j** was active against the *Bacillus subtilis* and the growth was found to be inhibited at very low concentration 10 µg/ml and MIC 7.01 µg/ml.

Table 2: Time and dose dependent growth inhibition assay compounds (7a-j) on pathogenic microorganism

Entry	Compound	MIC (µM)		
		<i>E. coli</i>	<i>S. aureus</i>	<i>Bacillus subtilis</i>
1.	(7a)	14.5	-	-
2.	(7b)	6.3	7.8	7.4
3.	(7c)	12.4	10.6	-
4.	(7d)	8.3	-	9.20
5.	(7e)	12.2	-	-
6.	(7f)	4.6	9.1	-
7.	(7g)	7.25	6.8	-
8.	(7h)	-	15.9	12.4
9.	(7i)	5.8	8.4	4.5
10.	(7j)	-	-	7.01

4. CONCLUSION

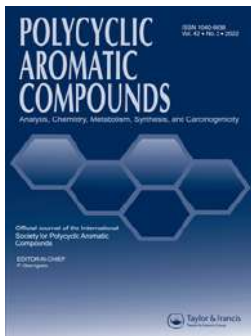
In summary, we synthesized N2-((1r,4r)-4-amino-cyclohexyl)-N6-(substitutedphenyl)-9-cyclopentyl-9H-purin-2,6-diamine derivatives (**7a-j**). Synthesized derivatives showed moderate to good inhibition of antimicrobial activity. These analogues are chemically tractable and hence provide ample opportunities for further modification to obtain potent anti-microbial agents. The isolated yield of the N2-((1r,4r)-4-aminocyclohexyl)-N6-(substitutedphenyl)-9-cyclopentyl-9H-purin-2,6-diamine derivatives (**7a-j**) are excellent.

5. ACKNOWLEDGMENT

All authors are grateful to the Department of Postgraduate Studies and Research in Chemistry, S. B. E. S. College of Science, Aurangabad, Vasant Rao Naik Mahavidyalaya, Aurangabad for providing laboratory facilities and Indian Institute of Chemical Technology, Hyderabad for spectral data.

6. REFERENCES

1. Rida SM, Ashour FA, El-Hawash SA, El-Semary MM, Badr MH. *Arch Pharm (Weinheim)*, 2007; **340**: 185-194.
2. Zaza G, Yang W, Kager L, Cheok M, Downing J. *Blood*, 2004, **104**:1435-144.
3. Robak T, Lech-Maranda E, Korycka A, Robak E. *Curr. Med. Chem.*, 2006, **13**:3165-3189.
4. Schwartz RS. *World J Surg*, 2006, **24**:783-786.
5. Carey NH, Mandel HG. *J. Biol. Chem.*, 1961, **236**:520-524.
6. Mars U, Larsson BS. *Pigment Cell Res*, 1995, **8**:194-201.
7. Rubina K, Abele E, Arsenyan P, Abele R, Veveris M. *Metal Based Drugs*, 2001, **8**:85-93.
8. Rosemeyer H. *Chemistry & Biodiversity*, 2004, **1**:361-401.
9. Nair, V, Bera B, Earl RK. *Nucleosides, nucleotides & nucleic acids*, 2003, **22**:115-127.
10. Holy A, Gunter J, Dvorakova H, Masojidkova M, Andrei G, Snoeck R, et al. *J. Med. Chem.*, 1999, **42**:2064-2086.
11. Avila JL, Rojas T, Avila A, Polegre MA, Robins RK. *Antimicrob. Agents Chem.*, 1987, **31**:447-451.
12. Raic-Malic S, Hergold-Brundic A, Nagl A, Grdisa M, Pavelic K, Clercq ED. *J. Med. Chem.*, 1999, **42**:2673-2678.






Pyridine-1,3,4-Thiadiazole-Schiff Base Derivatives, as Antioxidant and Antimitotic Agent: Synthesis and *in Silico* ADME Studies

Amit A. Pund, Mubarak H. Shaikh, Badrinarayan G. Chandak, Vijay N. Bhosale & Baban K. Magare

To cite this article: Amit A. Pund, Mubarak H. Shaikh, Badrinarayan G. Chandak, Vijay N. Bhosale & Baban K. Magare (2022): Pyridine-1,3,4-Thiadiazole-Schiff Base Derivatives, as Antioxidant and Antimitotic Agent: Synthesis and *in Silico* ADME Studies, Polycyclic Aromatic Compounds, DOI: [10.1080/10406638.2022.2026988](https://doi.org/10.1080/10406638.2022.2026988)



To link to this article: <https://doi.org/10.1080/10406638.2022.2026988>

 View supplementary material 

 Published online: 17 Jan 2022.

 Submit your article to this journal 

 Article views: 34

 View related articles 

 View Crossmark data 



Pyridine-1,3,4-Thiadiazole-Schiff Base Derivatives, as Antioxidant and Antimitotic Agent: Synthesis and *in Silico* ADME Studies

Amit A. Pund^a , Mubarak H. Shaikh^b , Badrinarayan G. Chandak^c , Vijay N. Bhosale^a , and Baban K. Magare^a

^aUG, PG and Research Centre, Department of Chemistry, Shivaji Arts, Commerce and Science College, Kannad. Dist., Aurangabad, India; ^bDepartment of Chemistry, Radhabai Kale Mahila Mahavidyalaya, Ahmednagar, India; ^cDepartment of Pharmaceutical chemistry, Y. B. Chavan College of Pharmacy, Aurangabad, India

ABSTRACT

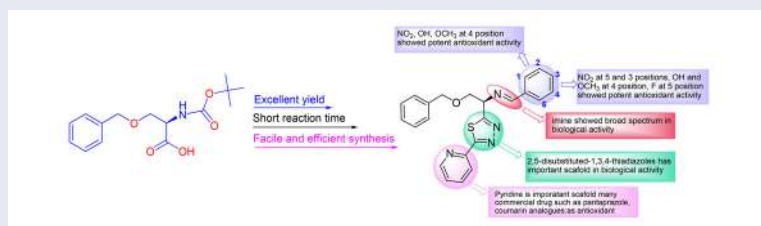
An efficient method developed for the synthesis of asymmetric (*S*)-*N*-benzylidene-2-(benzyloxy)-1-(5-(pyridin-2-yl)-1,3,4-thiadiazol-2-yl)ethanamine derivatives with excellent yield in short reaction time. The antioxidant and antimetabolic activities were estimated and strongly correlated with the potential of Ascorbic acid and Methotrexate respectively. All the synthesized molecules were characterized using various spectral techniques including FTIR, ¹H NMR, ¹³C NMR, and Mass spectrometry. The drug-likeness properties were studied using *in silico* ADME parameters. All the compounds have an acceptable range of values which indicated good drug-like characteristics based on Lipinski's rule of five and to be orally active. The present method is quite easy along with simple operation and offers many benefits including short reaction time, easy work-up, excellent yield, reduced waste production as well as cost effective. In addition structure-activity relationships of **AP-1** to **AP-10** derivatives have been described.

ARTICLE HISTORY

Received 20 October 2021
Accepted 30 December 2021

KEYWORDS

Antioxidant; antimetabolic; asymmetric synthesis; *in silico* ADME parameters; structure-activity relationships



Introduction

The heterocyclic compounds with five-membered heterocyclic ring have acquired impressive interest on account of their wide scope of helpful pharmacological properties. Amongst these five membered heterocyclic compounds, 2,5-disubstituted-1,3,4-thiadiazoles are associated with diverse biological activities probably due to the presence of $-N=C-S-$ group. The backbone of these article is the combination of biologically active scaffolds containing pyridine, 1,3,4-thiadiazole and

CONTACT Baban K. Magare magrebk75@gmail.com; amitchem0512@gmail.com UG, PG and Research Centre, Department of Chemistry, Shivaji Arts, Commerce and Science College, Kannad. Dist., Aurangabad, India

Supplemental data for this article is available online at <https://doi.org/10.1080/10406638.2022.2026988>.

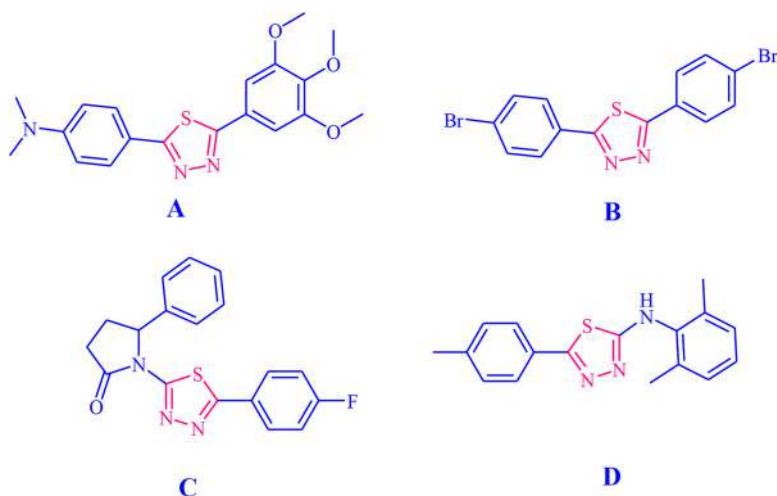


Figure 1. 1,3,4-Thiadiazole heterocycles containing reported molecules.

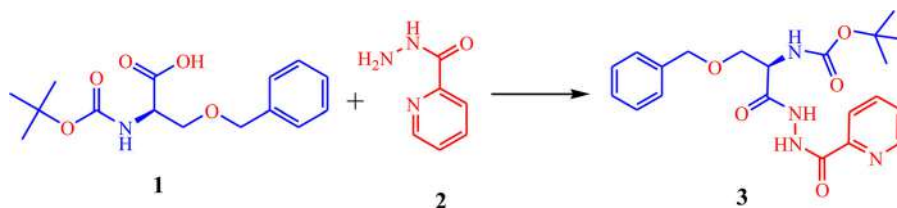
imine moiety. The 1,3,4-thiadiazoles ring system is widely distributed in a broad variety of important compounds with significant pharmacological properties such as antitubercular,¹ antimicrobial,² antifungal,³ antiparasitic,⁴ antiviral,⁵ anti-inflammatory and analgesic,⁶ COX and LOX inhibitory activities,⁷ antiproliferative,⁸ anticonvulsant,⁹ antidepressant,¹⁰ epilepsy,¹¹ Parkinson's disease.¹² Thiadiazole containing drugs like Acetazolamide, Methazolamide, Cefazolin, Sulfamethizole and Megazol are available in market.¹³ Furthermore, an azomethine group exhibited broad spectrum in pharmacological properties, perhaps engaged with the formation of a hydrogen bond with the active centers of cell constituents and interferes in normal cell metabolism.^{14a-j}

Moreover, antimetabolic agents are classified into three major classes. First one is microtubule-stabilizing agents, these agents prevent the depolymerization of tubulin subunits through binding with fully formed microtubules. The remaining two other classes functioning by binding to tubulin monomers and inhibiting their polymerization into microtubules.¹⁵ Noteworthy, the 2,5-disubstituted-1,3,4-thiadiazole moiety is the backbone in many drugs including antimetabolic agents 4-(5-(3,4,5-trimethoxyphenyl)-1,3,4-thiadiazol-2-yl)-N,N-dimethylbenzenamine (A),¹⁶ antioxidant agent 2,5-bis(4-bromophenyl)-1,3,4-thiadiazole (B),¹⁷ 1-(5-(4-fluorophenyl)-1,3,4-thiadiazol-2-yl)-5-phenylpyrrolidin-2-one (C),¹⁸ N-(2,6-dimethylphenyl)-5-p-tolyl-1,3,4-thiadiazol-2-amine (D)¹⁹ (Figure 1).

There are numerous reports have been available for the construction of thiadiazole and Schiff's base molecules, the synthesis of 2,5-disubstituted thiadiazole containing imine moiety are rare.

As a part of our ongoing work and in view of above challenges, previously we reported the synthesis of asymmetric (*S*)-*N*-benzylidene-2-(benzyloxy)-1-(5-(pyridin-2-yl)-1,3,4-thiadiazol-2-yl)ethanamine derivatives (AP-1 to AP-10) *via* amide coupling using *N,N'*-carbonyldiimidazole (CDI) and evaluated *in vitro* anti-microbial activities.²⁰ The formation of 2,5-disubstituted-1,3,4-thiadiazole ring could be possible by cyclocondensation of diacyl hydrazine using Lawesson's Reagent (LR) or phosphorus pentasulfide²¹ as thionating agent in the presence of tetrahydrofuran (THF) and toluene as solvent. This reaction is always carried out in warm condition and yield of product is moderate and it is very difficult to maintain purity due to harsh reaction conditions such as temperature and workup.

The amide coupling of hydrazide and acid moiety to afford diacylhydrazine have been reported using 1-ethyl-3-(3-dimethylaminopropyl) carbodiimide hydrochloride (EDC.HCl)^{22a-g} which requires column chromatography for purification. Another reagent 2-(1*H*-benzotriazole-1-yl)-1,1,3,3-tetramethylammonium tetrafluoroborate (TBTU)^{23a-b} has identified to react with acid and



Scheme 1. Synthesis of diacyl hydrazine (**3**)

hydrazide but yield of isolated product is not reasonable. Moreover, *N,N'*-diisopropylcarbodiimide (DIPC)^{24a-b} and thionyl chloride^{25a-b} were used as coupling reagents for the same reaction of hydrazide and acid but removal of unreacted *N,N'*-diisopropyl carbodiimide and thionyl chloride was quite difficult. The CDI^{26a-c} was also used for coupling to obtain amide bond and unreacted CDI can be removed with water. By taking the advantage of above reactions we have reported efficient synthesis of the target compounds (**AP-1** to **AP-10**) using condensation of (*S*)-2-(benzyloxy)-1-[5-(pyridin-2-yl)-[1,3,4]-thiadiazol-2yl]ethanamine (**4**) with substituted benzaldehyde in isopropyl alcohol (IPA). The purified product was isolated by simple acidification of 2% aqueous hydrochloric acid with simple workup operation, excellent yield in short reaction time.

Result and discussion

In continuation of our earlier work²⁰ herein, we focused on facile and efficient synthesis of 1,2,3-thiadiazole-imine hybrids with excellent yield in short reaction time. This is facile, efficient and environmentally benign green protocol which avoids use of strong dehydrating agents, generation of wastes. Moreover, targeted compounds (**AP-1** to **AP-10**) were evaluated for *in vitro* antioxidant and antimetabolic activities. In addition to this, we performed *in silico* ADME prediction for the synthesized compounds. The target compounds were prepared in four steps from the commercially available cheap and potentially active starting material *N*-*boc*-*O*-benzyl-*L*-tyrosine (**1**).

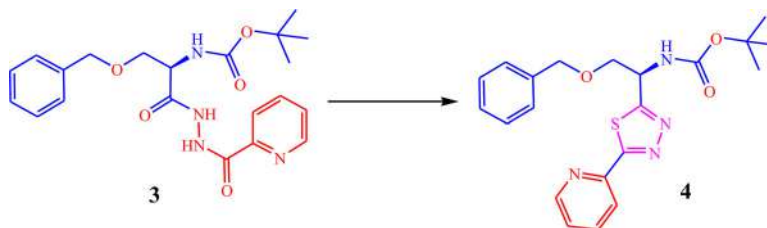
Initially, the coupling of acid (**1**) and hydrazide (**2**) to form diacyl hydrazine (**3**) have been investigated using EDC.HCl, *N*-Methylmorpholine (NMM) and hydroxybenzotriazole (HOBT) in the presence of DMF (**Scheme 1**). In order to optimize the reaction conditions, initially we carried out the reaction between acid (**1**) and hydrazide (**2**) as a model reaction. Optimum reaction conditions for the synthesis of **3** was designed and developed using various type of coupling reagents, different temperature, time and solvents (**Table 1**).

The coupling of **1** and **2** to form **3** is possible at 20–30 °C optimum temperature. Initially, Steglich esterification carried out using DCC and reaction was completed in 3 h with 85% yield of product (**Table 1**, entry 1). During this coupling reaction, dicyclohexylurea (DCU) was formed as a by-product. After completion of the reaction it was very difficult to remove DCU and unreacted DCC from the product. Moreover, we used another amide coupling reagent, 1-[Bis(dimethylamino)methylene]-1*H*-1,2,3-triazolo[4,5-*b*]pyridinium-3-oxidehexafluorophosphate (HATU) and required 6 h for the completion of reaction to get 90.2% yield (**Table 1**, entry 2). Furthermore another coupling reagent CDI was used and the product was formed in 1 h with 96% yield (**Table 1**, entry 3). Finally, the amide coupling was carried out by using EDC. HCl. The reaction was completed in 30 min with maximum yield of product (97%), mild reaction conditions and easy work up procedure (**Table 1**, entry 4). It was simply isolated by filtration and by-product EDC urea and unreacted EDC. HCl washed out in mother liquor.

In next step, cyclization of **3** was carried out in the presence of Lowesson's reagent (LR) and phosphorus pentasulfide to form 2,5-disubstituted-1,3,4-thiadiazole ring (**Scheme 2**).

Table 1. Screening of different coupling reagent and their effect on reaction time and yield on the synthesis of **3**.

Sr. No.	Coupling agent	Reaction time	% Yield for Compound 3
1	DCC	3 h	85.3%
2	HATU	6 h	90.2%
3	CDI	1 h	96%
4	EDC.HCl	30 min	97%

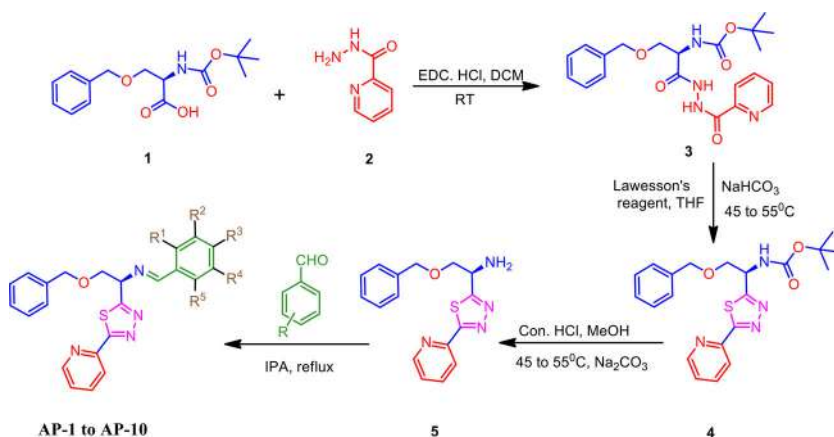
**Scheme 2.** Synthesis of 2,5-disubstituted, 1,3,4-thiadiazole ring**Table 2.** Screening of different cyclization reagent and their effect on reaction time for synthesis of **4**.

Sr. No.	Reagent	Reaction temperature (°C)	Reaction time (hr)	Solvent	Remarks
1	Lowessons Reagent	75–80	4.0	Toluene	Reaction done but a yield of 4 is 50% w/w
2	Phosphorus Pentasulfide	75–80	6.0	Toluene	Sticky mass observed and more impurity observed on TLC
3	Lawesson's Reagent	60–70	8.0	Toluene	Reaction done but yield of 4 is 30% w/w
4	Phosphorus Pentasulfide	60–70	8.0	Toluene	Sticky mass observed and more impurity observed on TLC
5	Lawesson's Reagent	45–55	6.0	THF	Reaction done but a yield of compound 4 is 74% w/w
6	Phosphorus Pentasulfide	45–55	8.0	THF	Reaction done and yield of compound 4 is 70% w/w

The experiment was carried out in THF and toluene as solvents at various temperatures. The screening of cyclization reagents and their effect on reaction time and yield for the synthesis of **4** was tabulated in Table 2. It was observed that the best results were accomplished with THF and LR at 45–55 °C temperature. The reaction was completed in 6 h and yield was 74% (Table 2, entry 5). Whereas in case of phosphorus pentasulfide, reaction was completed but low yield was observed as compared to LR. At higher temperature conditions, maximum impurities were observed on TLC (Table 2, entry 1-4) hence optimum temperature was set to 45–55 °C. Moreover, reaction was also carried out using phosphorus pentasulfide in toluene, but reaction mass become sticky and non-stirable (Table 2, entry 2 and 4). Therefore, it was concluded that the cyclization of compound **3** successfully achieved using LR at temperature 45–55 °C in THF to form 2,5-disubstituted-1,3,4-thiadiazole ring compound **4** (Table 2, entry 6).

Finally, the title compounds (**AP-1** to **AP-10**) have been prepared after boc-deprotection of **4** in acidic condition afforded **5**. The synthesis of **AP-1** to **AP-10** was outlined in Scheme 3.

Synthesis of asymmetric (*S*)-*N*-benzylidene-2-(benzyloxy)-1-(5-(pyridin-2-yl)-1,3,4-thiadiazol-2-yl)ethanamine derivatives (**AP-1** to **AP-10**) were investigated from (*S*)-2-Benzyloxy-1-(5-pyridin-2-yl-[1,3,4]-thiadiazol-2-yl)-ethanamine (**5**) and substituted aldehydes. The reaction mixture was



Scheme 3. Synthesis of asymmetric (*S*)-*N*-benzylidene-2-(benzyloxy)-1-(5-(pyridin-2-yl)-1,3,4-thiadiazol-2-yl)ethanamine derivatives (AP-1 to AP-10)

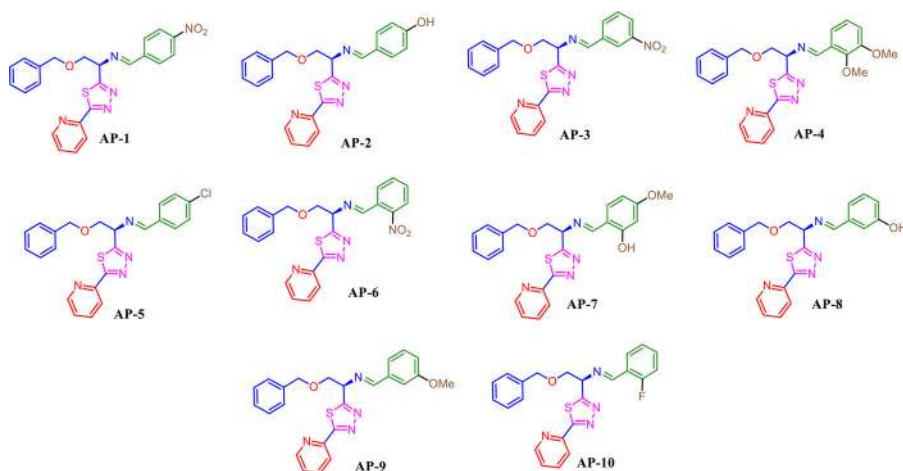


Figure 2. Structures of all the synthesized derivatives AP-1 to AP-10.

refluxed in IPA for 9-12 h. After completion of reaction, pure compounds were obtained using acidic treatment with excellent yield (92-97%) in short reaction time. All synthesized molecules were well identified and characterized using various spectral techniques including FTIR, ¹H NMR, ¹³C NMR, and Mass spectrometry. Structures of all the synthesized compounds were shown in Figure 2.

Biological evaluation

Antioxidant activity

The AP-1 to AP-10 were tested for their antioxidant property using free stable radical and commercially available organic nitrogen radical as 2, 2-diphenyl-1-picrylhydrazyl (DPPH). All the synthesized compounds exhibited excellent antioxidant activity. However, the compounds which exhibited relatively good antioxidant activities as compared with standard antioxidant drug Ascorbic acid (80.40 μg/ml). AP-1, AP-6 and AP-8 to AP-10 with their % inhibition at 150 μg/ml

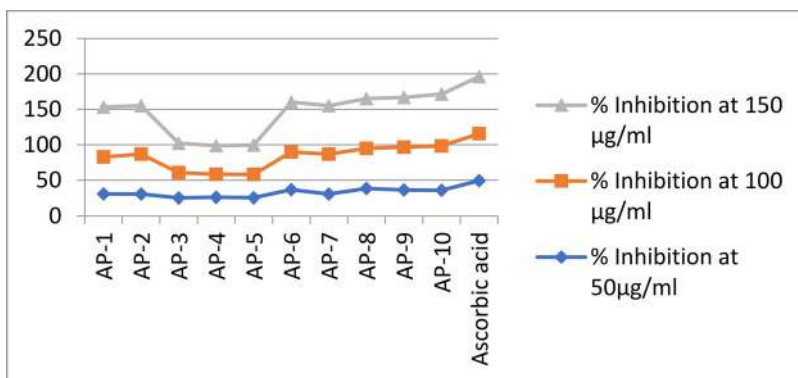
Table 3. DPPH scavenging activity of AP-1 to AP-10.

CONCENTRATION	% Inhibition at 50µg/ml	% Inhibition at 100 µg/ml	% Inhibition at 150 µg/ml
Control	0	0	0
AP-1	30.6	52.28	70.42
AP-2	30.45	56.48	68.21
AP-3	25.12	35.66	41.32
AP-4	26.10	32.28	40.30
AP-5	25.46	32.68	41.45
AP-6	36.60	53.28	70.42
AP-7	30.45	56.48	68.21
AP-8	38.45	56.48	70.21
AP-9	36.15	60.52	70.21
AP-10	35.90	62.48	73.21
Ascorbic acid	49.40	66.33	80.40

Table 4. Statistical analysis of DPPH scavenging activity.

Goodness of fit	
R square	0.5983
F	16.54
DFn,DFd	1,10
P Value	0.0019
Deviation from horizontal	Significant

was 70.42, 70.42, 70.21, and 73.21, respectively (Table 3). The AP-1, AP-6, AP-8 to AP-10 showed good assay against antioxidant activity, it may be due to nitro group at *ortho-para* position and hydroxy and methoxy at *meta* position as well as fluorine at *ortho* position. Statistical analysis of DPPH scavenging activity is showed in Table 4. The graph of antioxidant activity of AP-1 to AP-10 showed in Graph 1.

**Graph 1.** Antioxidant activity of AP-1 to AP-10.

Antimitotic activity

The results of antimitotic activity have expressed as a reduction in *Allium cepa* root length.²⁷ In this activity, a mixture of DMSO and water was used as control and Methotrexate as reference standard. At the beginning (zero time), no significant difference ($P > 0.05$) was found in mitotic percent amongst different samples, as showed in Table 5. However, after 48 h of incubation (concentration 500 ppm), the compounds AP-3, AP-8 and AP-9 showed significant antimitotic activity as compared to a standard drug ($P < 0.05$). This may be attributed due to presence of *meta*

Table 5. Results of the antimetabolic assay for AP-1 to AP-10.

Compound	Concentration $\mu\text{g/ml}$	Root Length in (cm)		
		0 h	48 h	96 h
AP-1	10	3.1	3.4	3.8
AP-2	10	3.1	3.3	3.8
AP-3	10	3.2	4.2	4.5
AP-4	10	3.2	3.8	4.0
AP-5	10	3.2	3.6	4.0
AP-6	10	3.1	3.8	3.9
AP-7	10	3.1	4.0	4.2
AP-8	10	3.2	4.1	4.2
AP-9	10	3.2	3.8	4.2
AP-10	10	3.1	3.4	3.9
Methotrexate	10	3.2	3.9	4.0

substitution of nitro, hydroxy and methoxy on benzene ring. The result of the antimetabolic assay for AP-1 to AP-10 has mentioned in Table 5.

Structure-activity relationship (SAR)

Ten new Schiff base derivatives, bearing hetero aromatic ring pyridine, 1,3,4-thiadiazole and substituted aromatic ring were synthesized and evaluated *in vitro* for antioxidant and antimetabolic activities. In order to enhance the potency of Schiff base derivatives, we elucidated the structure-activity relationship (SAR) based on the mode of action. We used electron donating and electron withdrawing substituted aromatic aldehydes to study, its effect on the biological activity. The nitro substitution at *ortho* and *para* position, hydroxy and methoxy moiety at *meta* position and fluorine substitution at *ortho* position in Schiff base derivatives showed potent antioxidant activity. The compound AP-4 in which methoxy group present at *meta* and *ortho* position exhibited two-fold more antioxidant activity as compared to standard drug. Similarly, compound AP-3 (nitro group at *meta* position) and compound AP-5 (chloro group at *para* position) exhibited near about two-fold more antioxidant activity as compared to the standard drug. In compound AP-1, AP-3, and AP-6 nitro group present *para*, *meta*, and *ortho* position respectively; though all these three compounds having nitro group at different position, compound AP-3 exhibited excellent antioxidant activity due to presence of nitro functional group at *meta* position. These results confirm that the activity varies depending on the various substituents present on the phenyl rings. Diverse substituted forms of hetero aromatic ring are tolerated on the Schiff base derivative and the presence or orientation of -OH at *ortho* and *para* position, -Cl at *para* position, -NO₂ at *meta* position, -OCH₃ at *ortho*, *para*, and *meta* position in the hetero aromatic ring affected the antioxidant activity.

Moreover, the compounds AP-1, AP-2, AP-6 and AP-10 showed significant antimetabolic activity as compared to a standard drug ($P < 0.05$). This may be attributed due to presence of substitution of -NO₂, -OH, and -F on benzene ring. In compound AP-1, AP-3 and AP-6, NO₂ group present *para*, *meta* and *ortho* position respectively though all these three compounds having -NO₂ at different position, compound AP-1 and AP-6 exhibited excellent antimetabolic activity. These results confirm that the activity varies depending on the various substituents present on the phenyl rings.

Diverse substituted forms of hetero aromatic ring are tolerated on the Schiff base derivative and the presence or orientation of -NO₂ and -OH functional group at *ortho* and *para* position, -Cl at *para* position, -OCH₃ substitution at *ortho*, *meta*, and *para* position as well as -F substitution at *ortho* position in the hetero aromatic ring affected the antimetabolic activity.

Table 6. Pharmacokinetic parameters of compounds **AP-1** to **AP-10**.

Entry	% ABS	TPSA (Å ²)	n-R OT B	MV	MW	miLog P	n-ON	n-OHN H	Lipinski violation	Drug-likeness model score
Rule	–	–	–	–	< 500	≤ 5	< 10	< 5	≤ 1	–
AP-1	72.39	106.10	9	382.52	445.5	3.99	8	0	0	–0.73
AP-2	81.22	80.50	8	367.21	416.5	3.55	6	1	0	–0.19
AP-3	72.39	106.10	10	399.32	459.5	3.56	8	0	0	–0.54
AP-4	81.83	78.74	10	410.28	460.5	3.85	7	0	0	0.09
AP-5	88.21	60.27	8	372.72	434.9	4.71	5	0	0	0.06
AP-6	72.39	106.10	9	382.52	445.8	3.94	8	0	0	–0.96
AP-7	78.04	89.74	9	392.75	446.5	4.00	9	1	0	0.16
AP-8	81.22	80.50	8	367.21	416.5	3.53	8	1	0	–0.01
AP-9	85.02	69.51	9	384.73	430.5	4.07	6	0	0	0.06
AP-10	88.20	60.27	8	364.12	418.5	4.15	5	0	0	–0.56

Note: % ABS: Percentage absorption, TPSA: Topological polar surface area, n-ROTB: Number of rotatable bonds, MV: Molecular volume, MW: Molecular weight, miLogP: Logarithm of partition coefficient of a compound between n-octanol and water, n-ON Acceptors: Number of hydrogen bond acceptors, n-OHNH donors: Number of hydrogen bonds donors.

In silico ADME Prediction

Based on Lipinski's rule of five, the drug-likeness properties were analyzed by ADME parameters using Molinspiration online property calculation toolkit²⁸ and data are summarized in Table 6.

All the compounds exhibited values and showed good drug-like characteristics based on Lipinski's rule of five and to be likely orally active. The data obtained for all the synthesized compounds were within the range of accepted values. None of the synthesized compounds violated Lipinski's rule of five. The parameters like the number of rotatable bonds and total polar surface area were linked with the intestinal absorption and results showed all synthesized compounds had good absorption ranging from 72.39% to 88.20%. The *in-silico* assessment of all the synthesized compounds showed very good pharmacokinetic properties, which is reflected in their physicochemical values, thus ultimately enhancing the pharmacological properties of these molecules. The molecule likely to be developed as an orally active drug candidate and should not show more than one violation of the following four criteria: miLog P (octanol-water partition coefficient) ≤5, molecular weight ≤500, number of hydrogen bond acceptors ≤10, and number of hydrogen bond donors ≤5.²⁹ The larger value of the drug-likeness model score reflects the higher probability of molecule to be active. All the tested compounds **AP-1** to **AP-10** were followed the criteria of an orally active drug, and therefore, these compounds may have a good potential for eventual development as oral agents.

Experimental

Material and methods

The starting material (2S)-3-(benzyloxy)-2-[(tert-butoxycarbonyl) amino] propanoic acid or *N*-*boc*-*O*-benzyl-*L*-serine obtained from Alichem and 2-hydrazinopyridine and phosphorus pentasulfide from Sigma Aldrich. Anhydrous sodium carbonate and other chemicals were obtained from SDFCL. The anhydrous solvents were obtained from Rankem. The reactions were monitored by TLC (Silica gel60, GF254, Merck) and visualized under UV light chamber. The melting points of synthesized compounds were recorded on melting point apparatus (Veego, Model-VMP-AD). The IR spectra were recorded on Shimadzu FTIR-8400S spectrometer. The ¹H NMR and ¹³C NMR spectra were run on a Bruker spectrophotometer at 500 MHz and 125 MHz, respectively. The elemental (C, H, and N) analyses were measured on Perkin-Elmer 2400.

General procedure for the synthesis of compound 3

In three neck 250 ml round bottom flask, 2-hydrazinopyridine (**2**) (20 gm, 1.0 mol) and (2S)-3-(benzyloxy)-2-[(*tert*-butoxycarbonyl) amino] propanoic acid (**1**) (45.3 gm, 1.1 mol) was stirred in water (100 ml). In this stirred solution added HOBt (1.97 gm, 0.1 mol) followed by addition of NMM (22.45 gm, 1.52 mol). Then EDC.HCl (41.98 gm, 1.5 mol) was added lot wise and whole reaction was stirred for 30 minutes at 20–30 °C. The reaction was monitored by TLC (DCM:MeOH: 9:1), after reaction completion, the reaction mixture was filtrated and dried to get white compound (**3**) as white solid, yield 58.65 gm (97%), mp 187 °C. IR spectrum, ν , cm^{-1} : 1242.16 (C–N), 1421.54 (C=C), 699.91 (C–S), 2980.02 (C–H), 1695.43 (C=O), 1070.49 (C–O). ^1H NMR spectrum, δ , ppm (J, Hz): 10.12 s (1H, NH), 9.16 s (1H, NH), 8.59–8.58 d ($J=5$ Hz, 1H, H-2 pyridine), 8.16–8.15 d ($J=5$ Hz, 1H, H-5 pyridine), 7.88–7.85 t (1H, H-4 pyridine), 7.48–7.46 t (1H, H-3 pyridine), 7.35–7.29 m (5H, Ar-H), 5.43 s (1H, NH-Boc), 4.60 s (2H, CH_2 -Ph), 4.51–4.49 t (1H, CH-N-Boc), 3.97–3.96 d ($J=5$ Hz, 1H, CH=N), 3.67–3.66 d ($J=5$ Hz, 1H, CH), 1.47 s (9H, Boc) and NH proton confirmed by D_2O exchange. ^{13}C -NMR spectrum δ , ppm: 167.3, 160.6, 148.5, 148.1, 137.4, 137.2, 128.5, 128.0, 127.9, 126.8, 122.5, 73.6, 69.3, 28.2. Anal. calcd for $\text{C}_{21}\text{H}_{26}\text{N}_4\text{O}_5$: C 60.86, H 6.32, N 13.52, O 19.30, found: C 60.85, H 6.33, N 13.52.

General procedure for the synthesis of Compound 5

In a three neck 250 ml round bottom flask diacylhydrazine derivative (**3**) (50 gm 1.0 mol), sodium carbonate (12.8 gm 1.0 mol) and Lowessons reagent (29.31 gm, 0.6 mol), in THF (150 mL) were stirred at 45–55 °C for 6 hours. The reaction was monitored by TLC (DCM:MeOH, 9:1) after completion of reaction, quenched with 5% sodium bicarbonate solution (500 mL) and product so obtained was extracted in ethylacetate (250 mL). After layer separation, the ethylacetate layer was distilled out undervacuum. The obtained residue dissolved in methanol (50 mL) and added 35% aqueous hydrochloric acid solution (100 mL, warmed 50–75 °C temperature for 8 hours. After reaction completion by TLC (DCM:MeOH, 9:1) and it was cooled to room temperature and added water (500 mL). The two layers were separated, aqueous layer was collected in two neck 1000 ml round bottom flask and pH 8.5 to 9.5 adjust by using 10% aqueous sodium hydroxide solution. The product thus obtained and was extracted in DCM and the DCM layer washed with water and concentrated and obtained residue was purified by silica gel chromatography to get compound (**5**) as dark brown color solid, yield 27.88 gm (68%), mp: 160 °C. IR spectrum, ν , cm^{-1} : 1245.53 (C–N), 1431.14 (C=C), 700.98 (C–S), 3061.86 (C–H), 3376.11 (N–H). ^1H NMR spectrum, δ , ppm (J, Hz): 8.64–8.63 d ($J=5$ Hz, 1H, H-2 pyridine), 8.33–8.31 d ($J=10$ Hz, 1H, H-5 pyridine), 7.84–7.81 t (1H, H-4 pyridine), 7.37–7.28 m (6H, Ar-H and H-3 pyridine), 4.67–4.66 t (1H, CH–N), 4.60 s (2H, CH_2 -Ph), 3.92–3.90 d ($J=10$ Hz, 1H, CH=N), 3.76–3.73 d ($J=15$ Hz, 1H, CH), 2.23 s (2H, NH_2) and NH proton confirmed by D_2O exchange. ^{13}C -NMR spectrum δ , ppm: 175.7, 170.7, 149.7, 149.3, 137.5, 137.0, 128.4, 127.8, 127.7, 125.1, 120.7, 73.8, 73.4, 52.2. ESMS ($M+1$): 313. Anal. calcd for $\text{C}_{16}\text{H}_{16}\text{N}_4\text{OS}$: C 61.52, H 5.16, N 17.93, S 10.26, found: C 61.53, H 5.16, N 17.92, S 10.27.

General procedure for synthesis of compounds AP-1 to AP-10

To a solution of corresponding 1.0 mol of (S)-2-Benzyloxy-1-(5-pyridin-2-yl-[1,3,4] thiadiazol-2-yl)-ethylamine (**5**) in 5 ml IPA, 0.98 mol substituted benzaldehyde was added and refluxed for 8–12 hours. The progress of reaction was monitored by TLC (DCM:MeOH, 9.5:0.5). Reaction quenched using 25 ml water (confirmed qty) and product was extracted in DCM and organic layer washed with 3 ml 2% aqueous hydrochloric acid solution. The obtained residue was suspended in MTBE to get **AP-1** to **AP-10** compounds.

(S)-[2-Benzyloxy-1-(5-pyridin-2-yl-[1,3,4]-thiadiazol-2-yl)-ethyl]-(4-nitro-benzylidene)-amine (AP-1)

Brown color solid; Yield: 96%; M.p.: 196–198 °C; IR (KBr ν , cm^{-1}): 1201 (C–N), 1521.84 & 1342.46 (NO_2), 1400.32 (C=C), 1651.07 (C=N), 698.23 (C–S), 1107.14 (C–O), 3172.90 (C–H). ^1H NMR spectrum, δ , ppm (J, Hz): 8.65–8.64 d ($J=5$ Hz, 1H, pyridine H-2), 8.36 s (1H, N=CH), 8.34–8.32 m (3H, pyridine H-5, 4-nitrobenzene H-3 & 5), 7.89–7.83 t (3H, pyridine H-4, 4-nitrobenzene H-2 & 6), 7.40–7.37 t (1H, pyridine H-3), 7.29–7.26 m (5H, Ar-H), 5.13–5.11 t (1H, CH–N=C), 4.61 s (2H, CH_2 -ph), 4.16–4.13 d ($J=15$ Hz, 1H, CH), 3.90–3.89 t (1H, CH). ^{13}C -NMR spectrum δ , ppm: 171.9, 171.1, 162.1, 152.7, 149.8, 149.5, 149.1, 140.7, 137.5, 137.3, 129.6, 129.4, 128.5, 127.9, 127.7, 125.4, 124.3, 123.9, 120.8, 73.5, 72.8, 69.4. ES-MS, $m/z=447.1$ [$M+1$]. Anal. calcd for $\text{C}_{23}\text{H}_{19}\text{N}_5\text{O}_3\text{S}$: C, 62.01; H, 4.30; N, 15.72; S, 7.20; Found: C, 62.00; H, 4.31; N, 15.73; S, 7.21.

(S)-4-{[2-Benzyloxy-1-(5-pyridin-2-yl-[1,3,4]-thiadiazol-2-yl)-ethylimino]-methyl}-phenol (AP-2)

Off white color solid; Yield: 93%; M.p.: 158–160 °C; IR (KBr ν , cm^{-1}): 1224.80 (C–N), 1276.88 (OH), 1444.68 (C=C), 1639.49 (C=N), 683.81 (C–S), 1064.71 (C–O), 3066.82 (C–H). ^1H NMR spectrum, δ , ppm (J, Hz): 8.65–8.64 d ($J=5$ Hz, 1H, pyridine H-2), 8.36–8.34 m (2H, N=CH and pyridine H-5), 7.87–7.83 t (1H, pyridine H-4), 7.69–7.68 d ($J=5$ Hz, 2H, 4-hydroxybenzene H-2 & 6), 7.40–7.37 t (1H, pyridine H-3), 7.29–7.26 m (4H, Ar-H), 6.89–6.88 d ($J=5$ Hz, 2H, 4-hydroxybenzene H-3 & 5), 6.33 bs (1H, OH), 5.13–5.11 t (1H, CH–N=C), 4.61 s (2H, CH_2 -Ph), 4.16–4.13 d ($J=15$ Hz, 1H, CH), 3.90–3.89 t (1H, CH). ^{13}C -NMR spectrum δ , ppm: 173.6, 170.8, 163.9, 152.2, 149.7, 149.2, 137.6, 137.4, 130.6, 128.4, 128.0, 127.8, 125.4, 120.9, 115.7, 73.5, 73.3, 69.2. ES-MS, $m/z=417.1$ [$M+1$]; Anal. calcd for $\text{C}_{23}\text{H}_{20}\text{N}_4\text{O}_2\text{S}$: C, 66.33; H, 4.84; N, 13.45; S, 7.70; Found: C, 66.33; H, 4.83; N, 13.44; S, 7.70.

(S)-[2-Benzyloxy-1-(5-pyridin-2-yl-[1,3,4]-thiadiazol-2-yl)-ethyl]-(3-nitro-benzylidene)-amine (AP-3)

Light brown color solid; Yield: 94%; M.p.: 200–203 °C; IR (KBr ν , cm^{-1}): 1205.51 (C–N), 1527.62 & 1350.17 ($-\text{NO}_2$), 1436.97 (C=C), 1645.28 (C=N), 686.66 (C–S), 1091.71 (C–O), 3086.11 (C–H). ^1H NMR spectrum, δ , ppm (J, Hz): 8.65–8.63 d ($J=10$ Hz, 1H, pyridine H-2), 8.51 s (1H, 3-Nitrobenzene H-2), 8.36 s (1H, N=CH), 8.35–8.34 d ($J=5$ Hz, 1H, pyridine H-5), 8.21–8.20 d ($J=5$ Hz, 1H, 3-Nitrobenzene H-4), 7.86–7.85 d ($J=5$ Hz, 1H, 3-Nitrobenzene H-6), 7.84–7.82 t (1H, pyridine H-4), 7.53–7.51 d.d ($J=10$ Hz, 1H, 3-Nitrobenzene H-5), 7.38–7.36 t (1H, pyridine H-3), 7.29–7.27 m (5H, Ar-H), 5.13–5.11 t (1H, CH–N=C), 4.61 s (2H, CH_2 -Ph), 4.16–4.13 d ($J=15$ Hz, 1H, CH), 3.90–3.89 t (1H, CH). ^{13}C -NMR spectrum δ , ppm: 173.6, 170.8, 163.9, 152.2, 149.7, 149.2, 137.6, 137.4, 130.6, 128.4, 128.0, 127.8, 125.4, 120.9, 115.7, 73.5, 73.3, 69.2. ES-MS, $m/z=447.2$ [$M+1$]; Anal. calcd for $\text{C}_{23}\text{H}_{19}\text{N}_5\text{O}_3\text{S}$: C, 62.01; H, 4.30; N, 15.72; S, 7.20; Found: C, 62.02; H, 4.31; N, 15.72; S, 7.19.

(S)-[2-Benzyloxy-1-(5-pyridin-2-yl-[1,3,4]-thiadiazol-2-yl)-ethyl]-(2,3-dimethoxy-benzylidene)-amine (AP-4)

Dark brown color Solid; Yield: 93%; M.p.: 191–194 °C; IR (KBr ν , cm^{-1}): 1234.07 (C–N), 1454.80 (C=C), 1645.82 (C=N), 699.91 (C–S), 1030.08 (C–O), 2936.26 (C–H). ^1H NMR spectrum, δ , ppm (J, Hz): 8.64–8.63 d ($J=10$ Hz, 1H, pyridine H-2), 8.37 s (1H, N=CH), 8.35–8.34 d ($J=5$ Hz, 1H, pyridine H-5), 7.86–7.82 d ($J=5$ Hz, 1H, 3-Nitrobenzene H-6), 7.53–7.52 d

($J = 5$ Hz, 1H, 2,3-dimethoxy benzene H-6), 7.38–7.36 t (1H, pyridine H-3), 7.29–7.24 m (5H, Ar-H), 6.99–6.98 d ($J = 5$ Hz, 1H, 2,3-dimethoxy benzene H-4), 6.91–6.90 d ($J = 5$ Hz, 1H, 2,3-dimethoxy benzene H-4), 5.15–5.14 t (1H, CH-N), 4.61 s (2H, CH₂-Ph), 4.17–4.14 d ($J = 15$ Hz, 1H, CH), 3.98 s (3H, O-CH₃), 3.94 s (3H, O-CH₃), 3.90–3.88 t (t, 1H, CH). ¹³C-NMR spectrum δ , ppm: 173.3, 170.9, 163.9, 152.1, 149.8, 149.8, 137.2, 137.2, 128.6, 128.4, 127.9, 127.7, 125.3, 124.0, 120.9, 73.5, 69.4, 56.2; ES-MS, m/z : 461.1 [M + 1]; Anal. calcd for C₂₅H₂₄N₄O₃S: C, 65.20; H, 5.25; N, 12.17; S, 6.96; Found: C, 65.21; H, 5.26; N, 12.17; S, 6.96.

(S)-[2-Benzyloxy-1-(5-pyridin-2-yl-[1,3,4]-thiadiazol-2-yl)-ethyl]-(2-chloro-benzylidene)-amine (AP-5)

Light yellow color solid; Yield: 95%; M.p. = 95–98 °C; IR (KBr ν , cm⁻¹): 1203.58 (C-N), 827.46 (Cl), 1431.18 (C=C), 1651.07 (C=N), 698.23 (C-S), 1111.00 (C-O), 3059.10 (C-H). ¹H NMR spectrum, δ , ppm (J, Hz): 8.65–8.64 d ($J = 5$ Hz, 1H, pyridine H-2), 8.37 s (1H, N=CH), 8.35–8.33 dd ($J = 10$ Hz, 1H, pyridine H-5), 7.86–7.83 t (1H, pyridine H-4), 7.78–7.76 d ($J = 10$ Hz, 2H, 4-chlorobenzene H-2 & 6), 7.43–7.39 d ($J = 20$ Hz, 2H, 4-chlorobenzene H-3 & 5), 7.39–7.37 t (1H, pyridine H-3), 7.28–7.26 m (5H, Ar-H), 5.17–5.16 t (1H, CH-N=C), 4.60 s (2H, CH₂-Ph), 4.17–4.14 d ($J = 15$ Hz, 1H, CH), 3.88–3.84 t (1H, CH). ¹³C-NMR spectrum δ , ppm: 172.7, 170.9, 163.0, 152.1, 149.8, 149.3, 137.7, 137.5, 137.2, 133.9, 130.9, 129.9, 129.5, 129.0, 128.5, 128.4, 127.8, 127.8, 127.7, 125.3, 120.8, 73.4, 69.3. ES-MS, m/z : 435.1 [M + 1]. Anal. calcd for C₂₃H₁₉ClN₄O₃S: C, 63.51; H, 4.40; N, 12.88; S, 7.37; Found: C, 63.50; H, 4.40; N, 12.87; S, 7.37.

(S)-[2-Benzyloxy-1-(5-pyridin-2-yl-[1,3,4]-thiadiazol-2-yl)-ethyl]-(2-nitro-benzylidene)-amine (AP-6)

Reddish brown color solid; Yield: 95%; M.p.: 128–130 °C; IR (KBr ν , cm⁻¹): 1210.47 (C-N), 1281.35 (OH), 1455.59 (C=C), 1644.10 (C=N), 699.05 (C-S), 1045.98 (C-O), 3064.83 (C-H). ¹H NMR spectrum, δ , ppm (J, Hz): 8.65–8.63 d ($J = 10$ Hz, 1H, pyridine H-2), 8.37 s (1H, N=CH), 8.35–8.34 d ($J = 5$ Hz, 1H, pyridine H-5), 8.23–8.22 d ($J = 5$ Hz, 1H, 2-Nitrobenzene H-3), 7.86–7.85 d ($J = 5$ Hz, 1H, 2-Nitrobenzene H-6), 7.84–7.82 t (1H, pyridine H-4), 7.53–7.51 d.d ($J = 10$ Hz, 2-Nitrobenzene H-4 & 5), 7.38–7.36 t (1H, pyridine H-3), 7.29–7.27 m (5H, Ar-H), 5.15–5.14 t (1H, CH-N=C), 4.61 s (2H, CH₂-Ph), 4.17–4.14 d ($J = 15$ Hz, 1H, CH), 3.91–3.88 t (1H, CH). ¹³C-NMR spectrum δ , ppm: 171.9, 171.1, 162.1, 152.0, 149.3, 149.3, 137.5, 137.2, 131.1, 129.6, 129.4, 128.5, 127.9, 127.7, 125.4, 124.3, 123.9, 121.8, 73.5, 72.8, 69.4. ES-MS, m/z : 447.1 [M + 1]. Anal. calcd for C₂₃H₁₉N₅O₃S: C, 62.01; H, 4.30; N, 15.72; S, 7.20; Found: C, 62.00; H, 4.31; N, 15.72; S, 7.19.

(S)-2-{[2-Benzyloxy-1-(5-pyridin-2-yl-[1,3,4]-thiadiazol-2-yl)-ethylimino]-methyl}-5-methoxyphenol (AP-7)

Off white solid; Yield: 92%; M.p.: 273–274 °C; IR (KBr ν , cm⁻¹): 1210.20 (C-N), 1455.59 (C=C), 1695.80 (C=N), 699.76 (C-S), 1098.20 (C-O), 2983.64 (C-H). ¹H NMR spectrum, δ , ppm (J, Hz): 8.65–8.64 d ($J = 5$ Hz, pyridine H-2), 8.36–8.34 m (2H, N=CH and pyridine H-5), 7.87–7.83 t (1H, pyridine H-4), 7.40–7.38 t (1H, pyridine H-3), 7.38–7.36 d ($J = 10$ Hz, 1H, 2-hydroxy-4-methoxybenzene H-6), 7.29–7.26 m (5H, Ar-H), 6.42–6.40 d ($J = 10$ Hz, 1H, 2-hydroxy-4-methoxybenzene H-5), 6.28 s (1H, 2-hydroxy-4-methoxybenzene H-3), 6.03 bs (1H, OH), 5.13–5.10 t (1H, CH-N=C), 4.61 s (2H, CH₂-Ph), 4.16–4.13 d ($J = 15$ Hz, 1H, CH), 4.01 s (3H, O-CH₃), 3.90–3.86 t (1H, CH). ¹³C-NMR spectrum δ , ppm: 173.3, 170.9, 163.9, 154.6, 152.1, 149.9, 149.5, 137.3, 137.2, 130.2, 128.6, 128.4, 127.9, 127.9, 127.8, 125.3, 124.0, 120.9, 110.5, 109.3,

74.0, 69.5, 56.3. ES-MS, m/z : 445.1 $[M + 1]$. Anal. calcd for $C_{24}H_{22}N_4O_3S$: C, 64.56; H, 4.97; N, 12.55; S, 7.18; Found: C, 64.55; H, 4.98; N, 12.55; S, 7.17.

(S)-3-{[2-Benzyloxy-1-(5-pyridin-2-yl-[1,3,4]-thiadiazol-2-yl)-ethylimino]-methyl}-phenol (AP-8)

Brown color solid; Yield: 93%; M.p.: 183–185 °C; IR (KBr ν , cm^{-1}): 1210.47 (C–N), 1281.35 (OH), 1455.59 (C=C), 1644.10 (C=N), 699.05 (C–S), 1045.98 (C–O), 3064.83 (C–H). 1H NMR spectrum, δ , ppm (J, Hz): 8.65–8.64 d ($J=5$ Hz, 1H, pyridine H-2), 8.36–8.34 m (2H, N=CH and pyridine H-5), 7.87–7.83 t (1H, pyridine H-4), 7.40–7.37 t (1H, pyridine H-3), 7.29–7.26 m (5H, Ar-H), 7.19–7.18 d ($J=5$ Hz, 1H, 3-hydroxybenzene H-6), 7.16–7.14 t (1H, 3-hydroxybenzene H-5), 7.13–7.12 d ($J=5$ Hz, 1H, 3-hydroxybenzene H-4), 6.89–6.88 d ($J=5$ Hz, 1H, 3-hydroxybenzene H-3), 6.33 bs (1H, OH), 5.13–5.11 t (1H, CH–N=C), 4.61 s (2H, CH_2 -Ph), 4.16–4.13 d ($J=15$ Hz, 1H, CH), 3.90–3.86 t (1H, CH). ^{13}C -NMR spectrum δ , ppm: 173.7, 170.8, 163.9, 153.2, 149.7, 149.2, 137.6, 137.4, 130.0, 128.4, 128.0, 127.8, 121.6, 118.2, 116.2, 73.5, 973.4, 69.2. ES-MS, m/z : 417.1 $[M + 1]$. Anal. calcd for $C_{23}H_{20}N_4O_2S$: C, 66.33; H, 4.84; N, 13.45; S, 7.70; Found: C, 66.34; H, 4.84; N, 13.45; S, 7.71.

(S)-[2-Benzyloxy-1-(5-pyridin-2-yl-[1,3,4]-thiadiazol-2-yl)-ethyl]-(3-methoxy-benzylidene)-amine (AP-9)

Brown color solid; Yield: 92%; M.p.: 146–149 °C; IR (KBr ν , cm^{-1}): 1247.75 (C–N), 1432.48 (C=C), 1645.93 (C=N), 699.69 (C–S), 1178.81 (C–O), 3063.39 (C–H). 1H NMR spectrum, δ , ppm (J, Hz): 8.65–8.63 d ($J=10$ Hz, 1H, pyridine H-2), 8.37 s (1H, N=CH), 8.35–8.34 d ($J=5$ Hz, 1H, pyridine H-5), 7.86–7.82 t (1H, pyridine H-4), 7.51–7.50 d ($J=5$ Hz, 1H, 3-dimethoxy benzene H-6), 7.37–7.36 t (1H, pyridine H-3), 7.29–7.25 m (5H, Ar-H), 7.14 s (1H, 3-dimethoxy benzene H-2), 7.00–6.99 d ($J=5$ Hz, 1H, 3-dimethoxy benzene H-4), 6.92–6.90 d ($J=10$ Hz, 1H, 3-dimethoxy benzene H-3), 5.15–5.14 t (1H, CH–N), 4.61 s (2H, CH_2 -Ph), 4.16–4.13 d ($J=15$ Hz, 1H, CH), 3.99 s (3H, O– CH_3), 3.91–3.88 t (1H, CH). ^{13}C -NMR spectrum δ , ppm: 172.8, 170.2, 163.9, 161.0, 152.1, 149.9, 149.9, 141.0, 137.3, 137.2, 130.0, 128.6, 128.4, 127.9, 127.9, 127.8, 125.3, 124.0, 120.9, 117.0, 113.4, 74.0, 73.5, 69.5, 55.0. ES-MS, m/z : 431.1 $[M + 1]$. Anal. calcd for $C_{24}H_{22}N_4O_2S$: C, 66.96; H, 5.15; N, 13.01; S, 7.45; Found: C, 66.97; H, 5.15; N, 13.00; S, 7.45.

(S)-[2-Benzyloxy-1-(5-pyridin-2-yl-[1,3,4]-thiadiazol-2-yl)-ethyl]-(2-fluoro-benzylidene)-amine (AP-10)

Pale yellow color solid; Yield: 94%; M.p.: 129–131 °C. IR (KBr ν , cm^{-1}): 1203.77 (C–N), 1010.31 (Ph–F), 1431.74 (C=C), 1651.00 (C=N), 698.23 (C–S), 1112.00 (C–O), 3060.00 (C–H). 1H NMR spectrum, δ , ppm (J, Hz): 8.65–8.64 d (1H, $J=10$ Hz, pyridine H-2), 8.36 s (1H, N=CH), 8.35–8.34 d ($J=5$ Hz, 1H, pyridine H-5), 7.87–7.83 t (1H, pyridine H-4), 7.58–7.56 d ($J=10$ Hz, 1H, 2-fluorobenzene H-6), 7.38–7.36 t (1H, pyridine H-3), 7.29–7.26 m (6H, 2-fluorobenzene H-4 and Ar), 7.04–7.02 t (1H, 2-fluorobenzene H-5), 6.94–6.92 t (1H, 2-fluorobenzene H-3), 5.13–5.10 t (1H, CH–N), 4.61 s (2H, CH_2 -Ph), 4.16–4.13 d ($J=15$ Hz, 1H, CH), 3.90–3.86 t (1H, CH). ^{13}C -NMR spectrum δ , ppm: 173.3, 170.9, 163.9, 162.0, 152.1, 149.7, 149.8, 137.3, 137.2, 132.8, 130.2, 128.6, 128.4, 127.7, 127.7, 127.8, 125.3, 124.0, 120.9, 115.0, 74.0, 73.4, 69.4, 56.3. ES-MS, m/z : 419.1 $[M + 1]$. Anal. calcd for $C_{23}H_{19}FN_4OS$: C, 66.01; H, 4.58; N, 13.39; S, 7.66; Found: C, 66.00; H, 4.58; N, 13.39; S, 7.66.

Biological

Antioxidant activity

In this method, 0.1 mM solution of 2, 2-diphenyl-1-picrylhydrazyl (DPPH) in methanol was prepared. The 1.0 ml of this solution was added into 3 ml solution of hybrid compounds (**AP-1** to **AP-10**) in dimethyl sulfoxide (DMSO) at different concentrations (50,100 &150 $\mu\text{g}/\text{ml}$) mentioned in Table 3. The mixtures were shaken vigorously and allowed to stand at 25-30 °C for 30 minutes. The absorbance was dignified at 517 nm by using a UV-VIS spectrophotometer. The Ascorbic acid used as a reference standard and DMSO as a control. The lower absorbance values of the compounds indicate higher free radical scavenging activity. The capability of scavenging DPPH radical was calculated by using the following formula:

$$\text{DPPH scavenging effect (\% inhibition)} = (A_0 - A_1)/A_0 \times 100$$

where A_0 is the absorbance of the control reaction and A_1 is the absorbance in the presence of selected sample of compounds. All the tests were performed in triplicates and the data are expressed as mean \pm standard deviation (SD). The results of the scavenging activity were statistically evaluated by one-way analysis of variance (ANOVA) which is designed to compare the means of independent samples, simultaneously the DPPH assay³⁰ is a simple and sensitive method to study antioxidant activity. This assay is based on the theory, that a hydrogen donor is an antioxidant and it measures compounds that are radical scavengers. The assay shows the mechanism by which DPPH radical accepts hydrogen from an antioxidant. The antioxidant effect is proportional to the disappearance of DPPH radicals in test samples. Monitoring DPPH with a UV spectrometer has become the most commonly used method because of its simplicity and accuracy. DPPH radical shows a strong absorption maximum at 517 nm (purple). The color turns from purple to yellow followed by the formation of DPPH upon absorption of hydrogen from an antioxidant. This reaction is stoichiometric concerning the number of hydrogen atoms absorbed. Hence, the antioxidant effect can be easily calculated by following the decrease of UV absorption at 517 nm.

Antimitotic activity

The model used for this activity was *Allium cepa* root tip meristem mode in which onion bulbs were cleaned and kept with root tips in the beaker containing distilled water till the tips grew up to 2–3 cm. Then these bulbs were expelled from the water and put on a layer of tissue paper to remove an excess of water. The solutions were divided into groups, the first group served as control (DMSO) 0.6 ml and distilled water volume adjusted to 600 ml, the second group target compounds dissolved in DMSO of concentration 10 $\mu\text{g}/\text{ml}$. The third group methotrexate also dissolved in DMSO of concentration 10 $\mu\text{g}/\text{ml}$ was used as a standard drug. The grown root tips were dipped into solutions mentioned above and these were stored at temperature 25 ± 2 °C for 96 h of direct daylight. The test sample was changed day by day with new ones. The length of roots developed during incubation (recently showing up roots excluded), root number, and the mitotic index was recorded after 96 h. The percent of root growth inhibition was calculated by

$$\text{Percent of root growth inhibition} = \text{Control} - \text{Test} \times 100.$$

The EC_{50} value was calculated by plotting treatment concentration versus mean of root length as a percentage of the water control group.

In silico ADME prediction

An important task in drug design and discovery is to early prediction of drug-likeness properties, as it resolves the cost and time in drug development and discovery. Due to the inadequate drug-

likeness properties of many active agents with a significant biological activity have failed in clinical trials.

In silico ADME is significant tool to predict properties regarding drug development. Absorption (% ABS) was calculated by:

$$\% \text{ ABS} = 109 - (0.345 \times \text{TPSA})$$

Conclusion

Facile, efficient synthetic route has been developed for the synthesis of compounds **3**, **4** and **AP-1** to **AP-10**. This practical protocol is easy, simple, eco-friendly and required less time for reaction completion with higher yield. The antimutagenic properties of final compounds were evaluated and results showed that, **AP-3**, **AP-8** and **AP-9** showed significant antimutagenic activity as compared with standard drug which is attributed the presence of *meta* substitution of nitro, hydroxy and methoxy on benzene ring. The **AP-1**, **AP-6**, **AP-8** to **AP-10** showed good assay against antioxidant activity, it might be due to nitro group at *ortho* and *para* position and hydroxy and methoxy at *meta* position as well as fluorine at *ortho* position. Finally, *insilico* ADME prediction, the **AP-1** to **AP-10** showed a good drug linkage score.

Acknowledgments

The authors are gratefully acknowledged to Dr. Rahul Ingle, Institute of Drug Metabolism and Pharmaceutical Analysis, Zhejiang University, Hangzhou (China) and Dr. Gajanan Sonawane, Principal, Rajesh Bhaiyya Tope College of Pharmacy, Aurangabad (India) for his kind support during work. The Authors also gratefully acknowledged to Ms. Rajashri Pund-Nale, Department of Zoology, Bhaskar Pandurang Hivale Education Society's Ahmednagar College, Ahmednagar for support during biological evaluation.

Disclosure statement

The authors declare no conflict of interest.

ORCID

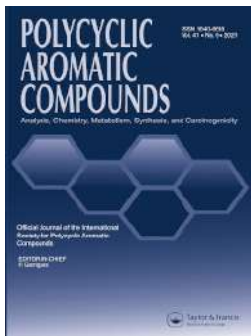
Amit A. Pund  <http://orcid.org/0000-0002-3406-6783>
Mubarak H. Shaikh  <http://orcid.org/0000-0002-1190-2371>
Badrinarayan G. Chandak  <http://orcid.org/0000-0001-7449-7062>
Vijay N. Bhosale  <http://orcid.org/0000-0002-1983-8458>
Baban K. Magare  <http://orcid.org/0000-0001-6719-0441>

References

1. S. Chitra, N. Paul, S. Muthusubramanian, P. Manisankar, P. Yogeewari, and D. Sriram, "Synthesis of 3-Heteroarylthioquinoline Derivatives and Their in Vitro Antituberculosis and Cytotoxicity Studies," *European Journal of Medicinal Chemistry* 46, no. 10 (2011): 4897–903. no.
2. K. Zamani, K. Faghihi, T. Tofghi, and M. R. Shariatzadeh, "Synthesis and Antimicrobial Activity of Some Pyridyl and Naphthyl Substituted 1, 2, 4-Triazole and 1, 3, 4-Thiadiazole Derivatives," *Turkish Journal of Chemistry* 28, no. 1 (2004): 95–100.
3. C. Camoutsis, A. Geronikaki, A. Ciric, M. Sokovic, P. Zoumpoulakis, and M. Zervou, "Sulfonamide-1,2,4-Thiadiazole Derivatives as Antifungal and Antibacterial Agents: Synthesis, Biological Evaluation, Lipophilicity, and Conformational Studies," *Chemical & Pharmaceutical Bulletin* 58, no. 2 (2010): 160–7. no.
4. A. Liesen, T. de Aquino, C. Carvalho, V. Lima, J. de Araujo, J. de Lima, A. de Faria, E. de Melo, A. Alves, E. Alves, et al. "Synthesis and Evaluation of anti-Toxoplasma gondii and Antimicrobial Activities of

- Thiosemicarbazides, 4-thiazolidinones and 1,3,4-thiadiazoles ,” *European Journal of Medicinal Chemistry* 45, no. 9 (2010): 3685–91. no.
5. S. Kucukguzel, I. Kucukguzel, E. Tatar, S. Rollas, F. Sahin, M. Gulluce, EDe. Clercq, and L. Kabasakal, “Synthesis of Some Novel Heterocyclic Compounds Derived from Diflunisal Hydrazone as Potential anti-Infective and anti-Inflammatory Agents,” *European Journal of Medicinal Chemistry* 42, no. 7 (2007): 893–901. no.
 6. S. Schenone, C. Brullo, O. Bruno, F. Bondavalli, A. Ranise, W. Filippelli, B. Rinaldi, A. Capuano, and G. Falcone, “New 1,3,4-Thiadiazole Derivatives Endowed with Analgesic and Anti-inflammatory Activities ,” *Bioorganic & Medicinal Chemistry* 14, no. 6 (2006): 1698–705. no.
 7. M. Mullican, M. Wilson, D. Connor, C. Kostlan, D. Schrier, and R. Dyer, “Design of 5-(3,5-di-tert-butyl-4-hydroxyphenyl)-1,3,4-thiadiazoles, -1,3,4-Oxadiazoles, and -1,2,4-triazoles as Orally-Active, Nonulcerogenic Antiinflammatory Agents ,” *Journal of Medicinal Chemistry* 36, no. 8 (1993): 1090–9.
 8. J. Matysiak, and A. Opolski, “Synthesis and Antiproliferative Activity of N-substituted 2-amino-5-(2,4-dihydroxyphenyl)-1,3,4-thiadiazoles ,” *Bioorganic & Medicinal Chemistry* 14, no. 13 (2006): 4483–9.
 9. M. Yar, and M. Akhter, “Synthesis and Anticonvulsant Activity of Substituted Oxadiazole and Thiadiazole Derivatives,” *Polish Pharmaceutical Society* 66, no. 4 (2009): 393–7.
 10. M. Yusuf, R. A. Khan, and B. Ahmed, “Syntheses and anti-Depressant Activity of 5-Amino-1, 3, 4-Thiadiazole-2-Thiol Imines and Thiobenzyl Derivatives,” *Bioorganic & Medicinal Chemistry* 16, no. 17 (2008): 8029–34.
 11. W. Reiss, and K. Oles, “Acetazolamide in the Treatment of Seizures,” *The Annals of Pharmacotherapy* 30, no. 5 (1996): 514–9.
 12. R. Uitti, “Medical Treatment of Essential Tremor and Parkinson’s Disease,” *Geriatrics (Basel, Switzerland)* 53, no. 5 (1998): 46–8.
 13. A. Tahghighi, and F. Babalouei, “Thiadiazoles: The Appropriate Pharmacological Scaffolds with Leishmanicidal and Antimalarial Activities: A Review,” *Iranian Journal of Basic Medical Sciences* 20, no. 6 (2017): 613–22.
 14. a) K. Mounika, B. Anupama, J. Pragathi, C.Gyanakumari, “Synthesis, Characterization and Biological Activity of a Schiff Base Derived from 3-Ethoxy Salicylaldehyde and 2-Amino Benzoic Acid and Its Transition Metal Complexes,” *Journal of Molecular Modeling*, 19, no. 2 (2013): 2,727–524. (b) A. Chaubey, S.Pandeya, “Synthesis & Anticonvulsant Activity (Chemo Shock) of Schiff and Mannich Bases of Isatin Derivatives with 2-Amino Pyridine (Mechanism of Action),” *International Journal of PharmTech Research* 4(2012): 590–598.)c) T. Aboul-Fadl, F. Mohammed, E. Hassan, “Synthesis, Antitubercular Activity and Pharmacokinetic Studies of Some Schiff Bases Derived from 1-Alkylisatin and Isonicotinic Acid Hydrazone (INH),” *Archives of Pharmacal Research* 26 (2003): 778–784. [Mismatch] d) R. Miri, N.Razzaghi-Asl, M. Mohammad, “QM Study and Conformational Analysis of an Isatin Schiff Base as a Potential Cytotoxic Agent,” *Journal of Molecular Modeling* 19 (2013):727–735.e) S. Sondhi, N. Singh, A. Kumar, O. Lozach, L. Meijer, “Synthesis, Anti-inflammatory, Analgesic and Kinase (CDK-1, CDK-5 and GSK-3) Inhibition Activity Evaluation of Benzimidazole/Benzoxazole Derivatives and Some Schiff’s Bases,” *Bioorganic & Medicinal Chemistry* 14 (2006): 3758–3765.f) R. Chinnasamy, R. Sundararajan, S.Govindaraj, “Synthesis, Characterization, and Analgesic Activity of Novel Schiff Base of Isatin Derivatives,” *Journal of Advanced Pharmaceutical Technology & Research* 1 (2010): 342–347.g) D. Wei, N. Li, G. Lu, K. Yao, “Synthesis, Catalytic and Biological Activity of Novel Dinuclear Copper Complex with Schiff Base,” *Science China Chemistry* 49(2006): 225–229. h) P. Avaji, C. Kumar, S. Patil, K.Shivananda, C.Nagaraju, “Synthesis, Spectral Characterization, In-vitro Microbiological Evaluation and Cytotoxic Activities of Novel Macrocyclic bis Hydrazone,” *European Journal of Medicinal Chemistry* 44 (2009): 3552–3559.j) K.Venugopala, B. Jayashree, “Synthesis of Carboxamides of 20-amino-40-(6-bromo-3-coumarinyl)-thiazole as Analgesic and Anti-inflammatory Agents. *Indian Journal of Heterocyclic Chemistry* 12, no. 4 (2003): 307–310.
 15. D. Sylvie, “Antimitotic Chalcones and Related Compounds as Inhibitors of Tubulin Assembly,” *Anti-Cancer Agents in Medicinal Chemistry* 9, no. 3 (2009): 336.
 16. B. Szczepankiewicz, G. Liu, H. Jae, A. Tasker, I. Gunawardana, T. Geldern, S. Gwaltney, J. R. Wu-Wong, L. Gehrke, W. Chiou, et al. “New Antimitotic Agents with Activity in Multi-Drug-Resistant Cell Lines and in Vivo Efficacy in Murine Tumor Models,” *Journal of Medicinal Chemistry* 44, no. 25 (2001): 4416–30. no.
 17. M. N. K. Zabiulla, A. B. Begum, M. Sunil, and S. Ara Khanum, “Synthesis, Docking and Biological Evaluation of Thiadiazole and Oxadiazole Derivatives as Antimicrobial and Antioxidant Agents,” *Results in Chemistry* 2, (2020): 100045.
 18. A. Joseph, C. Shah, S. Sharad Kumar, A. Treasa Alex, N. Maliyakkal, S. Moorkoth, and J. E. Mathew, “Synthesis, in Vitro Anticancer and Antioxidant Activity of Thiadiazole Substituted Thiazolidin-4-Ones,” *Acta Pharmaceutica (Zagreb, Croatia)* 63, no. 3 (2013): 397–408. no.

19. I. Khan, S. Ali, S. Hameed, N. Hasan Rama, M. Tahir Hussain, A. Wadood, R. Uddin, Z. Ul-Haq, A. Khan, S. Ali, et al. "Synthesis, Antioxidant Activities and Urease Inhibition of Some New 1,2,4-triazole and 1,3,4-thiadiazole Derivatives," *European Journal of Medicinal Chemistry* 45, no. 11 (2010): 5200–7.
20. A. Pund, S. Saboo, G. Sonawane, A. Dukale, and B. Magare, "Synthesis of 2, 5-Disubstituted-1, 3, 4-Thiadiazole Derivatives from (2S)-3-(Benzyloxy)-2-[(Tert-Butoxycarbonyl) Amino] Propanoic Acid and Evaluation of anti-Microbial Activity," *Synthetic Communications* 50, no. 24 (2020): 3854–64.
21. (a) Y. Hu, C. Li, M. Wang, H. Yang, and L. Zhu, "1,3,4-Thiadiazole: Synthesis, Reactions, and Applications in Medicinal, Agricultural, and Materials Chemistry," *Chemical Reviews*, 114 no. 10 (2014): 5572–5610. (b) G. Nagendra, R. Lamani, N. Narendra, and V. Sureshbabu, "A Convenient Synthesis of 1, 3, 4-Thiadiazole and 1, 3, 4-oxadiazole based Peptidomimetics Employing Diacylhydrazines Derived from Amino Acids," *Tetrahedron Letters* 51, no. 48 (2010): 6338–6341.
22. (a) G. Samala, R. Nallangi, P. B. Devi, S. Saxena, R. Yadav, J. P. Sridevi, P. Yogeewari, and D. Sriram, "Design and Synthesis of 1, 5-and 2, 5-Substituted Tetrahydrobenzazepinones as Novel Potent and Selective Integrin $\alpha V\beta 3$ Antagonists," *Bioorganic & Medicinal Chemistry* 22, no. 15 (2014): 4223–1341.
23. (a) F. Barthels, G. Marincola, T. Marciniak, M. Konhauser, S. Hammerschmidt, J. Bierlmeier, U. Distler, P. Wich, S. Tenzer, D. Schwarzer, and W. Ziebuhr, "Asymmetric disulfanylbenzamides as irreversible and selective inhibitors of Staphylococcus aureus sortase A," *Chem. Med. Chem.* 15, no. 10 (2020): 839–850. (b) M. Al-Ghorbani, G. Pavankumar, P. Naveen, P. Thirusangu, B. Prabhakar, and S. Khanum, "Synthesis and an Angiolytic Role of Novel Piperazine–Benzothiazole Analogues on Neovascularization, a Chief Tumoral Parameter in Neoplastic Development," *Bioorganic Chemistry* 65, (2016) : 110–7.
24. (a) S. Terracciano, G. Lauro, A. Russo, M. Vaccaro, A. Vassallo, M. De Marco, B. Ranieri, A. Rosati, M. Turco, R. Riccio, and G. Bifulco, "Discovery and Synthesis of the First Selective BAG Domain Modulator of BAG3 as an Attractive Candidate for the Development of a New Class of Chemotherapeutics," *Chemical Communications* 54, no. 55 (2018): 7613–7616. (b) S. Khattab, S. Moneim, A. Bekhit, A. El Massry, S. Hassan, A. El-Faham, H. Ahmed, and A. Amer, "Exploring New Selective 3-benzylquinoxaline-based MAO-A Inhibitors: Design, Synthesis, Biological Evaluation and Docking Studies," *European Journal of Medicinal Chemistry* 93 (2015): 308–320.
25. (a) Y. Gorak, N. Obushak, V. Matiichuk, and R. Lytvyn, "Synthesis, Antibacterial and Antileishmanial Activity, Cytotoxicity, and Molecular Docking of New Heteroleptic Copper (I) Complexes with Thiourea Ligands and Triphenylphosphine," *Russian Journal of General Chemistry* 88, no. 3 (2018). (b) A. Saeed, M. Hussain, and M. Qasim, "Novel N-acyl/aroyl-2-(5-phenyl-2H-tetrazol-2-yl) acetohydrazides: Synthesis and Characterization," *Turkish Journal of Chemistry* 38, no. 3 (2014): 436–442.
26. (a) H. Lai, D. Dou, S. Aravapalli, T. Teramoto, G. Lushington, T. Mwania, K. Alliston, D. Eichhorn, R. Padmanabhan, and W. Groutas, "Design, Synthesis and Characterization of Novel 1, 2-Benzisothiazol-3 (2H)-one and 1, 3, 4-oxadiazole hybrid derivatives: Potent Inhibitors of Dengue and West Nile virus NS2B/NS3 Proteases," *Bioorganic & medicinal chemistry* 21, no. 1 (2013): 102–113. (b) E. Lacivita, P. Giorgio, A. Colabufo, B. Francesco, P. Roberto, N. Mauro, and L. Marcello, "Design, Synthesis, Lipophilic Properties, and Binding Affinities of Potential Ligands in Positron Emission Tomography (PET) for Visualization of Brain Dopamine D4 Receptors," *Chemistry & biodiversity* 11, no. 2 (2014): 299–310. (c) H. Staab, "New Methods of Preparative Organic Chemistry IV. Syntheses Using Heterocyclic Amides (Azolides)," *Angewandte Chemie International*, 1 no 7 (1962): 1962.
27. G. Nagendra, R. Lamani, N. Narendra, and V. Sureshbabu, "A Convenient Synthesis of 1,3,4-Thiadiazole and 1,3,4-Oxadiazole Based Peptidomimetics Employing Diacylhydrazines Derived from Amino Acids," *Tetrahedron Letters* 51, no. 48 (2010): 6338–41.
28. Molinspiration Chemo informatics, Brastislava, Slovak Republic, 2014, <http://www.molinspiration.com/cgi-bin/properties>.
29. B. Kashid, H. P. Salunkhe, B. Dongare, K. More, V. Khedkar, and Anil A. Ghanwat, "Synthesis of Novel of 2, 5-disubstituted 1, 3, 4- Oxadiazole Derivatives and their in vitro Anti-inflammatory, Anti-oxidant Evaluation, and Molecular Docking Study," *Bioorganic & Medicinal Chemistry Letters* 30, no. 12 (2020): 127136.
30. (a) C. Tschierske, D. Girdziunaite, "Synthese von 1, 3, 4-Thiadiazol-derivaten," *Journal fur Praktische Chemie*, 333, no. 1 (1991): 135–137. (b) Y. Lijuan, M. Li, S. Ruan, X. Xu, Z. Wang, and S. Wang, "Highly Efficient Coumarin-derived Colorimetric Chemosensors for Sensitive Sensing of Fluoride Ions and Their Applications in Logic Circuits," *Spectrochimica Acta Part A: Molecular and Biomolecular Spectroscopy* 255 (2021): 119718.






[DBUH][OAc]-Catalyzed Domino Synthesis of Novel Benzimidazole Incorporated 3,5-Bis (Arylidene)-4-Piperidones as Potential Antitubercular Agents

Dnyaneshwar D. Subhedar, Mubarak H. Shaikh, Amol A. Nagargoje, Dhiman Sarkar, Vijay M. Khedkar & Bapurao B. Shingate



To cite this article: Dnyaneshwar D. Subhedar, Mubarak H. Shaikh, Amol A. Nagargoje, Dhiman Sarkar, Vijay M. Khedkar & Bapurao B. Shingate (2021): [DBUH][OAc]-Catalyzed Domino Synthesis of Novel Benzimidazole Incorporated 3,5-Bis (Arylidene)-4-Piperidones as Potential Antitubercular Agents, Polycyclic Aromatic Compounds, DOI: [10.1080/10406638.2021.1995008](https://doi.org/10.1080/10406638.2021.1995008)

To link to this article: <https://doi.org/10.1080/10406638.2021.1995008>

 View supplementary material 

 Published online: 23 Oct 2021.

 Submit your article to this journal 

 View related articles 

 View Crossmark data 



[DBUH][OAc]-Catalyzed Domino Synthesis of Novel Benzimidazole Incorporated 3,5-Bis (Arylidene)-4-Piperidones as Potential Antitubercular Agents

Dnyaneshwar D. Subhedar^a, Mubarak H. Shaikh^{a,b}, Amol A. Nagargoje^c, Dhiman Sarkar^d, Vijay M. Khedkar^e, and Bapurao B. Shingate^a

^aDepartment of Chemistry, Dr. Babasaheb Ambedkar Marathwada University, Aurangabad, Maharashtra, India;

^bDepartment of Chemistry, Radhabai Kale Mahila Mahavidyalaya, Ahmednagar, Maharashtra, India;

^cDepartment of Chemistry, Khopoli Municipal Council College, Khopoli, Maharashtra, India; ^dCombichem Bioresource Centre, Organic Chemistry Division, CSIR-National Chemical Laboratory, Pune, Maharashtra, India;

^eSchool of Pharmacy, Vishwakarma University, Pune, Maharashtra, India

ABSTRACT

A series of new benzimidazole incorporated 3,5-bis (arylidene)-4-piperidones were synthesized by using aryl aldehydes, piperidinone, 2-(chloromethyl)-benzimidazole and DBU acetate [DBUH][OAc] act as a catalyst under solvent free condition in excellent yields. The synthesized compounds were screened for their *in vitro* antimycobacterial activity against *M. tuberculosis* H37Ra (MTB) and *M. bovis* BCG strains. The compounds **4a**, **4b**, **4e**, **4i**, **4k** and **4l** are highly potent against both the strains. Most of the active compounds are non-cytotoxic against MCF-7, A549, HCT 116 and THP-1 cell lines. Furthermore, a molecular docking study of these compounds was carried out to investigate their binding pattern with the target, active site of mycobacterial enoyl-acyl carrier protein reductase (Inh A). Therefore, these compounds can be subjected for further optimization and drug development which could give promising chemical leads for treatment of TB.

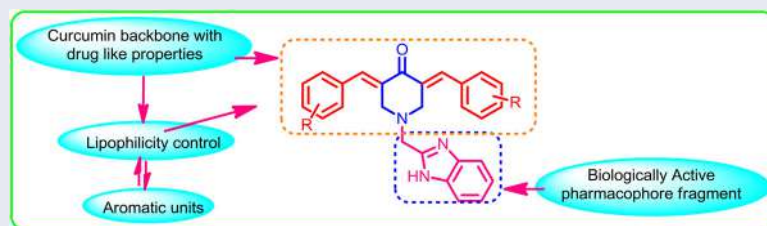
ARTICLE HISTORY

Received 2 May 2021

Accepted 13 October 2021

KEYWORDS


Curcumin; antitubercular activity; cytotoxicity; ionic liquid; multicomponent reactions



Introduction

Mycobacterium Tuberculosis (MTB) bacteria causes Tuberculosis (TB), mostly affect the lungs. Nearly 10 million people fell ill with TB worldwide in 2009, in which 1.2 million children, 3.2 million women and 5.6 million men. Health providers ignored child and adolescent TB because it is difficult to diagnose and treat. In 2019, nearly, 87% new TB cases found in 30 countries, among them only eight countries are responsible for the two thirds of the total, with India

CONTACT Bapurao B. Shingate  bapushingate@gmail.com  Department of Chemistry, Dr. Babasaheb Ambedkar Marathwada University, Aurangabad, Maharashtra 431 004, India.

 Supplemental data for this article can be accessed online at <http://dx.doi.org/10.1080/10406638.2021.1995008>

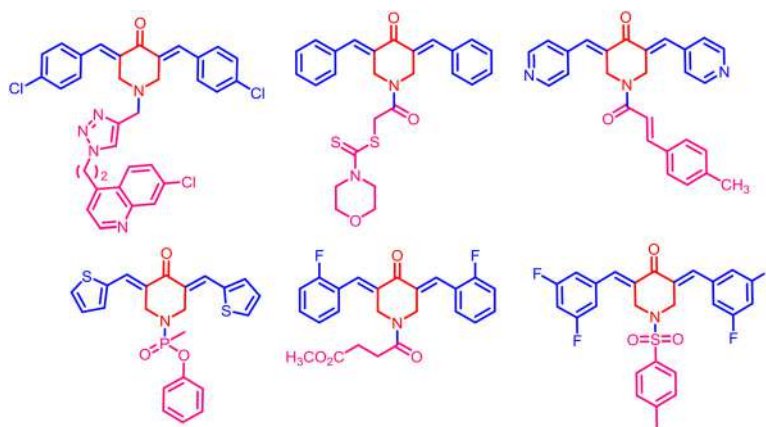


Figure 1. Active monocarbonyl curcumin analogues bearing *N*-substituted piperidone moiety.

leading the count, followed by Indonesia, China, the Philippines, Pakistan, Nigeria, Bangladesh and South Africa. Multidrug-resistant TB (MDR-TB) is the biggest public health crisis and a health security threat worldwide. In 2019, globally total 2,06,030 people detected with multidrug- or rifampicin-resistant TB (MDR/RR-TB) which is 10% higher from 186 883 in 2018.¹ Near about 2% TB incidence is falling globally along with 9% cumulative reduction between 2015 and 2019. This was less than half way to the End TB Strategy milestone of 20% reduction between 2015 and 2020. Between 2000 and 2009 it is estimated that 60 million lives were saved through TB diagnosis and treatment. United Nations Sustainable Development Goals (SDGs) health target is to Wind-up the TB epidemic by 2030.¹

Curcumin [(1,7-bis(4-hydroxy-3-methoxyphenyl)1,6-heptadien-3,5-dion)], a natural component of the rhizome of *Curcuma longa*, proved to be a powerful chemopreventive.² The monocarbonyl curcumin analogues shows wide range of multiple biological activities.³ The substituents on nitrogen of arylidene-piperidones with various heterocycles systems were reported with different bioactivities such as anticancer,⁴ antitubercular,⁵ antiinflammatory,⁶ antileishmanial,⁷ antioxidant⁸ and antidiabetic activity.⁹ They also exhibits topoisomerase II alpha inhibitors,^{10a} a proinflammatory cytokines,^{10b} murine and human macrophages cell lines^{10c} and nitric oxide inhibitors.^{10d} The representative structures of biologically active monocarbonyl curcumin analogues/bis arylidene having *N*-substituted piperidinone moieties are given in Figure 1.

Benzimidazole a privileged pharmacophore, possesses an array of biological activities^{11a,b} including tubulin polymerization,^{12a} anticancer,^{12b} antidiabetic,^{12c} antimicrobial,^{12d} antimycobacterial,^{12e} anti-inflammatory,^{12f} anti-HIV,^{12g} antiprotozoal,^{12h} analgesic,¹²ⁱ antimalarial,^{12j} antihistaminic^{12k} and antiviral^{12l} activity. Some of the marketed drugs containing benzimidazole nucleus are albendazole (antiprotozoal), nocardazole (anticancer), lerisetron (antihistaminic), andibendeb (phosphodiesterase inhibitor), veliarib (anticancer), maribavir (antiviral) are shown in Figure 2.

Multicomponent reactions (MCRs) permits rapid access to combinatorial libraries of organic molecules¹³ for lead structure identification and optimization in drug discovery.¹⁴ The implementation of several transformations in a single manipulation is highly compatible with the goals of sustainable and green chemistry.¹⁵ A variety of ionic liquids have been extensively applied in heterocyclic synthesis as a solvent or catalysts.¹⁶ The [DBUH][OAc] received considerable attention because, it is an inexpensive, nontoxic catalyst as well as solvent for many organic transformations in excellent yields.¹⁷

We have recently reported the synthesis of 3,5-bis (arylidene)-4-piperidones (Figure 3A) as antitubercular agent (MTB H37Ra and *M. bovis* BCG strain with MIC values 1.89–26.37 and 2.69–29.14 mg/mL, respectively),^{18a} monocarbonyl curcumin analogues bearing propargyl ether

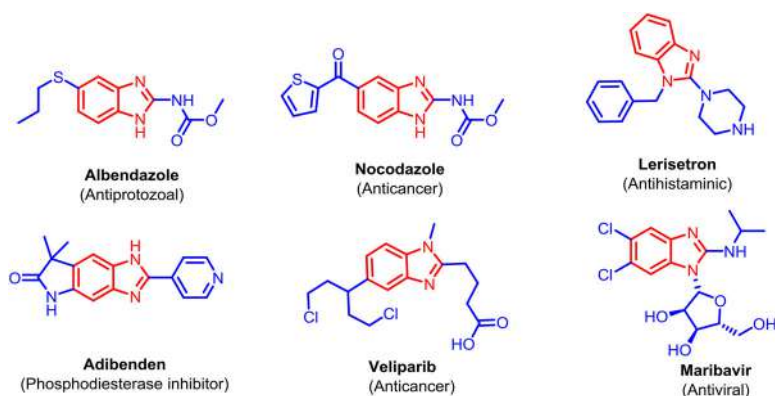


Figure 2. Benzimidazoles containing drugs available in market.

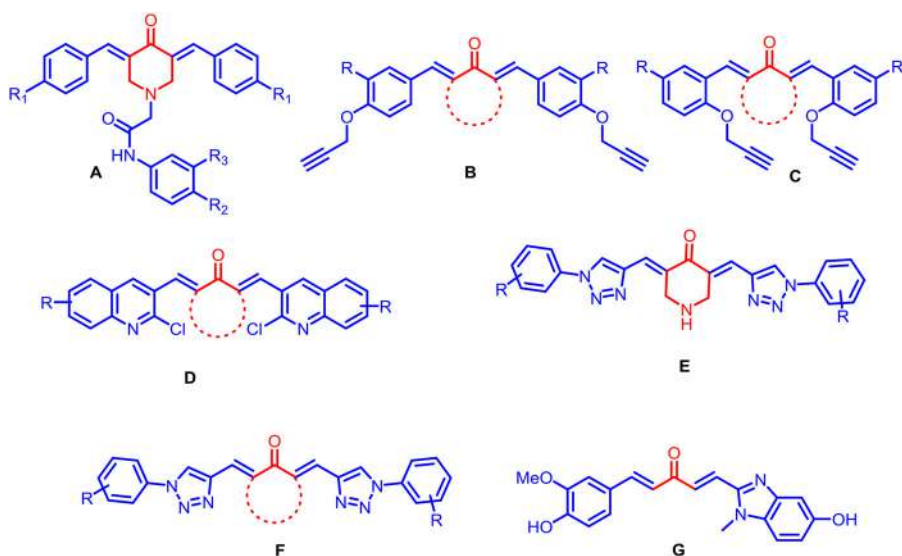


Figure 3. Developed an approach toward the synthesis of curcumin mimics.

(Figure 3B and 3C) (MIC 12.5–175 $\mu\text{g}/\text{mL}$)^{18b} and quinoline (Figure 3D)^{18c} (MIC 6.25–200 $\mu\text{g}/\text{mL}$) based monocarbonyl curcumin analogues as antifungal agents, 1,2,3-triazole incorporated monocarbonyl curcumin analogues^{18d} (Figure 3E) (MIC 6.25–>25 $\mu\text{g}/\text{mL}$) and α,α' -bis(1H-1,2,3-triazol-5-ylmethylene) ketones^{18e} (Figure 3F) as potent antitubercular (MIC 3.125–>25 $\mu\text{g}/\text{mL}$) and antioxidant agents (MIC 15.49 \pm 0.24–71.09 \pm 0.25).

Literature survey reveals that, Lee and coworkers reported synthesis of substituted benzimidazolyl curcumin mimics and their anticancer activity¹⁹ (Figure 3G). However, there is no report on antitubercular activity of benzimidazole incorporated 3,5-bis(arylidene)-4-piperidone derivatives.

In view of the above and continuation of our research programme on the development of new methodology for the synthesis of bioactive heterocyclic compounds,^{18,20} herein, we would like to report the synthesis of new benzimidazole incorporated arylidene-piperidone derivatives and their biological evaluation for antibacterial, antitubercular and cytotoxic activity. In addition to this, we have also studied the molecular binding interactions with enoyl-acyl carrier protein reductase enzyme (Inh A) for most active compound.

Table 1. Optimization of solvent and reaction temperature.

Entry	Solvent	Time (h)	Temp (°C)	Yield ^a (%)
1	DMSO	9	rt	63
2	EtOH	7.5	rt	55
3	MeOH	7	rt	59
4	DMF	6.5	rt	74
5	CH ₃ CN	8	rt	61
6	Toulene	7.5	rt	75
7	Solvent-free	4	rt	85

Reaction conditions: **1a** (2 mmol), **2** (1 mmol), **3** (1 mmol) and 20 mol% [DBUH][OAc].

^aIsolated yield.

Results and discussion

Chemistry

To optimize the best reaction condition for condensation-alkylation, the benzaldehyde **1a**, piperidinone **2**, and 2-(chloromethyl)-benzimidazole **3** in the presence of [DBUH][OAc] as a medium/catalyst was considered for model reaction (Scheme 1). Firstly, we have screened different solvents for model reaction *viz.* DMSO, EtOH, MeOH, DMF, CH₃CN and Toluene at room temperature provides low yield of product (Table 1, Entries 1–6). Under the solvent-free condition, the desired product **4a** was obtained in 85% yield (Table 1, Entry 7).

The amount of catalyst plays a vital role to carry the reaction in forward direction. Further investigation was carried out to determine the quantity of [DBUH][OAc]. An increase in the amount of [DBUH][OAc] from 5 to 20 mol% led to an increase in the yield (Table 2, entries 2–5). The use of 25 mol% of [DBUH][OAc] did not improve the yield (Table 2, entry 6). However, when reaction was carried out in the absence of [DBUH][OAc], no product was obtained (Table 2, entry 1). It proves that a [DBUH][OAc] may be essential for better catalytic activity.

Because [DBUH][OAc] can play a role of acid or a base or both simultaneously, as a nucleophile. Thus, the optimum conditions required the use of [DBUH][OAc] as 20 mol % at room temperature.

To check the eco friendliness of [DBUH][OAc], we recycled the ionic liquid [DBUH][OAc] for five times, Table 3. The reaction proceeded cleanly with good yields (85, 83, 80, 80 and 75%); although a weight loss of ~5% of [DBUH][OAc] was observed from cycle to cycle due to mechanical loss (Table 3, entries 1–5).

The structure of **4a** has been established on the basis of IR, ¹H, ¹³C NMR and HRMS. In the IR spectrum of **4a** displayed characteristic signal for C=O at 1647 cm⁻¹. In the ¹H NMR spectrum for **4a** exhibited a sharp singlet resonating at δ 4.95 ppm for two protons, has been assigned to methylene protons attached to benzimidazole. The peak observed at δ 4.56 ppm for the four protons of the piperidone ring. ¹³C NMR spectrum was also in good agreement with the proposed structure displaying characteristic signals for C=O and two CH₂ group at δ 188.4, 56.8 and 51.4 ppm, respectively.

Using the above optimized reaction conditions, the scope and efficiency of this approach was explored for the synthesis of other new benzimidazole based 3,5-bis(arylidene)-4-piperidones with electron donating and withdrawing groups on phenyl ring in excellent yields (Scheme 2). The structures of all the derivatives are confirmed by physical data and spectral analysis.

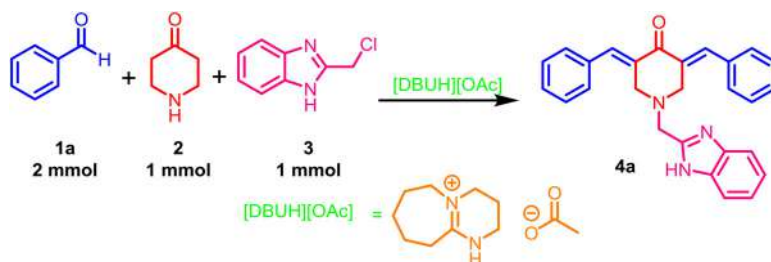
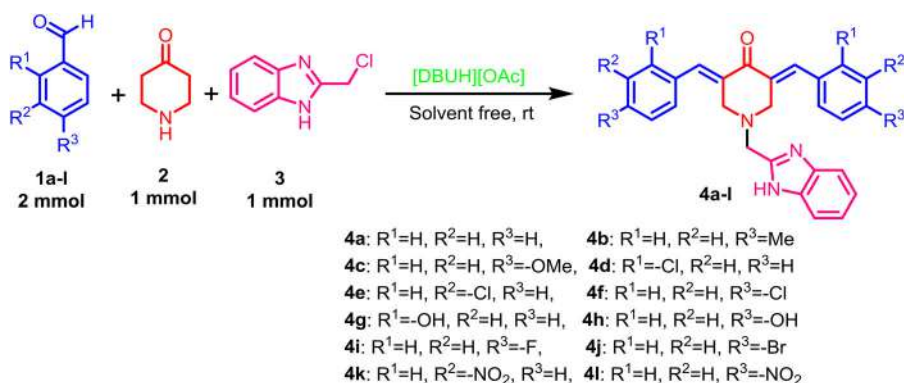
A plausible mechanistic pathway (Scheme 3) is proposed to illustrate the synthesis of monocarbonyl curcumin analogues catalyzed by [DBUH][OAc]. The initial step is believed to be the protonation of the aldehyde **I** by ionic liquid [DBUH][OAc] to form intermediate **II**, which facilitates the nucleophilic attack of piperidinone to promote the formation of C-C bond to yield intermediate **IV**. The subsequent elimination of H₂O molecule by the reaction of intermediate **IV** to yield compound **V**. The final step involves deprotonation of intermediate **V** followed by 2-

Table 2. The effect of [DBUH][OAc] loading on model reaction **4a**^a.

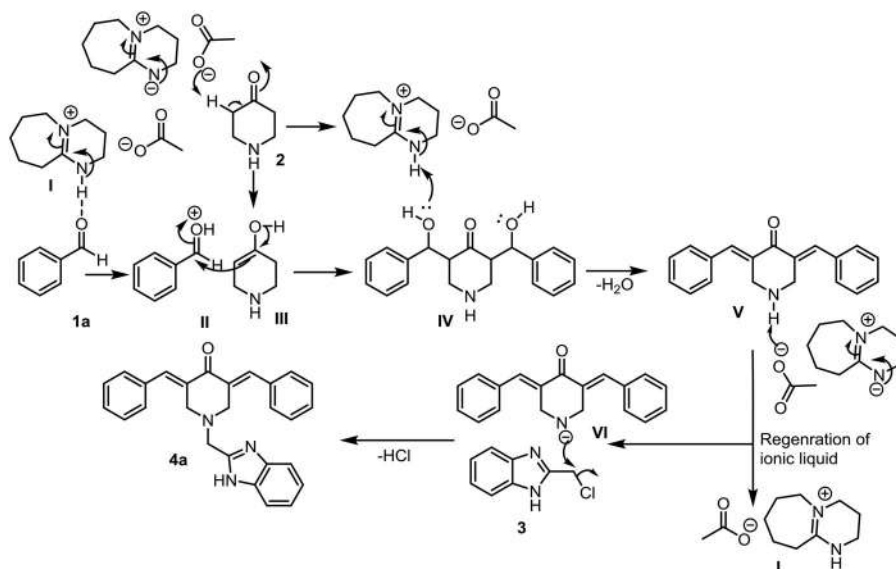
Entry	Catalyst (mol%)	Yield (%) ^b
1	No Catalyst	Trace
2	5	50
3	10	65
4	15	73
5	20	85
6	25	85

^aReaction conditions: **1a** (2 mmol), **2** (1 mmol), **3** (1 mmol), rt, 4 h.^bIsolated yield.**Table 3.** Reusability of [DBUH][OAc] in the synthesis of **4a**^a.

Entry	Reaction cycle	Isolated yield (%) ^b
1	1st (fresh run)	85
2	2nd cycle	83
3	3rd cycle	80
4	4th cycle	80
5	5th cycle	75

^aReaction conditions: **1a** (2 mmol), **2** (1 mmol), **3** (1 mmol), [DBUH][OAc] (20 mol%), rt, 4 h.^bIsolated yield.**Scheme 1.** Model reaction.**Scheme 2.** Synthesis of benzimidazole incorporated 3,5-bis(arylidene)-4-piperidones **4a-l**.

(chloromethyl)-1*H*-benzo[*d*]imidazole (**3**) expedites the formation of C-N bond to yield compound **4a** by the elimination of HCl molecule by the nucleophilic attack of nitrogen to the carbon group to promote C-N bond formation, accelerated by ionic liquid [DBUH][OAc] eventually leads to the formation of final product **4a**.



Scheme 3. Plausible mechanistic catalytic cycle for the synthesis of compound **4a**.

Biological evaluation

Antitubercular activity

In a standard primary screening, all the newly synthesized compounds **4a–l** were evaluated for their *in vitro* antitubercular activity against *MTB* H37Ra and *M. bovis* BCG strains at concentrations of 30, 10 and 3 $\mu\text{g/mL}$ using an established XTT Reduction Menadione assay (XRMA) and NR (Nitrate reductase) assay, respectively.²¹ Compounds showing 90% inhibition of bacilli at or lower than 30 $\mu\text{g/mL}$ were selected for further dose response curve (Tables S1–S13, [supplementary material](#)). Rifampicin was used as standard drug and the obtained results are presented in Table 4.

The compounds **4a**, **4b**, **4e**, **4i**, **4k** and **4l** (MIC = 1.37, 0.64, 2.46, 1.3, 1.38 and 2.19 $\mu\text{g/mL}$, respectively) were found to be highly active against *MTB* H37Ra strain. Similarly, compounds **4a**, **4b**, **4e**, **4i**, **4k** and **4l** (MIC = 1.36, 3.15, 2.5, 1.33, 2.3 and 2.52 $\mu\text{g/mL}$, respectively) were found to be active against *M. bovis* BCG. Remaining all the compounds (MIC = >30 $\mu\text{g/mL}$) were found to be less active against both the strains. According to the data, the activity depends on the substituents present on phenyl rings.

For *MTB* H37Ra and *M. bovis* BCG strains, the compound **4a** showed promising antitubercular activity with MIC values 1.37 and 1.36 $\mu\text{g/mL}$, respectively. The compound **4b** ($R^3 = \text{Me}$) showed very promising antitubercular activity as compared to remaining with MIC value of 0.64 and 3.15 $\mu\text{g/mL}$, against the *MTB* H37Ra and *M. bovis* BCG strains, respectively. The compound **4e** ($R^2 = \text{Cl}$) showed significant antimycobacterial activity with MIC value of 2.46 and 2.5 $\mu\text{g/mL}$, against both the strains. Remaining chloro containing compounds does not displayed significant change in antitubercular activity. The position of *chloro*- group is considered to be important on the phenyl ring for activity. For compound **4i** ($R^3 = \text{OH}$), the MIC values 1.3 and 1.33 $\mu\text{g/mL}$, showed excellent antitubercular activity. The presence of nitro group in compounds **4k** and **4l** displays prominent antitubercular activity with MIC values 1.38 and 2.19 $\mu\text{g/mL}$, against the *MTB* H37Ra strain and 2.3 and 2.52 $\mu\text{g/mL}$, against the *M. bovis* BCG strain respectively. The similar type of trend was occurred for active compounds **4a**, **4b**, **4c**, **4i**, **4k** and **4l** with lower IC_{50} values against both the strains. However, all the synthesized compounds exhibited poor activity compared to the standard antitubercular drug Rifampicin.

Table 4. *In vitro* antitubercular activity of **4a-l** ($\mu\text{g/mL}$).

Cpd	<i>MTB</i> H37Ra		<i>M. bovis</i> BCG		Glide score	Glide energy (Kcal/mol)	H-bonding (Å)	π - π /cation- π stacking (Å)
	MIC	IC ₅₀	MIC	IC ₅₀				
4a	1.37	0.11	1.36	0.11	-9.760	-58.003	Thr196 (2.085)	Tyr158(5.096), Phe149(4.349)
4b	0.64	0.18	3.15	1.3	-8.956	-49.971	Ile194 (2.158)	Tyr158(5.350), Trp222(4.825)
4c	>30	>30	>30	>30	-7.853	-41.635	-	Tyr158(5.363)
4d	>30	>30	>30	>30	-9.375	-46.883	-	Phe149(4.331)
4e	2.46	0.25	2.5	0.21	-8.135	-55.35	Thr196 (1.866)	Tyr158(5.161), Phe149(4.331)
4f	>30	>30	>30	>30	-7.802	-41.562	-	Tyr158(5.276)
4g	>30	>30	>30	>30	-7.842	-41.521	-	Tyr158(5.003)
4h	>30	>30	>30	>30	-7.347	-41.117	-	Tyr158(5.062)
4i	1.3	0.13	1.33	0.11	-9.442	-54.663	-	Tyr158(5.096), Phe149(4.296)
4j	>30	>30	>30	>30	-7.685	-41.863	-	Tyr158(5.309)
4k	1.38	0.09	2.3	0.09	-9.957	-59.653	Thr196 (2.034)	Tyr158(5.230), Phe149(4.378)/Phe149(5.573)
4l	2.19	0.24	2.52	0.13	-8.799	-46.538	Ile194 (2.074)	Tyr158(5.224), Trp222(5.018)/ Tyr158(5.572)
RP	0.045	0.0017	0.017	0.0015	-	-	-	-

Cpd: Compound; RP: Rifampicin.

Cytotoxicity

After identifying a good number of active antitubercular leads, the compounds were tested against human cell lines, MCF-7, A549, HCT-116 and THP-1 using MTT assay²² with paclitaxel as a positive control. The cytotoxicity results are expressed in terms of GI₅₀ indicating the 50% growth inhibition concentration (Table 5). None of the active compounds exhibited any significant cytotoxic effects against all the cell lines, suggesting a great potential for their *in vivo* use as antimycobacterial agents.

Antibacterial activity

The most active antitubercular compounds **4a**, **4b**, **4e**, **4i**, **4k** and **4l** were further confirmed from their dose dependent effect against four bacteria strains Gram-negative and Gram-positive bacteria.²³ The most promising compounds **4a**, **4b**, **4i**, **4k** and **4l** showed strong specificity against *MTB* and BCG as compared to **4e** (Table 6). The results clearly indicates that, compounds **4a**, **4b**, **4i**, **4k** and **4l** are mycobacteria specific and that can be explored further for potential antitubercular drug.

Molecular docking study

All compounds were successfully docked into the active site of mycobacterial InhA. The docking score of most active compounds **4a**, **4b**, **4e**, **4i**, **4k** and **4l** was found to be -9.760, -8.956, -8.135, -9.442, -9.957 and -8.799 respectively, which were comparable with respect to *in vitro* antitubercular activity. We have discussed only the docking study of most active compound **4k**. The interactions of **4k** with the active site of mycobacterial InhA is shown in Figure 4. The lowest energy docking pose of **4k** revealed the presence of hydrogen bonding interactions between nitrogen of imidazole ring and Thr196 with a distance of 2.034 Å. Also, highly hydrophobic π - π stacking interactions were observed between phenyl ring and Tyr158 and Phe149 and also π - π stacking interaction between nitro group and Phe149. These hydrogen binding and π stacking interactions helps in predilection of these ligands within the active site which increases the steric and electrostatic interactions of ligands with the amino acid residues present within the active site of mycobacterial InhA.

The compound **4k** was stabilized within the active site through favorable van der Waals interactions observed with Met199 (-3.783 kcal/mol), Ala198 (-0.773 kcal/mol), Thr196 (-2.165 kcal/

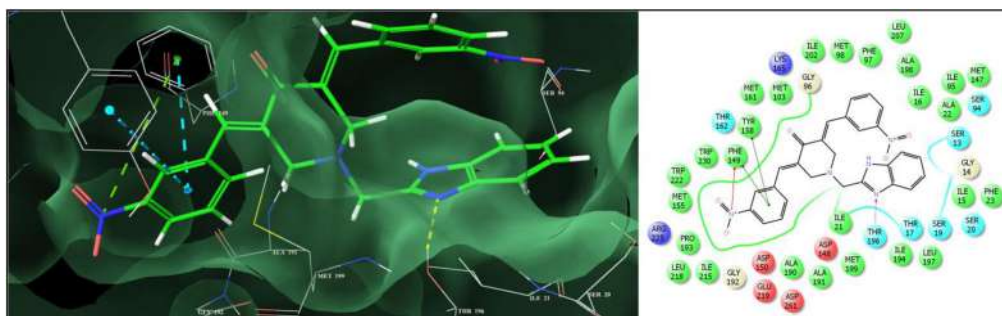
Table 5. *In vitro* cytotoxicity of active compounds (GI₅₀ in $\mu\text{g/mL}$).

Compound	MCF-7	A549	HCT-116	THP-1
4a	>100	>100	>100	>100
4b	>100	>100	>100	>100
4e	>100	>100	>100	>100
4i	>100	>100	>100	>100
4k	>100	>100	>100	>100
4l	>100	>100	>100	>100
Rifampicin	>100	>100	>100	>100
Paclitaxel	0.0048	0.0035	0.0260	0.1374

GI₅₀ indicates concentration to inhibit 50% growth of cells.

Table 6. *In vitro* antibacterial activity (MIC in $\mu\text{g/mL}$).

Compound	<i>E. coli</i>	<i>P. fluorescens</i>	<i>S. aureus</i>	<i>B. subtilis</i>
4a	>30	>30	>30	>30
4b	>30	>30	>30	>30
4e	7.86	8.66	9.46	10.26
4i	>30	>30	>30	>30
4k	>30	>30	>30	>30
4l	>30	>30	>30	>30
Ampicillin	4.17 \pm 1.04	12.47 \pm 1.28	2.86 \pm 0.78	29.53 \pm 1.88
Kanamycin	3.34 \pm 0.41	1.01 \pm 0.09	> 61.92	2.78 \pm 0.85

**Figure 4.** 3D and 2D view of binding of **4k** with the active site of mycobacterial InhA.

mol), Ile194 (−2.334 kcal/mol), Pro193 (−3.911 kcal/mol), Gly192 (−1.982 kcal/mol), Ala191 (−1.793 kcal/mol), Lys165 (−1.254 kcal/mol), Met161 (−2.452 kcal/mol), Tyr158 (−2.711 kcal/mol), Phe149 (−5.313 kcal/mol), Met147 (−1.241 kcal/mol), Phe97 (−0.931 kcal/mol), Gly96 (−1.218 kcal/mol), Ile95 (−1.561 kcal/mol), Ser94 (−1.603 kcal/mol) and Ile21 (−1.484 kcal/mol) residues. Also, several strong electrostatic interactions were observed with Met199 (−4.544 kcal/mol), Ala198 (−0.811 kcal/mol), Thr196 (−1.842 kcal/mol), Ile194 (−3.533 kcal/mol), Pro193 (−4.558 kcal/mol), Gly192 (−2.501 kcal/mol), Ala191 (−2.531 kcal/mol), Lys165 (−1.155 kcal/mol), Met161 (−2.831 kcal/mol), Tyr158 (−3.306 kcal/mol), Phe149 (−4.791 kcal/mol), Met147 (−0.926 kcal/mol), Phe97 (−0.994 kcal/mol), Gly96 (−1.272 kcal/mol), Ile95 (−2.193 kcal/mol), Ser94 (−4.620 kcal/mol) and Ile21 (−0.908 kcal/mol) which fits the compound **4k** in to the cavity of InhA and leads to its firm binding with docking score of −9.957 and was found to be most potent among the series. From, the docking studies it is clear that these compounds have significant binding with the active site of mycobacterial InhA.

Conclusion

A series of new benzimidazole incorporated 3,5-bis (arylidene)-4-piperidones were synthesized by using aryl aldehydes, piperidinone, 2-(chloromethyl)-benzimidazole and [DBUH][OAc] act as a

catalyst under solvent free condition in excellent yields. The synthesized compounds were screened for their *in vitro* antimycobacterial activity against *M. tuberculosis* H37Ra (*MTB*) and *M. bovis* BCG strains. The compounds **4a**, **4b**, **4e**, **4i**, **4k** and **4l** are highly potent against both the strains. Most of the active compounds are non-cytotoxic against MCF-7, A549, HCT 116 and THP-1 cell lines. Furthermore, a molecular docking study of these compounds was carried out to investigate their binding pattern with the target, active site of mycobacterial enoyl-acyl carrier protein reductase (Inh A) and can be developed as oral drug candidate.

Experimental

All the solvents and reagents were purchased from commercial suppliers, Spectrochem Pvt. Ltd., Rankem India Ltd. and Sigma Aldrich, and were used without further purification. The completion of the reactions was monitored by thin-layer chromatography (TLC) on aluminum plates coated with silica gel 60 F₂₅₄, 0.25 mm thickness (Merck). The detection of the components was made by exposure to iodine vapors or UV light. Melting points were determined by open capillary methods and are uncorrected. ¹H NMR & ¹³C NMR spectra were recorded in DMSO-*d*₆ on a Bruker DRX-400 MHz spectrometer. IR spectra were recorded using a Bruker ALPHA ECO-ATR FTIR spectrometer. High-resolution mass spectra (HRMS) were recorded on Agilent 6520 (QTOF) mass spectrometer.

General procedure for (3*E*,5*E*)-1-((1*H*-benzo[*d*]imidazol-2-yl)methyl)-3,5-dibenzylidenepiperidin-4-one derivatives (**4a-l**)

In a 50 mL round bottom flask, aromatic aldehydes (1 mmol), piperidin-4-one (1 mmol) and 2-(chloromethyl)-1*H*-benzo[*d*]imidazole (1 mmol) and 20 mol% [DBUH][OAc] was stirred at room temperature under solvent-free condition for 4 h. The progress of the reaction was monitored using thin layer chromatography (TLC) (Petroleum ether: Ethyl acetate 1:1). After completion of reaction water was added the reaction mixture was further stirred for 5 min. The solid obtained was removed by filtration, washed with water and then recrystallized from ethanol. The water was removed from filtrate under reduced pressure to recover [DBUH][OAc], which was then reused in subsequent cycles. The identity of the products was confirmed by IR, ¹H NMR, ¹³C NMR and HRMS spectra.

(3*E*,5*E*)-1-((1*H*-Benzo[*d*]imidazol-2-yl)methyl)-3,5-dibenzylidenepiperidin-4-one (**4a**)

The compound **4a** was obtained from **1a**, **2** and **3** as yellow solid; Mp: 214–216 °C; Yield: 85%; IR (cm⁻¹): 1647, 1564, 1486 and 1427; ¹H NMR (400 MHz, DMSO-*d*₆, δ ppm): 9.55 (s, 1H, NH), 7.85 (s, 2H, -C=CH), 7.77–7.66 (m, 6H, Ar-H), 7.56–7.53 (m, 6H, Ar-H), 7.41–7.40 (d, 2H, J = 4 Hz, -Ar-H), 4.95 (s, 2H, -CH₂) and 4.56 (s, 4H, -CH₂); ¹³C NMR (100 MHz, DMSO-*d*₆, δ ppm): 188.4, 156.2, 137.0, 135.7, 132.6, 129.0, 126.0, 122.4, 121.8, 120.1, 119.6, 117.6, 105.7, 56.8 and 51.4; HRMS (ESI-qTOF): Calcd for C₂₇H₂₃N₃O [M + K]⁺, 444.1388, found: 444.1367.

(3*E*,5*E*)-1-((1*H*-Benzo[*d*]imidazol-2-yl)methyl)-3,5-bis(4-methylbenzylidene) piperidin-4-one (**4b**)

The compound **4b** was obtained from **1b**, **2** and **3** as yellow solid; Mp: 212–214 °C; Yield: 80%; ¹H NMR (400 MHz, DMSO-*d*₆, δ ppm): 7.83 (s, 2H, -C=CH), 7.54–7.47 (m, 6H, Ar-H), 7.27–7.23 (m, 6H, Ar-H), 4.94 (s, 2H, -CH₂), 4.49 (s, 4H, -CH₂) and 2.35 (s, 6H, CH₃). Calcd for C₂₉H₂₈N₃O [M + H]⁺, 434.2232, found: 434.0875.

(3E,5E)-1-((1H-Benzo[d]imidazol-2-yl)methyl)-3,5-bis(4-methoxybenzylidene)piperidin-4-one (4c)

The compound **4c** was obtained from **1c**, **2** and **3** as yellow solid; Mp: 245–247 °C; Yield: 79%; ¹HNMR (400 MHz, DMSO-*d*₆, δ ppm): 7.93 (s, 2H, -C=CH), 7.59–7.55 (m, 6H, Ar-H), 7.27–7.25 (m, 2H, Ar-H), 7.12–7.11 (m, 4H, Ar-H), 5.01 (s, 2H, -CH₂), 4.35 (s, 4H, -CH₂) and 3.80 (s, 6H, OCH₃). Calcd for C₂₉H₂₈N₃O₃ [M + H]⁺, 467.2164, found: 467.2631.

(3E,5E)-1-((1H-Benzo[d]imidazol-2-yl)methyl)-3,5-bis(2-chlorobenzylidene) piperidin-4-one (4d)

The compound **4d** was obtained from **1d**, **2** and **3** as yellow solid; Mp: 220–222 °C; Yield: 80%; ¹HNMR (400 MHz, DMSO-*d*₆, δ ppm): 8.06 (s, 2H, -C=CH), 7.64–7.57 (m, 4H, Ar-H), 7.42–7.25 (m, 8H, Ar-H), 5.10 (s, 2H, -CH₂) and 4.58 (s, 4H, -CH₂).

(3E,5E)-1-((1H-Benzo[d]imidazol-2-yl)methyl)-3,5-bis(3-chlorobenzylidene) piperidin-4-one (4e)

The compound **4e** was obtained from **1e**, **2** and **3** as yellow solid; Mp: 178–180 °C; Yield: 78%; ¹HNMR (400 MHz, DMSO-*d*₆, δ ppm): 7.75 (s, 2H, -C=CH), 7.70–7.65 (m, 4H, Ar-H), 7.49–7.40 (m, 6H, Ar-H), 7.34–7.32 (m, 2H, Ar-H), 4.66 (s, 2H, -CH₂) and 4.09 (s, 4H, -CH₂).

(3E,5E)-1-((1H-Benzo[d]imidazol-2-yl)methyl)-3,5-bis(4-chlorobenzylidene) piperidin-4-one (4f)

The compound **4f** was obtained from **1f**, **2** and **3** as yellow solid; Mp: 232–234 °C; Yield: 82%; ¹HNMR (400 MHz, DMSO-*d*₆, δ ppm): 8.11 (s, 2H, -C=CH), 7.89–7.87 (m, 2H, Ar-H), 7.74–7.58 (m, 10H, Ar-H), 4.64 (s, 2H, -CH₂) and 4.00 (s, 4H, -CH₂).

(3E,5E)-1-((1H-Benzo[d]imidazol-2-yl)methyl)-3,5-bis(2-hydroxybenzylidene)piperidin-4-one (4g)

The compound **4g** was obtained from **1g**, **2** and **3** as yellow solid; Mp: 242–244 °C; Yield: 81%. Calcd for C₂₇H₂₃N₃O₃ [M + H]⁺, 438.1773, found: 438.0804.

(3E,5E)-1-((1H-Benzo[d]imidazol-2-yl)methyl)-3,5-bis(4-hydroxybenzylidene)piperidin-4-one (4h)

The compound **4h** was obtained from **1h**, **2** and **3** as yellow solid; Mp: 210–212 °C; Yield: 83%; ¹HNMR (400 MHz, DMSO-*d*₆, δ ppm): 8.34 (s, 2H, -C=CH), 7.33–7.32 (m, 2H, Ar-H), 7.89–7.82 (m, 6H, Ar-H), 7.71–7.67 (m, 2H, Ar-H), 7.40–7.38 (m, 2H, Ar-H), 4.83 (s, 2H, -CH₂) and 4.39 (s, 4H, -CH₂).

(3E,5E)-1-((1H-Benzo[d]imidazol-2-yl)methyl)-3,5-bis(4-fluorobenzylidene) piperidin-4-one (4i)

The compound **4i** was obtained from **1i**, **2** and **3** as yellow solid; Mp: 195–197 °C; Yield: 72%; ¹HNMR (400 MHz, DMSO-*d*₆, δ ppm): 7.87 (s, 2H, -C=CH), 7.66–7.64 (m, 2H, Ar-H),

7.58–7.33 (m, 6H, Ar-H), 6.92–6.91 (m, 4H, Ar-H), 4.79 (s, 2H, -CH₂) and 4.26 (s, 4H, -CH₂). Calcd for C₂₇H₂₂F₂N₃O [M + H]⁺, 442.1686, found: 442.0526.

(3E,5E)-1-((1H-Benzo[d]imidazol-2-yl)methyl)-3,5-bis(4-bromobenzylidene)piperidin-4-one (4j)

The compound **4j** was obtained from **1j**, **2** and **3** as yellow solid; Mp: 253–255 °C; Yield: 80%; ¹HNMR (400 MHz, DMSO-*d*₆, δ ppm): 7.89 (s, 2H, -C=CH), 7.65–7.63 (m, 6H, Ar-H), 7.48–7.47 (m, 4H, Ar-H), 7.33–7.31 (m, 2H, Ar-H), 4.68 (s, 2H, -CH₂) and 4.32 (s, 4H, -CH₂).

(3E,5E)-1-((1H-Benzo[d]imidazol-2-yl)methyl)-3,5-bis(3-nitrobenzylidene) piperidin-4-one (4k)

The compound **4k** was obtained from **1k**, **2** and **3** as yellow solid; Mp: 209–211 °C; Yield: 75%; ¹HNMR (400 MHz, DMSO-*d*₆, δ ppm): 8.45 (s, 2H, -C=CH), 8.26 (s, 2H, Ar-H), 7.88–7.56 (m, 8H, Ar-H), 7.30–7.26 (m, 2H, Ar-H), 4.81 (s, 2H, -CH₂) and 4.38 (s, 4H, -CH₂). Calcd for C₂₇H₂₁N₅O₅ [M + H]⁺, 495.4950, found: 495.3476.

(3E,5E)-1-((1H-benzo[d]imidazol-2-yl)methyl)-3,5-bis(4-nitrobenzylidene)piperidin-4-one (4l)

The compound **4l** was obtained from **1l**, **2** and **3** as yellow solid; Mp: 228–230 °C; Yield: 80%; ¹HNMR (400 MHz, DMSO-*d*₆, δ ppm): 7.90 (s, 2H, -C=CH), 7.60–7.58 (m, 6H, Ar-H), 7.31–7.20 (m, 6H, Ar-H), 4.69 (s, 2H, -CH₂) and 4.10 (s, 4H, -CH₂). Calcd for C₂₇H₂₁N₅O₅ [M + H]⁺, 495.1543, found: 495.1063.

Experimental protocol for biological activity

Antitubercular testing using the XRMA protocol

All the synthesized compounds were screened for their *in vitro* activity against *MTB* H37Ra (ATCC 25177) and *M. bovis* BCG (ATCC 35743) using two-fold dilution technique, in order to determine the actual minimum inhibitory concentration (MIC). Activity against *MTB* was determined through the XTT reduction menadione assay (XRMA) reading absorbance at 470 nm as per the protocol developed earlier.²¹ The nitrate reductase (NR) assay was performed to estimate inhibition of *M. bovis* BCG by compounds. Absorbance for the NR assay was measured at 540 nm. *In vitro* activity against *MTB* and *M. bovis* BCG at active (8 days) and dormant (12 days) stages was performed using the XRMA and NR assay, respectively, as described above. Percentage inhibition was calculated using the following formula:

$$\% \text{ inhibition} = \left[\frac{(\text{control} - \text{CMP})}{(\text{control} - \text{blank})} \right] \times 100$$

where ‘control’ is the activity of mycobacteria without compounds, ‘CMP’ is the activity of mycobacteria in the presence of compounds and ‘blank’ is the activity of the culture medium without mycobacteria.

Cytotoxicity assay

To check the selectivity, active derivatives **4a**, **4b**, **4e**, **4i**, **4k** and **4l** were assayed for their cytotoxic effects in three different cell lines MCF-7, A549 and HCT 116 using MTT assay²² (Table 5). The cell lines were maintained under standard cell culture conditions under 5% CO₂ at 37 °C in

95% air humidified environment. Each concentration was tested in duplicates in a single experiment. GI_{50}/GI_{90} values were calculated using Origin Pro Software.

Antibacterial activity

All bacterial cultures were first grown in Lysogeny Broth (LB) media at 37 °C at 180 RPM. Once the culture reaches 1 O.D, it is used for antibacterial assay. Bacterial strains *E. coli* (NCIM 2688), *Pseudomonas fluorescens* (NCIM 2036) as gram-negative and *B. subtilis* (NCIM 2079), *S. aureus* (NCIM 2010) as gram-positive were obtained from NCIM (NCL, Pune) and were grown in Luria Burtony medium from Himedia, India. The assay was performed in 96 well plates after 8 and 12 h. for gram negative and gram-positive bacteria respectively. 0.1% of 1 OD culture at 620 nm was used for screening.²³ 0.1% inoculated culture was added in to each well of 96 well plates containing the compounds to be tested. Optical density for each plate was measured at 620 nm after 8 h for gram negative bacteria and after 12 h for gram positive bacteria.

Molecular docking study

Docking studies were carried out to predict the probable mechanism of action of antitubercular activity of our synthesized imidazole incorporated curcumin conjugates. Docking studies were performed using crystal structure of mycobacterium tuberculosis enoyl-acyl carrier protein reductase (InhA) (PDB ID: 1ZID) using Glide module (Grid-Based Ligand Docking with Energetics Program) of Schrodinger molecular modeling package.²⁴ All the ligand structure were drawn in Maestro 9.3²⁵ and were prepared using *Ligand Preparation* tool²⁶ which gives the low-energy conformers, 3D structures with correct chirality's for each successfully processed input structure. The imported protein was further purified. After, careful examination, the water molecules were deleted. Ionization and tautomeric state of amino acid residues were rectified and H-atoms atoms were added wherever necessary. Missing residues of the side chain were added using Prime.²⁷ Initially, during protein refinement orientation of polar hydrogens, flip terminal amides and histidine's and protein protonation states were optimized. Further, existing steric clashes present within the protein were relaxed using the OPLS-2005 force field present in the impact refinement module. Minimization was terminated when the energy converged or the root mean square deviation reached a maximum cut off of 0.30 Å.²⁸

Further, the active site of receptor was identified by generating grid around the native ligand ZID. Native ligand was selected and a grid box of size of around 20 Å was encompassed around it, so that there will be maximum inclusion of active site of mycobacterial InhA.

Before subjecting the benzimidazole incorporated 3,5-bis (arylidene)-4-piperidones (4a-4l) for molecular docking, the protocol was validated by extracting the co-crystallized ligand and redocking it into the active site of InhA using the above discussed setup. The best docked conformation of the native ligand was re-produced with a rmsd of less than 1 Å compared to the experimentally observed conformation (Figure 12S) which validates the molecular docking protocol adopted for the molecules being investigated herein.

Acknowledgments

DDS and MHS are very much grateful to the Council of Scientific and Industrial Research (CSIR), New Delhi for the award of senior research fellowship. Authors thank Schrödinger Inc. for providing the GLIDE software to perform the molecular docking study. Authors are also thankful to the Head, Department of Chemistry, Dr. Babasaheb Ambedkar Marathwada University, for providing laboratory facility.

Disclosure statement

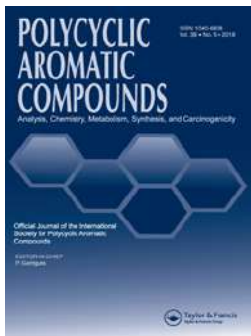
No potential conflict of interest was reported by the authors.

References

1. Global Tuberculosis Control: WHO Report. 2020.
2. M. A. Bill, C. Bakan, D. M. Benson, J. Fuchs, G. Young, and G. B. Lesinski, "Curcumin Induces Proapoptotic Effects against Human Melanoma Cells and Modulates the Cellular Response to Immunotherapeutic Cytokines," *Molecular Cancer Therapeutics* 8, no. 9 (2009): 2726–35.
3. K. Bairwa, J. Grover, M. Kania, and S. M. Jachak, "Recent Developments in Chemistry and Biology of Curcumin Analogues," *RSC Advances* 4, no. 27 (2014): 13946–78; and references cited therein.
4. (a) S. K. Kandi, S. Manohar, C. E. Velez-Gerena, B. Zayas, S. V. Malhotra, and D. S. Rawat, "C5-Curcuminoid-4-Aminoquinoline based Molecular Hybrids: Design, Synthesis and Mechanistic Investigation of Anticancer Activity," *New Journal of Chemistry* 39, no. 1 (2015): 224–234;(b) N. K. Paul, M. Jha, K. S. Bhullar, H. P. V. Rupasinghe, J. Balzarini, and A. Jha, "All Trans 1-(3-Arylacryloyl)-3,5-Bis(Pyridin-4-Ylmethylene)Piperidin-4-Ones as Curcumin-Inspired Antineoplastics," *European Journal of Medicinal Chemistry* 87 (2014): 461–470;(c) H. L. Qin, J. Leng, C. P. Zhang, I. Jantan, M. W. Amjad, M. Sher, M. N. Hassan, M. A. Hussain, and S. N. A. Bukhari, "Synthesis of α,β -Unsaturated Carbonyl-Based Compounds, Oxime and Oxime Ether Analogs as Potential Anticancer Agents for Overcoming Cancer Multidrug Resistance by Modulation of Efflux Pumps in Tumor Cells," *Journal of Medicinal Chemistry* 59 (2016): 3549–3561.
5. P. R. Baldwin, A. Z. Reeves, K. R. Powell, R. J. Napier, A. I. Swimm, A. Sun, K. Giesler, B. Bommarius, T. M. Shinnick, J. P. Snyder, et al. "Monocarbonyl Analogs of Curcumin Inhibit Growth of Antibiotic Sensitive and Resistant Strains of Mycobacterium Tuberculosis," *European Journal of Medicinal Chemistry* 92 (2015): 693–9.
6. P. Yu, L. Dong, Y. Zhang, W. Chen, S. Xu, Z. Wang, X. Shan, J. Zhou, Z. Liu, and G. Liang, "Design, Synthesis and Biological Activity of Novel Asymmetric C66 Analogs as Anti-Inflammatory Agents for the Treatment of Acute Lung Injury," *European Journal of Medicinal Chemistry* 94 (2015): 436–46.
7. M. Samim, S. Naqvi, I. Arora, F. J. Ahmad, and A. Maitra, "Antileishmanial Activity of Nanocurcumin," *Therapeutic Delivery* 2, no. 2 (2011): 223–30.
8. Q. Li, J. Chen, S. Luo, J. Xu, Q. Huang, and T. Liu, "Synthesis and Assessment of the Antioxidant and Antitumor Properties of Asymmetric Curcumin Analogues," *European Journal of Medicinal Chemistry* 93 (2015): 461–9.
9. (a) S. N. A. Bukhari, I. Jantan, V. H. Masand, D. T. Mahajan, M. Sher, M. N. Hassan, and M. W. Amjad, "Synthesis of α, β -Unsaturated Carbonyl-Based Compounds as Acetylcholinesterase and Butyrylcholinesterase Inhibitors: Characterization, Molecular Modeling, QSAR Studies and Effect Against Amyloid β -Induced Cytotoxicity," *European Journal of Medicinal Chemistry* 83 (2014): 355–365;(b) X. Yuan, H. Li, H. Bai, Z. Su, Q. Xiang, C. Wang, B. Zhao, Y. Zhang, Q. Zhang, Y. Chu, and Y. Huang, "Synthesis of Novel Curcumin Analogues for Inhibition of 11β -Hydroxysteroid Dehydrogenase Type 1 with Anti-diabetic Properties," *European Journal of Medicinal Chemistry* 77 (2014): 223–230.
10. (a) A. Jha, K. M. Duffield, M. R. Ness, S. Ravoori, G. Andrews, K. S. Bhullar, H. P. V. Rupasinghe, and J. Balzarini, "Curcumin-Inspired Cytotoxic 3,5-Bis(Arylmethylene)-1-(N-(Ortho-Substituted Aryl)Maleamoyl)-4-Piperidones: A Novel Group of Topoisomerase II Alpha Inhibitors," *Bioorganic & Medicinal Chemistry* 23, no. 19 (2015): 6404–6417;(b) S. N. A. Bukhari, G. Lauro, I. Jantan, G. Bifulco, and M. W. Amjad, "Pharmacological Evaluation and Docking Studies of α,β -Unsaturated Carbonyl Based Synthetic Compounds as Inhibitors of Secretory Phospholipase A₂, Cyclooxygenases, Lipoxygenase and Proinflammatory Cytokines," *Bioorganic Medicinal Chemistry* 22 (2014): 4151–4161;(c) M. F. F. M. Aluwi, K. Rullah, B. M. Yamin, S. W. Leong, M. N. A. Bahari, S. J. Lim, S. M. M. Faudzi, J. Jalil, F. Abas, N. M. Fauzi, N. H. Ismail, I. Jantan, and K. W. Lam, "Synthesis of Unsymmetrical Monocarbonyl Curcumin Analogs with Potent Inhibition on Prostaglandin E2 Production in LPS-Induced Murine and Human Macrophages Cell Lines," *Bioorganic & Medicinal Chemistry Letters* 26 (2016): 2531–2538;(d) S. M. M. Faudzi, S. W. Leong, F. Abas, M. F. F. M. Aluwi, K. Rullah, K. W. Lam, S. Ahmad, C. L. Tham, K. Shaari, and N. H. Lajis, "Synthesis, Biological Evaluation and QSAR Studies of Diarylpentanoic Acid Analogues as Potential Nitric Oxide Inhibitors," *Medicinal Chemistry Communications* 6 (2015): 1069–1080.
11. (a) G. Yadav and S. Ganguly, "Structure Activity Relationship (SAR) Study of Benzimidazole Scaffold for Different Biological Activities: A Mini-Review," *European Journal of Medicinal Chemistry* 97 (2015): 419–443;(b) S. Tahlan, S. Kumar, and B. Narasimhan, "Pharmacological Significance of Heterocyclic 1H-Benzimidazole Scaffolds: A Review," *BMC Chemistry* 13 (2019):101.

12. (a) Y. T. Wang, Y. J. Qin, N. Yang, Y. L. Zhang, C. H. Liu, and H. L. Zhu, "Synthesis, Biological Evaluation, and Molecular Docking Studies of Novel 1-Benzene Acyl-2-(1-Methylindol-3-yl)-Benzimidazole Derivatives as Potential Tubulin Polymerization Inhibitors," *European Journal of Medicinal Chemistry* 99 (2015): 125–137; (b) T. S. Reddy, H. Kulhari, G. Reddy, V. Bansal, A. Kamal, and R. Shukla, "Design, Synthesis and Biological Evaluation of 1,3-Diphenyl-1H-Pyrazole Derivatives Containing Benzimidazole Skeleton as Potential Anticancer and Apoptosis Inducing Agents," *European Journal of Medicinal Chemistry* 101 (2015): 790–805; (c) Y. K. Yoon, M. A. Ali, A. C. Wei, T. S. Choon, and R. Ismail, "Synthesis and Evaluation of Antimycobacterial Activity of New Benzimidazole Aminoesters," *European Journal of Medicinal Chemistry* 93 (2015): 614–624; (d) K. Gobis, H. Foks, M. Serocki, E. A. Kope, and A. Napiorkowska, "Synthesis and Evaluation of In Vitro Antimycobacterial Activity of Novel 1H-Benzo[d]imidazole Derivatives and Analogues," *European Journal of Medicinal Chemistry* 89 (2015): 13–20; (e) Y. Bansal, M. Kaur, and O. Silakari, "Benzimidazole-Ibuprofen/Mesalamine Conjugates: Potential Candidates for Multifactorial Diseases," *European Journal of Medicinal Chemistry* 89 (2015): 671–682; (f) D. Seenaiyah, P. R. Reddy, G. M. Reddy, A. Padmaja, V. Padmavathi, and N. S. Krishna, "Synthesis, Antimicrobial and Cytotoxic Activities of Pyrimidinyl Benzoxazole, Benzothiazole and Benzimidazole," *European Journal of Medicinal Chemistry* 77 (2014): 1–7; (g) R. V. Shingalapur, K. M. Hosamani, R. S. Keri, and M. H. Hugar, "Derivatives of Benzimidazole Pharmacophore: Synthesis, Anticonvulsant, Antidiabetic and DNA Cleavage Studies," *European Journal of Medicinal Chemistry* 45 (2010): 1753–1759; (h) A. S. Alpan, S. Parlar, L. Carlino, A. H. Tarikogullari, V. Alptuzun, and H. S. Gunes, "Synthesis Biological Activity and Molecular Modeling Studies on 1H-Benzimidazole Derivatives as Acetylcholinesterase Inhibitors," *Bioorganic Medicinal Chemistry* 21 (2013): 4928–4937; (i) E. P. Jesudason, S. K. Sridhar, E. J. P. Malar, P. Shanmugapandiyam, M. Inayathullah, V. Arul, D. Selvaraj, and R. Jayakumar, "Synthesis, Pharmacological Screening, Quantum Chemical and In Vitro Permeability Studies of N-Mannich Bases of Benzimidazoles Through Bovine Cornea," *European Journal of Medicinal Chemistry* 44 (2009): 2307–2312; (j) P. Bandyopadhyay, M. Sathe, S. N. Tikar, R. Yadav, P. Sharma, A. Kumar, and M. P. Kaushik, "Synthesis of Some Novel Phosphorylated and Thiophosphorylated Benzimidazoles and Benzothiazoles and Their Evaluation for Larvicidal Potential to *Aedes Albopictus* and *Culex Quinquefasciatus*," *Bioorganic & Medicinal Chemistry Letters* 24 (2014): 2934–2939; (k) X. J. Wang, M. Y. Xi, J. H. Fu, F. R. Zhang, G. F. Cheng, D. L. Yin, and Q. D. You, "Synthesis, Biological Evaluation and SAR Studies of Benzimidazole Derivatives as H1-Antihistamine Agents," *Chinese Chemical Letters* 23 (2012): 707–710; (l) J. R. Hwu, R. Singha, S. C. Hong, Y. H. Chang, A. R. Das, I. Vliegen, E. D. Clercq, and J. Neyts, "Synthesis of New Benzimidazole-Coumarin Conjugates as Antihepatitis C Virus Agents," *Antiviral Research* 77 (2008): 157–162.
13. B. H. Rotstein, S. Zaretsky, V. Rai, and A. K. Yudin, "Small Heterocycles in Multicomponent Reactions," *Chemical Reviews* 114, no. 16 (2014): 8323–59; and references cited therein.
14. A. Domling, W. Wang, and K. Wang, "Chemistry and Biology of Multicomponent Reactions," *Chemical Reviews* 112, no. 6 (2012): 3083–135; and references cited therein.
15. N. Isambert, M. M. S. Duque, J. C. Plaquevent, Y. Genisson, J. Rodriguez, and T. Constantieux, "Multicomponent Reactions and Ionic Liquids: A Perfect Synergy for Eco-Compatible Heterocyclic Synthesis," *Chemical Society Reviews* 40, no. 3 (2011): 1347–57.
16. M. A. P. Martins, C. P. Frizzo, A. Z. Tier, D. N. Moreira, N. Zanatta, and H. G. Bonaccorso, "Update 1 of: Ionic Liquids in Heterocyclic Synthesis," *Chemical Reviews* 114, no. 20 (2014): PR1–PR70; and references cited therein.
17. [DBUH][OAc] catalyzed organic transformations see: (a) X. T. Cao, L. Qiao, H. Zheng, H. Y. Yang and P. F. Zhang, "A efficient protocol for the synthesis of thioamides in [DBUH][OAc] at room temperature," *RSC Advances* 8 (2018): 170–175; (b) R. Bhupathi, B. Madhu, B. R. Devi, V. R. R. Chittireddy and P. K. Dubey, "DBU acetate mediated: one-pot multi component syntheses of dihydropyrano [3, 2-c] quinolones," *Journal of Heterocyclic Chemistry* 53 (2016): 1911–1916; (c) X. T. Cao, P. F. Zhang and H. Zheng, "Metalfree catalytic synthesis of diaryl thioethers under mild conditions," *New Journal of Chemistry* 40 (2016): 6762–6767; (d) J. Hu, J. Ma, Z. Zhang, Q. Zhu, H. Zhou, W. Lu and B. Han, "A route to convert CO₂: synthesis of 3,4,5-trisubstituted oxazolones," *Green Chemistry* 17 (2015): 1219–1225; (e) S. H. Jayaprakash, B. S. Krishna, S. S. Sudha, N. B. Reddy, P. Sreelakshmi, K. M. K. Reddy and C. S. Reddy, "Ionic liquid-promoted phosphamichael reaction: convenient access to β -Nitrophosphonates," *Synthetic Communications* 45 (2015): 2083–2091; (f) D. D. Subhedar, M. H. Shaikh, B. B. Shingate, L. Nawale, D. Sarkar, V. M. Khedkar, F. A. K. Khan and J. N. Sangshetti, "Quinolidene-rhodanine conjugates: Facile synthesis and biological evaluation," *European Journal of Medicinal Chemistry* 125 (2017): 385–399; (g) B. Yu, H. Zhang, Y. Zhao, S. Chen, J. Xu, L. Hao and Z. Liu, "DBU-based ionic-liquid-catalyzed carbonylation of o-phenylenediamines with CO₂ to 2-benzimidazolones under solvent-free conditions," *ACS Catalysis* 3 (2013): 2076–2082; (h) D. D. Subhedar, M. H. Shaikh, B. B. Shingate, L. Nawale, A. Yeware, D. Sarkar and V. M. Khedkar, "Novel tetrazoloquinoline-thiazolidinone conjugates as possible antitubercular agents: synthesis and molecular docking," *Medicinal Chemical Communications* 7 (2016): 1832–1848.

18. (a) D. D. Subhedar, M. H. Shaikh, A. A. Nagargoje, S. V. Akolkar, S. G. Bhansali, D. Sarkar and B. B. Shingate, "Amide-linked monocarbonyl curcumin analogues: efficient synthesis, antitubercular activity and molecular docking study", *Polycyclic Aromatic Compounds* (2020) <https://doi.org/10.1080/10406638.2020.1852288>; (b) A. A. Nagargoje, S. V. Akolkar, D. D. Subhedar, M. H. Shaikh, J. N. Sangshetti, V. M. Khedkar and B. B. Shingate, "Propargylated monocarbonyl curcumin analogues: synthesis, bioevaluation and molecular docking study", *Medicinal Chemistry Research* 29 (2020): 1902–1913; (c) Amol A. Nagargoje, Satish V. Akolkar, Madiha M. Siddiqui, Dnyaneshwar D. Subhedar, Jaiprakash N. Sangshetti, Vijay M. Khedkar, and Bapurao B. Shingate, "Synthesis and Bioevaluation of α , α' -Bis (1H-1, 2, 3-triazol-5-ylmethylene) Ketones," *Chemistry & Biodiversity* 17, no. 2 (2020): e1900624–820; (d) T. R. Deshmukh, S. P. Khare, V. S. Krishna, D. Sriram, J. N. Sangshetti and B. B. Shingate, "Synthesis of 1, 2, 3-triazole incorporated monocarbonyl curcumin analogues as potent antitubercular, antifungal and antioxidant agents", *Chemistry & Biology Interface*, 9 (2019): 59–70; (e) T. R. Deshmukh, V. S. Krishna, D. Sriram, J. N. Sangshetti and B. B. Shingate, "Synthesis and bioevaluation of α , α' -bis (1H-1, 2, 3-triazol-5-ylmethylene) ketones", *Chemical Papers*, 74 (2020): 809–820.
19. H. B. Woo, Y. W. Eom, K. S. Park, J. Ham, C. M. Ahn, and S. Lee, "Synthesis of Substituted Benzimidazolyl Curcumin Mimics and Their Anticancer Activity," *Bioorganic & Medicinal Chemistry Letters* 22, no. 2 (2012): 933–6.
20. (a) S. V. Akolkar, A. A. Nagargoje, V. S. Krishna, D. Sriram, J. N. Sangshetti, M. Damale, and B. B. Shingate, "New *N*-Phenylacetamide-Incorporated 1,2,3-Triazoles: [Et₃NH][OAc]-Mediated Efficient Synthesis and Biological Evaluation," *Bioorganic & Medicinal Chemistry Letters* 26, no. 7 (2016): 1704–22091; (b) D. D. Subhedar, M. H. Shaikh, M. A. Arkile, A. Yeware, D. Sarkar, and B. B. Shingate, "Facile Synthesis of 1, 3-Thiazolidin-4-Ones as Antitubercular Agents," *Bioorganic & Medicinal Chemistry Letters* 26 (2016): 1704–1708; (c) D. D. Subhedar, M. H. Shaikh, L. Nawale, A. Yeware, D. Sarkar, F. A. K. Khan, J. N. Sangshetti, and B. B. Shingate, "Novel Tetrazoloquinoline-Rhodanine Conjugates: Highly Efficient Synthesis and Biological Evaluation," *Bioorganic & Medicinal Chemistry Letter* 2016, 26, 2278–2283; (d) D. D. Subhedar, M. H. Shaikh, F. A. K. Khan, J. N. Sangshetti, V. M. Khedkar, and B. B. Shingate, "Facile Synthesis of New *N*-Sulfonamidyl-4-Thiazolidinone Derivatives and Their Biological Evaluation," *New Journal of Chemistry* 40 (2016): 3047–3058; (e) D. D. Subhedar, M. H. Shaikh, L. Nawale, A. Yeware, D. Sarkar, and B. B. Shingate, "[Et₃NH][HSO₄] Catalyzed Efficient Synthesis of 5-Arylidene-Rhodanine Conjugates and Their Antitubercular Activity," *Research on Chemical Intermediate* 42 (2016): 6607–6626; (f) M. H. Shaikh, D. D. Subhedar, F. A. K. Khan, J. N. Sangshetti, and B. B. Shingate, "[Et₃NH][HSO₄]-Catalyzed One-Pot, Solvent-Free Synthesis and Biological Evaluation of α -Amino Phosphonates," *Research on Chemical Intermediate* 42(2016): 5115–5131.
21. U. Singh, S. Akhtar, A. Mishra, and D. Sarkar, "A Novel Screening Method Based on Menadione Mediated Rapid Reduction of Tetrazolium Salt for Testing of anti-Mycobacterial Agents," *Journal of Microbiological Methods* 84, no. 2 (2011): 202–7.
22. D. Sreekanth, A. Syed, S. Sarkar, D. Sarkar, B. Santhakumari, A. Ahmad, and I. Khan, "Production, Purification and Characterization of Taxol and 10DAB III from a New Endophytic Fungus *Gliocladium* sp. Isolated from the Indian Yew Tree, *Taxus Baccata*," *Journal of Microbiology and Biotechnology* 19, no. 11 (2009): 1342–7.
23. R. Singh, L. U. Nawale, M. Arkile, U. U. Shedbalkar, S. A. Wadhvani, D. Sarkar, and B. A. Chopade, "Chemical and Biological Metal Nanoparticles as Antimycobacterial Agents: A Comparative Study," *International Journal of Antimicrobial Agents* 46, no. 2 (2015): 183–8.
24. Glide Version 5.8 (New York, NY: Schrodinger LLC, 2012).
25. Maestro Version 9.3 (New York, NY: Schrodinger LLC, 2012).
26. LigPrep Version 2.5 (New York, NY: Schrodinger LLC, 2012).
27. Prime Version 3.1 (New York; NY: Schrodinger LLC, 2012).
28. (a) R. A. Friesner, J. L. Banks, R. B. Murphy, T. A. Halgren, J. J. Klicic, D. T. Mainz, M. P. Repasky, E. H. Knol, M. Shelley, J. K. Perry, D. E. Shaw, P. Francis, and P. S. Shenkin, "Glide: A New Approach for Rapid, Accurate Docking and Scoring. 1. Method and Assessment of Docking Accuracy," *Journal of Medicinal Chemistry* 47 (2004): 1739–1749; (b) T. A. Halgren, R. B. Murphy, R. A. Friesner, H. S. Beard, L. L. Frye, W. T. Pollard, and J. L. Banks, "Glide: A New Approach for Rapid, Accurate Docking and Scoring. 2. Enrichment Factors in Database Screening," *Journal of Medicinal Chemistry* 47 (2004): 1750–1759.




Synthesis and Biological Evaluation of 2-(4,5,6,7-Tetrahydrobenzo[c]isoxazol-3-yl)-4*H*-Chromen-4-Ones

Sujata G. Dengale, Hemantkumar N. Akolkar, Nirmala R. Darekar, Mubarak H. Shaikh, Keshav K. Deshmukh, Sadhana D. Mhaske, Bhausahab K. Karale, Dipak N. Raut & Vijay M. Khedkar


To cite this article: Sujata G. Dengale, Hemantkumar N. Akolkar, Nirmala R. Darekar, Mubarak H. Shaikh, Keshav K. Deshmukh, Sadhana D. Mhaske, Bhausahab K. Karale, Dipak N. Raut & Vijay M. Khedkar (2021): Synthesis and Biological Evaluation of 2-(4,5,6,7-Tetrahydrobenzo[c]isoxazol-3-yl)-4*H*-Chromen-4-Ones, Polycyclic Aromatic Compounds, DOI: [10.1080/10406638.2021.1982733](https://doi.org/10.1080/10406638.2021.1982733)

To link to this article: <https://doi.org/10.1080/10406638.2021.1982733>

 View supplementary material 

 Published online: 27 Sep 2021.


 Submit your article to this journal 

 View related articles 

 View Crossmark data 



Synthesis and Biological Evaluation of 2-(4,5,6,7-Tetrahydrobenzo[c]isoxazol-3-yl)-4H-Chromen-4-Ones

Sujata G. Dengale^a, Hemantkumar N. Akolkar^b , Nirmala R. Darekar^c, Mubarak H. Shaikh^c, Keshav K. Deshmukh^a, Sadhana D. Mhaske^d, Bhasusaheb K. Karale^b, Dipak N. Raut^e, and Vijay M. Khedkar^f

^aDepartment of Chemistry, Sangamner Nagarpalika Arts, D. J. Malpani Commerce and B. N. Sarada Science College, Sangamner, Maharashtra, India; ^bDepartment of Chemistry, Abasaheb Marathe Arts & New Commerce, Science, College, Rajapur, Maharashtra, India; ^cDepartment of Chemistry, Radhabai Kale Mahila Mahavidyalaya, Ahmednagar, Maharashtra, India; ^dDepartment of Chemistry, Dadapatil Rajale College, Pathardi, Maharashtra, India; ^eDepartment of Pharmacognosy, Amrutvahini College of Pharmacy, Sangamner, Maharashtra, India; ^fSchool of Pharmacy, Vishwakarma University, Pune, Maharashtra, India

ABSTRACT

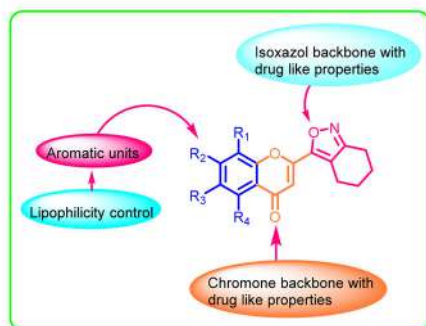
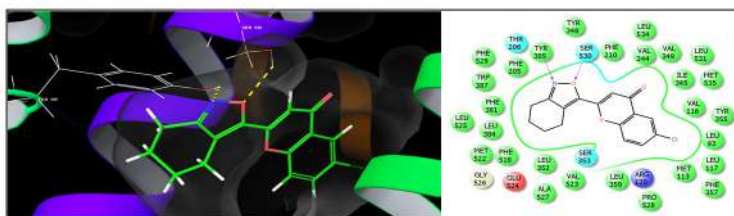
A new series of 2-(4,5,6,7-tetrahydrobenzo[c]isoxazol-3-yl)-4H-chromen-4-ones **5a-e** were synthesized from 1-(2-hydroxyphenyl)-3-(4,5,6,7-tetrahydrobenzo[c]isoxazol-3-yl)propane-1,3-diones **4a-e** in presence of acetic acid and conc. HCl. Compounds **4a-e** were synthesized by Baker-Venkataraman rearrangement from 2-acetylphenyl 4,5,6,7-tetrahydrobenzo[c]isoxazole-3-carboxylate **3a-e** in presence of pyridine and KOH and compounds **3a-e** were synthesized from 4,5,6,7-tetrahydrobenzo[c]isoxazole-3-carboxylic acid **1** and substituted 2-hydroxy acetophenone **2a-e**. All the synthesized compounds were characterized with the help of IR, ¹H NMR, ¹³C NMR and mass spectroscopic techniques. All the compounds were screened for their *in vitro* anti-inflammatory activities. Furthermore, molecular docking study against COX-2 enzyme could provide valuable insight into the binding affinity of these molecules and the type of thermodynamic interactions governing their binding.

ARTICLE HISTORY

Received 27 February 2021
Accepted 9 September 2021

KEYWORDS

β -Diketones; anti-inflammatory screening; COX-2 enzyme; molecular docking; ADME



Introduction

Isoxazole is oxygen and nitrogen containing five membered heterocyclic compounds. It contains one Carbon-Nitrogen double bond and one Carbon-Carbon double bond contribute to the unsaturated property of the molecule. The incorporation of isoxazole moiety may contribute to the improved efficacy, less toxicity, and increased pharmacokinetics profiles.¹ Isoxazole exhibits various pharmacological activities such as cytotoxic,² anti-diabetic,³ anti-inflammatory,⁴ antibacterial,⁵ antifungal,⁶ antitumor,⁷ antiviral,⁸ antitubercular.⁹ There are several drugs in market available as drugs containing isoxazole such as oxacillin, sulfamethoxazole, sulfisoxazole, drazoxolon, HWA-486 and NVP-AUY922 (Figure 1).

Chromones are the oxygen containing heterocyclic compounds with benzofused γ -pyrone ring, with the parent compound being chromone (4*H*-chromene-4-one, 4*H*-1-benzopyran-4-one). The derivatives of chromone are the most significant heterocyclic compounds in variety of natural products and medicinal agents. Chromone derivatives have variety of biological activities such as nematocidal,¹⁰ antitumor¹¹ antioxidant,¹² antibacterial,¹³ anticancer,¹⁴ anti-Alzheimer¹⁵ and anti-inflammatory activity¹⁶ etc. There are some marketed drugs having chromone as core heterocyclic ring like khellin act as herbal folk medicine, disodium cromoglycate used in treatment of asthma,¹⁷ flavoxate in smooth-muscle relaxant and apigenin as a skin cancer chemo preventive agent (Figure 2).

1,3-Diketones opens wide prospects for the design of a variety of organic compounds due to its high reactivity, including those structurally related to natural ones. For COX-2 inhibitions the β -diketone scaffold is a very important key intermediate which is a non-steroidal anti-inflammatory agent of the coxib family. The functionalized beta-diketones are clinically important molecules showing antiviral,¹⁸ antibacterial,¹⁸ antitumor,¹⁹ anti-inflammatory,²⁰ anticancer²⁰ and antioxidant²¹ activities. Gill *et al.*, reported some novel chromones incorporated isoxazole moieties and evaluated for their antimicrobial activity.²² Wang *et al.* reported the synthesis of isoxazole-linked norcantharidin analogues of substituted chromones.²³

In continuation of our earlier work²⁴ on synthesis and biological properties of various heterocyclic moieties, herein, a small focused library of 2-heteryl chromones incorporated molecules.

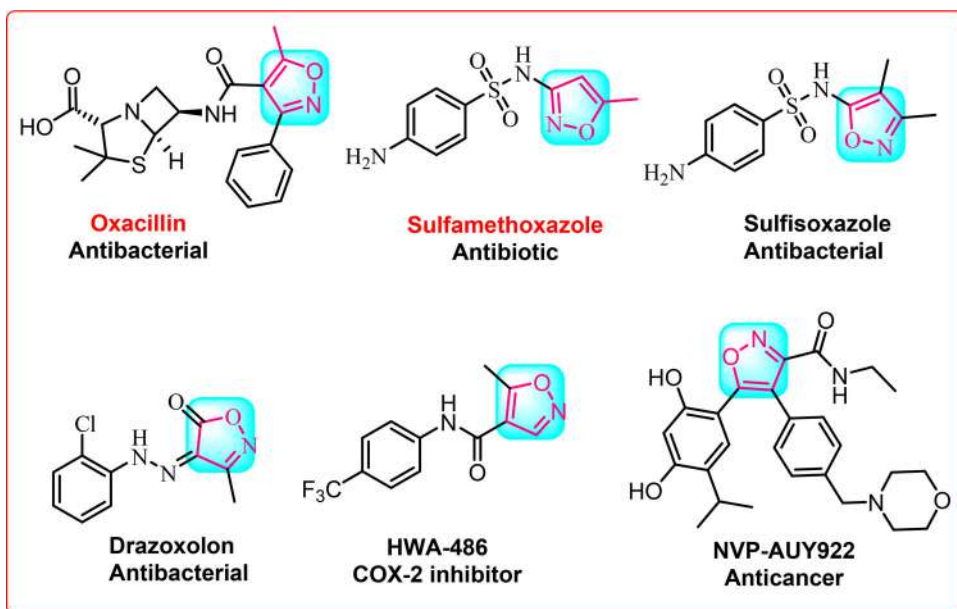


Figure 1. Isoxazole-containing drugs.

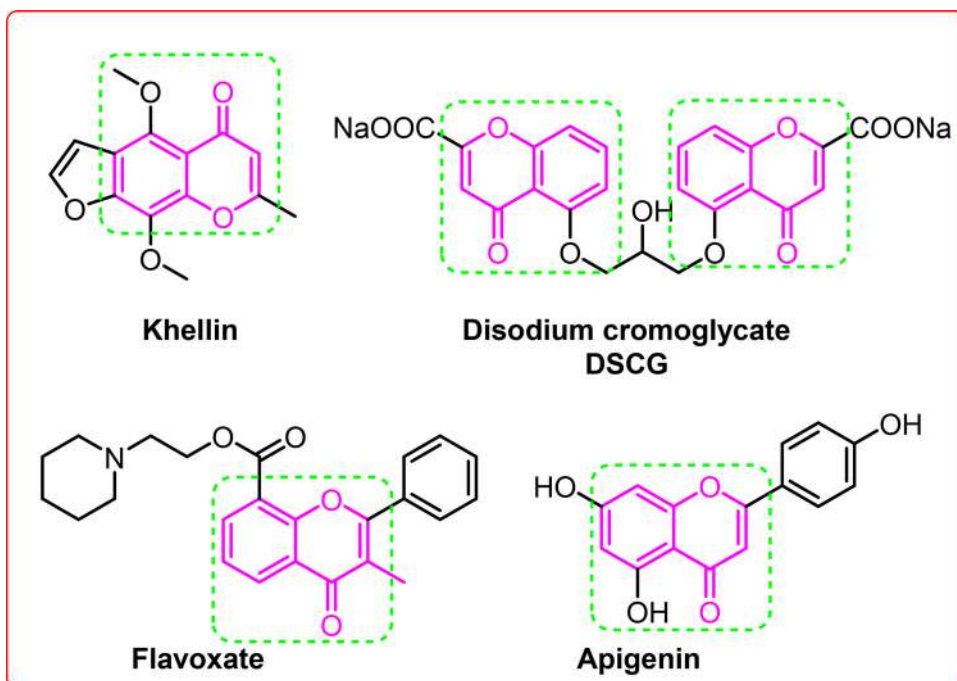


Figure 2. Chromone containing marketed drugs.

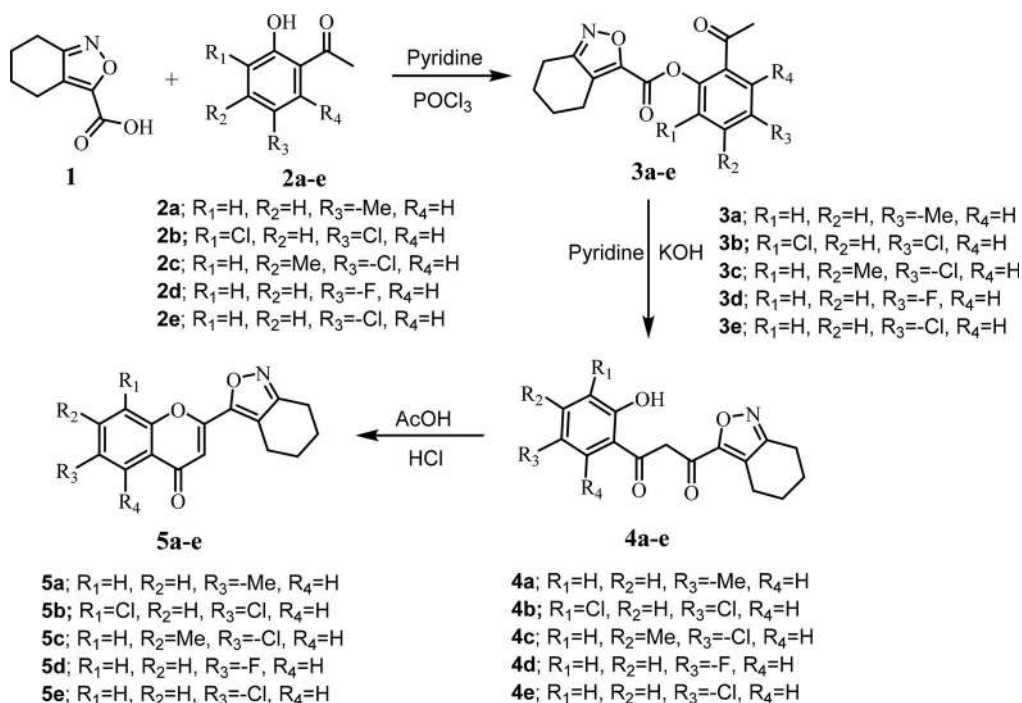
Considering the biological importance of isoxazole, chromones and β -diketones, we construct conjugated isoxazole, chromones and β -diketones in one molecular framework to enhance the anti-inflammatory and antioxidant activity with minimizing the side effects. In addition to this, we have also performed *in silico* molecular docking study against COX-2 enzyme and ADME prediction for the synthesized compounds.

Results and discussion

Chemistry

In the present study, we have described the synthesis of new 2-(4,5,6,7-tetrahydrobenzo[*c*]isoxazol-3-yl)-4*H*-chromen-4-ones (**5a-e**). Initially, a series of 2-acetylphenyl 4,5,6,7-tetrahydrobenzo[*c*]isoxazole-3-carboxylate **3a-e** were synthesized from 4,5,6,7-tetrahydrobenzo[*c*]isoxazole-3-carboxylic acid **1** and substituted 2-hydroxy acetophenone **2a-e** in POCl₃ and dry pyridine (Scheme 1). Further, compounds **3a-e** undergoes Baker-Venkataraman transformation to give 1-(2-Hydroxyphenyl)-3-(4,5,6,7-tetrahydrobenzo[*c*]isoxazol-3-yl)propane-1,3-diones (**4a-e**). Finally, the cyclodehydration of compounds **4a-e** in presence of acetic acid and conc. HCl gives corresponding 2-(4,5,6,7-tetrahydrobenzo[*c*]isoxazol-3-yl)-4*H*-chromen-4-ones (**5a-e**) in a good yield. (Scheme 1).

The formation of 2-acetylphenyl 4,5,6,7-tetrahydrobenzo[*c*]isoxazole-3-carboxylate **3a-e** were confirmed by ¹H NMR, ¹³C NMR and mass spectra. In the ¹H NMR spectrum of compound **3a**, the two singlets observed at δ 2.41 and 2.52 ppm for the -CH₃ group attached to the phenyl and carbonyl carbon respectively. The ¹³C NMR spectrum of compound **3a** revealed that the peak appears at δ 197.89 ppm is due to the presence of carbonyl carbon. Structure of compound **3a** also confirmed by molecular ion peak at *m/z* 300.11 (M + H)⁺. Similarly, the synthesis of 1-(2-hydroxyphenyl)-3-(4,5,6,7-tetrahydrobenzo[*c*]isoxazol-3-yl)propane-1,3-diones **4a-e** were also confirmed by the spectral techniques. In the ¹H NMR spectrum of compound **4a**, the singlet observed at δ 16.12 ppm confirms the presence of enolic-OH proton. The ¹³C NMR spectrum of compound **4a** showed the peak at δ 196.80 ppm confirms the presence of carbonyl carbon. Further, the structure of compound **4a** also confirmed by molecular ion peak at *m/z* 300.16 (M + H)⁺.



Scheme 1. Synthesis of 2-(4,5,6,7-tetrahydrobenzo[*c*]isoxazol-3-yl)-4*H*-chromen-4-ones (**5a-e**)

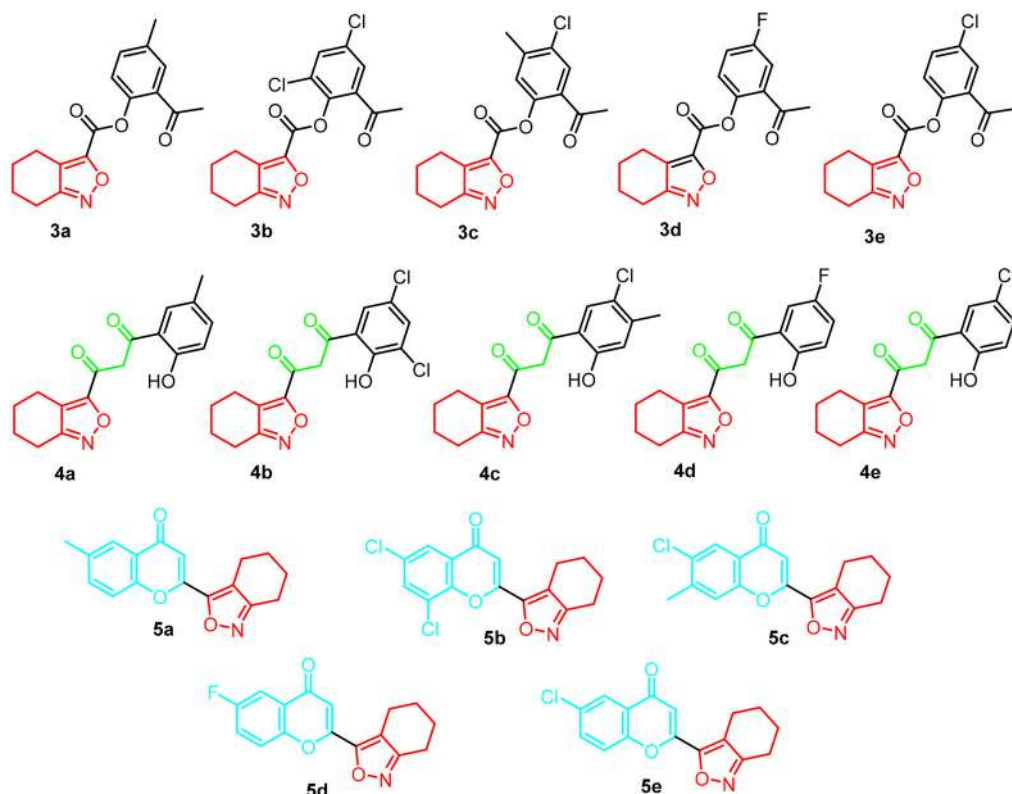


Figure 3. Structures of all the synthesized derivatives.

Finally, the formation of 2-(4,5,6,7-tetrahydrobenzo[*c*]isoxazol-3-yl)-4*H*-chromen-4-ones (**5a-e**) were confirmed by the various spectral techniques. In the ^1H NMR spectrum, the formation of chromone ring in compound **5a** confirmed by the singlet peak observed at δ 6.58 ppm for the proton present on chromone ring. The ^{13}C NMR spectrum of compound **5a** showed that the signal appears at δ 176.67 ppm for carbonyl carbon of chromone ring. Structure of compound **5a** also confirmed by mass spectra, molecular ion peak observed at m/z 282.15 ($\text{M} + \text{H}$) $^+$. Similarly, all the synthesized compounds were characterized by the spectral analysis. Structures of all the synthesized derivatives shown in Figure 3.

Biological evaluation

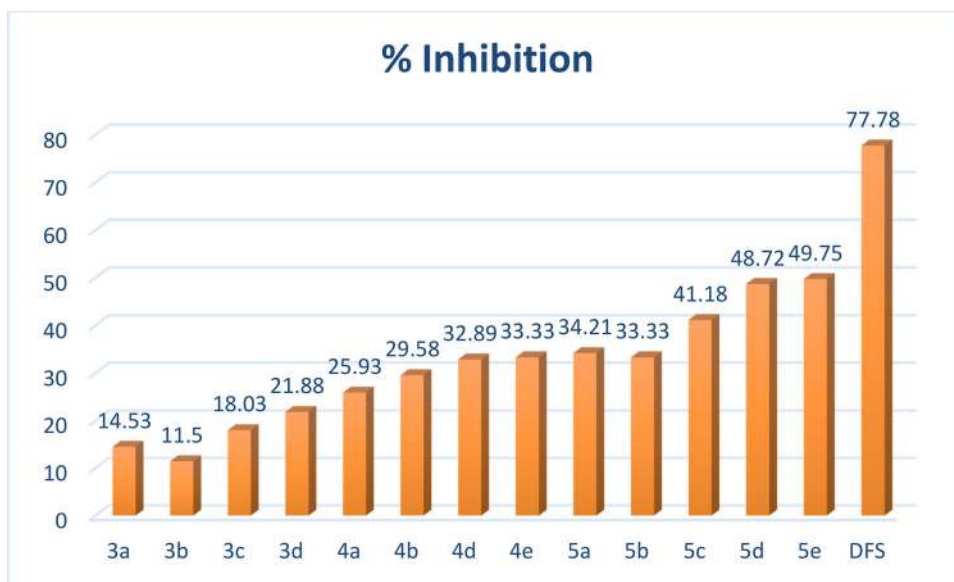
Anti-inflammatory activity

All the synthesized compounds were screened for their *in vitro* anti-inflammatory activities in comparison to standard drug Diclofenac sodium. Inflammation is related to pain and inflammation of surrounding tissues that involves elevated protein denaturation, vascular permeability and membrane alterations.²⁸ Non-steroidal anti-inflammatory drugs (NSAIDs) including diclofenac sodium are common choice of the drugs. Role of inhibition of protein denaturation carried out by such drug is reported²⁸ and ability of reversal of enhanced plasma protein coagulation is also seen in drug-treated animals. Previous literature²⁸ on *in vitro* anti-inflammatory activity demonstrated the application of bovine serum albumin model in para-medical research.

Table 1. *In vitro* anti-inflammatory (percent of inhibition), anti-oxidant activity (MIC in $\mu\text{g/mL}$) and molecular docking score.

Cpd	Anti-inflammatory	Anti-oxidant	Glide Score	Glide energy (Kcal/mol)	H-bonding (\AA)
3a	14.53	153.507	-7.881	-34.912	Ser530(2.599)
3b	11.50	309.5597	-7.189	-31.726	Ser530(2.731)
3c	18.03	141.9384	-8.001	-36.449	Ser530(2.538)
3d	21.88	142.1429	-8.107	-37.199	Ser530(2.051), Tyr385(2.653)
3e	NT	NT	-6.741	-28.606	Ser530(2.579)
4a	25.93	214.75	-8.178	-36.065	Ser530(1.701)
4b	29.58	269.3371	-8.294	-38.031	Ser530(1.864)
4c	NT	NT	-6.649	-27.864	Ser530(2.307, 2.639), Tyr385(2.575)
4d	32.89	239.507	-8.668	-39.907	Ser530(2.561)
4e	33.33	157.8333	-8.726	-40.076	Ser530(2.567)
5a	34.21	471.598	-9.121	-42.596	Ser530(2.181), Tyr385(2.596)
5b	33.33	882.875	-9.031	-41.868	Ser530(2.232), Tyr385(2.614)
5c	41.18	650.475	-9.177	-44.257	Ser530(2.466), Tyr385(2.369)
5d	48.72	628.325	-9.577	-47.365	Ser530(2.013), Tyr385(2.729)
5e	49.75	NT	-9.638	-48.518	Ser530(2.215), Tyr385(2.628)
DFS	77.78	-	-	-	-
AA	-	41.69611	-	-	-

Cpd: Compounds; DFS: Diclofenac sodium; AA: Ascorbic acid.

**Figure 4.** The percent inhibition of compounds *in vitro* anti-inflammatory model.

Among all the synthesized compounds, 2-(4,5,6,7-tetrahydrobenzo[*c*]isoxazol-3-yl)-4*H*-chromen-4-ones (**5a-e**) compound **5c**, **5d** and **5e** all other compounds exhibited moderate anti-inflammatory activity compare to the standard drug diclofenac sodium. (Table 1).

The percent inhibition of compounds *in vitro* anti-inflammatory model shown in Figure 4.

Anti-oxidant activity by DPPH

According to the DPPH assay, all the synthesized compound displays comparable antioxidant activity than standard drug Ascorbic acid (Table 1). The percent inhibition of compounds *in vitro* antioxidant model shown in Figure 5.

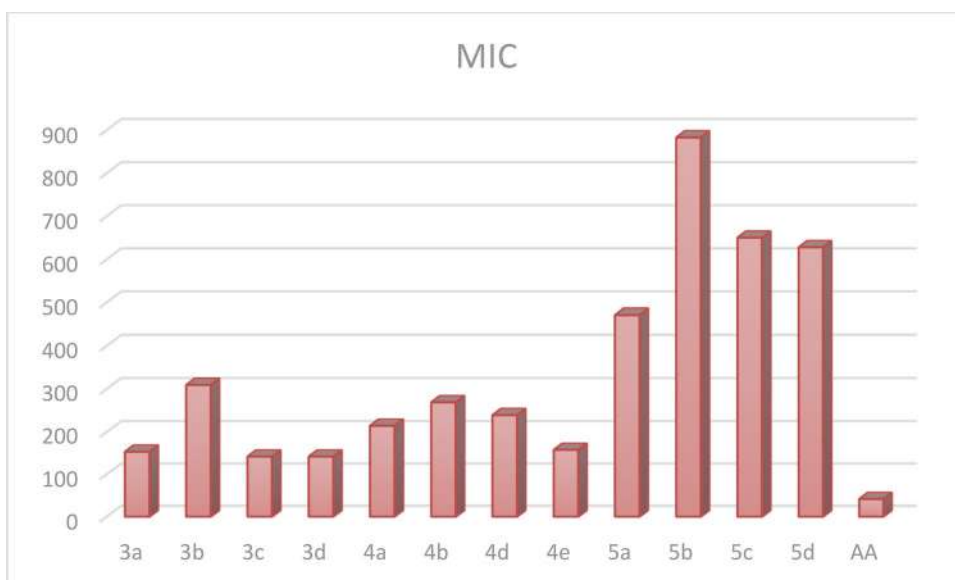


Figure 5. The percent inhibition of compounds *in vitro* antioxidant model.

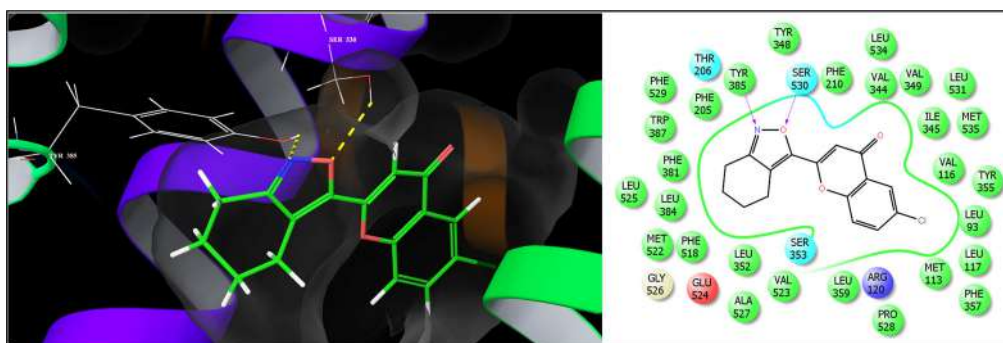


Figure 6. Binding mode of **5e** at the active site of COX-2 (on right side: the pink lines represent the hydrogen bonding interactions).

Computational study

Molecular docking

A perusal of the docked complexes of chromones derivatives (**3a-3e**, **4a-4e**, **5a-5e**) revealed that they could snugly fit into the active site of COX-2 engaging a series of bonded and non-bonded interactions. Their binding affinity was found to be in agreement with the observed anti-inflammatory activity with active compounds showing relatively higher binding compared to compounds with moderate activity (Table 1). Quantitative analysis of the per-residue interactions between one of the most active molecule **5e** (Figure 6) and the residues lining the active site of the enzyme was carried out to identify the most significantly interacting residues and the nature of thermodynamic interactions governing their affinity to COX-2.

The lowest energy docked complex of **5e** showed that molecule could aptly bind to the target protein with high binding affinity (Glide docking score of -9.638 /intermolecular binding energy of -48.518 kcal/mol) interactions at co-ordinates close to the co-crystallized ligand. The major driving force for mechanical interlocking of this molecule into the active site was observed to be

favorable van der Waals interactions observed with Ser530(-2.359 kcal/mol), Ala527(-4.548 kcal/mol), Gly526(-2.363 kcal/mol), Val523(-2.387 kcal/mol), Met522(-1.969 kcal/mol), Phe518(-1.035 kcal/mol), Trp387(-1.482 kcal/mol), Tyr385(-2.183 kcal/mol), Leu384(-1.135 kcal/mol), Phe381(-1.213 kcal/mol) and Leu352(-1.088 kcal/mol) residues through the 4,5,6,7-tetrahydrobenzo[c]isoxazol-3-yl component while the 6-Chloro-4H-chromen-4-one component of the molecule engaged in similar type of interactions with Leu534(-1.018 kcal/mol), Leu531(-3.071 kcal/mol), Tyr355(-1.296 kcal/mol), Ser353(-1.794 kcal/mol) and Val349(-3.014 kcal/mol). The enhanced binding affinity is also attributed to a favorable electrostatic interaction with Ser530(-1.729 kcal/mol), Glu524(-1.479 kcal/mol), Glu510(-1.045 kcal/mol) and Tyr385(-1.833 kcal/mol). Along with these non-bonded interactions, **5e** also portrayed two very close hydrogen bonding interactions through the isoxazole ring, firstly with Ser530(2.215 Å) and second with Tyr385(2.628 Å) residues. Such hydrogen bonding interactions "anchor" the ligand guiding its orientation into the 3D space of the active site and further facilitates the non-bonded interactions. A similar mode and type of bonded and non-bonded interactions were involved in stabilizing the complexes of other compounds with COX-2 speculating an identical mechanism of action (Figure 1S-14S). This *in silico* binding affinity data suggest that structural modifications in the isoxazole clubbed chromen-4-one scaffold directed toward improving the steric and electrostatic interactions along with other bonded interactions *viz.* Hydrogen bonding can lead to compounds with improved binding affinity toward COX-2.

In silico ADME prediction

Important task for the lead compounds is early prediction of drug likeness properties, as it resolves the cost and time of drug development and discovery. Due to the inadequate drug likeness properties of many active agents with a significant biological activity have failed in clinical trials.²⁶ On the basis of Lipinski's rule of five, the drug likeness properties were analyzed by ADME parameters using Molinspiration online property calculation toolkit²⁷ and data are summarized in Table 2.

All the compounds exhibited noteworthy values for the various parameters analyzed and showed good drug-like characteristics based on Lipinski's rule of five and its variants that characterized these agents to be likely orally active. For all the synthesized compound, the data obtained

Table 2. Pharmacokinetic parameters of (4a-e, 5a-e & 6a-e) compounds.

Entry	% ABS	TPSA (Å ²)	n-ROTB	MV	MW	miLog P	n-ON	n-OHNH	Lipinski violation	Drug-likeness model score
Rule	–	–	–	–	< 500	≤ 5	< 10	< 5	≤ 1	–
3a	85.05	69.41	4	269.30	299.33	3.64	5	0	0	0.34
3b	85.05	69.41	4	279.81	354.19	4.48	5	0	0	0.16
3c	85.05	69.41	4	282.84	333.77	4.25	5	0	0	0.32
3d	85.05	69.41	4	257.67	303.29	3.36	5	0	0	0.31
3e	85.05	69.41	4	266.28	319.74	3.87	5	0	0	0.37
4a	81.26	80.40	4	268.58	299.33	3.14	5	1	0	0.42
4b	81.26	80.40	4	279.09	354.19	3.77	5	1	0	0.31
4c	81.26	80.40	4	282.11	333.77	3.75	5	1	0	0.24
4d	81.26	80.40	4	256.95	303.29	2.86	5	1	0	0.50
4e	81.26	80.40	4	265.55	319.74	3.37	5	1	0	0.60
5a	89.59	56.24	1	250.33	281.31	3.94	4	0	0	0.43
5b	89.59	56.24	1	260.84	336.17	4.78	4	0	0	-0.07
5c	89.59	56.24	1	263.87	315.76	4.55	4	0	0	0.37
5d	89.59	56.24	1	238.70	285.27	2.69	4	0	0	0.57
5e	89.59	56.24	1	247.31	301.73	4.17	4	0	0	0.65

% ABS: Percentage absorption, TPSA: Topological polar surface area, n-ROTB: Number of rotatable bonds, MV: Molecular volume, MW: Molecular weight, miLogP: Logarithm of partition coefficient of compound between n-octanol and water, n-ON Acceptors: Number of hydrogen bond acceptors, n-OHNH donors: Number of hydrogen bonds donors.

were within the range of accepted values. None of the synthesized compounds violated the Lipinski's rule of five. The parameters like the number of rotatable bonds and total polar surface area are linked with the intestinal absorption; results showed that all synthesized compounds had good absorption. The larger the value of the drug likeness model score, the higher is also probability that the particular molecule will be active. The *in-silico* assessment of all the synthetic compounds has shown that they have very good pharmacokinetic properties, which is reflected in their physicochemical values, thus ultimately enhancing pharmacological properties of these molecules.

Conclusion

A new series of 2-(4,5,6,7-tetrahydrobenzo[c]isoxazol-3-yl)-4H-chromen-4-ones **5a-e** were synthesized from 1-(2-hydroxyphenyl)-3-(4,5,6,7-tetrahydrobenzo[c]isoxazol-3-yl)propane-1,3-diones **4a-e** in presence of acetic acid and conc. HCl. Compounds **4a-e** were synthesized by Baker-Venkataraman rearrangement from 2-acetylphenyl 4,5,6,7-tetrahydrobenzo[c]isoxazole-3-carboxylate **3a-e** in presence of pyridine and KOH and compounds **3a-e** were synthesized from 4,5,6,7-tetrahydrobenzo[c]isoxazole-3-carboxylic acid **1** and substituted 2-hydroxy acetophenone **2a-e**. All the synthesized compounds were characterized with the help of IR, ¹H NMR, ¹³C NMR and mass spectroscopic techniques. All the compounds were screened for their *in vitro* anti-inflammatory activities. Furthermore, *in-silico* molecular docking study against COX-2 enzyme and ADME properties of the synthesized compounds also carried out. The results of *in silico* binding affinity study were found to be in agreement with the *in vitro* data suggesting that these molecules could serve as a pertinent starting point for structure-based optimization of this novel scaffold and therefore efforts are under way to optimize scaffold for arriving at potent molecules with improved anti-inflammatory and selectivity.

Experimental

All organic solvents were acquired from commercial sources and used as received. The melting points were measured on a DBK melting point apparatus and are uncorrected. IR spectra were recorded on Shimadzu IR Affinity 1S (ATR) FTIR spectrophotometer. ¹H NMR (500 MHz) and ¹³C NMR (125 MHz) spectra were recorded on Bruker Advance neo 500 spectrophotometers using TMS as an internal standard and DMSO-*d*₆ as solvent and chemical shifts were expressed as δ ppm units. Mass spectra were obtained on Waters, Q-TOF micromass (ESI-MS) mass spectrometer.

General procedure for the synthesis of 2-acetylphenyl 4,5,6,7-tetrahydrobenzo[c]isoxazole-3-carboxylate (**3a-e**)

A mixture of 4,5,6,7-tetrahydrobenzo[c]isoxazole-3-carboxylic acid **1** (0.001 mol) and substituted 2-hydroxy acetophenone **2a-e** (0.001 mol) were taken in dry round bottom flask and dissolved in 10 mL dry pyridine. The reaction mixture was then cooled to 0 °C. To this solution, POCl₃ (0.01 mol) was added drop-wise maintaining temperature below 5 °C. Then the reaction mixture was kept overnight at RT under stirring. It was then poured over crushed ice with vigorous stirring. The crude solid product was separated by filtration and washed with ice-cold water followed by ice cold solution of dil. NaOH and finally again washed with ice cold water. The crude solid product purified by crystallization from ethyl alcohol to get pure compounds **3a-e**.

General procedure for the synthesis of benzoxazole β diketones (**4a-e**)

Compound **3a-e** (0.05 mol) was taken in 15 mL dry pyridine, and to this reaction mixture an excess of powdered KOH (0.1 mol) was added with constant stirring and the reaction mixture

was stirred at RT for 3 hr. Thereafter the contents were poured over crushed ice and acidified with dil. HCl. The resulting product was separated by filtration and purified by crystallization from ethanol to afforded **4a-e**.

General procedure for the 6-methyl-2-(4, 5, 6, 7-tetrahydrobenzo[c]isoxazol-3-yl)-4H-chromen-4-one (5a-e)

Compound **4a-e** (1 mmol) taken in acetic acid (5 mL) and to this conc. HCl (1 mL) was added. Reaction mixture was heated under reflux for 2 hr. After completion of heating, the reaction mixture was cooled and poured over crushed ice. The resulting product was separated by filtration and purified by crystallization from ethanol to give **5a-e**.

2-Acetyl-4-methylphenyl 4,5,6,7-tetrahydrobenzo[c]isoxazole-3-carboxylate (3a)

Yield: 61%; White solid; mp: 172-174 °C; ¹H NMR (500 MHz, DMSO-D6): δ = 1.71-1.79 (m, 4H), 2.41 (s, 3H, Ar-CH₃), 2.52 (s, 3H, -CH₃), 2.76-2.81 (m, 4H), 7.27-7.29 (d, 1H, J = 10 Hz, Ar-H), 7.50-7.52 (d, 1H, J = 10 Hz, Ar-H), 7.84-7.86 (d, 1H, J = 10 Hz, Ar-H); ¹³C NMR (100 MHz, DMSO-D6): δ = 197.9, 162.6, 156.0, 153.0, 145.6, 137.0, 134.7, 131.7, 130.0, 124.1, 123.3, 29.6, 21.7, 21.7, 21.4, 20.8, 20.6; MS (ESI-MS): m/z 300.11 (M + H)⁺.

2-Acetyl-4, 6-dichlorophenyl 4,5,6,7-tetrahydrobenzo[c]isoxazole-3-carboxylate (3b)

Yield: 61%; White solid; mp: 120-122 °C; ¹H NMR (500 MHz, DMSO-D6): δ = 2.36 (s, 1H, -CH₃), 2.70-2.68 (dd, 4H, Ar-H), 2.76-2.73 (dd, 4H, Ar-H), 7.88 (d, 2H, J = 2.5 Hz, Ar-H), 7.99 (d, 2H, J = 2.5 Hz, Ar-H); ¹³C NMR (100 MHz, DMSO-D6): δ 162.8, 162.4, 154.9, 154.0, 152.1, 151.2, 147.2, 141.3, 132.6, 131.1, 131.0, 129.0, 128.8, 124.8, 123.4, 111.6, 21.5, 21.5, 21.4, 21.4, 20.5, 20.4.

2-Acetyl-4-chloro-5-methylphenyl 4,5,6,7-tetrahydrobenzo[c]isoxazole-3-carboxylate (3c)

Yield: 61%; White solid; mp: 122-124 °C; ¹H NMR (500 MHz, DMSO-D6): δ = 1.79-1.70 (m, 4H), 2.41 (s, 3H, Ar-CH₃), 2.62 (s, 3H, -CH₃), 2.76-2.81 (m, 4H), 7.47 (s, 1H, Ar-H), 8.07 (s, 1H, Ar-H); ¹³C NMR (100 MHz, DMSO-D6): δ = 196.5, 162.7, 155.7, 152.7, 146.3, 142.8, 131.8, 131.5, 129.3, 126.9, 123.6, 29.6, 21.7, 21.6, 21.4, 20.6, 20.2; MS (ESI-MS): m/z 334.11 (M + H)⁺.

2-Acetyl-4-fluorophenyl 4, 5, 6, 7-tetrahydrobenzo[c]isoxazole-3-carboxylate (3d)

Yield: 61%; White solid; mp: 68-70 °C; ¹H NMR (500 MHz, DMSO-D6): δ = 1.70-1.81 (m, 4H, Ar-H), 2.51 (s, 1H, -CH₃), 2.77-2.81 (m, 4H, Ar-H), 7.50 (dd, 1H, J = 3 Hz & 9 Hz, Ar-H), 7.57-7.61 (m, 1H, Ar-H), 7.88-7.91 (dd, 1H, J = 3 Hz & 9 Hz, Ar-H); ¹³C NMR (100 MHz, DMSO-D6): δ = 197.0, 162.7, 161.1, 159.1, 155.9, 152., 143.8, 143.7, 131.9, 131.9, 126.5, 126.5, 123.5, 121.1, 120.9, 118.0, 117.6, 29.7, 21.7, 21.6, 21.4, 20.6; MS (ESI-MS): m/z 304.12 (M + H)⁺.

2-Acetyl-4-chlorophenyl 4,5,6,7-tetrahydrobenzo[c]isoxazole-3-carboxylate (3e)

Yield: 61%; White solid; mp: 108-110 °C; ¹H NMR (500 MHz, DMSO-D6): δ = 1.71-1.80 (m, 4H), 2.56 (s, 3H, -CH₃), 2.77-2.81 (m, 4H), 7.48-7.50 (d, 1H, J = 10 Hz, Ar-H), 7.78-7.80 (dd, 1H, J = 10 Hz, Ar-H), 8.08-8.09 (d, 1H, J = 5 Hz, Ar-H); ¹³C NMR (100 MHz, DMSO-D6): δ = 197.0, 162.7, 155.6, 152.7, 146.4, 134.0, 132.0, 131.7, 130.9, 126.5, 123.6, 29.8, 21.7, 21.6, 21.4, 20.6; MS (ESI-MS): m/z 320.11 (M + H)⁺.

1-(2-Hydroxy-5-methylphenyl)-3-(4,5,6,7-tetrahydrobenzo[c]isoxazol-3-yl) propane-1,3-dione (4a)

Yield: 61%; Yellow solid; mp: 90-92 °C; ¹H NMR (500 MHz, DMSO-D₆): δ = 1.64-1.76 (m, 8H), 2.26 (s, 3H), 2.62-2.82 (m, 8H), 2.97 (d, *J* = 16.5 Hz, 1H), 3.34 (d, *J* = 16.5 Hz, 1H), 7.0 (d, 1H, *J* = 8.5 Hz, Ar-H), 7.44 (dd, 1H, *J* = 8 & 2 Hz, Ar-H), 7.71 (d, 1H, *J* = 2 Hz, 10.89 (s, 1H, -O-H), 15.85 (broad singlet, 1H, enolic-OH); MS (ESI-MS): *m/z* 300.16 (M + H)⁺.

1-(3,5-Dichloro-2-hydroxyphenyl)-3-(4,5,6,7-tetrahydrobenzo[c]isoxazol-3-yl)propane-1,3-dione (4b)

Yield: 61%; White solid; mp: 220-222 °C; ¹H NMR (500 MHz, DMSO-D₆): δ = 1.68-1.76 (m, 8H, Ar-H), 2.69-2.82 (m, 8H, Ar-H), 3.10 (d, *J* = 16 Hz, 1H), 3.50 (d, *J* = 16 Hz, 1H), 7.18 (s, 1H, enol-olefinic proton), 7.71 (d, 1H, *J* = 2 Hz), 7.85 (s, 1H), 7.97 (s, 1H, enolic -OH), 8.00 (d, 1H, *J* = 2 Hz, 1H), 8.64 (s, 1H), 11.92 (keto-OH); ¹³C NMR (100 MHz, DMSO-D₆): δ = 188.7, 162.6, 162.3, 161.5, 152.2, 135.8, 134.4, 128.2, 126.4, 124.4, 124.2, 123.0, 112.6, 100.2, 46.9, 22.3, 21.9, 21.8, 21.7, 21.6, 21.5, 20.8, 19.9; MS (ESI-MS): *m/z* 354.10 (M + H)⁺.

1-(5-Chloro-2-hydroxy-4-methylphenyl)-3-(4,5,6,7-tetrahydrobenzo[c]isoxazol-3-yl)propane-1,3-dione(4c)

Yield: 61%; White solid; mp: 150-152 °C; ¹H NMR (500 MHz, DMSO-D₆): δ = 1.68-1.76 (m, 4H, Ar-H), 2.69-2.82 (m, 4H, Ar-H), 3.51(d, 2H, -CH₂), 4.83(S, 1H, -OH),7.96 (d, 1H, *J* = 5 Hz, Ar-H), 8.003(d, 1H, *J* = 2 Hz, Ar-H), 15.97 (broad singlet, 1H, enolic-OH); ¹³C NMR (100 MHz, DMSO-D₆): δ = 189.1, 183.3, 174.3, 162.9, 162.5, 161.4, 157.9, 157.8, 156.2, 145.2, 143.2, 129.1, 127.2, 125.5, 124.4, 122.2, 121.4, 120.3, 120.1, 119.5, 112.3, 99.3, 99.2, 47.1, 22.3, 22.0, 21.9, 21.7, 21.6, 21.5, 20.9, 20.6, 20.5, 19.9; MS (ESI-MS): *m/z* 334.13 (M + H)⁺.

1-(5-Fluoro-2-hydroxyphenyl)-3-(4,5,6,7-tetrahydrobenzo[c]isoxazol-3-yl)propane-1,3-dione(4d)

Yield: 61%; White solid; mp: 172-174 °C; ¹H NMR (500 MHz, DMSO-D₆): δ = 4.64 (S, 1H, olefinic proton), 11.13 (S, 1H, enolic -OH proton); ¹³C NMR (100 MHz, DMSO-D₆): δ = 189.7, 183.2, 174.7, 162.9, 162.5, 161.4, 157.9, 156.7, 156.3, 155.5, 154.7, 154.0, 124.2, 124.0, 122.3, 122.1, 121.4, 121.0, 120.9, 120.8, 120.7, 120.5, 119.4, 119.3, 114.9, 114.7, 112.3, 111.3, 111.1, 99.5, 99.2, 47.1, 22.3, 22.0, 21.9, 21.7, 21.6, 21.5, 20.9, 20.6, 19.8; MS (ESI-MS): *m/z* 304.15 (M + H)⁺.

1-(5-Chloro-2-hydroxyphenyl)-3-(4, 5, 6, 7-tetrahydrobenzo[c]isoxazol-3-yl) propane-1, 3-dione (4e)

Yield: 61%; White solid; mp: 150-152 °C ¹H NMR (500 MHz, DMSO-D₆): δ = 4.63 (S, 1H, olefinic proton), 11.39 & 11.25 (bs 2H, phenolic -OH & keto-enol tautomeric proton); ¹³C NMR (100 MHz, DMSO-D₆): δ = 189.4, 182.8, 174.9, 162.7, 162.5, 161.4, 157.9, 157.8, 156.3, 136.4, 134.5, 128.7, 126.5, 125.2, 123.7, 121.9, 121.7, 121.2, 120.5, 119.9, 112.4, 99.6, 99.3, 47.1, 22.3, 21.9, 21.8, 21.7, 21.6, 21.5, 20.9, 20.6, 19.8; MS (ESI-MS): *m/z* 320.13 (M + H)⁺.

6-Methyl-2-(4,5,6,7-tetrahydrobenzo[c]isoxazol-3-yl)-4H-chromen-4-one (5a)

Yield: 61%; White solid; ¹H NMR (500 MHz, DMSO-D₆): δ ppm 1.75-1.78 (m, 6H), 2.43 (s, 3H, -CH₃), 2.43-2.46 (m, 3H), 6.67(s, 1H, chromone), 3.02 (s, 2H), 7.63-7.68 (m, 2H, Ar-H), 7.84-7.86 (d, 1H, *J* = 10 Hz, Ar-H); ¹³C (100 MHz, DMSO-D₆): δ ppm = 176.67, 162.78, 162.53, 154.76, 154.05, 153.50, 137.07, 136.27, 136.18, 124.68, 124.61, 123.75, 121.98, 120.86, 119.06, 118.79, 118.32, 108.81, 21.98, 21.73, 21.61, 21.49, 20.91, 20.49; MS (ESI-MS): *m/z* 282.15 (M + H)⁺ .

6,8-Dichloro-2-(4,5,6,7-tetrahydrobenzo[c]isoxazol-3-yl)-4H-chromen-4-one(5b)

Yield: 61%; White solid; ¹H NMR (500 MHz, DMSO-D₆): δ ppm 1.78-1.79 (m, 5H), 2.77-2.78 (m, 2H), 2.98-3.00 (m, 2H), 6.84 (s, 1H, chromone), 7.95-7.96 (d, *J* = 5 Hz, 1H, Ar-H), 8.25(s, 1H,

Ar-H); ^{13}C (100 MHz, DMSO-D₆): δ ppm = 162.73, 134.66, 126.21, 124.44, 123.66, 119.16, 108.86, 21.96, 21.70, 21.49, 20.77; MS (ESI-MS): m/z 336.08 (M + H)⁺.

6-Chloro-7-methyl-2-(4,5,6,7-tetrahydrobenzo[c]isoxazol-3-yl)-4H-chromen-4-one (5c)

Yield: 61%; White solid; ^1H NMR (500 MHz, DMSO-D₆): δ ppm 1.78-1.79 (m, 6H), 2.77 (s, 3H, -CH₃), 2.95 (m, 2H), 6.73 (s, 1H, chromone), 7.87 (s, 1H, Ar-H), 7.98 (s, 1H, Ar-H); ^{13}C NMR (100 MHz, DMSO-D₆): δ ppm = 144.24, 124.64, 118.49, 116.24, 109.00, 107.00, 21.96, 21.74, 21.48, 20.54; MS (ESI-MS): m/z 316.12(M + H)⁺.

6-Fluoro-2-(4,5,6,7-tetrahydrobenzo[c]isoxazol-3-yl)-4H-chromen-4-one (5d)

Yield: 61%; White solid; ^1H NMR (500 MHz, DMSO-D₆): δ ppm 1.78-1.79(m, 4H), 2.77-2.79 (d, 2H, $J = 10\text{Hz}$), 2.93-2.96 (d, 2H, $J = 15\text{Hz}$), 6.73(s, 1H, chromone), 7.73-7.75 (m, 1H, Ar-H), 7.77-7.79 (d, $J = 4\text{Hz}$, 1H, Ar-H), 7.87-7.89 (d, $J = 10\text{Hz}$, 1H, Ar-H); ^{13}C (100 MHz, DMSO-D₆): δ ppm = 176.14, 162.60, 158.75, 154.56, 153.90, 152.90, 125.30, 125.24, 123.43, 123.22, 121.94, 121.87, 118.72, 110.23, 110.04, 108.24, 21.95, 21.73, 21.48, 20.49; MS (ESI-MS): m/z 286.13(M + H)⁺.

6-Chloro-2-(4,5,6,7-tetrahydrobenzo[c]isoxazol-3-yl)-4H-chromen-4-one (5e)

Yield: 61%; White solid; ^1H NMR (500 MHz, DMSO-D₆): δ ppm 1.77-1.80 (m, 4H), 2.76-2.79 (m, 2H), 2.92-2.95 (m, 2H), 6.74 (s, 1H, chromone), 7.82-7.84 (d, $J = 10\text{Hz}$, 1H, Ar-H), 7.90-7.92 (m, 1H, Ar-H), 7.98-7.99 (d, $J = 5\text{Hz}$, 1H, ArH); (100 MHz, DMSO-D₆): δ ppm = 175.68, 162.60, 154.47, 154.38, 153.91, 135.12, 130.94, 125.17, 124.40, 121.57, 118.81, 108.85, 21.94, 21.72, 21.48, 20.50; MS (ESI-MS): m/z 302.12 (M + H)⁺.

Anti-inflammatory activity

All the synthesized compounds were screened for their in vitro anti-inflammatory activities according to the literature procedure²⁸ with slight modification in the procedure using bovine serum albumin (BSA) as protein and the standard drug diclofenac sodium. A volume of 1 ml of diclofenac sodium at concentrations 50, 100, 200, 400, 800, and 1,000 $\mu\text{g}/\text{mL}$ and synthetic compounds was allowed to homogenized separately with 1 mL of aqueous solution of BSA (5%) and incubated for 15 minutes at 27°C. The mixture of distilled water and BSA was used as the control. Denaturation of the proteins was caused by placing the mixture in a water bath for 10 minutes at 70°C. The denaturation of all samples was carried out. The mixture was cooled within the ambient room temperature, and the activity of each mixture was measured at 660 nm by measuring extent of turbidity in terms of percent inhibition in each sample tube. Each test was conducted thrice and mean of the readings were recorded. The following formula was used to calculated inhibition percentage:

$$\% \text{inhibition} = (\text{absorbance of control} - \text{absorbance of sample}) / (\text{absorbance of control}) \times 100$$

Antioxidant activity

Various concentrations (50, 100, 150 $\mu\text{g}/\text{mL}$) were prepared by dilution method. The mixture was shaken vigorously and allowed to stand at room temp for 30 min. then, absorbance was measured at 255 nm. by using spectrophotometer (UV-VIS Shimadzu). Reference standard compounds being used was ascorbic acid and experiment was done in triplicate. The IC₅₀ value of the sample, which is the concentration of sample required to inhibit 50% of the DPPH free radical, was calculated using Log dose inhibition curve. Lower absorbance of the reaction mixture indicated higher

free radical activity. The percent DPPH scavenging effect was calculated by using following equation:

DPPH scavenging effect (%) or Percent inhibition = $A_0 - A_1 / A_0 \times 100$.

Where A_0 was the Absorbance of control reaction and A_1 was the Absorbance in presence of test or standard sample.

Molecular docking

A very promising level of anti-inflammatory activity demonstrated by the title compounds in the *in vitro* assay paved the way to gain an insight into the plausible mechanism of action. The *in-silico* techniques of molecular docking are now a well-established approach for evaluation of binding affinity of a bioactive molecule toward the target protein and predict the type of thermodynamic interactions between the compounds and the active site amino acids to rationalize the obtained biological results. With this objective, Cyclo-oxygenase 2 (COX-2) was chosen as the model protein to perform the molecular docking study for the title compounds. Critical in the inflammation pathway, Cyclo-oxygenase 2 (COX-2) is essential for the formation of prostanoids including thromboxane and prostaglandins which mediate the inflammation and pain. Molecular docking study was performed using the standard protocol implemented in the GLIDE (Grid-based Ligand Docking with Energetics) module of the Schrödinger Molecular modeling package.²⁵ The three-dimensional X-ray crystal structure of cyclooxygenase-2 (COX-2) enzyme complexed with its inhibitor Diclofenac was retrieved from the Protein Data Bank (www.rcsb.org/1PXX) and subjected to docking against the title compounds.

In silico ADME

In the present study, we have calculated molecular volume (MV), molecular weight (MW), logarithm of partition coefficient (miLog P), number of hydrogen bond acceptors (n-ON), number of hydrogen bonds donors (n-OH/NH), topological polar surface area (TPSA), number of rotatable bonds (n-ROTB) and Lipinski's rule of five²⁹ using Molinspiration online property calculation toolkit.²⁷ Absorption (% ABS) was calculated by: % ABS = $109 - (0.345 \times \text{TPSA})$.³⁰ Drug-likeness model score (a collective property of physico-chemical properties, pharmacokinetics and pharmacodynamics of a compound is represented by a numerical value) was computed by MolSoft software.³¹

Acknowledgement

Authors are thankful to Schrödinger Inc. for providing the GLIDE program to perform the molecular docking study.

Disclosure statement

No potential conflict of interest was reported by the authors.

ORCID

Hemantkumar N. Akolkar  <http://orcid.org/0000-0003-0882-1324>

References

1. J. Zhu, J. Mo, H. Z. Lin, Y. Chen, and H. P. Sun, "The Recent Progress of Isoxazole in Medicinal Chemistry," *Bioorganic & Medicinal Chemistry* 26, no. 12 (2018): 3065–75.
2. A. Oubella, Y. A. Itto, A. Auhmani, A. Riahi, A. Robert, J. C. Dara, H. Morjani, C. A. Parish, and M. Esseffar, "Diastereoselective Synthesis and Cytotoxic Evaluation of New Isoxazoles and Pyrazoles with Monoterpenic Skeleton," *Journal of Molecular Structure* 1198, (2019): 126924.
3. J. P. Nie, Z. Qu, Y. Chen, J. H. Chen, Y. Jiang, M. Jin, Y. Yu, W. Y. Niu, H. Duan, and N. Qin, "Discovery and anti-Diabetic Effects of Novel Isoxazole Based Flavonoid Derivatives," *Fitoterapia* 142, (2020): 104499.
4. K. A. E. Abdelall, "Synthesis and Biological Evaluations of Novel Isoxazoles and Furoxan Derivative as anti-Inflammatory Agents," *Bioorganic Chemistry* 94, (2020): 103441.
5. D. Zhang, J. Jia, L. Meng, W. Xu, L. Tang, and J. Wang, "Synthesis and Preliminary Antibacterial Evaluation of 2-Butyl Succinate-Based Hydroxamate Derivatives Containing Isoxazole Rings," *Archives of Pharmacal Research* 33, no. 6 (2010): 831–42.
6. Maria M. M. Santos, Natália Faria, Jim Iley, Simon J. Coles, Michael B. Hursthouse, M. Luz Martins, and Rui Moreira, "Reaction of Naphthoquinones with Substituted Nitromethanes. Facile Synthesis and Antifungal Activity of naphtho[2,3-d]isoxazole-4,9-diones," *Bioorganic & Medicinal Chemistry Letters* 20, no. 1 (2010): 193–5.
7. Ki Deok Shin, Mi-Young Lee, Dae-Seop Shin, Sangku Lee, Kwang-Hee Son, Sukhoon Koh, Young-Ki Paik, Byoung-Mog Kwon, and Dong Cho Han, "Blocking Tumor Cell Migration and Invasion with Biphenyl Isoxazole Derivative KRIBB3, a Synthetic Molecule That Inhibits Hsp27 Phosphorylation," *The Journal of Biological Chemistry* 280, no. 50 (2005): 41439–48.
8. Z. Yang, P. Li, and X. Gan, "Novel Pyrazole-Hydrazone Derivatives Containing an Isoxazole Moiety: Design, Synthesis, and Antiviral Activity," *Molecules* 23, (2018): 1798.
9. N. V. Balaji, B. HariBabu, V. U. Rao, G. V. Subbaraju, K. P. Nagasree, and M. M. K. Kumar, "Synthesis, Screening and Docking Analysis of Hispolon Pyrazoles and Isoxazoles as Potential Antitubercular Agents," *Current Topics in Medicinal Chemistry* 19, no. 9 (2019): 662–82.
10. W. Li, J. Li, H. Shen, J. Cheng, Z. Li, and X. Xu, "Synthesis, Nematicidal Activity and Docking Study of Novel Chromone Derivatives Containing Substituted Pyrazole," *Chinese Chemical Letters* 29, no. 6 (2018): 911–4.
11. Y. Duan, Y. Jiang, F. Guo, L. Chen, L. Xu, W. Zhang, and B. Liu, "The Antitumor Activity of Naturally Occurring Chromones: A Review," *Fitoterapia* 135, (2019): 114–29.
12. C. Demetgul, and N. Beyazit, "Synthesis, Characterization and Antioxidant Activity of Chitosan-Chromone Derivatives," *Carbohydrate Polymers* 181, (2018): 812–7.
13. J. N. Modranka, E. Nawrot, and J. Graczyk, "In Vivo Antitumor, in Vitro Antibacterial Activity and Alkylating Properties of Phosphorohydrazone Derivatives of Coumarin and Chromone," *European Journal of Medicinal Chemistry* 41, no. 11 (2006): 1301–9.
14. C. Sun, C. Chen, S. Xu, J. Wang, Y. Zhu, D. Kong, H. Tao, M. Jin, P. Zheng, and W. Zhu, "Synthesis and Anticancer Activity of Novel 4-Morpholino-7,8-Dihydro-5H-Thiopyrano[4,3-d]Pyrimidine Derivatives Bearing Chromone Moiety," *Bioorganic & Medicinal Chemistry* 24, no. 16 (2016): 3862–9.
15. P. Baruah, M. A. Rohman, S. O. Yesylevskyy, and S. Mitra, "Therapeutic Potency of Substituted Chromones as Alzheimer's Drug: Elucidation of Acetylcholinesterase Inhibitory Activity through Spectroscopic and Molecular Modelling Investigation," *BioImpacts: BI* 9, no. 2 (2019): 79–88. BI,
16. H. Liu, R. Xu, L. Feng, W. Guo, N. Cao, C. Qian, P. Teng, L. Wang, X. Wu, Y. Sun, et al. "A Novel Chromone Derivative with anti-Inflammatory Property via Inhibition of ROS-Dependent Activation of TRAF6-ASK1-p38 Pathway," *PLoS One* 7, no. 8 (2012): e37168.
17. N. C. Netzer, T. Kupper, H. W. Voss, and A. H. Eliasson, "The Actual Role of Sodium Cromoglycate in the Treatment of Asthma-a Critical Review," *Sleep & Breathing = Schlaf & Atmung* 16, no. 4 (2012): 1027–32.
18. J. Sheikh, H. Juneja, V. Ingle, P. Ali, and T. B. Hadda, "Synthesis and in Vitro Biology of Co(II), Ni(II), Cu(II) and Zinc(II) Complexes of Functionalized Beta-Diketone Bearing Energy Buried Potential Antibacterial and Antiviral O,O Pharmacophore Sites," *Journal of Saudi Chemical Society* 17, no. 3 (2013): 269–76.
19. T. V. Deepthi, and P. Venugopalan, "Synthesis, Characterization and Biological Studies on Ni^{II} and Cu^{II} Complexes of Two Novel α,β -Unsaturated 1,3-Diketones Related to Curcuminoids," *Inorganica Chimica Acta* 450, (2016): 243–50.
20. V. Porchezhiyan, D. Kalaivani, J. Shobana, and S. E. Noorjahan, "Synthesis, Docking and in Vitro Evaluation of l-Proline Derived 1,3-Diketones Possessing anti-Cancer and anti-Inflammatory Activities," *Journal of Molecular Structure* 1206, (2020): 127754.
21. T. Nishiyama, S. Shiotsu, and H. Tsujita, "Antioxidative Activity and Active Site of 1,3-Indandiones with the β -Diketone Moiety," *Polymer Degradation and Stability* 76, no. 3 (2002): 435–9.

22. P. V. Badadhe, L. R. Patil, S. S. Bhagat, A. V. Chate, D. W. Shinde, M. D. Nikam, and C. H. Gill, "Synthesis and Antimicrobial Screening of Some Novel Chromones and Pyrazoles with Incorporated Isoxazole Moieties," *Journal of Heterocyclic Chemistry* 50, (2013): n/a-1004.
23. W. Wang, L. Deng, C. Hu, Y. Zhang, Y. Li, and S. Zuo, "Synthesis of Isoxazole-Linked Norcantharidin Analogues of Substituted Chromones," *Journal of Heterocyclic Chemistry* 54, no. 3 (2017): 1806-11.
24. (a) S. G. Dengale, H. N. Akolkar, B. K. Karale, N. R. Darekar, S. D. Mhaske, M. H. Shaikh, D. N. Raut and K. K. Deshmukh, "Synthesis of 3-(trifluoromethyl)-1-(perfluorophenyl)-1H-pyrazol-5(4H)-one derivatives via Knoevenagel condensation and their biological evaluation," *Journal of the Chinese Chemical Society*, 68 (2021): 657-668; (b) S. P. Kunde, K. G. Kanade, B. K. Karale, H. N. Akolkar, S. S. Arbuj, P. V. Randhavane, S. T. Shinde, M. H. Shaikh and A. K. Kulkarni, "Nanostructured N doped TiO₂ efficient stable catalyst for Kabachnik-Fields reaction under microwave irradiation," *RSC Advances*, 10 (2020): 26997-27005; (c) H. N. Akolkar, S. J. Takate, K. K. Deshmukh, B. K. Karale, N. R. Darekar, V. M. Khedkar and M. H. Shaikh "Design, Synthesis and Biological Evaluation of Novel Furan & Thiophene Containing Pyrazolyl Pyrazolines as Antimalarial Agents," *Polycyclic Aromatic Compounds*, <https://doi.org/10.1080/10406638.2020.1821231>; (d) M. H. Shaikh, D. D. Subhedar, S. V. Akolkar, A. A. Nagargoje, V. M. Khedkar, D. Sarkar and B. B. Shingate, "Tetrazoloquinoline-1, 2, 3-Triazole Derivatives as Antimicrobial Agents: Synthesis, Biological Evaluation and Molecular Docking Study," *Polycyclic Aromatic Compounds*, <https://doi.org/10.1080/10406638.2020.1821229>.
25. (a) *Schrodinger Suite 2015-4 QM-Polarized Ligand Docking protocol; Glide version 6.9*, Schrodinger, LLC, New York, NY, 2006; *Jaguar version 9.0*, Schrodinger, LLC, New York, NY, 2015; *QSite version 6.9*, Schrodinger, LLC, New York, NY, 2015; (b) R. A. Friesner, R. B. Murphy, M. P. Repasky, L. L. Frye, J. R. Greenwood, T. A. Halgren, P. C. Sanschagrin and D. T. Mainz, "Extra precision glide: Docking and scoring incorporating a model of hydrophobic enclosure for protein-ligand complexes," *Journal of Medicinal Chemistry*, 2149 (2006): 6177-6196 and related references cited therein.
26. S. Zhang, Y. Luo, L. Q. He, Z. J. Liu, A. Q. Jiang, Y. H. Yang, and H. L. Zhu, "Synthesis, Biological Evaluation, and Molecular Docking Studies of Novel 1,3,4-Oxadiazole Derivatives Possessing Benzotriazole Moiety as FAK Inhibitors with Anticancer Activity," *Bioorganic & Medicinal Chemistry* 21, no. 13 (2013): 3723-9.
27. Molinspiration Chemoinformatics Bratislava, Slovak Republic, Available from: <http://www.molinspiration.com/cgi-bin/properties> 2014.
28. (a) P. Padmanabhan and S. N. Jangle, "Evaluation of in-vitro anti-inflammatory activity of herbal preparation, a combination of four medicinal plants," *International Journal of Basic and Applied Medical Sciences*, 2 (2012): 109-116; (b) Y. Mizushima and M. Kobayashi, "Interaction of anti-inflammatory drugs with serum proteins, especially with some biologically active proteins," *Journal of Pharmacy and Pharmacology*, 20 (1968): 169-73; (c) G. Elias and M. N. Rao, "Inhibition of albumin denaturation and anti-inflammatory activity of dehydrozingerone and its analogs," *Indian Journal of Experimental Biology*, 26 (1988): 540-542; (d) S. F. D. Nguemngang, E. G. Tsafack, M. Mbiantcha, A. Gilbert, A. D. Atsamo, N. W. Yousseu, M. M. V. Matah, C. F. Adjouzem, "In vitro anti-inflammatory and in vivo antiarthritic activities of aqueous and ethanolic extracts of *Dioscorea thollonii* Cogn. (Melastomataceae) in rats," *Evidence-Based Complementary and Alternative Medicine* 15(2019); (e) K. D. P. P. Gunathilake, K. K. D. S. Ranaweera and H. P. Vasantha Rupasinghe, "In vitro anti-inflammatory properties of selected green leafy vegetables," *Biomedicines* 6 (2018): 107-116; (f) N. H. Grant, H. E. Alburn and C. Kryzanasuskas, "Stabilization of serum albumin by anti-inflammatory drugs," *Biochemical Pharmacology* 19 (1970): 715-722.
29. C. A. Lipinski, L. Lombardo, B. W. Dominy, and P. J. Feeney, "Experimental and Computational Approaches to Estimate Solubility and Permeability in Drug Discovery and Development Settings," *Advanced Drug Delivery Reviews* 46, no. 1-3 (2001): 3-26.
30. Yuan H. Zhao, Michael H. Abraham, Joelle Le, Anne Hersey, Chris N. Luscombe, Gordon Beck, Brad Sherborne, and Ian Cooper, "Rate Limited Steps of Human Oral Absorption and QSAR Studies," *Pharmaceutical Research* 19, no. 10 (2002): 1446-57.
31. Drug-likeness and molecular property prediction, available from: <http://www.molsoft.com/mprop/>


[Et₃NH][HSO₄]-Catalyzed One-Pot Solvent Free Syntheses of Functionalized [1,6]-Naphthyridines and Biological Evaluation

Mubarak H. Shaikh, Dnyaneshwar D. Subhedar, Vijay M. Khedkar & Bapurao B. Shingate

To cite this article: Mubarak H. Shaikh, Dnyaneshwar D. Subhedar, Vijay M. Khedkar & Bapurao B. Shingate (2021): [Et₃NH][HSO₄]-Catalyzed One-Pot Solvent Free Syntheses of Functionalized [1,6]-Naphthyridines and Biological Evaluation, Polycyclic Aromatic Compounds, DOI: [10.1080/10406638.2021.1970587](https://doi.org/10.1080/10406638.2021.1970587)



To link to this article: <https://doi.org/10.1080/10406638.2021.1970587>

 View supplementary material 

 Published online: 02 Sep 2021.

 Submit your article to this journal 

 Article views: 60

 View related articles 

 View Crossmark data 



[Et₃NH][HSO₄]-Catalyzed One-Pot Solvent Free Syntheses of Functionalized [1,6]-Naphthyridines and Biological Evaluation

Mubarak H. Shaikh^{a,b}, Dnyaneshwar D. Subhedar^a, Vijay M. Khedkar^c, and Bapurao B. Shingate^a

^aDepartment of Chemistry, Dr. Babasaheb Ambedkar Marathwada University, Aurangabad, Maharashtra, India; ^bDepartment of Chemistry, Radhabai Kale Mahila Mahavidyalaya, Ahmednagar, Maharashtra, India; ^cDepartment of Pharmaceutical Chemistry, School of Pharmacy, Vishwakarma University, Pune, Maharashtra, India

ABSTRACT

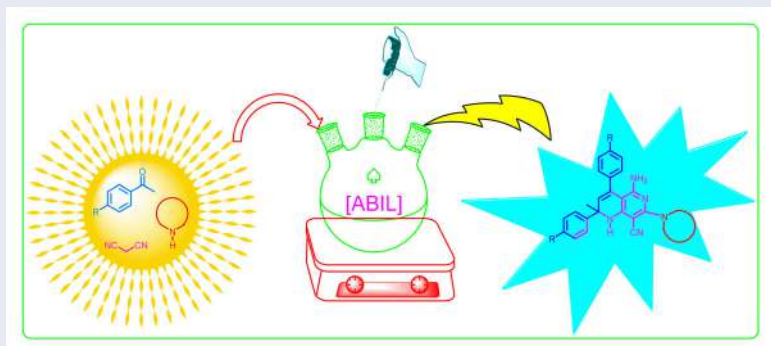
We have developed a convenient one-pot multicomponent synthesis of highly functionalized [1,6]-naphthyridines under solvent free condition using [Et₃NH][HSO₄] in excellent yield. This protocol offers several advantages, including short reaction time, simple experimental workup procedure and no toxic byproducts, avoids the use of toxic organic solvents and anhydrous conditions. Further, we have screened the synthesized naphthyridines for *in vitro* antibacterial, antifungal and antioxidant activity. Furthermore, a molecular docking study of these compounds was carried out to investigate their binding pattern with the target, β -Ketoacyl-acyl carrier protein synthase III (FabH). Finally, the ADME parameters for these compounds showed good drug like properties and can be developed as oral drug candidates.

ARTICLE HISTORY

Received 13 April 2021
Accepted 14 August 2021

KEYWORDS


Antimicrobial; Antioxidant; FabH; ADME; Naphthyridines; [Et₃NH][HSO₄]; multicomponent reactions



Introduction

Naphthyridine is a bicyclic heterocycle containing a pyridine ring fused to that of the dihydropyridine ring. According to literature survey, we found that the methods which are used for the synthesis of the functionalized [1,6]-naphthyridines and their benzo/heterofused analogues involves either multistep sequences or inert atmosphere, lengthy reaction time, expensive catalyst and laborious work up. Being a multifunctional entity, it finds application in nearly every field of laboratory, industrial and medicinal chemistry. Naphthyridines continued to be of great interest due to a wide spectrum of their biological activities such as used in agrochemicals,¹

CONTACT Bapurao B. Shingate  bapushingate@gmail.com  Department of Chemistry, Radhabai Kale Mahila Mahavidyalaya, Ahmednagar, Maharashtra, India.

 Supplemental data for this article can be accessed online at <https://doi.org/10.1080/10406638.2021.1970587>

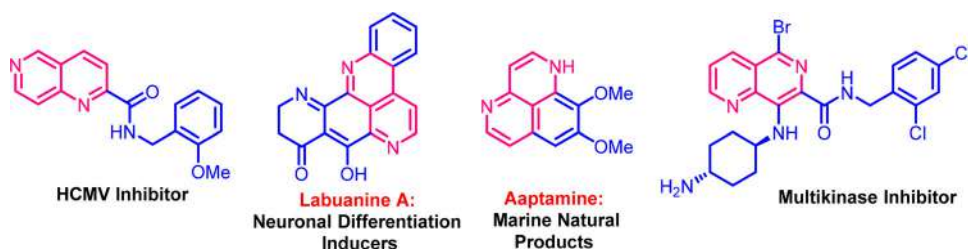


Figure 1. Pharmacologically active naphthyridine based active compounds.

pharmaceuticals,¹ and fluorescent probes.² Currently, numerous naphthyridine-containing molecules exhibited medicinal properties for the prevention and treatment of Alzheimer's disease (AD),³ bacterial infections,⁴ heart failure,⁵ angiogenic disorder,⁶ cancer,⁷ parasitic infections⁸ and viral infections⁹ have been reported. Therefore, the construction of naphthyridines have received increasing attention recently.¹⁰ Human cytomegalovirus (HCMV) is a species-specific DNA virus belonging to the herpesviridae family. The structures of pharmacologically active naphthyridine based compounds are shown in Figure 1.

Nowadays, greener reaction media has gaining more importance to perform organic transformations safely. Ionic liquids referred as 'designer solvent' due to their physical and chemical properties, and can be adjusted by a careful choice of cation and anion. Ionic liquid has been turned to be a kind of promising alternative medium for various chemical processes due to its good solvating capability, non-inflammability, negligible vapor pressure, ease of recyclability, controlled miscibility and high thermal stability.¹¹ In particular, acidic Bronsted ionic liquids [ABILs] are of special importance, because they possess simultaneously the proton acidity and the characteristic properties of ionic liquids.¹² ABILs offer environmentally friendly catalytic properties due to the combination of the advantages of liquid acids and solid acids, such as uniform acid sites, stability in water and air, easy separation and reusability. The ionic liquid has been proved to be a very excellent catalyst as well as solvent for many organic transformations.¹³

Triethylammonium Hydrogen Sulfate [$\text{Et}_3\text{NH}][\text{HSO}_4]$ (TEAHS) ionic liquid has been proved to be a very excellent catalyst as well as solvent for many organic transformations such as for the synthesis of quinoline,¹³ coumarin,¹⁴ biscoumarins,¹⁵ 1,8-dioxo-octahydroxanthenes,¹⁶ thiazolidine and oxazolidine,¹⁷ hydrazone,¹⁸ 4,4'-(arylmethylene)bis(1*H*-pyrazol-5-ols),¹⁹ functionalized aminoalkyl and amidoalkyl naphthol,²⁰ β -amino carbonyl pyrimidines,²¹ xanthene,²² 3,4-Dihydropyrimidin-2(1*H*)-one²³ derivatives and in hydrolytic reaction,²⁴ 3,4,5-substituted furan-2(5*H*)-ones²⁵ and α -amino phosphonates.²⁶

The approach to functionalized [1,6]-naphthyridines and their benzo/heterofused analogues presented herein offers an unprecedented coupling which leads to the construction of both the nitrogen containing rings during the synthesis without starting from any nitrogen containing heterocyclic moiety. Recently, Shen and coworkers described the synthesis of naphtho[2,3-*b*][1,6]naphthyridines catalyzed by acetic acid.^{27a} Zhang et. al. described synthesis of 1,6-naphthyridine-2,5-dione derivatives under ultrasound irradiation in water with acetic acid as catalyst^{27b} and recycle heterogeneous solid acid catalyst.^{27c} Vennila et. al. synthesized new 10-methoxy dibenzo[*b,h*][1,6]naphthyridine carboxylic acid from 3-methoxyaniline by a new route.^{27d} A survey of the literature shows that the majority of the strategies involve either multistep sequences,^{27e-j} or expensive catalysts,^{27g-j,28} inert atmosphere,^{27f,g,28a} lengthy reaction time,^{27g,h} and laborious workup.^{27f-h}

However, [$\text{Et}_3\text{NH}][\text{HSO}_4]$ has not been explored yet for the synthesis of functionalized [1,6]-naphthyridines *via* multicomponent reaction. Therefore, in continuation of our work on the development of novel synthetic methodologies for organic transformations,^{26,29} we employed [$\text{Et}_3\text{NH}][\text{HSO}_4]$ as an acidic Bronsted ionic liquid as a green, efficient, and recyclable catalyst as well as a solvent for the synthesis of functionalized [1,6]-naphthyridines. Further, we have screened

the synthesized naphthyridines for *in vitro* antimicrobial and antioxidant activity. In order to rationalize the promising data obtained from antimicrobial screening and to gain an insight into plausible mechanism of action, a molecular docking study was performed against a critical target, β -Ketoacyl-acyl carrier protein synthase III (FabH) which could provide clustered solutions on binding mode and various thermodynamic interactions governing the binding affinity.

Results and discussion

Chemistry

In search of the best experimental reaction conditions, reaction of acetophenone **1a**, malononitrile **2** and piperidine **3a** in ecofriendly solvent free condition using ionic liquid $[\text{Et}_3\text{NH}][\text{HSO}_4]$ at 80–90 °C was considered as a standard model reaction (Scheme 1). Initially, the reaction was carried out in absence of the catalyst, the product **4a** was formed in trace amount (Table 1, entry 1).

To determine the appropriate concentration of the catalyst $[\text{Et}_3\text{NH}][\text{HSO}_4]$, the model reaction at different concentrations of $[\text{Et}_3\text{NH}][\text{HSO}_4]$ such as 5, 10, 15, 20 and 25 mol% has been carried out. The functionalized [1,6]-naphthyridine formed in 60, 80, 85, 93 and 93% yields, respectively in given times (Table 1, entries 2–6). The increase in concentration of catalyst from 20 to 25 mol% does not increase the yield of product. This indicates that, 20 mol% of $[\text{Et}_3\text{NH}][\text{HSO}_4]$ is sufficient for the reaction by considering yield of product.

To evaluate the effect of solvents, dichloromethane (DCM), THF, 1,4-dioxane, toluene, CH_3CN and EtOH were used for the model reaction. It has been observed that, the use of solvents retards the rate of reaction and affords the desired product in lower yields than that for neat reaction condition (Table 2, entry 1–6).

To check the ecofriendliness of $[\text{Et}_3\text{NH}][\text{HSO}_4]$, we recycled the ionic liquid $[\text{Et}_3\text{NH}][\text{HSO}_4]$ for five times Table 3. The reaction proceeded cleanly with good yields (93, 93, 92, 90, 90 and 85%); although a weight loss of ~5% of $[\text{Et}_3\text{NH}][\text{HSO}_4]$ was observed from cycle to cycle due to mechanical loss (Table 3, entries 1–6).

With these optimized reaction conditions for model reaction i.e., 20 mol% $[\text{Et}_3\text{NH}][\text{HSO}_4]$ catalyst, 80–90 °C and solvent-free conditions, we have synthesized a series of functionalized



Scheme 1. Standard model reaction

Table 1. Effect of concentration of catalyst and time^a.

Entry	$[\text{Et}_3\text{NH}][\text{HSO}_4]$ (mol %)	Time (Min)	Yield ^b (%)
1	–	60	Trace
2	5	60	60
3	10	45	80
4	15	15	85
5	20	10	93
6	25	10	93

^aReaction conditions: Acetophenone **1a** (2 mmol), malononitrile **2** (2 mmol), piperidine **3a** (1 mmol), solvent-free at 80–90 °C.

^bIsolated yield.

Table 2. Screening of solvents.

Entry	Solvent	Yield ^a (%)
1	DCM	44
2	THF	46
3	1,4-Dioxane	48
4	Toluene	55
5	Acetonitrile	58
6	Ethanol	60
7	Solvent free	93

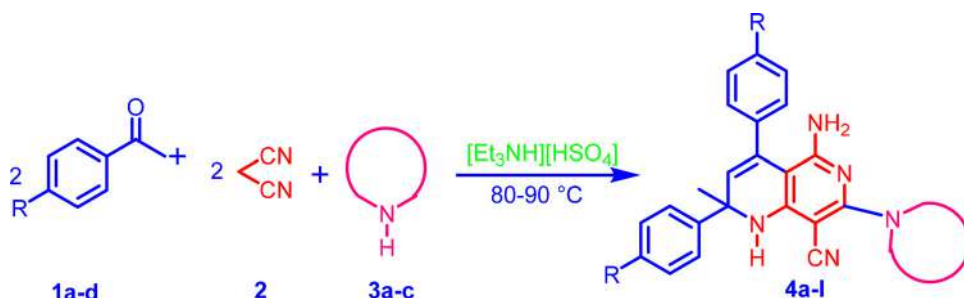
Reaction conditions: Acetophenone **1a** (2 mmol), malononitrile **2** (2 mmol), piperidine **3a** (1 mmol) in 20 mol% [Et₃NH][HSO₄].
^aIsolated yield.

Table 3. Reusability of catalyst for model reaction.

Entry	Run	Time ^a (Min)	Yield ^b
1	Fresh	10	93
2	1	10	93
3	2	10	92
4	3	10	90
5	4	10	90
6	5	15	85

^aReaction progress monitored by TLC.

^bIsolated yield.

**Scheme 2.** Synthesis of functionalized [1,6]-naphthyridines **4a-l**.

[1,6]-naphthyridines (**4b-l**) by reacting acetophenones (**1a-d**), malononitrile (**2**) and secondary amines (**3a-c**) in excellent yields (Scheme 2, Figure 2).

The formation of functionalized [1,6]-naphthyridines **4a-l** have been confirmed by physical data³⁰ and spectroscopic methods such as ¹H NMR, ¹³C NMR and mass. According to the ¹H NMR spectrum of representative compound **4a**, the singlet observed at δ 1.65 ppm for proton of methyl group, the multiplet observed at δ 1.48-1.55 ppm confirms the six protons from three methylene groups present in piperidine ring and multiplet observed at δ 3.44 ppm for methylene four proton attached to the nitrogen heteroatom. Similarly, broad singlet observed at δ 4.92 ppm for -NH₂ protons. In addition, a singlet observed at δ 5.57 ppm assigned to -NH proton present in [1,6]-naphthyridine and singlet for alkene proton observed at δ 6.74 ppm confirmed the formation of [1,6]-naphthyridine ring. Furthermore, all the aromatic protons appeared at expected chemical shifts and integral values. The synthesis of [1,6]-naphthyridine was further confirmed by ¹³C NMR spectral data **4a**, in which the carbon signals of methylene group is resonated at δ 24.3 ppm. The signal observed at δ 30.9 ppm indicates the presence of methyl carbon. The signals at δ 48.7 ppm indicate the presence of methylene carbon attached to the nitrogen heteroatom. The signal observed at δ 56.5 ppm indicates the tertiary carbon atom on which methyl and phenyl ring is present. In addition to this the signal observed at δ 118.7 indicates the presence of carbon in -CN group, while all other carbons gave signals at expected values.

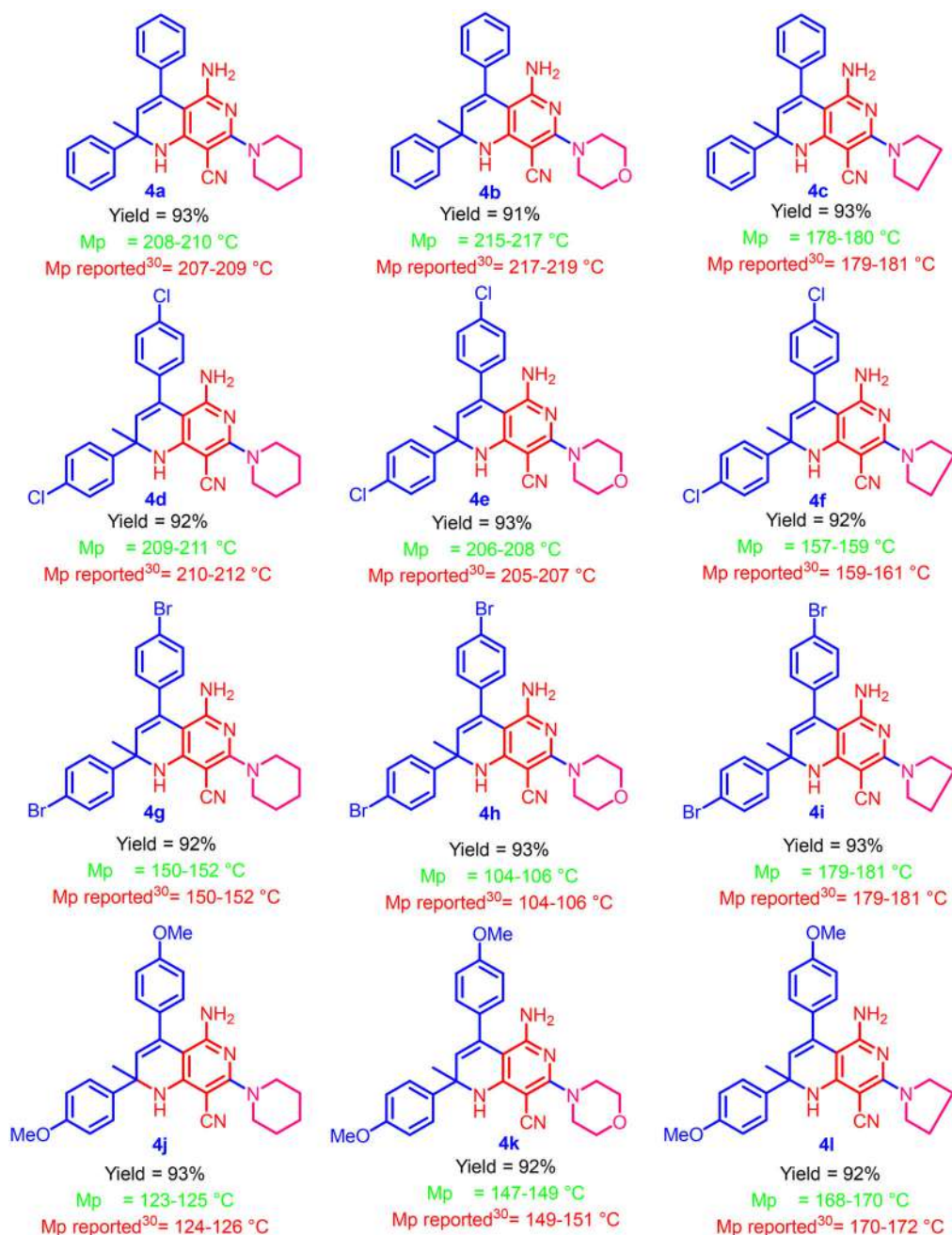


Figure 2. Structures, yields and melting point of the [1,6]-naphthyridines (4a-l).

Biological evaluation

Antibacterial activity

The functionalized [1,6]-naphthyridines **4a-l** were screened for antibacterial activity against the two Gram positive and two Gram negative bacterial strains and results are shown in Table 4.

For bacterial strain *S. aureus*, the compounds **4g**, **4h**, and **4j** shows excellent inhibitory activity with MIC value 4 µg/mL, which is equivalent to the clinical drug ampicillin (MIC 4 µg/mL).

Table 4. *In vitro* antimicrobial (MIC) and antioxidant activities (IC₅₀) of **4a-l** (μg/mL).

Compound	Gram + ve bacteria		Gram -ve bacteria		Antifungal activity			DPPH IC ₅₀
	SA	ML	EC	PF	CA	FO	AF	
4a	16	32	32	32	16	32	64	21.3
4b	8	16	32	32	16	32	64	27.3
4c	16	8	16	8	16	16	64	22.1
4d	8	8	16	8	32	16	32	18.1
4e	8	16	4	4	16	64	32	19.3
4f	8	16	8	4	16	32	16	18.9
4g	4	32	4	8	16	16	16	16.1
4h	4	8	32	8	32	64	64	16.3
4i	8	8	32	32	16	32	32	16.4
4j	4	16	8	16	16	16	16	25.3
4k	8	8	4	8	64	16	16	30.2
4l	8	8	4	16	64	64	64	20.3
Ampicilin	4	16	4	2	–	–	–	–
Kanamycin	2	2	2	2	–	–	–	–
Miconazole	–	–	–	–	16	16	16	–
Fluconazole	–	–	–	–	2	2	4	–
BHT	–	–	–	–	–	–	–	16.5

SA: *Staphylococcus aureus*; ML: *Micrococcus luteus*; EC: *Escherichia coli*; PF: *Pseudomonas fluorescens*; CA: *Candida albicans*; FO: *Fusarium oxysporum*; AF: *Aspergillus flavus*; BHT: Butylated Hydroxy Toluene.

For bacterial strain *M.luteus*, compounds **4c**, **4d**, **4h**, **4i**, **4k** and **4l** exhibit two-fold antibacterial activity with MIC value 8 μg/mL and compounds **4b**, **4e**, **4f** and **4j** with MIC value 16 μg/mL exhibited equivalent activity as compared to the clinical drug ampicilin (MIC 16 μg/mL). For bacterial strain *E. coli* compounds **4e**, **4g**, **4k** and **4l** with MIC value 4 μg/mL exhibited equivalent activity as compared to the clinical drug ampicilin (MIC 4 μg/mL) and for *P. fluorescens*, all the synthesized compounds exhibited moderate antibacterial activity compared to the standard antibacterial drugs.

Antifungal activity

In case of antifungal activity, all the synthesized [1,6]-naphthyridines **4a-l** shows good to moderate activity against all the tested fungal strains (Table 4).

Compounds **4a**, **4b**, **4c**, **4e**, **4f**, **4g**, **4i** and **4j** with MIC value 16 μg/mL exhibited equivalent activity compared with the standard drug miconazole against the fungicidal strain *C. albicans*. Compounds **4c**, **4d**, **4g**, **4j** and **4k** with MIC value 16 μg/mL exhibited equivalent activity compared with the standard drug miconazole against the fungicidal strain *F. oxysporum*. Compounds **4f**, **4g**, **4j** and **4k** with MIC value 16 μg/mL exhibited equivalent activity compared to the standard antibacterial drug miconazole for the fungicidal strain *A. flavus*.

Antioxidant activity

All the synthesized compounds **4a-l** shows moderate antioxidant activity as compared to the standard drug BHT (Table 4). The compounds **4g** (IC₅₀= 16.1 μg/mL), **4h** (IC₅₀= 16.3 μg/mL) and **4i** (IC₅₀= 16.4 μg/mL) have shown excellent activity as compared to standard drugs BHT (IC₅₀= 16.5 μg/mL). Remaining compounds exhibit good to moderate antioxidant activity as compared to standard drugs BHT.

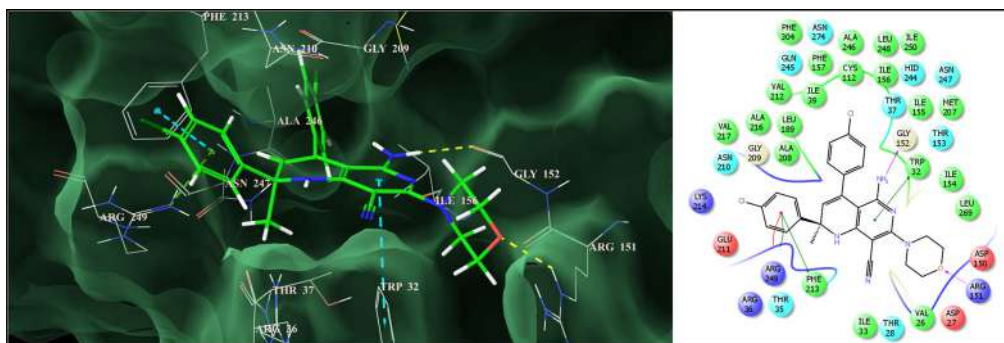
Computational study

Molecular docking

In an effort to elucidate the plausible mechanism for antimicrobial activity demonstrated by the naphthyridines investigated herein and guide further SAR, molecular docking was performed

Table 5. Molecular docking study results- Glide score, Glide energy, H- bond and π - π stacking.

Comp	Glide Score	Glide energy (Kcal/mol)	H-bond (Å)	π - π / cation- π stacking(Å)
4a	-7.001	-39.539	Gly152(2.104)	Arg249(2.507), Phe213(2.501)/Arg249(2.507)
4b	-7.015	-40.353	Gly152(2.067), Arg151(2.055)	Arg249(2.09), Phe213(2.47), Trp32(2.34)/ Arg249(2.09)
4c	-7.128	-43.49	Gly152(2.048)	Arg249(2.264), Phe213(2.572) /Arg249(2.264)
4d	-7.024	-42.043	Gly152(2.140)	Arg249(1.891), Phe213(2.471), Trp32(2.549)/ Arg249(1.891)
4e	-8.640	-49.152	Gly152(2.067), Arg151(2.111)	Arg249(2.053), Phe213(2.471), Trp32(2.582)/ Arg249(2.053)
4f	-8.102	-46.223	Gly152(2.160)	Arg249(1.878), Phe213(2.415), Trp32(2.626)/ Arg249(1.878)
4g	-8.635	-49.095	Gly152(2.072)	Arg249(1.997), Phe213(2.496), Trp32(2.564)/ Arg249(1.997)
4h	-8.164	-46.336	Gly152(1.979), Arg151(2.118)	Arg249(2.188), Phe213(2.458), Trp32(2.598)/ Arg249
4i	-7.101	-41.869	Gly152(2.086)	Arg249(1.921), Phe213(2.462), Trp32(2.622)/ Arg249(1.921)
4j	-8.197	-46.117	Gly152(1.9777)	Arg249(2.214), Phe213(2.487), Trp32(2.58)/ Arg249(2.214)
4k	-8.194	-46.423	Gly152(1.959), Arg151(2.067)	Arg249(2.275), Phe213(2.441), Trp32(2.602)/ Arg249(2.275)
4l	-8.139	-46.904	Gly152(2.0998)	Arg249(2.03), Phe213(2.472)/Arg249

**Figure 3.** Binding mode of **4e** into the active site of beta-ketoacyl-acyl carrier protein synthase III (on right side: the pink lines represent the hydrogen bonding interactions; the green lines represent π - π stacking interaction while red line represent cation- π stacking interaction).

against β -ketoacyl-acyl carrier protein synthase III (FabH) (PDB code: 1HNJ) using the standard protocol implemented in the GLIDE (Grid-based LIgand Docking with Energetics) program of the Schrodinger Molecular modeling package (Schrodinger, LLC, New York, NY, 2018).³¹ FabH is a condensing enzyme that plays an essential and regulatory role in bacterial fatty acid biosynthesis wherein it initiates the fatty acid elongation cycles and is involved in the feedback regulation of the biosynthetic pathway *via* product inhibition. FabH catalyzes the condensation of CoA-attached acetyl group and an ACP-attached malonyl group, yielding acetoacetyl-ACP as its final product. The essentiality of FabH for bacterial viability and due to their central roles in the fatty acid biosynthetic pathway qualifies FabH as an excellent molecular target.³²

All the naphthyridines were observed to be nicely bound to the active site of FabH with excellent binding affinity (average Glide docking score of -7.778 and Glide binding energy of -44.795 kcal/mol) and engaged in several close interactions (Table 5).

A detailed investigation of the per-residue interactions for one of most active analogs **4e** showed that it could snugly fit into the active site of FabH through an extensive network of steric and electrostatic interactions (Figure 3).

A significant network of van der Waals interactions were observed with Asn247(-2.479 Kcal/mol), Gly209(-2.887 Kcal/mol), Met207(-3.179 Kcal/mol), Ile156(-2.643 Kcal/mol), Gly152(-2.615 Kcal/mol), Thr37(-1.127 Kcal/mol) and Trp32(-4.727 Kcal/mol) residues through the 5-amino-2-methyl-1,2-dihydro-[1,6]naphthyridine nucleus while the morpholine side chain exhibited a similar chain of interactions with Arg151(-2.939 Kcal/mol), Thr28(-1.115 Kcal/mol), Asp27(-1.032 Kcal/mol) and Val26(-1.543 Kcal/mol) residues. Even the 2,4-bis-(4-chloro-phenyl) side chain also showed significant van der Waals interactions with Arg249(-2.276 Kcal/mol),

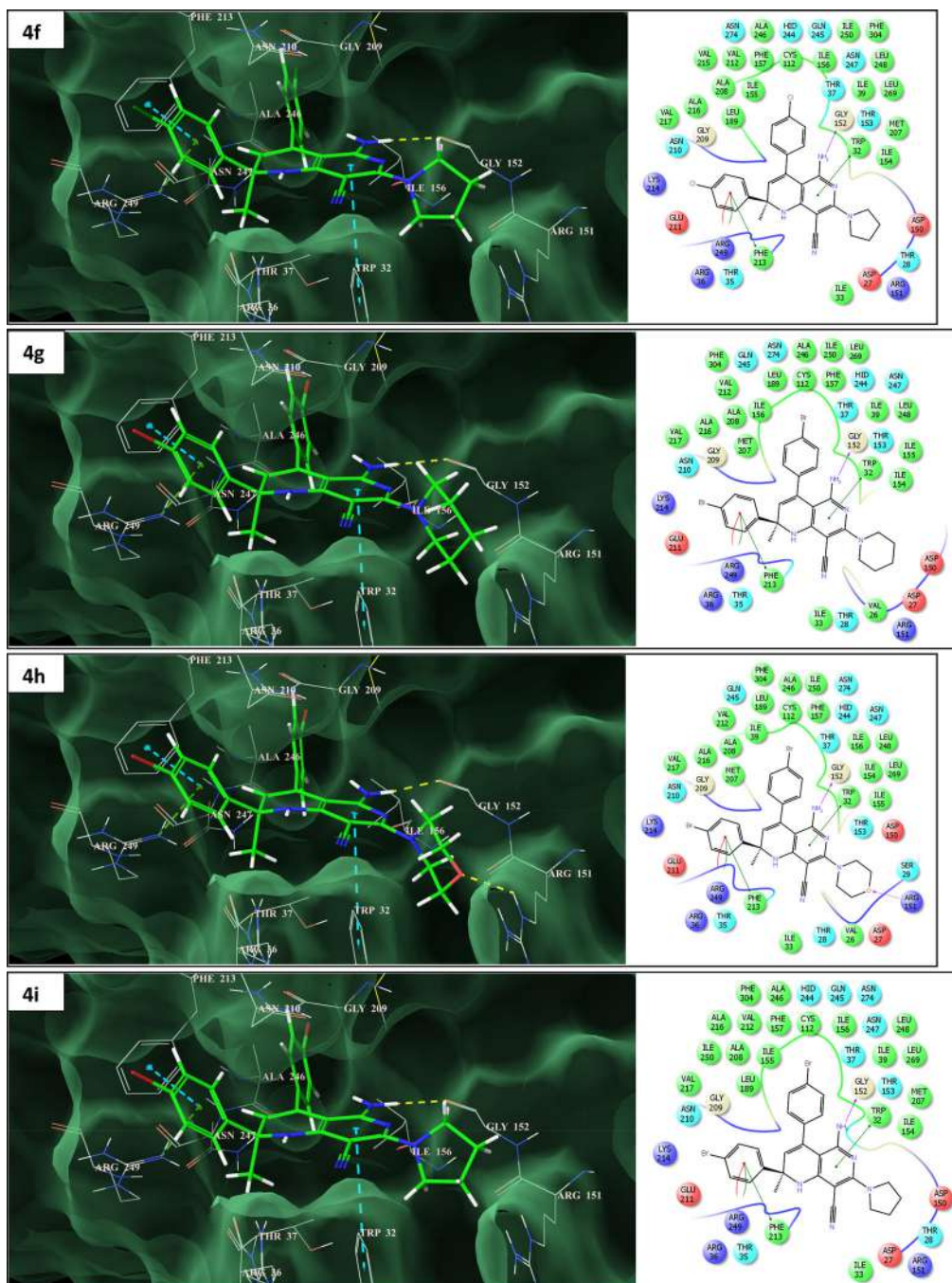


Figure 4. Continued

3.678 Kcal/mol) residues. Furthermore, it was observed to be stabilized into the active site through two prominent hydrogen bonding interactions: first through the amino group ($-NH_2$) of the naphthyridine ring with Gly152(2.067 Å) and second through the oxygen atom of the morpholine side chain with Arg151(2.111 Å). The compound has also exhibited significant π - π stacking interactions through Arg249(2.053 Å), Phe213(2.471 Å) and Trp32(2.582 Å) as well as a cation- π

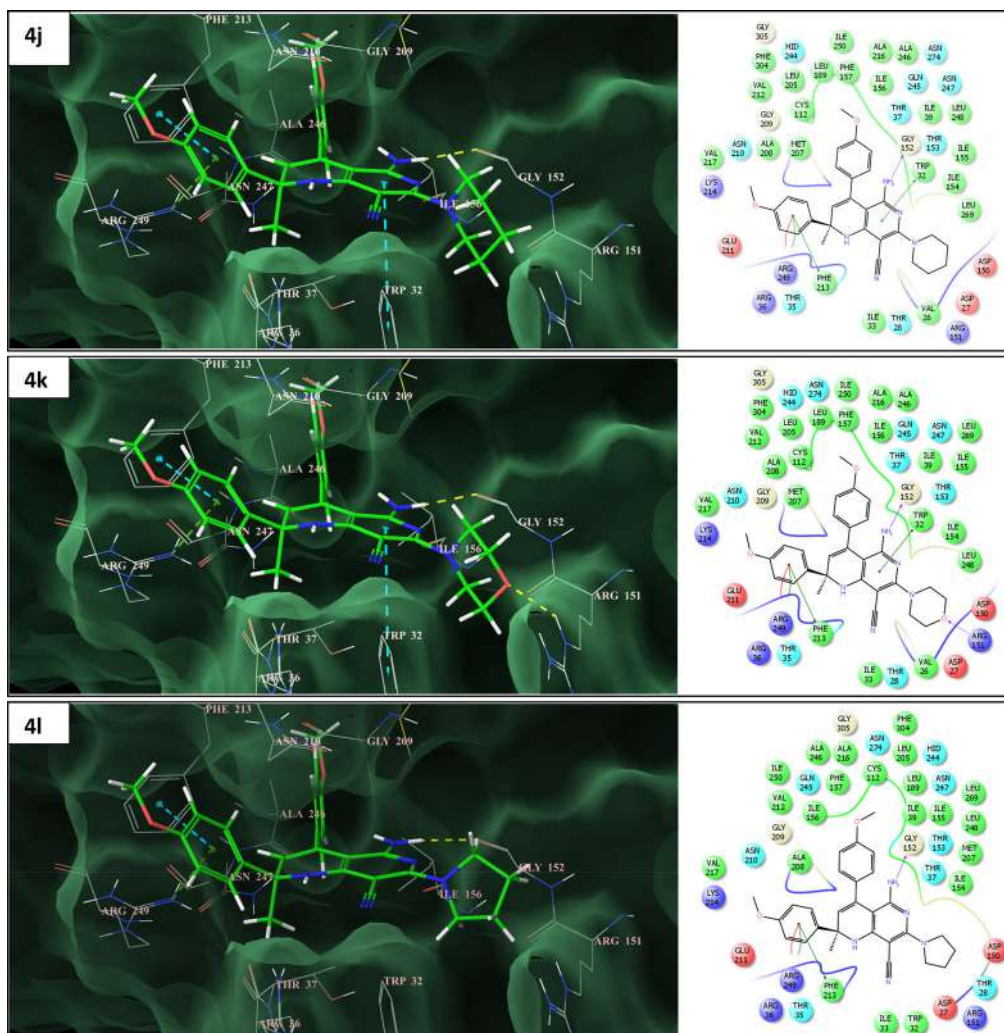


Figure 4. Continued

stacking interaction through Arg249(2.053 Å). Such hydrogen bonding and π stacking interactions serves as an anchor to stabilize the ligand into the 3D space of the active site and also facilitate the non-bonded (steric and electrostatic) interactions. A similar network of bonded and non-bonded interactions were observed for the other naphthyridines (Figure 4) as well indicating that these molecules could exhibit their antimicrobial action through inhibiting FabH and could be optimized further to arrive at selective and potent antimicrobial agents.

In silico ADME prediction

The success of a drug is determined not only by good efficacy but also by an acceptable ADME (absorption, distribution, metabolism and excretion) profile. A computational study of all the synthesized **4a-l** was performed for prediction of ADME properties and the value obtained is presented in Table 6. It is observed that, the compounds exhibited a good % ABS (% absorption) ranging from 72.54 to 82.10% (Table 6). Furthermore, only compounds **4g** and **4i** violated

Table 6. Molecular properties of compounds **4a-4l**.

Entry	% ABS	TPSA (Å ²)	n-ROTB	MV	MW	log p	n-ON	n-OHND	Lipinski violations	Drug-likeness model score
Rule	–	–	–	–	<500	≤5	<10	<5	≤1	–
4a	82.10	77.97	3	398.85	421.55	4.07	5	3	0	0.41
4b	78.91	87.21	3	391.03	423.52	3.01	6	3	0	0.10
4c	82.10	77.97	3	382.04	407.52	3.57	5	3	0	0.42
4d	82.10	77.97	3	425.92	490.44	5.43	5	3	1	0.74
4e	78.91	87.21	3	418.10	492.41	4.37	6	3	0	0.44
4f	82.10	77.97	3	409.12	476.41	4.92	5	3	0	0.77
4g	82.10	77.97	3	434.62	579.34	5.69	5	3	2	0.45
4h	78.91	87.21	3	426.80	581.31	4.63	6	3	1	0.16
4i	82.10	77.97	3	417.81	565.31	5.18	5	3	2	0.48
4j	75.72	96.44	5	449.94	481.60	4.18	7	3	0	0.41
4k	72.54	105.67	5	442.12	483.57	3.12	8	3	0	0.12
4l	75.72	96.44	5	433.13	467.57	3.68	7	3	0	0.41

Cpd, Compounds, % ABS: percentage absorption, TPSA: topological polar surface area, n-ROTB: number of rotatable bonds, MV: molecular volume, MW: molecular weight, milogP: logarithm of partition coefficient of compound between n-octanol and water, n-ON acceptors: number of hydrogen bond acceptors, n-OHND donors: number of hydrogen bonds donors.

Lipinski's rule of five ($\log p$). All the tested compounds followed the criteria for orally active drug and therefore, these compounds may have a good potential for eventual development as oral agents.

Conclusions

We have developed a convenient one-pot multicomponent synthesis of highly functionalized [1,6]-naphthyridines under solvent free condition using $[\text{Et}_3\text{NH}][\text{HSO}_4]$ in high yields. We have screened the synthesized naphthyridines for *in vitro* antimicrobial and antioxidant activity. This solvent-free domino reaction proceeded smoothly in good to excellent yields and offered several other advantages including short reaction time, simple experimental workup procedures and no toxic byproducts, avoids the use of catalyst, toxic organic solvents and anhydrous conditions.

Molecular docking analysis revealed that these naphthyridines exhibited excellent binding affinity toward crucial microbial target β -Ketoacyl-acyl carrier protein synthase III (FabH) engaging in several close and significant bonded and non-bonded interactions. Furthermore, analysis of the ADME parameters for synthesized compounds showed good drug like properties and can be developed as oral drug candidate. The *in silico* results were found to be in harmony with experimentally observed MIC results which provide a strong platform to optimize this scaffold to arrive at selective and potent antimicrobial agents targeting FabH.

Experimental

Synthesis of $[\text{Et}_3\text{NH}][\text{HSO}_4]$

The synthesis of ionic liquid was carried out in a 100 mL round-bottom flask, which was immersed in a recirculating heated water-bath and fitted with a reflux condenser. Sulfuric acid (98%) (1.96 g, 0.02 mol) was added drop wise from triethylamine (2.02 g, 0.02 mol) stirring at 60 °C for 1 h. After the addition, the reaction mixture was stirred for an additional period of 1 h at 70 °C to ensure the reaction had proceeded to completion. The traces of water were removed by heating the residue at 80 °C in high vacuum until the weight of the residue remains constant.

Triethylammonium hydrogen sulfate $[\text{Et}_3\text{NH}][\text{HSO}_4]$: ¹H NMR (300 MHz, DMSO *d*₆): d (ppm) 1.15-1.19 (t, 9H), 3.04-3.12 (m, 6H), 8.98 (s, 1H); ¹³C NMR (75 MHz, DMSO *d*₆): d (ppm) 8.88, 46.40.

General procedure for preparation of [1,6]-naphthyridines (4a-l)

A mixture of ketone **1a-d** (2 mmol), malononitrile **2** (2 mmol) and amine **3a-c** (1 mmol) in 20 mol% [Et₃NH][HSO₄] were heated at 80-90 °C for 10-15 minutes. The reaction was monitored by TLC using ethyl acetate:hexane as a solvent system. The reaction mixture was quenched with crushed ice and extracted with ethyl acetate (2 × 25 mL). The organic extracts were washed with brine (2 × 25 mL) and dried over anhydrous sodium sulfate. The solvent was evaporated under reduced pressure to afford the corresponding crude compounds. The obtained crude compounds were recrystallized using ethanol-ethylacetate solvent system. The residual ionic liquid was washed with diethyl ether, dried under vacuum at 100 °C and reused for subsequent reactions. The recovered ionic liquid could be used for 5 times without much loss of catalytic activity.

5-Amino-2-methyl-2,4-diphenyl-7-piperidin-1-yl-1,2-dihydro-[1,6]-naphthyridine-8-carbonitrile (4a): A mixture of acetophenone **1a** (2 mmol), malononitrile **2** (2 mmol) and piperidine **3a** (1 mmol) in 20 mol% [Et₃NH][HSO₄] were heated at 80-90 °C for 10 min to give [1,6]-naphthyridine **4a** in 93% yield as white solid. Mp 207-209 °C (recrystallized from EtOH-EtOAc); ¹H NMR (300 MHz, DMSO-*d*₆, δ ppm): 1.55 (*bs*, 6*H*), 1.65 (*s*, 3*H*), 3.44 (*s*, 4*H*), 4.92 (*bs*, 2*H*), 5.57 (*s*, 1*H*), 6.74 (*s*, 1*H*), 7.14-7.23 (*m*, 3*H*), 7.27-7.38 (*m*, 5*H*) and 7.43 (*d*, 2*H*, *J* = 7.5 Hz). ¹³C NMR (75 MHz, DMSO-*d*₆, δ ppm): 24.3, 25.7, 30.9, 48.7, 56.5, 68.6, 90.6, 118.7, 124.7, 126.6, 126.9, 127.8, 127.9, 128.2, 128.5, 132.6, 138.8, 148.7, 154.7, 154.8 and 161.6.

5-Amino-2-methyl-7-morpholin-4-yl-2,4-diphenyl-1,2-dihydro-[1,6]-naphthyridine-8-carbonitrile (4b): A mixture of acetophenone **1a** (2 mmol), malononitrile **2** (2 mmol) and morpholine **3b** (1 mmol) in 20 mol% [Et₃NH][HSO₄] were heated at 80-90 °C for 10 min to give [1,6]-naphthyridine **4b** in 91% yield as cream colored solid. Mp 217-219 °C (recrystallized from EtOH-EtOAc); ¹H NMR (300 MHz, DMSO-*d*₆, δ ppm): 1.66 (*s*, 3*H*), 3.34-3.37 (*m*, 2*H*), 3.47-3.52 (*m*, 2*H*), 3.62 (*bs*, 4*H*), 5.02 (*bs*, 2*H*), 5.60 (*s*, 1*H*), 6.88 (*s*, 1*H*), 7.14-7.23 (*m*, 3*H*), 7.27-7.35 (*m*, 5*H*) and 7.43 (*d*, 2*H*, *J* = 7.8 Hz). ¹³C NMR (75 MHz, DMSO-*d*₆, δ ppm): 30.9, 48.2, 56.5, 66.1, 69.2, 91.0, 124.7, 126.6, 127.4, 128.0, 128.3, 128.5, 132.4, 154.7, 154.8 and 161.6.

5-Amino-2-methyl-2,4-diphenyl-7-pyrrolidin-1-yl-1,2-dihydro-[1,6]-naphthyridine-8-carbonitrile (4c): A mixture of acetophenone **1a** (2 mmol), malononitrile **2** (2 mmol) and pyrrolidine **3c** (1 mmol) in 20 mol% [Et₃NH][HSO₄] were heated at 80-90 °C for 15 min to give [1,6]-naphthyridine **4c** in 93% yield as light yellow solid. Mp 179-181 °C (recrystallized from EtOH-EtOAc); ¹H NMR (300 MHz, DMSO-*d*₆, δ ppm): 1.65 (*s*, 3*H*), 1.77-1.86 (*m*, 4*H*), 3.46-3.49 (*m*, 2*H*), 3.58-3.61 (*m*, 2*H*), 4.83 (*bs*, 2*H*), 5.52 (*s*, 1*H*), 6.40 (*s*, 1*H*), 7.14-7.23 (*m*, 3*H*), 7.27-7.36 (*m*, 5*H*) and 7.44 (*d*, 2*H*, *J* = 7.8 Hz). ¹³C NMR (75 MHz, DMSO-*d*₆, δ ppm): 25.1, 31.0, 48.6, 56.5, 66.0, 89.7, 119.4, 124.8, 126.0, 127.9, 128.0, 128.3, 128.5, 132.8, 139.2, 148.8, 155.0 and 157.4.

5-Amino-2,4-bis-(4-chloro-phenyl)-2-methyl-7-morpholin-4-yl-1,2-dihydro-[1,6]naphthyridine-8-carbonitrile (4e): A mixture of 4-chloroacetophenone **1b** (2 mmol), malononitrile **2** (2 mmol) and morpholine **3b** (1 mmol) in 20 mol% [Et₃NH][HSO₄] were heated at 80-90 °C for 15 min to give [1,6]-naphthyridine **4e** in 93% yield as cream colored solid. Mp 205-207 °C (recrystallized from EtOH-EtOAc); ¹H NMR (300 MHz, DMSO-*d*₆, δ ppm): 1.65 (*s*, 3*H*), 3.35-3.39 (*m*, 2*H*), 3.49-3.55 (*m*, 2*H*), 3.58-3.64 (*m*, 4*H*), 5.18 (*bs*, 2*H*), 5.63 (*s*, 1*H*), 7.00 (*s*, 1*H*), 7.22 (*d*, 2*H*, *J* = 8.1 Hz), 7.36 (*t*, 4*H*, *J* = 7.6 Hz) and 7.44 (*d*, 2*H*, *J* = 8.7 Hz). ¹³C NMR (75 MHz, DMSO-*d*₆, δ ppm): 30.4, 48.1, 56.2, 66.1, 68.9, 98.8, 117.7, 118.4, 126.8, 127.1, 128.0, 128.1, 129.8, 121.2, 132.0, 132.3, 137.0, 147.4, 154.7 and 161.6. HRMS calculated [M + H]⁺ for C₂₆H₂₄N₅OCl₂: 492.0915, found: 492.0905, [M + Na]⁺ for C₂₆H₂₃N₅OCl₂Na: 515.0703, found: 515.0693.

5-Amino-2,4-bis-(4-chloro-phenyl)-2-methyl-7-pyrrolidin-1-yl-1,2-dihydro-[1,6]-naphthyridine-8-carbonitrile (4f): A mixture of 4-chloroacetophenone **1b** (2 mmol), malononitrile **2** (2 mmol) and pyrrolidine **3c** (1 mmol) in 20 mol% [Et₃NH][HSO₄] were heated at 80-90 °C for 15 min to give [1,6]-naphthyridine **4f** in 92% yield as white solid. Mp 159-161 °C (recrystallized from EtOH-EtOAc); ¹H NMR (300 MHz, DMSO-*d*₆, δ ppm): 1.64 (*s*, 3*H*), 1.79-1.85 (*m*, 4*H*), 3.49 (*bs*, 2*H*), 3.58 (*bs*, 2*H*), 4.95 (*bs*, 2*H*), 5.54 (*s*, 1*H*), 6.57 (*s*, 1*H*), 7.21 (*d*, 2*H*, *J* = 8.1 Hz), 7.35 (*t*,

4H, $J=8.1$ Hz) and 7.43 (*d*, 2H, $J=8.4$ Hz). ^{13}C NMR (75 MHz, DMSO- d_6 , δ ppm): 25.1, 30.5, 48.5, 56.1, 65.9, 89.5, 119.2, 126.8, 128.1, 128.2, 129.8, 131.2, 132.3, 137.5, 147.5, 154.8, 154.9 and 157.5. LCMS calculated $[\text{M} + \text{H}]^+$ for $\text{C}_{26}\text{H}_{24}\text{N}_5\text{Cl}_2$: 476.15, found: 476.20,

Experimental protocol for biological activity

Antibacterial activity

The antimicrobial susceptibility testing of newly synthesized compounds were performed *in vitro* against bacterial strains *viz.*, Gram-positive *Staphylococcus Aureus* (ATCC No. 29737), *Micrococcus Luteus* (ATCC No. 398) and Gram-negative *Escherichia Coli* (NCIM No. 2256) and *Pseudomonas Fluorescens* (NCIM No. 2173) respectively, to find out minimum inhibitory concentration (MIC).³³ The MIC was defined as the lowest concentrations of compound that completely inhibit the growth of each strain. Serial two-fold dilutions of all samples were prepared in triplicate in micro titer plates and inoculated with suitably prepared cell suspension to achieve the required initial concentration. Serial dilutions were prepared for screening. Dimethylsulfoxide (DMSO) was used as solvent control. Ampicilin, kanamycin & chloramphenicol were used as a standard antibacterial drug. The concentration range of tested compounds and standard was 128-0.5 $\mu\text{g}/\text{mL}$. The plates were incubated at 37 °C for all micro-organisms; absorbance at 595 nm was recorded to assess the inhibition of cell growth after 24 h. The compounds which are showing promising antibacterial activity were selected for MIC studies. The MIC was determined by assaying at 128, 64, 32, 16, 8, 4, 2, 1 and 0.5 $\mu\text{g}/\text{mL}$ concentrations along with standards at the same concentrations.

Antifungal activity

The antifungal activity was evaluated against different fungal strains such as *Aspergillus Niger* (NCIM No. 1196), *Penicillium Chrysogenum* (NCIM No. 723) and *Curvularia Lunata* (NCIM No. 1131).³³ Fluconazole, miconazole and amphotericin B were used as standard drugs for the comparison of antifungal activity. The plates were incubated at 37 °C for all micro-organisms; absorbance at 410 nm was recorded to assess the inhibition of cell growth after 48 h. The lowest concentration inhibiting growth of the organisms was recorded as the MIC. DMSO was used as a solvent or negative control. In order to clarify any effect of DMSO on the biological screening, separate studies were carried out with solutions alone of DMSO and showed no activity against any microbial strains. The compounds which are showing promising antifungal activity were selected for MIC studies. The MIC was determined by assaying at 128, 64, 32, 16, 8, 4, 2, 1 and 0.5 $\mu\text{g}/\text{mL}$ concentrations along with standards at the same concentrations.

DPPH radical scavenging activity

The hydrogen atom or electron donation ability of some compounds were measured from the bleaching of the purple colored methanol solution of DPPH.³⁴ The spectrophotometric assay uses the stable radical DPPH as a reagent. 1 mL of various concentrations of the test compounds (5, 10, 25, 50 and 100 $\mu\text{g}/\text{mL}$) in methanol was added to 4 mL of 0.004% (w/v) methanol solution of DPPH. The reaction mixture was incubated at 37 °C. The scavenging activity on DPPH was determined by measuring the absorbance at 517 nm after 30 min. All tests were performed in triplicate and the mean values were entered. The percent of inhibition (I %) of free radical production from DPPH was calculated by the following equation

$$\% \text{ of scavenging} = [(A_{\text{control}} - A_{\text{sample}}) / (A_{\text{sample}} \times 100)]$$

Where, A_{control} is the absorbance of the control (DPPH radical without test sample)

A_{sample} is the absorbance of the test sample (DPPH radical with test sample). The control contains all reagents except the test samples.

ADME prediction

In the present study, we have calculated molecular volume (MV), molecular weight (MW), logarithm of partition coefficient ($\text{miLog } P$), number of hydrogen bond acceptors (n-ON), number of hydrogen bonds donors (n-OHNH), topological polar surface area (TPSA), number of rotatable bonds (n-ROTB) and Lipinski's rule of five³⁵ using Molinspiration online property calculation toolkit.³⁶ Absorption (% ABS) was calculated by: % ABS = $109 - (0.345 \times \text{TPSA})$.³⁷ Drug-likeness model score (a collective property of physico-chemical properties, pharmacokinetics and pharmacodynamics of a compound is represented by a numerical value) was computed by MolSoft software.³⁸ A molecule likely to be developed as an orally active drug candidate should show no more than one violation of the following four criteria: $\text{miLog } P$ (octanol-water partition coefficient) ≤ 5 , molecular weight ≤ 500 , number of hydrogen bond acceptors ≤ 10 and number of hydrogen bond donors ≤ 5 .³⁹

Acknowledgement

The authors M.H.S. and D.D.S. are very much grateful to the Council of Scientific and Industrial Research (CSIR), New Delhi for the award of Senior Research Fellowship. Authors are also thankful to the University Grants Commission and Department of Science & Technology, New Delhi for financial support under UGC-SAP and DST-FIST schemes. Authors also thank Schrodinger Inc. for GLIDE software to perform the molecular docking studies.

Disclosure statement

No potential conflict of interest was reported by the authors.

References

1. B. M. Teipel, J. Teixido, R. Pascual, M. Mora, J. Pujola, T. Fujimoto, J. I. Borrell, and E. L. Michelotti, "2-Methoxy-6-Oxo-1,4,5,6-Tetrahydropyridine-3-Carbonitriles: Versatile Starting Materials for the Synthesis of Libraries with Diverse Heterocyclic Scaffolds," *J. Combinatorial Chemistry* 7, no. 3 (2005): 436–48.
2. Y. Zhang, R. Sun, X. Kang, D. H. Wang, and Y. Chen, "A Water-Soluble 1,8-Naphthyridine-Based Imidazolium Molecular Gripper for Fluorescence Sensing and Discriminating of GMP," *Dyes and Pigments* 174, (2020): 108103.
3. J. Fiorito, J. Vendome, F. Saeed, A. Staniszewski, H. Zhang, S. Yan, S. X. Deng, O. Arancio, and D. W. Landry, "Identification of a Novel 1,2,3,4-Tetrahydrobenzo[b][1,6]naphthyridine Analogue as a Potent Phosphodiesterase 5 Inhibitor with Improved Aqueous Solubility for the Treatment of Alzheimer's Disease," *Journal of Medicinal Chemistry* 60, no. 21 (2017): 8858–75.
4. C. D. d. M. Oliveira-Tintino, S. R. Tintino, D. F. Muniz, C. R. D. S. Barbosa, R. L. S. Pereira, I. M. Begnini, R. A. Rebelo, L. E. da Silva, S. L. Mireski, M. C. Nasato, et al. "Do 1,8-Naphthyridine Sulfonamides Possess an Inhibitory Action Against Tet(K) and MsrA Efflux Pumps in Multiresistant Staphylococcus Aureus Strains?," *Microbial Pathogenesis* 147, (2020): 104268.
5. E. L. Meredith, O. Ardayfio, K. Beattie, M. R. Dobler, I. Enyedy, C. Gaul, V. Hosagrahara, C. Jewell, K. Koch, W. Lee, et al. "Identification of Orally Available Naphthyridine Protein Kinase D Inhibitors," *Journal of Medicinal Chemistry* 53, no. 15 (2010): 5400–21.
6. X. Y. Mu, J. Xu, Y. J. Zhou, Y. L. Li, Y. Liu, and X. S. Wang, "Convenient Synthesis of Naphtho[1,6]Naphthyridine Derivatives under Catalyst-Free Conditions," *Research on Chemical Intermediates* 41, no. 3 (2015): 1703–14.
7. T. Chen, L. S. Zhuo, P. F. Liu, W. R. Fang, Y. Li, and W. Huang, "Discovery of 1,6-Naphthyridinone-Based MET Kinase Inhibitor Bearing Quinoline Moiety as Promising Antitumor Drug Candidate," *European Journal of Medicinal Chemistry* 192 (2020): 112174.

8. Michael G. Thomas, Manu De Rycker, Richard J. Wall, Daniel Spinks, Ola Epemolu, Sujatha Manthri, Suzanne Norval, Maria Osuna-Cabello, Stephen Patterson, Jennifer Riley, et al. "Identification and Optimization of a Series of 8-Hydroxy Naphthyridines with Potent In Vitro Antileishmanial Activity: Initial SAR and Assessment of In Vivo Activity," *Journal of Medicinal Chemistry* 63, no. 17 (2020): 9523–39.
9. Kevin M. Peese, Christopher W. Allard, Timothy Connolly, Barry L. Johnson, Chen Li, Manoj Patel, Margaret E. Sorensen, Michael A. Walker, Nicholas A. Meanwell, Brian McAuliffe, et al. "5,6,7,8-Tetrahydro-1,6-Naphthyridine Derivatives as Potent HIV-1-Integrase-Allosteric-Site Inhibitors," *Journal of Medicinal Chemistry* 62, no. 3 (2019): 1348–61.
10. V. Litvinov, "Advances in the Chemistry of Naphthyridines," *Advances in Heterocyclic Chemistry* 91 (2006): 189–300.
11. M. V. Fedorov, and A. A. Kornyshev, "Ionic Liquids at Electrified Interfaces," *Chemical Reviews* 114, no. 5 (2014): 2978–3036.
12. X. X. Han, H. Du, C. T. Hung, L. L. Liu, P. H. Wu, D. H. Ren, S. J. Huang, and S. B. Liu, "Syntheses of Novel Halogen-Free Bronsted-Lewis Acidic Ionic Liquid Catalysts and Their Applications for Synthesis of Methyl Caprylate," *Green Chemistry* 17, no. 1 (2015): 499–508.
13. Z. N. Siddiqui, and K. Khan, "[Et₃NH][HSO₄]-Catalyzed Efficient, Eco-Friendly, and Sustainable Synthesis of Quinoline Derivatives via Knoevenagel Condensation," *ACS Sustainable Chemistry & Engineering* 2, no. 5 (2014): 1187–94.
14. Z. K. Jaber, B. Masoudi, A. Rahmani, and K. Alborzi, "Triethylammonium Hydrogen Sulfate [Et₃NH][HSO₄] as an Efficient Ionic Liquid Catalyst for the Synthesis of Coumarin Derivatives," *Polycyclic Aromatic Compounds* 40, no. 1 (2020): 99–107.
15. S. K. Patil, D. V. Awale, M. M. Vadiyar, S. A. Patil, S. C. Bhise, and S. S. Kolekar, "Simple Protic Ionic Liquid [Et₃NH][HSO₄] as a Proficient Catalyst for Facile Synthesis of Biscoumarins," *Research on Chemical Intermediates* 43, no. 10 (2017): 5365–76.
16. Z. Zhou, and X. Deng, "[Et₃NH][HSO₄] Catalyzed Efficient and Green Synthesis of 1,8-Dioxo-Octahydroxanthenes," *Journal of Molecular Catalysis A: Chemical* 367 (2013): 99–102.
17. Ali Mohammed Malla, Mehtab Parveen, Faheem Ahmad, Shaista Azaz, and Mahboob Alam, "Et₃NH][HSO₄]-Catalyzed Eco-Friendly and Expeditious Synthesis of Thiazolidine and Oxazolidine Derivatives," *RSC Advances* 5, no. 25 (2015): 19552–69.
18. M. Parveen, S. Azaz, A. M. Malla, F. Ahmad, P. Sidonio, P. da Silva, and M. R. Silva, "Solvent-Free, [Et₃NH][HSO₄] Catalyzed Facile Synthesis of Hydrazone Derivatives," *New Journal of Chemistry* 39, no. 1 (2015): 469–81.
19. Z. Zhou, and Y. Zhang, "An Eco-Friendly One-Pot Synthesis of 4,4'-(Arylmethylene)Bis(1*h*-Pyrazol-5-Ols) Using [Et₃NH][HSO₄] as a Recyclable Catalyst," *Journal of the Chilean Chemical Society* 60, no. 3 (2015): 2992–6.
20. E. Hadadianpour, and B. Pouramiri, "Facile, Efficient and One-Pot Access to Diverse New Functionalized Aminoalkyl and Amidoalkyl Naphthol Scaffolds via Green Multicomponent Reaction Using Triethylammonium Hydrogen Sulfate ([Et₃NH][HSO₄]) as an Acidic Ionic Liquid under Solvent-Free Conditions," *Molecular Diversity* 24, no. 1 (2020): 241–52.
21. N. S. Suryawanshi, P. Jain, M. Singhal, and I. Khan, "Mannich Synthesis under Ionic Liquid [Et₃NH][HSO₄] Catalysis," *IOSR Journal of Applied Chemistry* 1, no. 2 (2012): 18–23.
22. F. G. Nikfarjam, M. M. Hashemi, and A. Ezabadi. "One-Pot Synthesis of Biologically Important Xanthene Derivatives Using [(Et₃N)₂SO][HSO₄]₂ as a Novel and Green IL-Based Catalyst under Solvent-Free Conditions," *Journal of Nanomedicine* 3, no. 1 (2020) 1020.
23. B. Pouramiri, R. Fayazi, and E. T. Kermani, "Facile and Rapid Synthesis of 3,4-Dihydropyrimidin-2(1*h*)-One Derivatives Using [Et₃NH][HSO₄] as Environmentally Benign and Green Catalyst," *Iranian Journal of Chemistry and Chemical Engineering* 37 (2018): 159–67.
24. J. Weng, C. Wang, H. Li, and Y. Wang, "Novel Quaternary Ammonium Ionic Liquids and Their Use as Dual Solvent-Catalysts in the Hydrolytic Reaction," *Green Chemistry* 8, no. 1 (2006): 96–9.
25. S. Salahi, M. T. Maghsoodlou, N. Hazeri, M. Lashkari, R. Doostmohammadi, A. Kanipour, F. Farhadpour, and A. Shojaei, "Two Ammonium Ionic Liquids as Efficient Catalysts for the One-Pot Green Synthesis of 3,4,5-Substituted Furan-2(5*H*)-Ones," *Bulgarian Chemical Communications* 48 (2016): 364–8.
26. M. H. Shaikh, D. D. Subhedar, F. A. K. Khan, J. N. Sangshetti, and B. B. Shingate, "[Et₃NH][HSO₄]-Catalyzed One-Pot, Solvent-Free Synthesis and Biological Evaluation of α -Amino Phosphonates," *Research on Chemical Intermediates* 42, no. 5 (2016): 5115–31.
27. (a) C. Li, F. Zhang and Z. Shen, "An Efficient Strategy for the Synthesis of Naphtho[2,3-*b*][1,6]Naphthyridines Promoted by Acetic Acid", *Synlett* 32 (2021): 1117–1122;(b) C. Li, C. Qi and F. Zhang, "An Efficient Strategy for the Synthesis of 1,6-Naphthyridine-2,5-Dione Derivatives Under Ultrasound Irradiation" *Synlett* 31 (2020): 1313–1317; (c) C. Li, C. Qi and F. Zhang, "Ultrasonic Promoted Synthesis of 1,6-Naphthyridine Derivatives Catalyzed by Solid Acid in Water" *Tetrahedron Letters* 61 (2020):

- 152144; (d) K. N. Vennila, B. Selvakumar, V. Satish, D. Sunny, S. Madhuri and K. P. Elango, "Structure-Based Design, Synthesis, Biological Evaluation, and Molecular Docking of Novel 10-Methoxy Dibenzo[b,h][1,6]Naphthyridinecarboxamides" *Medicinal Chemistry Research* 30 (2021): 133–141; (e) S. Vanlaer, A. Voet, C. Gielens, M. D. Maeyer and F. Compennolle, "Bridged 5,6,7,8-Tetrahydro-1,6-Naphthyridines, Analogues of Huperzine A: Synthesis, Modelling Studies and Evaluation as Inhibitors of Acetylcholinesterase", *European Journal of Organic Chemistry* (2009): 643–654; (f) J. A. Turner, "A General Approach to the Synthesis of 1,6-, 1,7-, and 1,8-Naphthyridines", *Journal of Organic Chemistry* 55 (1990): 4744–4750; (g) Q. Zhang, Q. Shi, H. R. Zhang and K. K. Wang, "Synthesis of 6H-indolo[2,3-b][1,6]Naphthyridines and Related Compounds as the 5-aza Analogues of Ellipticine Alkaloids", *Journal of Organic Chemistry* 65 (2000): 7977–7983; (h) H. Suzuki, N. Sakai, R. Iwahara, T. Fujiwaka, M. Satoh, A. Kakehi and T. Konakahara, "Novel synthesis of 7-fluoro-8-(trifluoromethyl)-1H-1,6-Naphthyridin-4-One Derivatives: Intermolecular Cyclization of an *N*-silyl-1-Azaallyl Anion with Perfluoroalkene and Subsequent Intramolecular Skeletal Transformation of the Resulting Pentasubstituted Pyridines", *Journal of Organic Chemistry* 72 (2007): 5878–5881; (i) Y. Zhou, J. A. Porco and J. K. Snyder, "Synthesis of 5,6,7,8-Tetrahydro-1,6-Naphthyridines and Related Heterocycles by Cobalt-Catalyzed [2+2+2] Cyclizations", *Organic Letters* 9 (2007): 393–396; (j) V. J. Colandrea and E. M. Naylor, "Synthesis and Regioselective Alkylation of 1,6- and 1,7-Naphthyridines", *Tetrahedron Letters* 41 (2000): 8053–8057.
28. (a) A. Chandra, B. Singh, S. Upadhyay and R. M. Singh, "Copper-Free Sonogashira Coupling of 2-Chloroquinolines with Phenyl Acetylene and Quick Annulation to benzo[b][1,6]Naphthyridine Derivatives in Aqueous Ammonia", *Tetrahedron*, 64, no. 51 (2008): 11680–11685; (b) G. Sabitha, E. R. Reddy, C. Maruthi and J. S. Yadav, "Bismuth(III) Chloride-Catalyzed Intramolecular Hetero-Diels-Alder Reactions: A Novel Synthesis of Hexahydrodibenzo[b,h][1,6]Naphthyridines", *Tetrahedron Letters* 43 (2002): 1573–1575.
29. (a) S. V. Akolkar, A. A. Nagargoje, V. S. Krishna, D. Sriram, J. N. Sangshetti, M. Damale and B. B. Shingate, "New *N*-Phenylacetamide-Incorporated 1,2,3-triazoles: [Et₃NH][OAc]-Mediated Efficient Synthesis and Biological Evaluation", *RSC Advances*, 9, no. 38 (2019): 22080–22091; (b) D. D. Subhedar, M. H. Shaikh, M. A. Arkile, A. Yeware, D. Sarkar and B. B. Shingate, "Facile Synthesis of 1,3-thiazolidin-4-ones as Antitubercular Agents" *Bioorganic & Medicinal Chemistry Letters* 26 (2016): 1704–1708; (c) D. D. Subhedar, M. H. Shaikh, B. B. Shingate, L. Nawale, D. Sarkar, V. M. Khedkar, F. A. K. Khan and J. N. Sangshetti, "Quinolidene-Rhodanine Conjugates: Facile Synthesis and Biological Evaluation", *European Journal of Medicinal Chemistry* 125 (2017): 385–399; (d) D. D. Subhedar, M. H. Shaikh, L. Nawale, A. Yeware, D. Sarkar, F. A. K. Khan, J. N. Sangshetti and B. B. Shingate, "Novel Tetrazoloquinoline-Rhodanine Conjugates: Highly Efficient Synthesis and Biological Evaluation", *Bioorganic & Medicinal Chemistry Letters* 26 (2016): 2278–2283; (e) D. D. Subhedar, M. H. Shaikh, F. A. K. Khan, J. N. Sangshetti, V. M. Khedkar and B. B. Shingate, "Facile Synthesis of new *N*-sulfonamidyl-4-Thiazolidinone Derivatives and Their Biological Evaluation", *New Journal of Chemistry* 40 (2016): 3047–3058; (f) D. D. Subhedar, M. H. Shaikh, L. Nawale, A. Yeware, D. Sarkar, and B. B. Shingate, "[Et₃NH][HSO₄] Catalyzed Efficient Synthesis of 5-Arylidene-Rhodanine Conjugates and Their Antitubercular Activity", *Research on Chemical Intermediate* 42 (2016): 6607–6626; (g) D. D. Subhedar, M. H. Shaikh, A. A. Nagargoje, S. V. Akolkar, S. G. Bhansali, D. Sarkar and B. B. Shingate, "Amide-Linked Monocarbonyl Curcumin Analogues: Efficient Synthesis, Antitubercular Activity and Molecular Docking Study", *Polycyclic Aromatic Compounds* (2020).
30. (a) C. Mukhopadhyaya, P. Das and R. J. Butcher, "An Expeditious and Efficient Synthesis of Highly Functionalized [1,6]-Naphthyridines Under Catalyst-Free Conditions in Aqueous Medium", *Organic Letters*, 13, no. 17 (2011): 4664–4667; (b) A. M. A. Hameed, "Rapid Synthesis of 1,6-Naphthyridines by Grindstone Chemistry", *Environmental Chemistry Letters* 13 (2015): 125–129; (c) P. Das, T. Chaudhuri, and C. Mukhopadhyaya, "Pseudo-Five-Component Domino Strategy for the Combinatorial Library Synthesis of [1,6] Naphthyridines-an on-Water Approach" *ACS Combinatorial Science*, 16 (2014): 606–613.
31. (a) *Schrodinger Suite 2015-4 QM-Polarized Ligand Docking protocol; Glide version 6.9* (Schrodinger, LLC: New York, NY, 2006); *Jaguar version 9.0* (Schrodinger, LLC: New York, NY, 2015); *QSite version 6.9* (Schrodinger, LLC: New York, NY, 2015); (b) R. A. Friesner, R. B. Murphy, M. P. Repasky, L. L. Frye, J. R. Greenwood, T. A. Halgren, P. C. Sanschagrin and D. T. Mainz, "Extra Precision Glide: Docking and Scoring Incorporating a Model of Hydrophobic Enclosure for Protein-Ligand Complexes," *Journal of Medicinal Chemistry*, 49, no. 21 (2006): 6177–6196.
32. X. Qiu, C. A. Janson, W. W. Smith, M. Head, J. Lonsdale, and A. K. Konstantinidis, "Refined Structures of Beta-Ketoacyl-Acyl Carrier Protein Synthase III," *Journal of Molecular Biology* 307, no. 1 (2001): 341–56.
33. NCCLS (National Committee for Clinical Laboratory Standards), Performance standards for antimicrobial susceptibility testing: twelfth informational supplement, 2002, 1-56238-454-6 M100-S12(M7).
34. M. Burits, and F. Bucar, "Antioxidant Activity of Nigella Sativa Essential Oil," *Phytotherapy Research* 14, no. 5 (2000): 323–8.



35. C. A. Lipinski, L. Lombardo, B. W. Dominy, and P. J. Feeney, "Experimental and Computational Approaches to Estimate Solubility and Permeability in Drug Discovery and Development Settings," *Advanced Drug Delivery Reviews* 46, no. 1–3 (2001): 3–26.
36. Molinspiration Chemoinformatics Brastislava, Slovak Republic, Available from: <http://www.molinspiration.com/cgi-bin/properties>; 2014.
37. Y. H. Zhao, M. H. Abraham, J. Le, A. Hersey, C. N. Luscombe, G. Beck, B. Sherborne, and I. Cooper, "Rate Limited Steps of Human Oral Absorption and QSAR Studies," *Pharmaceutical Research* 19, no. 10 (2002): 1446–57.
38. Drug-likeness and molecular property prediction, available from: <http://www.molsoft.com/mprop/>
39. P. Ertl, B. Rohde, and P. Selzer, "Fast Calculation of Molecular Polar Surface Area as a Sum of Fragment-Based Contributions and Its Application to the Prediction of Drug Transport Properties," *Journal of Medicinal Chemistry* 43, no. 20 (2000): 3714–7.


Synthesis and Biological Evaluation of Novel Asymmetric (*E*)-3-(4-(Benzyloxy) Phenyl)-2-((Substituted Benzylidene) Amino)-1-(Thiazolidin-3-yl) Propan-1-One and Computational Validation by Molecular Docking and QSTR Studies

Amit A. Pund, Suresh T. Gaikwad, Mazahar Farooqui, Rajashri A. Pund-Nale, Mubarak H. Shaikh & Baban K. Magare


To cite this article: Amit A. Pund, Suresh T. Gaikwad, Mazahar Farooqui, Rajashri A. Pund-Nale, Mubarak H. Shaikh & Baban K. Magare (2022): Synthesis and Biological Evaluation of Novel Asymmetric (*E*)-3-(4-(Benzyloxy) Phenyl)-2-((Substituted Benzylidene) Amino)-1-(Thiazolidin-3-yl) Propan-1-One and Computational Validation by Molecular Docking and QSTR Studies, Polycyclic Aromatic Compounds, DOI: [10.1080/10406638.2022.2046615](https://doi.org/10.1080/10406638.2022.2046615)

To link to this article: <https://doi.org/10.1080/10406638.2022.2046615>

 View supplementary material 

 Published online: 15 Mar 2022.





 Submit your article to this journal 

 View related articles 

 View Crossmark data 



Synthesis and Biological Evaluation of Novel Asymmetric (*E*)-3-(4-(Benzyloxy) Phenyl)-2-((Substituted Benzylidene) Amino)-1-(Thiazolidin-3-yl) Propan-1-One and Computational Validation by Molecular Docking and QSTR Studies

Amit A. Pund^a , Suresh T. Gaikwad^b, Mazahar Farooqui^c , Rajashri A. Pund-Nale^d, Mubarak H. Shaikh^e , and Baban K. Magare^a 

^aUG, PG and Research Centre, Department of Chemistry, Shivaji Arts, Commerce and Science College Kannad, Dist. Aurangabad, Maharashtra, India; ^bDepartment of Chemistry, Dr. Babasaheb Ambedkar Marathwada University, Aurangabad, Maharashtra, India; ^cPost Graduate and Research Centre, Maulana Azad College of Arts, Science and Commerce, Aurangabad, Maharashtra, India; ^dDepartment of Zoology, Bhaskar Pandurang Hivale Education Society's Ahmednagar College, Ahmednagar, Maharashtra, India; ^eP.G. and Research, Department of Chemistry, Radhabai Kale Mahila Mahavidyalaya, Ahmednagar, Maharashtra, India

ABSTRACT



A novel series of asymmetric of (*E*)-3-(4-(benzyloxy) phenyl)-2-((substituted benzylidene) amino)-1-(thiazolidin-3-yl) propan-1-one derivatives (**AAP-1** to **AAP-10**) have been efficiently synthesized from (*S*)-2-amino-3-(4-(benzyloxy)phenyl)-1-(thiazolidin-3-yl)propan-1-one (**4**) and various substituted aldehydes by conventional as well as microwave irradiation method. The structure of newly synthesized compounds were confirmed by IR, ¹H NMR, ¹³C NMR, and Mass spectroscopic methods, further evaluated for their *in vitro* antimicrobial activities. Among these series, the compounds **AAP-2**, **AAP-4**, **AAP-5**, **AAP-7**, **AAP-8**, **AAP-9**, and **AAP-10**, showed excellent anti-bacterial activities against Gram-positive bacteria like *Staphylococcus aureus* (SA), *Lysinibacillus sphaericus* (LS), *Bacillus subtilis* (BS) and *Klebsiella aerogenes* (KA), *Pseudomonas Aeruginosa* (PA), *Chromobacterium violaceum* (CV) as Gram-negative bacteria as compared to standard Ciprofloxacin. The compounds **AAP-1**, **AAP-4**, **AAP-5**, **AAP-6**, **AAP-7**, and **AAP-8** exhibited good antifungal activities against *Fusarium oxysporum* (FO), *Rhizoctonia solani* (RS), *Colletotrichum capsici* (CC) strains as compared to standard Fluconazole. Molecular docking studies of final compounds were performed using Auto Dock Vina software against Lanosterol 14 α -demethylase (CYP51A1) enzyme and crystal 4WMZ and showed effective binding affinity of these molecules with enzymes. Quantitative structure toxicity relationship study of target compounds were studied by various computational animal models and defined oral rat LD₅₀ values for cytotoxicity. The **AAP-2**, **AAP-4**, **AAP-5**, and **AAP-7** to **AAP-10** showed low toxicity. In addition, the pharmacokinetic of target compounds were studied and revealed acceptable good drug-likeness score properties as well as follow Lipinski's rule of five.


ARTICLE HISTORY

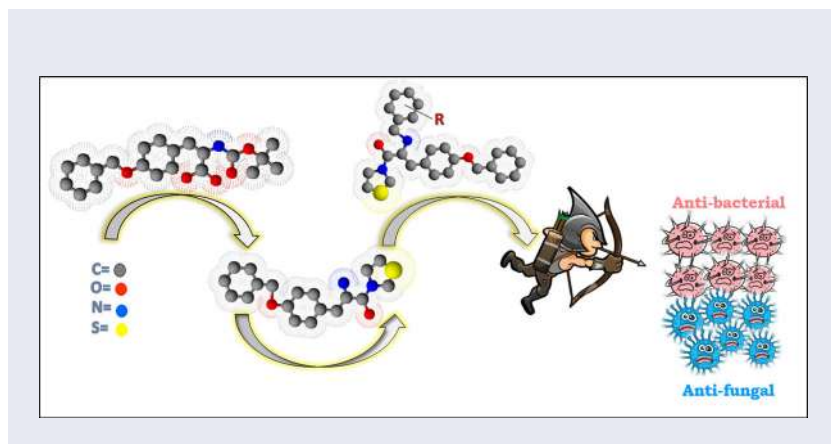
Received 15 March 2021
Accepted 16 February 2022

KEYWORDS

1,3-thiazolidine; antimicrobial; microwave irradiation; oral rat LD₅₀; molecular docking

CONTACT Baban K. Magare  magrebk75@gmail.com  UG, PG and Research Centre, Department of Chemistry, Shivaji Arts, Commerce and Science College, Kannad. Dist. Aurangabad, Maharashtra 431103, India.

 Supplemental data for this article can be accessed online at <https://doi.org/10.1080/10406638.2022.2046615>



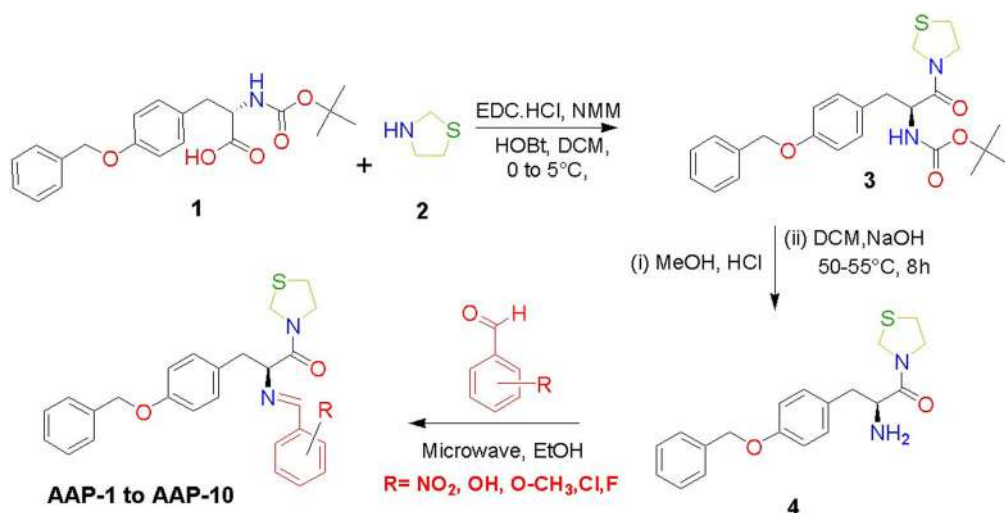
Introduction

The synthesis of novel agents to combat resistant bacteria and fungi has become one of the most important areas of antimicrobial research today.¹ Due to generic mutation, microorganisms become resistant to all standard antibiotic drugs and could only be treated with potentially active drugs. The 1,3-thiazolidine is an important class of heterocyclic compounds and its composites are key components of many drugs and present in natural products. This moiety is core part of magnificent antibiotics drugs like antibiotic penicillin and Tenepliptin (Figure 1).²

It is noteworthy that the 1,3-thiazolidine is exhibited potent activity against Gram-positive pathogens like *Staphylococci*, *Enterococci*, and *Streptococci*.³ The mechanism of action perceived that, thiazolidine bound to the bacterial sub units of 50S ribosomal and inhibition of the 70S ribosomal initiation complex formations.⁴ Furthermore positive charge on nitrogen atom of 1,3-thiazolidine ring tends to protonate and would be expected to play a significant role on the inhibition of viral or cellular enzymes, which are essential for viral imitation.⁵ Recently, the 1,3-thiazolidine ring containing heterocyclic compounds have been reported as antifungal,⁶ antimalarial,⁷ anti-HIV,⁸ anticancer,⁹ antiviral,¹⁰ antitubercular,¹¹ and antimicrobial.¹²⁻¹⁵ The diverse pharmaceutical activities of 1,3-thiazolidine have received the attention and incorporated with other functionality. In addition, tyrosine amino acid is a key neurotransmitter like epinephrine, norepinephrine, dopamine, and used as a starting material for many reactions due to easy availability and low cost. The importance of tyrosine compound has been described by James et al. and reported the structure-activity relationships of tyrosine-based inhibitors of autotaxin (ATX).¹⁶ Furthermore, the azomethine group has attracted significant attention due to their wide diversity in medical implications. It has been synthesized via condensation of primary amines with active carbonyl compounds. Many Schiff bases have been reported to possess significant biological properties such as antimicrobial,^{17,18} antibacterial,¹⁹ antifungal,²⁰ antitumor,²¹ anti-inflammatory,²² anti-HIV,²³ anticonvulsant,²⁴ anticancer,²⁵ anti-malarial,²⁶ antiviral,²⁷ and analgesic.²⁸



Figure 1. Thiazolidine moiety containing marketed drugs.



Scheme 1. Synthetic scheme of target compounds (AAP-1 to AAP-10).

This observations enforced us to design and synthesis a small library of the Schiff bases containing thiazolidine ring from Boc-O-benzyl-L-tyrosine (**1**) in three steps. The coupling of 1,3-thiazolidine with substituted carboxylic acid was reported by using bromo tripyrrolidine phosphonium hexafluorophosphate,²⁹ *N,N*-dicyclohexyl carbodiimide (DCC) and 4-dimethylaminopyridine (DMAP) as coupling agents in dimethylformamide solvent^{30,31} whereas *N*-(3-Dimethylaminopropyl)-*N*-ethylcarbodiimide hydrochloride (EDC.HCl), *N*-methylmorpholine (NMM), hydroxybenzotriazole (HOBT) in different solvents.^{32,33} The boc deprotection of amines were carried out using trifluoroacetic acid, hydrogen bromide, tetra-*n*-butyl ammonium fluoride, boron trifluoride etherate and hydrochloric acid.³⁴ The formation of Schiff base derivatives were reported by condensation of aldehydes and amines acidic condition by using conventional method in 1948.³⁵

In view of continuous efforts on design and synthesis of biologically active molecules, we herein reported the efficient synthesis of novel series of asymmetric of (*E*)-3-(4-(benzyloxy)-phenyl)-2-((substituted-benzylidene)-amino)-1-(thiazolidin-3-yl) propan-1-one derivatives (**AAP-1** to **AAP-10**) by the reaction of novel amine and various substituted aromatic aldehydes by conventional as well as microwave irradiation methods.³⁶ Further, these compounds have been evaluated for their antimicrobial activities. In addition, the quantitative structure toxicity relationship (QSTR) as well as molecular docking study were carried out for better understanding of effective binding. Furthermore, *in silico* ADME predictions for good drug like properties of newly synthesized compounds were studied.

Results and discussion

Chemistry

Amide coupling of 1,3-thiazolidine and *N*-boc-O-benzyl-L-tyrosine (**1**) was carried out using EDC.HCl and HOBT in DCM with NMM as base (Scheme 1). The obtained crude product was crystallized using IPE to afford pure *S*-tert-butyl-3-(4-(benzyloxy) phenyl)-1-oxo-1-(thiazolidin-3-yl) propan-2-ylcarbamate (**3**) with excellent yield (95%). In next stage novel amine **4** was obtained by boc deprotection of **3** using aqueous hydrochloric acid solution. Finally targeted compounds were achieved by condensation of amine **4** with various substituted aromatic aldehydes under microwave irradiation at 560 W for 2–3 min with excellent yield of 92–98%. The purity and

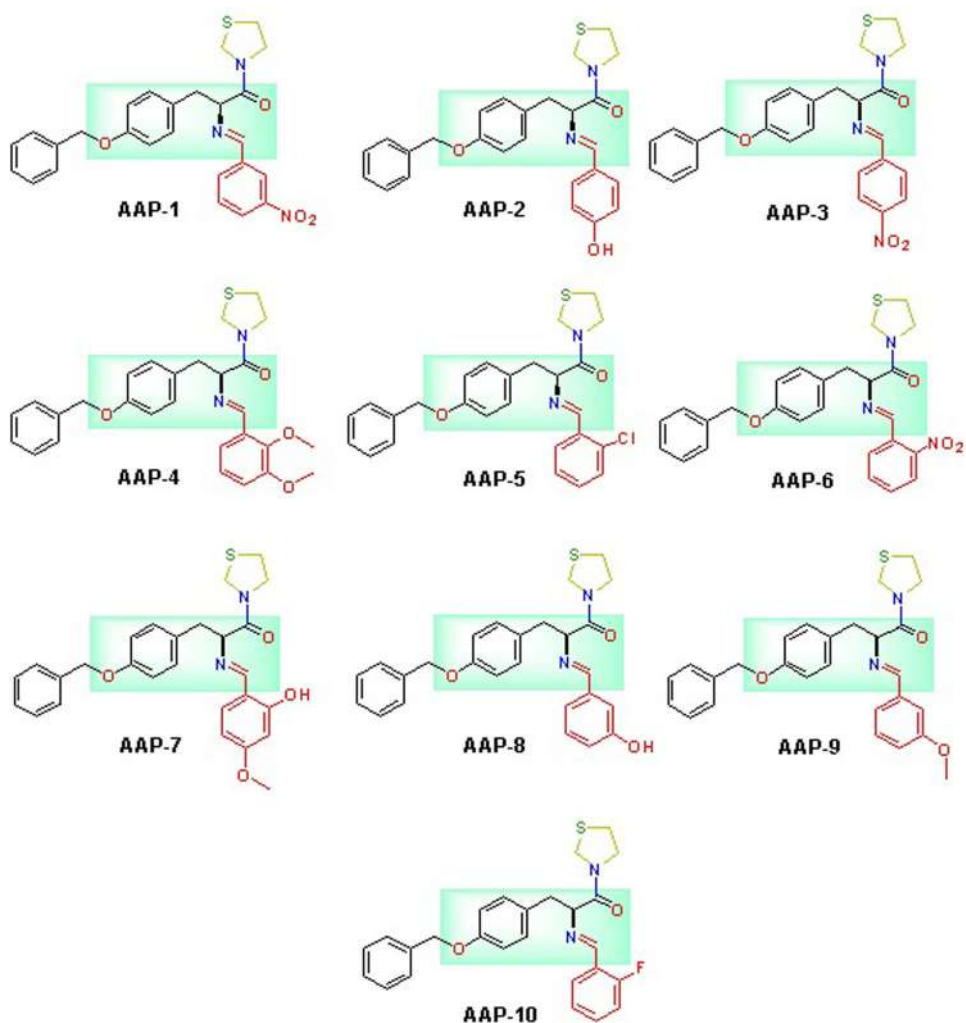


Figure 2. The structural representation of synthesized compounds.

identity were unambiguously established with the help of elemental analysis, ^1H NMR, ^{13}C NMR, mass spectroscopy, and FTIR. The structures of the novel derivatives are shown in [Figure 2](#).

Biological evaluation

Antibacterial activity

The ready-made Tryptic soya broth and Malt extract broth medium were used for antibacterial activity.³⁷ The final compounds were tested against *Staphylococcus aureus* (SA), *Lysinibacillus sphaericus* (LS), *Bacillus subtilis* (BS) (Gram-positive bacteria), and *Klebsiella aerogenes* (KA), *Pseudomonas Aeruginosa* (PA), *Chromobacterium violaceum* (CV) (Gram-negative bacteria). The results of MIC for antibacterial activity of targeted compounds were showed in [Table 1](#). The AAP-2, AAP-4, AAP-5, AAP-7, AAP-8, AAP-9, and AAP-10 title compounds which has hydroxyl, methoxy, chloro, fluoro functional groups showed good to excellent MIC activity against Gram-negative bacteria and Gram-positive bacteria, conversely the compounds AAP-1,

Table 1. Antibacterial activity of target compounds.

Compounds	MIC in $\mu\text{g/mL}$					
	Gram -ve bacteria			Gram + ve bacteria		
	<i>K. A.</i>	<i>P. A.</i>	<i>C. V.</i>	<i>S. A.</i>	<i>L. S.</i>	<i>B. S.</i>
AAP-1	38	40	41	35	40	30
AAP-2	20	21	17	27	20	18
AAP-3	35	36	30	39	37	29
AAP-4	19	20	20	28	20	17
AAP-5	19	19	18	27	21	18
AAP-6	35	41	26	31	26	22
AAP-7	18	19	17	29	23	20
AAP-8	19	22	18	28	21	19
AAP-9	20	20	16	26	21	21
AAP-10	21	19	17	28	22	19
Ciprofloxacin	22	23	19	29	23	21

K.A.: *Klebsiella aerogenes*; *P.A.*: *Pseudomonas Aeruginosa*; *C.V.*: *Chromobacterium violaceum*; *S.A.*: *Staphylococcus aureus*; *L.S.*: *Lysinibacillus sphaericus*; *B.S.*: *Bacillus subtilis*. Negative control (Dimethyl sulfoxide) – no activity. Values are indicated in $\mu\text{g/mL}$.

Table 2. Antifungal activity of target compounds.

Compounds	Minimum inhibitory concentration in $\mu\text{g/mL}$ (MIC)		
	<i>F.O.</i>	<i>R. S.</i>	<i>C. C.</i>
AAP-1	17	14	15
AAP-2	21	18	17
AAP-3	26	23	29
AAP-4	19	14	15
AAP-5	15	13	17
AAP-6	18	15	15
AAP-7	19	15	16
AAP-8	18	14	15
AAP-9	19	15	18
AAP-10	19	16	17
Fluconazole	19	15	17

F.O.: *Fusarium oxysporum*; *R.S.*: *Rhizoctonia solani*; *C.C.*: *Colletotrichum capsici*. Negative control (Dimethyl sulfoxide) – no activity. Values are indicated in $\mu\text{g/mL}$.

AAP-3, and AAP-6 which has nitro substituent at *meta*, *para* and *ortho* position, respectively, on the benzene ring showed lower activity as compared to Ciprofloxacin as reference drug (Table 1).

Antifungal activity

The ready-made Muller Hinton agar medium used for evaluation of antifungal activities,³⁸ *Fusarium oxysporum* (FO), *Rhizoctonia solani* (RS), *Colletotrichum capsici* (CC) were used as fungal pathogens. The results of antifungal activities of targeted compounds were showed in Table 2. The compounds AAP-1, AAP-4, AAP-5, AAP-6, AAP-7, and AAP-8 showed good antifungal activity as compared to standard Fluconazole drug. The good and enhanced antibacterial and antifungal activities of title compounds may be attributed due to the presence of 1,3-thiazolidine incorporated with imine moiety and different functional groups.

QSTR study

The QSTR study of new compounds were carried out with the help of Toxicity Estimation Software Tool (T.E.S.T). In 2005, according to Hodge and Sterner³⁹ toxicity scale predicted on

Table 3. Hodge and Sterner scale for LD₅₀ (Oral, Rat, mg/kg) toxicity.

Sr. No.	Term for toxicity	LD ₅₀ (Rat, Oral) Value in mg/kg
1	Extremely toxic	>1
2	Highly toxic	1 to 50
3	Moderately toxic	50 to 500
4	Slightly toxic	500 to 5000
5	Practically nontoxic	5000 to 15,000

Table 4. QSTR derived Oral Rat LD₅₀ value for target compounds.

Compound	Predicted LD50 (Oral, Rat, mg/kg) in male rat	Oral rat LD ₅₀ - Log10 (mol/kg) in male rat	Result
AAP-1	1<	1<	Extremely toxic
AAP-2	1503.16	2.47	Slightly toxic
AAP-3	1<	1<	Extremely toxic
AAP-4	1406.88	2.54	Slightly toxic
AAP-5	1259.89	2.57	Slightly toxic
AAP-6	1<	1<	Extremely toxic
AAP-7	1564.37	2.48	Slightly toxic
AAP-8	1509.77	2.47	Slightly toxic
AAP-9	1454.99	2.50	Slightly toxic
AAP-10	1244.84	2.56	Slightly toxic

the basis of LD₅₀ (Oral, Rat, mg/kg) and showed in Table 3. Predicted Oral rat LD₅₀ values of final compounds were calculated from consensus method and showed in Table 4.

The LD 50 values calculated by following arithmetic method

n = total number of animal in a group.

a = the difference between two successive doses of administered extract/substance.

b = the average number of dead animals in two successive doses.

LD₁₀₀ = Lethal dose causing the 100% death of all test animals.

The results of oral rat LD₅₀ showed that the compounds **AAP-2**, **AAP-4**, **AAP-7**, **AAP-8**, **AAP-9**, and **AAP-10** has slight toxicity. It is revealed that the compounds with nitro group at ortho, meta, and para position on benzene ring (**AAP-1**, **AAP-3**, and **AAP-6**) possess extreme toxicity.

Computational study

Molecular docking

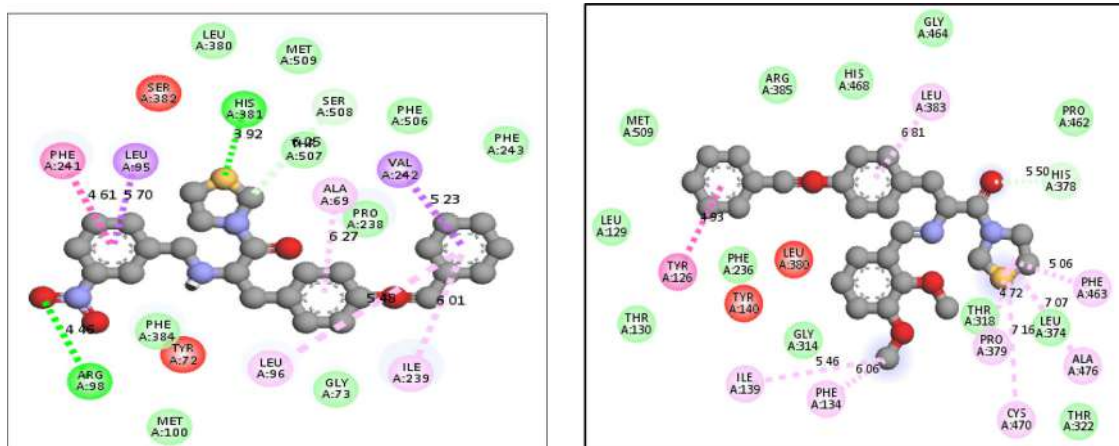
Molecular docking was performed to evaluate the antifungal activity of target compounds by using Auto Dock Vina (<http://vina.scripps.edu>) software.⁴⁰ Before screening the biologically activity, the molecular docking study was carried out by using a crystal 4WMZ is a chain structure of Baker's yeast and whose ligand is fluconazole and protein Lanosterol 14 α -demethylase (CYP51A1) enzyme which is the class of cytochrome P450 superfamily of enzymes. The molecular docking results of target compounds are summarized in Table 5.

Molecular docking study showed that designed compounds fit in the active site cavity of CYP51A1 occupying energetically favorable position to the co-crystallized ligand. The binding affinities were co-related well with the experimentally observed antifungal activity and found that there is good agreement between the values. All the newly synthesized compounds revealed effective interaction between active sites and proteins. The compound **AAP-1** exhibited highest binding affinity (-10.3) whereas **AAP-4** showed lowest binding affinity (-8.1).

The binding affinity indicates that, there is highest binding affinity towards amino acids due to excellent binding at nitrogen and oxygen sites. The representative molecular docking of **AAP-1** and **AAP-4** are showed in Figure 3.

Table 5. Molecular docking results of target compounds.

Compound	Binding affinity	rmsd/		Binding with amino acids		
		ub	rmsd/lb	Hydrogen bond	Hydrophobic interaction	π - π cation- π
AAP-1	-10.3	15.038	11.951	HIS 381, ARG 98	ILE 239, LEU 96, ALA 69, PHE 241, SER 508	VAL 242, LEU 95.
AAP-2	-8.8	17.261	14.096	ARG 385	LYS 151, ILE 139, CYS 470, PHE 463, ALA 747, PRO 379	VAL 311, LEU 383
AAP-3	-9.2	17.335	11.608	ARG 98, HIS 381	LEU 95, ALA 69, LEU 380, PRO 238,	MET 509, PHE 241
AAP-4	-8.1	13.166	10.491	ILE 139, PHE 134	PHE 463, ALA 47, CYS 470, PRO 379,	TYR 126, LEU 383
AAP-5	-9.5	14.238	9.478	PRO 238	PH241, TYR 126	MET 509, LEU 95
AAP-6	-9.6	8.188	3.606	LYS 151, HIS 468	HIS 378, LEU 380, LEU 383, LYS 151	TYR 126
AAP-7	-8.5	6.221	3.378	PHE 506	ILE 239, PRO 238, MET 509, TYR 126, PHE 384, ALA 125, PHE 241	PH 241, TYR 7, LEU 95
AAP-8	-10.1	6.381	2.422	GLY 47, PRO 462	CYC 470, ILE 139, LYS 151, VAL311, LEU 158, ALA 47, PRO 37	CYS 470
AAP-9	-8.2	1.933	1.481	ILE 139, PHE 134.	PHE 463, ALA 47, CYS 470, PRO 379,	TYR 126, LEU 383
AAP-10	-9.5	7.626	3.660	HIS 381, TYR 507	TYR 126, PRO 238, PHE 241	MET 590, LEU 95.

**Figure 3.** The representative molecular docking of AAP-1 and AAP-4.

The effective interaction between hydrogen bonding, hydrophobic and π - π interaction with amino acid are represented in Figure 3.

In silico ADME prediction

It's very prime task in medicinal chemistry to predict early the drug likeness properties, because it resolves the cost and time of drug development and discovery. Though most of compounds have significant biological activities, have failed in their clinical trials due to the inadequate drug likeness properties. On the basis of Lipinski's rule of five, the drug likeness properties were analyzed by ADME parameters using mol inspiration online property calculation toolkit.⁴¹

All the newly synthesized compounds exhibited significant values for the various parameters analyzed and showed good drug-like characteristics based on Lipinski's rule of five and characterized to be likely orally active. None of the synthesized compounds violated the Lipinski's rule of five and results were within the range of accepted values. The parameters like the number of rotatable bonds and total polar surface area are linked with the intestinal absorption, results showed that all synthesized compounds were good absorption. The *in silico* assessment emphasizes to be good pharmacokinetic properties, which is reflected in their physicochemical values, thus, ultimately enhancing pharmacological properties of these molecules.

Table 6. Pharmacokinetic parameters of **AAP-1 to AAP-10** compounds.

Entry	% ABS	TPSA (Å ²)	n-ROTB	MV	MW	miLog <i>P</i>	n-ON	n-OHNNH	Lipinski violation	Drug-likeness model score
Rule	–	–	–	–	<500	≤5	<10	<5	≤1	–
AAP-1	78.7	87.7	9	422.3	475.6	4.88	7	0	0	–0.60
AAP-2	87.6	62.1	8	407.0	446.6	4.46	5	1	0	–0.08
AAP-3	78.7	87.7	9	422.3	475.6	4.90	7	0	0	–0.74
AAP-4	88.2	60.4	10	450.1	490.6	4.76	6	0	0	0.24
AAP-5	94.5	41.9	8	412.5	465.0	5.57	4	0	1	–0.18
AAP-6	78.7	87.7	9	422.3	475.6	4.85	7	0	0	–0.88
AAP-7	84.4	71.4	9	432.6	476.6	4.91	6	1	0	–0.06
AAP-8	87.6	62.1	8	407.0	446.6	4.44	5	1	0	0.07
AAP-9	91.3	51.1	9	424.5	460.6	4.97	5	0	0	–0.13
AAP-10	94.5	41.9	8	403.9	448.6	5.06	4	0	1	–0.39

% ABS: Percentage absorption, TPSA: Topological polar surface area, n-ROTB: Number of rotatable bonds, MV: Molecular volume, MW: Molecular weight, miLog *P*: Logarithm of partition coefficient of compound between n-Octanol and water, n-ON Acceptors: Number of hydrogen bond acceptors, n-OHNNH donors: Number of hydrogen bonds donors.

In present study, we have calculated molecular volume (MV), molecular weight (MW), logarithm of partition coefficient (miLog *P*), number of hydrogen bond acceptors (n-ON), number of hydrogen bonds donors (n-OHNNH), topological polar surface area (TPSA), number of rotatable bonds (n-ROTB), and Lipinski's rule of five using Molinspiration online property calculation toolkit. Absorption (% ABS) was calculated by: % ABS = 109 – (0.345 × TPSA). Drug-likeness model score (a collective property of physic-chemical properties, pharmacokinetics and pharmacodynamics of a compound is represented by numerical value) was computed by MolSoft software (Table 6).

Conclusion

In summary, we designed and synthesized the new 1, 3-thiazolidine based (*E*)-3-(4-(benzyloxy) phenyl)-2-((substituted benzylidene) amino)-1-(thiazolidin-3-yl) propan-1-one derivatives from novel (*S*)-2-amino-3-(4-(benzyloxy)phenyl)-1-(thiazolidin-3-yl)propan-1-one (**4**) and different substituted aldehydes using microwave irradiation at 560 W. The structures were confirmed by IR, Mass, ¹H NMR, and ¹³C NMR spectroscopic methods. It is seen that **AAP-4**, **AAP-5**, **AAP-7**, and **AAP-8** displayed excellent antibacterial and antifungal activities. Moreover, the molecular docking was carried out with crystal 4WMZ and enzyme CYP51A1 by using Auto Dock software and study revealed that compounds **AAP-1** showed highest binding affinity (–10.3) whereas **AAP-4** showed lowest binding affinity (–8.1). These studies revealed that there is good agreement with experimental antifungal activity results. In addition, the QSTR study showed that **AAP-2**, **AAP-4**, **AAP-5**, and **AAP-7** to **AAP-10** compounds have slight toxicity. Further analysis of the ADME parameters predicted good drug like properties and can be developed as oral drug candidate. All these results suggested that the new compounds have potent antimicrobial activity and can be further optimized as a lead molecule.

Experimental

General

General procedure synthesis of (*S*)-*tert*-butyl-3-(4-(benzyloxy) phenyl)-1-oxo-1-(thiazolidin-3-yl) propan-2-ylcarbamate (**3**)

To a stirred mixture of (*S*)-2-[(2-methylpropan-2-yl)oxycarbonylamino]-3-(4-phenylmethoxyphenyl)propanoic acid (**1**) (50 g, 0.135 mol) and 1,3-thiazolidine (**2**) (13.2 g, 0.148 mol) in DCM (250 mL), HOBt (0.91 g, 0.007 mol) followed by *N*-methylmorpholine (20.4 g, 0.202 mol) were added at 0–5 °C and stirred for 10 min. EDC.HCl (33.6 g, 0.175 mol) was added lot wise and

stirred for 3.0 h at 5–10 °C. Progress of reaction was monitored by TLC (DCM: MeOH:: 9:1). After reaction completion, water (250 mL) was added to quench and extracted with DCM. The organic layer was washed with 10% brine solution (250 mL) and concentrated under vacuum. The residue treated with IPE (200 mL), filtrated and dried to obtain compound (**3**) as white solid. (56.6 g, 95%); M.P.: 184–186 °C. IR (KBr, ν_{\max} , cm^{-1}): 695.92 (C-S), 1172.11 (C-O), 1239.73 (C-N), 1444.55 (C=C), 2911.63 and 2883.20 (H-C-C=O), 3382.03 (N-H). ^1H NMR (400 MHz, DMSO- d_6 , δ ppm): 7.41–7.31 (m, 5H, Ar-H), 7.10–7.08 (d, 2H, $J=8$ Hz, Ar-H), 6.89–6.87 (d, 2H, $J=8$ Hz, Ar-H), 5.14 (s, 3H, O-CH₂-Ar and NH-Boc), 4.74–4.72 (t, 1H, $J=4$ Hz, N-CH), 4.36 (s, 3H, N-CH₂-S of thiazolidine), 3.63–3.61 (t, 2H, $J=4$ Hz, N-CH₂ of thiazolidine), 3.16–3.13 (dd, 1H, $J=4$ Hz, 8 Hz, CH₂-Ar), 2.96–2.94 (t, 2H, $J=4$ Hz, S-CH₂ of thiazolidine), 2.87–2.84 (dd, 1H, $J=4$ Hz, 8 Hz, CH₂-Ar), 1.39 (s, 9H, Boc). ^{13}C -NMR (125 MHz, DMSO- d_6 , δ ppm): 170.54, 159.23, 157.53, 140.94, 133.55, 129.07, 127.41, 114.87, 77.08, 69.92, 56.12, 55.83, 54.12, 38.71, 28.81. ES-MS m/z 443.3 (M+H)⁺. Analytical calculated formula for C₂₄H₃₀N₂O₄S; C, 65.13; H, 6.83; N, 6.33; O, 14.46; S, 7.25; Found: C, 65.14; H, 6.82; N, 6.34; S, 7.24.

General procedure for synthesis of (S)-2-amino-3-(4-(benzyloxy)phenyl)-1-(thiazolidin-3-yl)propan-1-one (4**)**

The (S)-tert-butyl-3-(4-(benzyloxy)phenyl)-1-oxo-1-(thiazolidin-3-yl)propan-2-ylcarbamate (**3**) (55 g, 0.123 mol) and 15% aqueous hydrochloric acid solution (165 mL) in methanol (165 mL) was stirred at 50–55 °C for 8 h. Progress of reaction was monitored by TLC (DCM: MeOH: : 9:1). After reaction completion, water (550 mL) and DCM (220 mL) were added. The aqueous layer was collected in round bottom flask and product is extracted in DCM (275 mL) after adjusting pH 9–9.5 by using 10% aqueous sodium hydroxide solution. The organic layer was washed with 10% sodium chloride solution (275 mL) and concentrated under vacuum to obtain compound (**4**) as brown color thick sirup. (38 g, 90%); M.P.: 153–156 °C. IR (KBr, ν_{\max} , cm^{-1}): 697.35 (C-S), 1177.79 (C-O), 1241.35 (C-N), 1455.76 (C=C), 2924.73 and 3030.45 (H-C-C=O), 3646.81 (N-H). ^1H NMR (400 MHz, DMSO- d_6 , δ ppm): 7.41–7.32 (m, 5H; Ar-H), 7.11–7.09 (d, 2H, $J=8$ Hz, Ar-H), 6.89–6.87 (d, 2H, $J=8$ Hz, Ar-H), 5.14 (s, 2H, O-CH₂-Ar-H), 4.74–4.72 (t, 1H, $J=4$ Hz, N-CH), 4.37 (s, 2H, N-CH₂-S of thiazolidine), 3.64–3.62 (t, 2H, $J=4$ Hz, N-CH₂ of thiazolidine), 3.15–3.12 (dd, 1H, $J=4$ Hz, 8 Hz, CH₂-Ar), 2.97–2.95 (t, 2H, $J=4$ Hz, S-CH₂ of thiazolidine), 2.88–2.85 (dd, 1H, $J=4$ Hz, 8 Hz, CH₂-Ar), 2.19 (s, 2H, NH₂). ^{13}C -NMR (125 MHz, DMSO- d_6 , δ ppm): 171.94, 159.26, 141.24, 133.57, 129.09, 127.44, 114.78, 78.10, 56.05, 55.13, 54.01, 39.00. ES-MS m/z 343.2 (M+H)⁺. Analytical calculated formula for C₂₄H₃₀N₂O₄S; C, 65.13; H, 6.83; N, 6.33; O, 14.46; S, 7.25; Found: C, 66.66; H, 6.47; N, 8.19; S, 9.37.

General procedure for the synthesis compounds AAP-1 to AAP-10

To a 25 mL single neck round bottom flask, the (S)-2-amino-3-(4-(benzyloxy) phenyl)-1-(thiazolidin-3-yl) propan-1-one (**4**) (1.0 eq.) and aromatic aldehyde (0.98 eq.) in ethanol (5.0 times) were put in microwave reaction vessel equipment with magnetic stirrer and irradiated at 560 W for 2–3 min.³⁶ The reaction was monitored by TLC (DCM: MeOH: : 9:1). After completion of reaction, the cold water was added (20 times) in reaction mixture. The product was then extracted with DCM (5 times). The organic layer washed with 2% aqueous hydrochloric acid solution (3 times) and concentrated under vacuum and residue was allowed to suspend in IPE. It is, then, filtered and purified by column chromatography (mobile phase: Ethyl acetate: hexane: : 1:9) to obtain compounds **AAP-1** to **AAP-10**.

Characterization of synthesized compounds (AAP-1 to AAP-10)**(E)-2-(3-nitrobenzylideneamino)-3-(4-(benzyloxy)phenyl)-1-(thiazolidin-3-yl)propan-1-one**

(AAP-1): White solid; (1.32 g, 95%); M.P.: 100–104 °C. IR (KBr, ν_{\max} , cm^{-1}): 696.89 (C-S), 1174.17 (C-O), 1243.92 (C-N), 1366.41 & 1509.48 (NO_2), 1417.72 (C=C), 1638.52 (C=N), 2931.43 and 2766.70 (H-C-C=O). ^1H NMR (400 MHz, DMSO- d_6 , δ ppm): 8.55 (s, 1H, Ar-H of 3-nitrobenzene), 8.26–8.25 (d, 1H, $J=4$ Hz, Ar-H of 3-nitrobenzene), 8.04 (s, 1H, N=CH), 8.02–8.01 (d, 1H, $J=4$ Hz, Ar-H of 3-nitrobenzene), 7.56–7.54 (t, 1H, $J=4$ Hz, Ar-H of 3-nitrobenzene), 7.42–7.31 (m, 5H, Ar-H), 7.11–7.09 (d, 2H, $J=8$ Hz, Ar-H), 6.88–6.86 (d, 2H, $J=8$ Hz, Ar-H), 5.04 (s, 2H; O- CH_2 -Ar), 4.64–4.62 (t, 1H, $J=4$ Hz, N-CH), 4.46 (s, 2H, N- CH_2 -S of thiazolidine), 3.63–3.61 (t, 2H, $J=4$ Hz, N- CH_2 of thiazolidine), 3.16–3.13 (dd, 1H, $J=4$ Hz, 8 Hz, CH_2 -Ar), 2.96–2.94 (t, 2H, $J=4$ Hz, S- CH_2 of thiazolidine), 2.87–2.84 (dd, 1H, $J=4$ Hz, 8 Hz, CH_2 -Ar). ^{13}C -NMR (125 MHz, DMSO- d_6 , δ ppm): 169.45, 160.41, 157.23, 148.58, 140.94, 139.58, 137.28, 135.02, 130.85, 129.07, 128.59, 128.00, 127.41, 123.99, 114.87, 73.87, 69.93, 49.12, 48.05, 38.71, 31.31. ES-MS m/z 477.3 ($\text{M} + \text{H}$) $^+$. Analytical calculated formula for $\text{C}_{26}\text{H}_{25}\text{N}_3\text{O}_4\text{S}$: C, 65.67; H, 5.30; N, 8.84; O, 13.46; S, 6.74; Found: C, 65.68; H, 5.30; N, 8.83; S, 6.73.

(E)-2-(4-hydroxybenzylideneamino)-3-(4-(benzyloxy)phenyl)-1-(thiazolidine-3-yl)propan-1-one

(AAP-2): White solid; (1.24 g, 95%); M.P.: 151–156 °C. IR (KBr, ν_{\max} , cm^{-1}): 695.84 (C-S), 1175.59 (C-O), 1250.32 (C-N), 1382.03 (OH), 1454.29 (C=C), 1625.61 (C=N), 2956.99 and 2843.15 (H-C-C=O). ^1H NMR (400 MHz, DMSO- d_6 , δ ppm): 9.96 (s, 1H, OH), 8.02 (s, 1H, N=CH), 7.51–7.49 (d, 1H, $J=8$ Hz, Ar-H of 4-hydroxybenzene), 7.42–7.31 (m, 5H, Ar-H), 7.10–7.08 (d, 2H, $J=8$ Hz, Ar-H), 6.89–6.87 (d, 2H, $J=8$ Hz, Ar-H), 6.80–6.78 (d, 1H, $J=8$ Hz, Ar-H of 4-hydroxybenzene), 5.03 (s, 2H, O- CH_2 -Ar), 4.65–4.63 (t, 1H, $J=4$ Hz, N-CH), 4.45 (s, 2H, N- CH_2 -S of thiazolidine), 3.63–3.61 (t, 2H, $J=4$ Hz, N- CH_2 of thiazolidine), 3.14–3.11 (dd, 1H, $J=4$ Hz, 8 Hz, CH_2 -Ar), 2.94–2.92 (t, 2H, $J=4$ Hz, S- CH_2 of thiazolidine), 2.84–2.81 (dd, 1H, $J=4$ Hz, 8 Hz, CH_2 -Ar). ^{13}C -NMR (125 MHz, DMSO- d_6 , δ ppm): 169.44, 162.64, 160.55, 157.21, 137.23, 130.87, 130.15, 128.56, 127.94, 127.64, 127.23, 115.69, 114.66, 73.87, 69.93, 49.08, 48.09, 38.80, 31.28. ES-MS m/z 447.3 ($\text{M} + \text{H}$) $^+$. Analytical calculated formula for $\text{C}_{26}\text{H}_{26}\text{N}_2\text{O}_5\text{S}$: C, 69.93; H, 5.87; N, 6.27; O, 10.75; S, 7.18; Found: C, 69.94; H, 5.86; N, 6.26; S, 7.19.

(E)-2-(4-nitrobenzylideneamino)-3-(4-(benzyloxy)phenyl)-1-(thiazolidin-3-yl)propan-1-one

(AAP-3): White solid; (1.34 g, 97%); M.P.: 89–93 °C. IR (KBr, ν_{\max} , cm^{-1}): 697.09 (C-S), 1174.77 (C-O), 1243.72 (C-N), 1369.47 & 1499.96 (NO_2), 1419.72 (C=C), 1688.02 (C=N), 2832.93 and 2726.72 (H-C-C=O). ^1H NMR (400 MHz, DMSO- d_6 , δ ppm): 8.29–8.28 (d, 2H, $J=4$ Hz, Ar-H of 4-nitrobenzene), 8.04 (s, 1H, N=CH), 7.94–7.92 (d, 2H, $J=8$ Hz, Ar-H of 4-nitrobenzene at position 2), 7.40–7.31 (m, 5H, Ar-H), 7.12–7.10 (d, 2H, $J=8$ Hz, Ar-H), 6.88–6.86 (d, 2H, $J=8$ Hz, Ar-H), 5.04 (s, 2H, CH_2 -Ar), 4.63–4.61 (t, 1H, $J=4$ Hz, N-CH), 4.46 (s, 2H, N- CH_2 -S of thiazolidine), 3.67–3.64 (t, 2H, $J=6$ Hz, N- CH_2 of thiazolidine), 3.20–3.17 (dd, 1H, $J=4$ Hz, 8 Hz, CH_2 -Ar), 2.94–2.92 (t, 2H, $J=4$ Hz, S- CH_2 of thiazolidine), 2.85–2.82 (dd, 1H, $J=4$ Hz, 8 Hz, CH_2 -Ar). ^{13}C -NMR (125 MHz, DMSO- d_6 , δ ppm): 169.41, 160.59, 157.23, 149.28, 140.94, 137.28, 130.85, 129.07, 128.59, 128.00, 127.41, 123.91, 114.88, 73.87, 69.93, 49.12, 48.05, 38.71, 31.31. ES-MS m/z 476.3 ($\text{M} + \text{H}$) $^+$. Analytical calculated formula for $\text{C}_{26}\text{H}_{25}\text{N}_3\text{O}_4\text{S}$: C, 65.67; H, 5.30; N, 8.84; O, 13.46; S, 6.74; Found: C, 65.66; H, 5.31; N, 8.85; S, 6.75.

(E)-2-(2,3-dimethoxybenzylideneamino)-3-(4-(benzyloxy)phenyl)-1-(thiazolidin-3-yl)propan-1-one

(AAP-4): White solid; (1.34 g, 94%); M.P.: 199–203 °C; IR (KBr, ν_{\max} , cm^{-1}): 696.87 (C-S), 1190.18 (C-O), 1258.35 (C-N), 1426.35 (C=C), 1648.35 (C=N), 2926.76 and 2832.40 (H-C-C=O). ^1H NMR (400 MHz, DMSO- d_6 , δ ppm): 8.06 (s, 1H, N=CH), 7.42–7.31 (m, 5H, Ar-H), 7.12–7.10 (d, 3H, $J=8$ Hz, Ar-H (2H) and Ar-H (1H) of 2,3-dimethoxybenzene), 6.99–6.97 (d, 1H, $J=8$ Hz, Ar-H of 2,3-dimethoxybenzene), 6.89–6.87 (d, 2H, $J=8$ Hz, Ar-H), 6.68–6.66 (m, 1H, Ar-H of 2,3-dimethoxybenzene), 5.03 (s, 2H; O- CH_2 -Ar), 4.64–4.62 (t, 1H, $J=4$ Hz, N-CH), 4.47 (s, 2H, N- CH_2 -S of thiazolidine), 3.78 (s, 6H, O- CH_3), 3.66–3.63 (t, 2H, $J=4$ Hz, N- CH_2 of thiazolidine), 3.16–3.12 (dd, 1H, $J=4$ Hz, 8 Hz, CH_2 -Ar), 2.94–2.92 (t, 2H, $J=4$ Hz, S- CH_2 of

thiazolidine), 2.87–2.84 (dd, 1H, $J=4$ Hz, 8 Hz, $\text{CH}_2\text{-Ar}$). $^{13}\text{C-NMR}$ (125 MHz, DMSO-d_6 , δ ppm): 169.40, 162.66, 157.45, 150.03, 137.02, 130.88, 129.95, 128.59, 127.47, 124.15, 123.01, 117.03, 114.75, 73.89, 69.62, 55.40, 49.18, 48.15, 38.90, 31.34. ES-MS m/z 491.3 ($\text{M} + \text{H}$)⁺. Analytical calculated formula for $\text{C}_{28}\text{H}_{30}\text{N}_2\text{O}_4\text{S}$: C, 68.55; H, 6.16; N, 5.71; O, 13.04; S, 6.54; Found: C, 68.53; H, 6.15; N, 5.72; S, 6.54.

(E)-2-(2-chlorobenzylideneamino)-3-(4-(benzyloxy)phenyl)-1-(thiazolidin-3-yl)propan-1-one (AAP-5): White solid; (1.30 g, 96%); M.P.: 146–151 °C. IR (KBr, ν_{max} , cm^{-1}): 695.64 (C-S), 826.65 (Cl), 1177.61 (C-O), 1245.97 (C-N), 1427.73 (C=C), 1638.17 (C=N), 2933.37 and 2876.10 (H-C-C=O). $^1\text{H NMR}$ (400 MHz, DMSO-d_6 , δ ppm): 8.02 (s, 1H, N=CH), 7.63–7.60 (t, 2H, $J=4$ Hz, Ar-H of 2-chlorobenzene), 7.40–7.32 (m, 7H, Ar-H (5H) and Ar-H (2H) of 2-chlorobenzene), 7.10–7.08 (d, 2H, $J=8$ Hz, Ar), 6.87–6.85 (d, 2H, $J=8$ Hz, Ar), 5.04 (s, 2H, $\text{CH}_2\text{-Ar}$), 4.65–4.63 (t, 1H, $J=4$ Hz, N-CH), 4.45 (s, 2H, N- $\text{CH}_2\text{-S}$ of thiazolidine), 3.63–3.61 (t, 2H, $J=4$ Hz, N- CH_2 of thiazolidine), 3.14–3.11 (dd, 1H, $J=4$ Hz, 8 Hz, $\text{CH}_2\text{-Ar}$), 2.94–2.92 (t, 2H, $J=4$ Hz, S- CH_2 of thiazolidine), 2.84–2.81 (dd, 1H, $J=4$ Hz, 8 Hz, $\text{CH}_2\text{-Ar}$). $^{13}\text{C-NMR}$ (125 MHz, DMSO-d_6 , δ ppm): 169.51, 160.58, 157.51, 137.20, 136.96, 134.07, 130.83, 129.18, 128.93, 128.58, 127.96, 127.44, 114.79, 73.86, 69.93, 49.19, 48.12, 38.76, 31.32. ES-MS m/z 465.3 ($\text{M} + \text{H}$)⁺. Analytical calculated formula for $\text{C}_{26}\text{H}_{25}\text{ClN}_2\text{O}_2\text{S}$: C, 67.16; H, 5.42; Cl, 7.62; N, 6.02; O, 6.88; S, 6.90; Found: C, 67.17; H, 5.43; N, 6.01; S, 6.91.

(E)-2-(2-nitrobenzylideneamino)-3-(4-(benzyloxy)phenyl)-1-(thiazolidin-3-yl)propan-1-one (AAP-6): White solid; (1.36 g, 98%); M.P.: 165–169 °C. IR (KBr, ν_{max} , cm^{-1}): 697.00 (C-S), 1204.67 (C-O), 1242.99 (C-N), 1319.31 & 1514.17 (NO_2), 1419.72 (C=C), 1640.15 (C=N), 2946.03 and 2769.38 (H-C-C=O). $^1\text{H NMR}$ (400 MHz, DMSO-d_6 , δ ppm): 8.23–8.22 (d, 1H, $J=4$ Hz, Ar-H of 2-nitrobenzene), 8.03 (s, 1H, N=CH), 7.90–7.88 (d, 1H, $J=8$ Hz, Ar-H of 2-nitrobenzene), 7.80–7.72 (m, 2H, Ar-H, 2-nitrobenzene), 7.40–7.27 (m, 5H, Ar-H) 7.14–7.11 (d, 2H, $J=12$ Hz, Ar-H), 6.89–6.87 (d, 2H, $J=8$ Hz, Ar-H), 5.03 (s, 2H, $\text{CH}_2\text{-Ar}$), 4.66–4.64 (t, 1H, $J=4$ Hz, N-CH), 4.46 (s, 2H, N- $\text{CH}_2\text{-S}$ of thiazolidine), 3.67–3.65 (t, 2H, $J=4$ Hz, N- CH_2 of thiazolidine), 3.19–3.15 (dd, 1H, $J=4$ Hz, 8 Hz, $\text{CH}_2\text{-Ar}$), 3.01–2.98 (t, 2H, $J=4$ Hz, S- CH_2 of thiazolidine), 2.92–2.89 (dd, 1H, $J=4$ Hz, 8 Hz, $\text{CH}_2\text{-Ar}$). $^{13}\text{C-NMR}$ (125 MHz, DMSO-d_6 , δ ppm): 169.59, 160.45, 157.28, 148.68, 137.30, 135.01, 132.07, 130.85, 129.07, 128.59, 127.41, 121.31, 114.87, 73.89, 69.98, 49.14, 48.05, 38.74, 31.28. ES-MS m/z 476.3 ($\text{M} + \text{H}$)⁺. Analytical calculated formula for $\text{C}_{26}\text{H}_{25}\text{N}_3\text{O}_4\text{S}$: C, 65.67; H, 5.30; N, 8.84; O, 13.46; S, 6.74; Found: C, 65.65; H, 5.31; N, 8.83; S, 6.75.

(E)-2-(2-hydroxy-4-methoxybenzylideneamino)-3-(4-(benzyloxy)phenyl)-1-(thiazolidin-3-yl)propan-1-one (AAP-7): White solid; (1.30 g, 93%); M.P. 134–138 °C. IR (KBr, ν_{max} , cm^{-1}): 696.24 (C-S), 1172.19 (C-O), 1237.91 (C-N), 1375.61 (OH), 1444.35 (C=C), 1641.95 (C=N), 2933.67 and 2880.30 (H-C-C=O). $^1\text{H NMR}$ (400 MHz, DMSO-d_6 , δ ppm): 10.04 (s, 1H, OH), 8.07 (s, 1H, N=CH), 7.42–7.30 (m, 6H Ar-H (5H) and Ar-H (1H) of 2-hydroxy-4-methoxybenzene), 7.10–7.06 (d, 2H, $J=8$ Hz, Ar), 6.90–6.88 (d, 2H, $J=8$ Hz, Ar), 6.42–6.41 (d, 1H, $J=4$ Hz, Ar-H of 2-hydroxy-4-methoxybenzene), 6.28 (s, 1H, Ar-H of 2-hydroxy-4-methoxybenzene), 5.04 (s, 2H, $\text{CH}_2\text{-Ar}$), 4.64–4.62 (t, 1H, $J=4$ Hz, N-CH), 4.46 (s, 2H, N- $\text{CH}_2\text{-S}$ of thiazolidine), 3.76 (s, 3H, O- CH_3), 3.64–3.62 (t, 2H, $J=4$ Hz, N- CH_2 of thiazolidine), 3.15–3.12 (dd, 1H, $J=4$ Hz, 8 Hz, $\text{CH}_2\text{-Ar}$), 2.96–2.93 (t, 2H, $J=4$ Hz, S- CH_2 of thiazolidine), 2.86–2.83 (dd, 1H, $J=4$ Hz, 8 Hz, $\text{CH}_2\text{-Ar}$). $^{13}\text{C-NMR}$ (125 MHz, DMSO-d_6 , δ ppm): 169.54, 165.56, 163.75, 160.70, 157.64, 136.92, 133.13, 130.64, 128.58, 127.97, 127.45, 116.89, 114.94, 106.77, 101.11, 74.02, 69.95, 55.43, 49.13, 48.12, 38.74, 31.34. ES-MS m/z 477.1 ($\text{M} + \text{H}$)⁺. Analytical calculated formula for $\text{C}_{27}\text{H}_{28}\text{N}_2\text{O}_4\text{S}$: C, 68.04; H, 5.92; N, 5.88; O, 13.43; S, 6.73; Found: C, 68.05; H, 5.92; N, 5.87; S, 6.74.

(E)-2-(3-hydroxybenzylideneamino)-3-(4-(benzyloxy)phenyl)-1-(thiazolidin-3-yl)propan-1-one (AAP-8): White solid; (1.26 g, 96%); M.P.: 106–108 °C. IR (KBr, ν_{max} , cm^{-1}): 695.34 (C-S), 1175.59 (C-O), 1257.32 (C-N), 1382.23 (OH), 1454.22 (C=C), 1636.61 (C=N), 2959.29 and 2893.95 (H-C-C=O). $^1\text{H NMR}$ (400 MHz, DMSO-d_6 , δ ppm): 9.59 (s, 1H, OH), 8.06 (s, 1H,

N = CH), 7.42–7.31 (m, 5H, Ar-H), 7.24–7.21 (m, 1H, Ar-H of 3-hydroxybenzene), 7.12–7.09 (m, 3H, Ar-H (2H) and Ar-H (1H) of 3-hydroxybenzene), 7.05–7.03 (d, 1H, $J = 8$ Hz, Ar-H of 3-hydroxybenzene), 6.88–6.86 (d, 3H, $J = 8$ Hz, Ar-H (2H) and Ar-H (1H) and Ar-H (1H) of 3-hydroxybenzene), 5.04 (s, 2H, CH₂-Ar), 4.64–4.62 (t, 1H, $J = 4$ Hz, N-CH), 4.46 (s, 2H, N-CH₂-S of thiazolidine), 3.64–3.62 (t, 2H, $J = 4$ Hz, N-CH₂ of thiazolidine), 3.16–3.13 (dd, 1H, $J = 4$ Hz, 8 Hz, CH₂-Ar), 2.95–2.93 (t, 2H, $J = 4$ Hz, S-CH₂ of thiazolidine), 2.87–2.84 (dd, 1H, $J = 4$ Hz, 8 Hz, CH₂-Ar). ¹³C-NMR (125 MHz, DMSO-d₆, δ ppm): 169.38, 161.94, 160.37, 157.23, 137.29, 130.77, 130.19, 128.60, 127.97, 127.64, 127.27, 120.27, 115.99, 114.69, 73.87, 69.63, 49.08, 48.09, 38.80, 31.28. ES-MS m/z 447.5 (M + H)⁺. Analytical calculated formula for C₂₆H₂₆N₂O₃S: C, 69.93; H, 5.87; N, 6.27; O, 10.75; S, 7.18; Found: C, 69.93; H, 5.86; N, 6.28; S, 7.19.

(E)-2-(3-methoxybenzylideneamino)-3-(4-(benzyloxy)phenyl)-1-(thiazolidin-3-yl)propan-1-one (AAP-9): White solid; (1.28 g, 95%); M.P.: 176–180 °C. IR (KBr, ν_{\max} , cm⁻¹): 696.74 (C-S), 1170.35 (C-O), 1248.72 (C-N), 1426.81 (C=C), 1639.34 (C=N), 2932.67 and 2876.41 (H-C-C=O). ¹H NMR (400 MHz, DMSO-d₆, δ ppm): 8.07 (s, 1H, N = CH), 7.62–7.61 (d, 2H, $J = 4$ Hz, Ar-H of 3-methoxybenzene), 7.42–7.31 (m, 5H, Ar-H), 7.10–7.07 (d, 3H, $J = 12$ Hz, Ar-H (2) and Ar-H (1H) of 3-methoxybenzene), 6.99–6.97 (d, 2H, $J = 8$ Hz, Ar-H of 3-methoxybenzene), 6.90–6.88 (d, 2H, $J = 8$ Hz, Ar-H), 5.03 (s, 2H, CH₂-Ar), 4.64–4.62 (t, 1H, $J = 4$ Hz, N-CH), 4.45 (s, 2H, N-CH₂-S of thiazolidine), 3.77 (s, 3H, O-CH₃), 3.65–3.63 (t, 2H, $J = 4$ Hz, N-CH₂ of thiazolidine), 3.16–3.12 (dd, 1H, $J = 4$ Hz, 8 Hz, CH₂-Ar), 2.95–2.92 (t, 2H, $J = 4$ Hz, S-CH₂ of thiazolidine), 2.86–2.84 (dd, 1H, $J = 4$ Hz, 8 Hz, CH₂-Ar). ¹³C-NMR (125 MHz, DMSO-d₆, δ ppm): 169.48, 162.60, 157.44, 137.03, 130.82, 130.05, 128.56, 127.93, 127.45, 124.15, 114.72, 113.99, 73.81, 69.64, 55.39, 49.17, 48.25, 38.88, 31.33. ES-MS m/z 461.3 (M + H)⁺. Analytical calculated formula for C₂₇H₂₈N₂O₃S: C, 70.41; H, 6.13; N, 6.08; O, 10.42; S, 6.96; Found: C, 70.42; H, 6.12; N, 6.06; S, 6.97.

(E)-2-(2-fluorobenzylideneamino)-3-(4-(benzyloxy)phenyl)-1-(thiazolidin-3-yl)propan-1-one (AAP-10): Dark brown solid (1.21 g, 92%); M.P.: 99–102 °C. IR (KBr, ν_{\max} , cm⁻¹): 695.89 (C-S), 1197.70 (Ar-F), 1227.79 (C-O), 1252.08 (C-N), 1427.93 (C=C), 1628.99 (C=N), 2999.13 and 2973.18 (H-C-C=O). ¹H NMR (400 MHz, DMSO-d₆, δ ppm): 8.11 (s, 1H, N = CH), 7.82–7.81 (d, 1H, $J = 4$ Hz, Ar-H of 2-fluorobenzene), 7.44–7.30 (m, 5H, Ar-H), 7.22–7.17 (m, 1H, Ar-H of 2-fluorobenzene), 7.10–7.05 (m, 3H, Ar-H (2H) and Ar-H (1H) of 2-fluorobenzene), 6.88–6.86 (d, 3H, $J = 8$ Hz, Ar-H (2H) and Ar-H (1H) of 2-fluorobenzene), 5.00 (s, 2H, CH₂-Ar), 4.63–4.61 (t, 1H, $J = 4$ Hz, N-CH), 4.46 (s, 2H, N-CH₂-S of thiazolidine), 3.65–3.63 (t, 2H, $J = 4$ Hz, N-CH₂ of thiazolidine), 3.16–3.13 (dd, 1H, $J = 4$ Hz, 8 Hz, CH₂-Ar), 2.95–2.93 (t, 2H, $J = 4$ Hz, S-CH₂ of thiazolidine), 2.87–2.84 (dd, 1H, $J = 4$ Hz, 8 Hz, CH₂-Ar). ¹³C-NMR (125 MHz, DMSO-d₆, δ ppm): 169.43, 160.39, 157.23, 137.27, 131.28, 130.79, 128.67, 127.96, 127.64, 127.29, 124.08, 120.27, 116.20, 73.88, 69.79, 49.10, 48.11, 38.81, 32.08. ES-MS m/z 449.2 (M + H)⁺. Analytical calculated formula for C₂₆H₂₅FN₂O₂S: C, 69.62; H, 5.62; F, 4.24; N, 6.25; O, 7.13; S, 7.15; Found: C, 69.63; H, 5.63; N, 6.25; S, 7.15.

Biological activity procedure

Minimum inhibitory concentration

The ready-made Tryptic Soya broth and Malt extract broth medium (30 g) was suspended in distilled water (100 mL) and warmed until it dissolved completely. The test tube as well as medium tubes were autoclaved at a pressure of 1.0 bar for 30 min. A set of sterilized test tubes with Tryptic Soya broth and Malt extract broth medium was capped with cotton plugs. The newly synthesized compounds were dissolved in dimethyl sulfoxide (DMSO) and in first test tube added 100 μ g/mL concentration of the newly synthesized compounds and which was serially diluted. A fixed volume of 0.5 mL of overnight culture was added in all the test tubes which were incubated at 37 °C for 24 h. After 24 h these tubes were measured for turbidity. For the antifungal assay, the ready-made Muller Hinton agar medium (30 g) was suspended in distilled water (100 mL) and

warmed until it dissolved completely. The medium and glass petri dishes were autoclaved at a pressure of 1.0 bar for 30 min. under sterilized conditions in a Laminar flow chamber; the medium was poured into sterile petri dishes. The 0.5 mL of the culture of fungal spore suspension was injected and uniformly spread over the agar surface with a sterile glass rod. The newly synthesized compounds solution were prepared in DMSO. After inoculation, cups were lifted out with 6-mm sterile cork borer and the lids of the dishes were replaced. To each cup, different concentrations of test solution of each synthesized compounds were added. Controls were maintained with DMSO and fluconazole. The treated and the controls were kept at 27–28 °C for 60–84 h. The minimum inhibitory concentration (MIC) was recorded in µg/mL. Three to four replicates were maintained for each treatment.

Molecular docking

Molecular docking of the protein–ligand complexes was executed with the help of AutoDock Vina (<http://vina.scripps.edu>) software. PDB sum and CASTp servers used for identification of ligand-binding site of each complex. This process was used to make binding of its crystal with ligand in a similar region to avoid the binding with other areas. With the help of AutoDock tools the ligand coordinates and protein were separated from each complex, the ligand structures and protein were processed to a format as pdbqt files (Recognized by ADT), by adding Gasteiger charges, all hydrogen atoms and merging the non-polar hydrogen atoms. By using babel in AutoDock the hydrogens are added to the receptor and ligand structures. The AutoDock, an inbuilt tool in the ADT were used for determined by the number of torsions for the ligand. The torsional root for the ligand molecule is usually branches with rotatable bonds surface of rigid part of the ligand molecule. The AutoDock frequently tries to detect the root for the molecule unless the user specifies it. In this process, AutoDock was automatically selected its root. As per the information from the PDB sum and CastP servers the grid box was sited. Auto grid were computed the atom specific affinity maps for all ligand atom types, electrostatic and desolvation potentials. The docking simulation consisted of 100 iterations by Genetic Algorithm methods for every protein ligand pair. Lamarckian Genetic Algorithm, local search method in AutoDock was used to set population size 150 with 25 million energy evaluations. All the other factors like the number of generations, the maximum number of top individuals to persist to the next generation, the crossover rate and mutation rate were set to their default value. The binding energy was analysis after total minimum energy resulting from the 100 docking runs.

Acknowledgements

This research work is dedicated to my dear father late Mr. Ashok Trambak Pund and friends late Mr. Somanath Darkunde and late Dr. Nilesh Patil. Authors are thankful to Principal, Shivaji Arts, Commerce and Science College Kannad, District Aurangabad (M.S.) for availing research laboratory and FTIR facilities. Authors also thankful to Mr. Prathmesh Pramod Deshpande for support and Mr. Vijay Maskar, Sprint testing solution, Mumbai for characterization of samples.

Disclosure statement

No potential conflict of interest was reported by the authors.

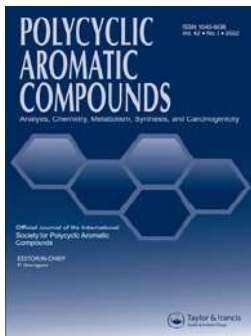
ORCID

Amit A. Pund  <http://orcid.org/0000-0002-3406-6783>
Mazahar Farooqui  <http://orcid.org/0000-0003-2236-6639>
Mubarak H. Shaikh  <http://orcid.org/0000-0002-1190-2371>
Baban K. Magare  <http://orcid.org/0000-0001-6719-0441>

References

1. Y. Hu, Z. Xu, S. Zhang, Wu Xiang, D. Jun-Wei, Lv Zao-Sheng, and F. Lian-Shun, "Recent Developments of Coumarin-Containing Derivatives and Their Anti-Tubercular Activity," *European Journal of Medicinal Chemistry* 136 (2017): 122–30. doi:10.1016/j.ejmech.2017.05.004.
2. S. Musrat, S. Ayushi, S. Jay, A. Dinesh, and A. Shikha, "Saturated Five-Membered Thiazolidines and Their Derivatives: From Synthesis to Biological Applications," *Topics in Current Chemistry* 378, no. 2 (2020): 1–90.
3. M. Nasr, M. Gineinah, and E. El-Bendary, "Synthesis and In Vitro Antibacterial Evaluation of Novel Imidazo[2',1':5,1]-1,2,4-Triazolo[4,3-c]-Quinazoline Derivatives Of 5-Thioxo-1, 2, 4-Triazole, 4-Oxothiazolidine, and Their Open-Chain Counterparts," *Archiv Der Pharmazie* 336, no. 12 (2003): 560–6. doi:10.1002/ardp.200300809.
4. B. Belleau, L. Brasili, L. Chan, M. DiMarco, B. Zacharie, N. Nguyen-Ba, H. Jenkinson, J. Coates, and J. Cameron, "A Novel Class of 1, 3-Oxathiolane Nucleoside Analogues Having Potent Anti-HIV Activity," *Bioorganic & Medicinal Chemistry Letters* 3, no. 8 (1993): 1723–8. doi:10.1016/S0960-894X(00)80050-5.
5. M. Peterson and R. Vince, "Synthesis and Biological Evaluation of 4-Purinylypyrrolidine Nucleosides," *Journal of Medicinal Chemistry* 34, no. 9 (1991): 2787–97. doi:10.1021/jm00113a017.
6. K. Obydenov, A. Khamidullina, A. Galushchinskiy, A. Shatunova, M. Kosterina, T. Kalina, Z. Fan, T. Glukhareva, and Y. Morzherin, "Discovery of Methyl (5 Z)-[2-(2,4,5-Trioxopyrrolidin-3-ylidene)-4-Oxo-1,3-Thiazolidin-5-Ylidene]Acetates as Antifungal Agents against Potato Diseases," *Journal of Agricultural and Food Chemistry* 66, no. 24 (2018): 6239–45. doi:10.1021/acs.jafc.8b02151.
7. V. Solomon, W. Haq, K. Srivastava, S. Puri, and B. Katti, "Synthesis and Antimalarial Activity of Side Chain Modified 4-Aminoquinoline Derivatives," *Journal of Medicinal Chemistry* 50, no. 2 (2007): 394–8. doi:10.1021/jm061002i.
8. M. Barreca, A. Chimirri, L. Luca, A. Monforte, P. Monforte, A. Rao, M. Zappala, J. Balzarini, E. Clercq, C. Pannecouque, et al. "Discovery of 2,3-Diaryl-1,3-Thiazolidin-4-Ones as Potent Anti-HIV-1 Agents," *Bioorganic & Medicinal Chemistry Letters* 11, no. 13 (2001): 1793–6. doi:10.1016/S0960-894X(01)00304-3.
9. N. Fuloria, V. Singh, M. Shaharyar, and M. Ali, "Synthesis, Characterization and Biological Studies of New Schiff Bases and Azetidinone Derived from Propionic Acid Derivatives," *Asian Journal of Chemistry*. 20, no. 8 (2008): 6457–62.
10. G. Kucukguzel, A. Kocatepe, E. Clercq, F. Sahin, and M. Gulluce, "Synthesis and Biological Activity of 4-Thiazolidinones, Thiosemicarbazides Derived from Diflunisal Hydrzide," *European Journal of Medicinal Chemistry* 41, no. 3 (2006): 353–9. doi:10.1016/j.ejmech.2005.11.005.
11. Ş. G. Küçükğüzel, E. E. Oruç, S. Rollas, F. Şahin, and A. Özbek, "Synthesis, Characterization and Biological Activity of Novel 4-Thiazolidinones, 1,3,4-Oxadiazoles and Some Related Compounds," *European Journal of Medicinal Chemistry* 37, no. 3 (2002): 197–206. doi:10.1016/S0223-5234(01)01326-5.
12. P. Vicini, A. Geronikaki, K. Anastasia, M. Incerti, and F. Zani, "Cyclobutane Derivatives as Potent NK1 Selective Antagonists," *Bioorganic & Medicinal Chemistry Letters* 16, no. 14 (2006): 3859–64.
13. K. V. G. C. Sekhar, V. S. Rao, A. S. Reddy, R. Sunandini, and V. S. A. Kumar Satuluri, "Solvent Free Microwave Accelerated Synthesis of Heterocyclic Thiazolidin-4-Ones as Anti-Microbial and Anti-Fungal Agents," *Bulletin of the Korean Chemical Society* 31, no. 5 (2010): 1219–22. doi:10.5012/bkcs.2010.31.5.1219.
14. B. M. Gurupadaya, M. Gopal, B. Padmashali, and Y. N. Manohara, "Synthesis and Pharmacological Evaluation of Azetid-2-Ones and Thiazolidin-4-Ones Encompassing Benzothiazole," *Indian Journal of Pharmaceutical Sciences* 70, no. 5 (2008): 572–7. doi:10.4103/0250-474X.45393.
15. D. Visagaperumal, K. Jaya, R. Vijayaraj, and N. Anbalagan, "Microwave Induced Synthesis of Some New 3-Substituted-1,3-Thiazolidin-4-Ones for Their Potent Anti-Microbial and Antitubercular Activities," *International Journal of ChemTech Research* 1, no. 4 (2009): 1048–51.
16. J. East, A. Kennedy, J. Tomsig, A. De Leon, K. Lynch, and T. Macdonald, "Synthesis and Structure-Activity Relationships of Tyrosine-Based Inhibitors of Autotaxin (ATX)," *Bioorganic & Medicinal Chemistry Letters* 20, no. 23 (2010): 7132–6. doi:10.1016/j.bmcl.2010.09.030.
17. J. Cobb, S. Blanchard, E. Boswell, K. Brown, P. Charifson, J. Cooper, J. Collins, M. Dezube, B. Henke, E. Hull-Ryde, et al. "N-(2-Benzoylphenyl)-L-Tyrosine PPARgamma Agonists. 3. Structure-Activity Relationship and Optimization of the N-Aryl Substituent," *Journal of Medicinal Chemistry* 41, no. 25 (1998): 5055–69. doi:10.1021/jm980414r.
18. A. Pund, S. Saboo, G. Sonawane, A. Dukale, and B. Magare, "Synthesis of 2,5-Disubstituted-1,3,4-Thiadiazole Derivatives from (2S)-3-(Benzyloxy)-2-[(Tert-Butoxycarbonyl)Amino] Propanoic Acid and Evaluation of Anti-Microbial Activity," *Synthetic Communications* 50, no. 24 (2020): 3854–64. doi:10.1080/00397911.2020.1817488.
19. B. Kahveci, O. Bekircan, and S. Karaoglu, "Synthesis and Anti-Microbial Activity of Some 3-Alkyl-4-(Arylmethyleneamino)-4,5-Dihydro-1H-1,2,4-Triazol-5-Ones," *Indian Journal of Chemistry* 40, no. B (2005): 2614–7.
20. O. Bekircan, B. Kahveci, and M. Kucuk, "Synthesis and Anticancer Evaluation of Some New Unsymmetrical 3,5-Diaryl-4H-1,2,4-Triazole Derivatives," *Turkish Journal of Chemistry* 30 (2006): 29–40.

21. M. Singh, and C. Dash, "Synthesis of Some New Schiff Bases Containing Thiazole and Oxazole Nuclei and Their Fungicidal Activity," *Pesticides* 22, no. 11 (1988): 33–7.
22. S. Holla, K. Shivananda, S. Shenoy, and G. Antony, "Studies on Aryl Furan Derivatives: Part VII. Synthesis and Characterization of Some Mannich Bases Carrying Halophenylfuryl Moieties as Promising Antibacterial Agents," *Farmaco* 53 (1998): 531–5.
23. S. Holla, B. Veerendra, K. Shivananda, and B. Poojary, "Synthesis Characterization and Anticancer Activity Studies on Some Mannich Bases Derived from 1,2,4-Triazoles," *European Journal of Medicinal Chemistry* 38, no. 7–8 (2003): 759–67. doi:[10.1016/S0223-5234\(03\)00128-4](https://doi.org/10.1016/S0223-5234(03)00128-4).
24. E. Gokce, G. Bakir, F. Sahin, E. Kupeli, and E. Yesilada, "Synthesis of New Mannich Bases of Arylpyridazinones as Analgesic and Anti-Inflammatory Agents," *Arzneimittel Forschung* 55 (2005): 318–25.
25. R. Dimmock, S. Jonnalagadda, A. Phillips, E. Erciyas, K. Shyam, and A. Semple, "Anticonvulsant Properties of Some Mannich Bases of Conjugated Arylidene Ketones," *Journal of Pharmaceutical Sciences* 81, no. 5 (1992): 436–40. doi:[10.1002/jps.2600810509](https://doi.org/10.1002/jps.2600810509).
26. F. Lopes, R. Capela, J. O. Gonçalves, P. N. Horton, M. B. Hursthouse, J. Iley, C. M. Casimiro, J. Bom, and R. Moreira, "Amidomethylation of Amodiaquine: Antimalarial N-Mannich Base Derivatives," *Tetrahedron Letters* 45, no. 41 (2004): 7663–6. doi:[10.1016/j.tetlet.2004.08.093](https://doi.org/10.1016/j.tetlet.2004.08.093).
27. J. Knabe, P. Buch, and W. Schmit, "Derivatives of Barbituric Acid Cytostatic and CNS Activities of Chiral Barbiturate Mannich-Bases," *Archiv Der Pharmazie* 316, no. 12 (1983): 1051–3. doi:[10.1002/ardp.19833161216](https://doi.org/10.1002/ardp.19833161216).
28. R. Islam, J. Abedin, M. Hossain, and H. Duddeck, "Synthesis of 1-Methyl Bis-Dioxopyrolino [2,3:2,3:2,3:6,5] Benzene and Its Heterocycles via Thiocarbohydrazone, Thiosemicarbazone," *Journal of the Bangladesh Chemical Society* 11 (1998): 71–8.
29. E. Michel, H. John, and T. Elizabeth, "FAP Inhibitors," (WO2007085895A2, filed August 31, 2006, and issued August 02, 2007).
30. N. Andersen, J. Cadahia, V. Previtali, J. Bondebjerg, C. Hansen, A. Hansen, T. Andresen, and M. Clausen, "Methotrexate Prodrugs Sensitive to Reactive Oxygen Species for the Improved Treatment of Rheumatoid Arthritis," *European Journal of Medicinal Chemistry* 156 (2018): 738–46. doi:[10.1016/j.ejmech.2018.07.045](https://doi.org/10.1016/j.ejmech.2018.07.045).
31. C. Decicco and P. Grover, "Total Asymmetric Synthesis of the Potent Immunosuppressive Marine Natural Product Microcolin A," *The Journal of Organic Chemistry* 61, no. 10 (1996): 3534–41. doi:[10.1021/jo952123l](https://doi.org/10.1021/jo952123l).
32. N. Kumar, S. Devineni, K. Aggile, P. Gajjala, P. Kumar, and S. Dubey, "Facile New Industrial Process for Synthesis of Tenelegliptin through New Intermediates and Its Optimization with Control of Impurities," *Research on Chemical Intermediates* 44, no. 1 (2018): 567–84. doi:[10.1007/s11164-017-3120-3](https://doi.org/10.1007/s11164-017-3120-3).
33. T. Yoshida, F. Akahoshi, H. Sakashita, H. Kitajima, M. Nakamura, S. Sonda, M. Takeuchi, Y. Tanaka, N. Ueda, S. Sekiguchi, et al. "Discovery and Preclinical Profile of Tenelegliptin (3-[(2S,4S)-4-[4-(3-Methyl-1-Phenyl-1H-Pyrazol-5-yl)Piperazin-1-yl]Pyrrolidin-2-Ylcarbonyl]Thiazolidine): A Highly Potent, Selective, Long-Lasting and Orally Active Dipeptidyl Peptidase IV Inhibitor for the Treatment of Type 2 Diabetes," *Bioorganic & Medicinal Chemistry* 20, no. 19 (2012): 5705–19. doi:[10.1016/j.bmc.2012.08.012](https://doi.org/10.1016/j.bmc.2012.08.012).
34. A. Karmakar, M. Basha, G. Babu, M. Botlagunta, N. Malik, R. Rampulla, A. Mathur, and A. Gupta, "Tertiary-Butoxycarbonyl (Boc)-A Strategic Group for N-Protection/Deprotection in the Synthesis of Various Natural/Unnatural N-Unprotected Aminoacid Cyanomethyl Esters," *Tetrahedron Letters* 59, no. 48 (2018): 4267–71. doi:[10.1016/j.tetlet.2018.10.041](https://doi.org/10.1016/j.tetlet.2018.10.041).
35. O. Bekircan and H. Bektas, "Synthesis of Schiff and Mannich Bases of Isatin Derivatives with 4-Amino-4,5-Dihydro-1H-1,2,4-Triazole-5-Ones," *Molecules (Basel, Switzerland)* 13, no. 9 (2008): 2126–35. doi:[10.3390/molecules13092126](https://doi.org/10.3390/molecules13092126).
36. H. Jiyaul, S. Vandana, C. Dheeraj, L. Hassane, and Q. Mumtaz, "Microwave-Induced Synthesis of Chitosan Schiff Bases and Their Application as Novel and Green Corrosion Inhibitors, Experimental and Theoretical Approach," *ACS Omega* 3 (2018): 5654–68.
37. K. Campbell, C. Helbing, M. Florkowsk, and B. Campbell, "The Reaction of Grignard Reagents with Schiff Bases," *Journal of the American Chemical Society* 70, no. 11 (1948): 3868–70. doi:[10.1021/ja01191a099](https://doi.org/10.1021/ja01191a099).
38. S. Magaldi, C. Mata-Essayag, C. Capriles, C. Perez, M. Colella, C. Olaizola, and Y. Ontiveros, "Well Diffusion for Antifungal Susceptibility Testing," *International Journal of Infectious Diseases* 8, no. 1 (2004): 39–45. doi:[10.1016/j.ijid.2003.03.002](https://doi.org/10.1016/j.ijid.2003.03.002).
39. M. Ahmed, "Acute Toxicity (Lethal Dose 50 Calculation) of Herbal Drug Somina in Rats and Mice," *Pharmacology & Pharmacy* 06, no. 03 (2015): 185–9. doi:[10.4236/pp.2015.63019](https://doi.org/10.4236/pp.2015.63019).
40. S. Zhang, Y. Luo, L. He, Z. Liu, A. Jiang, Y. Yang, and H. Zhu, "Synthesis, Biological Evaluation, and Molecular Docking Studies of Novel 1,3,4-Oxadiazole Derivatives Possessing Benzotriazole Moiety as FAK Inhibitors with Anticancer Activity," *Bioorganic & Medicinal Chemistry* 21, no. 13 (2013): 3723–9. doi:[10.1016/j.bmc.2013.04.043](https://doi.org/10.1016/j.bmc.2013.04.043).
41. A. Pund, M. Shaikh, B. Chandak, V. Bhosale, and B. Magare, "Pyridine-1,3,4-Thiadiazole-Schiff Base Derivatives, as Antioxidant and Antimitotic Agent: Synthesis and *in Silico* ADME Studies," *Polycyclic Aromatic Compounds* (2022): 1–6. doi:[10.1080/10406638.2022.2026988](https://doi.org/10.1080/10406638.2022.2026988).



New 1,2,3-Triazole-Tethered Thiazolidinedione Derivatives: Synthesis, Bioevaluation and Molecular Docking Study

Mubarak H. Shaikh, Dnyaneshwar D. Subhedar, Satish V. Akolkar, Amol A. Nagargoje, Ashish Asrondkar, Vijay M. Khedkar & Bapurao B. Shingate

To cite this article: Mubarak H. Shaikh, Dnyaneshwar D. Subhedar, Satish V. Akolkar, Amol A. Nagargoje, Ashish Asrondkar, Vijay M. Khedkar & Bapurao B. Shingate (2022): New 1,2,3-Triazole-Tethered Thiazolidinedione Derivatives: Synthesis, Bioevaluation and Molecular Docking Study, Polycyclic Aromatic Compounds, DOI: [10.1080/10406638.2022.2069132](https://doi.org/10.1080/10406638.2022.2069132)

To link to this article: <https://doi.org/10.1080/10406638.2022.2069132>



Published online: 01 May 2022.



Submit your article to this journal [↗](#)





View related articles [↗](#)



View Crossmark data [↗](#)



New 1,2,3-Triazole-Tethered Thiazolidinedione Derivatives: Synthesis, Bioevaluation and Molecular Docking Study

Mubarak H. Shaikh^{a,b} , Dnyaneshwar D. Subhedar^a, Satish V. Akolkar^a, Amol A. Nagargoje^a, Ashish Asrondkar^c, Vijay M. Khedkar^d , and Bapurao B. Shingate^a

^aDepartment of Chemistry, Dr. Babasaheb Ambedkar Marathwada University, Aurangabad, Maharashtra, India;

^bDepartment of Chemistry, Radhabai Kale Mahila Mahavidyalaya, Ahmednagar, Maharashtra, India; ^cHaffkine Institute for Training, Research and Testing, Mumbai, Maharashtra, India; ^dDepartment of Pharmaceutical Chemistry, School of Pharmacy, Vishwakarma University, Pune Maharashtra, India

ABSTRACT

In search of new active molecules, a small focused library of 1,2,3-triazoles based 2,4-thiazolidinedione derivatives has been efficiently prepared *via* the click chemistry approach. Several derivatives were exhibited excellent anti-inflammatory activity compared to the standard drug. Further, the synthesized compounds were found to have potential antioxidant activity. Furthermore, to rationalize the observed biological activity data, the molecular docking study has also been carried out against the active site of inflammation enzyme PPAR γ , which revealed a significant correlation between the binding score and biological activity for these compounds. The results of the *in vitro* and *in silico* study suggest that the triazole incorporated 2,4-thiazolidinedione derivatives may possess the ideal structural requirements for the further development of novel therapeutic agents.

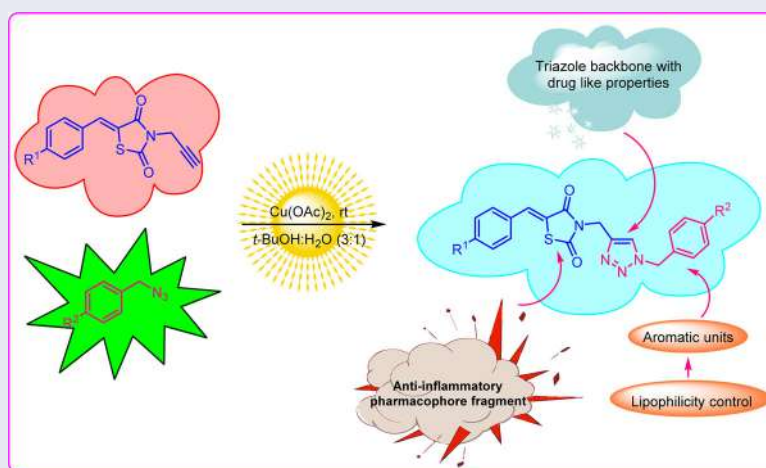
ARTICLE HISTORY

Received 18 January 2022

Accepted 11 April 2022

KEYWORDS

Click chemistry; 1,2,3-triazoles; anti-inflammatory activity; antioxidant activity; 2,4-thiazolidinedione



Introduction

There are numerous biologically active molecules with nitrogen, sulfur and oxygen heteroatoms that have always drawn the attention of chemists over the years mainly because of their biological importance, therefore, extensive research is still needed to improve their properties and to reduce

their adverse effects. Thiazolidinone is considered as a biologically important active scaffold that possesses almost all types of biological activities.¹ Thiazolidine-2,4-dione (TZDs) are a class of insulin sensitizing drugs which include ciglitazone, pioglitazone and rosiglitazone. Apart from their known antidiabetic activity,² the ability of TZDs to contribute to cancer therapy has been evidenced by numerous *in vitro* and *in vivo* studies,³ antibacterial and antifungal activity,⁴ aldose reductase inhibitory activity,⁵ antimicrobial activity,⁶ anti-inflammatory activity,⁷ oncostatic,⁸ anti-cancer activity⁹ and tuberculostatic activity.¹⁰

The involvement of PPAR γ in inflammatory processes was first suggested by the antagonism between the activities of proinflammatory cytokines and PPAR γ . Additionally, macrophage activation is inhibited by several PPAR γ agonists.¹¹ Therefore; this receptor is an attractive target for the development of anti-inflammatory agents due to its key roles at various stages in the inflammatory process. The two thiazolidines share a common thiazolidine-2,4-dione structure that is responsible for the majority of their pharmacological effects, including anti-inflammatory effects.¹² It has been shown that PPAR γ trans-represses the expression of pro-inflammatory mediators at the transcriptional level, by inhibiting inducible nitric oxide synthase (iNOS), NF- κ B, STAT and activation protein-1 (AP-1) signaling.¹³ Thus, drugs with anti-inflammatory properties such as TZDs (clubbed with triazole) can probably reduce the risk of inflammation-induced problems.

Antioxidant therapies are gaining importance due to their ability to retard disease progression by reducing the damage caused by free radical oxidative stress in a patient.¹⁴ Physiological levels of reactive oxygen species (ROS) play a vital role as signaling molecules to mediate numerous biological functions causing alterations in cell growth, gene expression and host defence.¹⁵ Under inflammatory conditions, the presence of excess reactive oxygen species (O₂, OH⁻, H₂O₂, NO, ONOO⁻) can initiate damage to nucleic acids, proteins, carbohydrates and lipids in many types of cells including macrophages.¹⁶ Increased oxidative stress-induced production of ROS, overwhelming the antioxidant defence system, has been implicated in the pathogenesis of various disorders including atherosclerosis,¹⁷ cancer,¹⁸ asthma,¹⁹ rheumatoid arthritis,²⁰ ischemia-reperfusion injury,²¹ neurodegenerative diseases,²² inflammation,²³ myocardial infarction and also aging.²⁴

Triazoles are stable to acidic/basic hydrolysis and also reductive/oxidative conditions, indicative of a high aromatic stabilization. This moiety is relatively resistant to metabolic degradation. Over the past two decades, 1,2,3-triazole and its derivatives have attracted continued interest in the medicinal field and are reported to possess a wide range of biological activities such as antifungal,²⁵ antitubercular,²⁶ antiallergic,²⁷ a anti-HIV activity,²⁷ b α -glucosidase inhibitor,⁹ antimicrobial,²⁸ anticoccidiostats,²⁹ anticonvulsant,³⁰ antimalarial,³¹ antiviral³² and antimycobacterial,³³ antitumor,³⁴ antiproliferative efficacy³⁵ and anticancer activity.³⁶ Similarly, copper oxide chitosan nanocomposite has been used for green regioselective synthesis of [1,2,3]triazoles.³⁷ Triazole has been used to improve the pharmacokinetic properties of the desired drug.³⁸

Barros et. al., synthesized arylidene-thiazolidine-2,4-diones and assayed *in vivo* to investigate their anti-inflammatory activities.³⁹ These compounds showed considerable biological efficacy when compared to rosiglitazone, a potent and well-known agonist of PPAR γ . In recent years, a library of thiazolidinedione derivatives conjugated with triazole skeleton was synthesized and proved to possess different bioactivity such as α -glucosidase inhibition,⁹ anticancer,⁹ hypoglycemic,⁴⁰ antibacterial,^{41a} and antifungal activity^{41b} (Figure 1).

The search for new anti-inflammatory and antioxidant agents will consequently remain as an important and challenging task for medicinal chemists. The combination of two pharmacophores into a single molecule is an effective and commonly used direction in modern medicinal chemistry for the exploration of novel and highly active compounds. In continuation of our earlier work⁴² on the synthesis and biological properties of various heterocyclic moieties, herein, a small focused library of 1,2,3-triazole incorporated molecules have been efficiently prepared by click chemistry. Considering the biological importance of 2,4-thiazolidinediones and 1,2,3-triazoles, we

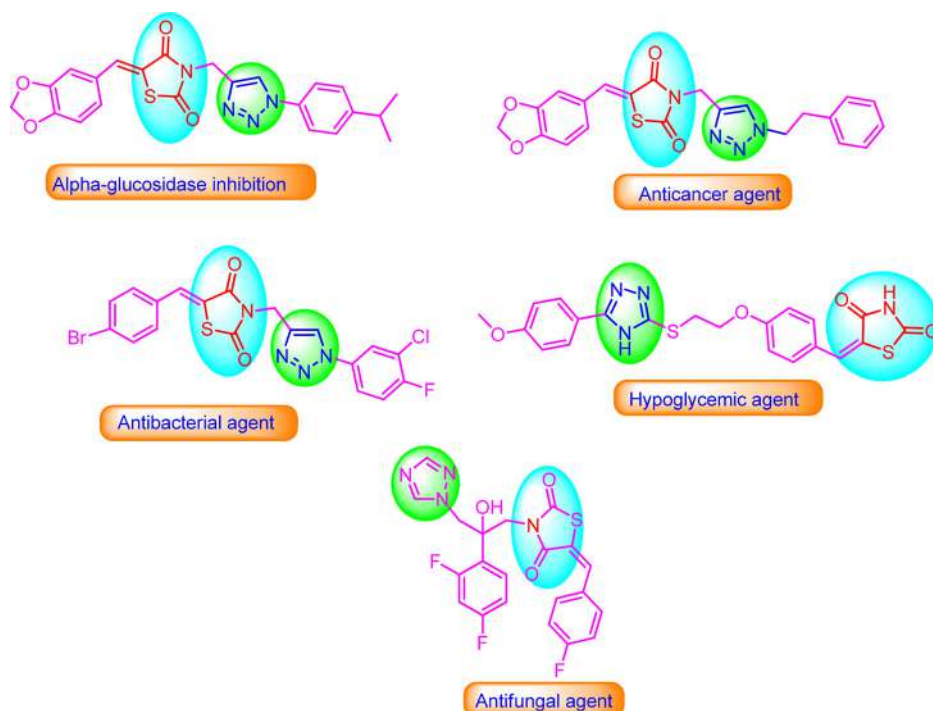


Figure 1. Thiazolidinedione derivatives clubbed with triazole shows different biological activity.

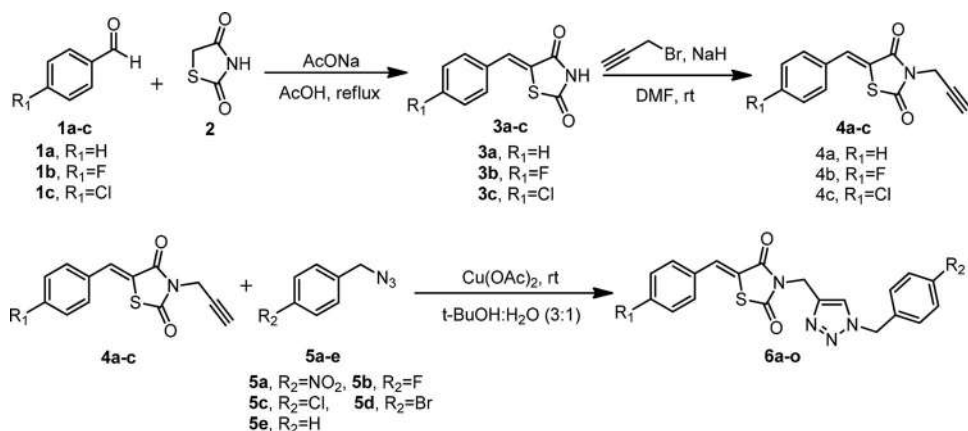
construct conjugated thiazolidinedione with 1,2,3-triazoles in one molecular framework through a methylene linkage to enhance the anti-inflammatory activity with minimizing the side effects. In addition to this, we have also performed molecular docking study and *in silico* ADME prediction for the synthesized compounds.

Results and discussion

Chemistry

We have described a protocol for the syntheses of a series of new (*Z*)-5-benzylidene-3-((1-(4-substitutedbenzyl)-1*H*-1,2,3-triazol-4-yl)methyl)thiazolidine-2,4-diones **6a-o** as a potential anti-inflammatory and antioxidant agents from commercially available starting materials (Scheme 1). These compounds were formed by the fusion of substituted (*Z*)-5-benzylidene-3-(prop-2-yn-1-yl)thiazolidine-2,4-dione **4a-c** and benzyl azides **5a-e** via click chemistry (Scheme 1). The substituted (*Z*)-5-benzylidene-3-(prop-2-yn-1-yl)thiazolidine-2,4-diones **4a-c** were prepared in two steps, in the first step, (*Z*)-5-benzylidenethiazolidine-2,4-diones **3a-c** were prepared by Knoevenagel condensation reaction between benzaldehydes **1a-c** and 2,4-thiazolidinedione **2** under reflux conditions in acetic acid using sodium acetate as the base. In the second step, (*Z*)-5-benzylidene thiazolidine-2,4-dione **3a-c** have been alkylated with propargyl bromide in the presence of K_2CO_3 as a base in *N,N*-dimethylformamide (DMF) afforded the corresponding (*Z*)-5-benzylidene-3-(prop-2-yn-1-yl)thiazolidine-2,4-diones **4a-c** in good to excellent yield.

Finally, the Huisgen's CuAAC reaction has been performed on (*Z*)-5-benzylidene-3-(prop-2-yn-1-yl)thiazolidine-2,4-dione **4a-c** and benzyl azides **5a-e** in the presence of $Cu(OAc)_2$ in *t*-BuOH- H_2O (3:1) at room temperature for 22-30 h gave the corresponding 1,4-disubstituted-1,2,3-triazole based 2,4-thiazolidinedione derivatives **6a-o** in quantitative isolated yield (90-92%) (Scheme 1).



Scheme 1. Synthesis of 1,4-disubstituted-1,2,3-triazole based 2,4-thiazolidinedione derivatives.

The formation of compounds **6a-o** was confirmed by physical data and spectral analysis. In the ¹H NMR spectrum of compound **6b**, the two methylene groups attached to nitrogen showed singlet at δ 4.89 and 5.55 ppm. In addition to this, the signal observed at δ 8.18 ppm indicates the presence of olefinic proton. In the ¹³C NMR spectrum for compound **6b**, the signals at δ 37.2 and 52.6 ppm indicate the presence of methylene carbon attached to the nitrogen of 2,4-thiazolidinedione and triazole ring, respectively. Furthermore, two characteristics carbon signals exhibited at δ 165.7 and 167.5 ppm due to the -N-C=O and -S-C=O groups, respectively. The formation of compound **6b** has been confirmed by the HRMS spectrum. For compound **6b**, the calculated mass for [M+H]⁺ is 395.0978 and in HRMS, the [M+H]⁺ peak was observed at 395.0981. Furthermore, to expand the series, 1,4-disubstituted-1,2,3-triazole-2,4-thiazolidinedione derivatives **6a-o** with various substituents have been prepared by the cycloaddition reaction of (Z)-5-benzylidene-3-(prop-2-yn-1-yl)thiazolidine-2,4-dione **4a-c** and benzyl azides **5a-e** (Scheme 1 and Table 1) under similar reaction condition in good to excellent yields.

Biological evaluation

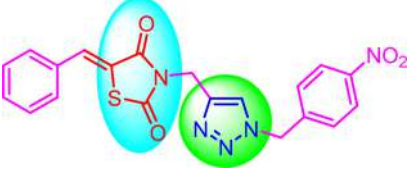





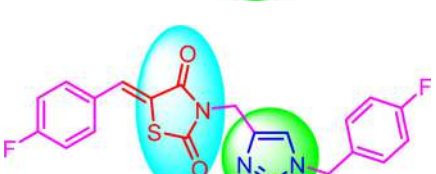
Anti-inflammatory activity

The newly synthesized 1,2,3-triazole incorporated 2,4-thiazolidinedione derivatives **6c**, **6d**, **6e** and **6o** (EC₅₀ range = 0.6483 ± 0.221-0.8519 ± 0.281 μg/mL) exhibited excellent anti-inflammatory activity as compared to the standard drug diclofenac sodium (Table 1).

Remaining compounds were found to show less anti-inflammatory activity. Compound **6c** (EC₅₀ = 0.8519 ± 0.281 μg/mL), **6d** (EC₅₀ = 0.7034 ± 0.349 μg/mL) and **6e** (EC₅₀ = 0.6483 ± 0.221 μg/mL) from **6a-e** were found to display more anti-inflammatory activity than standard drug DFS. When NO₂ group at R² in compound **6a**, (EC₅₀ = 8.668 ± 2.63 μg/mL) and fluoro- at R² in compound **6b** (EC₅₀ = 11.66 ± 1.22 μg/mL) did not show any significant change in activity. Replacement of R² = Cl group led to increase in activity (compound **6c**, EC₅₀ = 0.8519 ± 0.281 μg/mL). Again, when bromo- group is at R² in compound **6d** (EC₅₀ = 0.7034 ± 0.349 μg/mL) further increases the anti-inflammatory activity compared to the standard DFS. Surprisingly, the compound **6e** (EC₅₀ = 0.6483 ± 0.221) in which R₁ = H and R₂ = H exhibited excellent anti-inflammatory activity among all the synthesized compounds.








Among the **6f-j** series, all the five compounds (EC₅₀ range = 31.43 ± 0.192-57.80 ± 0.224 μg/mL) have shown less potent anti-inflammatory activity compared with standard drug DFS. There is no significant variation observed while varying the substituent like, NO₂, Cl, F and Br on the phenyl ring system (Table 1). Compound **6o** (EC₅₀ = 0.8416 ± 0.239 μg/mL) from **6k-6o** series

Table 1. *In vitro* anti-inflammatory activity and antioxidant activity of compounds **6a-o**.

Compound	Structure	Anti-inflammatory		Antioxidant	
		EC ₅₀ (μg/mL)	μM	IC ₅₀ (μg/mL)	μM
6a		8.668 ± 2.63	21.27	30.20	74.12
6b		11.66 ± 1.22	30.65	39.43	103.64
6c		0.8519 ± 0.281	2.15	22.48	56.64
6d		0.7034 ± 0.349	1.59	16.30	36.93
6e		0.6483 ± 0.221	1.79	20.41	56.31
6f		47.23 ± 0.881	111.01	16.78	39.44
6g		31.43 ± 0.192	78.88	12.55	31.49


(continued)

Table 1. Continued.

Compound	Structure	Anti-inflammatory		Antioxidant	
		EC ₅₀ (μg/mL)	μM	IC ₅₀ (μg/mL)	μM
6h		57.80 ± 0.224	139.32	15.19	36.61
6i		47.49 ± 0.116	103.39	19.20	41.8
6j		32.64 ± 0.191	85.80	13.82	36.33
6k		65.93 ± 0.180	149.20	17.18	38.88
6l		17.76 ± 0.350	42.81	27.23	65.63
6m		6.630 ± 0.241	15.37	33.30	77.20
6n		10.96 ± 0.182	23.04	19.28	40.52

(continued)

Table 1. Continued.

Compound	Structure	Anti-inflammatory		Antioxidant	
		EC ₅₀ (μg/mL)	μM	IC ₅₀ (μg/mL)	μM
6o		0.8416 ± 0.239	1.77	29.23	73.64
DFS	–	0.7227 ± 0.250	2.27	–	–
BHT	–	–	–	16.47	74.74

Values are expressed as mean ± standard deviation (n = 3); DFS: Diclofenac Sodium; BHT: Butylated Hydroxy Toluene; NT: Not tested

bearing R¹ = Cl and R² = H group was found to be display excellent anti-inflammatory activity compared to the standard drug DFS. Replacement of *nitro*- group at R² in compound **6k**, (EC₅₀ = 65.93 ± 0.180 μg/mL), *fluoro*- at R² in compound **6l** (EC₅₀ = 17.76 ± 0.350 μg/mL) and *bromo*- at R² in **6n** (EC₅₀ = 10.96 ± 0.182 μg/mL) did not show any significant change in the activity. In compound **6m**, (EC₅₀ = 6.630 ± 0.241 μg/mL), the replacement of the *chloro*- group at a R² led to decrease in the activity.

Antioxidant activity

According to the DPPH assay, compounds **6d** (IC₅₀ = 16.3 μg/mL), **6f** (IC₅₀ = 16.78 μg/mL), **6g** (IC₅₀ = 12.53 μg/mL), **6h** (IC₅₀ = 15.19 μg/mL) and **6j** (IC₅₀ = 13.82) show excellent antioxidant activity compared to the standard antioxidant drug BHT (IC₅₀ = 16.47 μg/mL) (Table 1). Compound **6d** (IC₅₀ = 16.3 μg/mL) from **6a-e** series bearing R² = Br group was found to be display more antioxidant activity than standard drug BHT. Replacement of R² = F group led to decrease in activity by two-fold (compound **6b**, IC₅₀ = 39.43 μg/mL). Replacement of NO₂ group at R² in compound **6a**, (IC₅₀ = 30.2 μg/mL) and *chloro*- at R² in compound **6c** (IC₅₀ = 27.3 μg/mL) did not show any significant change in activity. When hydrogen is at R² in compound **6e** (IC₅₀ = 20.41 μg/mL) exhibited satisfactory antioxidant, activity compared to the standard BHT. Among **6f-j** series, all the five compounds (IC₅₀ range = 12.55-19.2 μg/mL) have shown good activity when compared with standards. There is no significant variation observed while varying the substituent like, NO₂, Cl, F and Br. Compound **6g** (IC₅₀ = 12.55 μg/mL) bearing R¹ and R² = F group was found to be most active antioxidant agent among synthesized compounds than standard drug BHT. From **6k-o** series, all compounds (IC₅₀ range = 17.18-33.3 μg/mL) except **6k** (IC₅₀ = 17.18 μg/mL) showed less potent activity when compared with standards.

Computational study

Molecular docking study

The most appropriate approach for gauging the accuracy of a docking protocol is to monitor how closely the lowest energy binding pose predicted by the scoring function resembles the experimentally observed binding mode in the PDB. The molecular docking protocol adopted in the current study was validated by extracting the native ligand from the crystal structure and re-docking it to the binding site of PPARγ. The root means square deviation (RMSD) between the X-ray conformation of native ligand and the conformation predicted by docking into crystal structure was found to be less than 1 Å, validating the reliability of and reproducibility of the docking

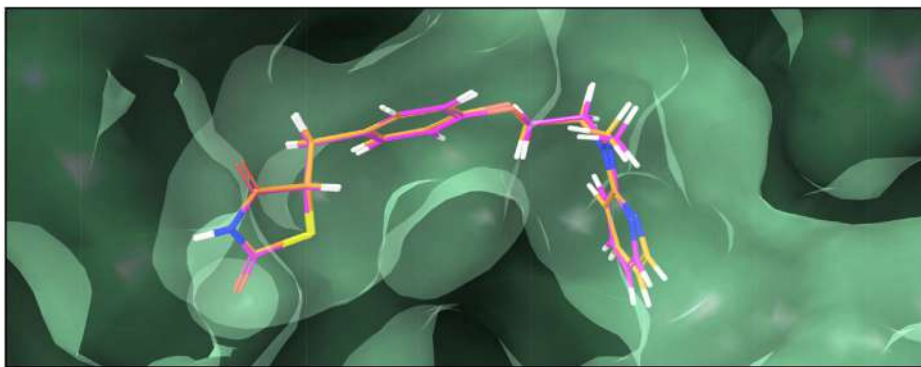


Figure 2. Overlay of the best scoring poses for the co-crystallized ligand-Rosiglitazone obtained by docking (orange carbon) against the X-ray bound conformation (pink carbon).

procedure in reproducing the experimentally observed binding mode for molecules investigated herein. The overlay of the experimentally observed binding mode of the native ligand over its best docked conformation is shown in [Figure 2](#).

The level of anti-inflammatory activities demonstrated by 2,4-thiazolidinedione-1,2,3-triazole derivatives motivated us to gain an insight into molecular interactions that govern the binding of these molecules with the target enzyme PPAR γ . In the absence of available resources to carry out the enzyme-based experimental studies, molecular docking study has gained significant attention to identify the targets for different ligands and provides an alternative approach to understand the thermodynamic events involved in the binding of molecules to the active site of the target enzyme which thereby helps to rationalize their experimentally observed biological activity.

Molecular docking study revealed that all the 1,2,3-Triazole incorporated 2,4-Thiazolidinedione derivatives investigated herein, snugly fitted into the active site of PPAR γ with very similar orientations occupying coordinates very close to that of the native ligand in the crystal structure and their resulting complexes were stabilized by a network of steric and electrostatic interactions ([Figure 3](#)). Their binding energies were also found to be very favorable ranging from -50.869 kcal/mol to -27.09 kcal/mol while the docking score ranged from -8.51 to -6.21 . The docking score for the native ligand Rosiglitazone was found to be -9.511 with a binding energy of -58.26 kcal/mol. We could observe a statistically significant correlation between the experimental anti-inflammatory activities and the molecular docking scores wherein the active analogues exhibited higher docking scores while those with relatively low inhibition were also predicted to have a lower score.

Furthermore, a detailed per-residue interaction analysis between the enzyme and the docked 1,2,3-Triazole incorporated 2,4-Thiazolidinedione derivatives were carried out to identify the most significantly interacting residues and provide an explanation for the observed difference in binding affinity for these molecules through which we can speculate regarding the detailed binding patterns in the cavity. For the sake of brevity, we have illustrated this analysis only for the most active analogue **6e** ([Figure 4](#)) while the results for other derivatives and their binding modes shown in ([Table 2](#)) and molecular docking images shown in [Figure 5](#).

The lowest energy docking pose of the most active analogue **6e** into the active site of PPAR γ revealed that it binds to the enzyme with a significantly higher binding affinity (docking score: -8.51 , binding energy: -50.869 kcal/mol) which can be explained in terms of the specific bonded and non-bonded per-residue interactions with the residues shaping the active site. The per residue-ligand interaction energy distribution showed that the compound is stabilized within the active site of PPAR γ through an extensive network of van der Waals interactions with Met348 (-1.80 kcal/mol), Ile341 (-3.74 kcal/mol), Leu330 (-2.90 kcal/mol), Arg288 (-4.51 kcal/mol), Gly284 (-3.41 kcal/mol), Ile281 (-2.87 kcal/mol) and Arg280 (-1.04 kcal/mol) residues through

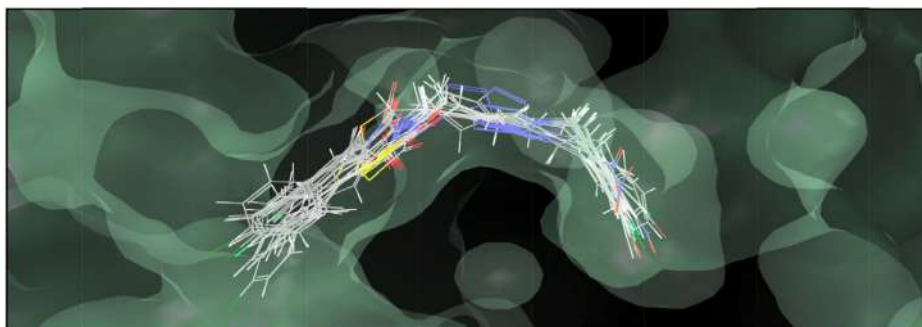


Figure 3. Binding modes of 1,2,3-Triazole incorporated 2,4-Thiazolidinedione Derivatives into the active site of human peroxisome proliferator-activated receptor gamma (PPAR γ).

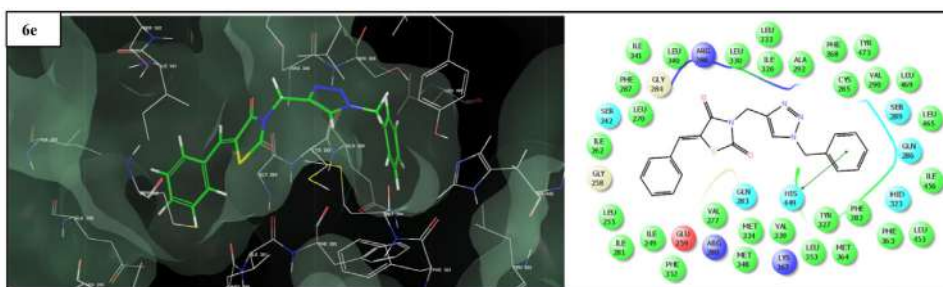


Figure 4. Binding mode of **6e** into the active site of human peroxisome proliferator-activated receptor gamma (PPAR γ) (the π - π stacking interaction has been represented using green lines).

benzylidethiazolidine-2,4-dione section of the molecule while 1-benzyl-1*H*-1,2,3-triazol-4-yl component was engaged in favorable van der Waals interactions with Tyr473 (-1.28 kcal/mol), Leu453(-1.18 kcal/mol), His449(-2.14 kcal/mol), Met364(-2.75 kcal/mol), Tyr327(-2.85 kcal/mol), Ile326(-2.74 kcal/mol), His323(-1.51 kcal/mol), Ser289(-2.39 kcal/mol), Gln286(-3.15 kcal/mol), Cys285(-8.85 kcal/mol), Phe282(-2.25 kcal/mol) residues. Analysis of the polar contacts i.e. electrostatic interactions revealed multiple closed contacts with Lys367 (-1.21 kcal/mol), Met364(-1.02 kcal/mol) and Arg288(-4.86 kcal/mol) residues. The enhanced binding affinity of **6e** is also attributed to its position in the π -interaction space (π - π stacking) of His449(2.46 Å). This type of the π - π stacking interaction serves as an "anchor", guiding the 3D orientation of the ligand in the active site of the enzyme and thereby aid the steric and electrostatic interactions within. Thus, a strong network of thermodynamic interactions observed with PPAR γ account for its good *in silico* affinity and provides a clue for its significant *in vitro* anti-inflammatory activity.

A similar network of thermodynamic interaction was consistently observed for other 1,2,3-Triazole incorporated 2,4-Thiazolidinedione derivatives investigated herein as well but decreasing gradually with their observed anti-inflammatory activity. The per-residue interaction energy distribution revealed that the primary driving force for mechanical interlocking was the steric complementarity between the ligand and the active site residues of PPAR γ which is reflected in the relatively higher number of favorable van der Waals interaction over other components contributing to the overall binding scores. The binding pattern predicted by docking and the per-residue interaction energy distribution along with the glide score and the glide energy indicates that these 1,2,3-Triazole incorporated 2,4-Thiazolidinedione derivatives have a good affinity toward the active site of PPAR γ enzyme making them pertinent starting points for further structure-based design efforts.

Table 2. Results of the per-residue interaction analysis for the 2,4-thiazolidinedione-1,2,3-triazole derivatives with the active site of human PPAR γ .

Cpd	Docking score	Binding energy	Per-residue interaction energy analysis		
			Van der Waals (Kcal/mol)	Electrostatic (Kcal/mol)	π - π stacking (Å)
6a	-7.63	-44.861	His449(-1.88), Met364(-2.02), Phe363(-1.69), Met348(-2.12), Ser342(-1.20), Ile341(-3.18), Leu330(-2.68), Tyr327(-2.29), Ile326(-2.38), Ser289(-2.29), Arg288(-4.10), Gln286(-2.93), Cys285(-6.97), Gly284(-2.93), Phe282(-1.80), Ile281(-2.46), Arg280(-1.32)	His 449 (-1.13), Lys 367 (-1.10), Arg 288 (-3.24), Glu 259 (-1.16)	Tyr327 (2.37), His449 (2.41)
6b	-7.23	-41.783	His449(-2.00), Met364(-1.98), Ser342(-1.97), Ile341(-3.09), Leu330(-3.19), Tyr327(-2.16), Ile326(-2.14), Glu291(-1.61), Ser289(-2.34), Arg288(-3.35), Phe287(-2.33), Gln286(-2.41), Cys285(-5.96), Gly284(-2.60), Phe282(-1.52), Ile281(-2.07), Arg280(-1.16)	Glu291 (-1.75), Arg288(-2.61),	Tyr327(2.10), His449(2.56), Phe287(2.59)
6c	-8.214	-47.368	Tyr473(-1.10), His449(-2.07), Met364(-2.50), Met348(-2.29), Ile341(-3.68), Leu330(-2.74), Tyr327(-2.32), Ile326(-2.71), His323(-1.40), Ser289(-2.67), Arg288(-3.29), Gln286(-3.06), Cys285(-7.06), Gly284(-3.23), Phe282(-1.84), Ile281(-2.62), Arg280(-1.07)	Met364(-1.16), Arg288(-2.94), Cys285(-1.02),	His449(2.24)
6d	-8.50	-49.006	Tyr473(-1.25), His449(-2.13), Met364(-2.20), Met348(-1.73), Ile341(-3.70), Leu330(-2.91), Tyr327(-2.25), Ile326(-2.54), His323(-1.46),	Met364(-1.15), Arg288(-4.17), Glu259(-1.05)	His449(2.98)

(continued)

Table 2. Continued.

Cpd	Docking score	Binding energy	Per-residue interaction energy analysis		
			Van der Waals (Kcal/mol)	Electrostatic (Kcal/mol)	π - π stacking (Å)
6e	-8.51	-50.869	Ser289(-2.17), Arg288(-3.40), Gln286(-2.23), Cys285(-8.37), Gly284(-3.53), Phe282(-2.26), Ile281(-2.02), Arg280(-1.08),	Lys367 (-1.21), Met364(-1.02), Arg288(-4.86),	His449 (2.46)
			Tyr473 (-1.28), Leu453(-1.18), His449(-2.14), Met364(-2.75), Met348 (-1.80), Ile341(-3.74), Leu330(-2.90), Tyr327(-2.85), Ile326(-2.74), His323(-1.51), Ser289(-2.39), Arg288(-4.51), Gln286(-3.15), Cys285(-8.85), Gly284(-3.41), Phe282(-2.25), Ile281(-2.87), Arg280(-1.04)		
6f	-6.54	-33.63	Tyr473 (-0.97), His449(-1.37), Met364(-1.75), Met348(-1.11), Ile341(-3.11), Leu330(-2.89), Tyr327(-2.04), Ile326(-1.75), Glu291(-1.58), Ser289(- 2.17), Arg288(-3.08), Phe287(-2.64), Gln286(-2.10), Cys285(-5.27), Gly284(-2.36), Phe282(-1.16), Ile281(-1.31)	Glu291(-1.307), Arg288(-1.534),	Tyr327(2.19), His449(2.55), Phe287(2.63)
			His449(-1.85), Met364(-1.77), Phe363(-1.36), Ser342(-1.93), Ile341(-3.10), Leu330(-3.02), Tyr327(-2.11), Ile326(-1.95), Glu291(-1.40), Ser289(-2.23), Arg288(-3.17), Phe287(-2.89), Gln286(-2.17), Cys285(-5.58), Gly284(-2.37), Phe282(-1.31), Ile281(-1.99), Arg280(-1.14)	Glu291 (-1.59), Arg288(-1.187),	Tyr327(2.13), His449(2.24), Phe287(2.81)
6g	-7.00	-38.548	His449(-1.85), Met364(-1.77), Phe363(-1.36), Ser342(-1.93), Ile341(-3.10), Leu330(-3.02), Tyr327(-2.11), Ile326(-1.95), Glu291(-1.40), Ser289(-2.23), Arg288(-3.17), Phe287(-2.89), Gln286(-2.17), Cys285(-5.58), Gly284(-2.37), Phe282(-1.31), Ile281(-1.99), Arg280(-1.14)	Glu291 (-1.59), Arg288(-1.187),	Tyr327(2.13), His449(2.24), Phe287(2.81)
6h	-6.61	-30.544	His449(-1.16), Met364(-1.29),	Glu291(-1.43), Arg288(-1.05)	His449(2.68), Phe287(2.64)

(continued)

Table 2. Continued.

Cpd	Docking score	Binding energy	Per-residue interaction energy analysis		
			Van der Waals (Kcal/mol)	Electrostatic (Kcal/mol)	π - π stacking (Å)
6i	-6.44	-32.484	Ile341(-3.34), Leu330(-2.17), Tyr327(-2.05), Ile326(-1.21), Glu291(-1.57), Ser289(-1.28), Arg288(-2.71), Phe287(-2.39), Gln286(-2.05), Cys285(-4.04), Gly284(-2.09), Phe282(-1.15), Ile281(-1.08)	Glu291(-1.74), Arg288(-1.16)	His449(2.52), Phe287(2.62)
			His449(-1.29), Met364(-1.57), Met348(-1.08), Ile341(-3.05), Leu330(-2.79), Tyr327(-2.01), Ile326(-1.47), Glu291(-1.61), Ser289(-2.68), Arg288(-3.09), Phe287(-2.48), Gln286(-2.13), Cys285(-5.28), Gly284(-2.16), Phe282(-1.15), Ile281(-1.03)		
6j	-6.99	-37.868	Tyr473 (-1.04), His449(-1.63), Met364(-1.74), Met348(-1.19), Ile341(-3.12), Leu330(-2.901), Tyr327(-2.07), Ile326(-1.86), Ser289(-2.22), Arg288(-3.12), Phe287(-2.78), Gln286(-2.10), Cys285(-5.35), Gly284(-2.24), Phe282(-1.27), Ile281(-1.92), Arg280(-1.13)	Arg288(-1.74), Cys285(-1.59),	Tyr327(2.29), His449(2.35),
			His449(-1.48), Met364(-1.14), Ile341(-3.14), Leu330(-1.14), Tyr327(-2.21), Ile326(-1.15), Arg288(-2.23), Phe287(-1.18), Cys285(-3.25), Gly284(-1.83), Phe282(-1.02), Ile281(-1.03), Arg280(-1.39)		
6k	-6.21	-27.09	His449(-1.48), Met364(-1.14), Ile341(-3.14), Leu330(-1.14), Tyr327(-2.21), Ile326(-1.15), Arg288(-2.23), Phe287(-1.18), Cys285(-3.25), Gly284(-1.83), Phe282(-1.02), Ile281(-1.03), Arg280(-1.39)	Lys367(-1.03), Arg288(-1.30)	Tyr327(2.68),
			His449(-1.95), Met364(-1.93), Phe363(-1.39), Ser342(-1.96)		
6l	-7.11	-40.497	His449(-1.95), Met364(-1.93), Phe363(-1.39), Ser342(-1.96)	Glu291 (-1.85), Arg288(-2.47)	His449(2.71)

(continued)

Table 2. Continued.

Cpd	Docking score	Binding energy	Per-residue interaction energy analysis		
			Van der Waals (Kcal/mol)	Electrostatic (Kcal/mol)	π - π stacking (Å)
6m	-7.837	-45.878	Ile341(-3.02), Leu330(-3.13), Tyr327(-2.16), Ile326(-2.10), Glu291(-1.68), Ser289(-2.32), Arg288(-3.62), Phe287(-2.31), Gln286(-2.22), Cys285(-5.73), Gly284(-2.60), Phe282(-1.50), Ile281(-2.05), Arg280(-1.14)		
			Tyr473(-1.04), His449(-1.99), Met364(-2.08), Met348(-2.12), Ile341(-3.35), Leu330(-2.70), Tyr327(-2.38), Ile326(-2.70), His323(-1.40), Ser289(-2.41), Arg288(-3.02), Gln286(-2.92), Cys285(-7.08), Gly284(-3.12), Phe282(-1.96), Ile281(-2.57), Arg280(-1.07)	Met364(-1.07), Arg288(-3.36)	His449(2.21)
6n	-7.36	-42.482	His449(-2.05), Met364(-2.04), Met348(-2.22), Ser342(-1.20), Ile341(-3.16), Leu330(-2.49), Tyr327(-2.14), Ile326(-2.16), Ser289(-2.38), Arg288(-3.46), Gln286(-2.66), Cys285(-6.23), Gly284(-2.75), Phe282(-1.72), Ile281(-2.36), Arg280(-1.28)	Met364 (-1.08), Arg288(-2.98)	His449(4.57)
6o	-8.37	-48.86	His449(-2.11), Met364(-1.77), Met348(-1.86), Ile341(- 3.637), Leu330(-2.87), Tyr327(-2.26), Ile326(- 2.72), Ser289(-1.60), Arg288(-3.16), Gln286(-2.66), Cys285(-8.42), Gly284(-2.99), Phe282(-2.18), Ile281(- 2.72), Arg280(-1.07), Glu259(-1.24), 255(-1.37)	Lys367(-1.22), Met364(-1.09), Arg288(-4.28)	His449(3.18)

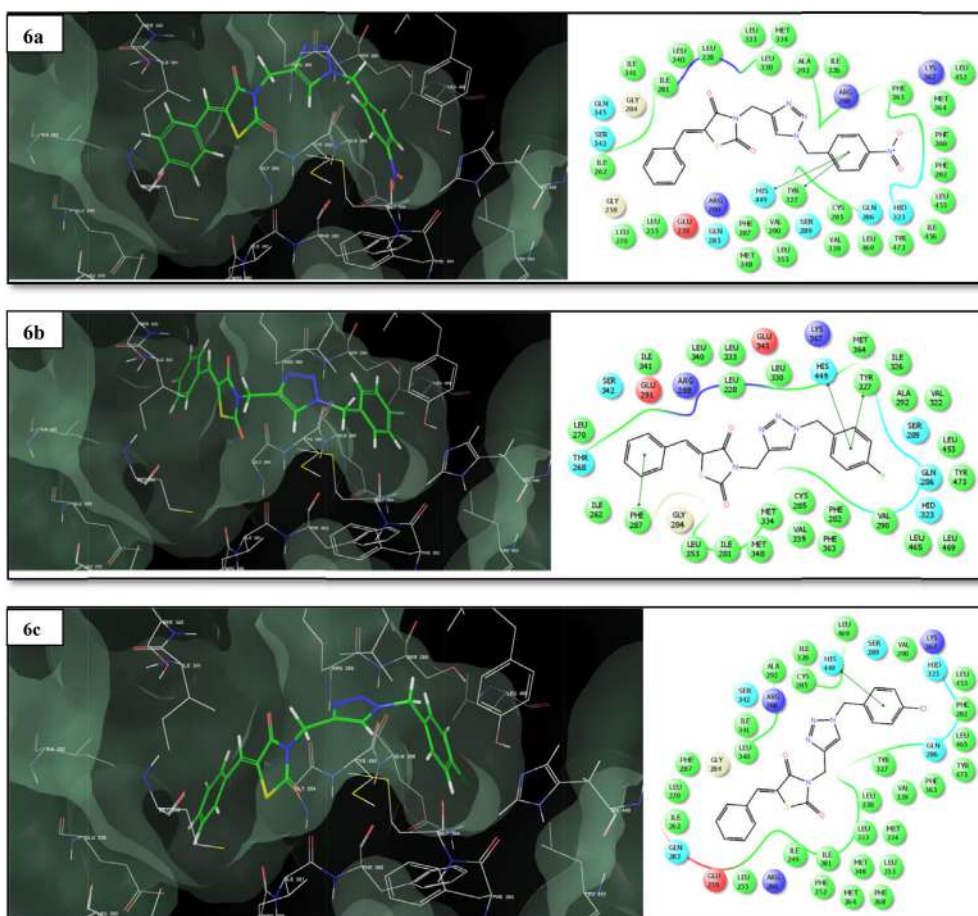


Figure 5. Binding mode of compounds into the active site of human peroxisome proliferator-activated receptor gamma (PPAR γ) (the π - π stacking interaction has been represented using green lines).

ADME properties

The success of a drug is determined not only by good efficacy but also by an acceptable ADME (absorption, distribution, metabolism and excretion) profile. A computational study of all the synthesized compounds was performed for the prediction of ADME properties and the value obtained is presented in Table 3. It is observed that compounds exhibited a good % ABS (% absorption) ranging from 69.11 to 85.02%.

Furthermore, none of the synthesized derivatives violates Lipinski's rule of five ($\text{miLog } P \leq 5$). A molecule likely to be developed as an orally active drug candidate should not show more than one violation of the following four criteria: $\text{miLog } P$ (octanol-water partition coefficient) ≤ 5 , molecular weight ≤ 500 , number of hydrogen bond acceptors ≤ 10 and number of hydrogen bond donors ≤ 5 .⁴³ The larger the value of the drug-likeness model score, the higher is also the probability that the particular molecule will be active. All the tested compounds followed the criteria for orally active drugs and therefore, these compounds may have a good potential for eventual development as oral agents.

Conclusion

In conclusion, we have synthesized new 1,2,3-triazole based thiazolidinone derivatives *via* click chemistry approach and evaluated them for biological activity. The synthesized 1,2,3-Triazole

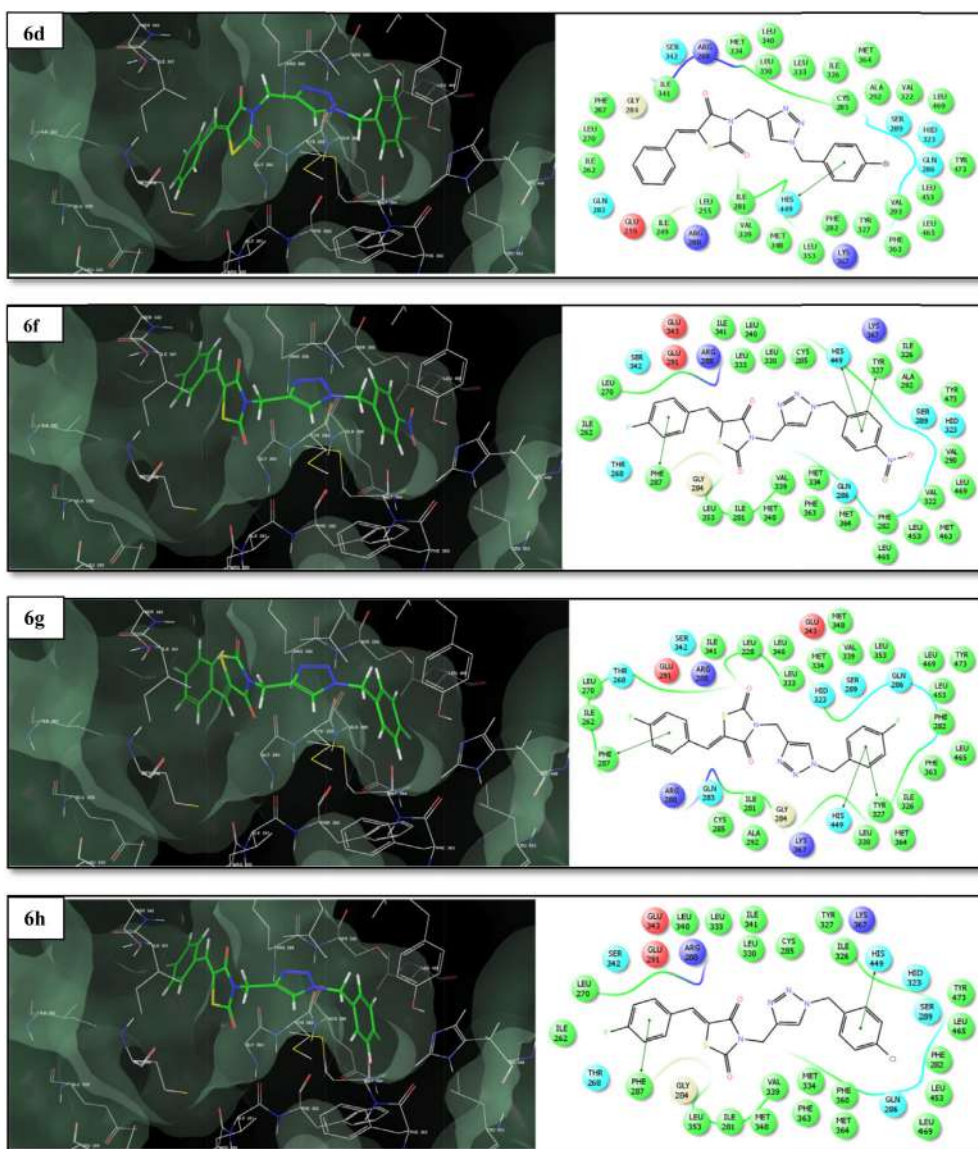


Figure 5. Continued.

incorporated 2,4-Thiazolidinedione derivatives exhibited promising anti-inflammatory activity. Compounds **6d** and **6e** display higher anti-inflammatory activity compared to the standard drug diclofenac sodium. Similarly, all the synthesized compound displays promising antioxidant activity as compared to the standard drug. Compounds **6d**, **6g**, **6h** and **6j** shows potential antioxidant activity ($IC_{50} = 12.55-16.30 \mu\text{g/mL}$) when compared with standard drug BHT. In addition to this, molecular docking study of 1,2,3-Triazole incorporated 2,4-Thiazolidinedione derivatives have a high affinity toward the active site of enzyme PPAR γ which provides a strong platform for new structure-based design efforts. Furthermore, analysis of the ADME parameters shows good drug-like properties and can be developed as an oral drug candidate. Thus, suggesting that compounds from the present series can be further optimized and developed as a lead molecule. Further work on the utilization of triazole incorporated thiazolidinedione derivatives leading to useful bioactive compounds is in progress.

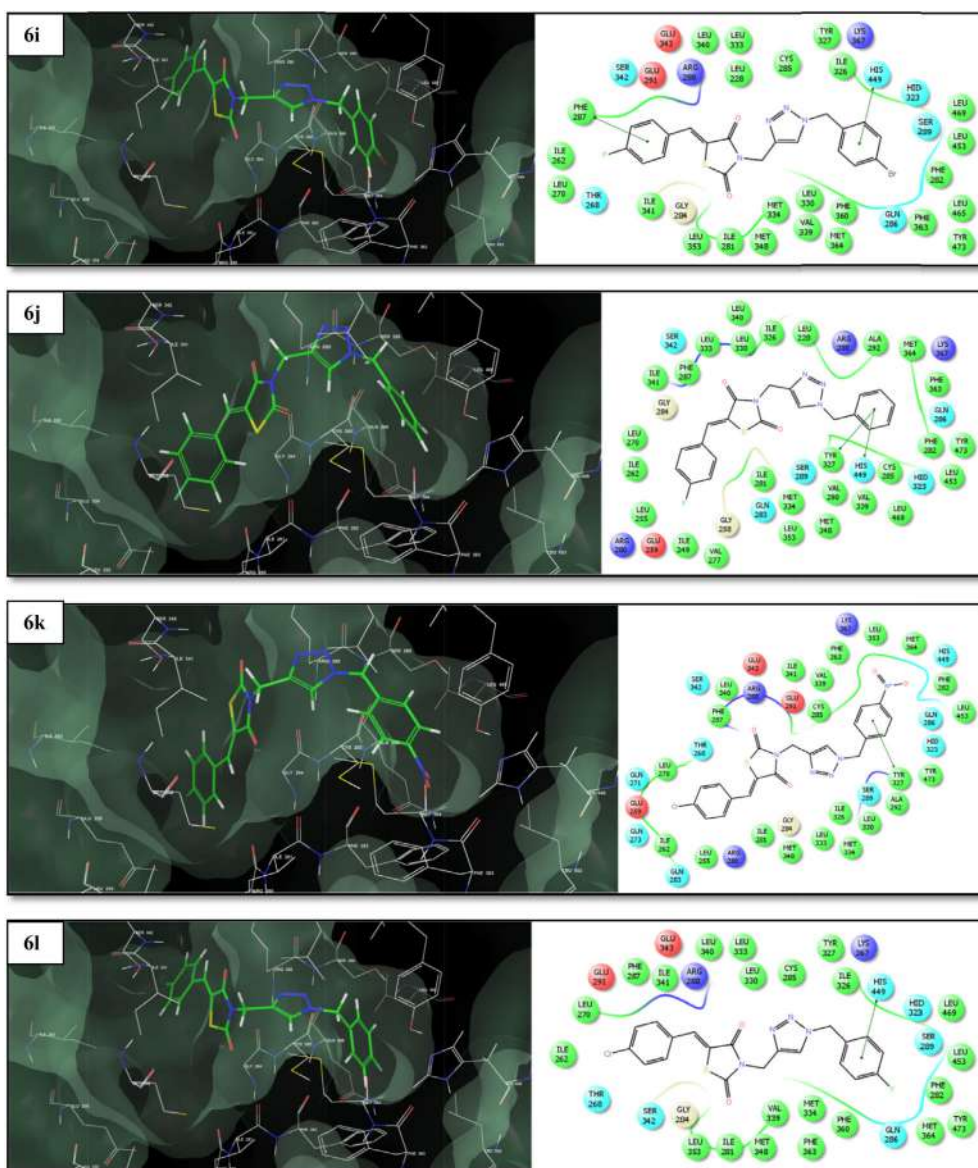


Figure 5. Continued.

Experimental section

General

All the solvents and reagents were purchased from commercial suppliers, Spectrochem Pvt. Ltd., Rankem India Ltd. and Sigma Aldrich which was used without further purification. The progress of each reaction was monitored by ascending thin layer chromatography (TLC) using TLC aluminum sheets, silica gel F₂₅₄ precoated, Merck, Germany and locating the spots using UV light as the visualizing agent or Iodine vapors. Melting points were taken in the open capillary method and are uncorrected. ¹H NMR spectra were recorded (DMSO-d₆) on Bruker Avance 400 NMR Spectrometer. ¹³C NMR and DEPT 135 spectra were recorded (DMSO-d₆) on Bruker Avance 100 NMR Spectrometer. Chemical shifts (δ) are reported in parts per million (ppm) using

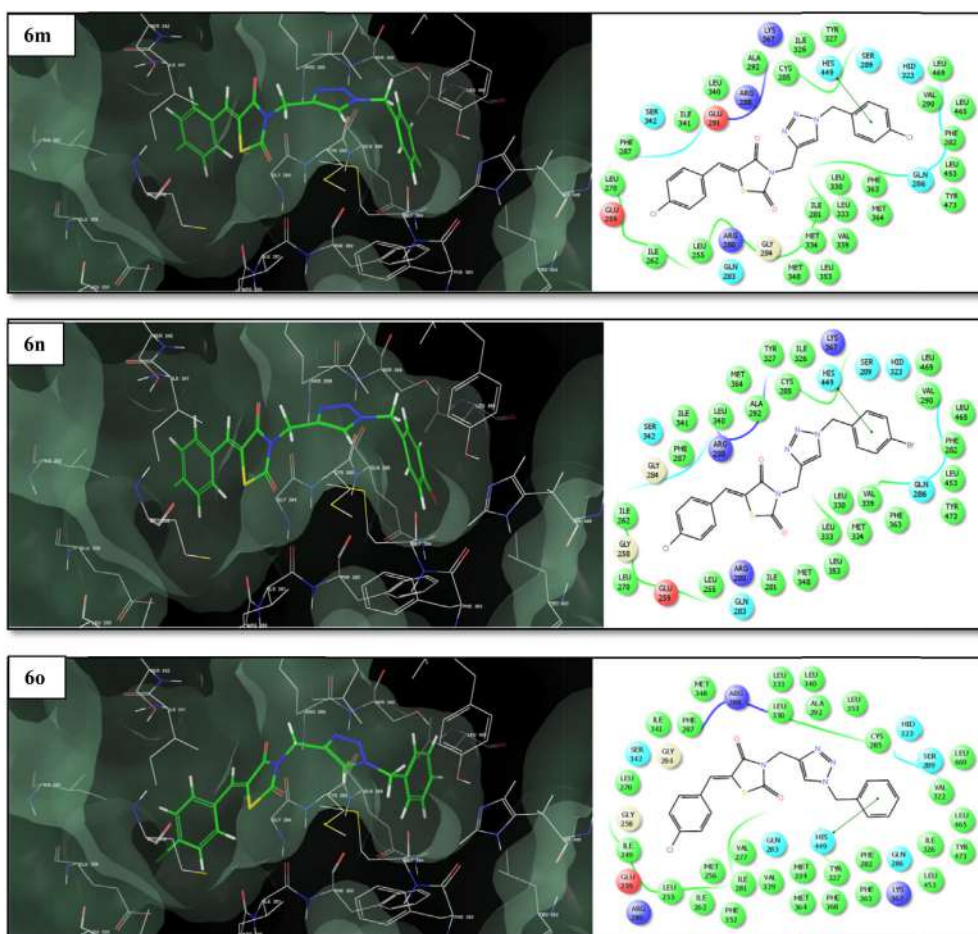


Figure 5. Continued.

Table 3. Pharmacokinetic parameters were important for good oral bioavailability and its drug – likeness model score.

Cpd Rule	% ABS	TPSA (Å ²)	n-ROTB	MV	MW	miLog P	n-ON	n-OHNN	Lipinski violation	drug likeness model score
	–	–	–	–	< 500	≤ 5	< 10	< 5	≤ 1	
6a	69.11	115.62	6	346.31	421.44	2.85	9	0	0	−0.14
6b	85.02	69.79	5	327.90	394.43	3.06	6	0	0	0.02
6c	85.02	69.79	5	336.51	410.89	3.57	6	0	0	0.19
6d	85.02	69.79	5	340.86	455.34	3.70	6	0	0	−0.17
6e	85.02	69.79	5	322.97	376.44	2.90	6	0	0	−0.23
6f	69.11	115.62	6	351.24	439.43	3.02	9	0	0	−0.02
6g	85.02	69.79	5	332.84	412.42	3.22	6	0	0	−0.09
6h	85.02	69.79	5	341.44	428.88	3.74	6	0	0	0.02
6i	85.02	69.79	5	345.79	473.33	3.87	6	0	0	−0.36
6j	85.02	69.79	5	327.90	394.43	3.05	6	0	0	0.02
6k	69.11	115.62	6	359.84	455.88	3.53	9	0	0	0.16
6l	85.02	69.79	5	341.44	428.88	3.73	6	0	0	0.02
6m	85.02	69.79	5	350.05	445.33	4.25	6	0	0	0.10
6n	85.02	69.79	5	354.39	489.78	4.38	6	0	0	−0.17
6o	85.02	69.79	5	336.51	410.89	3.57	6	0	0	0.19

Cpd: Compound, % ABS: Percentage Absorption, TPSA: Topological Polar Surface Area, nROTB: Number of Rotatable Bonds, MV: Molecular Volume, MW: Molecular Weight, miLogP: Logarithm of Partition Coefficient of Compound Between n-Octanol and Water, n-ON Acceptors: Number of Hydrogen Bond Acceptors, n-OHNN Donors: Number of Hydrogen Bonds Donors.

tetramethylsilane (TMS) as an internal standard. The splitting pattern abbreviations are designed as singlet (s); doublet (d); double doublet (dd); triplet (t); quartet (q) and multiplet (m). The mass spectra were recorded on Q-TOF micromass (YA-105) spectrometer in the ESI (Electrospray Ionization) modes.

General procedure for the synthesis of (Z)-5-benzylidenethiazolidine-2,4-dione (3a-c)

A mixture of aldehyde (10 mmol) **1a-c**, glacial acetic acid (10 mL), 2,4-thiazolidinedione **2** (10 mmol), and fused sodium acetate (20 mmol) was refluxed for 4-5 hr with constant stirring. The progress of the reaction was monitored by thin layer chromatography (*n*-Hexane/EtOAc 9:1). After completion of reaction indicated by TLC, it was allowed to cool at room temperature. Then ice cold water (50 mL) was added to it and whole reaction mass was stirred for 10 min and then filtered. The solid appeared was collected by simple filtration and washed with cold water. The crude compound was recrystallized using the ethanol/ethylacetate.

General procedure for synthesis of (Z)-5-benzylidene-3-(prop-2-yn-1-yl)thiazolidine-2,4-dione (4a-c). To the stirred solution of (Z)-5-benzylidenethiazolidine-2,4-dione (10 mmol) in *N,N*-dimethylformamide (DMF) (10 mL), K_2CO_3 (20 mmol) was added. The reaction mixture was stirred at room temperature for 30 minutes, which results in the corresponding anion. To this mixture, propargyl bromide (10 mmol) was added and stirred for 2 h. The progress of the reaction was monitored by TLC using ethyl acetate:hexane as a solvent system. The reaction was quenched by crushed ice. The obtained solid product was filtered and crystallized using ethanol/ethylacetate. The crystallized products were taken for the next step.

General procedure for synthesis of (Z)-5-benzylidene-3-((1-(4-substitutedbenzyl)-1H-1,2,3-triazol-4-yl)methyl)thiazolidine-2,4-dione (6a-o). To the solution of (Z)-5-benzylidene-3-(prop-2-yn-1-yl)thiazolidine-2,4-dione (**4a-c**) (1 mmol), benzyl azides **5a-e** (1 mmol) and copper diacetate ($Cu(OAc)_2$) (20 mole %) in *t*-BuOH- H_2O (3:1, 8 mL) and the resulting mixture was stirred at room temperature for 22-30 h. The progress of the reaction was monitored by TLC using ethyl acetate:hexane as a solvent system. The reaction mixture was quenched with crushed ice and extracted with ethyl acetate (2×25 mL). The organic extracts were washed with brine solution (2×25 mL) and dried over anhydrous sodium sulfate. The solvent was evaporated under reduced pressure to afford the corresponding crude compounds. The obtained crude compounds were crystallized using ethanol and ethyl acetate.

(Z)-5-Benzylidene-3-((1-(4-nitrobenzyl)-1H-1,2,3-triazol-4-yl)methyl)thiazolidine-2,4-dione (6a). The compound **6a** as a off white solid and was obtained *via* 1,3-dipolar cycloaddition between (Z)-5-benzylidene-3-(prop-2-yn-1-yl)thiazolidine-2,4-dione (**4a**) and 1-(azidomethyl)-4-nitrobenzene (**5a**) using 20 mol% of $Cu(OAc)_2$ in 26 h with 92% yield. Mp. 190 °C.

(Z)-5-Benzylidene-3-((1-(4-fluorobenzyl)-1H-1,2,3-triazol-4-yl)methyl)thiazolidine-2,4-dione (6b). The compound **6b** as a off white solid and was obtained *via* 1,3-dipolar cycloaddition between (Z)-5-benzylidene-3-(prop-2-yn-1-yl)thiazolidine-2,4-dione (**4a**) and 1-(azidomethyl)-4-fluorobenzene (**5b**) using 20 mol% of $Cu(OAc)_2$ in 26 h with 92% yield. Mp. 178-179 °C. IR (KBr) $\tilde{\nu}$: 653.6-783.8 (monosubstituted aromatic C-F stretching), 1599.8 (C=C stretching), 1685.52 (carbonyl carbon CN), 1754.21 (Carbonyl carbon CS), 2965.7 (Ar-H stretching). 1H NMR (400 MHz, DMSO- d_6 , ppm): δ 4.89 (s, 2H, CH_2 , methylene bridge between TZD and Triazole), 5.55 (s, 2H, CH_2 , methylene bridge between Triazole and phenyl ring), 7.18-7.38 (m, 2H, Ar-H at ortho position with respect to fluorine on phenyl), 7.39-7.49 (m, 2H, Ar-H at ortho position with respect to fluorine on phenyl), 7.50-7.56 (m, 3H, Ar-H fused with TZD), 7.62-7.64 (d, 2H, Ar-H fused

with TZD), 7.95 (s, 1H, Ar-H of triazole) and 8.18 (s, 1H, β -H of carbonyl). ^{13}C NMR (100 MHz, DMSO- d_6 , ppm): δ 37.2, 52.6 (methylene carbon between Triazole and phenyl ring), 116, 116.2, 121.6, 124.2, 129.9, 130.7, 130.8, 130.9, 131.3, 132.7, 133.4, 133.9, 141.9, 161.2, 163.6, 165.7 (Carbonyl carbon attached to the nitrogen) and 167.5 (Carbonyl carbon attached to the sulfur). HRMS calculated $[\text{M} + \text{H}]^+$ for $\text{C}_{20}\text{H}_{16}\text{N}_4\text{O}_2\text{SF}$: 395.0978, found: 395.0981; $[\text{M} + \text{Na}]^+$ for $\text{C}_{20}\text{H}_{15}\text{N}_4\text{O}_2\text{SFNa}$: 417.0798, found: 417.0802.

(Z)-5-Benzylidene-3-((1-(4-chlorobenzyl)-1H-1,2,3-triazol-4-yl)methyl)thiazolidine-2,4-dione (6c).

The compound **6c** as a off white solid and was obtained *via* 1,3-dipolar cycloaddition between (Z)-5-benzylidene-3-(prop-2-yn-1-yl)thiazolidine-2,4-dione (**4a**) and 1-(azidomethyl)-4-chlorobenzene (**5c**) using 20 mol% of $\text{Cu}(\text{OAc})_2$ in 26 h with 94% yield. Mp. 196 °C. ^1H NMR (400 MHz, DMSO- d_6 , ppm): δ 4.44 (s, 2H, CH_2 , methylene bridge between TZD and Triazole), 5.29 (s, 2H, CH_2 , methylene bridge between Triazole and phenyl ring), 7.48-7.88 (m, 9H, Ar-H), 8.26 (s, 1H, Ar-H of triazole) and 8.56 (s, 1H, β -H of carbonyl). ^{13}C NMR (100 MHz, DMSO- d_6 , ppm): δ 36 (methylene carbon between TZD and Triazole), 55.2 (methylene carbon between Triazole and phenyl ring), 141.5, 144.7, 151.1, 151.9, 152.6, 152.8, 156.2, 158.7 (Carbonyl carbon attached to the nitrogen) and 166.8 (Carbonyl carbon attached to the sulfur).

(Z)-5-Benzylidene-3-((1-(4-bromobenzyl)-1H-1,2,3-triazol-4-yl)methyl)thiazolidine-2,4-dione (6d).

The compound **6d** as a off white solid and was obtained *via* 1,3-dipolar cycloaddition between (Z)-5-benzylidene-3-(prop-2-yn-1-yl)thiazolidine-2,4-dione (**4a**) and 1-(azidomethyl)-4-bromobenzene (**5d**) using 20 mol% of $\text{Cu}(\text{OAc})_2$ in 28 h with 92% yield. Mp. 204-205 °C. ^1H NMR (400 MHz, DMSO- d_6 , ppm): δ 4.43 (s, 2H, CH_2 , methylene bridge between TZD and Triazole), 5.26 (s, 2H, CH_2 , methylene bridge between Triazole and phenyl ring), 7.39-7.41 (d, 2H, Ar-H at ortho position with respect to bromine on phenyl), 7.71-7.87 (m, 7H, Ar-H), 8.26 (s, 1H, Ar-H of triazole) and 8.55 (s, 1H, β -H of carbonyl). ^{13}C NMR (100 MHz, DMSO- d_6 , ppm): δ 36 (methylene carbon between TZD and Triazole), 55.2 (methylene carbon between Triazole and phenyl ring), 141.5, 142, 144.9, 151.9, 152.8, 153, 153.6, 154.7, 156.2 (Carbonyl carbon attached to the nitrogen) and 159.3 (Carbonyl carbon attached to the sulfur). HRMS calculated $[\text{M} + \text{H}]^+$ for $\text{C}_{20}\text{H}_{16}\text{N}_4\text{O}_2\text{SBr}$: 455.0177, found: 455.0172.

(Z)-3-((1-Benzyl-1H-1,2,3-triazol-4-yl)methyl)-5-benzylidenethiazolidine-2,4-dione (6e).

The compound **6e** as a off white solid and was obtained *via* 1,3-dipolar cycloaddition between (Z)-5-benzylidene-3-(prop-2-yn-1-yl)thiazolidine-2,4-dione (**4a**) and (azidomethyl)benzene (**5e**) using 20 mol% of $\text{Cu}(\text{OAc})_2$ in 22 h with 95% yield. Mp. 190 °C. ^1H NMR (400 MHz, DMSO- d_6 , ppm): δ 4.82 (s, 2H, CH_2 , methylene bridge between TZD and Triazole), 5.66 (s, 2H, CH_2 , methylene bridge between Triazole and phenyl ring), 7.82-8.26 (m, 10H, Ar-H), 8.65 (s, 1H, Ar-H of triazole) and 8.93 (s, 1H, β -H of carbonyl). ^{13}C NMR (100 MHz, DMSO- d_6 , ppm): δ 36.3 (methylene carbon between TZD and Triazole), 56.4 (methylene carbon between Triazole and phenyl ring), 141.9, 145.1, 150.4, 150.6, 151.3, 152.1, 153.1, 156.5, 157.1, 160.3 (Carbonyl carbon attached to the nitrogen) and 167 (Carbonyl carbon attached to the sulfur). HRMS calculated $[\text{M} + \text{H}]^+$ for $\text{C}_{20}\text{H}_{17}\text{N}_4\text{O}_2\text{S}$: 377.1072, found: 377.1073.

(Z)-5-(4-Fluorobenzylidene)-3-((1-(4-nitrobenzyl)-1H-1,2,3-triazol-4-yl)methyl) thiazolidine-2,4-dione (6f).

The compound **6f** as a off white solid and was obtained *via* 1,3-dipolar cycloaddition between (Z)-5-(4-fluorobenzylidene)-3-(prop-2-yn-1-yl)thiazolidine-2,4-dione (**4b**) and 1-(azidomethyl)-4-nitrobenzene (**5a**) using 20 mol% of $\text{Cu}(\text{OAc})_2$ in 28 h with 94% yield. Mp. 178-179 °C. ^1H NMR (400 MHz, DMSO- d_6 , ppm): δ 4.90 (s, 2H, CH_2 , methylene bridge between TZD and Triazole), 5.75 (s, 2H, CH_2 , methylene bridge between Triazole and phenyl ring), 7.36-7.52 (m, 4H, Ar-H), 7.68-7.71 (m, 2H, Ar-H at meta position with respect to nitro on phenyl), 7.96 (s, 1H,

Ar-H of triazole) and 8.21-8.25 (t, 3H, 1 β -H of carbonyl and 2 Ar-H at ortho position with respect to nitro on phenyl). HRMS calculated $[M + H]^+$ for $C_{20}H_{15}N_5O_4SF$: 440.0829, found: 440.0831.

(Z)-3-((1-(4-Fluorobenzyl)-1H-1,2,3-triazol-4-yl)methyl)-5-(4-fluorobenzylidene) thiazolidine-2,4-dione (6g). The compound **6g** as a off white solid and was obtained *via* 1,3-dipolar cycloaddition between (Z)-5-(4-fluorobenzylidene)-3-(prop-2-yn-1-yl)thiazolidine-2,4-dione (**4b**) and 1-(azidomethyl)-4-fluorobenzene (**5b**) using 20 mol% of $Cu(OAc)_2$ in 27 h with 92% yield. Mp. 198-200 °C.

(Z)-3-((1-(4-Chlorobenzyl)-1H-1,2,3-triazol-4-yl)methyl)-5-(4-fluorobenzylidene) thiazolidine-2,4-dione (6h). The compound **6h** as a off white solid and was obtained *via* 1,3-dipolar cycloaddition between (Z)-5-(4-fluorobenzylidene)-3-(prop-2-yn-1-yl)thiazolidine-2,4-dione (**4b**) and 1-(azidomethyl)-4-chlorobenzene (**5c**) using 20 mol% of $Cu(OAc)_2$ in 29 h with 90% yield. Mp. 135-136 °C.

(Z)-3-((1-(4-Bromobenzyl)-1H-1,2,3-triazol-4-yl)methyl)-5-(4-fluorobenzylidene) thiazolidine-2,4-dione (6i). The compound **6i** as a off white solid and was obtained *via* 1,3-dipolar cycloaddition between (Z)-5-(4-fluorobenzylidene)-3-(prop-2-yn-1-yl)thiazolidine-2,4-dione (**4b**) and 1-(azidomethyl)-4-bromobenzene (**5d**) using 20 mol% of $Cu(OAc)_2$ in 28 h with 92% yield. Mp. 154-156 °C. 1H NMR (400 MHz, $DMSO-d_6$, ppm): δ 4.43 (s, 2H, CH_2 , methylene bridge between TZD and Triazole), 5.26 (s, 2H, CH_2 , methylene bridge between Triazole and phenyl ring), 7.38-7.41 (d, 2H, Ar-H at ortho position with respect to fluorine on phenyl), 7.53-7.59 (m, 2H, Ar-H at meta position with respect to bromine on phenyl), 7.75-7.79 (m, 2H, Ar-H at meta position with respect to fluorine on phenyl), 7.93-7.97 (m, 2H, Ar-H at ortho position with respect to bromine on phenyl), 8.27 (s, 1H, Ar-H of triazole) and 8.55 (s, 1H, β -H of carbonyl). ^{13}C NMR (100 MHz, $DMSO-d_6$, ppm): δ 36.3 (methylene carbon between TZD and Triazole), 55.5 (methylene carbon between Triazole and phenyl ring), 136, 136.3, 141.4, 142.2, 145.2, 152.3, 152.4, 153.2, 155, 156.2, 159.5 (Carbonyl carbon attached to the nitrogen) and 167.1 (Carbonyl carbon attached to the sulfur). HRMS calculated $[M + H]^+$ for $C_{20}H_{15}N_4O_2SBr$: 473.0083, found: 473.0082.

(Z)-3-((1-Benzyl-1H-1,2,3-triazol-4-yl)methyl)-5-(4-fluorobenzylidene)thiazolidine-2,4-dione (6j). The compound **6j** as a off white solid and was obtained *via* 1,3-dipolar cycloaddition between (Z)-5-(4-fluorobenzylidene)-3-(prop-2-yn-1-yl)thiazolidine-2,4-dione (**4b**) and (azidomethyl)benzene (**5e**) using 20 mol% of $Cu(OAc)_2$ in 26 h with 93% yield. Mp. 174-176 °C. 1H NMR (400 MHz, $DMSO-d_6$, ppm): δ 4.80 (s, 2H, CH_2 , methylene bridge between TZD and Triazole), 5.64 (s, 2H, CH_2 , methylene bridge between Triazole and phenyl ring), 7.80-7.95 (m, 7H, Ar-H), 8.29-8.34 (m, 2H, Ar-H at meta position with respect to fluorine on phenyl), 8.64 (s, 1H, Ar-H of triazole) and 8.90 (s, 1H, β -H of carbonyl). ^{13}C NMR (100 MHz, $DMSO-d_6$, ppm): δ 36 (methylene carbon between TZD and Triazole), 56.2 (methylene carbon between Triazole and phenyl ring), 135.7, 136, 141.1, 144.8, 150.1, 150.3, 151.1, 152.1, 155.5, 155.9, 160 (Carbonyl carbon attached to the nitrogen) and 167 (Carbonyl carbon attached to the sulfur). HRMS calculated $[M + H]^+$ for $C_{20}H_{16}N_4O_2SF$: 395.0978, found: 395.0981.

(Z)-5-(4-Chlorobenzylidene)-3-((1-(4-nitrobenzyl)-1H-1,2,3-triazol-4-yl)methyl) thiazolidine-2,4-dione (6k). The compound **6k** as a off white solid and was obtained *via* 1,3-dipolar cycloaddition between (Z)-5-(4-chlorobenzylidene)-3-(prop-2-yn-1-yl)thiazolidine-2,4-dione (**4c**) and 1-(azidomethyl)-4-nitrobenzene (**5a**) using 20 mol% of $Cu(OAc)_2$ in 30 h with 94% yield. Mp. 184 °C.

(Z)-5-(4-Chlorobenzylidene)-3-((1-(4-fluorobenzyl)-1H-1,2,3-triazol-4-yl)methyl) thiazolidine -2,4-dione (6l). The compound **6l** as a off white solid and was obtained *via* 1,3-dipolar cycloaddition

between (Z)-5-(4-chlorobenzylidene)-3-(prop-2-yn-1-yl)thiazolidine-2,4-dione (**4c**) and 1-(azidomethyl)-4-fluorobenzene (**5b**) using 20 mol% of Cu(OAc)₂ in 30 h with 94% yield. Mp. 180 °C. ¹H NMR (400 MHz, DMSO-d₆, ppm): δ 4.87 (s, 2H, CH₂, methylene bridge between TZD and Triazole), 5.54 (s, 2H, CH₂, methylene bridge between Triazole and phenyl ring), 7.16-7.21 (m, 2H, Ar-H), 7.36-7.39 (m, 2H, Ar-H), 7.60-7.62 (m, 4H, Ar-H phenyl with chlorine), 7.93 (s, 1H, Ar-H of triazole) and 8.17 (s, 1H, β-H of carbonyl). ¹³C NMR (100 MHz, DMSO-d₆, ppm): δ 36.7 (methylene carbon between TZD and Triazole), 52.1 (methylene carbon between Triazole and phenyl ring), 115.5, 121.9, 123.7, 129.5, 130.4, 130.5, 131.8, 132.1, 132.2, 132.5, 135.4, 141.3, 160.7, 163.1, 165.1 (Carbonyl carbon attached to the nitrogen) and 166.7 (Carbonyl carbon attached to the sulfur).

(Z)-3-((1-(4-Chlorobenzyl)-1H-1,2,3-triazol-4-yl)methyl)-5-(4-chlorobenzylidene) thiazolidine-2,4-dione (6m). The compound **6m** as a off white solid and was obtained *via* 1,3-dipolar cycloaddition between (Z)-5-(4-chlorobenzylidene)-3-(prop-2-yn-1-yl)thiazolidine-2,4-dione (**4c**) and 1-(azidomethyl)-4-chlorobenzene (**5c**) using 20 mol% of Cu(OAc)₂ in 28 h with 92% yield. Mp. 168 °C. ¹H NMR (400 MHz, DMSO-d₆, ppm): δ 4.98 (s, 2H, CH₂, methylene bridge between TZD and Triazole), 5.56 (s, 2H, CH₂, methylene bridge between Triazole and phenyl ring), 7.31-7.33 (d, 2H, Ar-H), 7.41-7.43 (d, 2H, Ar-H), 7.58-7.65 (q, 4H, Ar-H), 7.94 (s, 1H, Ar-H of triazole) and 8.18 (s, 1H, β-H of carbonyl). HRMS calculated [M + H]⁺ for C₂₀H₁₅N₄O₂SCl₂: 445.0293, found: 445.0300.

(Z)-3-((1-(4-Bromobenzyl)-1H-1,2,3-triazol-4-yl)methyl)-5-(4-chlorobenzylidene) thiazolidine-2,4-dione (6n). The compound **6n** as a off white solid and was obtained *via* 1,3-dipolar cycloaddition between (Z)-5-(4-chlorobenzylidene)-3-(prop-2-yn-1-yl)thiazolidine-2,4-dione (**4c**) and 1-(azidomethyl)-4-bromobenzene (**5d**) using 20 mol% of Cu(OAc)₂ in 27 h with 90% yield. Mp. 176-178 °C.

(Z)-3-((1-Benzyl-1H-1,2,3-triazol-4-yl)methyl)-5-(4-chlorobenzylidene)thiazolidine-2,4-dione (6o). The compound **6o** as a off white solid and was obtained *via* 1,3-dipolar cycloaddition between (Z)-5-(4-chlorobenzylidene)-3-(prop-2-yn-1-yl)thiazolidine-2,4-dione (**4c**) and (azidomethyl)benzene (**5e**) using 20 mol% of Cu(OAc)₂ in 26 h with 93% yield. Mp. 168-169 °C. ¹H NMR (400 MHz, DMSO-d₆, ppm): δ 4.87 (s, 2H, CH₂, methylene bridge between TZD and Triazole), 5.54 (s, 2H, CH₂, methylene bridge between Triazole and phenyl ring), 7.28-7.34 (m, 5H, Ar-H), 7.58-7.62 (m, 4H, Ar-H), 7.93 (s, 1H, Ar-H of triazole) and 8.16 (s, 1H, β-H of carbonyl). ¹³C NMR (100 MHz, DMSO-d₆, ppm): δ 36.8 (methylene carbon between TZD and Triazole), 52.9 (methylene carbon between Triazole and phenyl ring), 121.9, 123.8, 128, 128.2, 128.8, 129.5, 132.1, 135.4, 135.9, 141.3, 165.1 (Carbonyl carbon attached to the nitrogen) and 166.7 (Carbonyl carbon attached to the sulfur). HRMS calculated [M + H]⁺ for C₂₀H₁₆N₄O₂SCL: 411.0682, found: 411.0684.

Experimental protocol for biological activity

Anti-inflammatory activity

Thiazolidinedione binding with PPAR γ has been suggested to play a down regulatory role in the treatment of inflammatory disorders. Thiazolidinedione gives potential anti-inflammatory activity by inhibiting monocyte/macrophage activation and expression of inflammatory molecules, i.e. interleukin (IL)-1 β , IL-6, tumor necrosis factor (TNF- α), inducible nitric oxide synthase and gelatinase B.⁴⁴ Anti-inflammatory agents act by either inhibiting lysosomal enzymes or by stabilizing lysosomal membranes, and HRBC membranes are similar to these lysosomal membrane components. Hence, the lysis of an HRBC membrane is taken as a measure of anti-inflammatory activity. *In vitro* anti-inflammatory activity was studied *via* the HRBC membrane stabilization

method against the standard drug diclofenac sodium (DFS).⁴⁵ Blood is collected from healthy volunteers. Fresh whole human blood was collected and it was mixed with equal volumes of sterilized Alsever's solution (Dextrose 2%, Sodium citrate 0.8%, Citric acid 0.05%, Sodium chloride 0.42% and Distilled water 100 mL). This blood solution was centrifuged for 10 mins at 3000 rpm and then washed three times with an equal volume of normal saline. The volume of the blood is measured and reconstituted as 10% v/v suspension with normal saline. The reaction mixture consists of 1.0 mL of the test sample of different concentrations in normal saline and 0.5 mL of 10% HRBC suspension, 1 mL of 0.2 M phosphate buffer, 1 mL hypo saline were incubated at 37 °C for 30 min and centrifuged for 30 min at 3000 rpm. The hemoglobin content of the supernatant solution was estimated at 560 nm spectrophotometrically. Each experiment was performed in triplicate and distilled water as control in this study. Where the blood control represents 100% lysis or zero percent stability, the percentage of HRBC hemolysis calculated by formula,

$$\% \text{ Haemolysis} = (\text{O. D. of Control} - \text{O. D. of Test sample}) / \text{O. D. of Control} \times 100$$

The concentration of a compound where 50% of its maximal effect is observed (EC₅₀) using graph pad prism was measured.

DPPH radical scavenging activity

Antioxidant activity of the synthesized compounds has been assessed *in vitro* by the 1,1-diphenyl-2-picrylhydrazyl (DPPH) radical scavenging assay.⁴⁶ Butylated hydroxytoluene (BHT) has been used as a standard drug for the comparison of antioxidant activity. The hydrogen atom or electron donation ability of the compounds was measured from the bleaching of the purple-colored methanol solution of 1,1-diphenyl-1-picrylhydrazyl (DPPH). The spectrophotometric assay uses the stable radical DPPH as a reagent. 1 mL of various concentrations of the test compounds (5, 10, 25, 50 and 100 µg/mL) in methanol was added to 4 mL of 0.004% (w/v) methanol solution of DPPH. After a 30 min incubation period at room temperature, the absorbance was measured against blank at 517 nm. The percent inhibition (I %) of free radical production from DPPH was calculated by the following equation.

$$\% \text{ of scavenging} = [(A \text{ control} - A \text{ sample}) / A \text{ blank}] \times 100$$

Where 'A control' is the absorbance of the control reaction (containing all reagents except the test compound) and 'A sample' is the absorbance of the test compound. Tests were carried at in triplicate.

Computational study

Molecular docking study

Grid-Based Ligand Docking with Energetics (Glide) module integrated with in the Small Drug Discovery Suite of Schrodinger molecular modeling software was used to study the binding mode of the title compounds into the active site of human peroxisome proliferator-activated receptor gamma (PPAR γ).⁴⁷

Grid-Based Ligand Docking with Energetics (Glide) module integrated in the Small Drug Discovery Suite of Schrodinger molecular modeling software was used to study the binding mode of the title compounds into the active site of human peroxisome proliferator-activated receptor gamma (PPAR γ). With this purpose, the three-dimensional X-ray structure of human peroxisome proliferator-activated receptor gamma (PPAR γ) in complex with Rosiglitazone (PDB code: 2PRG) was obtained from the Protein Data Bank (PDB) (<http://www.rcsb.org/pdb>). The *Protein Preparation Wizard* integrated in the software package was used to preprocess the enzyme structure for docking simulation which involved omitting the crystallographically observed water

molecules (since no water molecule was observed to be conserved), the addition of missing hydrogens and side-chain atoms and assigning the appropriate charge and protonation states. Hydrogen atoms were added corresponding to pH 7.0 considering the appropriate ionization states for the acidic and basic amino acid residues in the enzyme. Thereafter, the structure was subjected to energy minimization using the OPLS-2005 force field to relieve the steric clashes among the residues caused due to addition of hydrogen atoms until the RMSD (root mean square deviation) constraint was reached to 0.3 Å.

The 3D structures of the title compounds (**6a-o**) were sketched through the *build* panel in Maestro and optimized using the *LigPrep* utility which involves the addition of hydrogen atoms, adjusting realistic bond lengths and angles, correcting the chirality and generating several low energy 3D structures with various ionization states, tautomer's, stereo chemistries, and ring conformations from each molecule input followed by assignment of partial atomic charges using the OPLS-2005 force-field. The ligand structures thus obtained were finally refined by subjecting to energy minimization until it reached a RMSD cutoff of 0.01 Å.

After ensuring that the structures of both enzyme and ligands were in the correct form, the active site of the PPAR γ enzyme was defined using the *receptor grid generation* panel in Glide which generates two cubical boxes having a common centroid for organizing the calculations: a larger enclosing and a smaller binding box. With the non-covalently bound native ligand-Rosiglitazone in place, the active site grid was defined by a 12 \times 12 \times 12 Å box (centred on the centroid of Rosiglitazone) which was large enough to explore a large surface of the enzyme. The co-crystallized ligand serves as the reference coordinate as it signifies the active site of a molecule concerning the target. The optimized ligand structures were then subjected to docking simulations against the defined active site using with extra precision (i.e. GlideXP) scoring function to gauge their binding affinities. The output files generated in the form of the docking poses were visualized and analyzed for the key elements of interaction with the active site residues using the Maestro's Pose Viewer utility.

ADME prediction

In this study, we calculated molecular volume (MV), molecular weight (MW), logarithm of the partition coefficient (miLog *P*), number of hydrogen bond acceptors (n-ON), number of hydrogen bonds donors (n-OH/NH), topological polar surface area (TPSA), number of rotatable bonds (n-ROTB) and Lipinski's rule of five⁴⁸ using Molinspiration online property calculation toolkit.⁴⁹ Absorption (% ABS) was calculated by: % ABS = 109-(0.345 \times TPSA).⁵⁰ Drug-likeness model score (a collective property of physic-chemical properties, pharmacokinetics and pharmacodynamics of a compound is represented by a numerical value) was computed by MolSoft software.⁵¹

Acknowledgements

The authors M.H.S., D.D.S. and S.V.A. are very much grateful to the Council of Scientific and Industrial Research (CSIR), New Delhi for the award of Research Fellowship. Authors also thank Schrodinger Inc. for GLIDE software to perform the molecular docking studies.

Disclosure statement

No potential conflict of interest was reported by the authors.

Funding

Authors are thankful to the University Grants Commission and Department of Science & Technology, New Delhi for financial support under UGC-SAP and DST-FIST schemes.

ORCID

Mubarak H. Shaikh  <http://orcid.org/0000-0002-1190-2371>

Vijay M. Khedkar  <http://orcid.org/0000-0001-9982-7785>

References

1. A. K. Jain, A. Vaidya, V. Ravichandran, S. K. Kashaw, and R. M. Agrawal, "Recent Developments and Biological Activities of Thiazolidinone Derivatives: A Review," *Bioorganic & Medicinal Chemistry* 20, no. 11 (2012): 3378–95. doi:10.1016/j.bmc.2012.03.069.
2. (a) J. M. Lehmann, L. B. Moore, T. A. Smith-Oliver, W. O. Wilkinson, T. M. Wilson, and S. A. Kliewer, "An Antidiabetic Thiazolidinedione is a High Affinity Ligand for Peroxisome Proliferator-Activated Receptor γ (PPAR γ)," *Journal of Bioorganic Chemistry* 270 (1995): 12953–6; (b) R. Da Ros, R. Assaloni, and, A. Ceriello, "The Preventive Antioxidant Action of Thiazolidinediones: A New Therapeutic Prospect in Diabetes and Insulin Resistance," *Diabetic Medicine* 21 (2004): 1249–52.
3. (a) S. Kitamura, Y. Miyazaki, Y. Shinomura, S. Kondo, S. Kanayama, and Y. Matsuzawa, "Peroxisome Proliferator-Activated Receptor Gamma Induces Growth Arrest and Differentiation Markers of Human Colon Cancer Cells," *Japanese Journal of Cancer Research GANN* 96 (1999): 75–80. 90; (b) M. Li, T. W. Lee, T. S. Mok, T. D. Warner, A. P. Yim, and G. G. Chen, "Activation of Peroxisome Proliferator-Activated Receptor-Gamma by Troglitazone (TGZ) Inhibits Human Lung Cell Growth," *Journal of Cellular Biochemistry* (2005): 760–74;(c) C. W. Shiau, C. C. Yang, S. K. Kulp, K. F. Chen, C. S. Chen, J. W. Huang, and, and C. S. Chen, "Thiazolidinediones Mediate Apoptosis in Prostate Cancer Cells in Part through Inhibition of Bcl-xL/Bcl-2 Functions Independently of PPAR Gamma," *Cancer Research* 65 (2005):1561–9.
4. B. D. Oya, O. Ozen, M. Arzu, A. Nurten, A. Onur, K. Engin, and E. Rahmiye, "Synthesis and Antimicrobial Activity of Some New Thiazolyl Thiazolidine-2,4-Dione Derivative," *Bioorganic Medicinal Chemistry* 15 (2007): 6012–7.
5. (a) G. Bruno, L. Costantino, C. Curinga, R. Maccari, F. Monforte, F. Nicolò, R. Ottanà, and M. G. Vigorita, "Recent Studies of Aldose Reductase Enzyme Inhibition for Diabetic Complications," *Bioorganic & Medicinal Chemistry* 10, no. 4 (2002): 1077–352. doi:10.1016/S0968-0896(01)00366-2.
6. (a) V. V. Mulwad, A. A. Mir, and H. T. Parmar, "Synthesis and Antimicrobial Screening of 5-Benzylidene-2-Imino-3-(2-Oxo-2H-Benzopyran-6-yl-)Thiazolidine-4-One and Its Derivatives," *Indian Journal of Chemistry* 48B (2009): 137–141; (b) K. R. Alagawadi, and S. G. Alegaon, "Synthesis, Characterization and Antimicrobial Activity Evaluation of New 2,4-Thiazolidinediones Bearing Imidazo[2,1-b][1,3,4]Thiadiazole Moiety," *Arabian Journal Chemistry* 4 (2011): 465–72
7. S. Rekha, U. Shantharam, and V. Chandy, "Synthesis and Evaluation of Novel Thiazolidinedione for anti-Inflammatory Activity," *International Research Journal of Pharmacy* 2 (2011): 81–4.
8. F. Herrera, J. C. Mayo, V. Martin, R. M. Sainz, I. Antolin, and C. Rodriguez, "Cytotoxicity and Oncostatic Activity of the Thiazolidinedione Derivative CGP 52608 on central nervous system cancer cells," *Cancer Letters* 211, no. 1 (2004): 47–55. doi:10.1016/j.canlet.2004.03.036.
9. Y. Chinthala, A. Kumar, Domatti, A. Sarfaraz, S. P. Singh, N. K. Arigari, N. Gupta, S. K. V. N. Satya, J. K. Kumar, F. Khan, A. K. Tiwari, et al, "Synthesis, Biological Evaluation and Molecular Modeling Studies of Some Novel Thiazolidinediones with Triazole Ring," *European Journal of Medicinal Chemistry* 70 (2013): 308–14. doi:10.1016/j.ejmech.2013.10.005.
10. A. Verma, and S. K. Saraf, "4-thiazolidinone-a biologically active scaffold," *European Journal of Medicinal Chemistry* 43, no. 5 (2008): 897–905. doi:10.1016/j.ejmech.2007.07.017.
11. M. Ricote, A. C. Li, T. M. Willson, J. Kelly, and C. K. Glass, "The Peroxisome proliferator-activated receptor-gamma is a negative regulator of macrophage activation," *Nature* 391, no. 6662 (1998): 79–82. doi:10.1038/34178.
12. (a) T. M. Willson, and W. Wahli, "Peroxisome Proliferator-Activated Receptor Agonists," *Current Opinion in Chemical Biology* 1, no. 2 (1997): 235–241; (b) R. A. Komers, and, and A. Vrana, "Thiazolidinediones-Tools for the Research of Metabolic Syndrome X," *Physiological Research* 47 (1998):215–25. doi:10.1016/s1367-5931(97)80015-4.
13. P. Delerive, J. C. Fruchart, and B. Staels, "Peroxisome Proliferator-Activated Receptors in Inflammation Control," *The Journal of Endocrinology* 169, no. 3 (2001): 453–9. doi:10.1677/joe.0.1690453.
14. S. R. Maxwell, "Prospects for the Use of Antioxidant Therapies," *Drugs* 49, no. 3 (1995): 345–61. doi:10.2165/00003495-199549030-00003.
15. K. Bedard, and K. H. Krause, "The NOX Family of ROS-Generating NADPH Oxidases: Physiology and Pathophysiology," *Physiological Reviews* 87, no. 1 (2007): 245–313. doi:10.1152/physrev.00044.2005.

16. M. Valko, D. Leibfritz, J. Moncol, M. T. Cronin, M. Mazur, and J. Telser, "Free Radicals and Antioxidants in Normal Physiological Functions and Human Disease," *The International Journal of Biochemistry & Cell Biology* 39, no. 1 (2007): 44–87. doi:10.1016/j.biocel.2006.07.001.
17. (a) M. D. Stringer, P. G. Gorog, A. Freeman, and V. V. Kakkar, "Lipid Peroxides and Atherosclerosis," *BMJ (Clinical Research ed.)* 298, no. 6669 (1989): 281–4; (b) R. J. Perry, P. Watson, and, J. R. Hodges, "The Nature and Staging of Attention Dysfunction in Early (Minimal and Mild) Alzheimer's Disease: Relationship to Episodic and Semantic Memory Impairment," *Neuropsychologia* 38 (2000): 252–71. doi:10.1136/bmj.298.6669.281.
18. (a) B. Halliwell, and J. M. C. Gutteridge, *Free Radicals in Biology and Medicine*, 3rd ed. (Oxford University Press, USA, 1992); (b) C. P. Rajneesh, A. Manimaran, K. R. Sasikala, and P. Adikappan, "Lipid peroxidation and antioxidant status in patients with breast cancer," *Singapore Medicinal Journal* 49 (2008):640–3.
19. A. A. Andreadis, S. L. Hazen, S. A. Comhair, and S. C. Erzurum, "Oxidative and Nitrosative Events in Asthma," *Free Radical Biology & Medicine* 35, no. 3 (2003): 213–25. doi:10.1016/S0891-5849(03)00278-8.
20. S. B. Abramson, A. R. Amin, R. M. Clancy, and M. Attur, "The Role of Nitric Oxide in Tissue Destruction," *Best Practice & Research. Clinical Rheumatology* 15, no. 5 (2001): 831–45. doi:10.1053/berh.2001.0196.
21. J. M. McCord, "Oxygen-Derived Free Radicals in Postischemic Tissue Injury," *The New England Journal of Medicine* 312, no. 3 (1985): 159–63. doi:10.1056/NEJM198501173120305.
22. G. B. Bulkeley, "Free Radicals and Other Reactive Oxygen Metabolites: Clinical Relevance and the Therapeutic Efficacy of Antioxidant Therapy," *Surgery* 113 (1993): 479–83.
23. N. Sreejayan, and M. N. Rao, "Free Radical Scavenging Activity of Curcuminoids," *Arzneimittel-Forschung* 46, no. 2 (1996): 169–71.
24. M. H. Shaikh, D. D. Subhedar, V. M. Khedkar, P. C. Jha, F. A. K. Khan, J. N. Sangshetti, and B. B. Shingate, "1, 2, 3-Triazole Tethered Acetophenones: Synthesis, Bioevaluation and Molecular Docking Study," *Chinese Chemical Letters* 27, no. 7 (2016): 1058–63. doi:10.1016/j.ccl.2016.03.014.
25. M. H. Shaikh, D. D. Subhedar, M. Arkile, V. M. Khedkar, N. Jadhav, D. Sarkar, and B. B. Shingate, "Synthesis and Bioactivity of Novel Triazole Incorporated Benzothiazinone Derivatives as Antitubercular and Antioxidant Agent," *Bioorganic & Medicinal Chemistry Letters* 26, no. 2 (2016): 561–9. doi:10.1016/j.bmcl.2015.11.071.
26. N. Boechat, V. F. Ferreira, S. B. Ferreira, M. L. G. Ferreira, F. C. da Silva, M. M. Bastos, M. S. Costa, M. C. S. Lourenco, A. C. Pinto, A. U. Krettli, et al, "Novel 1,2,3-Triazole Derivatives for Use against Mycobacterium tuberculosis H37Rv (ATCC 27294) Strain," *Journal of Medicinal Chemistry* 54, no. 17 (2011): 5988–99. doi:10.1021/jm2003624.
27. (a) R. Kharb, P. C. Sharma, and M. S. Yar, "Pharmacological Significance of Triazole Scaffold," *Journal of Enzyme Inhibition and Medicinal Chemistry* 26, no. 1 (2011): 1–21; (b) L. S. Feng, M. J. Zheng, F. Zhao, and D. Liu, "1,2,3-Triazole Hybrids with anti-HIV-1 Activity," *Archiv Der Pharmazie* 354 (2021):e2000163. doi: 10.3109/14756360903524304.
28. M. H. Shaikh, D. D. Subhedar, B. B. Shingate, F. A. K. Khan, J. N. Khan, V. M. Khedkar, L. Nawale, D. Sarkar, G. R. Navale, and S. S. Shinde, "Synthesis, Biological Evaluation and Molecular Docking of Novel Coumarin Incorporated Triazoles as Antitubercular, Antioxidant and Antimicrobial Agents," *Medicinal Chemistry Research* 25, no. 4 (2016): 790–804. doi:10.1007/s00044-016-1519-9.
29. R. J. Bochis, J. C. Chabala, E. Harris, L. H. Peterson, L. Barash, T. Beattie, J. E. Brown, D. W. Graham, F. S. Wakszynski, M. Tischler, et al, "Benzylated 1,2,3-Triazoles as Anticoccidiostats," *Journal of Medicinal Chemistry* 34, no. 9 (1991): 2843–52. doi:10.1021/jm00113a024.
30. J. L. Kelley, C. S. Koble, R. G. Davis, E. W. Mc Lean, F. E. Soroko, and B. R. Cooper, "1-(Fluorobenzyl)-4-Amino-1H-1,2,3-Triazolo[4,5-c]Pyridines: Synthesis and Anticonvulsant Activity," *Journal of Medicinal Chemistry* 38, no. 20 (1995): 4131–4. doi:10.1021/jm00020a030.
31. R. Raj, P. Singh, P. Singh, J. Gut, P. J. Rosenthal, and V. Kumar, "Azide-Alkyne Cycloaddition en Route to 1H-1,2,3-Triazole-Tethered 7-Chloroquinoline-Isatin Chimeras: synthesis and Antimalarial Evaluation," *European Journal of Medicinal Chemistry* 62 (2013): 590–6. doi:10.1016/j.ejmech.2013.01.032.
32. Alessandro K. Jordão, Priscila P. Afonso, Vitor F. Ferreira, Maria C. B. V. de Souza, Maria C. B. Almeida, Cristiana O. Beltrame, Daniel P. Paiva, Solange M. S. V. Wardell, James L. Wardell, Edward R. T. Tiekink, et al, "Antiviral Evaluation of N-Amino-1,2,3-Triazoles against Cantagalo Virus Replication in Cell Culture," *European Journal of Medicinal Chemistry* 44, no. 9 (2009): 3777–83., doi:10.1016/j.ejmech.2009.04.046.
33. B. L. Wilkinson, H. Long, E. Sim, and A. J. Fairbanks, "Synthesis of Arabino Glycosyl Triazoles as Potential Inhibitors of Mycobacterial Cell Wall Biosynthesis," *Bioorganic & Medicinal Chemistry Letters* 18, no. 23 (2008): 6265–7. doi:10.1016/j.bmcl.2008.09.082.
34. S. M. Gomha, S. A. Ahmed, and A. O. Abdelhamid, "Synthesis and Cytotoxicity Evaluation of Some Novel Thiazoles, Thiadiazoles, and Pyrido[2,3-d][1,2,4]Triazolo[4,3-a]Pyrimidin-5(1H)-ones Incorporating Triazole Moiety," *Molecules (Basel, Switzerland)* 20, no. 1 (2015): 1357–76. doi:10.3390/molecules20011357.

35. H. R. M. Rashdan, S. M. Gomha, M. S. El-Gendey, M. A. El-Hashash, and A. M. M. Soliman, "Eco-Friendly One-Pot Synthesis of Some New Pyrazolo[1,2-b]Phthalazinediones with Antiproliferative Efficacy on Human Hepatic Cancer Cell Lines," *Green Chemistry Letters and Reviews* 11, no. 3 (2018): 264–74. doi:10.1080/17518253.2018.1474270.
36. E. M. H. Abbas, S. M. Gomha, and T. A. Farghaly, "Multicomponent Reactions for Synthesis of Bioactive Polyheterocyclic Ring Systems under Controlled Microwave Irradiation," *Arabian Journal of Chemistry* 7, no. 5 (2014): 623–9. doi:10.1016/j.arabjc.2013.11.036.
37. K. D. Khalil, S. M. Riyadh, S. M. Gomha, and I. Ali, "Synthesis, Characterization and Application of Copper Oxide Chitosan Nanocomposite for Green Regioselective Synthesis of [1,2,3]Triazoles," *International Journal of Biological Macromolecules* 130 (2019): 928–37. doi:10.1016/j.ijbiomac.2019.03.019.
38. M. Kume, T. Kubota, Y. Kimura, H. Nakashimizu, K. Motokawa, and M. Nakano, "Orally Active cephalosporins. II. Synthesis and structure-activity relationships of new 7 beta-[(Z)-2-(2-Aminothiazol-4-yl)-2-Hydroxyiminoacetamido]-Cephalosporins with 1,2,3-Triazole in C-3 Side Chain," *The Journal of Antibiotics* 46, no. 1 (1993): 177–92. doi:10.7164/antibiotics.46.177.
39. C. D. Barros, A. A. Amato, T. B. de Oliveira, K. B. R. Iannini, A. L. da Silva, T. G. da Silva, E. S. Leite, M. Z. Hernandez, M. C. A. de Lima, S. L. Galdino, et al, "Synthesis and Anti-inflammatory Activity of New Arylidene-Thiazolidine-2,4-Diones as PPAR Gamma Ligands," *Bioorganic & Medicinal Chemistry* 18, no. 11 (2010): 3805–11. doi:10.1016/j.bmc.2010.04.045.
40. A. K. M. Iqbal, A. Y. Khan, M. B. Kalashetti, N. S. Belavagi, Y. D. Gong, and I. A. M. Khazi, "Synthesis, Hypoglycemic and Hypolipidemic Activities of Novel Thiazolidinedione Derivatives Containing Thiazole/Triazole/Oxadiazole Ring," *European Journal of Medicinal Chemistry* 53 (2012): 308–15. doi:10.1016/j.ejmech.2012.04.015.
41. (a) J. Sindhu, H. Singh, J. M. Khurana, C. Sharma, and K. R. Aneja, "Multicomponent Domino Process for the Synthesis of Some Novel 5-(Arylidene)-3-((1-Aryl-1H-1,2,3-Triazol-4-yl)Methyl)-Thiazolidine-2,4-Diones Using PEG-400 as an Efficient Reaction Medium and Their Antimicrobial Evaluation," *Chinese Chemical Letters* 26, no. 1 (2015): 50–54; (b) S. Wu, Y. Zhang, X. He, X. Che, S. Wang, Y. Liu, Y. Jiang, N. Liu, G. Dong, J. Yao, Z. Miao, Y. Wang, W. Zhang, and C. Sheng, "From Antidiabetic to Antifungal: Discovery of Highly Potent Triazole-Thiazolidinedione Hybrids as Novel Antifungal Agents," *ChemMedChem* 9 (2014): 2639–46. doi:10.1016/j.cclct.2014.09.006.
42. (a) M. H. Shaikh, D. D. Subhedar, S. V. Akolkar, A. A. Nagargoje, V. M. Khedkar, D. Sarkar, B. B. Shingate, "Tetrazoloquinoline-1,2,3-Triazole Derivatives as Antimicrobial Agents: Synthesis, Biological Evaluation and Molecular Docking Study," *Polycyclic Aromatic Compounds*. doi:10.1080/10406638.2020.1821229 ; (b) M. H. Shaikh, D. D. Subhedar, M. Arkile, M. A. Yeware, F. A. K. Khan, J. N. Sangshetti, and B. B. Shingate, "Novel Benzylidenehydrazide-1, 2, 3-Triazole Conjugates as Antitubercular Agents: Synthesis and Molecular Docking," *Mini-Reviews in Medicinal Chemistry* 19 (2019): 1178–1194;(c) D. D. Subhedar, M. H. Shaikh, A. A. Nagargoje, S. V. Akolkar, S. G. Bhansali, D. Sarkar, and B. B. Shingate, "Amide-Linked Monocarbonyl Curcumin Analogues: Efficient Synthesis, Antitubercular Activity and Molecular Docking Study," *Polycyclic Aromatic Compounds* <https://doi.org/10.1080/10406638.2020.1852288>;(d) S. V. Akolkar, A. A. Nagargoje, M. H. Shaikh, M. Z. A. Warshagha, J. N. Sangshetti, M. G. Damale, and B. B. Shingate, "New N-Phenylacetamide-Linked 1,2,3-Triazole-Tethered Coumarin Conjugates: Synthesis, Bioevaluation, and Molecular Docking Study," *Archiv Der Pharmazie* 353 (2020):200016.
43. P. Ertl, B. Rohde, and P. Selzer, "Fast Calculation of Molecular Polar Surface Area as a Sum of Fragment-Based Contributions and Its Application to the Prediction of Drug Transport Properties," *Journal of Medicinal Chemistry* 43, no. 20 (2000): 3714–7. doi:10.1021/jm000942e.
44. H. Nadia Metwally, N. M. Rateb, and H. F. Zohdi, "A Simple and Green Procedure for the Synthesis of 5-Arylidene-4-Thiazolidinones by Grinding," *Green Chemistry Letters and Reviews* 4, no. 3 (2011): 225–8. doi: 10.1080/17518253.2010.544330.
45. J. Mahimaidoss, C. Antony, and A. R. Vincent, "Phytochemical Screening and Bioactivity Studies of *Phyllanthus Wightianus*," *Journal of Pharmacy Research* 6, no. 1 (2013): 188–92. doi:10.1016/j.jopr.2012.11.039.
46. M. Burits, and F. Bucar, "Antioxidant Activity of *Nigella Sativa* Essential Oil," *Phytotherapy Research* 14, no. 5 (2000): 323–8. doi:10.1002/1099-1573(200008)14:5<323::AID-PTR621>3.0.CO;2-Q.
47. (a) R. A. Friesner, J. L. Banks, R. B. Murphy, T. A. Halgren, J. J. Klicic, D. T. Mainz, M. P. Repasky, E. H. Knoll, M. Shelley, J. K. Perry, D. E. Shaw, P. Francis and P. S. Shenkin, "Glide: A New Approach for Rapid, Accurate Docking and Scoring. 1. Method and Assessment of Docking Accuracy," *Journal of Medicinal Chemistry* 47 (2004):1739–49; (b) R. A. Friesner, R. B. Murphy, M. P. Repasky, L. L. Frye, J. R. Greenwood, T. A. Halgren, P. C. Sanschagrin and D. T. Mainz, "Extra Precision Glide: Docking and Scoring Incorporating a Model of Hydrophobic Enclosure for Protein-Ligand Complexes," *Journal of Medicinal Chemistry* 49 (2006):6177–96;(c) T. A. Halgren, R. B. Murphy, R. A. Friesner, H. S. Beard, L. L. Frye, W. T.

- Pollard and J. L. Banks, "Glide: A New Approach for Rapid, Accurate Docking and Scoring. 2. Enrichment Factors in Database Screening," *Journal of Medicinal Chemistry* 47 (2004):1750–9.
48. C. A. Lipinski, F. Lombardo, B. W. Dominy, and P. J. Feeney, "Experimental and Computational Approaches to Estimate Solubility and Permeability in Drug Discovery and Development Settings," *Advanced Drug Delivery Reviews* 46, no. 1–3 (2001): 3–26.
 49. Molinspiration Chemoinformatics Brastislava, Slovak Republic, Available from: <http://www.molinspiration.com/cgi-bin/properties>, 2014.
 50. Yuan H. Zhao, Michael H. Abraham, Joelle Le, Anne Hersey, Chris N. Luscombe, Gordon Beck, Brad Sherborne, and Ian Cooper, "Rate Limited Steps of Human Oral Absorption and QSAR Studies," *Pharmaceutical Research* 19, no. 10 (2002): 1446–57. doi:10.1023/A:1020444330011.
 51. Drug-likeness and molecular property prediction, Available from: <http://www.molsoft.com/mprop/>.



SYNTHESIS AND ANTIBACTERIAL SCREENING OF THIAZOLYL PYRAZOLE CONTAINING CHROMONES AND AURONES

Nirmala R. Darekar^a, Bhausaheb K. Karale^a, Jaidip B. Wable^b, Hemantkumar N. Akolkar^{c,*}

^aDepartment of Chemistry, Radhabai Kale Mahila Mahavidyalaya, Ahmednagar, 414 001, Maharashtra, India.

^bDepartment of Chemistry, K.J.S.S.C. College, Vidyavihar, Mumbai, Maharashtra, India.

^cDepartment of Chemistry, Abasaheb Marathe Arts and New Commerce, Science College, Rajapur, Dist- Ratnagiri, 416 702, Maharashtra, India.

E-Mail: hemantakolkar@gmail.com (Corresponding Author)

ABSTRACT

Thiazolyl pyrazole anchored chalcones were converted into chromones and aurones. Formation of the target compounds was confirmed by spectral techniques like IR, ¹H NMR and mass spectrometry. The newly synthesized compounds were screened for their antibacterial activities.

KEYWORDS: Thiazole, pyrazole, chromones, aurones.

INTRODUCTION

1,3-Thiazole is well known sulphur and nitrogen containing five membered heterocyclic compound found in many clinically used drugs like Nizatidine, Meloxicam, Ritonavir, Tiazofurin, Bleomycin, Nitazoxanide, etc. Molecules containing thiazole nucleus are attractive targets for medicinal chemistry because of their wide spectrum of biological activities such as anti-inflammatory^{i, ii}, antibacterialⁱⁱⁱ, antiproliferativeⁱⁱⁱⁱ and adenosine receptor antagonists^v. Pyrazole and its derivatives are known to possess antibacterial^v, fungistatic^{vi}, and anti-inflammatory^{vii} activities. Chromone is an important class of oxygen-containing heterocyclic compounds and part of the flavonoid family. Chromone derivatives exhibit wide range of pharmacological activities such as antiallergic^{viii}, antitumor^{ix}, antimicrobial^x, antioxidant^{xi}, anti-inflammatory^{xii}, antiproliferative^{xiii}, etc. Aurones are found in some flowers, bark, seedlings, leaves and nectar of plant species. Recently aurones are known to have various biological activities such as anti-cancer^{xiv}, antioxidant^{xv}, anti-inflammatory^{xvi} and antimicrobial^{xvi}.

Various biological activities associated with thiazole, pyrazole, chromones and aurones prompted us to synthesize thiazolyl pyrazole anchored fluorinated chromones and aurones.

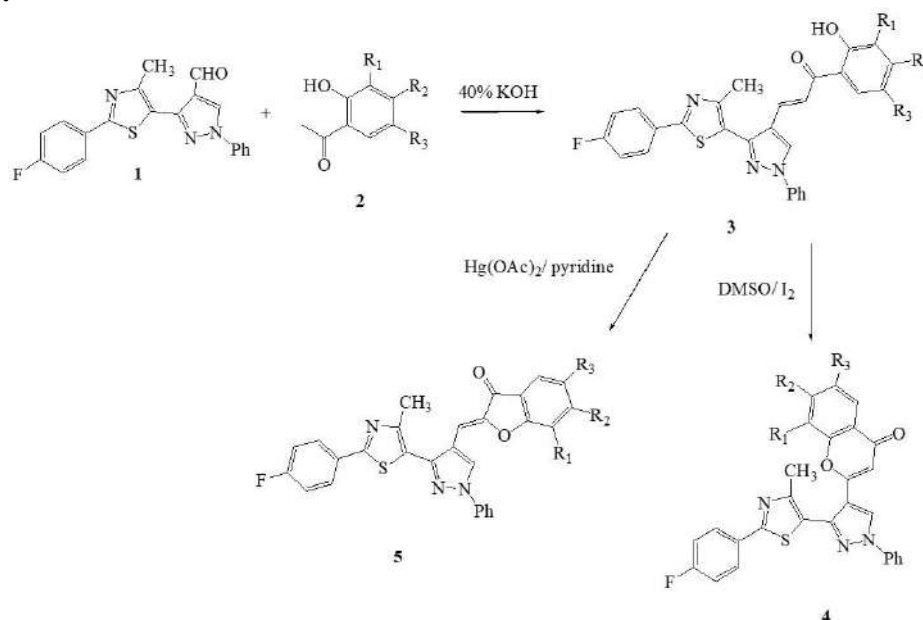
EXPERIMENTAL

Physical constants of all synthesized compounds were determined in open capillary tubes in liquid paraffin bath and are uncorrected. The IR spectra were recorded on Shimadzu IR Affinity-1S FTIR spectrophotometer. The NMR spectra were recorded on Varian NMR 400 MHz spectrometer (Varian Inc., Switzerland) and chemical shifts are given in δ ppm relative to TMS using deuterated DMSO and deuterated chloroform as solvents. Mass spectra were recorded on Water's Acquity Ultra Performance TQ Detector Mass Spectrometer.

RESULT AND DISCUSSION

Synthesis of (*E*)-3-(3-(2-(4-fluorophenyl)-4-methylthiazol-5-yl)-1-phenyl-1*H*-pyrazol-4-yl)-1-(2-hydroxyphenyl)prop-2-en-1-one **3** was carried out by known method^{x, xvii}. Compound **3** on reaction with DMSO/I₂ gave 2-(3-(2-(4-Fluorophenyl)-4-methylthiazol-5-yl)-1-phenyl-1*H*-pyrazol-4-yl)-4*H*-chromen-4-ones **4**. Also compound **3** on reaction with mercuric acetate in pyridine gave (*Z*)-2-((3-(2-(4-fluorophenyl)-4-methylthiazol-5-yl)-1-phenyl-1*H*-pyrazol-4-yl)methylene)benzofuran-3(2*H*)-ones **5**. All the synthesized compounds were characterized with the help of spectral techniques and screened for their antibacterial activities.

Scheme-1:



General procedure for the synthesis of 2-(3-(2-(4-fluorophenyl)-4-methylthiazol-5-yl)-1-phenyl-1*H*-pyrazol-4-yl)-4*H*-chromen-4-one **4**

Chalcone **3** (0.001 mol) was dissolved in 15 mL of DMSO containing catalytic amount of iodine. The contents were heated at 130°C for 2.5 hr and left overnight undisturbed. The reaction mixture was poured over crushed ice and separated solid product **4** was filtered, washed with cold water followed by 10% sodium thiosulphate solution and again with cold water. Product was recrystallized from ethanol.

2-(3-(2-(4-Fluorophenyl)-4-methylthiazol-5-yl)-1-phenyl-1*H*-pyrazol-4-yl)-6-methyl-4*H*-chromen-4-one (4a): IR: 3145 (=C-H), 1647 (C=O), 1597 (C=N), 1562 (C=C), 1246 (C-O-C), 1170 (Ar-F) cm⁻¹; ¹H NMR: δ 2.28 (s, 3H, Ar-CH₃), 2.36 (s, 3H, Thiazolyl-CH₃), 6.68 (s, 1H, Ar-H), 7.33 (t, 2H, *J* = 8Hz, Ar-H), 7.44 (t, 1H, Ar-H), 7.59 (t, 2H, *J* = 8Hz, Ar-H), 7.81 (s, 1H, Ar-H), 7.93-8.04 (m, 6H, Ar-H), 9.29 (s, 1H, pyrazolyl-H); Mass: *m/z* 494 [M+H]⁺.

6-Fluoro-2-(3-(2-(4-fluorophenyl)-4-methylthiazol-5-yl)-1-phenyl-1*H*-pyrazol-4-yl)-4*H*-

chromen-4-one (4b): IR: 3146 (=C-H), 1645 (C=O), 1597 (C=N), 1562 (C=C), 1240 (C-O-C), 1170 (Ar-F) cm^{-1} ; $^1\text{H NMR}$: δ 2.53 (s, 3H, Thiazolyl- CH_3), 6.67 (s, 1H, Ar-H), 7.23 (t, 2H, $J=8\text{Hz}$, Ar-H), 7.28-8.08 (m, 10H, Ar-H), 9.54 (s, 1H, pyrazolyl-H); Mass: m/z 498 $[\text{M}+\text{H}]^+$.

6-Chloro-2-(3-(2-(4-fluorophenyl)-4-methylthiazol-5-yl)-1-phenyl-1H-pyrazol-4-yl)-4H-chromen-4-one (4c): IR: 3150 (=C-H), 1646 (C=O), 1595 (C=N), 1559 (C=C), 1243 (C-O-C), 1169 (Ar-F) cm^{-1} ; $^1\text{H NMR}$: δ 2.54 (s, 3H, Thiazolyl- CH_3), 6.68 (s, 1H, Ar-H), 7.21 (t, 2H, $J=8\text{Hz}$, Ar-H), 7.26-8.11 (m, 10H, Ar-H), 9.53 (s, 1H, pyrazolyl-H); Mass: m/z 514 $[\text{M}+\text{H}]^+$.

6-Bromo-2-(3-(2-(4-fluorophenyl)-4-methylthiazol-5-yl)-1-phenyl-1H-pyrazol-4-yl)-4H-chromen-4-one (4d): IR: 3144 (=C-H), 1648 (C=O), 1596 (C=N), 1567 (C=C), 1241 (C-O-C), 1171 (Ar-F) cm^{-1} ; $^1\text{H NMR}$: δ 2.53 (s, 3H, Thiazolyl- CH_3), 6.67 (s, 1H, Ar-H), 7.23 (t, 2H, $J=8.4\text{Hz}$, Ar-H), 7.27-8.16 (m, 10H, Ar-H), 9.53 (s, 1H, pyrazolyl-H); Mass: m/z 558 $[\text{M}+\text{H}]^+$.

6,8-Dichloro-2-(3-(2-(4-fluorophenyl)-4-methylthiazol-5-yl)-1-phenyl-1H-pyrazol-4-yl)-4H-chromen-4-one (4e): IR: 3146 (=C-H), 1651 (C=O), 1597 (C=N), 1561 (C=C), 1243 (C-O-C), 1170 (Ar-F) cm^{-1} ; $^1\text{H NMR}$: δ 2.52 (s, 3H, Thiazolyl- CH_3), 6.66 (s, 1H, Ar-H), 7.21 (t, 2H, $J=8.4\text{Hz}$, Ar-H), 7.26-8.18 (m, 9H, Ar-H), 9.54 (s, 1H, pyrazolyl-H); Mass: m/z 548 $[\text{M}+\text{H}]^+$.

6-Chloro-2-(3-(2-(4-fluorophenyl)-4-methylthiazol-5-yl)-1-phenyl-1H-pyrazol-4-yl)-7-methyl-4H-chromen-4-one (4f): IR: 3147 (=C-H), 1650 (C=O), 1595 (C=N), 1562 (C=C), 1242 (C-O-C), 1170 (Ar-F) cm^{-1} ; $^1\text{H NMR}$: δ 2.32 (s, 3H, Ar- CH_3), 2.53 (s, 3H, Thiazolyl- CH_3), 6.67 (s, 1H, Ar-H), 7.22 (t, 2H, $J=8\text{Hz}$, Ar-H), 7.27-8.16 (m, 9H, Ar-H), 9.51 (s, 1H, pyrazolyl-H); Mass: m/z 528 $[\text{M}+\text{H}]^+$.

General procedure for the synthesis of (Z)-2-((3-(2-(4-fluorophenyl)-4-methylthiazol-5-yl)-1-phenyl-1H-pyrazol-4-yl)methylene)benzofuran-3(2H)-one 5

A mixture of chalcone **3** (0.015 mol) and mercuric acetate (0.015 mol) was dissolved in 15 mL dry pyridine. The reaction mixture was refluxed for 5-6 h. After completion of reaction (checked by TLC) contents were cooled to room temperature and poured over crushed ice and neutralized with conc. HCl. The solid product **5** was filtered and recrystallized from glacial acetic acid.

(Z)-2-((3-(2-(4-Fluorophenyl)-4-methylthiazol-5-yl)-1-phenyl-1H-pyrazol-4-yl)methylene)-5-methylbenzofuran-3(2H)-one (5a): IR: 3086 (=C-H), 1712 (C=O), 1647 (C=N), 1597 (C=C), 1222 (C-O-C), 1172 (Ar-F) cm^{-1} ; $^1\text{H NMR}$: δ 2.37 (s, 3H, Ar- CH_3), 2.52 (s, 3H, Thiazolyl- CH_3), 6.70 (s, 1H, Ar-H), 7.38 (t, 2H, $J=8\text{Hz}$, Ar-H), 7.43-7.52 (m, 2H, Ar-H), 7.58-7.66 (m, 4H, Ar-H), 8.02-8.06 (m, 4H, Ar-H), 9.216 (s, 1H, pyrazolyl-H); Mass: m/z 494 $[\text{M}+\text{H}]^+$.

(Z)-5-Fluoro-2-((3-(2-(4-fluorophenyl)-4-methylthiazol-5-yl)-1-phenyl-1H-pyrazol-4-yl)methylene)benzofuran-3(2H)-one (5b): IR: 3086 (=C-H), 1710 (C=O), 1645 (C=N), 1598 (C=C), 1223 (C-O-C), 1171 (Ar-F) cm^{-1} ; $^1\text{H NMR}$: δ 2.53 (s, 3H, Thiazolyl- CH_3), 6.71 (s, 1H, Ar-H), 7.34 (t, 2H, $J=9\text{Hz}$, Ar-H), 7.41-8.05 (m, 10H, Ar-H), 9.14 (s, 1H, pyrazolyl-H); Mass: m/z 498 $[\text{M}+\text{H}]^+$.

(Z)-5-Chloro-2-((3-(2-(4-fluorophenyl)-4-methylthiazol-5-yl)-1-phenyl-1H-pyrazol-4-yl)methylene)benzofuran-3(2H)-one (5c): IR: 3085 (=C-H), 1711 (C=O), 1646 (C=N), 1597 (C=C), 1221 (C-O-C), 1172 (Ar-F) cm^{-1} ; $^1\text{H NMR}$: δ 2.51 (s, 3H, Thiazolyl- CH_3), 6.70 (s, 1H, Ar-H), 7.33 (t, 2H, $J=9\text{Hz}$, Ar-H), 7.43-8.10 (m, 10H, Ar-H), 9.13 (s, 1H, pyrazolyl-H); Mass: m/z 514 $[\text{M}+\text{H}]^+$.

(Z)-5-Bromo-2-((3-(2-(4-fluorophenyl)-4-methylthiazol-5-yl)-1-phenyl-1H-pyrazol-4-yl)methylene)benzofuran-3(2H)-one (5d): IR: 3087 (=C-H), 1710 (C=O), 1648 (C=N), 1596 (C=C), 1221 (C-O-C), 1170 (Ar-F) cm^{-1} ; $^1\text{H NMR}$: δ 2.53 (s, 3H, Thiazolyl- CH_3), 6.71 (s, 1H), 7.35 (t, 2H, $J=9\text{Hz}$), 7.47-8.11 (m, 10H), 9.15 (s, 1H, pyrazolyl-H); Mass: m/z 558 $[\text{M}+\text{H}]^+$.

(Z)-5,7-Dichloro-2-((3-(2-(4-fluorophenyl)-4-methylthiazol-5-yl)-1-phenyl-1H-pyrazol-4-

yl)methylene)benzofuran-3(2H)-one (5e): IR: 3084 (=C-H), 1712 (C=O), 1647 (C=N), 1594 (C=C), 1223 (C-O-C), 1173 (Ar-F) cm^{-1} ; $^1\text{H NMR}$: δ 2.54 (s, 3H, Thiazolyl- CH_3), 6.72 (s, 1H, Ar-H), 7.33 (t, 2H, $J=9$ Hz, Ar-H), 7.42-8.07 (m, 9H, Ar-H), 9.12 (s, 1H, pyrazolyl-H); Mass: m/z 548 $[\text{M}+\text{H}]^+$.

(Z)-5-Chloro-2-((3-(2-(4-fluorophenyl)-4-methylthiazol-5-yl)-1-phenyl-1H-pyrazol-4-yl)methylene)-6-methylbenzofuran-3(2H)-one (5f): IR: 3085 (=C-H), 1710 (C=O), 1649 (C=N), 1596 (C=C), 1222 (C-O-C), 1170 (Ar-F) cm^{-1} ; $^1\text{H NMR}$: δ 2.31 (s, 3H, Ar- CH_3), 2.53 (s, 3H, Thiazolyl- CH_3), 6.71 (s, 1H, Ar-H), 7.33 (t, 2H, $J=9$ Hz, Ar-H), 7.44-8.09 (m, 9H, Ar-H), 9.13 (s, 1H, pyrazolyl-H); Mass: m/z 528 $[\text{M}+\text{H}]^+$.

Table-1: Physical data of the synthesized compounds

Compd	R ₁	R ₂	R ₃	M. P. (°C)	Yield (%)
4a	H	H	Me	155	64
4b	H	H	F	164	62
4c	H	H	Cl	157	68
4d	H	H	Br	120	64
4e	Cl	H	Cl	180	72
4f	H	Me	Cl	174	67
5a	H	H	Me	187	61
5b	H	H	F	182	59
5c	H	H	Cl	177	63
5d	H	H	Br	191	66
5e	Cl	H	Cl	196	69
5f	H	Me	Cl	170	62

BIOLOGICAL SCREENING

The antibacterial activity of synthesized compounds was against the standard Gram-negative bacteria, *Pseudomonas fluorescens* (NCIM 2059), *Escherichia coli* (NCIM 2576) and Gram-positive bacteria, *Bacillus subtilis* (NCIM 2162), *Staphylococcus aureus* (NCIM 2602). Ampicillin served as positive control for antibacterial activity. The *in vitro* preliminary screening values (% inhibition) against microorganisms tested are summarized in **Table 2**. All bacterial cultures were first grown in Luria Burtony media at 37⁰C at 180 rpm. Once the culture reaches 1 O.D., it is used for anti-bacterial assay. Bacterial strains *Pseudomonas fluorescens* (NCIM 2059), *Escherichia coli* (NCIM 2576) as Gram-negative and *Bacillus subtilis* (NCIM 2162), *Staphylococcus aureus* (NCIM 2602) as Gram-positive were obtained from NCIM (NCL, Pune) and were grown in Luria Burtony medium from Hi Media, India. The assay was performed in 96 well plates after 8 Hrs. and 12 Hrs. for Gram negative and Gram positive bacteria respectively¹⁴. 0.1 % of 1 O.D. culture at 620 nm was used for screening inoculated culture was added into each well of 96 well plate containing the compounds to be tested. Optical density for each plate was measured at 620nm after 8 hrs for Gram-negative bacteria and after 12 Hrs. for Gram- positive bacteria.

All the synthesized compounds were found to be inactive against gram negative bacterial strains of *P. fluorescens* and *E. coli*. All the synthesized compounds were found to be inactive against gram positive bacterial strains of *S. aureus*. Compounds **4d**, **4f** and **5d** showed good activity against gram positive bacterial strain of *B. subtilis* compared to the standard drug Ampicillin at a concentration of 100 $\mu\text{g/mL}$ also compound **5d** showed good activity at a concentration of 30 $\mu\text{g/mL}$ compared to the standard.

Table-2: Antibacterial screening of some synthesized compounds (% inhibition)

Comp	Gram Negative						Gram Positive					
	<i>P. fluorescens</i>			<i>E. coli</i>			<i>S. aureus</i>			<i>B. subtilis</i>		
	100	30	10	100	30	10	100	30	10	100	30	10
4a	-	-	-	-	-	-	-	-	-	-	-	-
4b	2.2	-	-	14.2	-	-	-	-	-	55.4	22.3	7.8
4c	-	-	-	-	-	-	-	-	-	-	-	-
4d	7.4	1.0	-	43.1	8.7	-	-	-	-	72.6	49.8	45.6
4e	-	-	-	-	-	-	-	-	-	-	-	-
4f	7.5	6.4	0.8	19.8	17.7	7.6	-	-	-	83.4	63.7	40.9
5a	-	-	-	-	-	-	-	-	-	-	-	-
5b	-	-	-	-	-	-	-	-	-	-	-	-
5c	-	-	-	-	-	-	-	-	-	-	-	-
5d	8.4	-	-	27.4	20.7	13.1	-	-	-	87.1	71.8	55.5
5e	4.4	-	-	13.1	-	-	13.7	-	-	55.6	54.7	19.6
5f	8.3	3.9	-	-	-	-	17.5	17.5	12.9	66.4	49.2	28.8
AMP	97.0	95.2	92.2	96.6	92.0	92.1	95.0	93.8	91.1	98.5	95.0	90.5

AMP-Ampicillin; Concentrations in µg/mL.

CONCLUSION

The main objective of this research work was to synthesize thiazole anchored chromones and aurones followed by their antibacterial activities. The newly synthesized compounds were characterized with the help of spectral techniques. Some of the compounds showed good to moderate activity towards bacterial species when compared to standard Ampicillin.

ACKNOWLEDGEMENT

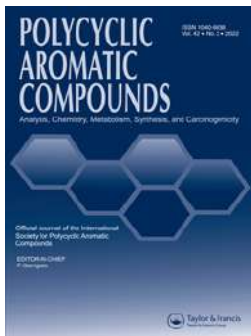
Authors are thankful to Dr. Dhiman Sarkar, National Chemical Laboratory, Pune and his team for providing biological screening.

REFERENCES

- i. Helal, M. H. M.; Salem, M. A.; El-Gaby, M. S. A. & Aljahdali, M.; Synthesis and biological evaluation of some novel thiazole compounds as potential anti-inflammatory agents; *Eur J Med Chem* 2013, **65**, 517-526.
- ii. Aggarwal, R.; Kumar, S.; Kaushik, P.; Kaushik, D. & Gupta, G. K.; Synthesis and pharmacological evaluation of some novel 2-(5-hydroxy-5-trifluoromethyl-4,5-dihydropyrazol-1-yl)-4-(coumarin-3-yl)thiazoles; *Eur J Med Chem* 2013, **62**, 508-514.
- iv. Grozav, A.; Gaina, L. I.; Pileczki, V.; Crisan, O.; Silaghi-Dumitrescu, L.; Therrien, B.; Zaharia, V. & Berindan-Neagoe, I.; The Synthesis and Antiproliferative Activities of New Arylidene-Hydrazinyl-Thiazole Derivatives; *Int J Mol Sci* 2014, **15**, 22059-22072.
- v. Muijlwijk-Koezen, J. E.; Timmerman, H.; Vollinga, R. C.; Drabbe Kunzel, J. F.; de Groote, M.; Visser, S. & Jzerman, A. P., Thiazole and thiadiazole analogues as a novel class of adenosine receptor antagonists; *J Med Chem* 2001, **44**, 749-762.
- vi. Berghot, M. A. & Moawad, E. B.; Convergent synthesis and antibacterial activity of pyrazole and pyrazoline derivatives of diazepam; *Eur J Pharm Sci* 2003, **20**, 173-176.
- vii. Sridhar, R.; Perumal, P. T.; Etti, S.; Shanmugam, G.; Ponnuswamy, M. N.; Prabavathy, V. R. & Mathivanan, N.; Design, synthesis and anti-microbial activity of

- 1H-pyrazole carboxylates; *Bioorg Med Chem Lett* 2004, **14**, 6035-6040.
- viii. Mohammed, K. O. & Nissan, Y. M.; Synthesis, molecular docking, and biological evaluation of some novel hydrazones and pyrazole derivatives as anti-inflammatory agents; *Chem Biol Drug Des* 2014, **84**, 473-488.
- ix. Oganesyanyan, E. T.; Saraf, A. S. & Ivchenko, A. V.; Synthesis and antiallergic activity of novel chromone derivatives; *Pharm Chem J* 1993, **27(1)**, 52-54.
- x. Kimura, Y.; Sumiyoshi, M.; Taniguchi, M. & Baba, K.; Antitumor actions of a chromone glucoside cnidimoside A isolated from *Cnidium japonicum*; *J Nat Med* 2008, **62(3)**, 308-313.
- xi. Hon, K. S.; Akolkar, H. N.; Karale B. K.; Synthesis and characterization of novel 2 (1-benzyl-3-[4-fluorophenyl]-1H-pyrazol-4-yl)-7-fluoro-4H-chromen-4-one derivatives; *J Heterocycl Chem* 2020, **57(4)**, 1692-1697.
- xii. Pietta, P. J.; Flavonoids as antioxidants; *J Nat Prod* 2000, **63**, 1035-1042.
- xiii. Kim, H. P.; Mani, I.; Iversen, L. & Ziboh, V. A.; Effects of naturally-occurring flavonoids and biflavonoids on epidermal cyclooxygenase and lipoxygenase from guinea-pigs; *Prostaglandins Leukot Essent Fatty Acids* 1998, **58**, 17-24.
- xiv. Ferry, D. R.; Smith, A.; Malkhandi, J.; Fyfe, D. W.; deTakats, P. G.; Anderson, D.; Baker, J. & Kerr, D. J.; Phase I clinical trial of the flavonoid quercetin: pharmacokinetics and evidence for in vivo tyrosine kinase inhibition; *Clin Cancer Res* 1996, **2**, 659-668.
- xv. Zheng, X.; Wang, H.; Liu, Y. M.; Yao, X.; Tong, M.; Wang, Y. H. & Liao, D. F.; Synthesis, Characterization, and Anticancer Effect of Trifluoromethylated Aurone Derivatives; *J Heterocycl Chem* 2015, **52**, 296-301.
- xvi. Detsi, A.; Majdalani, M.; Kontogiorgis, C. A.; Hadjipavlou-Litina, D. & Kefalas, P.; Natural and synthetic 2'-hydroxy-chalcones and aurones: synthesis, characterization and evaluation of the antioxidant and soybean lipoxygenase inhibitory activity; *Bioorg Med Chem* 2009, **17**, 8073-8085.
- xvii. Bandgar, B. P.; Patil, S. A.; Korbadi, B. L.; Biradar, S. C.; Nile, S. N. & Khobragade, C. N.; Synthesis and biological evaluation of a novel series of 2,2-bisaminomethylated aurone analogues as anti-inflammatory and antimicrobial agents; *Eur J Med Chem* 2010, **45**, 3223-3227.
- xviii. Akolkar, H.; Karale, B. and Darekar, N.; Synthesis and antibacterial screening of novel (E)-3-(3-(2-(4-fluorophenyl)-4-methylthiazol-5-yl)-1-phenyl-1H-pyrazol-4-yl)-1-(2-hydroxyphenyl)prop-2-en-1-ones; *Int. Res. J. Pharm.* 2019, **10(5)**, 196-199.
- xix. Singh, R.; Nawale, L.; Arkile, M.; Shedbalkar, U.; Wadhvani, S.; Sarkar, D. & Chopade, B.; Chemical and biological metal nanoparticles as antimycobacterial agents: A comparative study; *Int J Antimicrob Agents* 2015, **46(2)**, 183-188.

Received on May 26, 2022.




[Et₃NH][HSO₄]-Catalyzed One-Pot Solvent Free Syntheses of Functionalized [1,6]-Naphthyridines and Biological Evaluation

Mubarak H. Shaikh, Dnyaneshwar D. Subhedar, Vijay M. Khedkar & Bapurao B. Shingate

To cite this article: Mubarak H. Shaikh, Dnyaneshwar D. Subhedar, Vijay M. Khedkar & Bapurao B. Shingate (2021): [Et₃NH][HSO₄]-Catalyzed One-Pot Solvent Free Syntheses of Functionalized [1,6]-Naphthyridines and Biological Evaluation, Polycyclic Aromatic Compounds, DOI: [10.1080/10406638.2021.1970587](https://doi.org/10.1080/10406638.2021.1970587)


To link to this article: <https://doi.org/10.1080/10406638.2021.1970587>

 View supplementary material 

 Published online: 02 Sep 2021.

 Submit your article to this journal 

 Article views: 60

 View related articles 

 View Crossmark data 



[Et₃NH][HSO₄]-Catalyzed One-Pot Solvent Free Syntheses of Functionalized [1,6]-Naphthyridines and Biological Evaluation

Mubarak H. Shaikh^{a,b}, Dnyaneshwar D. Subhedar^a, Vijay M. Khedkar^c, and Bapurao B. Shingate^a

^aDepartment of Chemistry, Dr. Babasaheb Ambedkar Marathwada University, Aurangabad, Maharashtra, India; ^bDepartment of Chemistry, Radhabai Kale Mahila Mahavidyalaya, Ahmednagar, Maharashtra, India; ^cDepartment of Pharmaceutical Chemistry, School of Pharmacy, Vishwakarma University, Pune, Maharashtra, India

ABSTRACT

We have developed a convenient one-pot multicomponent synthesis of highly functionalized [1,6]-naphthyridines under solvent free condition using [Et₃NH][HSO₄] in excellent yield. This protocol offers several advantages, including short reaction time, simple experimental workup procedure and no toxic byproducts, avoids the use of toxic organic solvents and anhydrous conditions. Further, we have screened the synthesized naphthyridines for *in vitro* antibacterial, antifungal and antioxidant activity. Furthermore, a molecular docking study of these compounds was carried out to investigate their binding pattern with the target, β -Ketoacyl-acyl carrier protein synthase III (FabH). Finally, the ADME parameters for these compounds showed good drug like properties and can be developed as oral drug candidates.

ARTICLE HISTORY

Received 13 April 2021
Accepted 14 August 2021

KEYWORDS


Antimicrobial; Antioxidant; FabH; ADME; Naphthyridines; [Et₃NH][HSO₄]; multicomponent reactions



Introduction

Naphthyridine is a bicyclic heterocycle containing a pyridine ring fused to that of the dihydropyridine ring. According to literature survey, we found that the methods which are used for the synthesis of the functionalized [1,6]-naphthyridines and their benzo/heterofused analogues involves either multistep sequences or inert atmosphere, lengthy reaction time, expensive catalyst and laborious work up. Being a multifunctional entity, it finds application in nearly every field of laboratory, industrial and medicinal chemistry. Naphthyridines continued to be of great interest due to a wide spectrum of their biological activities such as used in agrochemicals,¹

CONTACT Bapurao B. Shingate  bapushingate@gmail.com  Department of Chemistry, Radhabai Kale Mahila Mahavidyalaya, Ahmednagar, Maharashtra, India.

 Supplemental data for this article can be accessed online at <https://doi.org/10.1080/10406638.2021.1970587>

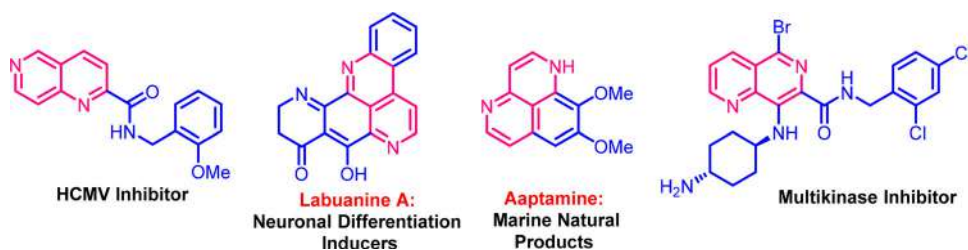


Figure 1. Pharmacologically active naphthyridine based active compounds.

pharmaceuticals,¹ and fluorescent probes.² Currently, numerous naphthyridine-containing molecules exhibited medicinal properties for the prevention and treatment of Alzheimer's disease (AD),³ bacterial infections,⁴ heart failure,⁵ angiogenic disorder,⁶ cancer,⁷ parasitic infections⁸ and viral infections⁹ have been reported. Therefore, the construction of naphthyridines have received increasing attention recently.¹⁰ Human cytomegalovirus (HCMV) is a species-specific DNA virus belonging to the herpesviridae family. The structures of pharmacologically active naphthyridine based compounds are shown in [Figure 1](#).

Nowadays, greener reaction media has gaining more importance to perform organic transformations safely. Ionic liquids referred as 'designer solvent' due to their physical and chemical properties, and can be adjusted by a careful choice of cation and anion. Ionic liquid has been turned to be a kind of promising alternative medium for various chemical processes due to its good solvating capability, non-inflammability, negligible vapor pressure, ease of recyclability, controlled miscibility and high thermal stability.¹¹ In particular, acidic Bronsted ionic liquids [ABILs] are of special importance, because they possess simultaneously the proton acidity and the characteristic properties of ionic liquids.¹² ABILs offer environmentally friendly catalytic properties due to the combination of the advantages of liquid acids and solid acids, such as uniform acid sites, stability in water and air, easy separation and reusability. The ionic liquid has been proved to be a very excellent catalyst as well as solvent for many organic transformations.¹³

Triethylammonium Hydrogen Sulfate [Et₃NH][HSO₄] (TEAHS) ionic liquid has been proved to be a very excellent catalyst as well as solvent for many organic transformations such as for the synthesis of quinoline,¹³ coumarin,¹⁴ biscoumarins,¹⁵ 1,8-dioxo-octahydroxanthenes,¹⁶ thiazolidine and oxazolidine,¹⁷ hydrazone,¹⁸ 4,4'-(arylmethylene)bis(1*H*-pyrazol-5-ols),¹⁹ functionalized aminoalkyl and amidoalkyl naphthol,²⁰ β -amino carbonyl pyrimidines,²¹ xanthene,²² 3,4-Dihydropyrimidin-2(1*H*)-one²³ derivatives and in hydrolytic reaction,²⁴ 3,4,5-substituted furan-2(5*H*)-ones²⁵ and α -amino phosphonates.²⁶

The approach to functionalized [1,6]-naphthyridines and their benzo/heterofused analogues presented herein offers an unprecedented coupling which leads to the construction of both the nitrogen containing rings during the synthesis without starting from any nitrogen containing heterocyclic moiety. Recently, Shen and coworkers described the synthesis of naphtho[2,3-*b*][1,6]naphthyridines catalyzed by acetic acid.^{27a} Zhang et. al. described synthesis of 1,6-naphthyridine-2,5-dione derivatives under ultrasound irradiation in water with acetic acid as catalyst^{27b} and recycle heterogeneous solid acid catalyst.^{27c} Vennila et. al. synthesized new 10-methoxy dibenzo[*b,h*][1,6]naphthyridine carboxylic acid from 3-methoxyaniline by a new route.^{27d} A survey of the literature shows that the majority of the strategies involve either multistep sequences,^{27e-j} or expensive catalysts,^{27g-j,28} inert atmosphere,^{27f,g,28a} lengthy reaction time,^{27g,h} and laborious workup.^{27f-h}

However, [Et₃NH][HSO₄] has not been explored yet for the synthesis of functionalized [1,6]-naphthyridines *via* multicomponent reaction. Therefore, in continuation of our work on the development of novel synthetic methodologies for organic transformations,^{26,29} we employed [Et₃NH][HSO₄] as an acidic Bronsted ionic liquid as a green, efficient, and recyclable catalyst as well as a solvent for the synthesis of functionalized [1,6]-naphthyridines. Further, we have screened

the synthesized naphthyridines for *in vitro* antimicrobial and antioxidant activity. In order to rationalize the promising data obtained from antimicrobial screening and to gain an insight into plausible mechanism of action, a molecular docking study was performed against a critical target, β -Ketoacyl-acyl carrier protein synthase III (FabH) which could provide clustered solutions on binding mode and various thermodynamic interactions governing the binding affinity.

Results and discussion

Chemistry

In search of the best experimental reaction conditions, reaction of acetophenone **1a**, malononitrile **2** and piperidine **3a** in ecofriendly solvent free condition using ionic liquid $[\text{Et}_3\text{NH}][\text{HSO}_4]$ at 80–90 °C was considered as a standard model reaction (Scheme 1). Initially, the reaction was carried out in absence of the catalyst, the product **4a** was formed in trace amount (Table 1, entry 1).

To determine the appropriate concentration of the catalyst $[\text{Et}_3\text{NH}][\text{HSO}_4]$, the model reaction at different concentrations of $[\text{Et}_3\text{NH}][\text{HSO}_4]$ such as 5, 10, 15, 20 and 25 mol% has been carried out. The functionalized [1,6]-naphthyridine formed in 60, 80, 85, 93 and 93% yields, respectively in given times (Table 1, entries 2–6). The increase in concentration of catalyst from 20 to 25 mol% does not increase the yield of product. This indicates that, 20 mol% of $[\text{Et}_3\text{NH}][\text{HSO}_4]$ is sufficient for the reaction by considering yield of product.

To evaluate the effect of solvents, dichloromethane (DCM), THF, 1,4-dioxane, toluene, CH_3CN and EtOH were used for the model reaction. It has been observed that, the use of solvents retards the rate of reaction and affords the desired product in lower yields than that for neat reaction condition (Table 2, entry 1–6).

To check the ecofriendliness of $[\text{Et}_3\text{NH}][\text{HSO}_4]$, we recycled the ionic liquid $[\text{Et}_3\text{NH}][\text{HSO}_4]$ for five times Table 3. The reaction proceeded cleanly with good yields (93, 93, 92, 90, 90 and 85%); although a weight loss of ~5% of $[\text{Et}_3\text{NH}][\text{HSO}_4]$ was observed from cycle to cycle due to mechanical loss (Table 3, entries 1–6).

With these optimized reaction conditions for model reaction i.e., 20 mol% $[\text{Et}_3\text{NH}][\text{HSO}_4]$ catalyst, 80–90 °C and solvent-free conditions, we have synthesized a series of functionalized



Scheme 1. Standard model reaction

Table 1. Effect of concentration of catalyst and time^a.

Entry	$[\text{Et}_3\text{NH}][\text{HSO}_4]$ (mol %)	Time (Min)	Yield ^b (%)
1	–	60	Trace
2	5	60	60
3	10	45	80
4	15	15	85
5	20	10	93
6	25	10	93

^aReaction conditions: Acetophenone **1a** (2 mmol), malononitrile **2** (2 mmol), piperidine **3a** (1 mmol), solvent-free at 80–90 °C.

^bIsolated yield.

Table 2. Screening of solvents.

Entry	Solvent	Yield ^a (%)
1	DCM	44
2	THF	46
3	1,4-Dioxane	48
4	Toluene	55
5	Acetonitrile	58
6	Ethanol	60
7	Solvent free	93

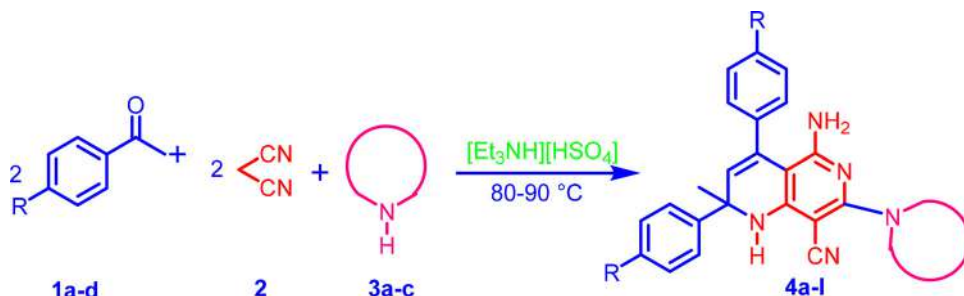
Reaction conditions: Acetophenone **1a** (2 mmol), malononitrile **2** (2 mmol), piperidine **3a** (1 mmol) in 20 mol% [Et₃NH][HSO₄].
^aIsolated yield.

Table 3. Reusability of catalyst for model reaction.

Entry	Run	Time ^a (Min)	Yield ^b
1	Fresh	10	93
2	1	10	93
3	2	10	92
4	3	10	90
5	4	10	90
6	5	15	85

^aReaction progress monitored by TLC.

^bIsolated yield.

**Scheme 2.** Synthesis of functionalized [1,6]-naphthyridines **4a-l**.

[1,6]-naphthyridines (**4b-l**) by reacting acetophenones (**1a-d**), malononitrile (**2**) and secondary amines (**3a-c**) in excellent yields (Scheme 2, Figure 2).

The formation of functionalized [1,6]-naphthyridines **4a-l** have been confirmed by physical data³⁰ and spectroscopic methods such as ¹H NMR, ¹³C NMR and mass. According to the ¹H NMR spectrum of representative compound **4a**, the singlet observed at δ 1.65 ppm for proton of methyl group, the multiplet observed at δ 1.48-1.55 ppm confirms the six protons from three methylene groups present in piperidine ring and multiplet observed at δ 3.44 ppm for methylene four proton attached to the nitrogen heteroatom. Similarly, broad singlet observed at δ 4.92 ppm for -NH₂ protons. In addition, a singlet observed at δ 5.57 ppm assigned to -NH proton present in [1,6]-naphthyridine and singlet for alkene proton observed at δ 6.74 ppm confirmed the formation of [1,6]-naphthyridine ring. Furthermore, all the aromatic protons appeared at expected chemical shifts and integral values. The synthesis of [1,6]-naphthyridine was further confirmed by ¹³C NMR spectral data **4a**, in which the carbon signals of methylene group is resonated at δ 24.3 ppm. The signal observed at δ 30.9 ppm indicates the presence of methyl carbon. The signals at δ 48.7 ppm indicate the presence of methylene carbon attached to the nitrogen heteroatom. The signal observed at δ 56.5 ppm indicates the tertiary carbon atom on which methyl and phenyl ring is present. In addition to this the signal observed at δ 118.7 indicates the presence of carbon in -CN group, while all other carbons gave signals at expected values.

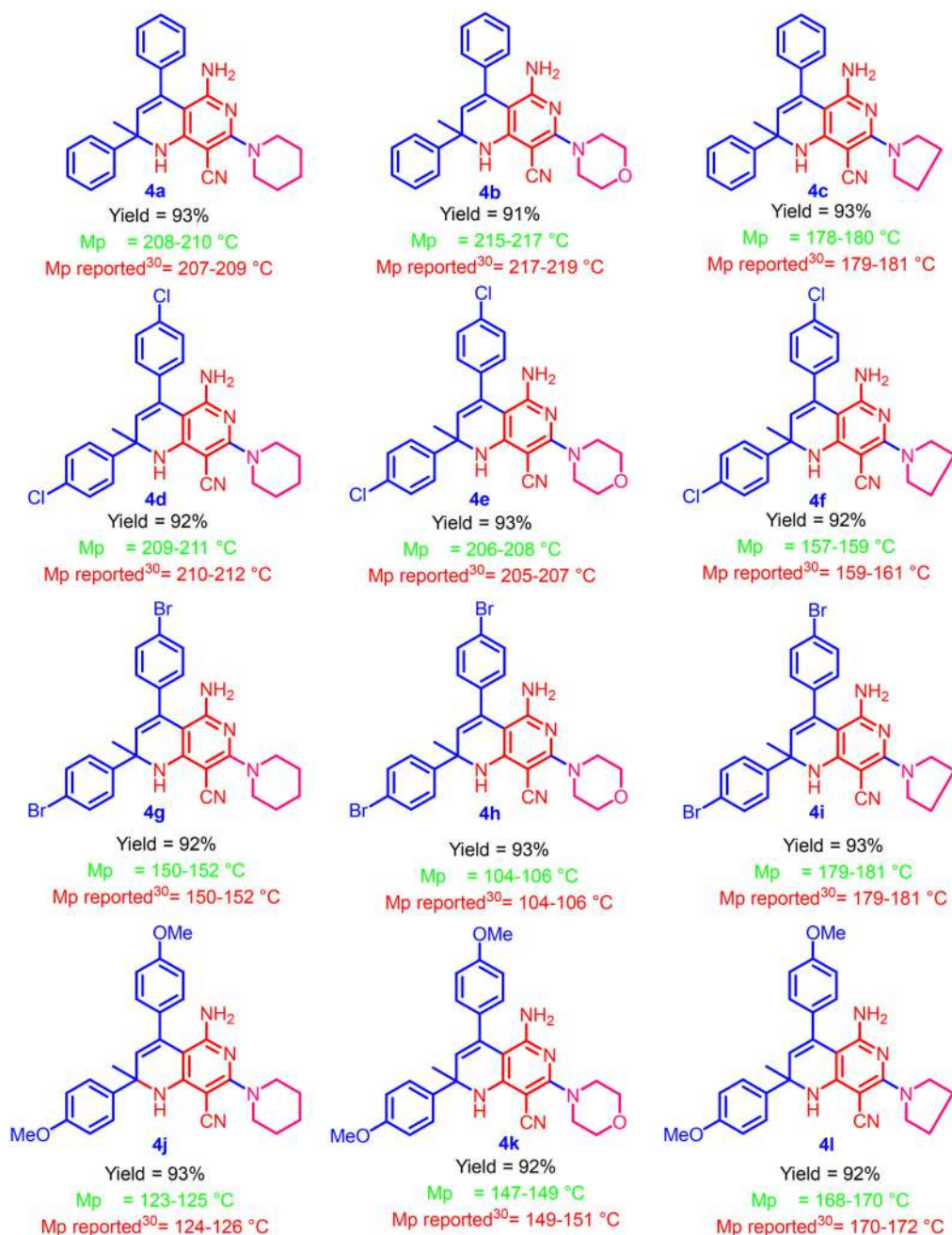


Figure 2. Structures, yields and melting point of the [1,6]-naphthyridines (4a-l).

Biological evaluation

Antibacterial activity

The functionalized [1,6]-naphthyridines **4a-l** were screened for antibacterial activity against the two Gram positive and two Gram negative bacterial strains and results are shown in Table 4.

For bacterial strain *S. aureus*, the compounds **4g**, **4h**, and **4j** shows excellent inhibitory activity with MIC value 4 µg/mL, which is equivalent to the clinical drug ampicillin (MIC 4 µg/mL).

Table 4. *In vitro* antimicrobial (MIC) and antioxidant activities (IC₅₀) of **4a-l** (μg/mL).

Compound	Gram + ve bacteria		Gram -ve bacteria		Antifungal activity			DPPH IC ₅₀
	SA	ML	EC	PF	CA	FO	AF	
4a	16	32	32	32	16	32	64	21.3
4b	8	16	32	32	16	32	64	27.3
4c	16	8	16	8	16	16	64	22.1
4d	8	8	16	8	32	16	32	18.1
4e	8	16	4	4	16	64	32	19.3
4f	8	16	8	4	16	32	16	18.9
4g	4	32	4	8	16	16	16	16.1
4h	4	8	32	8	32	64	64	16.3
4i	8	8	32	32	16	32	32	16.4
4j	4	16	8	16	16	16	16	25.3
4k	8	8	4	8	64	16	16	30.2
4l	8	8	4	16	64	64	64	20.3
Ampicilin	4	16	4	2	–	–	–	–
Kanamycin	2	2	2	2	–	–	–	–
Miconazole	–	–	–	–	16	16	16	–
Fluconazole	–	–	–	–	2	2	4	–
BHT	–	–	–	–	–	–	–	16.5

SA: *Staphylococcus aureus*; ML: *Micrococcus luteus*; EC: *Escherichia coli*; PF: *Pseudomonas fluorescens*; CA: *Candida albicans*; FO: *Fusarium oxysporum*; AF: *Aspergillus flavus*; BHT: Butylated Hydroxy Toluene.

For bacterial strain *M.luteus*, compounds **4c**, **4d**, **4h**, **4i**, **4k** and **4l** exhibit two-fold antibacterial activity with MIC value 8 μg/mL and compounds **4b**, **4e**, **4f** and **4j** with MIC value 16 μg/mL exhibited equivalent activity as compared to the clinical drug ampicilin (MIC 16 μg/mL). For bacterial strain *E. coli* compounds **4e**, **4g**, **4k** and **4l** with MIC value 4 μg/mL exhibited equivalent activity as compared to the clinical drug ampicilin (MIC 4 μg/mL) and for *P. fluorescens*, all the synthesized compounds exhibited moderate antibacterial activity compared to the standard antibacterial drugs.

Antifungal activity

In case of antifungal activity, all the synthesized [1,6]-naphthyridines **4a-l** shows good to moderate activity against all the tested fungal strains (Table 4).

Compounds **4a**, **4b**, **4c**, **4e**, **4f**, **4g**, **4i** and **4j** with MIC value 16 μg/mL exhibited equivalent activity compared with the standard drug miconazole against the fungicidal strain *C. albicans*. Compounds **4c**, **4d**, **4g**, **4j** and **4k** with MIC value 16 μg/mL exhibited equivalent activity compared with the standard drug miconazole against the fungicidal strain *F. oxysporum*. Compounds **4f**, **4g**, **4j** and **4k** with MIC value 16 μg/mL exhibited equivalent activity compared to the standard antibacterial drug miconazole for the fungicidal strain *A. flavus*.

Antioxidant activity

All the synthesized compounds **4a-l** shows moderate antioxidant activity as compared to the standard drug BHT (Table 4). The compounds **4g** (IC₅₀= 16.1 μg/mL), **4h** (IC₅₀= 16.3 μg/mL) and **4i** (IC₅₀= 16.4 μg/mL) have shown excellent activity as compared to standard drugs BHT (IC₅₀= 16.5 μg/mL). Remaining compounds exhibit good to moderate antioxidant activity as compared to standard drugs BHT.

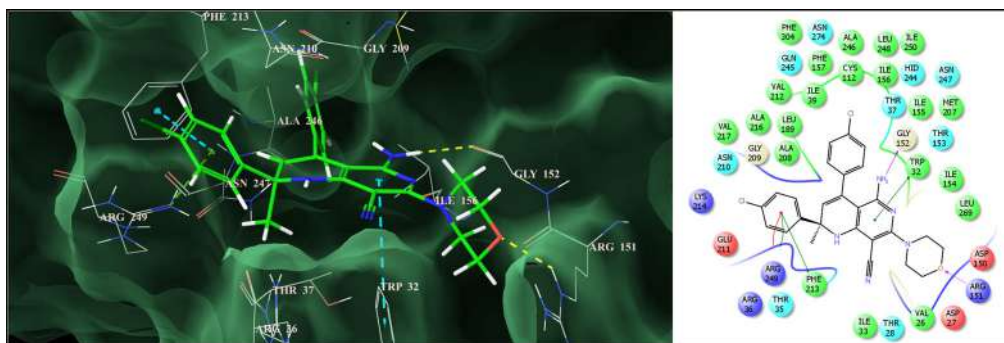
Computational study

Molecular docking

In an effort to elucidate the plausible mechanism for antimicrobial activity demonstrated by the naphthyridines investigated herein and guide further SAR, molecular docking was performed

Table 5. Molecular docking study results- Glide score, Glide energy, H- bond and π - π stacking.

Comp	Glide Score	Glide energy (Kcal/mol)	H-bond (Å)	π - π / cation- π stacking(Å)
4a	-7.001	-39.539	Gly152(2.104)	Arg249(2.507), Phe213(2.501)/Arg249(2.507)
4b	-7.015	-40.353	Gly152(2.067), Arg151(2.055)	Arg249(2.09), Phe213(2.47), Trp32(2.34)/ Arg249(2.09)
4c	-7.128	-43.49	Gly152(2.048)	Arg249(2.264), Phe213(2.572) /Arg249(2.264)
4d	-7.024	-42.043	Gly152(2.140)	Arg249(1.891), Phe213(2.471), Trp32(2.549)/ Arg249(1.891)
4e	-8.640	-49.152	Gly152(2.067), Arg151(2.111)	Arg249(2.053), Phe213(2.471), Trp32(2.582)/ Arg249(2.053)
4f	-8.102	-46.223	Gly152(2.160)	Arg249(1.878), Phe213(2.415), Trp32(2.626)/ Arg249(1.878)
4g	-8.635	-49.095	Gly152(2.072)	Arg249(1.997), Phe213(2.496), Trp32(2.564)/ Arg249(1.997)
4h	-8.164	-46.336	Gly152(1.979), Arg151(2.118)	Arg249(2.188), Phe213(2.458), Trp32(2.598)/ Arg249
4i	-7.101	-41.869	Gly152(2.086)	Arg249(1.921), Phe213(2.462), Trp32(2.622)/ Arg249(1.921)
4j	-8.197	-46.117	Gly152(1.9777)	Arg249(2.214), Phe213(2.487), Trp32(2.58)/ Arg249(2.214)
4k	-8.194	-46.423	Gly152(1.959), Arg151(2.067)	Arg249(2.275), Phe213(2.441), Trp32(2.602)/ Arg249(2.275)
4l	-8.139	-46.904	Gly152(2.0998)	Arg249(2.03), Phe213(2.472)/Arg249

**Figure 3.** Binding mode of **4e** into the active site of beta-ketoacyl-acyl carrier protein synthase III (on right side: the pink lines represent the hydrogen bonding interactions; the green lines represent π - π stacking interaction while red line represent cation- π stacking interaction).

against β -ketoacyl-acyl carrier protein synthase III (FabH) (PDB code: 1HNJ) using the standard protocol implemented in the GLIDE (Grid-based LIgand Docking with Energetics) program of the Schrodinger Molecular modeling package (Schrodinger, LLC, New York, NY, 2018).³¹ FabH is a condensing enzyme that plays an essential and regulatory role in bacterial fatty acid biosynthesis wherein it initiates the fatty acid elongation cycles and is involved in the feedback regulation of the biosynthetic pathway *via* product inhibition. FabH catalyzes the condensation of CoA-attached acetyl group and an ACP-attached malonyl group, yielding acetoacetyl-ACP as its final product. The essentiality of FabH for bacterial viability and due to their central roles in the fatty acid biosynthetic pathway qualifies FabH as an excellent molecular target.³²

All the naphthyridines were observed to be nicely bound to the active site of FabH with excellent binding affinity (average Glide docking score of -7.778 and Glide binding energy of -44.795 kcal/mol) and engaged in several close interactions (Table 5).

A detailed investigation of the per-residue interactions for one of most active analogs **4e** showed that it could snugly fit into the active site of FabH through an extensive network of steric and electrostatic interactions (Figure 3).

A significant network of van der Waals interactions were observed with Asn247(-2.479 Kcal/mol), Gly209(-2.887 Kcal/mol), Met207(-3.179 Kcal/mol), Ile156(-2.643 Kcal/mol), Gly152(-2.615 Kcal/mol), Thr37(-1.127 Kcal/mol) and Trp32(-4.727 Kcal/mol) residues through the 5-amino-2-methyl-1,2-dihydro-[1,6]naphthyridine nucleus while the morpholine side chain exhibited a similar chain of interactions with Arg151(-2.939 Kcal/mol), Thr28(-1.115 Kcal/mol), Asp27(-1.032 Kcal/mol) and Val26(-1.543 Kcal/mol) residues. Even the 2,4-bis-(4-chloro-phenyl) side chain also showed significant van der Waals interactions with Arg249(-2.276 Kcal/mol),

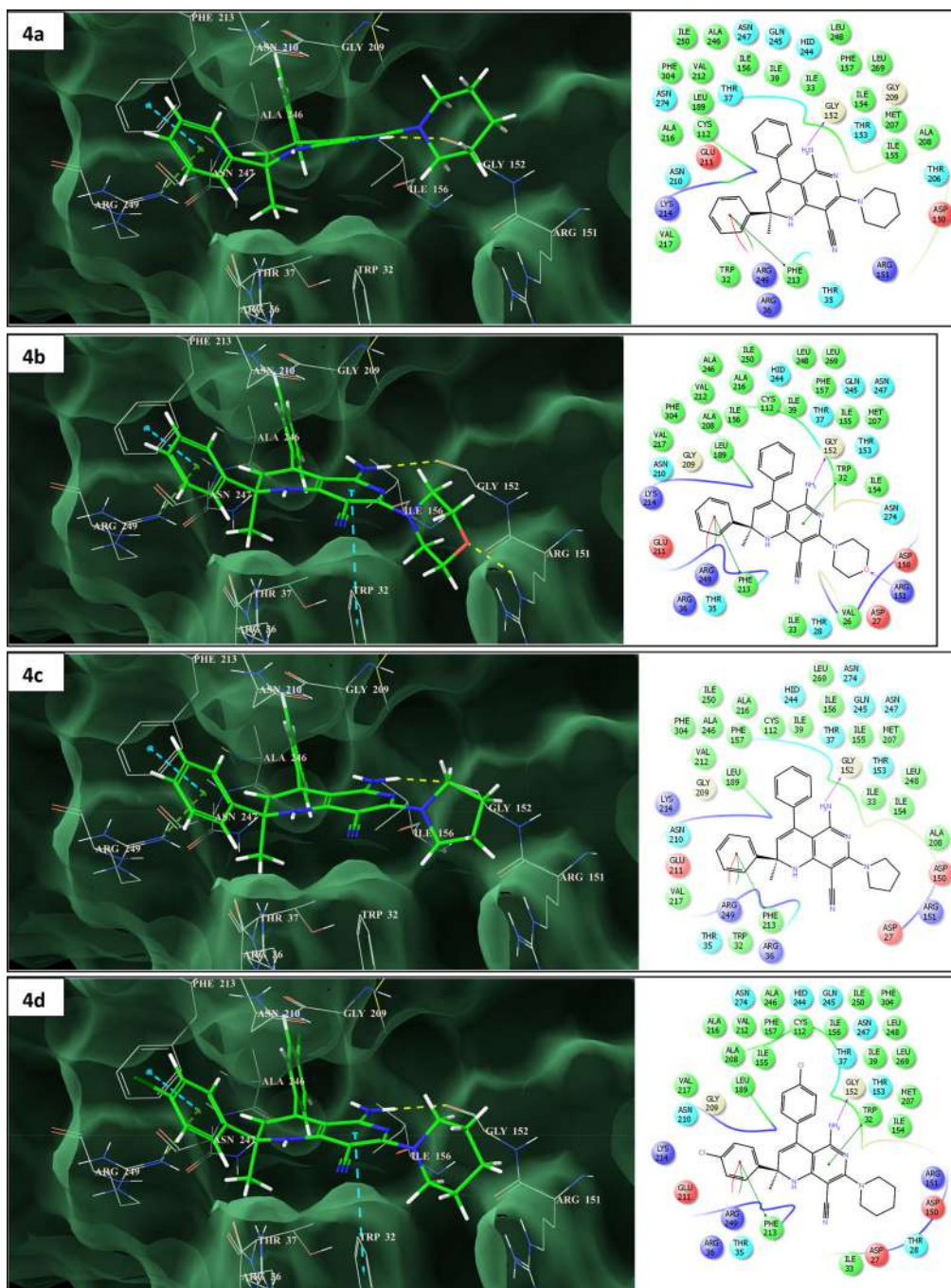


Figure 4. Binding mode of naphthyrindines into the active site of Beta-Ketoacyl-Acyl Carrier Protein Synthase III (on right side: the pink lines represent the hydrogen bonding interactions; the green lines represent π - π stacking interaction while red line represents cation- π stacking interaction).

Ala246(-1.569 Kcal/mol), Lys214(-1.015 Kcal/mol), Phe213(-5.249 Kcal/mol), Val212(-1.044 Kcal/mol), Asn210(-4.644 Kcal/mol) and Arg36(-3.542 Kcal/mol) residues of the active site. The enhanced binding affinity of **4e** is also attributed to significant electrostatic interactions observed with Arg249(-2.704 Kcal/mol), Lys214(-1.088 Kcal/mol), Gly152(-1.531 Kcal/mol) and Arg151(-

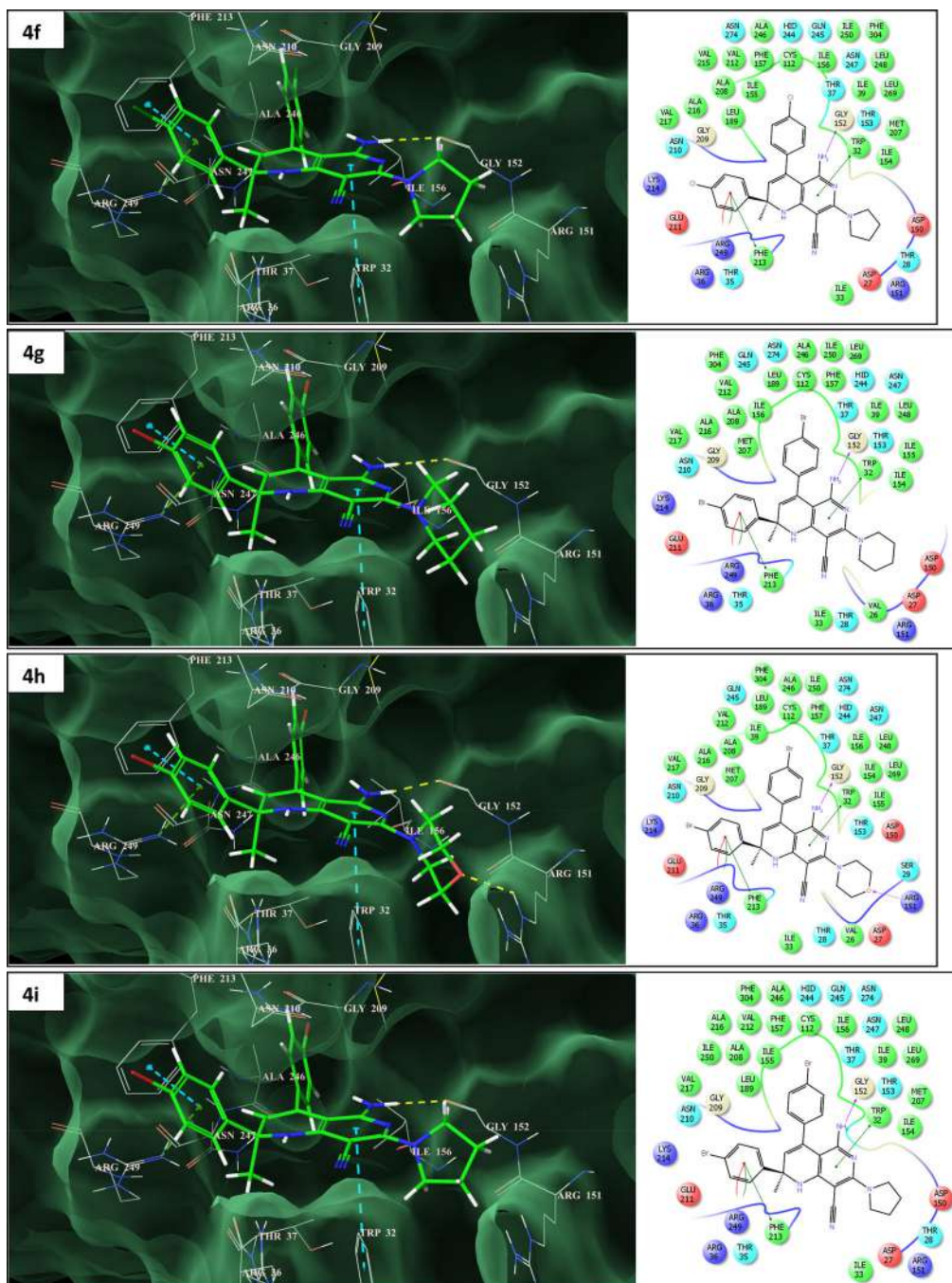


Figure 4. Continued

3.678 Kcal/mol) residues. Furthermore, it was observed to be stabilized into the active site through two prominent hydrogen bonding interactions: first through the amino group ($-NH_2$) of the naphthyridine ring with Gly152(2.067 Å) and second through the oxygen atom of the morpholine side chain with Arg151(2.111 Å). The compound has also exhibited significant π - π stacking interactions through Arg249(2.053 Å), Phe213(2.471 Å) and Trp32(2.582 Å) as well as a cation- π

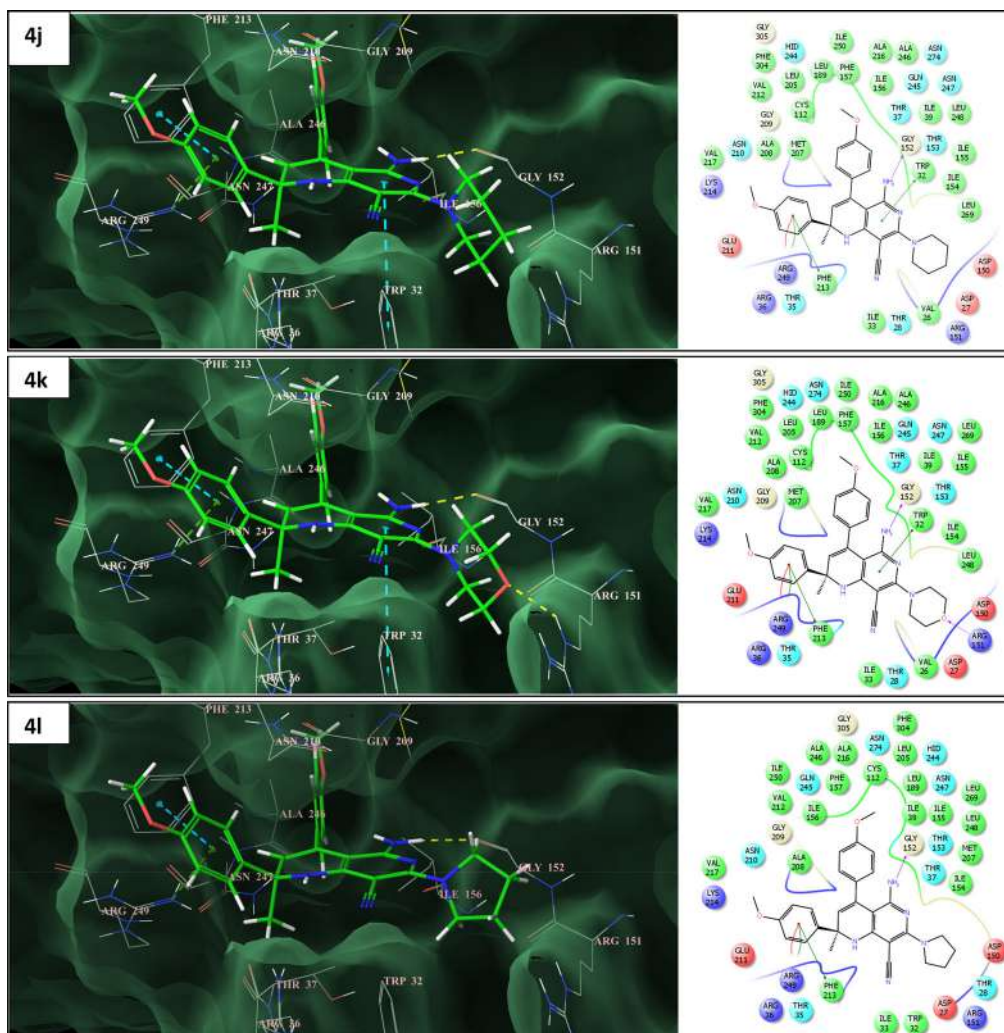


Figure 4. Continued

stacking interaction through Arg249(2.053 Å). Such hydrogen bonding and π stacking interactions serves as an anchor to stabilize the ligand into the 3D space of the active site and also facilitate the non-bonded (steric and electrostatic) interactions. A similar network of bonded and non-bonded interactions were observed for the other naphthyridines (Figure 4) as well indicating that these molecules could exhibit their antimicrobial action through inhibiting FabH and could be optimized further to arrive at selective and potent antimicrobial agents.

***In silico* ADME prediction**

The success of a drug is determined not only by good efficacy but also by an acceptable ADME (absorption, distribution, metabolism and excretion) profile. A computational study of all the synthesized **4a-l** was performed for prediction of ADME properties and the value obtained is presented in Table 6. It is observed that, the compounds exhibited a good % ABS (% absorption) ranging from 72.54 to 82.10% (Table 6). Furthermore, only compounds **4g** and **4i** violated

Table 6. Molecular properties of compounds **4a-4l**.

Entry	% ABS	TPSA (Å ²)	n-ROTB	MV	MW	log p	n-ON	n-OHND	Lipinski violations	Drug-likeness model score
Rule	–	–	–	–	<500	≤5	<10	<5	≤1	–
4a	82.10	77.97	3	398.85	421.55	4.07	5	3	0	0.41
4b	78.91	87.21	3	391.03	423.52	3.01	6	3	0	0.10
4c	82.10	77.97	3	382.04	407.52	3.57	5	3	0	0.42
4d	82.10	77.97	3	425.92	490.44	5.43	5	3	1	0.74
4e	78.91	87.21	3	418.10	492.41	4.37	6	3	0	0.44
4f	82.10	77.97	3	409.12	476.41	4.92	5	3	0	0.77
4g	82.10	77.97	3	434.62	579.34	5.69	5	3	2	0.45
4h	78.91	87.21	3	426.80	581.31	4.63	6	3	1	0.16
4i	82.10	77.97	3	417.81	565.31	5.18	5	3	2	0.48
4j	75.72	96.44	5	449.94	481.60	4.18	7	3	0	0.41
4k	72.54	105.67	5	442.12	483.57	3.12	8	3	0	0.12
4l	75.72	96.44	5	433.13	467.57	3.68	7	3	0	0.41

Cpd, Compounds, % ABS: percentage absorption, TPSA: topological polar surface area, n-ROTB: number of rotatable bonds, MV: molecular volume, MW: molecular weight, milogP: logarithm of partition coefficient of compound between n-octanol and water, n-ON acceptors: number of hydrogen bond acceptors, n-OHND donors: number of hydrogen bonds donors.

Lipinski's rule of five ($\log p$). All the tested compounds followed the criteria for orally active drug and therefore, these compounds may have a good potential for eventual development as oral agents.

Conclusions

We have developed a convenient one-pot multicomponent synthesis of highly functionalized [1,6]-naphthyridines under solvent free condition using $[\text{Et}_3\text{NH}][\text{HSO}_4]$ in high yields. We have screened the synthesized naphthyridines for *in vitro* antimicrobial and antioxidant activity. This solvent-free domino reaction proceeded smoothly in good to excellent yields and offered several other advantages including short reaction time, simple experimental workup procedures and no toxic byproducts, avoids the use of catalyst, toxic organic solvents and anhydrous conditions.

Molecular docking analysis revealed that these naphthyridines exhibited excellent binding affinity toward crucial microbial target β -Ketoacyl-acyl carrier protein synthase III (FabH) engaging in several close and significant bonded and non-bonded interactions. Furthermore, analysis of the ADME parameters for synthesized compounds showed good drug like properties and can be developed as oral drug candidate. The *in silico* results were found to be in harmony with experimentally observed MIC results which provide a strong platform to optimize this scaffold to arrive at selective and potent antimicrobial agents targeting FabH.

Experimental

Synthesis of $[\text{Et}_3\text{NH}][\text{HSO}_4]$

The synthesis of ionic liquid was carried out in a 100 mL round-bottom flask, which was immersed in a recirculating heated water-bath and fitted with a reflux condenser. Sulfuric acid (98%) (1.96 g, 0.02 mol) was added drop wise from triethylamine (2.02 g, 0.02 mol) stirring at 60 °C for 1 h. After the addition, the reaction mixture was stirred for an additional period of 1 h at 70 °C to ensure the reaction had proceeded to completion. The traces of water were removed by heating the residue at 80 °C in high vacuum until the weight of the residue remains constant.

Triethylammonium hydrogen sulfate $[\text{Et}_3\text{NH}][\text{HSO}_4]$: ¹H NMR (300 MHz, DMSO *d*₆): d (ppm) 1.15-1.19 (t, 9H), 3.04-3.12 (m, 6H), 8.98 (s, 1H); ¹³C NMR (75 MHz, DMSO *d*₆): d (ppm) 8.88, 46.40.

General procedure for preparation of [1,6]-naphthyridines (4a-l)

A mixture of ketone **1a-d** (2 mmol), malononitrile **2** (2 mmol) and amine **3a-c** (1 mmol) in 20 mol% [Et₃NH][HSO₄] were heated at 80-90 °C for 10-15 minutes. The reaction was monitored by TLC using ethyl acetate:hexane as a solvent system. The reaction mixture was quenched with crushed ice and extracted with ethyl acetate (2 × 25 mL). The organic extracts were washed with brine (2 × 25 mL) and dried over anhydrous sodium sulfate. The solvent was evaporated under reduced pressure to afford the corresponding crude compounds. The obtained crude compounds were recrystallized using ethanol-ethylacetate solvent system. The residual ionic liquid was washed with diethyl ether, dried under vacuum at 100 °C and reused for subsequent reactions. The recovered ionic liquid could be used for 5 times without much loss of catalytic activity.

5-Amino-2-methyl-2,4-diphenyl-7-piperidin-1-yl-1,2-dihydro-[1,6]-naphthyridine-8-carbonitrile (4a): A mixture of acetophenone **1a** (2 mmol), malononitrile **2** (2 mmol) and piperidine **3a** (1 mmol) in 20 mol% [Et₃NH][HSO₄] were heated at 80-90 °C for 10 min to give [1,6]-naphthyridine **4a** in 93% yield as white solid. Mp 207-209 °C (recrystallized from EtOH-EtOAc); ¹H NMR (300 MHz, DMSO-*d*₆, δ ppm): 1.55 (*bs*, 6H), 1.65 (*s*, 3H), 3.44 (*s*, 4H), 4.92 (*bs*, 2H), 5.57 (*s*, 1H), 6.74 (*s*, 1H), 7.14-7.23 (*m*, 3H), 7.27-7.38 (*m*, 5H) and 7.43 (*d*, 2H, *J* = 7.5 Hz). ¹³C NMR (75 MHz, DMSO-*d*₆, δ ppm): 24.3, 25.7, 30.9, 48.7, 56.5, 68.6, 90.6, 118.7, 124.7, 126.6, 126.9, 127.8, 127.9, 128.2, 128.5, 132.6, 138.8, 148.7, 154.7, 154.8 and 161.6.

5-Amino-2-methyl-7-morpholin-4-yl-2,4-diphenyl-1,2-dihydro-[1,6]-naphthyridine-8-carbonitrile (4b): A mixture of acetophenone **1a** (2 mmol), malononitrile **2** (2 mmol) and morpholine **3b** (1 mmol) in 20 mol% [Et₃NH][HSO₄] were heated at 80-90 °C for 10 min to give [1,6]-naphthyridine **4b** in 91% yield as cream colored solid. Mp 217-219 °C (recrystallized from EtOH-EtOAc); ¹H NMR (300 MHz, DMSO-*d*₆, δ ppm): 1.66 (*s*, 3H), 3.34-3.37 (*m*, 2H), 3.47-3.52 (*m*, 2H), 3.62 (*bs*, 4H), 5.02 (*bs*, 2H), 5.60 (*s*, 1H), 6.88 (*s*, 1H), 7.14-7.23 (*m*, 3H), 7.27-7.35 (*m*, 5H) and 7.43 (*d*, 2H, *J* = 7.8 Hz). ¹³C NMR (75 MHz, DMSO-*d*₆, δ ppm): 30.9, 48.2, 56.5, 66.1, 69.2, 91.0, 124.7, 126.6, 127.4, 128.0, 128.3, 128.5, 132.4, 154.7, 154.8 and 161.6.

5-Amino-2-methyl-2,4-diphenyl-7-pyrrolidin-1-yl-1,2-dihydro-[1,6]-naphthyridine-8-carbonitrile (4c): A mixture of acetophenone **1a** (2 mmol), malononitrile **2** (2 mmol) and pyrrolidine **3c** (1 mmol) in 20 mol% [Et₃NH][HSO₄] were heated at 80-90 °C for 15 min to give [1,6]-naphthyridine **4c** in 93% yield as light yellow solid. Mp 179-181 °C (recrystallized from EtOH-EtOAc); ¹H NMR (300 MHz, DMSO-*d*₆, δ ppm): 1.65 (*s*, 3H), 1.77-1.86 (*m*, 4H), 3.46-3.49 (*m*, 2H), 3.58-3.61 (*m*, 2H), 4.83 (*bs*, 2H), 5.52 (*s*, 1H), 6.40 (*s*, 1H), 7.14-7.23 (*m*, 3H), 7.27-7.36 (*m*, 5H) and 7.44 (*d*, 2H, *J* = 7.8 Hz). ¹³C NMR (75 MHz, DMSO-*d*₆, δ ppm): 25.1, 31.0, 48.6, 56.5, 66.0, 89.7, 119.4, 124.8, 126.0, 127.9, 128.0, 128.3, 128.5, 132.8, 139.2, 148.8, 155.0 and 157.4.

5-Amino-2,4-bis-(4-chloro-phenyl)-2-methyl-7-morpholin-4-yl-1,2-dihydro-[1,6]naphthyridine-8-carbonitrile (4e): A mixture of 4-chloroacetophenone **1b** (2 mmol), malononitrile **2** (2 mmol) and morpholine **3b** (1 mmol) in 20 mol% [Et₃NH][HSO₄] were heated at 80-90 °C for 15 min to give [1,6]-naphthyridine **4e** in 93% yield as cream colored solid. Mp 205-207 °C (recrystallized from EtOH-EtOAc); ¹H NMR (300 MHz, DMSO-*d*₆, δ ppm): 1.65 (*s*, 3H), 3.35-3.39 (*m*, 2H), 3.49-3.55 (*m*, 2H), 3.58-3.64 (*m*, 4H), 5.18 (*bs*, 2H), 5.63 (*s*, 1H), 7.00 (*s*, 1H), 7.22 (*d*, 2H, *J* = 8.1 Hz), 7.36 (*t*, 4H, *J* = 7.6 Hz) and 7.44 (*d*, 2H, *J* = 8.7 Hz). ¹³C NMR (75 MHz, DMSO-*d*₆, δ ppm): 30.4, 48.1, 56.2, 66.1, 68.9, 98.8, 117.7, 118.4, 126.8, 127.1, 128.0, 128.1, 129.8, 121.2, 132.0, 132.3, 137.0, 147.4, 154.7 and 161.6. HRMS calculated [M + H]⁺ for C₂₆H₂₄N₅OCl₂: 492.0915, found: 492.0905, [M + Na]⁺ for C₂₆H₂₃N₅OCl₂Na: 515.0703, found: 515.0693.

5-Amino-2,4-bis-(4-chloro-phenyl)-2-methyl-7-pyrrolidin-1-yl-1,2-dihydro-[1,6]-naphthyridine-8-carbonitrile (4f): A mixture of 4-chloroacetophenone **1b** (2 mmol), malononitrile **2** (2 mmol) and pyrrolidine **3c** (1 mmol) in 20 mol% [Et₃NH][HSO₄] were heated at 80-90 °C for 15 min to give [1,6]-naphthyridine **4f** in 92% yield as white solid. Mp 159-161 °C (recrystallized from EtOH-EtOAc); ¹H NMR (300 MHz, DMSO-*d*₆, δ ppm): 1.64 (*s*, 3H), 1.79-1.85 (*m*, 4H), 3.49 (*bs*, 2H), 3.58 (*bs*, 2H), 4.95 (*bs*, 2H), 5.54 (*s*, 1H), 6.57 (*s*, 1H), 7.21 (*d*, 2H, *J* = 8.1 Hz), 7.35 (*t*,

4H, $J=8.1$ Hz) and 7.43 (*d*, 2H, $J=8.4$ Hz). ^{13}C NMR (75 MHz, DMSO- d_6 , δ ppm): 25.1, 30.5, 48.5, 56.1, 65.9, 89.5, 119.2, 126.8, 128.1, 128.2, 129.8, 131.2, 132.3, 137.5, 147.5, 154.8, 154.9 and 157.5. LCMS calculated $[\text{M} + \text{H}]^+$ for $\text{C}_{26}\text{H}_{24}\text{N}_5\text{Cl}_2$: 476.15, found: 476.20,

Experimental protocol for biological activity

Antibacterial activity

The antimicrobial susceptibility testing of newly synthesized compounds were performed *in vitro* against bacterial strains *viz.*, Gram-positive *Staphylococcus Aureus* (ATCC No. 29737), *Micrococcus Luteus* (ATCC No. 398) and Gram-negative *Escherichia Coli* (NCIM No. 2256) and *Pseudomonas Fluorescens* (NCIM No. 2173) respectively, to find out minimum inhibitory concentration (MIC).³³ The MIC was defined as the lowest concentrations of compound that completely inhibit the growth of each strain. Serial two-fold dilutions of all samples were prepared in triplicate in micro titer plates and inoculated with suitably prepared cell suspension to achieve the required initial concentration. Serial dilutions were prepared for screening. Dimethylsulfoxide (DMSO) was used as solvent control. Ampicilin, kanamycin & chloramphenicol were used as a standard antibacterial drug. The concentration range of tested compounds and standard was 128-0.5 $\mu\text{g}/\text{mL}$. The plates were incubated at 37 °C for all micro-organisms; absorbance at 595 nm was recorded to assess the inhibition of cell growth after 24 h. The compounds which are showing promising antibacterial activity were selected for MIC studies. The MIC was determined by assaying at 128, 64, 32, 16, 8, 4, 2, 1 and 0.5 $\mu\text{g}/\text{mL}$ concentrations along with standards at the same concentrations.

Antifungal activity

The antifungal activity was evaluated against different fungal strains such as *Aspergillus Niger* (NCIM No. 1196), *Penicillium Chrysogenum* (NCIM No. 723) and *Curvularia Lunata* (NCIM No. 1131).³³ Fluconazole, miconazole and amphotericin B were used as standard drugs for the comparison of antifungal activity. The plates were incubated at 37 °C for all micro-organisms; absorbance at 410 nm was recorded to assess the inhibition of cell growth after 48 h. The lowest concentration inhibiting growth of the organisms was recorded as the MIC. DMSO was used as a solvent or negative control. In order to clarify any effect of DMSO on the biological screening, separate studies were carried out with solutions alone of DMSO and showed no activity against any microbial strains. The compounds which are showing promising antifungal activity were selected for MIC studies. The MIC was determined by assaying at 128, 64, 32, 16, 8, 4, 2, 1 and 0.5 $\mu\text{g}/\text{mL}$ concentrations along with standards at the same concentrations.

DPPH radical scavenging activity

The hydrogen atom or electron donation ability of some compounds were measured from the bleaching of the purple colored methanol solution of DPPH.³⁴ The spectrophotometric assay uses the stable radical DPPH as a reagent. 1 mL of various concentrations of the test compounds (5, 10, 25, 50 and 100 $\mu\text{g}/\text{mL}$) in methanol was added to 4 mL of 0.004% (w/v) methanol solution of DPPH. The reaction mixture was incubated at 37 °C. The scavenging activity on DPPH was determined by measuring the absorbance at 517 nm after 30 min. All tests were performed in triplicate and the mean values were entered. The percent of inhibition (I %) of free radical production from DPPH was calculated by the following equation

$$\% \text{ of scavenging} = [(A_{\text{control}} - A_{\text{sample}}) / (A_{\text{sample}} \times 100)]$$

Where, A_{control} is the absorbance of the control (DPPH radical without test sample)

A_{sample} is the absorbance of the test sample (DPPH radical with test sample). The control contains all reagents except the test samples.

ADME prediction

In the present study, we have calculated molecular volume (MV), molecular weight (MW), logarithm of partition coefficient ($\text{miLog } P$), number of hydrogen bond acceptors (n-ON), number of hydrogen bonds donors (n-OHNH), topological polar surface area (TPSA), number of rotatable bonds (n-ROTB) and Lipinski's rule of five³⁵ using Molinspiration online property calculation toolkit.³⁶ Absorption (% ABS) was calculated by: % ABS = $109 - (0.345 \times \text{TPSA})$.³⁷ Drug-likeness model score (a collective property of physico-chemical properties, pharmacokinetics and pharmacodynamics of a compound is represented by a numerical value) was computed by MolSoft software.³⁸ A molecule likely to be developed as an orally active drug candidate should show no more than one violation of the following four criteria: $\text{miLog } P$ (octanol-water partition coefficient) ≤ 5 , molecular weight ≤ 500 , number of hydrogen bond acceptors ≤ 10 and number of hydrogen bond donors ≤ 5 .³⁹

Acknowledgement

The authors M.H.S. and D.D.S. are very much grateful to the Council of Scientific and Industrial Research (CSIR), New Delhi for the award of Senior Research Fellowship. Authors are also thankful to the University Grants Commission and Department of Science & Technology, New Delhi for financial support under UGC-SAP and DST-FIST schemes. Authors also thank Schrodinger Inc. for GLIDE software to perform the molecular docking studies.

Disclosure statement

No potential conflict of interest was reported by the authors.

References

1. B. M. Teipel, J. Teixido, R. Pascual, M. Mora, J. Pujola, T. Fujimoto, J. I. Borrell, and E. L. Michelotti, "2-Methoxy-6-Oxo-1,4,5,6-Tetrahydropyridine-3-Carbonitriles: Versatile Starting Materials for the Synthesis of Libraries with Diverse Heterocyclic Scaffolds," *J. Combinatorial Chemistry* 7, no. 3 (2005): 436–48.
2. Y. Zhang, R. Sun, X. Kang, D. H. Wang, and Y. Chen, "A Water-Soluble 1,8-Naphthyridine-Based Imidazolium Molecular Gripper for Fluorescence Sensing and Discriminating of GMP," *Dyes and Pigments* 174, (2020): 108103.
3. J. Fiorito, J. Vendome, F. Saeed, A. Staniszewski, H. Zhang, S. Yan, S. X. Deng, O. Arancio, and D. W. Landry, "Identification of a Novel 1,2,3,4-Tetrahydrobenzo[b][1,6]naphthyridine Analogue as a Potent Phosphodiesterase 5 Inhibitor with Improved Aqueous Solubility for the Treatment of Alzheimer's Disease," *Journal of Medicinal Chemistry* 60, no. 21 (2017): 8858–75.
4. C. D. d. M. Oliveira-Tintino, S. R. Tintino, D. F. Muniz, C. R. D. S. Barbosa, R. L. S. Pereira, I. M. Begnini, R. A. Rebelo, L. E. da Silva, S. L. Mireski, M. C. Nasato, et al. "Do 1,8-Naphthyridine Sulfonamides Possess an Inhibitory Action Against Tet(K) and MsrA Efflux Pumps in Multiresistant Staphylococcus Aureus Strains?," *Microbial Pathogenesis* 147, (2020): 104268.
5. E. L. Meredith, O. Ardayfio, K. Beattie, M. R. Dobler, I. Enyedy, C. Gaul, V. Hosagrahara, C. Jewell, K. Koch, W. Lee, et al. "Identification of Orally Available Naphthyridine Protein Kinase D Inhibitors," *Journal of Medicinal Chemistry* 53, no. 15 (2010): 5400–21.
6. X. Y. Mu, J. Xu, Y. J. Zhou, Y. L. Li, Y. Liu, and X. S. Wang, "Convenient Synthesis of Naphtho[1,6]Naphthyridine Derivatives under Catalyst-Free Conditions," *Research on Chemical Intermediates* 41, no. 3 (2015): 1703–14.
7. T. Chen, L. S. Zhuo, P. F. Liu, W. R. Fang, Y. Li, and W. Huang, "Discovery of 1,6-Naphthyridinone-Based MET Kinase Inhibitor Bearing Quinoline Moiety as Promising Antitumor Drug Candidate," *European Journal of Medicinal Chemistry* 192 (2020): 112174.

8. Michael G. Thomas, Manu De Rycker, Richard J. Wall, Daniel Spinks, Ola Epemolu, Sujatha Manthri, Suzanne Norval, Maria Osuna-Cabello, Stephen Patterson, Jennifer Riley, et al. "Identification and Optimization of a Series of 8-Hydroxy Naphthyridines with Potent In Vitro Antileishmanial Activity: Initial SAR and Assessment of In Vivo Activity," *Journal of Medicinal Chemistry* 63, no. 17 (2020): 9523–39.
9. Kevin M. Peese, Christopher W. Allard, Timothy Connolly, Barry L. Johnson, Chen Li, Manoj Patel, Margaret E. Sorensen, Michael A. Walker, Nicholas A. Meanwell, Brian McAuliffe, et al. "5,6,7,8-Tetrahydro-1,6-Naphthyridine Derivatives as Potent HIV-1-Integrase-Allosteric-Site Inhibitors," *Journal of Medicinal Chemistry* 62, no. 3 (2019): 1348–61.
10. V. Litvinov, "Advances in the Chemistry of Naphthyridines," *Advances in Heterocyclic Chemistry* 91 (2006): 189–300.
11. M. V. Fedorov, and A. A. Kornyshev, "Ionic Liquids at Electrified Interfaces," *Chemical Reviews* 114, no. 5 (2014): 2978–3036.
12. X. X. Han, H. Du, C. T. Hung, L. L. Liu, P. H. Wu, D. H. Ren, S. J. Huang, and S. B. Liu, "Syntheses of Novel Halogen-Free Bronsted-Lewis Acidic Ionic Liquid Catalysts and Their Applications for Synthesis of Methyl Caprylate," *Green Chemistry* 17, no. 1 (2015): 499–508.
13. Z. N. Siddiqui, and K. Khan, "[Et₃NH][HSO₄]-Catalyzed Efficient, Eco-Friendly, and Sustainable Synthesis of Quinoline Derivatives via Knoevenagel Condensation," *ACS Sustainable Chemistry & Engineering* 2, no. 5 (2014): 1187–94.
14. Z. K. Jaber, B. Masoudi, A. Rahmani, and K. Alborzi, "Triethylammonium Hydrogen Sulfate [Et₃NH][HSO₄] as an Efficient Ionic Liquid Catalyst for the Synthesis of Coumarin Derivatives," *Polycyclic Aromatic Compounds* 40, no. 1 (2020): 99–107.
15. S. K. Patil, D. V. Awale, M. M. Vadiyar, S. A. Patil, S. C. Bhise, and S. S. Kolekar, "Simple Protic Ionic Liquid [Et₃NH][HSO₄] as a Proficient Catalyst for Facile Synthesis of Biscoumarins," *Research on Chemical Intermediates* 43, no. 10 (2017): 5365–76.
16. Z. Zhou, and X. Deng, "[Et₃NH][HSO₄] Catalyzed Efficient and Green Synthesis of 1,8-Dioxo-Octahydroxanthenes," *Journal of Molecular Catalysis A: Chemical* 367 (2013): 99–102.
17. Ali Mohammed Malla, Mehtab Parveen, Faheem Ahmad, Shaista Azaz, and Mahboob Alam, "Et₃NH][HSO₄]-Catalyzed Eco-Friendly and Expeditious Synthesis of Thiazolidine and Oxazolidine Derivatives," *RSC Advances* 5, no. 25 (2015): 19552–69.
18. M. Parveen, S. Azaz, A. M. Malla, F. Ahmad, P. Sidonio, P. da Silva, and M. R. Silva, "Solvent-Free, [Et₃NH][HSO₄] Catalyzed Facile Synthesis of Hydrazone Derivatives," *New Journal of Chemistry* 39, no. 1 (2015): 469–81.
19. Z. Zhou, and Y. Zhang, "An Eco-Friendly One-Pot Synthesis of 4,4'-(Arylmethylene)Bis(1*h*-Pyrazol-5-Ols) Using [Et₃NH][HSO₄] as a Recyclable Catalyst," *Journal of the Chilean Chemical Society* 60, no. 3 (2015): 2992–6.
20. E. Hadadianpour, and B. Pouramiri, "Facile, Efficient and One-Pot Access to Diverse New Functionalized Aminoalkyl and Amidoalkyl Naphthol Scaffolds via Green Multicomponent Reaction Using Triethylammonium Hydrogen Sulfate ([Et₃NH][HSO₄]) as an Acidic Ionic Liquid under Solvent-Free Conditions," *Molecular Diversity* 24, no. 1 (2020): 241–52.
21. N. S. Suryawanshi, P. Jain, M. Singhal, and I. Khan, "Mannich Synthesis under Ionic Liquid [Et₃NH][HSO₄] Catalysis," *IOSR Journal of Applied Chemistry* 1, no. 2 (2012): 18–23.
22. F. G. Nikfarjam, M. M. Hashemi, and A. Ezabadi. "One-Pot Synthesis of Biologically Important Xanthene Derivatives Using [(Et₃N)₂SO][HSO₄]₂ as a Novel and Green IL-Based Catalyst under Solvent-Free Conditions," *Journal of Nanomedicine* 3, no. 1 (2020) 1020.
23. B. Pouramiri, R. Fayazi, and E. T. Kermani, "Facile and Rapid Synthesis of 3,4-Dihydropyrimidin-2(1*h*)-One Derivatives Using [Et₃NH][HSO₄] as Environmentally Benign and Green Catalyst," *Iranian Journal of Chemistry and Chemical Engineering* 37 (2018): 159–67.
24. J. Weng, C. Wang, H. Li, and Y. Wang, "Novel Quaternary Ammonium Ionic Liquids and Their Use as Dual Solvent-Catalysts in the Hydrolytic Reaction," *Green Chemistry* 8, no. 1 (2006): 96–9.
25. S. Salahi, M. T. Maghsoodlou, N. Hazeri, M. Lashkari, R. Doostmohammadi, A. Kanipour, F. Farhadpour, and A. Shojaei, "Two Ammonium Ionic Liquids as Efficient Catalysts for the One-Pot Green Synthesis of 3,4,5-Substituted Furan-2(5*H*)-Ones," *Bulgarian Chemical Communications* 48 (2016): 364–8.
26. M. H. Shaikh, D. D. Subhedar, F. A. K. Khan, J. N. Sangshetti, and B. B. Shingate, "[Et₃NH][HSO₄]-Catalyzed One-Pot, Solvent-Free Synthesis and Biological Evaluation of α -Amino Phosphonates," *Research on Chemical Intermediates* 42, no. 5 (2016): 5115–31.
27. (a) C. Li, F. Zhang and Z. Shen, "An Efficient Strategy for the Synthesis of Naphtho[2,3-*b*][1,6]Naphthyridines Promoted by Acetic Acid," *Synlett* 32 (2021): 1117–1122; (b) C. Li, C. Qi and F. Zhang, "An Efficient Strategy for the Synthesis of 1,6-Naphthyridine-2,5-Dione Derivatives Under Ultrasound Irradiation" *Synlett* 31 (2020): 1313–1317; (c) C. Li, C. Qi and F. Zhang, "Ultrasonic Promoted Synthesis of 1,6-Naphthyridine Derivatives Catalyzed by Solid Acid in Water" *Tetrahedron Letters* 61 (2020):

- 152144; (d) K. N. Vennila, B. Selvakumar, V. Satish, D. Sunny, S. Madhuri and K. P. Elango, "Structure-Based Design, Synthesis, Biological Evaluation, and Molecular Docking of Novel 10-Methoxy Dibenzo[b,h][1,6]Naphthyridinecarboxamides" *Medicinal Chemistry Research* 30 (2021): 133–141; (e) S. Vanlaer, A. Voet, C. Gielens, M. D. Maeyer and F. Compennolle, "Bridged 5,6,7,8-Tetrahydro-1,6-Naphthyridines, Analogues of Huperzine A: Synthesis, Modelling Studies and Evaluation as Inhibitors of Acetylcholinesterase", *European Journal of Organic Chemistry* (2009): 643–654; (f) J. A. Turner, "A General Approach to the Synthesis of 1,6-, 1,7-, and 1,8-Naphthyridines", *Journal of Organic Chemistry* 55 (1990): 4744–4750; (g) Q. Zhang, Q. Shi, H. R. Zhang and K. K. Wang, "Synthesis of 6H-indolo[2,3-b][1,6]Naphthyridines and Related Compounds as the 5-aza Analogues of Ellipticine Alkaloids", *Journal of Organic Chemistry* 65 (2000): 7977–7983; (h) H. Suzuki, N. Sakai, R. Iwahara, T. Fujiwaka, M. Satoh, A. Kakehi and T. Konakahara, "Novel synthesis of 7-fluoro-8-(trifluoromethyl)-1H-1,6-Naphthyridin-4-One Derivatives: Intermolecular Cyclization of an *N*-silyl-1-Azaallyl Anion with Perfluoroalkene and Subsequent Intramolecular Skeletal Transformation of the Resulting Pentasubstituted Pyridines", *Journal of Organic Chemistry* 72 (2007): 5878–5881; (i) Y. Zhou, J. A. Porco and J. K. Snyder, "Synthesis of 5,6,7,8-Tetrahydro-1,6-Naphthyridines and Related Heterocycles by Cobalt-Catalyzed [2+2+2] Cyclizations", *Organic Letters* 9 (2007): 393–396; (j) V. J. Colandrea and E. M. Naylor, "Synthesis and Regioselective Alkylation of 1,6- and 1,7-Naphthyridines", *Tetrahedron Letters* 41 (2000): 8053–8057.
28. (a) A. Chandra, B. Singh, S. Upadhyay and R. M. Singh, "Copper-Free Sonogashira Coupling of 2-Chloroquinolines with Phenyl Acetylene and Quick Annulation to benzo[b][1,6]Naphthyridine Derivatives in Aqueous Ammonia", *Tetrahedron*, 64, no. 51 (2008): 11680–11685; (b) G. Sabitha, E. R. Reddy, C. Maruthi and J. S. Yadav, "Bismuth(III) Chloride-Catalyzed Intramolecular Hetero-Diels-Alder Reactions: A Novel Synthesis of Hexahydrodibenzo[b,h][1,6]Naphthyridines", *Tetrahedron Letters* 43 (2002): 1573–1575.
29. (a) S. V. Akolkar, A. A. Nagargoje, V. S. Krishna, D. Sriram, J. N. Sangshetti, M. Damale and B. B. Shingate, "New *N*-Phenylacetamide-Incorporated 1,2,3-triazoles: [Et₃NH][OAc]-Mediated Efficient Synthesis and Biological Evaluation", *RSC Advances*, 9, no. 38 (2019): 22080–22091; (b) D. D. Subhedar, M. H. Shaikh, M. A. Arkile, A. Yeware, D. Sarkar and B. B. Shingate, "Facile Synthesis of 1,3-thiazolidin-4-ones as Antitubercular Agents" *Bioorganic & Medicinal Chemistry Letters* 26 (2016): 1704–1708; (c) D. D. Subhedar, M. H. Shaikh, B. B. Shingate, L. Nawale, D. Sarkar, V. M. Khedkar, F. A. K. Khan and J. N. Sangshetti, "Quinolidene-Rhodanine Conjugates: Facile Synthesis and Biological Evaluation", *European Journal of Medicinal Chemistry* 125 (2017): 385–399; (d) D. D. Subhedar, M. H. Shaikh, L. Nawale, A. Yeware, D. Sarkar, F. A. K. Khan, J. N. Sangshetti and B. B. Shingate, "Novel Tetrazoloquinoline-Rhodanine Conjugates: Highly Efficient Synthesis and Biological Evaluation", *Bioorganic & Medicinal Chemistry Letters* 26 (2016): 2278–2283; (e) D. D. Subhedar, M. H. Shaikh, F. A. K. Khan, J. N. Sangshetti, V. M. Khedkar and B. B. Shingate, "Facile Synthesis of new *N*-sulfonamidyl-4-Thiazolidinone Derivatives and Their Biological Evaluation", *New Journal of Chemistry* 40 (2016): 3047–3058; (f) D. D. Subhedar, M. H. Shaikh, L. Nawale, A. Yeware, D. Sarkar, and B. B. Shingate, "[Et₃NH][HSO₄] Catalyzed Efficient Synthesis of 5-Arylidene-Rhodanine Conjugates and Their Antitubercular Activity", *Research on Chemical Intermediate* 42 (2016): 6607–6626; (g) D. D. Subhedar, M. H. Shaikh, A. A. Nagargoje, S. V. Akolkar, S. G. Bhansali, D. Sarkar and B. B. Shingate, "Amide-Linked Monocarbonyl Curcumin Analogues: Efficient Synthesis, Antitubercular Activity and Molecular Docking Study", *Polycyclic Aromatic Compounds* (2020).
30. (a) C. Mukhopadhyaya, P. Das and R. J. Butcher, "An Expeditious and Efficient Synthesis of Highly Functionalized [1,6]-Naphthyridines Under Catalyst-Free Conditions in Aqueous Medium", *Organic Letters*, 13, no. 17 (2011): 4664–4667; (b) A. M. A. Hameed, "Rapid Synthesis of 1,6-Naphthyridines by Grindstone Chemistry", *Environmental Chemistry Letters* 13 (2015): 125–129; (c) P. Das, T. Chaudhuri, and C. Mukhopadhyaya, "Pseudo-Five-Component Domino Strategy for the Combinatorial Library Synthesis of [1,6] Naphthyridines-an on-Water Approach" *ACS Combinatorial Science*, 16 (2014): 606–613.
31. (a) *Schrodinger Suite 2015-4 QM-Polarized Ligand Docking protocol; Glide version 6.9* (Schrodinger, LLC: New York, NY, 2006); *Jaguar version 9.0* (Schrodinger, LLC: New York, NY, 2015); *QSite version 6.9* (Schrodinger, LLC: New York, NY, 2015); (b) R. A. Friesner, R. B. Murphy, M. P. Repasky, L. L. Frye, J. R. Greenwood, T. A. Halgren, P. C. Sanschagrin and D. T. Mainz, "Extra Precision Glide: Docking and Scoring Incorporating a Model of Hydrophobic Enclosure for Protein-Ligand Complexes," *Journal of Medicinal Chemistry*, 49, no. 21 (2006): 6177–6196.
32. X. Qiu, C. A. Janson, W. W. Smith, M. Head, J. Lonsdale, and A. K. Konstantinidis, "Refined Structures of Beta-Ketoacyl-Acyl Carrier Protein Synthase III," *Journal of Molecular Biology* 307, no. 1 (2001): 341–56.
33. NCCLS (National Committee for Clinical Laboratory Standards), Performance standards for antimicrobial susceptibility testing: twelfth informational supplement, 2002, 1-56238-454-6 M100-S12(M7).
34. M. Burits, and F. Bucar, "Antioxidant Activity of Nigella Sativa Essential Oil," *Phytotherapy Research* 14, no. 5 (2000): 323–8.

35. C. A. Lipinski, L. Lombardo, B. W. Dominy, and P. J. Feeney, "Experimental and Computational Approaches to Estimate Solubility and Permeability in Drug Discovery and Development Settings," *Advanced Drug Delivery Reviews* 46, no. 1–3 (2001): 3–26.
36. Molinspiration Chemoinformatics Brastislava, Slovak Republic, Available from: <http://www.molinspiration.com/cgi-bin/properties>; 2014.
37. Y. H. Zhao, M. H. Abraham, J. Le, A. Hersey, C. N. Luscombe, G. Beck, B. Sherborne, and I. Cooper, "Rate Limited Steps of Human Oral Absorption and QSAR Studies," *Pharmaceutical Research* 19, no. 10 (2002): 1446–57.
38. Drug-likeness and molecular property prediction, available from: <http://www.molsoft.com/mprop/>
39. P. Ertl, B. Rohde, and P. Selzer, "Fast Calculation of Molecular Polar Surface Area as a Sum of Fragment-Based Contributions and Its Application to the Prediction of Drug Transport Properties," *Journal of Medicinal Chemistry* 43, no. 20 (2000): 3714–7.

Synthesis and Biological Evaluation of Indolyl Bis-chalcones as Anti-Breast Cancer and Antioxidant Agents

Pravin S. Bhale,^{1,*} Hemant V. Chavan,² Rupali S. Endait,³ Ashok T. Kadam,¹ Rajesh J. Bopalkar,¹ Mandar S. Gaikwad¹

¹ Department of Chemistry, Yeshwantrao Chavan Mahavidyalaya, Tuljapur, Dist-Osmanabad-413601, Maharashtra, India

² Department of Chemistry, A.S.P. College, Devrukh, Dist-Ratnagiri-415 804, Maharashtra, India

³ Department of Chemistry, Radhabai Kale Mahila Mahavidyalaya, Ahmednagar-414001, Maharashtra, India

* Corresponding author's e-mail address: bhale.ps@gmail.com

RECEIVED: March 23, 2021 * REVISED: July 21, 2021 * ACCEPTED: July 28, 2021

Abstract: A series of novel α -cyano substituted indolyl bis-chalcones (**3a–l**) has been synthesized and evaluated for their *in vitro* antitumor activity against the human breast cancer MCF7 (estrogen receptor-positive) and normal Vero cell lines using sulforhodamine B (SRB) assay method. Compounds **3a**, **3c** and **3d** showed potent activity (GI_{50} = 11.7, 15.3 and 17.9 μ M respectively) against the human breast cancer MCF7 cell line, which was almost as good as that of adriamycin (GI_{50} = < 0.1 μ M) whereas, screening against the normal Vero Monkey cell line showed moderate selectivity. Furthermore, all the synthesized compounds screened for their antioxidant potential against DPPH, NO, SOR, and H_2O_2 radicals. Most of the bis-chalcones exhibited significant DPPH (51.09–12.72 %) and NO (64.11–34.43 %) radical scavenging activity and modest activity against SOR (88.08–43.14 %) and H_2O_2 (80.13–56.0 %) radicals compared to the reference standard ascorbic acid (40.78 %, 42.63 %, 87.05 %, and 79.42 % respectively). Current study provides impetus for the development of highly potent indolyl bis-chalcone derivatives as anticancer leads.

Keywords: indolyl bis-chalcone, breast cancer, anti-cancer activity, antioxidant activity.

INTRODUCTION

PRESENTLY cancer is deemed to a principal worldwide health problem that leads to death.^[1] Although considerable progress is made in controlling the progression of this devastating disease, till the date an entire cure for cancer remains a dream. Most of the cancer treatment is the use of surgery, radiation and chemotherapy.^[2] Most of the marketed chemotherapeutic agents suffer from serious and sometimes intolerable toxic effects. So, the development of novel anticancer agents is a crucial need of time.^[3,4] Chalcone is one of the important scaffold exhibiting diverse biological activities such as anti-inflammatory,^[5] antimalarial,^[6] antileishmanicidal, antiviral, antifungal, antibacterial and anticancer.^[7,8] Different type of structural alterations was performed in the chalcones primary structure either by varying the aryl moieties or the enone linker. Another tactic which is not that typical in literature is to change the α -

position of the α,β -unsaturated carbonyl system. This is a promising idea since it should have a direct and straightforward influence on the reactivity (Figure 1). Examples of the effect of α -alteration on biological activity are also present. First time Edwards et al. reported that α -substituted chalcones are more potent than their unsubstituted counterparts.^[9] Lawrence et al. also improved cytotoxic effects of α -substituents such as phenyl, ester, cyano and fluoro groups on α,β -unsaturated carbonyl system.^[10] Kumar et. al. also reported α -cyano bis-indolyl chalcones as novel anticancer agents.^[11] Recently, our research group reported α -cyano substituted bis-indolyl chalcone^[12] and extended conjugated indolyl chalcones as potent anti-breast cancer agents.^[13] In continuation of our constant efforts to discover a potent anticancer agents,^[14–18] herein we have synthesized a series of novel α -cyano substituted indolyl bis-chalcone having phenyl ring as a spacer and *in vitro* evaluated for their anti-breast cancer and anti-oxidant activity (Scheme 1).

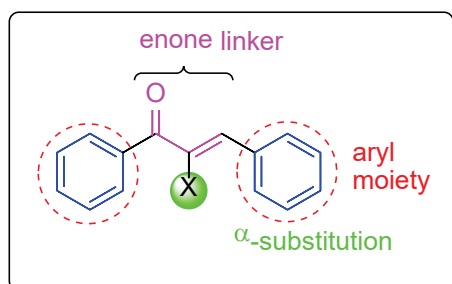


Figure 1. Chalcone framework.

EXPERIMENTAL

Materials and Methods

All the chemicals used for the synthesis were of synthetic grade and obtained from commercial sources. Development of the reactions was supervised by thin layer chromatography (TLC) using TLC plates (silica gel 60 F254, aluminum back, Merck). Visualization of TLC plate was achieved with UV light and or iodine vapors. All the solvents were dried using appropriate drying agents before use. Melting points were determined by open end capillary method and are uncorrected. All the ^1H NMR spectra were recorded in DMSO- d_6 / CDCl_3 and chemical shifts in ppm were reported on instrument Bruker AV-400 MHz, for ^1H NMR and 75 MHz for ^{13}C NMR relative to TMS as an internal standard. The IR spectra were recorded on Shimadzu FT-IR spectrophotometer by using 1 % potassium bromide discs. Mass spectra were obtained with a Shimadzu LCMS-2010EV (Shimadzu, Japan). Anticancer activities were performed under the supervision of Dr.JyotiKode, Scientific Officer, Tata Memorial Centre, Advanced Centre for Treatment Research and Education in Cancer (ACTREC), Kharghar, Navi Mumbai-410210.

Synthesis

GENERAL PROCEDURE FOR THE PREPARATION OF 3-CYANOACETYLINDOLE (2)

Indole **1** (0.117g, 1 mmol) was added to a solution prepared by dissolution of cyanoacetic acid (0.085g, 1 mmol) in Ac_2O (10 ml) at 50 °C. The solution was heated at 85 °C for 5 min. During that period 3-cyanoacetylindole **2** started to crystallize. After 5 more min, the mixture was allowed to cool and solid was collected, washed with methanol, and dried.^[12,13]

GENERAL PROCEDURE FOR THE PREPARATION OF INDOLYL BIS-CHALCONE (3a-I)

To a mixture of 3-cyanoacetylindole **2** (0.184g, 1 mmol) in ethanol (15 mL) was added piperidine (0.3 mL) and stirred for 5 min. Then isophthalaldehyde (0.134g, 1 mmol) was added and this mixture was heated to 80 °C for 1–3 h. After

completion of reaction, the desired indolyl bis-chalcone (**3a-I**) was obtained as precipitate. The obtained precipitate was filtered, washed with water and oven dried. It was column purified by column chromatography using silica gel mesh size, 100–200 and elution with 10 % ethyl acetate in hexane.

(2E,2'E)-3,3'-(1,3-PHENYLENE)BIS(2-(1H-INDOLE-3-CARBONYL)ACRYLONITRILE) (3a)

Pale yellow solid; 88 %; 264–266 °C; IR (cm^{-1}): 3251 (NH), 2218 (CN), 1652 (C=O), 1593(C=C); ^1H NMR (DMSO- d_6 , 400 MHz): δ = 11.69 (s, 2H, NH), 8.29–8.27 (m, 4H), 7.62 (d, J = 8.4 Hz, 2H), 7.48 (d, J = 8.4 Hz, 2H), 7.29 (d, J = 8.0 Hz, 2H), 7.20–7.16 (m, 5H), 6.64 (s, 1H); ^{13}C NMR (DMSO- d_6 , 75 MHz): δ = 184.5, 152.1, 138.0, 137.1, 135.2, 127.8, 127.1, 122.4, 121.6, 121.0, 119.5, 119.1, 115.5, 111.0, 110.3, 108.2; HRMS: 467.4052 (M+H)

(2E,2'E)-3,3'-(1,3-PHENYLENE)BIS(2-(2-METHYL-1H-INDOLE-3-CARBONYL)ACRYLONITRILE) (3b)

Yellow solid; 91 %; 302–304 °C; IR (cm^{-1}): 3258 (NH), 2200 (CN), 1608 (C=O), 1545 (C=C); ^1H NMR (DMSO- d_6 , 400 MHz): δ = 11.23 (s, 2H, NH), 8.18–8.15 (m, 2H), 7.65 (d, J = 7.6 Hz, 2H), 7.31–7.33 (m, 2H), 7.16–7.13 (m, 4H), 7.10–6.88 (m, 4H), 2.30 (s, 6H, - CH_3); ^{13}C NMR (DMSO- d_6 , 75 MHz): δ = HRMS: 495.1816 (M+H)

(2E,2'E)-3,3'-(1,3-PHENYLENE)BIS(2-(5-BROMO-1H-INDOLE-3-CARBONYL)ACRYLONITRILE) (3c)

Yellow solid; 89 %; 288–290 °C; IR (cm^{-1}): 3290 (NH), 3251 (NH), 2212 (CN), 2163 (CN), 1702 (C=O), 1690 (C=O); ^1H NMR (DMSO- d_6 , 400 MHz): δ = 11.52 (s, 2H, NH), 8.48 (s, 2H), 8.34 (s, 2H), 7.69–7.63 (m, 2H), 7.34 (d, J = 8.0 Hz, 2H), 7.09–6.99 (m, 3H), 6.94 (s, 1H), 6.79 (d, J = 8.8 Hz, 2H); ^{13}C NMR (DMSO- d_6 , 75 MHz): δ = 185.3, 153.6, 138.2, 136.8, 135.0, 128.2, 128.0, 127.7, 124.5, 122.6, 121.0, 115.4, 113.2, 113.0, 110.6, 108.2; HRMS: 622.8913 (M+H)

(2E,2'E)-3,3'-(1,3-PHENYLENE)BIS(2-(5-METHOXY-1H-INDOLE-3-CARBONYL)ACRYLONITRILE) (3d)

Pale yellow solid; 92 %; 264–266 °C; IR (cm^{-1}): 3281 (NH), 3245 (NH), 2220 (CN), 1635 (C=O); ^1H NMR (CDCl_3 , 400 MHz): δ = 11.63 (broad s, 2H, NH), 8.63 (s, 2H), 8.43 (s, 2H), 7.83–7.76 (m, 1H), 7.67 (d, J = 2.0 Hz, 2H), 7.48–7.46 (m, 2H), 7.33 (d, J = 8.8 Hz, 2H), 7.22–7.18 (m, 3H), 3.83 (s, 6H, OCH_3); ^{13}C NMR (CDCl_3 , 75 MHz): δ = HRMS: 527.1714 (M+H)

(2E,2'E)-3,3'-(1,3-PHENYLENE)BIS(2-(5-CYANO-1H-INDOLE-3-CARBONYL)ACRYLONITRILE) (3e)

Yellow solid; 87 %; 252–254 °C; IR (cm^{-1}): 3392(NH), 2221 (CN), 2185 (CN), 1592(C=O); ^1H NMR (DMSO- d_6 , 400 MHz): δ = 11.81 (broad s, 2H, NH), 8.62 (s, 2H), 7.76–7.69 (m, 4H), 7.47 (s, 2H), 7.34 (d, J = 7.4 Hz, 2H), 7.26–7.13 (m, 3H), 6.52

(s, 1H); ^{13}C NMR (DMSO- d_6 , 75 MHz): δ = 186.2, 153.3, 141.7, 138.7, 135.0, 128.4, 127.4, 127.0, 125.3, 123.6, 122.9, 118.5, 115.5, 111.4, 110.7, 108.2, 101.6; HRMS: 517.1323 (M+H)

(2E,2'E)-3,3'-(1,3-PHENYLENE)BIS(2-(5-NITRO-1H-INDOLE-3-CARBONYL)ACRYLONITRILE) (3f)

Yellow solid; 89 %; 270–272 °C; IR (cm^{-1}): 3165(NH), 2216 (CN), 1607 (C=O), 1515 (NO $_2$); ^1H NMR (DMSO- d_6 , 400 MHz): δ = 11.61 (broad s, 2H, NH), 8.68 (s, 2H), 8.60 (s, 2H), 8.31–8.28 (m, 2H), 7.77–7.76 (m, 1H), 7.48–7.44 (m, 2H), 7.25–7.19 (m, 5H); ^{13}C NMR (DMSO- d_6 , 75 MHz): δ = 184.7, 154.0, 143.2, 138.7, 135.2, 132.1, 128.5, 127.8, 127.0, 126.1, 122.8, 115.4, 114.2, 112.0, 110.3, 108.4; HRMS: 557.4122 (M+H)

(2E,2'E)-3,3'-(1,3-PHENYLENE)BIS(2-(1-METHYL-1H-INDOLE-3-CARBONYL)ACRYLONITRILE) (3g)

Pale yellow solid; 90 %; 264–266 °C; IR (cm^{-1}): 2219 (CN), 1614 (C=O), 1593 (C=C); ^1H NMR (DMSO- d_6 , 400 MHz): δ = 8.62 (d, J = 6.5 Hz, 2H), 8.36 (s, 2H), 7.45 (d, J = 7.6 Hz, 2H), 7.57–7.52 (m, 4H), 7.40 (d, J = 8.0 Hz, 4H), 7.21 (t, J = 7.6 Hz, 1H), 6.62 (s, 1H), 3.65 (s, 6H, NCH $_3$); ^{13}C NMR (DMSO- d_6 , 75 MHz): δ = 185.8, 153.7, 144.5, 139.3, 135.2, 128.5, 127.7, 124.5, 123.0, 122.7, 121.7, 119.8, 115.6, 110.7, 109.6, 108.2, 32.5; HRMS: 495.1816 (M+H)

(2E,2'E)-3,3'-(1,3-PHENYLENE)BIS(2-(1,2-DIMETHYL-1H-INDOLE-3-CARBONYL)ACRYLONITRILE) (3h)

Yellow solid; 92 %; 238–240 °C; IR (cm^{-1}): 2215 (CN), 1594 (C=O), 1576 (C=C); ^1H NMR (DMSO- d_6 , 400 MHz): δ = 8.14 (d, J = 6.4 Hz, 2H), 7.50 (s, 2H), 7.50–7.42 (m, 6H), 7.26–7.20 (m, 3H), 6.70 (s, 1H), 3.63 (s, 6H, NCH $_3$), 2.51 (s, 6H, CCH $_3$); ^{13}C NMR (DMSO- d_6 , 75 MHz): δ = 185.3, 168.6, 154.0, 140.3, 135.8, 128.5, 127.5, 126.2, 122.8, 121.8, 121.0, 119.7, 119.1, 115.5, 108.7, 103.0, 29.4, 12.2; HRMS: 523.4807 (M+H)

((2E,2'E)-3,3'-(1,3-PHENYLENE)BIS(2-(5-BROMO-1-METHYL-1H-INDOLE-3-CARBONYL)ACRYLONITRILE) (3i)

Yellow solid; 87 %; 268–270 °C; IR (cm^{-1}): 2226 (CN), 1642 (C=O), 1526 (C=C); ^1H NMR (DMSO- d_6 , 400 MHz): δ = 8.40 (s, 2H), 7.59–7.50 (m, 4H), 7.46 (d, J = 7.6 Hz, 2H), 7.31–7.23 (m, 4H), 7.24 (t, J = 7.6 Hz, 1H), 6.60 (s, 1H), 3.61 (s, 6H, NCH $_3$); ^{13}C NMR (DMSO- d_6 , 75 MHz): δ = 185.9, 154.4, 144.5, 135.3, 1351.1, 128.7, 128.2, 127.5, 124.3, 122.7, 121.0, 115.6, 113.2, 110.7, 110.0, 108.5, 32.6; HRMS: 653.0009 (M+1), 654.9952 (M+2), 655.2287 (M+3)

(2E,2'E)-3,3'-(1,3-PHENYLENE)BIS(2-(5-METHOXY-1-METHYL-1H-INDOLE-3-CARBONYL)ACRYLONITRILE) (3j)

Pale yellow solid; 90%; 270–272 °C; IR (cm^{-1}): 2216 (CN), 1621 (C=O), 1595 (C=C); ^1H NMR (CDCl $_3$, 400 MHz): δ = 8.40

(d, J = 4.0 Hz, 3H), 8.36 (s, 2H), 8.27 (dd, J = 8.0, 1.6 Hz, 2H), 8.00 (d, J = 2.8 Hz, 2H), 7.72 (t, J = 8.0, 7.6 Hz, 1H), 7.30 (d, J = 8.8 Hz, 2H), 7.04 (dd, J = 8.8, 2.4 Hz, 2H), 3.93 (s, 12H); ^{13}C NMR (CDCl $_3$, 75 MHz): δ = 185.8, 154.3, 154.0, 144.2, 135.1, 128.7, 128.3, 127.6, 127.2, 122.7, 115.5, 112.0, 110.4, 109.3, 108.3, 104.2, 55.4, 32.1; HRMS: 555.2027 (M+H)

(2E,2'E)-3,3'-(1,3-PHENYLENE)BIS(2-(5-CYANO-1-METHYL-1H-INDOLE-3-CARBONYL)ACRYLONITRILE) (3k)

Yellow solid; 92 %; 260–262 °C; IR (cm^{-1}): 2226 (CN), 2217 (CN), 1661 (C=O), 1621 (C=C); ^1H NMR (DMSO- d_6 , 400 MHz): δ = 8.32 (s, 2H), 7.80 (d, J = 6.8 Hz, 2H), 7.49 (s, 2H), 7.41–7.30 (m, 6H), 7.16 (t, J = 7.6 Hz, 1H), 6.67 (s, 1H), 3.68 (s, 6H, NCH $_3$); ^{13}C NMR (DMSO- d_6 , 75 MHz): δ = 186.1, 154.2, 144.2, 140.5, 135.0, 128.5, 127.4, 127.0, 125.2, 123.6, 122.8, 118.4, 115.8, 111.7, 110.4, 108.1, 101.4, 32.5; HRMS: 545.4930 (M+H)

(2E,2'E)-3,3'-(1,3-PHENYLENE)BIS(2-(1-METHYL-5-NITRO-1H-INDOLE-3-CARBONYL)ACRYLONITRILE) (3l)

Yellow solid; 88 %; 246–248 °C; IR (cm^{-1}): 2284 (CN), 1588 (C=O), 1563 (C=C), 1534 (NO $_2$); ^1H NMR (DMSO- d_6 , 400 MHz): δ = 9.10 (s, 2H), 8.32 (s, 2H), 8.10 (d, J = 8.0 Hz, 2H), 7.93 (d, J = 8.0 Hz, 2H), 7.46 (s, 2H), 7.48 (d, J = 7.6 Hz, 2H), 7.22 (t, J = 7.6 Hz, 1H), 6.39 (s, 1H), 3.56 (s, 6H, NCH $_3$); ^{13}C NMR (DMSO- d_6 , 75 MHz): δ = 185.3, 154.1, 144.0, 142.5, 135.6, 132.2, 128.5, 127.2, 127.0, 126.2, 122.4, 115.2, 114.0, 112.0, 110.3, 108.3, 32.6; HRMS: 585.5001 (M+H)

PROCEDURE OF THE SRB-ASSAY FOR ANTICANCER SCREENING

Tumor cells (human breast cancer cell line MCF-7, Source: NCI, USA and NCCS, Pune) were grown in tissue culture flasks in growth medium (RPMI-1640 with 2 mM glutamine, pH 7.4, 10 % fetal calf serum, 100 $\mu\text{g mL}^{-1}$ streptomycin, and 100 units mL^{-1} penicillin) at 37 °C under the atmosphere of 5 % CO $_2$ and 95 % relative humidity employing a CO $_2$ incubator. The cells at sub confluent stage were harvested from the flask by treatment with trypsin (0.05% trypsin in PBS containing 0.02 % EDTA) and placed in growth medium. The cells with more than 97 % viability (trypan blue exclusion) were used for cytotoxicity studies. An aliquot of 100 μL (5×10^3 cells/well) of cells were transferred to a well of 96-well tissue culture plate. The cells were allowed to grow for one day at 37 °C in a CO $_2$ incubator as mentioned above. The test materials at different concentrations (10^{-7} M, 10^{-6} M, 10^{-5} M, 10^{-4} M) were then added to the wells and cells were further allowed to grow for another 48 h. Suitable blanks and positive controls were also included. Each test was performed in triplicate. The cell growth was stopped by gently layering of 50 μL of 50 % trichloroacetic acid. The plates were incubated at 4 °C for

an hour to fix the cells attached to the bottom of the wells. Liquids of all the wells were gently pipette out and discarded. The plates were washed five times with doubly distilled water to remove TCA, growth medium, etc. and were air-dried. 100 μ L of SRB solution (0.4 % in 1 % acetic acid) was added to each well and the plates were incubated at ambient temperature for half an hour. The unbound SRB was quickly removed by washing the wells five times with 1 % acetic acid. Plates were air dried, tris-buffer (100 μ L of 0.01 M, pH 10.4) was added to all the wells and plates were gently stirred for 5 min on a mechanical stirrer. The optical density was measured on ELISA reader at 540 nm. The cell growth at absence of any test material was considered 100 % and in turn growth inhibition was calculated. GI₅₀ values were determined by regression analysis.

2,2-DIPHENYL-1-PICRYLHYDRAZYL (DPPH) RADICAL SCAVENGING ACTIVITY

In this method, 0.1 mM DPPH solution was prepared in methanol by adding 39.4 mg of DPPH in 1000 mL of methanol, and to 0.5 mL of this solution, 1.5 mL of test compounds of the dissolved in DMSO were added at various concentrations of all (1, 10, 100, 500 and 1000 μ g mL⁻¹). The mixtures were shaken vigorously and allowed to stand at room temperature for 30 minutes. Then the absorbance was measured at 517 nm using a UV-VIS spectrophotometer (Shimadzu, spectrophotometer). Vitamin-C was used as standard compound. Reduction in absorbance by test compounds and indicates radical scavenging activity. The scavenging activity by the DPPH radical was determined by

$$\text{DPPH}_{\text{scavenging effect (\% inhibition)}} = \frac{A_0 - A_1}{A_0} \cdot 100 \quad (1)$$

where A_0 is the absorbance of the control reaction, and A_1 is the absorbance test compound and vitamin C.

NITRIC OXIDE (NO) RADICAL SCAVENGING ACTIVITY

The various concentrations of test compounds (as 1, 10, 100, 500, and 1000 μ g mL⁻¹) were prepared in ethanol. To 0.5 mL of 10 mM sodium nitroprusside in phosphate buffered saline, to this, 1 mL of various concentrations of test compounds were mixed, and to this equal volume of freshly prepared Griess reagent was added, solution was then incubated at 25 °C for 3 h. Form this, 100 μ L of the reaction mixture was transferred to a 96-well plate, and the absorbance was read at 546 nm using a microplate reader (Biotek, Italy). Ascorbic acid was used as standard control.

The percentage of nitrite radical scavenging activity of test compounds was calculated by

$$\text{NO}_{\text{scavenging activity}} = \frac{A_c - A_1}{A_c} \cdot 100 \quad (2)$$

where A_c is the absorbance of control, and A_1 is absorbance of test compounds.

SUPEROXIDE RADICAL (SOR) SCAVENGING ASSAY

The reaction mixture consisting of 1mL of nitro blue tetrazolium (NBT) solution (156 mM NBT in phosphate buffer, pH 7.4), 1 mL NADH solution (468 mM NADH in phosphate buffer, pH 7.4), and 1mL of synthetic compound (1 mM) solution was mixed. The reaction was started by adding 1 mL of phenazine methosulfate (PMS) solution (60 mM PMS in phosphate buffer, pH 7.4) to the mixture. The reaction mixture was incubated at 25 °C for 5 min and the absorbance was measured at 560 nm against blank sample and compared with standards and percentage of inhibition was calculated using the same formula as above. Decreased absorbance of reaction mixture indicated increased SOR scavenging activity.

HYDROGEN PEROXIDE SCAVENGING (H₂O₂) ASSAY

A solution of H₂O₂ (40 mM) is prepared in phosphate buffer (50 mM, pH 7.4). The concentration of H₂O₂ was determined by measuring absorption at 230 nm using a spectrophotometer. Synthetic compound (1 mM) in DMSO was added to H₂O₂ and absorbance was measured at 230 nm after 10 min against a blank solution containing phosphate buffer without H₂O₂. The percentage inhibition of H₂O₂ was calculated by formula,

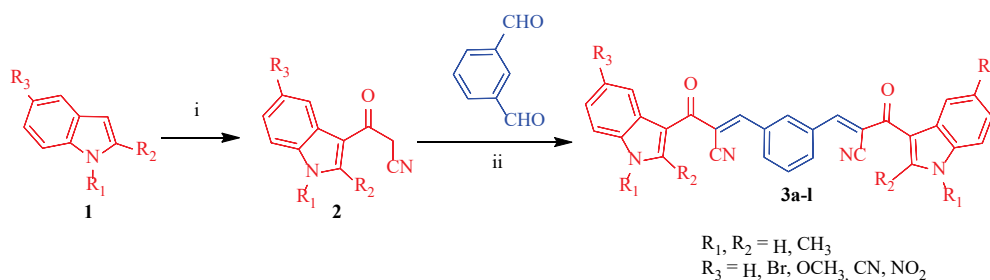
$$\% \text{ inhibition (H}_2\text{O)} = \frac{A_0 - A_1}{A_0} \cdot 100 \quad (3)$$

where A_0 is the absorbance of control and A_1 is the absorbance of test sample.

RESULTS AND DISCUSSION

Chemistry

In the current study, syntheses of novel α -cyano substituted bis-chalcones (**3a-l**) were accomplished by the Knoevenagel condensation of 3-cyanoacetyl indoles **2** with substituted 3-isophthalaldehyde in the presence of piperidine in ethanol (Scheme 1). The starting compound, namely 3-cyanoacetyl indoles **2** were synthesized in good yield from the reaction of substituted indoles **1** with cyanoacetic acid in presence of acetic anhydride using the method described in the literature with minor modifications.^[19] The obtained crude products were purified by column chromatography using silica gel mesh size, 100–200 and elution with 10 % ethyl acetate in hexane. The structures of target molecules were analyzed by IR, ¹H NMR and MS spectroscopic techniques.



Scheme 1. Synthesis of novel α -cyano substituted bis-chalcones. Reagents and conditions: i) CNCH_2COOH , $(\text{CH}_3\text{CO})_2\text{O}$, reflux; ii) piperidine, ethanol, 80°C , 1–3 h.

Biological Evaluation

IN VITRO ANTICANCER ACTIVITY

All the synthesized novel α -cyano substituted bis-chalcones (**3a–l**) were evaluated for their *in vitro* anticancer activity against human breast cancer cell line MCF-7 by employing the sulforhodamine B (SRB) assay method.^[20] It is worth mentioning that most of the compounds were significantly cytotoxic against MCF-7 compared to the standard drug adriamycin, with the concentration of the drug that produced 50 % inhibition of cell growth (GI_{50}). Three parameters such as GI_{50} , TGI and LC_{50} were determined during the screening process and the results summarized in Table 1.

Compound **3a**, **3c** and **3d** exhibited potent activity ($\text{GI}_{50} = 11.7$, 15.3 and $17.9\ \mu\text{M}$, respectively) against the MCF-7 cell line which was almost as good as that of standard drug adriamycin ($\text{GI}_{50} < 0.1\ \mu\text{M}$). On the other hand, all other α -cyano substituted bis-chalcones showed weak cytotoxicity ($\text{GI}_{50} = 79.1 - >100\ \mu\text{M}$) against MCF-7 cell line. A comparison of the TGI and LC_{50} concentrations of the compounds with Adriamycin were also done. All the α -cyano substituted bis-chalcones **3a–l** were inactive (TGI and $\text{LC}_{50} > 100\ \mu\text{M}$) like adriamycin against the MCF-7 cell line.

Many reported drugs impact the normal cell growth, which is a major disadvantage in the progress of anticancer drug development. Therefore, we have ensured the selectivity of some active compounds by *in vitro* screening against the normal Vero Monkey cell line. This cellular level screening results help to reveal the safety profile of active compounds. The cytotoxicity study showed that the GI_{50} values for **3a**, **3c** and **3d** are 65.1 , 70.6 and $55.3\ \mu\text{M}$, respectively (Table 1). This novel α -cyano substituted bis-chalcones showed moderate selectivity against cancer lines over normal cell line.

Structure activity relationship (SAR) study reveals that the presence of electron donating groups at 5-position of indole holds better anticancer potential over electron withdrawing groups. Compound **3a** with no substitution at 5-position of indole ring exhibited potent activity ($\text{GI}_{50} = 11.7\ \mu\text{M}$) against MCF-7 cell line. Considering the type of

substitution, compounds **3c** and **3d** containing bromo and methoxy group at 5-position of indole ring exhibited significant activity ($\text{GI}_{50} = 15.3$ and $17.9\ \mu\text{M}$) against MCF-7 cell line, however, decrease in activity was observed with cyano substitution. Comparing of GI_{50} values of **3a–d** ($\text{GI}_{50} = 11.7$, 47.2 , 15.3 and $17.9\ \mu\text{M}$, respectively) and **3g–j** ($\text{GI}_{50} = 79.1 - >100\ \mu\text{M}$), we may presume that free NH of indole is essential for activity.

To confirm the effect α -cyano substituted chalcone and α -cyano substituted bis-chalcone on cytotoxic potential, we have prepared three simple α -cyano substituted chalcone analogues of compounds **3a**, **3c** and **3d** by reacting suitable substituted 3-cyanoacetyl indole **2** with 3-(trifluoromethyl)benzaldehyde by refluxing in ethanol with the presence of piperidine. Comparison of the GI_{50} values against MCF-7 cancer cell line of α -cyano substituted chalcone and α -cyano substituted bis-chalcone were done. Bis-chalcone **3a**, **3c** and **3d** having phenyl ring as a spacer have increased the cytotoxic potential over their α -cyano substituted mono-indolyl chalcone analogues (Figure 2).

IN VITRO ANTIOXIDANT ACTIVITY

The series of bis-chalcone (**3a–l**) were evaluated for their direct scavenging activity against a variety of reactive oxygen and nitrogen species such as 2,2-diphenyl-2-picrylhydrazyl (DPPH), nitric oxide (NO) and superoxide (SOR), hydrogen peroxide (H_2O_2). Free radical scavenging

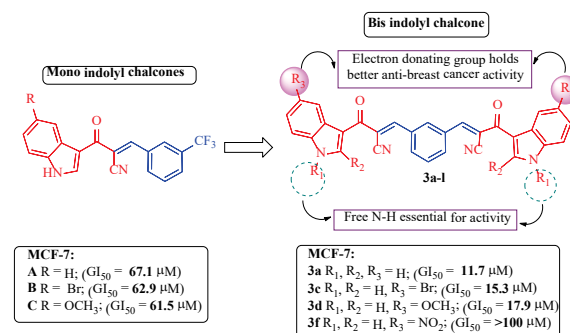
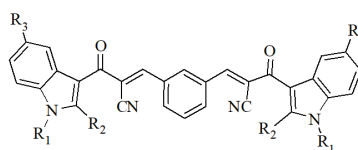


Figure 2. Comparison of anticancer activity of bis-indolyl chalcones over mono-indolyl chalcones.

Table 1. *In vitro* anticancer screening of α -cyano substituted bis-chalcones (**3a-l**) against human breast cancer cell line MCF-7^a and monkey normal kidney cell line Vero.



Compound	R ₁	R ₂	R ₃	MCF-7			Vero (normal)		
				LC ₅₀ ^(b)	TGI ^(c)	GI ₅₀ ^(d)	LC ₅₀	TGI	GI ₅₀
3a	H	H	H	> 100	> 100	11.7	> 100	> 100	65.1
3b	H	CH ₃	H	> 100	> 100	47.2	> 100	> 100	> 100
3c	H	H	Br	> 100	> 100	15.3	> 100	> 100	70.6
3d	H	H	OCH ₃	> 100	> 100	17.9	> 100	> 100	55.3
3e	H	H	CN	> 100	> 100	> 100	> 100	> 100	> 100
3f	H	H	NO ₂	> 100	> 100	> 100	> 100	> 100	> 100
3g	CH ₃	H	H	> 100	> 100	> 100	> 100	> 100	95.2
3h	CH ₃	CH ₃	H	> 100	> 100	79.1	> 100	> 100	> 100
3i	CH ₃	H	Br	> 100	> 100	> 100	> 100	> 100	> 100
3j	CH ₃	H	OCH ₃	> 100	> 100	88.0	> 100	> 100	78.1
3k	CH ₃	H	CN	> 100	> 100	> 100	> 100	> 100	> 100
3l	CH ₃	H	NO ₂	> 100	> 100	> 100	> 100	> 100	> 100
Adriamycin				100	11.0	< 0.1	>100	10.0	< 0.1

^(a) Concentrations in μ M.

^(b) Concentration of drug resulting in a 50 % reduction in the measured protein at the end of the drug treatment as compared to that at the beginning) calculated from $[(Ti - Tz) / Tz] \times 100 = -50$.

^(c) Drug concentration resulting in total growth inhibition (TGI) will calculated from $Ti = Tz$.

^(d) Growth inhibition of 50% (GI₅₀) calculated from $[(Ti - Tz) / (C - Tz)] \times 100 = 50$.

activity was measured in terms of percent inhibition by using reported procedure in literature and results are presented in Table 2. All the synthesized α -cyano substituted bis-chalcone have shown good to excellent scavenging activity against DPPH and NO radicals (Figure 3). The compounds **3d**, **3a**, **3c** and **3b** showed excellent DPPH free radical scavenging activity (51.09, 50.04, 46.90 and 41.10 %, respectively) as compared to standard ascorbic acid (AA) (40.78 %). Remaining compounds **3e-l** showed moderate to weak DPPH free radical scavenging activity (12.72–37.90 %). Compounds **3a-g** showed excellent NO free radical scavenging activity (42.67–63.11 %) as compared to standard ascorbic acid (42.63 %). All other compounds **3h-l** showed moderate NO free radical scavenging activity (34.43–41.30). Compound **3b** exhibited excellent activity (88.08 %) against SOR radical as compared to standard ascorbic acid (87.05 %). All other compounds were moderate SOR scavengers (43.14–85.92 %). Compound **3f** have shown excellent H₂O₂ radical scavenging activity (80.13 %), whereas all other compounds showed moderate activity (56.00–73.23 %).

Table 2. *In vitro* antioxidant activity of curcumin analogues (**3a-l**).

Entry	% inhibition at 1 mM			
	DPPH	NO	SOR	H ₂ O ₂
3a	50.04	62.64	80.16	66.11
3b	41.10	59.97	88.08	71.00
3c	46.90	44.18	60.55	69.05
3d	51.09	63.11	79.12	56.00
3e	37.90	59.25	54.99	59.12
3f	31.32	51.11	54.00	80.13
3g	30.11	42.67	81.40	71.14
3h	27.18	36.01	85.92	73.23
3i	29.13	37.17	43.14	64.57
3j	30.09	34.43	54.21	60.16
3k	12.72	40.00	65.12	56.98
3l	17.43	41.30	43.43	63.19
AA	40.78	42.63	87.05	79.42

CONCLUSION

We designed and synthesized a series of novel α -cyano substituted bis-indolyl chalcone derivatives and *in vitro* evaluated them for their cytotoxic potential against breast cancer (MCF-7) and normal Vero Monkey cell line. Compound **3a**, **3c** and **3d** showed strong activity against breast cancer as good as adriamycin. In general, the presence of electron donating groups at 5-position of indole ring over electron donating groups and free NH of indole are essential for activity. Antioxidant potential of synthesized compounds was also evaluated and most of the compounds exhibited significant DPPH and NO radical scavenging activity. The present investigation has thus provided impetus for the design and development of potent bis-indolyl chalcone derivatives as anticancer leads.

Acknowledgment. Authors express deep thank to Tata Memorial Centre, Advanced Centre for Treatment Research and Education in Cancer (ACTREC), Kharghar, Navi Mumbai-410210 for conducting the *in vitro* anticancer screening.

Supplementary Information. Supporting information to the paper is attached to the electronic version of the article at: <https://doi.org/10.5562/cca3758>.

PDF files with attached documents are best viewed with Adobe Acrobat Reader which is free and can be downloaded from Adobe's web site.

REFERENCES

- [1] M. H. El-Wakil, H.M. Ashour, M.N. Saudi, A. M. Hassan, I. M. Labouta, *Bioorg. Chem.* **2017**, *73*, 154–169.
<http://dx.doi.org/10.1016/j.bioorg.2017.06.009>
- [2] U. Bughani, S. Li, H.C. Joshi, *Recent Pat. Anti-Infect. Drug Discov.* **2009**, *4*, 164–182.
<https://doi.org/10.2174/157489109789318532>
- [3] E. Espinosa, P. Zamora, J. Feliu, M. G. Barón, *Cancer Treat. Rev.* **2003**, *29*, 515–523.
[https://doi.org/10.1016/S0305-7372\(03\)00116-6](https://doi.org/10.1016/S0305-7372(03)00116-6)
- [4] B. Mansoori, A. Mohammadi, S. Davudian, S. Shirjang, B. Baradaran, *Adv. Pharm. Bull.* **2017**, *7*, 339–348.
<http://dx.doi.org/10.15171/apb.2017.041>
- [5] C. Kontogiorgis, M. Mantzanidou, D. Hadjipavlou-Litina, *Mini. Rev. Med. Chem.* **2008**, *8*, 1224–1242.
<http://dx.doi.org/10.2174/138955708786141034>
- [6] A. Agarwal, K. Srivastava, S. Puri, P. M. S. Chauhan, *Bioorg. Med. Chem. Lett.* **2005**, *15*, 3133–3136.
<https://doi.org/10.1016/j.bmcl.2005.04.011>
- [7] X.-F. Liu, C.-J. Zheng, L.-P. Sun, X.-K. Liu, H.-R. Piao, *Eur. J. Med. Chem.* **2011**, *46*, 3469–3473.
<https://doi.org/10.1016/j.ejmech.2011.05.012>
- [8] M. Zoldakova, Z. Kornyei, A. Brown, B. Biersack, E. Madarász, R. Schobert, *BiochemPharmacol.* **2010**, *80*, 1487–1496.
<https://doi.org/10.1016/j.bcp.2010.07.046>
- [9] M. L. Edwards, D. M. Stemerick, P.S. Sunkara, *J. Med. Chem.* **1990**, *33*, 1948–1954.
<https://doi.org/10.1021/jm00169a021>
- [10] N. J. Lawrence, R. P. Patterson, L.-L. Ooi, D. Cook, S. Ducki, S., *Bioorg. Med. Chem. Lett.* **2006**, *16*, 5844–5848.
<https://doi.org/10.1016/j.bmcl.2006.08.065>
- [11] D. Kumar, N. Maruthi Kumar, M. P. Tantak, M. Ogura, E. Kusaka, T. Ito, *Bioorg. Med. Chem. Lett.* **2014**, *24*, 5170–5174.
<https://doi.org/10.1016/j.bmcl.2014.09.085>
- [12] P. S. Bhale, H. V. Chavan, S. B. Dongare, S. N. Shringare, Y. B. Mule, P. B. Choudhari, B. P. Bandgar, *Current Bioactive Compounds* **2018**, *14*, 299–308.
<https://doi.org/10.2174/1573407213666170428112855>
- [13] P. S. Bhale, H. V. Chavan, S. B. Dongare, S. N. Shringare, Y. B. Mule, S. S. Nagane, B. P. Bandgar, *Bioorg. Med. Chem. Lett.* **2017**, *27*, 1502–1507.
<https://doi.org/10.1016/j.bmcl.2017.02.052>
- [14] S. N. Shringare, H.V. Chavan, P. S. Bhale, S.B. Dongare, Y. B. Mule, N. D. Kolekar, B. P. Bandgar, *Croat. Chem. Acta* **2018**, *91*, 357–366.
<https://doi.org/10.5562/cca3393>
- [15] S. B. Dongare, B. P. Bandgar, P. S. Bhale, S. N. Shringare, H. V. Chavan, *Croat. Chem. Acta* **2019**, *92*, 1–9. <https://doi.org/10.5562/cca3418>
- [16] S. N. Shringare, H.V. Chavan, P. S. Bhale, S.B. Dongare, Y. B. Mule, S. B. Patil, B. P. Bandgar, *Med. Chem. Res.* **2018**, *27*, 1226–1237.
<https://doi.org/10.1007/s00044-018-2142-8>
- [17] P. S. Bhale, B. P. Bandgar, S. B. Dongare, S. N. Shringare, D. M. Sirsat, H. V. Chavan, *Phosphorus, Sulfur, and Silicon and the Related Elements* **2019**, *194*, 843–849.
<https://doi.org/10.1080/10426507.2019.1565760>
- [18] P. S. Bhale, H. V. Chavan, S. B. Dongare, S. T. Sankpal, B. P. Bandgar, *Anti-Cancer Agents in Medicinal Chemistry* **2018**, *18*, 757–764.
<https://doi.org/10.2174/1871520617666170912124258>
- [19] J. Slatt, I. Romero, J. Bergman, *Synthesis*, **2004**, *16*, 2760–2765.
<https://doi.org/10.1055/s-2004-831164>
- [20] P. Skehan, R. Strong, D. Scadiaro, A. Monks, J. McMahon, D. Vistica, J. T. Warren, H. Bokesch, S. Kenney, M. R. Boyed, *J. Natl. Cancer Inst.* **1990**, *82*, 1107–1112.
<https://doi.org/10.1093/jnci/82.13.1107>



Studies on Diversity of Soil Micro Fungi from Nashik City, Maharashtra, India

Bhagwat, M.G.^{1*}, Saler, R.S.²

¹Department of Botany, Radhabai Kale Mahila Mahavidyalaya, Ahmednagar, 414001, India

²Department of Botany, KRT Arts, BH Commerce and AM Science (KTHM) College, Nashik, 422002, India

ARTICLE INFO

Keywords:

Diversity
Fungi
Nashik
Soil

*Corresponding
author.

E-mail addresses:

manju.14.mb@gmail.com

ABSTRACT

Soil micro-organisms such as bacteria and fungi play an important role in soil fertility and promoting plant health. Soil harbors most of our planet's undiscovered biodiversity. The present study highlights the status of the diversity of soil fungi from Nashik city and adjoining places of Nashik city, Maharashtra, India. Soil samples of two ecosystems viz. Agricultural field and Barren lands from 5 localities were investigated for the diversity of fungi. A total of 40 species belonging to 23 genera were isolated from both ecosystem types. The microflora was isolated using the soil dilution plate count method on Czapek's Dox Agar medium supplemented with streptomycin. These fungi were diverse in their distribution and dominance. Identification and characterization of microflora were done with the help of available literature and manuals. The dominant genera recorded were *Aspergillus* and *Fusarium*. Potential pathogens like *Rhizoctonia bataticola*, *Fusarium oxysporum*, and *Aspergillus flavus* were also recorded during the investigation.

1. Introduction

It has been recognized for a long time that the soil is a favorable medium for life and life activities. Many investigators have undertaken the study of the soil flora to either study the micro-organisms found in the soil or the activities carried out by certain micro-organisms (Abbott, 1923, Alexander, 1977, Burges, 1958, Subramanian, 1952, Warcup, 1950). Biological diversity is the variability among the living organisms found in all sources such as air, water, and soil. Soil is a major component of the earth's ecosystem which comprises organic matter and a large number of microorganisms. Many biological processes are carried out in the soil. Microorganisms in the soil are beneficial in increasing soil fertility and plant growth as they take part in various biogeochemical processes. They decompose organic matter from humus, release nutrients, assimilate soil carbon and fix organic nutrients (Aneja, 2001, Basu et. al., 2021). The mycologists became more concerned of diversity of fungi as they have gained immense importance during recent years. However, fungi still are 'orphans' and trailing behind in the biodiversity stakes (Hawksworth, 1997). The present study aims to isolate microflora from different agricultural fields and barren lands of Nashik city and its outskirts. The study involves the collection of soil samples, isolation, and identification of fungal species.

2. Materials and Methods

2.1 Study area

Nashik is one of the fastest developing cities in the state of Maharashtra. It is situated on the banks of river Godavari and is popularly known as 'The Wine Capital of India'. The study area lies on 20.00°N latitude and 73.78°E longitude which has an average elevation of 700 meters. The temperature ranges from 11°C to 37°C and the annual rainfall is 812 mm. Type of soil found in the district is red soils and black cotton soils. Grapes, sugarcane, onion, tomato, wheat, etc. are the crops that are cultivated on a large scale.

Table 1: Soil samples collected from different localities of Nashik

Sample No.	Sampling location	No. of samples collected	Type of Ecosystem
1	Anandwali	2	Agriculture field and Barren Land
2	Chandshi	2	Agriculture field and Barren Land
3	Nashik city	2	Agriculture field and Barren Land
4	Nashik Road	2	Agriculture field and Barren Land
5	Wadala	2	Agriculture field and Barren Land

Table 2: Percentage contribution of fungal species in different ecosystems of Nashik

Sr. No.	Name of Fungal species	% Contribution									
		Agriculture field					Barren Land				
		1	2	3	4	5	1	2	3	4	5
1	<i>Alternaria alternata</i>	-	8	-	-	-	-	7.14	-	-	-
2	<i>Aspergillus carbonarius</i>	-	8	6.45	7.14	8	-	21.42	15	8.33	14.28
3	<i>Aspergillus flaviceps</i>	-	-	-	-	4	-	-	-	-	-
4	<i>Aspergillus flavus</i>	8.69	4	6.45	-	8	5.88	7.14	10	-	7.14
5	<i>Aspergillus fumigatus</i>	4.34	4	-	-	-	5.88	-	-	-	-
6	<i>Aspergillus nidulans</i>	-	-	9.67	7.14	-	-	-	10	4.16	-
7	<i>Aspergillus niger</i>	8.69	8	9.67	10.71	12	11.76	14.28	5	8.33	14.28
8	<i>Aspergillus petrakii</i>	-	4	-	-	-	5.88	7.14	-	-	-
9	<i>Aspergillus sclerotium</i>	4.34	-	-	3.57	-	-	-	-	8.33	-
10	<i>Aspergillus sulphureus</i>	-	-	-	-	4	-	-	-	-	-
11	<i>Aspergillus sydowii</i>	8.69	-	-	-	-	11.76	-	-	-	-
12	<i>Aspergillus ustus</i>	4.34	-	-	3.57	8	-	7.14	-	4.16	7.14
13	<i>Aureobasidium pullans</i>	-	-	-	3.57	-	-	-	-	-	-
14	<i>Biospora sp.</i>	-	-	3.22	-	-	-	-	-	4.16	-
15	<i>Chaetomium globosum</i>	-	4	-	-	-	-	-	-	-	-
16	<i>Cladosporium herbarum</i>	8.69	-	6.45	7.14	-	-	-	10	4.16	-
17	<i>Curvularia lunata</i>	-	8	6.45	-	4	-	7.14	5	-	-
18	<i>Fusarium moniliformae</i>	8.69	4	6.45	-	-	5.88	-	5	8.33	-
19	<i>Fusarium oxysporum</i>	8.69	4	3.22	3.57	4	11.76	14.28	-	-	7.14
20	<i>Fusarium rodlens</i>	-	4	-	3.57	-	-	-	-	-	-
21	<i>Fusarium semitectum</i>	-	-	3.22	7.14	-	-	-	-	-	-
22	<i>Helminthosporium tetramera</i>	4.34	-	-	-	8	-	-	-	-	-
23	<i>Mucor globosus</i>	-	-	6.45	-	8	-	-	10	8.33	7.14
24	<i>Mucor plumbeus</i>	-	4	-	7.14	8	11.76	-	-	4.16	14.28
25	<i>Myrothecium roridium</i>	-	-	-	3.57	-	-	-	-	-	-
26	<i>Neocosmospora vasinfecta</i>	-	8	-	7.14	-	-	7.14	-	12.5	-
27	<i>Penicillium brefeldianum</i>	-	-	3.22	-	-	-	-	-	-	-
28	<i>Penicillium funiculosum</i>	4.34	4	6.45	7.14	-	-	-	-	4.16	-
29	<i>Penicillium verrucosum</i>	-	-	3.22	-	-	-	-	5	-	-
30	<i>Phoma eupyrena</i>	4.34	4	3.22	-	-	-	-	-	-	-
31	<i>Phytophthora sp.</i>	-	-	-	7.14	-	-	-	-	8.33	-
32	<i>Pithomyces sp.</i>	-	-	-	3.57	-	-	-	-	8.33	-
33	<i>Rhizoctonia bataticola</i>	4.34	-	-	-	4	-	-	5	-	-
34	<i>Rhizopus stolonifer</i>	8.69	8	3.22	7.14	8	11.76	-	10	4.16	7.14
35	<i>Scedosporium sp.</i>	-	-	6.45	-	-	-	-	5	-	-
36	<i>Thielavia terricola</i>	-	-	6.45	-	-	-	-	5	-	-
37	<i>Torula herbarum</i>	-	-	-	-	4	-	-	-	-	-
38	<i>Trichoderma herzianum</i>	-	4	-	-	-	-	7.14	-	-	-
39	<i>Trichoderma viride</i>	8.69	8	-	-	8	11.76	-	-	-	21.42
40	<i>Zygorhynchus moelleri</i>	-	-	-	-	-	5.88	-	-	-	-

Table 3: Frequency of microflora in different ecosystems of Nashik

Sr. No.	Name of Fungal species	Agriculture field						% Contribution	Barren Land						% Contribution
		1	2	3	4	5	Total		1	2	3	4	5	Total	
1	<i>Alternaria</i>	-	2	-	-	-	2	1.51	-	1	-	-	-	1	1.12
2	<i>Aspergillus</i>	9	7	10	9	11	46	34.84	7	8	8	8	6	37	41.57
3	<i>Aureobasidium</i>	-	-	-	1	-	1	0.75	-	-	-	-	-	0	0
4	<i>Biospora</i>	-	-	1	-	-	1	0.75	-	-	-	1	-	1	1.12
5	<i>Chaetomium</i>	-	1	-	-	-	1	0.75	-	-	-	-	-	0	0
6	<i>Cladosporium</i>	2	-	2	2	-	6	4.54	-	-	2	1	-	3	3.37
7	<i>Curvularia</i>	-	2	2	-	1	5	3.78	-	1	1	-	-	2	2.24
8	<i>Fusarium</i>	4	3	4	4	1	16	12.12	3	2	1	2	1	9	10.11
9	<i>Helminthosporium</i>	1	-	-	-	2	3	2.27	-	-	-	-	-	0	0
10	<i>Mucor</i>	-	1	2	2	4	9	6.81	2	-	2	3	3	10	11.23
11	<i>Myrothecium</i>	-	-	-	1	-	1	0.75	-	-	-	-	-	0	0
12	<i>Neocosmospora</i>	-	2	-	2	-	4	3.03	-	1	-	3	-	4	4.49
13	<i>Penicillium</i>	1	1	4	2	-	8	6.06	-	-	1	1	-	2	2.24
14	<i>Phoma</i>	1	1	1	-	-	3	2.27	-	-	-	-	-	0	0
15	<i>Phytophthora</i>	-	-	-	2	-	2	1.51	-	-	-	2	-	2	2.24
16	<i>Pithomyces</i>	-	-	-	1	-	1	0.75	-	-	-	2	-	2	2.24
17	<i>Rhizoctonia</i>	1	-	-	-	1	2	1.51	-	-	1	-	-	1	1.12
18	<i>Rhizopus</i>	2	2	1	2	2	9	6.81	2	-	2	1	1	6	6.74
19	<i>Scedosporium</i>	-	-	2	-	-	2	1.51	-	-	1	-	-	1	1.12
20	<i>Thielavia</i>	-	-	2	-	-	2	1.51	-	-	1	-	-	1	1.12
21	<i>Torula</i>	-	-	-	-	1	1	0.75	-	-	-	-	-	0	0
22	<i>Trichoderma</i>	2	3	-	-	2	7	5.3	2	1	-	-	3	6	6.74
23	<i>Zygorhynchus</i>	-	-	-	-	-	0	0	1	-	-	-	-	1	1.12
	TOTAL	23	25	31	28	25	132		17	14	20	24	14	89	

2.2 Collection of Soil samples

The soil samples were collected from the Nashik city and adjoining places of the city. These were Anandwadi (1), Chandshi (2), Nashik city (3), Nashik Road (4), Wadala (5). From each locality 50 gm of soil sample was collected from a depth of 10-15 cms. The soil samples were collected from two ecological niches viz. the agricultural fields and barren lands. The collected soil samples were brought to the laboratory in sterile polythene bags and stored at 4°C until further use.

2.3 Isolation and identification of fungi

The soil fungi were isolated by using the soil dilution plate count method (Subba Rao, 2004) on Czapek's Dox Agar. 1 gm of soil sample was suspended in 200 ml of sterile autoclaved water. 1 ml of the microbial suspension was added to sterile Petri dishes upon which the Czapek's Dox Agar medium was

added by pour plate method. The fungi were identified with the help of literature (Barnett, 1998, Gilman, 2001, Nagamani et. al., 2006).

2.4 Statistical analysis

The number of colonies per plate in 1 gm of soil was calculated. The percentage contribution of each fungal species was calculated by using the following formula:

$$\% \text{ Contribution} = \frac{\text{Total no. of CFU of an individual sp.} \times 100}{\text{Total no. of CFU of all species}}$$

*CFU- Colony-forming unit

3. Results and Discussion

Diversity is the variation in the life forms of plants, animals, and microorganisms. Fungi are the important components of the

environment that have a significant role to play in the ecological processes (Chandrashekar, 2014). In the present study, a total of 221 fungal colonies were isolated from two ecosystem types viz. the agricultural fields and the barren lands. 40 species belonging to 23 genera were isolated from these sites of the localities under study (Table 1). Soil microbes play a very important role in biogeochemical processes which help to increase plant productivity (Aneja, 2001, Basu et al., 2021). Earlier studies indicate variations in the results. Maximum variation was observed in barren land soil, 65 species belonging to 30 genera were isolated from barren land samples (Wahegaonkar, et al., 2011). 162 fungal colonies of 10 fungal species were isolated from agriculture fields in Nanjangud taluka (Chandrashekar, 2014). The soil microflora in the agricultural fields and barren lands were observed. The most common and dominant among them like *Aspergillus* (34.84 % and 41.57 % in the agriculture field and barren land respectively), *Fusarium* (12.12 % and 10.11 % respectively), *Rhizopus* (6.81 % and 6.74 % respectively), *Mucor* (6.81 % and 10.11 % respectively) were isolated and characterized. Among others *Alternaria* (1.51 %), *Cladosporium* (4.54 %), *Curvularia* (3.78 %), *Helminthosporium* (2.27 %), *Penicillium* (6.06 %), *Trichoderma* (5.3 %) also contributed in the area (Table 3). Diversity was found to be higher in agricultural fields as compared to barren lands. The percentage contribution of each fungal species at different localities was analyzed statistically (Table 2). *Aspergillus niger*, *A. nidulans*, *Fusarium oxysporum*, *Mucor plumbeus*, *Rhizopus stolonifer*, and *Trichoderma viride* were the dominant species. The growth of other fungal species may have been prevented due to the toxins produced by *Aspergillus* species.

4. Conclusion

The result of the survey indicates that the Nashik city is characterized by a large proportion of Ascomycotina members which are among the more diverse groups of fungi and the occurrence of other groups is relatively rare. The total number of fungal species recorded from the agriculture fields was significantly greater than the number of fungal species recorded from the barren lands.

Acknowledgment

The authors are thankful to The University Grants Commission (UGC), New Delhi for providing the financial assistance to carry out the research work under the Major Research Project scheme.

Conflicts of interest

The authors declare that there are no conflicts of interest.

References

Abbott, E.V. 1923. Occurrence and action of fungi in soil. *Soil Sci.*, 16:207-216.

Alexander, M. 1977. *Introduction to Soil Microbiology*, John Wiley & Sons, New York.

Aneja, K.R. 2001. *Biochemical activities of microorganisms, Experiments in Microbiology, Plant Pathology and Biotechnology*, Newage International Publishers, 157-162.

Barnett, H.L. and Hunter, B.B. 1972. *Illustrated genera of Imperfect Fungi*, 2nd edn., Burgess Pub. Company, Minnesota.

Basu, S., Kumar, G., Chhabra, S., Prasad, R. 2021. *New and future Developments in Microbial Biotechnology and Bioengineering; Phytomicrobiome for Sustainable Agriculture*, 149-157.

Burges, A. 1958. *Microorganisms in the soil*. Hutchinson University Library, London.

Chandrashekar, M.A., Pai, S.K. and Raju, N.S. 2014. Fungal diversity of rhizosphere soils in different agriculture fields of Nanjangud taluk of Mysore district, Karnataka, India. *Int. J. Curr. Microbiol. App. Sci.*, 3(5):559-566.

Gilman, J.C. 1956-57. *A Manual of soil fungi*. 1st & 2nd ed. Iowa State University Press, Ame. Iowa.

Hawksworth, D.L. 1997. Orphans in botanical diversity. *Muelleria*. 10:111-123.

Nagamani, A., I. K. Kunwar, C. Manoharachary 2006. *Handbook of Soil Fungi*. I. K. International Pvt. Ltd., New Delhi.

Subba Rao, N.S. 2004. *Soil Microbiology*, Oxford & IBH, Publishing Co. Pvt. Ltd., New Delhi.

Subramanian, C. V. 1952. Fungi isolated and recorded from Indian soils. *Journal Madras Univ.* 22 B:206-212.

Wahegaonkar, N. Salunkhe, S. M., Palsingankar, P.L. and Shinde, S.Y. 2011. Diversity of fungi from soils of Aurangabad, MS, India., *Annals of Biological Research*, 2(2):198-205.

Warcup, J.H. 1950. The soil plate method for isolation of fungi from soil. *Nature*, London, 166:117-166.

Building evidence for conservation globally

Journal of Threatened Taxa



Open Access

10.11609/jott.2022.14.2.20539-20702
www.threatenedtaxa.org

26 February 2022 (Online & Print)
14(2): 20539-20702
ISSN 0974-7907 (Online)
ISSN 0974-7893 (Print)



ISSN 0974-7907 (Online); ISSN 0974-7893 (Print)

Publisher
Wildlife Information Liaison Development Society
www.wild.zooreach.org

Host
Zoo Outreach Organization
www.zooreach.org

No. 12, Thiruvannamalai Nagar, Saravanampatti - Kalapatti Road, Saravanampatti,
Coimbatore, Tamil Nadu 641035, India
Ph: +91 9385339863 | www.threatenedtaxa.org
Email: sanjay@threatenedtaxa.org

EDITORS

Founder & Chief Editor

Dr. Sanjay Molur

Wildlife Information Liaison Development (WILD) Society & Zoo Outreach Organization (ZOO),
12 Thiruvannamalai Nagar, Saravanampatti, Coimbatore, Tamil Nadu 641035, India

Deputy Chief Editor

Dr. Neelesh Dahanukar

Noida, Uttar Pradesh, India

Managing Editor

Mr. B. Ravichandran, WILD/ZOO, Coimbatore, India

Associate Editors

Dr. Mandar Paingankar, Government Science College Gadchiroli, Maharashtra 442605, India

Dr. Ulrike Streicher, Wildlife Veterinarian, Eugene, Oregon, USA

Ms. Priyanka Iyer, ZOO/WILD, Coimbatore, Tamil Nadu 641035, India

Dr. B.A. Daniel, ZOO/WILD, Coimbatore, Tamil Nadu 641035, India

Editorial Board

Dr. Russel Mittermeier

Executive Vice Chair, Conservation International, Arlington, Virginia 22202, USA

Prof. Mewa Singh Ph.D., FASc, FNA, FNAsc, FNAPsy

Ramanna Fellow and Life-Long Distinguished Professor, Psychobiology Laboratory, and
Institute of Excellence, University of Mysore, Mysuru, Karnataka 570006, India; Honorary
Professor, Jawaharlal Nehru Centre for Advanced Scientific Research, Bangalore; and Adjunct
Professor, National Institute of Advanced Studies, Bangalore

Stephen D. Nash

Scientific Illustrator, Conservation International, Dept. of Anatomical Sciences, Health Sciences
Center, T-8, Room 045, Stony Brook University, Stony Brook, NY 11794-8081, USA

Dr. Fred Pluthero

Toronto, Canada

Dr. Priya Davidar

Sigur Nature Trust, Chadapatti, Mavinahalla PO, Nilgiris, Tamil Nadu 643223, India

Dr. Martin Fisher

Senior Associate Professor, Battcock Centre for Experimental Astrophysics, Cavendish
Laboratory, JJ Thomson Avenue, Cambridge CB3 0HE, UK

Dr. John Fellowes

Honorary Assistant Professor, The Kadoorie Institute, 8/F, T.T. Tsui Building, The University of
Hong Kong, Pokfulam Road, Hong Kong

Prof. Dr. Mirco Solé

Universidade Estadual de Santa Cruz, Departamento de Ciências Biológicas, Vice-coordenador
do Programa de Pós-Graduação em Zoologia, Rodovia Ilhéus/Itabuna, Km 16 (45662-000)
Salobrinho, Ilhéus - Bahia - Brasil

Dr. Rajeev Raghavan

Professor of Taxonomy, Kerala University of Fisheries & Ocean Studies, Kochi, Kerala, India

English Editors

Mrs. Mira Bhojwani, Pune, India

Dr. Fred Pluthero, Toronto, Canada

Mr. P. Ilangoan, Chennai, India

Web Development

Mrs. Latha G. Ravikumar, ZOO/WILD, Coimbatore, India

Typesetting

Mr. Arul Jagadish, ZOO, Coimbatore, India

Mrs. Radhika, ZOO, Coimbatore, India

Mrs. Geetha, ZOO, Coimbatore, India

Fundraising/Communications

Mrs. Payal B. Molur, Coimbatore, India

Subject Editors 2019–2021

Fungi

Dr. B. Shivaraju, Bengaluru, Karnataka, India

Dr. R.K. Verma, Tropical Forest Research Institute, Jabalpur, India

Dr. Vatsavaya S. Raju, Kakatiya University, Warangal, Andhra Pradesh, India

Dr. M. Krishnappa, Jnana Sahyadri, Kuvempu University, Shimoga, Karnataka, India

Dr. K.R. Sridhar, Mangalore University, Mangalagangotri, Mangalore, Karnataka, India

Dr. Gunjan Biswas, Vidyasagar University, Midnapore, West Bengal, India

Plants

Dr. G.P. Sinha, Botanical Survey of India, Allahabad, India

Dr. N.P. Balakrishnan, Ret. Joint Director, BSI, Coimbatore, India

Dr. Shonil Bhagwat, Open University and University of Oxford, UK

Prof. D.J. Bhat, Retd. Professor, Goa University, Goa, India

Dr. Ferdinando Boero, Università del Salento, Lecce, Italy

Dr. Dale R. Calder, Royal Ontario Museum, Toronto, Ontario, Canada

Dr. Cleofas Cervancia, Univ. of Philippines Los Baños College Laguna, Philippines

Dr. F.B. Vincent Florens, University of Mauritius, Mauritius

Dr. Merlin Franco, Curtin University, Malaysia

Dr. V. Irudayaraj, St. Xavier's College, Palayamkottai, Tamil Nadu, India

Dr. B.S. Kholia, Botanical Survey of India, Gangtok, Sikkim, India

Dr. Pankaj Kumar, Kadoorie Farm and Botanic Garden Corporation, Hong Kong S.A.R., China

Dr. V. Sampath Kumar, Botanical Survey of India, Howrah, West Bengal, India

Dr. A.J. Solomon Raju, Andhra University, Visakhapatnam, India

Dr. Vijayasankar Raman, University of Mississippi, USA

Dr. B. Ravi Prasad Rao, Sri Krishnadevaraya University, Anantpur, India

Dr. K. Ravikumar, FRLHT, Bengaluru, Karnataka, India

Dr. Aparna Watve, Pune, Maharashtra, India

Dr. Qiang Liu, Xishuangbanna Tropical Botanical Garden, Yunnan, China

Dr. Noor Azhar Mohamed Shazili, Universiti Malaysia Terengganu, Kuala Terengganu, Malaysia

Dr. M.K. Vasudeva Rao, Shiv Ranjani Housing Society, Pune, Maharashtra, India

Prof. A.J. Solomon Raju, Andhra University, Visakhapatnam, India

Dr. Mandar Datar, Agharkar Research Institute, Pune, Maharashtra, India

Dr. M.K. Janarthanam, Goa University, Goa, India

Dr. K. Karthikeyan, Botanical Survey of India, India

Dr. Errol Vela, University of Montpellier, Montpellier, France

Dr. P. Lakshminarasimhan, Botanical Survey of India, Howrah, India

Dr. Larry R. Noblick, Montgomery Botanical Center, Miami, USA

Dr. K. Haridasan, Pallavur, Palakkad District, Kerala, India

Dr. Analinda Manila-Fajard, University of the Philippines Los Baños, Laguna, Philippines

Dr. P.A. Sinu, Central University of Kerala, Kasaragod, Kerala, India

Dr. Afroz Alam, Banasthali Vidyapeeth (accredited A grade by NAAC), Rajasthan, India

Dr. K.P. Rajesh, Zamorin's Guruvayurappan College, GA College PO, Kozhikode, Kerala, India

Dr. David E. Boufford, Harvard University Herbaria, Cambridge, MA 02138-2020, USA

Dr. Ritesh Kumar Choudhary, Agharkar Research Institute, Pune, Maharashtra, India

Dr. Navendu Page, Wildlife Institute of India, Chandrabani, Dehradun, Uttarakhand, India

Invertebrates

Dr. R.K. Avasthi, Rohtak University, Haryana, India

Dr. D.B. Bastawade, Maharashtra, India

Dr. Partha Pratim Bhattacharjee, Tripura University, Suryamaninagar, India

Dr. Kailash Chandra, Zoological Survey of India, Jabalpur, Madhya Pradesh, India

Dr. Ansie Dippenaar-Schoeman, University of Pretoria, Queenswood, South Africa

Dr. Rory Dow, National Museum of Natural History Naturalis, The Netherlands

Dr. Brian Fisher, California Academy of Sciences, USA

Dr. Richard Gallon, Ilandudno, North Wales, LL30 1UP

Dr. Hemant V. Ghate, Modern College, Pune, India

Dr. M. Monwar Hossain, Jahangirnagar University, Dhaka, Bangladesh

Mr. Jatishwor Singh Irungbam, Biology Centre CAS, Branišovská, Czech Republic.

Dr. Ian J. Kitching, Natural History Museum, Cromwell Road, UK

Dr. George Mathew, Kerala Forest Research Institute, Peechi, India

For Focus, Scope, Aims, and Policies, visit https://threatenedtaxa.org/index.php/JoTT/aims_scope

For Article Submission Guidelines, visit <https://threatenedtaxa.org/index.php/JoTT/about/submissions>

For Policies against Scientific Misconduct, visit https://threatenedtaxa.org/index.php/JoTT/policies_various

continued on the back inside cover

Cover: *Geodorum laxiflorum* Griff.—inflorescence (Orchidaceae) © Ashish Ravindra Bhojar.



First record and description of female *Onomarchus leuconotus* (Serville, 1838) (Insect: Orthoptera: Tettigoniidae) from peninsular India

Sunil M. Gaikwad¹ , Yogesh J. Koli²  & Gopal A. Raut³ 

¹Department of Zoology, Shivaji University, Kolhapur, Maharashtra 416004, India.

²Department of Zoology, Sant Rawool Maharaj College, Kudal, Maharashtra 416520, India.

³Department of Zoology, Radhabai Kale Mahila Mahavidyala, Ahmednagar, Maharashtra 414001, India.

¹smg_zoo@unishivaji.ac.in (corresponding author), ²dryjkoli@gmail.com, ³rautgopal189@gmail.com

Abstract: The members of family Tettigoniidae, commonly called katydids, generally exhibit mimicry and camouflage with shapes and colours similar to leaves. The genus *Onomarchus* Stal is mainly distributed in temperate and tropical Asia, and was earlier reported from Assam and West Bengal in India. The species *Onomarchus leuconotus* (Serville, 1838) is reported here for the first time in peninsular India from the Western Ghats (Chandoli National Park, Kolhapur, Maharashtra). This record extends the known geographical range of this species by about 1630 km. As its holotype is not described from India, the female of *O. leuconotus* is described here via detailed diagnostic characters, colour photographs and illustrations.

Keywords: Distribution, female description, katydid, *leuconotus*, Phaneropterinae.

During a survey of Orthoptera from the Western Ghats area, we came across a green Tettigoniid at Chandoli National Park of Kolhapur district, and identified it as *Onomarchus leuconotus*, not previously reported from peninsular India.

The genus *Onomarchus* Stal, 1874 is spread across temperate and tropical Asia, and so far represented by five species (<http://orthoptera.speciesfile.org>, accessed on 7 May 2021). From India, Shishodia et al. (2010) listed *Onomarchus bisulcatus* from Mizoram, and

Onomarchus leuconotus from Assam and West Bengal. Subsequently, Srinivasan and Prabakar (2012) reported *Onomarchus uninotatus* from Arunachal Pradesh. Serville (1838) described the male of *O. leuconotus*, while Barman (1993) provided minimum information about the diagnosis of this species and mentioned its locality as West Bengal (Kolkata) and Assam of India, as did Shishodia et al. (2010) who made a checklist without diagnosis and deposition records. Our report is the first record for the Western Ghats and peninsular India. Here we describe female *O. leuconotus* by giving detailed diagnostic characters, colour photographs and illustrations.

MATERIALS AND METHODS

Material examined: ZSUK.E.TT.07, 1 female, 15.xi.2012, Ukhalu, Chandoli National Park, Kolhapur, Maharashtra, India (Figure 1), 17.126°N and 73.860°E, 844 m, coll. Y.J. Koli, deposited in Department of Zoology, Shivaji University, Kolhapur. The specimen was studied under a Nikon stereozoom (SMZ 800) microscope and photographed using a Canon 550D camera with 100 mm lens. Measurements were done with digital Vernier

Editor: R.M. Sharma, Zoological Survey of India, Pune, India.

Date of publication: 26 February 2022 (online & print)

Citation: Gaikwad, S.M., Y.J. Koli & G.A. Raut (2022). First record and description of female *Onomarchus leuconotus* (Serville, 1838) (Insect: Orthoptera: Tettigoniidae) from peninsular India. *Journal of Threatened Taxa* 14(2): 20643–20647. <https://doi.org/10.11609/jott.7427.14.2.20643-20647>

Copyright: © Gaikwad et al. 2022. Creative Commons Attribution 4.0 International License. JoTT allows unrestricted use, reproduction, and distribution of this article in any medium by providing adequate credit to the author(s) and the source of publication.

Funding: Shivaji University, Kolhapur.

Competing interests: The authors declare no competing interests.

Acknowledgements: Authors are grateful to head, Department of Zoology, Shivaji University Kolhapur for providing necessary facilities; Dr. Sigfrid Ingrisch for the identification.



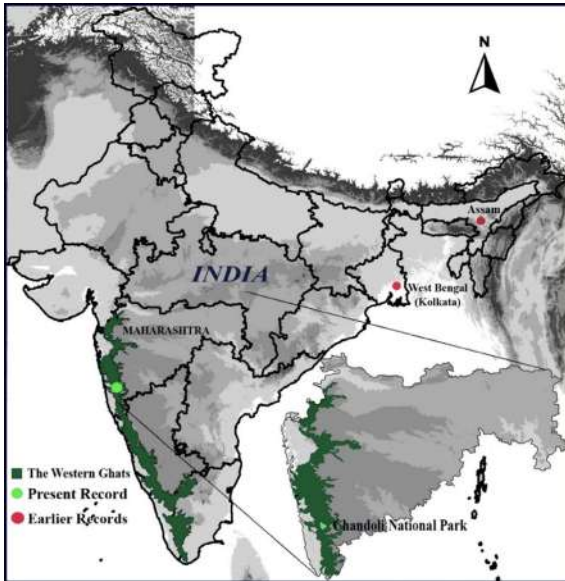


Figure 1. Distribution records of *Onomarchus leuconotus* in India.

calipers. The specimen was identified as *O. leuconotus* by using the original description (translated from French to English) of Serville (1838), De Jong (1939), Barman (1993), and images of the type specimen and keys on the website Orthoptera Species File (<http://orthoptera.speciesfile.org>). Dr. Sigfrid Ingrisch from The Alexander Koenig Zoological Research Museum in Germany confirmed the identification based on images of the specimen.

RESULTS

Description Female (Image 1 & 2):

Measurements (in mm): body length 82; pronotum 11; tegmen 75 & width 26; fore femur length 10, mid femur 12, hind femur 25, hind tibia 24; ovipositor length 30 & width 7 mm.

Diagnostics

Head: Lateral margins, starting from the lower margin of the eyes and antennal socket downwards along the genae, broadly yellowish-white; labrum and mandibular base whitish (Image 1A, E).

Pronotum: short, disc white, hind margin acutely angular, centrally one long and one slightly short transverse groove running downwards and short vertical groove intersect posterior transverse suture vertically (Image 2A).

Meso and Metasternum: mesosternum somewhat quadrate, metasternum subquadrate narrows posteriorly; two large pits are situated nearly in the

central area in both meso and metasterna and one very fine additional pit found near mesosternal caudal margin medially; pits in the metasternum joined by nearly straight grooves, mesosternal lateral pits joined to the medial pit by oblique grooves (Image 2B).

Legs: yellowish, fairly short; fore and mid femur barely dented below; fore femur bearing three spines on internal carina and 6 spines on external carina; mid femur bearing five spines on external carina and seven spines on internal carina; hind femur bearing five strong spines, broad at the base and hooked at tip and four small spines on external carina and 10 small spines on internal carina; hind tibia armed with five spines on the upper side and ventrally seven pairs of moderate spines, 4th pair separated.

Forewing: slightly leathery, undulating anteriorly, large, more than twice the length of the body (Image 1A). Venation (Image 2C): The costa (C) fine, unbranched, long, runs along the anterior margin; subcosta (Sc), branched into anterior short subcostal (Sc1) and long posterior subcostal (Sc2); the radius (R), most prominent, runs 2/3 distance and branched into anterior radius (R1) and posterior radius (R2); median (M) long runs parallel to radius for a short distance and then separates, reaching to the apical region; cubitus (Cu) forks at the base into long cubitus 1 (Cu1) and short cubitus 2 (Cu2), continues with a hind margin of tegmen; anals short, unbranched, 4 in number (A1, A2, A3, and A4).

Hindwing: large, hyaline, protruding beyond the tegmina at rest (Image 1A).

Abdomen: Last abdominal tergite short, transverse, subfused with epiproct; epiproct semicircular with shallow Y shaped furrow; cerci cylindrical, narrower towards the apex, sinuately curved outside before apex, apex obtuse dark coloured with a minute spinule; subgenital plate roughly triangular with basal angles rounded, basal half portion strongly raised in the midline, apical half portion with fine medial furrow, apex subtruncate, crenulated and obtusely projecting short lateral lobes (Image 1C,D); ovipositor large about four times longer than broad, sabre like, dorsal valves with seven oblique furrows at apex, 2/3 ventral valve and 1/3 dorsal valve dark black (Image 1B).

DISCUSSION

This species is distributed in India, Malaysia, Sumatra, Papua New Guinea, Java, China, Maluku, Indo-China, and Vietnam (<http://orthoptera.speciesfile.org>, accessed on 30 April 2021). This is the first illustrated report of this species from Western India, and the present record extends its known geographical range from Kolkata

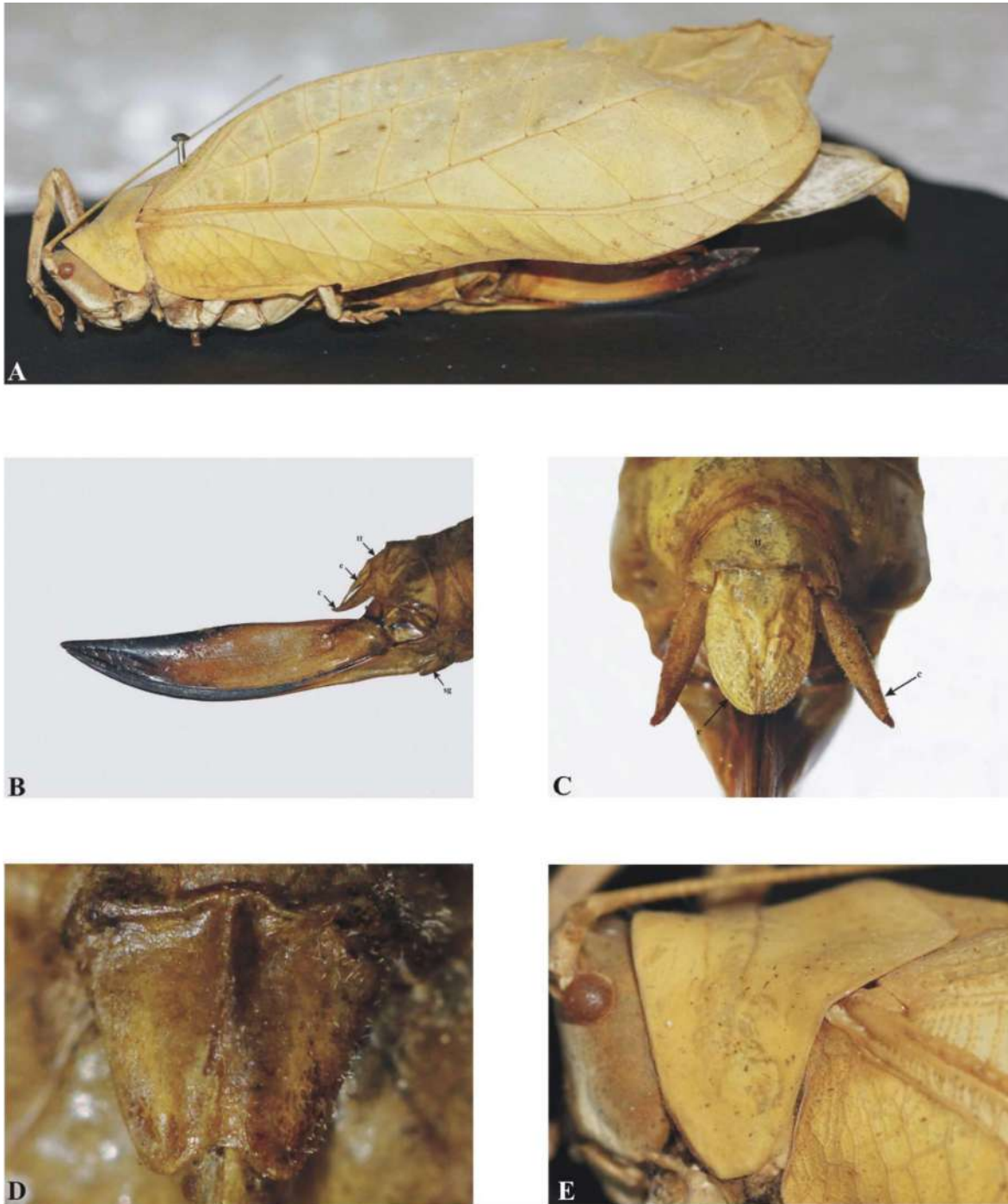


Image 1. A—*Onomarchus leuconotus* (lateral habitus of female) | B—Ovipositor | C—epiproct & abdominal apex with cerci (dorsal view) | D—subgenital plate (ventral view) | E—head- whitish gena & pronotum (lateral view). Abbreviation: tt—tenth abdominal tergite | e—epiproct | c—cercus | sg—subgenital plate. © Sunil Gaikwad.

to western India, a distance of about 1,630 km by air (Figure 1).

The holotype of *Onomarchus leuconotus* is from Java,

and the type specimen of this species is in the Natural History Museum, London. Serville originally described the *O. leuconotus* (male) in 1838 as *Pseudophyllus*

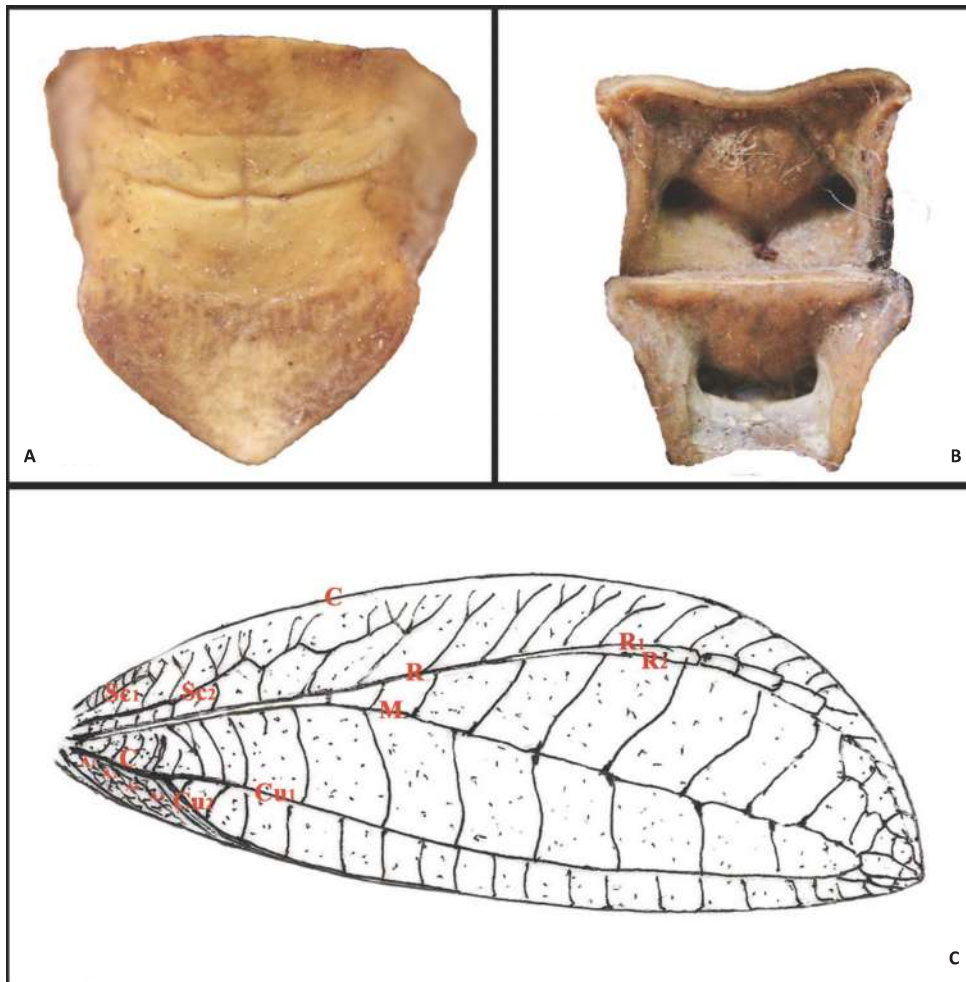


Image 2. *Onomarchus leuconotus*: A—pronotum with two horizontal & one vertical groove and acute angular hind margin (dorsal view) | B—meso and metasternum with deep pits | C—line drawing depicts right forewing venation- Costa (C); Subcosta 1 (Sc_1), Subcosta 2 (Sc_2); Radius (R), Radius 1 (R_1), Radius 2 (R_2); Median (M); Cubitus (C), Cubitus 1 (Cu_1), Cubitus 2 (Cu_2); Anals (A_1, A_2, A_3, A_4). © Sunil Gaikwad.

leuconotus in French. The same species was later described with three synonyms: *O. albisellatus* (Walker 1870), *O. latipennis* (Pictet & Saussure 1892) and *O. nobilis* (Brunner 1895), none described from India. However, Barman (1993) recorded *O. leuconotus* from India with scant diagnostics.

According to the original description by Serville (1838), elaborative diagnostics of de Jong (1939), images and keys on <http://orthoptera.speciesfile.org>, the specimen recorded from Chandoli National Park is treated here as *O. leuconotus*. The whitish genae, part of mouth and labrum; pronotal colour and shape; structure of meso- and metasternum; hind tibiae with strong 5 spines dorsally; broad tegmina and ovipositor in the present specimen are identical with *O. leuconotus*.

de Jong (1939) mentioned important characters for

identifying the three species of Serville. If hind tibia has five strong thorns on the dorso-internal margin, pronotum dorsally white, broad tegmen and ovipositor: *O. leuconotus*; if seven strong thorns on the dorso-internal margin of hind tibia, a white spot near the base of the tegmen and ovipositor five times as long as broad: *O. uninotus* and if six small thorns on hind and lot of white spots on tegmen and ovipositor is about six times longer than its thickness: *O. cretaceus*. Since the characters suggested for *O. uninotus* and *O. cretaceus*, are not found in our specimen and since our specimen contained the characters mentioned for *O. leuconotus* by de Jong (1939), our specimen proves to be *O. leuconotus*. Considering the thorns on the feet, it appears that only the large spines on the hind tibia are counted, mainly for *O. leuconotus*. However, while describing our specimen,

it has been found that in addition to large thorns, many small and blunt thorns are also found on femur and tibiae. It seems that the counting of the small spines has not been given importance thus information on this count is given here. Moreover, he mentioned additional character for *O. leuconotus* that narrow strip of little pits running from the lower margin of the eyes downwards along the genae, which is not found in the other species and the shape of the meso- and metasternum by line drawings. The characters and line drawings of meso- and meta-sternum given by de Jong (1939) are clear in our specimen. In addition, as per the revision of the Pseudophyllinae by Beier (1954), our specimen agrees best with *O. leuconotus* (Serville 1838). The smooth pronotum, the sinuate shape of the dorsal margin of the tegmen and its venation, and the white band at the genae agree with that species.

The pronotum has only one transverse groove in the anterior half of the disc, and the hind margin is acutely angular (de Jong 1939). The line drawing of pronotum on the website of Orthoptera species File (<http://orthoptera.speciesfile.org>) shows one transverse and one vertical groove, which intersect horizontal one. However, the pronotum of the specimen under study is having an additional short transverse groove. This is

probably because our specimen is female, it may have another groove in it, or it may not have been noticed, as the anterior transverse groove is indistinguishable.

REFERENCES

- Barman, R.S. (1993).** Insecta: Orthoptera: Tettigoniidae. Zoological Survey of India, Fauna of West Bengal, State Fauna Series 3(4): 355–367.
- Beier, M. (1954).** *Revision der Pseudophyllinen*. Instituto Español de Entomología, Madrid, 479 pp.
- Brunner, V.W. (1895).** *Monographie der Pseudophylliden*. Herausgegeben von der K.K. Zoologisch-Botanischen Gesellschaft in Wien, 282 pp.
- de Jong, C. (1939).** On Indo-Malayan Pterophyllinae (Orthoptera, Family Tettigoniidae). *Zoologische Mededelingen* 21(1): 1–109.
- Pictet, A. & H. de Saussure (1892).** *Iconographie des quelques sauterelles vertes*. Imprimerie Aubert-Schuchardt, Geneve, 28 pp, 1–3 plates.
- Serville, J.G.A. (1838 [1839]).** *Histoire naturelle des insectes. Orthoptères*. Librairie Encyclopédique de Roret, Paris, i-xviii (index), 776 pp, 1–14 plates.
- Shishodia, M.S., K. Chandra & S.K. Gupta (2010).** An annotated checklist of Orthoptera (Insecta) from India. *Records of Zoological Survey of India*. Occasional paper No. 314: 1–366.
- Srinivasan, G. & D. Prabakar (2012).** Additional records of Tettigoniidae from Arunachal Pradesh, India. *Journal of Threatened Taxa* 4(14): 3255–3268. <https://doi.org/10.11609/JoTT.o3065.3255-68>
- Walker, F. (1870).** *Catalogue of the specimens of Dermaptera Saltatoria in the collections of British Museum. Part III*. Printed for the Trustees of the British Museum, London, 604 pp.



JANABAI: AN IGNORED FEMINIST WRITER

Dr. Satish Govind Saykar Associate Professor Department of English Radhabai Kale Mahila Mahavidyalaya, Ahmednagar :: satishgsaykar@gmail.com

Abstract:

Up to the present time, we have read and discussed a lot on the Western feminism in the light of the texts such as *A Vindication of the Rights of Woman* (1792) by Mary Wollstonecraft, Virginia Woolf's *A Room of One's Own* (1929) or Simone de Beauvoir's *The Second Sex* (1949); but consciously the feminist critics have ignored the contribution of Indian feminist writers and critics. With the publication of Edward Said's *Orientalism* (1978) and *Culture and Imperialism* (1993) or Gayatri Chakravorty Spivak's 'Can the Subaltern Speak?' (1985), many feminists started rereading of literature from the feminist perspective. The present paper attempts to focus on Janabai's feminism through her revolt against the tradition, society and culture which is present in her works. Janabai makes the God to become woman and thereby asserting her superiority over the men and when she considers Him as her friend and supporter or she abuses Him, she talks of equality of both the sexes.

Keywords: *Varkari*, equality, feminism, marginalization

Saint Janabai belongs to the tradition of *Varkari* saint poets, the most influential bhakti sect among the Marathi-speaking people, in the way that T. S. Eliot expects in his essay 'Tradition and Individual Talent' (1919) that the writer to adhere to the tradition and contribute to the tradition with the help of one's talent. Being born in a poor family, she was handed over to Dama Shetty, the father of Saint Namdev, in whose house she was supposed to work as domestic servant. The *Varkari* sect believes in equality of all religions, castes, sects and sexes; but being a servant or *dasi*, she had to do never ending household work at home and she had to undergo the hard experiences of being a woman in the sense Gilles Deleuze and Felix Guattari defined in *A Thousand Plateaus: Capitalism and Schizophrenia* the term 'becoming woman' as 'becoming minor.' According to them, in the patriarchal society, man gets all the rights and the woman continuously undergoes the torture, exploitation and marginalization. The hardships of being a woman and the work burden at home finds fine expression in Janabai's writing whereby she rises as one of the leading Indian feminist writer who revolt the traditional views and assert the plight of women.

Like Saint Meera, Saint Janabai considers the God Vithoba as her friend, lover, supporter and a constant helpmate in her regular domestic work. She is very naïve that she considers that it is God Vithhal who helps her in carrying and heating the bath water, sweeping the courtyard and scratching her head when the lice bite her. Her belief was in work like Saint Savata Mali who used to find the God in all the living and non-living objects around him. Her poetry is sensitive which describes the everyday life of ordinary women consisting of both the joys and strains at the same time. She loves the God by heart and wants to be one with Him. She tries to be a free bird by becoming one with the God. It means that she rejects her identity as a common woman or *dasi* by becoming one with the God. Once she becomes one with God, she becomes powerful in all ways and has no any restrictions of the family, society or religion. Her poetry depicts her journey from the slavery to freedom and margin to the centre. Vidyut Bhagwat wisely points out in her article 'Marathi Literature as a Source for Contemporary Feminism' that her poetry is "full of references to the hard chores which she had to perform, which deprived her of the space necessary for a dialogue with her own emancipatory God." (Bhagwat, 1995:26)

The women were considered secondary to men due to the patriarchal family system as a result of which the women were marginalized in family, society and religion. No doubt, the marginalization was

not based on merit; but on the sex which reminds us of Simone de Beauvoir's famous sentence that says 'One is not born, but rather becomes, a woman' which means a woman's attitude towards her body and bodily functions changes over the years due to the influence of family, society and religion. Even the *Varkari* sect was not an exception to it. She had some limitations in her worship to God; but her belief in God was not flexible. She loved the God by heart. Whenever she was in work, she used to utter the name of God. She writes about herself:

Whether grain grinding or pounding; Your name, Oh Infinite, I am chanting.
Your name is with me constantly; Not forgetting it even momentarily.
My only perennial occupation; Is Almighty's name recitation.
My mother, father, brother, sister; You are, O Sudarshan Chakra holder.
On your feet is focused my attention; So says Sant Namdeo's handmaden.
(m.facebook.com)

As a woman, she was not supposed to use Veena. Even, she was not free from the restrictions of the society specially designed for women. But, she revolts against the traditions where she threatens the God by saying that she, having her pallav down to her shoulder, will enter the crowded marketplace.

I will let my saree slip
from my head to the shoulders
Hold my head high and walk
into the market-place
Taking cymbals in hand and veena on
shoulder I will go
Let me see who forbids me
I have opened a shop in Pandharpur
put oil on my wrist now
Jam declares herself a prostitute
Leaving you O God, this 'home' (Bhagwat, 1995:26)

Her worship of God Vithoba and the poetry she sang in praise of Him became the cause for jealousy against her. She was triple marginalized in the Spivak sense in 'Can the Subaltern Speak?'. First, she was born in a low caste family. Secondly, she was an orphan and finally she was a woman. One can imagine about the status of a low caste woman working as *dasi*. She was not allowed to worship the God because she was *dasi* and had never-ending work to do. She was victimized at two levels. First, the patriarchal system had restricted her life for she was born a woman; even, the *Varkari* sect did not allow her to shoulder Veena. She was revolutionary by nature. She decided to fight against the customs and traditions as a result of which she let her *pallav* fall on the shoulder when every woman was forced to hide their heads under their pallavas. The falling of pallav on the shoulder was not at home; but in the marketplace which shows how determined she was to fight against the traditions. Secondly, Veena was not allowed to women; but she took it upon her shoulder and wandered in the main peth in Pandharpur. She considers the God Vithoba as her soulmate or her life partner like Saint Meera who thought of God Krishn as her husband.

It is uncommon that we find here in Janabai's *Abhanga* that she expresses what is inexpressible. It was a time when (and now also) woman could assert of becoming a slut by wandering in the marketplace having Cymbals in hand and veena upon her shoulder for the sake of even God. She does not fear of what the people will say about her which shows her love for God. She is so involved in God Vithoba that she felt His presence around her like Savata Mali who considered his well, bullocks, string, vegetables and everything, living and nonliving, as the various forms of God. She thinks that the

God helps her in performing her duties such as sweeping the floor, collecting the dirt, casting it away. She is indebted to Him for the favour He had done to her. She writes:

Jani sweeps the floor, The Lord collects the dirt,
Carries it upon His head, And casts it away.
Won over by devotion, The Lord does lowly chores!
Says Jani to Vithoba, How shall I pay your debt? (Tr.Vilas Sarang)

As she looks at the God Vithoba in a way which shows her feminine sensibility. Feminization of male is also a way of the feminists. In the process of feminization she considers the God as mother of all the saints. Like a loving mother, the God accompanies his children. In this regard, Saint Janabai writes:

My Vitthal has many children
with him is a merry crowd.
Nivriddhi rides on his shoulder
he holds Sopan by the hand.
Dnyaneshwar walks in front
beautiful Mukta close behind
Gora the potter rides his hip
Cokha is in his very heart
Vunka [Banka?] clings to his waist
Nama holds his smallest finger
Jani says, Oh Gopala,
it is a festival of your dear ones. (Zelliot 80)

If we look at the description of God having one on the shoulder, one aside, the other walking in front, one behind, the next on the hip, the other clinging to his waist and so on shows Him in the feminine form. By showing the God in feminine form, she revolts against the patriarchy. It can be considered as her wish to womanize the world or the quest for the matriarchal system where woman is at the centre and others are at margin. With the rise of patriarchal system, the woman lost her importance at home and society and she was marginalized. The process of marginalization of women was the result of *Manusmriti* that formed the laws for the behavior of women. The right of woman over her own body was taken away and it was told her that her body belongs to her would be husband and it is her duty to keep the purity of her body to be seduced by her husband after marriage. Due to the patriarchal system, she had no right of inheritance in her father's property and her body was the sole property of her husband. It means that she belonged to nowhere and she had no rights at all. By womanizing the God, she had tried to increase the importance of women.

On the other level, she might have thought that if she considers the God as a mother, He will be caring and loving her continuously because mother stands for the Creator, nurturer or goddess. She writes:

As a kite roams in the sky
And still thinks of its young ones
Or as a mother is trapped in the household work
And yet longs for a child
Or as a female monkey climbs from tree to tree
And yet clasps its young ones
So is mother Vithoba to us. Says a Jani. (Bhagwat 26)

By making the mother-daughter relationship between her and the God, she tries to be one with God. All her actions result due to the influence of God upon her. She writes:

Of God my meat and drink I make,
God is the bed on which I lie.
God is whate'er I give or take;
God's constant fellowship have I
For God is here and God is there,-
No place that empty is of him.
Yea, lady Vitha, I declare,
I fill the world up to the brim.

(www.southasiaarchive.com)

Saint Janabai becomes free to abuse the God by making Him her supporter, companion, mother or lover. By womanizing the God, she enjoys the status of equality. When she attains equality with God, she becomes superior to all men because they are inferior to God. She gets this superiority status not to overpower others but to enjoy her own rights. Though she rebelled against the tradition and asserted her identity, she is not recognized for her contribution to feminism, neither Eastern nor the Western. Though her *Abhangas* have the power to transform the society and make it ready to revolt against the ill traditions which had marginalized the women for ages. Her *Abhangas* are not even taken for explanations in *Kirtanas* by various groups of *Varkaris*. Even the translators have closed their eyes and not taken her *Abhangas* for translation as a result of which she remains an ignored feminist.

Bibliography

- Bhagwat, Vidyut. 'Marathi Literature as a Source for Contemporary Feminism.' *Economic and Political Weekly*, Volume 30:17, April 1995, pp. 24-29. Web. 15 Feb. 2020.
- Deleuze, Gilles and Felix Guattari. *A Thousand Plateaus Capitalism and Schizophrenia*. Tr. Brian Massumi. University of Minnesota Press Minneapolis: London. Web. 28 August 2015.
- Eliot, T. S. 'Tradition and the Individual Talent.' 1919. Web. 15 Feb. 2020.
- Of God my meat and drink I make. n.d. Web. 15 Feb. 2020.
- Tharu, Susie and K. Lalita, eds., *Women Writing in India: 600 B.C to the Present. Volume 1: 600 B.C to the Early Twentieth Century*. New York: Feminist Press, 1991. Print.
- Whether Grain Grinding or Pounding. m.facebook.com. n.d. Web. 15 Feb. 2020.
- Zelliot, Eleanor. 'The Early Voices of Untouchables: The Bhakti Saints.' *Stigma to Assertion : Untouchability, Identity and Politics in Early and Modern India*. ed. by Mikael Aktor and Robert Deliège. Museum Tusulanum Press: 2008. Web. 15 Feb. 2020.

RNI MAHAR

36829-2010



ISSN- 2229-4929

Peer Reviewed

Akshar Wangmay

International Research Journal

UGC-CARE LISTED

Issue – IV, Volume-III

October 2021

Chief Editor

Dr. Nanasaheb Suryawanshi

AKSHAR WANGMAY

International Peer Reviewed Journal

UGC CARE LISTED JOURNAL

October – 2021

Issue-IV, Volume-III

Chief Editor

Dr. Nanasaheb Suryawanshi

PRATIK PRAKASHAN, PRANAV, RUKMENAGAR, THODGA ROAD AHMEDPUR,
DIST. LATUR, -433515, MAHARASHTRA

Editorial Board

Dr. Mahendra S. Kadam

Dr. Netaji B. Kokate

Dr. Balasaheb V. Das

Mr. Zakirhusen B. Mulani

The Editors shall not be responsible for originality and thought expressed in the papers. The author shall be solely held responsible for the originality and thoughts expressed in their papers.

© All rights reserved with the Editors

Price: Rs.1000

CONTENTS

Sr. No.	Paper Title	Page No.
1	Articulation of Feminism in Marathi Literature Dr. Saykar Satish Govind	1-3
2	The Phenomenon Of Code-mixing in Sami Ahmad Khan's Novel Aliens in Delhi Mr. Bapuso. S. Savase , Dr. I. M. Khairdi	4-6
3	Cultural Loss and Exodus of Kashmiri Pandits in the Poetry of Aga Shahid Ali Waseem Majid , Dr.Suresh Kumar	7-9
4	Portrayal of Brahmin Women- A critical study of Abburi Chaya Devi's select short stories Chaitra N S Murthy , Nivedita , Prof. Rachel Bari	10-12
5	Amalgamation of Myth and Indian Culture in Karnad's play Nagamandala: In special reference to man woman relationship Mr. Pradip Gunderao Kolhe	13-15
6	Conceptualizing Ambedkar's Thoughts on Thinking beyond Gender in Kavita Kane's Karna's Wife: The Outcaste Queen Chaithra T, Dr. Veena M. K	16-18
7	Indian Culture and Psyche: A Study of Sudhir Kakar's The Ascetic of Desire Amit Maruti Bamane, Dr. Ashok Babar	19-22
8	A Study of Contemporary Women in Shobha De's Sultry Days V. Hamsaveni , Dr. M. Maheswari	23-24
9	Meticulous Presentation of Embracing Womanism as the Redemptive Power of Culture, Love and Healing in Alice Walker's Novels. Veena J	25-27
10	Public Sculpture in the Cultural Ambit: An Assessment Dr. Binoy Paul	28-30
11	The Concept of Love and Forgiveness in Judith Mcnaught's Historical Romance Fiction Whitney, My Love Mrs. S. Shalini	31-32
12	Exploring Cultural Aspects in Amitav Ghosh's Sea of Poppies Mr.R.B.Palke, Dr.H.K.Awtade	33-34
13	Translation: Types, Methods and Approaches Mr. More S.S.	35-37
14	Conflicts in Ngugi Wa Thiong'O's "The River Between." Miss. Rangrez S. B.	38-40
15	The Theme of Family Disintegration in Shanta Gokhale's Avinash Todkar Shrishailya T	41-43
16	Culture, Poetics, and Politics of Food in the Select Short Stories of C.S. Lakshmi Priyanka Sharma, Dr. Rani Rathore	44-45
17	The Old Man in the Piazza: As the Silenced Voice of the Immigrants Aliya Parveen a Mulla	46-47
18	Getting Close To the Text in the Cinematic Adaptation of 'The White Tiger' Imteyaz Ahmad Khan	48-50
19	Use of ICT in English Language, Literature and Translation Dr. Vaibhav Harishchandra Waghmare	51-56
20	Momentousness of Minor Characters in the Plays of Kalidasa and Shakespeare: A Selective Study Dr. Sumita Mandal	57-60
21	Significance of Literature as a Tool to Appreciate Legal Studies Akil ali Saiyed, Jimmy Jose	61-63
22	Living Life to the Fullest: Towards an Understanding of Disabled Children's Childhood Studies Ms. Noble A. Paliath	64-66
23	Multiculturalism as a Religious Diversity Shashikala G.T	67-69

Articulation of Feminism in Marathi Literature

Dr. Saykar Satish Govind

Associate Professor, Department of English, Radhabai Kale Mahila Mahavidyalaya, Ahmednagar
satishgsaykar@gmail.com

Abstract

Feminism has a long tradition in India in general and Maharashtra in particular. The work done by *Mahatma* Jotiba Phule and Savitribai Phule by following the ideals of *Chhatrapati* Shivaji Maharaj and *Rajmata* Jijau to educate the women to reform the society initiated feminism in literature and Tarabai Shinde, Mukta Salve, Bahinabai Chaudhari and other anonymous women writers have tried their level best to state the suppression, oppression, marginalization that women have to undergo. The present paper depicts the life and sufferings of widows with the help of the women's narratives. The selected two essays are reprinted by Baba Padmanji as an appendices to his Novel *Yamuna Paryatan* (*Yamuna Journey*). The novel is sub titled as "An Elucidation of the Condition of Widows in India." He asserts that 'there can be no substitute for a description of women's woes and anxieties made by women themselves.' The true value of his Novel, Baba Padmanji thinks, would have been heightened a hundred times if it had been written by an educated Yamuna on her own. The present essay deals with the merciless treatment of widows and the movement for widow remarriage. Women's narratives often depict her life as a problem and advocate the need for her independence and the women's education like Savitribai Phule who was of the opinion that education transforms a person into a human being. The selected essays provide a vibrant sense of what women went through and how the horrors were caused on widows.

In the patriarchal society, a woman has to sacrifice her life for the family, culture and Society; but she is not treated as a human being. She always remains an obedient daughter, a devoted wife and a caring mother. The condition of women is depicted in her poem by Sughra Humayun Mirza, an Urdu poetess. She highlights that nobody cares for her. Her life is so trivial that nobody sheds tears even after her death. Throughout her life she is ignored. Nobody takes notice of her work, devotion and sacrifice. It is always a woman's unfulfilled desire that her work should be recognised. She writes: My last wish is this, that those who care for me, May strew a few flowers on my grave when I am gone. (Sughra, 380)

The first essay entitled 'A speech made by a woman at a women's meeting organised by the Prarthana Samaj, Bombay' is a speech read by a woman at the meeting of women organised by the Prarthana Samaj, and was published in the *Subodh Patrika* of 7th August 1881. The speech begins: See how terrible is this custom of not allowing widows to remarry. Women have to suffer great misery because of this. Besides, incidents like infanticide are extremely common, for widows are tremendously scared of the social stigma. (1881:357) The woman speaks so efficiently and still feels that she is not experienced enough to talk on all the miseries of the Hindu women. It means she thinks that what she had seen or experienced about the miseries of the Hindu women is all about a drop in the sea. First, she talks about the widow who is considered to be an inauspicious and polluting. To see the face of a widow in the morning is considered as an ill omen. She is not allowed to walk around in the house and is considered a thing and not a human being: "So the poor thing is forbidden walk around in the house." (1881:357) When any woman loses her husband, her hairs are shaved off and widowhood becomes her only identity forever though she is fifteen years old. She has to live all her life in despair due to many limitations and restrictions. She cannot wear pretty saris or ornaments. Neither she can mix with other people nor can she attend the religious ceremonies. And she has to leave all her life sitting in a corner. Even her parents consider her like a grit in the eye. They say: "Why was this wicked girl born in the first place? And if she was born, why didn't she die after birth? If our son-in-law had been alive, we would have given him our second daughter." (1881:357)

What a woman can do when her own parents wish her to die and their son in law to be alive. "Why was I ever born? What's the point of being alive? I'm not yet fifteen- and look at what a terrible condition I am in! No good clothes to wear, no mixing with people, no permission even to talk with anyone! Even my parents hate. People frown when they see me. What's the point of having been born?" (1881:357) This is not enough but she has to endure many more hardships. No one can cover all those hardships in a single piece of writing. The speaker throws light on the difference between male and female. If the man's first wife dies, he can marry the second and if she also dies, he can marry the third one. He is free to eat, drink, laugh and enjoy every pleasure; but the unfortunate widow is not allowed even one of them. The woman speaker questions:

"When God created them, he created them as equals. Can it be called God's justice that one is allowed every freedom while the other is forbidden to have any? This great injustice is really a result of the ignorance of our people." (1881:358) Like a great reformist, she advises the women to help the women as

much as one can. She assures that if widow remarriage takes place, there will be a positive change for women. She asks to encourage the widows for remarriage. She points out that the young girls are married to old men which results in the increasing number of young widows. If we have the custom of widow remarriage, the number of young widows will go down and there will be several other advantages. And most important is not to create any problem for widows. 'The plight of Hindu widows as described by a widow herself' is an essay that was published in *The Gospel in All Lands* in April 1889. The anonymous essayist begins her essay: "And since ours is a well-to-do, why, even wealthy caste, our regulations in this regard are extremely strict." (359) She refers to four major castes among the Hindus out of which she was born in *Kayastha* family which is the third in the hierarchy and more infamous for its ill-treatment of widows. She accepts the fact that widows are suffered anywhere; but states that the customs of *Kayastha* are very terrible if compared with other castes. When her husband dies, the wife is tortured severely. She tells an experience that she had before she became a widow. She participated in funeral procession. It was 3 o'clock in the summer afternoon when the people reached after completing all the funeral rites. People who were on the way used to take regular intervals for water and rest. But the poor widow could not ask for water fearing to lose her honour. The women surrounded her did not feel pity for her. At the end she became unconscious but still the torch event on. They dragged her throughout the road and kept nagging at her by saying: "Are you only widow in the world? What's the point of weeping now! Your husband is gone forever!" (360) When the woman did not have the strength to crawl, they tied her up into a bundle as if of rags and then dragged her off. She was one of the close relatives of the writer but no one dare to help her. One woman somehow manages to bring 1 glass of water for her. When the widow saw her, she ran to her like a beast and drinks the water. Then she fell at the feet of the woman who had given her the water and said: "Sister, I'll never forget what you have done for me. You are like a god to me. You have given my life back to me. But please go away quickly. If anybody comes to know of what you have done, both of us will have to pay for it. I, at least, will not let this out." (360) The Torture of a widow continues in many ways. She has to only once a day for a year after her husband's death. Many a times she has to keep fast completely on several days. Once she is back from the funeral of her husband, nobody visits her apart from the barber women. She has to stick her up in the corner. On writing of the condition of widows in general, she writes: "Oh, cruel corner, all of us widows know you so thoroughly well. And we never remember you unless we are grieved." (361)

A widow is like a living corpse. She has no rights in the home. All her relatives torture her. Even her mother says her as 'a mean creature'. (361) Her mother-in-law opines that the widow is a horrible snake who bit to her son and killed him. Her sister in law says: "I will not cast even a glance at this luckless, ill-fated creature! I will not even speak a word to her." (361) The widow is taken as responsible for the death of her husband. Her relatives say: "What a shameless woman! How callous! She cries because she wants a husband." (361) The writer considers it as an unendurable situation that no one can understand how painful it is unless she experiences it. On the eleventh and thirteenth day, the Brahmin comes to demand money, oil or many other things. If the widow is unable she has to promise that she will pay immediately. Sometimes the widow has to work as servant doing the household jobs to earn money to pay the Brahmins their dues. Even the barber women also demand money from the widow. The writer clearly the condition of women in general. She writes: "Thus, there is nothing in our fate but suffering from birth to death. When our husbands are alive, we are there slaves; when they die, our fate is even worse." (361) After six weeks she is given the same clothes that she wore when she became widow. She frightens to see those clothes again as if she had been widowed again. The widowed life of a woman consists of beating, torture and harassment and she needs to depend on others. In *kayastha*, a woman has neither a right to inherit her father's property nor does she get her husband's property. The marginalization is extreme in case of widows though it is a matter of her death. The writer observes: If a woman dies when her husband is still alive, her body is decorated with ornaments and new clothes, and then cremated. But when a widow dies, her body is just wrapped up in plain white cloth and cremated. It is reasoned that if a widow goes to the other world in ornaments and new clothes, her husband will not accept her there. (362-363)

Many women prefer to die before the death of their husbands. Some women commit suicide after the death of husband to avoid the dishonor and torture of widowhood. The writer comment on the ban on the custom of sati and asserts that many women who could have died a cruel but quick death when their husbands died now have to face an agonizingly slow death. To conclude it can be said that the women are marginalized because of their sex and have to live a life of slavery when their husbands are alive. The death of the husband brings torture, marginalization, suffering, sorrow and unhappiness in the life of a widow. Both the life and death of husband decorate their life with torture, harassment, agony and the

women have to bear the pangs of death throughout their death. The social customs of child marriage and ban on widow remarriage are responsible for the worsening condition of women. Widows should be supported by the family members and society and their exploitation in the name of religion and customs be stopped. Then and then only in the words of Bahinabai Chaudhari "but the wrists can still/ wrestle with fate." (Bahinabai Chaudhri, 355)

Works Cited

1. Anonymous (1881). 'A Speech Made by a Woman at a Women's Meeting Organized by the Prarthana Samaj, Bombay.' Tr. Maya Pandit. *Women Writing in India: 600 BC to the Early Twentieth Century*. (Ed.) Susie Tharu and K. Lalita. Volume I. Second Edition. OUP: New Delhi, 1993. P-357-358. Print.
2. Anonymous (1889). 'The plight of Hindu Widows as Described by a Widow Herself.' Tr. Maya Pandit. *Women Writing in India: 600 BC to the Early Twentieth Century*. (Ed.) Susie Tharu and K. Lalita. Volume I. Second Edition. OUP: New Delhi, 1993. P-358-363. Print.
3. Mirza, Sughra Humayaun. 'Who will care to visit my grave when I am gone.' Tr. Syed Sirajuddin. *Women Writing in India: 600 BC to the Early Twentieth Century*. (Ed.) Susie Tharu and K. Lalita. Volume I. Second Edition. OUP: New Delhi, 1993. P-379-380. Print.
4. Chaudhari, Bahinabai. Now I Remain for Myself. Tr. Shanta Gokhale. *Women Writing in India: 600 BC to the Early Twentieth Century*. (Ed.) Susie Tharu and K. Lalita. Volume I. Second Edition. OUP: New Delhi, 1993. Print.

Education and Society

Special Issue

UGC CARE LISTED PERIODICAL
ISSN 2278-6864

शिक्षण आणि समाज
Education and Society
Since 1977

The Quarterly dedicated to the policy of “Education for Social
Development and Social Development through Education”



Indian Institute of Education

J. P. Naik Path, Kothrud, Pune-38

Indian Institute of Education

Founders

Prof. J. P Naik and Dr. Chitra Naik

Shri. S. D. Gokhale, Administrator

Editorial Board

Dr. Jayasing Kalake, Editor

Dr. P. N. Gaikwad, Executive Editor

Dr. Prakash Salavi, Assistant Executive Editor

Dr. S. M. (Raja) Dixit

Prof. V. N. Bhandare

Dr. Sharmishtha Matkar

Shailja Sawant, Secretary



Publisher

Indian Institute of Education

J.P. Naik Path, 128/2, Kothrud, Pune 411038.

Contact No. 8805159904

Web-site: www.iiepune.org

E-Mail: shikshananisamaj1977@gmail.com

E-Mail: iiepune1948@gmail.com

Distributor

Writers Community (WC Publishers)

Website: www.writerscommunity.in

E-Mail: info@writerscommunity.in

‘Shikshan ani Samaj’ (Education & Society), the educational Quarterly is owned, printed and published by the Indian Institute of Education, Pune. It is printed at Pratima Offset, 1B, Devgiri Estate, S.No. 17/1B, Plot No. 14, Kothrud Industrial Area, Kothrud, Pune 411038 and Published at Indian Institute of Education, J.P. Naik Path, 128/2, Kothrud, Pune 411038. Editor: Dr. Jayasing N. Kalake

Opinions or views or statements and conclusions expressed in the articles which are published in this issue are personal of respective authors. The Editor, Editorial Board and Institution will not be responsible for the same in any way.

The Loopholes in Syllabus Design and Textbook Production

Dr. Satish Govind Saykar

Associate Professor, Department of English, Radhabai Kale

Mahila Mahavidyalaya, Ahmednagar. E-mail:

satishgsaykar@gmail.com

Abstract:

Syllabus design is one of the major aspects of curriculum that is designed by the policy makers that consists of academicians, politicians, administrative officers, philosophers, psychologists, sportsperson and many others. The syllabus is designed by the respective Board of Studies taking into account the things those are stated in the curricula designed for the concerned stage. Curriculum is rather a broader term as syllabus is merely a part of it. The syllabus states the learning objectives, learning experiences and evaluation method that is to be adopted to check whether the learning objectives have been fulfilled or not. Here formative assessment serves the purpose and if it is found that the objectives are not fulfilled, the teacher has to devise new ways or methods to provide the proper learning experiences in such a way through which the learning objectives can be achieved. As we know that the success of teaching, learning and evaluation is totally dependent on the achievement of the objectives; they need to be clearly stated in the syllabus along with the list of contents to be taught to a particular class. Unfortunately, now a day we find many loopholes in syllabus design and textbook production. The unavoidable politics in academia is also one of the reasons of failure of teaching and learning process. The present paper attempts to point out the loopholes in syllabus design and textbook production. The classes for which the textbook is not prescribed and only the list of contents is provided are facing many problems. Not only students but the teachers also are unable to decide the scope and limitation of any content as a result of which it leads to confusion which is dangerous for the teaching-learning process.

Keywords: *Syllabus, textbook, loopholes*

Introduction:

The syllabus framing process starts with the things that are stated in Curriculum. Generally, any syllabus framing committee sets the objectives for the particular class or subject as the case may be. The objectives must be stated in a very simple and clear language. The clarity while stating the objectives decides the success or failure of the course. Moreover, the objectives must be flawless as it becomes the public document. Let us have a look at the revised syllabus of *Structure of English T. Y. B. A. Special Paper III (S-3)* of Savitribai Phule Pune University, Pune.

The objectives are stated clearly but; there are some mistakes. Each objective starts with 'To.....' which is a good thing; but when the sentence ends nowhere is there a full stop. It is not expected and accepted from the Syllabus Framing Committee. As the purpose is not only to find out the faults, it can be said that the objectives are clearly stated.

After setting the objectives, the syllabus framing committee has to meditate as to how and what should be taught in the class. One may call it the selection of the contents to be taught throughout the year, because there is a close

<p>Revised Course Structure of English T.Y.B.A. Special Paper III (S-3) (w. e. f. 2015-16) Title of the Paper: Appreciating Novel</p> <p>1) Objectives:</p> <p>a) To introduce students to the basics of novel as a literary form</p> <p>b) To expose students to the historical development and nature of novel</p> <p>c) To make students aware of different types and aspects of novel</p> <p>d) To develop literary sensibility and sense of cultural diversity in students</p> <p>e) To expose students to some of the best examples of novel</p>

Fig 1 Objectives

relationship among the objectives, experiences and the evaluation pattern as is shown in

Fig 2. So it is clear that the committee may select the novels and some topics from the background such as ‘the elements of novel.’

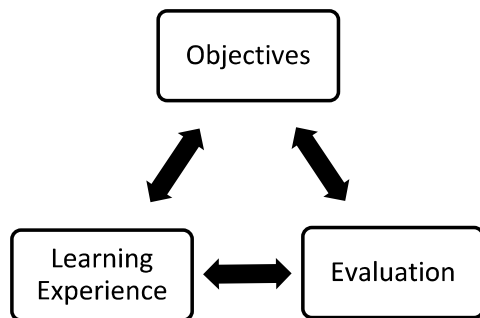


Fig-2: Furst's (1958) Paradigm-Interrelationship between Objectives, Learning Experience and Evaluation

Finally, the committee sets the evaluation pattern for the course which may assess the knowledge of a student and his or her ability to apply his knowledge. If all the three things are apt and flawless, the teaching and learning process will be successful and the objectives will be achieved.

Analysis of the Syllabus:

The syllabus selected for analysis is of B.A. III English Special Language and Linguistics (CBCS) Discipline Specific Elective Semester V –

Paper XI (DSE - E15) of Shivaji University, Kolhapur. (See Appendix I)

Merits of the Syllabus:

1. The objectives are set in a simple and clear language.
2. Course outcomes are also given clearly.
3. The list of contents to be learnt is given.
4. Enough scope is given for internal assessment.
5. Division of teaching hours is specified aptly.
6. List of reference books is also given to help the teachers and students.
7. Evaluation pattern is also given at the end along with the weightage to be given to different topics.

Demerits of the Syllabus:

1. The objectives and the list of contents do not match perfectly.
2. It seems that the objectives are designed either enthusiastically or are taken from somewhere else.
3. It is possible that the work to set the

objectives and content are given to two different people and it's not a team work.

4. The principle of 'Objectives to Selection of Content' is not followed.
5. There is no topic selected to teach to achieve the objective 'To make the students familiar with varieties of the English language.'
6. Due to demerit no. 5, the course outcome: 'Students are familiar with varieties of the English language' has no value at all because this can never be attained.
7. The list of topics is given; but to know the scope and limitation of the topic one has to ask other teachers or the members of Board of Studies or wait for the Self Instruction Material (SIM) which is published by the University for Distance Education Students. It

should have been self explanatory.

The textbook helps both the students and teachers in such a situation; but the textbook also has some limitations. Even it has to go through many stages such as selection of writing team, editorial board, proof readers and so on. In academics everything has some political implication as a result of which instead of quality other things may be unfair get undue importance.

Analysis of the Textbook:

The textbook selected for analysis is of *Ability Enhancement Compulsory Course (CBCS) For B. A. Part III English for Communication (Compulsory English)*. Shivaji University: Kolhapur. (See Appendix II)

Merits of the Textbook:

1. The book is written strictly adhering to the syllabus.
2. It clears the scope and limitation of each module.
3. Exercises are given wherever possible.

4. It is written in a simple language.
5. It takes into account the needs of even the slow learners.
6. The reading lists are provided for the advanced learners.
7. It is a good mixture of prose, poetry and units from communication skills.

Demerits of the Textbook:

1. More exercises could have been added in it.
2. Some topics can be written more effectively.

Suggestions to overcome the loopholes in syllabus design and textbook creation:

1. The number of members should be increased in the syllabus forming committee.
2. There should be a regional balance to be able to serve the needs of the students.
3. Quality should be the sole criterion for the selection of the members of syllabus forming committee.

4. Instead of separate responsibility, team work should be promoted.
5. Some experienced or superannuated teachers should be appointed if required.
6. Some new and enthusiastic teachers may be appointed on such committees.
7. The right combination of the new and experienced persons can be the best solution.
8. In a textbook, the topics with equal weightage should be given equal space. Sometimes one topic takes fifteen pages and the other takes four to five pages.
9. If there is scarcity of content, more exercises taking into account the evaluation pattern can be set.
10. Maximum academics and minimum politics can be the solution to every problem.

Conclusion:

The future of the students depends on the success or failure of teaching, learning and evaluation process as a result of which the role of the syllabus designing committee is very important. The syllabus committees may be reformed if necessary to pave the way towards the bright future. Minimizing the political interference and groupism among the academicians can result in the development of the students.

Bibliography:

Bhambar S.B.(ed.) Ability Enhancement Compulsory Course (CBCS) For B. A. Part III

En English for Communication (Compulsory English). Shivaji University: Kolhapur, 2020. Print.

http://cup.edu.in/school_education/data/E-content__module/AFLPDF/AFL020.pdf

<http://www.unishivaji.ac.in/syllabusnew/Off-Campus-humanities>

<http://dhanyanaveen88.blogspot.com/2014/02/objective-based-instruction.html>

http://www.unipune.ac.in/Syllabi_PDF/revised-2015/arts/TYBA_English_22-06-15.pdf

Appendix I

Shivaji University, Kolhapur

B.A. III English Special

Language and Linguistics (CBCS) Discipline Specific Elective

From June 2020 onwards

Language and Linguistics Semester V - Paper XI (DSE - E 15)

Course Objectives:

- To orient students to the concept of communication.
- To make the students familiar with varieties of the English language.
- To acquaint students with different levels of the study of language.
- To study the basic units of grammar.

Course Outcomes:

- Students know the concept of communication.
- Students are familiar with varieties of the English language.
- Students know different levels of study of the English language.

- Students know basic units of grammar.

Semester V - Paper XI DSE - E 15

Module I

Language and Communication

- i. Definitions and characteristics of language
- ii. Human and Animal communication systems (Special reference to Hockett's 7 characteristics of language)

Module II Phonology

Module III Morphology

Module IV Words

*Note: Semester V: 10 Marks for Internal Evaluation: STUDENTS' SEMINAR

Division of Teaching Hours: 4
Modules X 15 Periods = 60
Periods

Reference Books:

Balasubramaniam, T. A Textbook of English Phonetics for Indian Students, Delhi: MacMillan, 1981.
Bansal, R.K. & Harrison, J.B., Spoken English, Hyderabad: Orient Longman, 2000.

Hockett, C.F., A Course in Modern Linguistics, MacMillan, 1963.

Hudson, Richard, Sociolinguistics, Cambridge: Cambridge University Press, 1996.

Jones, Daniel, English Pronouncing Dictionary, ELBS Edition.

Leech et al, English Grammar Today: a New Introduction, Hyderabad: MacMillan, 2010.

Lyons, John, Language and Linguistics: An Introduction, Cambridge: Cambridge University Press, 1981.

Quirk, R., Greenbaum, S., Leech, G. & Svartvik, J., A Comprehensive Grammar of English, New Delhi: Pearson, 2010.

Quirk, Randolph & Greenbaum, Sidney, A University Grammar of English, New Delhi: Pearson, 2015.

Radford, A., Atkinson, M., Britain, D., Clahsen, H. & Spencer, A. Linguistics: An Introduction, Cambridge: Cambridge University Press, 1999.

Trask, R. L, Key Concepts in Language and Linguistics, London: Routledge, 1999.

Verma, S.K. & Krishnaswamy, N., Modern Linguistics, Hyderabad: Oxford University Press, 1989.

Velayudhan, S. & Mohanan, K. P., An Introduction to the Phonetics and Structure of English, New Delhi: Somaiya Pub. Pvt. Ltd., 1977

**QUESTION PAPER
PATTERN From June 2020
onwards**

LANGUAGE AND LINGUISTICS (CBCS) Discipline Specific Elective Semester V –Paper XI (DSE - E15)

Q. 1 Objective type

a) Three term labels

(3)

b) Transcription of words with primary stress

(3)

c) Conversion of the given transcriptions into the conventional spellings

(2)

Q.2 a) Write short notes (2/3) (to be set on **Module I**)

(10)

b) Morphological Analysis giving labels (2/4)

(4)

Q.3 a) Identification of word formation/morphological processes

(4)

d) Identification of word classes

(4)

Q.4. Write short notes (2/4) (2 each to be set on **Module II & IV**)

(10)

Appendix II Ability Enhancement Compulsory Course (CBCS) For B. A. Part III English for Communication (Compulsory English) CONTENTS

-----SEMESTER V -----

Module I

3

A) Interview Skills

B) The Interview - V. V. John

Module II

27

A) Grammar for Competitive Examinations

B) The Lottery - Shirley Jackson

Module III

67

A) Writing Skills for Competitive Examinations

B) After Twenty Years - O' Henry

Module IV

99

A) I Shall Return to This Bengal - Jibanananda Das

B) Song of Youth - A. P. J. Abdul Kalam

C) The Orphan Girl - Henry Derozio

----- SEMESTER VI -----

Module V

115

- A) Group Discussion
- B) The Lighthouse Keeper of
Aspinwall -Henry Sienkiewicz

Module VI

144

- A) Note Making and Note
Taking
- B) Three Questions - Leo
Tolstoy

Module VII

168

- A) Media Writing
- B) Eight Rupees - Murli Das
Melwani

Module VIII

205

- A) The Mystic Drum - Gabriel
Okara
- B) Two Dead Soldiers - Jean
Arasanayagam
- C) Bora Ring - Judith Wright

• PATTERN OF QUESTION
PAPER 220

VIEWS ABOUT NATURE IN ANITA DESAI'S THE VILLAGE BY THE SEA

Mr. Ramdas Vitthal Barve Head and Associate Professor Department of English Radhabai Kale Mahila Mahavidyalaya Ahmednagar.414001 (Maharashtra) : rvbarve9997@gmail.com

Abstract:

There is a vast and eternal relationship between human beings and nature. Nature plays an important role in human life; it is the basis of how our society is functioning. Personally and collectively there is a relationship with life and the world. It can support and inspire people struggling to find a foundational base for the development of productive societies and a healthy human–earth relationship. We have to find new ways to live and to run our economies for healthy human and ecological communities. Nature provides natural resources and energy resources to human beings. Nature has had a great influence on creative writers from the earliest developmental stages of human beings. They depicted its flora and fauna, beauty and charm, cyclical seasons of the year such as spring, summer, autumn and winter and the natural phenomena around them

Keywords: Flora and fauna, ecology, pandanus, Thul, urbanization, etc.

Introduction:

Anita Desai, the most distinguished Indian writer in English was born on 24 June 1937 in Jaipur, India. Her mother, Toni Nime was German and father was Bengali businessman, D. N. Mazumdar and she married Ashvin Desai. Her children were taken to Thul for weekends, where Desai set her novel *The Village by the Sea*. For that work she won the 1983 Guardian Children's Fiction Prize. She received a Sahitya Akademi Award in 1978 for her novel *Fire on the Mountain*. Tondon writes about her imagination and creative power as,

“She is endowed with soundless imaginative resourcefulness and creative vitality ... but within this limited world she reveals amazing variety and profundity.”¹

Presentation of Nature in *The Village by the Sea*:

The title of the novel, *The Village by the Sea* sounds close to nature and the ‘village’ and the ‘sea’ are important part of the ecosystem. Desai’s elegant pictures of sky in the monsoon and evening and the giant sea increase the beauty of the novel. Anita Desai seems to be related with the cultural life of India and influenced by the beauty of nature in many chapters of the novel. The beauty of nature is one of the themes of this novel. She seems to be entrapped by the serenity of nature at the very beginning of the novel where she captures the scenery of the sandy shore, blue water and waves of the sea, fragrant flowers and the colorful birds. Thul is a very calm place where man and nature develop their relationship with the lush paddy fields, calm waters, dense forests, and the vast sea. While living in such an enchanting locality, we get pleasure from natural objects and listening to the melodious songs of the wild birds. The natural tranquility of Thul contrasts with the artificialities of urban life. Thus, Desai appears to be an ardent lover of ecology and nature. While studying Anita Desai’s *The Village by the Sea*, the researcher has taken into consideration a verdict of M. K. Naik, he comments,

“This is true of Anita Desai also...but the snatches of sunshine, the sudden revealing and guiding lights, do not want either.”²

At the beginning of the novel, the opening scene is described to be an unstable environment. This is reflected by the setting of the waves and how they are portrayed to be 'unstable' as the author uses phrases such as 'high tide' and 'low tide' to show the instabilities of human life. At the exposition,

Mr. Ramdas Vitthal Barve Head and Associate Professor Department of English Radhabai Kale
Mahila Mahavidyalaya Ahmednagar. (Maharashtra) : rvbarve9997@gmail.com

Abstract:

It is universally acknowledged that there is a relationship between man and nature. Man has lived and is living in the company of nature. The cycle of seasons has an effect on human life. Man has experienced the beneficial as well as the destructive aspects of nature. Nature is part of the ecological system. There is the influence of nature on literature and a relationship of people with other humans and with natural communities which bring notions of mutual respect and fairness. The living beings on the earth are dependents on their own community as well nature and living and non-living beings. In the community, they share their emotions among them about nature and its resourcefulness to them. In nature, we come across with different forms of life and economy which depend on the earth. Nature has had a great influence on creative writers from the earliest developmental stages of human beings.

Key words: Nature, ecosystem, ecology, nectar, calamities, Rukmani, etc.

Introduction:

Kamala Markandaya, the most popular Indian novelist, journalist and social worker was born into a Hindu-Brahmin family in a small town in Mysore in 1924. She is known for writing about culture clashes between Indian urban and rural societies. Her first published novel, *Nectar in a Sieve* (1954), was a bestseller and cited as an American Library Association Notable Book in 1955. In this researcher paper, the researcher tried to investigate that being the woman novelist, how Markandaya is the part of nature. She is from an Indian rural and rustic background so her novels are also set in the same background where her character grows, develops and earns life in the company of nature. The Indian writer, Rebecca Angom observes,

“Kamala Markandaya is one of the major first generation Indian women novelists writing in English. She is also one of the finest and most distinguished Indian novelists in English of the post- colonial era.”¹

Representation of Nature in *Nectar in a Sieve*:

Markandaya depicts how the peasants and villagers in rural India fall prey to the cruelty of nature. The novel shows how nature can bring destruction to the lives of peasants. The people in the village face severe loss of crops not only because of constant rain but drought. She compares nature with a wild animal for which a man works in his entire life. Actually, nature gives its aid to all humans and others. Rukmani's faith in Nature makes her hope for the time when it will be better. The novelist also states the threat of flood and the destruction of paddy crop by the rain as,

“...but Nathan and I watched with heavy hearts while the waters rose and rose and the tender green of the paddy field sank under and was lost.” (p.41)²

In title of the research paper ‘figuring nature’ is one of the important issues the researcher has taken for study. Keeping in mind this issue A. V. Krishna Rao and K. Madhavi Menon's view about nature is taken into consideration that compare Markandaya's novel with Thomas Hardy,

“In fact, the plot or the causality that articulates the story is provided by Nature herself. Like in a typical Hardy novel, Nature spaniels this simple family like a foe.”³

शोध दिशा

ISSN 0975-735X

विश्वस्तरीय शोध-पत्रिका

केंद्रीय हिंदी संस्थान, आगरा से अनुदान प्राप्त

UGC APPROVED CARE LISTED JOURNAL

विश्वविद्यालय अनुदान आयोग द्वारा मान्यता प्राप्त शोध पत्रिका

शोध अंक 55

जुलाई-सितंबर 2021

300.00 रुपए

संपादकीय कार्यालय

हिंदी साहित्य निकेतन, 16 साहित्य विहार,
बिजनौर 246701 (उ०प्र०)

फोन : 01342-263232, 09557746346

ई-मेल : shodhdisha@gmail.com

वेब साइट : www.hindisahityaniketan.com

क्षेत्रीय कार्यालय

हरियाणा

डॉ० मीना अग्रवाल

ए-402, पार्क व्यू सिटी-2 सोहना रोड,

गुड़गाँव (हरियाणा)

फोन : 0124-4076565, 07838090237

दिल्ली एन०सी०आर०

डॉ० अनुभूति

सी-106, शिवकला अपार्टमेंट्स

बी 9/11, सेक्टर 62, नोएडा

फोन : 09958070700

(सभी पद मानद एवं अवैतनिक हैं।)

संपादक

डॉ० गिरिराजशरण अग्रवाल

07838090732

प्रबंध संपादक

डॉ० मीना अग्रवाल

संयुक्त संपादक

डॉ० शंकर क्षेम

उपसंपादक

डॉ० अशोककुमार

डॉ० कनुप्रिया प्रचण्डिया

कला संपादक

गीतिका गोयल/ डॉ० अनुभूति

विधि परामर्शदाता

अनिलकुमार जैन, एडवोकेट

आर्थिक परामर्शदाता

ज्योतिकुमार अग्रवाल, सी०ए०

शुल्क

आजीवन (दस वर्ष): व्यक्तिगत : पाँच हजार रुपए

संस्थागत : छह हजार रुपए

वार्षिक शुल्क : आठ सौ रुपए

यह प्रति : तीन सौ रुपए

प्रकाशित सामग्री से संपादकीय सहमति आवश्यक नहीं है। पत्रिका से संबंधित सभी विवाद केवल बिजनौर स्थित न्यायालय के अधीन होंगे। शुल्क की राशि 'शोध दिशा' बिजनौर के नाम भेजें। (सन् 1989 से प्रकाशन-क्षेत्र में सक्रिय)

स्वत्वाधिकारी, मुद्रक, प्रकाशक डॉ० गिरिराजशरण अग्रवाल द्वारा श्री लक्ष्मी ऑफसेट प्रिंटर्स, बिजनौर 246701 से मुद्रित एवं 16 साहित्य विहार, बिजनौर (उ०प्र०) से प्रकाशित। पंजीयन संख्या : UP HIN 2008/25034

संपादक : डॉ० गिरिराजशरण अग्रवाल

ISSN 0975-735X

जुलाई-सितंबर 2021

हिंदी तथा मराठी दलित रंगभूमि : एक तुलनात्मक अध्ययन

डॉ० राजाराम दादा कानडे

हिंदी विभागाध्यक्ष,

एस०एस०जी०एम० कॉलेज,

कोपरगाँव (अहमदनगर) महाराष्ट्र

हिंदी तथा मराठी दलित रंगभूमि की स्थिति-गति, नाट्याशय में व्यक्त साम्य-वैषम्य, प्रेरणाएँ तथा मंचीयता आदि बातों में कई जिज्ञासाएँ उभरना स्वाभाविक प्रतीत होता है। इस अर्थ में हिंदी तथा मराठी रंगभूमि में नई सोच के प्रति अध्ययन विश्लेषण करने का अवसर मिलने की संभावना है। दलित नाटक का उद्देश्य मनोरंजन कम और समाज सुधार ही अधिक रहा है। दलित नाटककारों ने पुरानी गलत रूढ़ि, परंपरा, अंधविश्वास, दैववाद, पापपुण्य, जातिभेद एवं धर्मभीरुता में व्याप्त झूठापन पर प्रकाश डाला है। साथ ही दलितेतर पात्रों के अहंकार पर प्रकाश डाला है।

1. रंगभूमि का अर्थ एवं परिभाषा

रंगमंच और रंगभूमि ये एक-दूसरे के पर्यायी शब्द हैं। रंगभूमि एक साकार कला है। इसकी परिधि में रंगशाला, नाटक, पात्र, वेशभूषा, अभिनय, मंचीय उपकरण आ जाते हैं। यह शब्द अंग्रेजी 'थिएटर' शब्द से विकसित है। 'रंग' शब्द खासतौर पर नाटक विधा से संबंधित है। 'रंगभूमि से तात्पर्य तमाशा या जलसे का स्थान, नाटक खेलने की जगह नाट्यशाला, अखाड़ा, युद्धस्थल, मल्लशाला, रणभूमि है।" किसी भी सुशोभित वस्तु का स्थान ऊँचा होता है ताकि सबका ध्यान उसकी तरफ आकृष्ट हो जाए। उसकी तरफ देखने में सुविधा हो सके। इसी स्थल को मंच कहते हैं। आचार्य भरतमुनि ने रंगभूमि को नाटक मानकर उसका विशेष अर्थ इन शब्दों में व्यक्त किया है, 'संसार में न ऐसा कोई ज्ञान है, न ऐसी कला है, न शिल्प न ही योग जो नाटक में अभिनीत न हो सके।' अर्थात् नाटक ही रमणीय विधा है। उसमें विश्व के ज्ञान की हर इकाई मौजूद है। यह एक ऐसी काव्य विधा है जिसके बिना मनुष्य जीवन अधूरा लगता है। इस अर्थ में साठोत्तरी हिंदी नाटककार मोहन राकेश ने कहा है, 'रंगमंच नाटक से बाहर होता नहीं। हर नाटक का रंगमंच नाटक के साथ ही जन्म लेता है। इसलिए रंगमंच की तलाश नाटक से बाहर नहीं हो सकती।' अर्थात् नाटक तथा उसका मंच सबको एक साथ प्रभावित करता है।

2. दलित रंगभूमि की परिभाषा

दलितों में स्वाभिमान, आत्मविश्वास, स्वत्व जगाने हेतु दलित रंगभूमि का गठन हुआ है। यही कारण है कि यह न्यायी-निराली-प्रस्थापितों से पृथक् है। प्रसिद्ध मराठी दलित नाटककार प्रा० दत्ता भगत ने कहा है, 'अंबेडकरी विचार अर्जित करने पर प्राप्त जीवन संबंधि दृष्टि के जरिए स्वयं के जीवन अनुभव की तलाश करना ही दलित नाटक है।" अंबेडकरी विचार दृष्टि में जीवन अनुभव की तलाश है जो दलित रंगभूमि है। यही दलितों की विचार संपत्ति है। इसी कारण भि०शि० शिंदे ने कहा है कि 'गुलाम को उसकी गुलामी का अहसास कराओ ताकि वह विद्रोह करेगा। यह

पैगाम देनेवाली भूमि को ही दलित रंगभूमि कहेंगे।⁵ दलितों को अपनी गुलामी का अहसास देना जरूरी था। इसका सस्ता माध्यम नाटक ही है। दलितों को उसकी जाति-व्यवस्था को नकारने तथा विज्ञानवादी विचारों के अनुसरण में कर्मवादी बनने की दिशा देने का कार्य डॉ० बी०आर० अंबेडकर ने किया और दलित साहित्यकारों ने उनके विचार जनमानस तक पहुँचाने का प्रयास नाटक के माध्यम से किया है। इसलिए अनेक परिभाषाओं पर विमर्श करने के उपरांत हम यह कह सकते हैं कि 'दलित रंगभूमि डॉ० बी०आर० अंबेडकर के विचारों के अनुसरण का मीठा फल है जिसके प्रति दलितों में अपनापन है, उसमें दलित जीवन की अनुभूति तथा दलितत्व को दूर करने हेतु प्रास्थापितों के अहंकार के खिलाफ क्रांति की चेतना मौजूद है।'

3. दलित रंगभूमि की परंपरा तथा पूर्वरंग

दलित कई युगों से ब्राह्मणवाद से पीड़ित है। उनकी मृतवत हालत में जान डालने का साहस केवल अंबेडकरी विचारों में हैं। इस हेतु दलित साहित्यकारों ने दलित नाटकों का सृजन किया जिसकी परंपरा बहुत पुरानी प्रतीत होती है जो जनरुचि रंगभूमि, तमाशा, सत्यशोधक एवं अंबेडकरी जलसों में देखी जा सकती है। यही दलित रंगभूमि का पूर्वरंग है। इससे यह स्पष्ट होता है कि दलित रंगभूमि की नींव लोककलाएँ हैं। जैसे—

बामणा घरी लिवणं
कुणव्या घरी दाणं आणि
म्हारा घरी गाणं।⁶

महारादि दलितों के घर गीत गाने की प्रथाएँ रूढ़ थीं। पारिवारिक सदस्यों के लालन-पालन के लिए नृत्य-गान जैसी कलाएँ दलितों द्वारा रक्षित थीं। यही कारण है कि लोकरंगभूमि का विकास हुआ है। इसका ही एक प्रचलित नाम 'तमाशा' है। 'तमाशा' लोकप्रिय कला को आम आदमियों ने काफी उन्नत किया है। इसमें जनप्रतिबद्धता देखी जाती है। 'इस कला की रक्षा उपेक्षित गरीब, दलित कलाकारों ने की हैं। इस दृष्टि से प्रथम व्यक्ति उमा बाबा माँग सावळजकर है, उनका मशहूर कवित्त 'मोहन बटाव' है जिसे 1960 ई० में अभिव्यक्त किया था।⁷ युगीन परिवेश की तहत तमाशा में कई परिवर्तन हुए हैं जो समयानुसार होता रहा है। अब उसका रुझान केवल संगीत बारी की ओर है इसे ही 'संगीत जलसा' कहते हैं।

'जलसा' अरबी भाषा का पुल्लिंग शब्द है। उसका अर्थ गाने की, बजाने की सभा अथवा गाने की महफिल है। दलितों ने उपदेशात्मक गीत, पद, लावणी आदि के नाद-लयबद्धता को इस ढंग में प्रस्तुत किया कि सबका ध्यान इसकी तरफ आकृष्ट होता गया और जलसाकारों की संख्या बढ़ती गई। जलसा दो रूपों में विकसित हुआ। उसका बहुचर्चित रूप सत्यशोधक जलसा रहा है जो सत्यान्वेषण के लिए महात्मा फुले के विचारों के अनुसरण की गतिविधि तथा नतीजा संबंधी प्रबोधन व्यक्त है। महात्मा फुले के विचार ने कटु औषधि के समान मरीज पर असरदार प्रभाव किया है। परिणामतः अंबेडकरी जलसा का जन्म हुआ है। दूसरे शब्दों में सत्यशोधक जलसा की विकसित अवस्था 'अंबेडकरी जलसा' है जिसकी शुरुआत 1930 ई० के पश्चात् हो गई। इसके बारे में भीमराव करडक ने यह कहा है, 'डॉ० बाबासाहेब अंबेडकर राजकीय सभा में जो मौलिक उपदेश देते थे तथा जो पैगाम देते थे उन उपदेशात्मक विचार तथा पैगाम का अनुवाद ही अंबेडकरी जलसा है।'⁸ डॉ० अंबेडकर के विचार, उच्चार, आदेश, तत्त्वज्ञान और दलित मुक्ति आंदोलन को

केंद्र में रखकर अंबेडकरी जलसे निर्माण हुए हैं। उनमें अनेक नए तथा कुछ पुराने जलसाकारों सत्यशोधक विचारकों ने अंबेडकरी जलसा के निर्माण का परिवेश तैयार किया है जिसमें कवि गोपालबाबा वलंगकर, प्रथम दलित पत्रकार किसन फागुजी बनसोडे, शिवराम जानबा कांबळे, हरिभाऊ तोरणे, गणेश गवई, शाहीर भाऊ फक्कड, रामजी रामटेके, रामचंद्र हरि बनसोडे आदि आरंभिक जलसाकार प्रमुख हैं। वैसे अंबेडकरी जलसाकारों की दो पीढियाँ हैं। इसकी दूसरी पीढी के जलसाकारों की लंबी सूची है। इनका दलित रंगभूमि पल्लवन में बहुत योगदान रहा है।

4. हिंदी मराठी दलित रंगभूमि का परिचय

दलित रंगभूमि में अंबेडकरी विचारों का स्मरण देने का प्रयास रहा है। स्पष्ट है कि इसमें दलितों में आत्मचिंतन, आत्मविकास, आत्मविश्वास एवं अभिमान जगाने और अपना स्वाभिमान निर्माण करने का प्रयास है। हिंदी रंगभूमि का विकास मराठी दलित रंगभूमि के प्रभाव स्वरूप है। भारतवर्ष का स्वातंत्र्योत्तर काल मराठी दलित नाटकों का 'उत्कर्ष काल' रहा है जिसका हिंदी दलित नाटककारों पर असर होना स्वाभाविक है। हिंदी तथा मराठी दलित नाटक या रंगभूमि का परिचय संक्षेप में इस प्रकार है।

(अ) शीर्षक बोध के दलित नाटक—शीर्षक पढ़ते ही पाठक को जब नाटक का आशय समझने में विलंब नहीं लगता वे नाट्य शीर्षक सुंदर तथा बोधगम्य माने जाते हैं। माताप्रसाद के लगभग सभी नाटक इस तरह के हैं। हिंदी के दलित नाट्य साहित्य को सबसे अधिक नाटक देने वाले हिंदी दलित नाटककार 'माताप्रसाद' हैं। उनके नाटक सरल एवं शीर्षक बोधगम्य के हैं। 'अछूत का बेटा', 'धर्म के नाम पर धोखा', 'वीरांगना झलकारी बाई', 'वीरांगना ऊदो देवी पासी', 'तडप मुक्ति की', 'अंतहीन बेडियाँ', 'हम एक हैं', 'संत शिरोमणि गुरु रविदास', महादानी राजा बलि', 'दिल्ली के गद्दी पर खुसरो भंगी', 'जातियों का जंजाल' आदि-शीर्षक नाटक हैं। मोहनदास नैमिशराय का 'हैलो कामरेड', राजकुमार सांभरिया का 'उजास' नाटक तथा सुशीला टाकभौरे का 'नंगा सत्य' नाटक शीर्षक बोध के हैं। मराठी दलित रंगभूमि में शीर्षक बोध के नाटक 'तनमाजोरी', 'देवनवरी', 'गांधी-आंबेडकर', 'वांझमाती', 'किरवंत', 'काळोखाच्या गर्भात', 'बामनवाडा', 'साक्षीपुरम', 'इथे माणसाला स्थान नाही', 'कैफियत', 'न्याय', 'सूर्यास्त', 'हत्याकांड' आदि हैं।

(आ) समस्या प्रधान दलित नाटक—भारतवर्ष की प्रमुख समस्याओं में भ्रष्टाचार, बाह्याडंबर, अंधविश्वास, बेरोजगार, जातिवाद आदि हैं। हिंदी दलित नाटकों में ये सारी समस्याएँ चित्रित हैं। रामअवतार पाल का 'एकलव्य', एन०आर० सागर का 'अंतिम अवरोध', रत्नकुमार सांभरिया का 'वीमा', 'उजास' नाटक जाति अंत या जाति निर्मूलन हेतु लिखे गए हैं। अर्थात् इसमें जाति अभिमानियों के षड्यंत्र पर प्रकाश डाला है। माताप्रसाद के 'अछूत का बेटा' तथा 'प्रतिशोध' शीर्षक नाटक समस्याप्रधान हैं। रूप नारायण सोनकर का नाटक 'एक दलित डिप्टी कलेक्टर' नामक है जो दलित ब्राह्मण की मानसिकता पर प्रकाश डालता है। जातिअभिमानियों की गद्दारी के प्रति दलितों को सतर्क करने हेतु तडप मुक्ति की, अंतिम अवरोध, संत शिरोमणि गुरु रविदास आदि नाटक लिखे गए।

भारत का मूलनिवासी होने के बावजूद दलितों को अपनी मूलभूत जरूरतों को पूर्ण करने हेतु कठिन परिस्थितियों का सामना करना पड़ रहा है। आखिर इसके लिए जिम्मेदार कौन है? इस प्रश्न के उत्तर में दलित नाटक सामाजिक, आर्थिक, राजनीतिक, शैक्षिक, सांस्कृतिक उलझनों पर प्रकाश डालते हैं। इस दृष्टि से मराठी दलित नाटक-मारेश्वर बी तांबे का 'प्रेमप्रताप', नामदेव व्हटकर का

‘वाट चुकली’ दत्ता भगत के नाटक ‘खेलिया’ तथा ‘वाटा-पळवाटा’, प्रेमानंद गज्जी के नाटक ‘तनमाजोरी’, ‘देवनवरी’, ‘सफेद बुधवार’ आदि हैं। संजय पवार का ‘कोण म्हणतं टक्का दिला’, रामनाथ चव्हाण का ‘पारध’, बामनवाडा, साक्षीपुरम, प्रज्ञा दया पवार का ‘धादांत खैरलांजी’ एवं माधव कोंडविलकर का ‘मुक्काम पोस्ट देवाचे गोठणे’ आदि समस्या प्रधान नाटक हैं।

(इ) सम्यक क्रांति के दलित नाटक—दलित नाटककारों की नाटयकृतियों में नए जमाने के बाबासाहेब डॉ० अंबेडकर बोल रहे हैं, शिक्षा-संगठन एवं संघर्ष का बोध दे रहे हैं। सम्यक क्रांति बोध के हिंदी दलित नाटक रत्नकुमार सांभरिया के ‘वीमा’ तथा ‘उजास’ नाटक तथा मोहनदास नैमिशराय का ‘हैलो कामरेड’ नाटक, माताप्रसाद के ‘अंतिम अवरोध’, ‘अछूत का बेटा’ आदि नाटक हैं तो मराठी दलित नाटकों में ‘सूर्यास्त’, ‘वाटा-पळवाटा’, ‘काळोखाच्या गर्भात’, ‘मन्वंतर’, ‘आम्ही देशाचे मारेकरी’, ‘थांबा रामराज्य येतय’ आदि नाटक प्रमुख हैं।

5. दलित रंगभूमि की वर्तमान स्थिति

दलित रंगभूमि व्यक्ति की सामाजिक, धार्मिक, आर्थिक, सांस्कृतिक, ऐतिहासिक, राजनीतिक अज्ञान को मिटाने का प्रयास में कार्यरत हैं। यह प्रयास नित्य अन्याय, शोषण, अमानवीयता के प्रति दलितों को सजग करता है ‘हम ही स्वयं के उद्धारकर्ता हैं। इसी भूमिका में उन्नत होने से अंधेरे में से उजाला की ओर ले जानेवाला प्रकाशपुत्र होने का बोध दलित रंगभूमि पर हो गया और वह दलित नाटकों के माध्यम से संभव हुआ।¹⁰ धर्मभीरुता व्यक्ति को गुलामी की तरफ ले जाती है। इसलिए दलितों ने कर्मवादिता वृत्ति की ओर विशेष ध्यान देकर राजनीति में शामिल होना अनिवार्य समझा है। इस हेतु कुछ दलित नाटक लिखे गए हैं।

भारत देश के विभिन्न प्रदेशों में कई प्रसिद्ध लोक कलाकार हैं जिनका वर्तमानकालीन अस्तित्व एक पेटबोली कलाकार हैं जो गाँव-कस्बों तथा नगरों में अपनी कलाओं का प्रदर्शन करके दर्शकों का मनोरंजन करते हैं। हिंदी नाट्य साहित्य में दलित विमर्श तो हुआ मगर विमर्श के अनुसार मंचीय विकास नहीं हो पाया। मराठी दलित नाटकों में जितना विकास हुआ है उतना हिंदी में नहीं हो पाया। इस संबंध में डॉ० माधव सोनटक्के की राय है, ‘बीसवीं शती के अंतिम और इक्कीसवीं शती के प्रथम दशक में स्वयं नाट्यविधा ही दम तोड़ती हुई दिखाई दे रही है। झुग्गी-झोपड़ी में केबल टी०वी० सुंदर सपने बेच रहा है। ऐसे परिवेश में अनगढ़ यथार्थ को लेकर आनेवाला नाटक रंगीनियों में फँसे दर्शकों को अपनी ओर फिर से खींचने में कहाँ तक सफल होगा—कहा नहीं जा सकता।¹¹

हमारे देश के नगर दिन दूनी और रात चौगुनी उन्नति कर रहे हैं किसके कारण गाँवों की तबाही हो रही है। यही कारण है कि हिंदी तथा मराठी दलित नाटक नगरों-महानगरों में विकसित हैं। हिंदी तथा मराठी दलित रंगभूमि की वर्तमान स्थिति कुछ समाधानकारक नहीं है। इसके कतिपय कारण इसप्रकार हैं—

1. दलित रंगभूमि की शून्य गति
2. दलित नेता-कार्यकर्ताओं का नजरअंदाज
3. दलितेतर समाज से दलित रंगभूमि दूर
4. विशिष्ट जाति कहकर भेदभाव का भ्रम फैलाने की साजिश
5. दलित रंगकर्मी के प्रति स्नेह का अभाव

6. हिंदी तथा मराठी दलित रंगभूमि में तुलना

मानवी जीवनमूल्य तथा संवैधानिक मूल्य रक्षा हेतु दलित नाटक लिखे गए हैं जिसका मूलाधार डॉ० बी०आर० अंबेडकर का व्यक्तित्व कृतित्व है। दोनों नाटकों में कुछ साम्य तथा वैषम्य हैं जो इसप्रकार हैं—

(क) **दलित रंगभूमि का उद्भव काल**—हिंदी की दलित नाट्यलेखन परंपरा मराठी की तरह पारंपरिक है। मराठी दलित नाटकों की शुरुआत 1955 के उपरांत है जिसका प्रभाव हिंदी नाटकों पर पड़ा और हिंदी दलित नाट्यलेखन को गति 1980 के उपरांत मिली है। दोनों रंगभूमियों की पूर्व परंपराएँ देहाती होकर भी दलित रंगभूमि का विकास नागरी संस्कृति की देन है।

(ख) **नाट्यशय में साम्य-वैषम्य**—हिंदी तथा मराठी दलित नाटक पौराणिक, ऐतिहासिक, सामाजिक, धार्मिक धरातल पर लिखे गए समस्या प्रधान नाटक हैं। इनमें दलित तथा दलितेतर के बीच जीवनमूल्य के संघर्ष का चित्रण है। हिंदी में दलित नाटकों की संख्या मराठी दलित नाटकों की तुलना में कम है। रत्नकुमार सांभरिया के 'वीमा' तथा 'उजास' नाटक मौलिक इसलिए लगते हैं कि इन नाटकों में अंबेडकरी विचार एवं नए विचारों में समन्वय है। रूपनारायण सोनकर के नाटकों में यथार्थता, दलित समस्या तथा ब्राह्मणवादी विचारधारा पर प्रकाश डाला गया है। माताप्रसाद के नाटकों में कई विचार प्रवाह चित्रित हैं। उन्होंने गांधीवाद तथा अंबेडकरवादी विचार प्रस्तुत किए हैं। मोहनदास नैमिशराय के नाटकों में जातिवादी व्यवस्था के सिक्कजे में दलित युवा-युवती का संघर्ष चित्रित है। उनका शिक्षा-संघर्षरत दलित युवा पीढ़ी की त्रासदी की वजह पर प्रकाश डालने का प्रयास है। 'अंतिम अवरोध' एवं 'एकलव्य' नाटक के नाटककारों ने जातिअभिमानियों की साजिश पर प्रकाश डाला है।

आशय-विषय तथा मौलिकता की दृष्टि से मराठी दलित नाटक असरदार हैं। मराठी दलित नाटककारों ने अंबेडकरी विचारों का ही अनुसरण किया है। उन्होंने प्रामाणिकता से अंबेडकरी विचार प्रस्तुत करने का ही प्रयास किया है। दोनों नाटकों में विषय-विविधताएँ हैं। हिंदी तथा मराठी दलित नाटकों का लेखन दलित तत्त्वों के अनुसार हुआ है। मराठी नाटकों में इन तत्त्वों की पहचान तुरंत होती है। वैसे हिंदी दलित नाटकों में उसकी पहचान करनी पड़ती है।

(ग) **हिंदी तथा मराठी दलित नाटका का वैषम्यबोध**—दोनों भाषाओं के दलित नाटकों में प्रभाव, प्रेरणाएँ तथा मंचन में विषमता नजर आती हैं।

(अ) **प्रेरणाएँ**—हिंदी दलित नाटकों की प्रेरणाओं में मध्ययुगीन कवि रैदास, कबीर तथा आधुनिक काल के डॉ० बी० आर० अंबेडकर, काशीराम, मायावती की राजनीति का प्रभाव रहा है। इस बात के लिए अपवाद मोहनदास नैमिशराय तथा रत्नकुमार सांभरिया रहे हैं। इनके नाटक अंबेडकरी चेतना के हैं। मराठी दलित नाटकों में अंबेडकरी चेतना प्रमुखता से झलकती है। इसका कारण भी स्पष्ट है कि मराठी दलित नाटकों के कुछ लेखक अंबेडकरी विचारक की प्रथम पीढ़ी के अनुयायी हैं। इन्होंने अंबेडकर के साथ स्वाधीनता तथा जाति निर्मूलन के आंदोलन में शामिल होकर स्वाभिमानी जिंदगी का अनुभव किया था। अंबेडकरी विचारक की दूसरी पीढ़ी ने भी अथक मेहनत करके अंबेडकरी विचारों को जनमानस तक पहुँचाने का प्रयास किया है। इसलिए इन नाटकों में वेदना, विद्रोह, नकार, विज्ञाननिष्ठ तथा मानवता की झाँकियाँ स्पष्ट नजर आती हैं।

(आ) मंचीयता का प्रभाव—'मंचीयता' की दृष्टि से हिंदी दलित नाटक इतने सफल नहीं हैं जितना मराठी दलित रंगभूमि रही है। कारण स्पष्ट है कि मराठी दलित नाटक का आधार तमाशा, सत्यशोधक जलसे तथा अंबेडकरी जलसा के साथ ही दलित पेंथर का सामाजिक आंदोलन है। मराठी दलित रंगभूमि का सूत्रपात 1950 के पश्चात् रहा है और 1955 से लेकर 1980 तक इस रंगभूमि ने जनमानस पर काफी प्रभाव किया। हिंदी प्रदेशों में दलित नाटककारों की कमियाँ तथा हिंदी प्रदेशों में जातिअभिमानियों के बढ़ते अत्याचार के कारण दलित रंगभूमि विकसित नहीं हो पाई। इन प्रदेशों में दलित नाट्य-सृजन करने में विलंब हुआ, अर्थात् यह 1980 के आसपास शुरू हुआ माताप्रसाद तथा रूप नारायण सोनकर के नाटकों का मंचन हुआ। परंतु इसी दौरान दूरदर्शन घर-घर में रंगीन सपने लोगों को दिखा रहा था और लोग उसमें अधिक रममान हुए थे। अतः 1980 के उपरांत दलित रंगभूमि जनमानस पर अमिट प्रभाव नहीं कर सकी।

इसप्रकार दलित रंगभूमि में कई योग, वियोग, इतिहास, वर्तमान तथा विज्ञानों की चर्चा हुई है। दलित रंगभूमि को उन्नत करने का कार्य अंबेडकरी अनुयायियों, विभिन्न जलसाकारों तथा दलित पेंथर के सामाजिक प्रतिबद्धता के रचनाकारों ने किया है। दलित जो भारत का मूल निवासी है। इसलिए दलितों में राष्ट्रीय चेतना पहले से है। दलित रंगभूमि असली देशद्रोही का पर्दाफाश करने का प्रयास करती है। इसलिए उसे उन्नत करना सबका कर्तव्य है। हिंदी तथा मराठी दलित नाटककारों ने दलित समस्याओं को चित्रित करके सामाजिक सत्य पर विमर्श करने हेतु अंबेडकरी चेतना को मुखरित किया है। यही दलित तथा दलितेतर समाज की उन्नति का सरल, सुगम रास्ता है। इसलिए दलित रंगभूमि को उन्नत करना अनिवार्य है।

संदर्भ

1. एस० कुमार, संपादक-हिंदी विश्वकोश, बी०आर० पब्लिकेशन हाउस, दरियागंज, 2011, पृ० 8227
2. डॉ० बाबासाहेब पोवार, नाट्यविज्ञान और लाल के नाटक', महालक्ष्मी, कोल्हापूर, 2004, पृ० 2
3. वहीं, पृ० 13
4. डॉ० ईश्वर नंदपुरे, दलित नाटक आणि रंगभूमी', पिंपळापुरे अण्ड कंपनी, नागपूर, 1997, पृ० 27.
5. डॉ० शशिकांत खिलारे, आंबेडकरी चळवळ आणि दलित नाटक, प्रज्ञाप्रबोध, सांगली, 2013, पृ०121
6. वहीं, पृ० 124
7. डॉ० मधुकर मोकाशी, दलित रंगभूमी आणि नाट्य चळवळ, स्नेहवर्धन प्रकाशन, पुणे, 2000, पृ० 10
8. डॉ० भगवान ठाकुर, आंबेडकरी जलसे, सुगावा प्रकाशन, पुणे, 2005, पृ० 101
9. सर्वेश कुमार मौर्य, हिंदी दलित एकांकी संचयन, स्वराज प्रकाशन, नई दिल्ली, 2012, पृ० 223
10. डॉ० ईश्वर नंदपुरे, दलित नाटक आणि रंगभूमि, पृ० 166
11. डॉ० माधव सोनटक्के, नाट्यालोचन, विकास प्रकाशन, कानपुर 2008, पृ० 37

मो० 9518747195, 9423202603

ईमेल : rajsaurvgaurav@gmail.com

जायकवाडी बांध आंदोलन में जिला अहमदनगर के साम्यवादी दल का योगदान

★ प्रा.डॉ. विघाटे गणेश शंकर ★★ डॉ.राजाराम कानडे

सारांश:

जायकवाडी जलसिंचन परियोजना में सरकार की भूमिका और विस्थापित लोगों पर हुए सितम के कारण, विस्थापितों का पुनर्वास संबंधी प्रश्नों की ओर सरकार का नजरअंदाज की वजह से उभरा जन आंदोलन को सही अंजाम देने की भूमिका में अहमदनगर जिले के साम्यवादी दल के योगदान को उजागर करने के प्रयोजन में प्रस्तुत शोध आलेख पाठक, संशोधक को आंदोलन के प्रति सजग करेगा। इसमें जन आंदोलन के बढ़ते प्रभाव के कारण सरकार द्वारा पारित विभिन्न अधिनियम की जानकारी है। साथ ही आंदोलन कर्मियों का विश्वास कायम रखने के प्रयास में साम्यवादी अनुयायियों का अथक प्रयास ही मानवतावादी विचारधारा की तरफ पाठक को ले जाता है।

महत्त्वपूर्ण शब्द:

महाराष्ट्र राज्य सरकार तथा साम्यवादी भूमिका की फल निष्पत्ति.

उद्देश्य:

1. जायकवाडी जलसिंचन परियोजना निर्माण में सरकार की भूमिका पर प्रकाश डालना।
2. बांध निर्माण कार्य में पीड़ितों की मानसिकता को उजागर करना एवं जन आंदोलन के विषय पर प्रकाश डालना।
3. साम्यवादी विचारकों की भूमिका और उनका मानवतावादी प्रयास की दिशा पर प्रकाश डालना।
4. जायकवाडी बांध निर्माण एवं जन आंदोलन की शुरुआत और पुनर्वास संबंधी अधिनियम के प्रति वाचक कोसजग करना।
5. बांध पीड़ितों के आंदोलन की दिशा और फलनिष्पत्ति का अध्ययन करना।

प्रस्तावना:

महाराष्ट्र की मशहूर नदी गोदावरीके तट पे स्थित 'पैठण' के समीप स्थापितजायकवाडी बांध के कारण विस्थापित हुए किसान, खेती मजदूरों के आवास के प्रश्नों पर अहमदनगर के साम्यवादी विचार दलने बांध पीड़ितों के आंदोलन हेतु बिगुल बजाया जो अहमदनगर जिले के किसान आंदोलन एक यशस्वी आंदोलन के रूप में समझा जाता है। बेघर भूमिहीन किसान तथा मजदूरों की विपन्न अवस्था में वे बांध के वास्ते मृत्यु' को गले लगान सके, पुनर्वासके साथ बांध योजना इस तत्व के अनुसरण में अहमदनगर के साम्यवादी दल के अनुयायियों ने 'गोदावरी बांध परिषद' की सहयोग में राज्यव्यापी आंदोलन जारी रखने का ऐलान किया और उसे जिम्मेदारी के साथ निभाया।

1. जायकवाडी बांध योजना का ऐलान

तत्कालीन जलसंधारण मंत्री शंकरराव चौहान ने जनवरी 1965 में ख्यातनाम नदी गोदावरी एवं पैठण के पश्चिम दिशा में स्थित 'कावसन' गांव में जायकवाडी बांध निर्माण करने का ऐलान किया। जायकवाडी बांध की ऊंचाई 120 फीट और लंबाई 7मीलथी। इसकी बृहददीवारलगभग 120 फीट की थी। इस बांध से उपलब्ध पानी लगभग 25 मील दूर और 12 से लेकर 15 मील चौड़ाई के अहाते में रहनेवाला था।बांध का कुल खर्चा 70 करोड़ था। बांध की एक ओर 115 मील तथा दूसरी ओर 178 मील की दो नहरे निकालने का ऐलान किया गया।' सामान्यतः यह बांध मराठवाड़ा के अकाल को दूर करके वहां

★ इतिहास विभागाध्यक्ष,राधाबाई काळे महिला महाविद्यालय, अहमदनगर

★ ★ हिंदी विभागाध्यक्ष एस.एस.जी.एम.कॉलेज,कोपरगांव, जि. अहमदनगर

शैक्षिक, व्यवसायिक, औद्योगिक विकास की दृष्टि के तहत बांध निर्माण किया जा रहा था।¹ इस बांध परियोजना से मराठवाड़ा की 7.5 लाख एकड़ जमीन जलसिंचनमें आने वाली थी।² इसलिए जायकवाडी बांध परियोजना मराठवाड़ा के चहुँमुखी विकास की एक मौलिक चाबी प्रतीत हो रही थी।

2. जायकवाडी बांध पीड़ितों के सत्याग्रह आंदोलन की नींव

महाराष्ट्र के तत्कालीन मुख्यमंत्री यशवंतराव चौहान ने 7 दिसंबर 1960 में स.गो.बर्वे की अध्यक्षता में समिति गठित की थी।³ प्रस्तुत समिति ने पुनर्वास के बारे में निम्न सूचनाएं दी—बांध परियोजना में जिन किसानों की जमीन शासन ने अपने कब्जे में की हैं, उनके लिये पुनर्वास योजना तैयार करना और परियोजना के साथ ही मंजूर होना अनिवार्य है।⁴ गुल्हाटी समिति के सम्मुख महाराष्ट्र की ओर से महाराष्ट्र शासन ने अकाल से पीड़ितों को इस योजना में सबसे पहले हक देने का मुद्दा प्रस्तुत किया था। लेकिन जायकवाडी बांध के ऐलान में शासन ने इसके बारे में कोई भी प्रारूपण प्रस्तुत नहीं किया। अतः 1962 की बर्वे सिंचन समिति की सिफारिशों को रोकने की संभावनाएं किसानों में तीव्र होने लगी। इस बांध के कारण शेवगांव, नेवासा, पैठण तथा गंगापुर जैसे चार तहसीलों के 66 गांव, 7 लाख किंवटल से ज्यादा जवार फसल देने वाली 92 हजार एकड़ उपजाऊ जमीन और लगभग एक लाख से ज्यादा लोग बेघर होने वाले थे। इनमें से शेवगांव तहसील के 20 और नेवासा तहसील के 24 गांव बांध में डूबने वाले थे।⁵ स्वातंत्र्योत्तर महाराष्ट्र में वीर, पानशेत तथा कोयना इन बांध पीड़ितों के ढेर सारे प्रश्नों को सरकार ने अनदेखा किया था। इसलिए कई लोग दिशाहीन हो गए थे अतः 'वीर' बांध परियोजना परिषद के सामने भारतीय कम्युनिस्ट दल के कॉमरेड वसंतराव तुळपुळे ने 'पहले पुनर्वास फिर बांध' यह नारा देकर बांधों के आंदोलन का बिगुल बजाया था।⁶

बांध परियोजना निर्माण और उससे संबंधित प्रश्नों के कारण विपन्न किसानों ने नापसंदगी दिखाई। पैठण में आयोजित कांग्रेस की सभा में अहमदनगर के कांग्रेस अध्यक्ष घुले पाटील ने शंकरराव चव्हाण की निंदा की। उनकी राय द्रष्टव्य है, "जायकवाडी बांध परियोजना की जगह जब निश्चित की गई तब शंकर चव्हाण और बाळासाहेब भारदे ने बांध की जगह यदि बदलने का प्रस्ताव भी सामने आया तो वे उसका जमकर विरोध करते क्योंकि शेवगांव, नेवासा तथा पैठण इन तहसीलों में साम्यवादी दल का काफी प्रभाव था और उनका प्रभाव या असर कम करने हेतु उनकी धनयुक्त जमीन को जल परियोजना में डूबने पर उन्हें बेघर करने का एक सुअवसर प्राप्त हो रहा था। इसलिए सत्ताधारियों ने अपनी पूरी शक्ति इस कार्य में लगाई।⁷

साम्यवादियों ने 1 मार्च 1965 में शेवगांव तहसील के 'आगरनांदुर' में बांध पीड़ितों की एक सभा कॉमरेड नाना पाटील की अगुवाई में आयोजित की। इस परिषद में 'गोदावरी बांध परिषद' की स्थापना की गई। इस संगठन के सचिव कॉमरेड वसंतराव तुळपुळे, अध्यक्ष कॉमरेड विश्वनाथ कर्डिले थे। पुनर्वास प्रश्नके बारे में 'गोदावरी बांध परिषद' में कई मांगें स्वीकृत की गईं।

1. पुनर्वास का आलेखन तैयार करके उसे बांध परियोजना में स्थान मिलना चाहिए।
2. बांध में जिनकी जमीन जाने वाली है, उन्हें उतनी ही जमीन नहर पानी की मिलनी चाहिए।
3. जमीन का कब्जा लेते समय नई जमीन हक का ठहराव शीघ्र तैयार होना चाहिए।
4. पुनर्वास बांध योजना में गैर किसान को समाकर उन्हें उचित आर्थिक मदद करनी चाहिए।
5. बांध विकास में तबाह हो गई जमीन पर जितना भी कर्ज का बोझ हो उसे मिटाया जाए।
6. सरकार बांध पीड़ितों की संतानों को मुफ्त में शिक्षा देने का ऐलान करें।

सरकार ने उपर्युक्त बातों की ओर गौर करके उनपर यथाशीघ्र अमल करके उन्हें पूर्ण किया जाए।⁸ साथ इन मांगों की पूर्ति हेतु किसानों ने आंदोलन के लिए तैयार होने का नारा दिया।

3. जायकवाडी बांध और सत्याग्रह आंदोलन का प्रारंभ:

संगमनेरककॉमरेड दत्ता देशमुख ने जायकवाडी बांध पीड़ितों के असंतोष का अध्ययन करके 'गोदावरी परियोजना व महाराष्ट्र शासन' इस प्रकाशित निबंध में जायकवाडी बांध योजनाअशासकीय होने तथा गलत जगह पर निर्माण करने के प्रति मुहर लगाई।⁹ सरकार ने इस खयाल की ओर अनदेखा किया। इसलिए कॉमरेड विश्वनाथ पाटील कर्डिले एवं कॉमरेड एकनाथ भागवत केमोरचा में तत्कालीन मुख्यमंत्री वसंतराव नाईक बांध स्थल को देखने हेतु पधारे उस वक्त साम्यवादियों ने 2000 किसानों के मोर्चा में उन्हें आवेदन दिया।

महाराष्ट्र राज्य के सब बांध पीड़ितों की सभा का आयोजन दिनांक 26 तथा 27 जून 1965 को हुआ। जिसकी अध्यक्षता कॉमरेड डांगे ने की और यह सभा 'महाराष्ट्र राज्य बांध और पुनर्वास परिषद' तथा साम्यवादी दल के निर्देशन में हुई। इसमें काकासाहेब गाडगीळ ने जायकवाडी बांध योजनाका सबसे ज्यादा फायदा महाराष्ट्र के अलावा आंध्र प्रदेश को होने वाली बात कहकर इस योजना पर प्रश्नचिह्न लगाने का प्रयास किया। इसलिए गोदावरी घाटमें बन रहे महाराष्ट्र केबांधों का अधिक खर्चा उठाने संबंधी प्रस्ताव यदि आ भी जाता है तो उसे मंजूर करने का सवाल निर्माण न हो इस लिये तत्कालीन केंद्रीय जलसंधारन मंत्री के.एल.राव नेजायकवाडी बांध को अतिशीघ्र मंजूरी दी। परिणामतः गोदावरी का ज्यादातर पानी आंध्र प्रदेश को ही मिलने वाला है यह निश्चितहो गया।¹⁰

बाँध और पुनर्वास परिषदकेआदेश मुताबिक 29 जुलाई 1965 में मुंबई कोअहमदनगर जिले के हजारों बांध पीड़ित किसानों का विधानसभा पर मोरचानिकाला। उन्होंने सरकार को यह इशारा दिया कि पुनर्वास के प्रश्नों को कानून के तौर पर हक प्रदान नहीं किया तो प्रस्तुत बांध योजना को रोका जाएगा। महाराष्ट्र शासन ने इस बात की ओर अनदेखा करके जायकवाडी बांध परियोजना निर्माण हेतु भूमिपूजन समारोह को 18 अक्टूबर 1965 में प्रधानमंत्री लाल बहादुर शास्त्री के कर कमलों से निश्चित किया। साम्यवादी दल ने इस समारोह के खिलाफ बिगुल बजाया। पुलिसों की सजगता में भूमि पूजन के पहले कॉमरेड एकनाथ भागवत, कॉमरेड अचपळराव लांडेपाटील, कॉमरेड शशिकांत कुलकर्णी आदि साम्यवादी अनुयायियों को गिरफ्तार कर नासिक के हरसुल नामक कारागृह में बंद किया और भूमि पूजा समारोह संपन्न होने पर उन्हें रिहा किया।¹¹ इससे यह स्पष्ट होता है कि सरकार की ऐसी मनचाही भूमिका में कहीं ना कहीं उनकी तानाशाही भूमिका प्रतीत होती है। गोदावरी बांध परिषद द्वारा नियुक्त सभासद मंडल नेभुतपूर्व प्रधानमंत्री लाल बहादुर शास्त्री के सामने बांध पीड़ितों के प्रश्न प्रकट किए जिसे प्रधानमंत्री लाल बहादुर शास्त्री ने अपनी स्वीकृति दी। "जिन बांध पीड़ितों को जिस गांव में पुनर्वासके लिए जमीन मिलेगी वहाँ जलसिंचन तथा पीने के लिए यथा योग्य पानी की सुविधा मिले।" उन्होंने इसकी सूचना महाराष्ट्र शासन को दी।¹² इसके बावजूद महाराष्ट्र सरकार ने परियोजना पीड़ितों के लिए यथा योग्य सुविधाएं न देने के कारण 18 मार्च 1966 में हो गई महाराष्ट्र राज्य बांध परिषद की कार्यकारी मंडल की सभा में पुनर्वास के अधिनियम के लिए गोदावरी बांध परिषद ने सत्याग्रह की राह पर कूच करके गोदावरी बांध कार्य रोकने का निर्णय लिया।¹³

ऊपरी फैसले के मुताबिक 14 मई 1966 को कॉमरेड रामराव पाटील थोरात के अगुवाई में, 19 मई को एरंडगांव के सरपंच कॉमरेड चंद्रभान पाटील के अगुआपन में; 26 मई को नेवासा तहसील के वकीलराव लंघे, 2 जून 1966 को कॉमरेड विश्वनाथ पाटील कर्डिले के आगुआपन में सत्याग्रह किए जिसमें क्रमशः 29, 77, 130, 114 अनुयायी प्रतिभागी हुए थे और इन्हें कई दिनों का कारावास भी हुआ था।¹⁴ 9 जून को श्रमिक महिला परिषद की अध्यक्ष वत्सलाबाई भागवत, अंजनाबाई दादा पाटील, सीताबाई काशीनाथ कर्डिले और सत्यभामा विश्वनाथ पाटील के आगुआपन में 101 किसान महिला सत्याग्रही की टुकड़ी ने सत्याग्रह करके बांध का कारोबार पूर्ण रूप से बंद किया। हालाँकि क्रेन वाहक डोजर तथा रोडरोलर को अपने कब्जे में करने वाली 24 महिलाओं को पुलिस ने हिरासत में लिया था। शेष महिलाओं

ने पूरा दिन क्रेन वाहक के सम्मुख बैठकर अपना आंदोलन किया। शाम पाँच बजे आयोजित की गई सभा में अगले आंदोलन के स्वरूप की दिशा तय करने में अपने पारिवारिक सदस्यों को भी इस आंदोलन में प्रतिभागी करने का नारा दिया गया।¹⁵ महिलाओं के इसी प्रयास में आंदोलन को एक मौलिक दिशा मिल गई।

4. जायकवाडी बांध और पुनर्वास में सरकार की भूमिका:

महाराष्ट्र शासन ने 'जायकवाडी बांध परियोजना' के ऐलान के पश्चात बांध पीड़ितों के पुनर्वास संबंधी एकयोजनाबनाई। जिसके अनुसार सरकार ने 1884 के भूसंपादन अधिनियम के तहत 1000 रुपये की क्षतिपूर्ति की रकम देनी चाही। मगर यह मदद विलंब से मिलने के कारण बांध पीड़ितों का असंतोष बढ़ गया। इसलिए सन 1965 में सरकार ने 'पुनर्वास मंडल' की स्थापना की। इसका कार्यक्षेत्र केवल बांध पीड़ितों को क्षतिपूर्ति के लिए आर्थिक बँटवारा ही थाना की पुनर्वास की कानूनी योजना बनाना। उसमें उन्होंने 1 एकड़ के लिए 1000 रुपये के बदले 2000 रुपये कर दिए थे फिर भी महंगाई के परिप्रेक्ष्य में यह रकम काफी न थी इसलिए आंदोलन जारी रहा।¹⁶

'महाराष्ट्र राज्य बांध एवं पुनर्वास परिषद' का दूसरा अधिवेशन अहमदनगर में 18 मार्च 1969 में कॉमरेड डांगे की अध्यक्षता में संपन्न हुआ। इस अधिवेशन के परिणाम स्वरूप सरकार ने किसानों की क्षतिपूर्ति की केवल नाममात्र रकम बढ़ाकर विद्रोही लोगों को खुश करने की कोशिश की। इसमें किसानों के जमीन का उचित साक्ष्यपत्र न देना, भ्रष्टाचार तथा किसानों के अज्ञान का नाजायद फायदा लेकर किसानों के कानूनी हक को नकारने कार्य प्रशासकीय अधिकारी कर रहे थे यह इल्जाम कॉमरेड डांगे ने किया। डांगे की राय से किसानों के लिए 'पुनर्वास कानून' ही एकमात्र राहत देने में सक्षम है। उसके लिए आवश्यक अधिनियम की आवश्यकता है और बांधपीड़ितों पर हो रहे सितम को रोकने हेतु उन्होंने एक कार्यक्रम सप्ताह का नारा दिया। इसके अनुसार 2 से लेकर 9 अप्रैल तक महाराष्ट्र में जहाँ कहीं पुनर्वास के प्रश्न हैं उन तहसिलों में सप्ताह में हर रोज सैकड़ों किसानों का जमघट तहसीलदार कार्यालय या कचहरी के सामने करने का ऐलान किया।¹⁷ यदि सरकार इसकी ओर अनदेखा करेगी तब महाराष्ट्र के प्रशासकीय अधिकारी तथा मंत्रीगण को रोकने की बात तय हो गई।

परिषद के आदेश के अनुसार शेवगांव में 9 अप्रैल को कॉमरेड विश्वनाथ कर्डिले के आगुआपन में पहले 98 और बाद में 68 किसानों ने 144 दफा खारिज करके कचहरी के सम्मुख सत्याग्रह किया। पी.बी. कडुपाटील की आगुआपन में राहुरी में 45 किसानों के सहयोग में सत्याग्रह किया। उन्हें 7 दिनों का कारावास मिला। जिन्हें कारावास मिला उनमें पुणे की कॉमरेड कमलाबाई भागवत, कॉमरेड विश्वनाथ कर्डिले, कॉमरेड बाबासाहेब नागवडे, कॉमरेड वकील राव लंधे, कॉमरेड पी.बी. कडु, कॉमरेड चंद्रभान थोरात आदि का समावेश था।¹⁸ इन्हें येरवड़ा कारागृह में भेज दिया गया। इस तरह क्षतिपूर्ति के प्रयास में सरकार की ओर से केवल नाममात्र प्रयास हुआ जिसका खंडन साम्यवाद के अनुयायियों ने बलपूर्वक करके आंदोलन को योग्य दिशा दी।

5. बांध पीड़ितों को जमीन और आर्थिक क्षतिपूर्ति करने का अधिनियम:

जायकवाडी बांध पीड़ितों के निरंतर आंदोलन के कारण महाराष्ट्र सरकार को इसकी ओर ध्यान आकृष्ट करना पड़ा। जायकवाडी बांध में भूमिहीन हुए किसानों, मजदूरों अथवा वंचितों को जमीन देने का फैसला लिया गया। नये पुनर्वास में पाठशाला, बिजली, पीने का पानी, अस्पताल आदि अत्यावश्यक सुविधाएँ नए गांव में स्थापित करने में सरकारके कटिबद्ध होने का ऐलान है। अगले छह माह में शेवगांव, नेवासा तहसील के बांध को 30 हजार एकड़ जमीन का बँटवारा किया जाएगा। इसकी घोषणा तत्कालीन राज्य पुनर्वासमंत्री माननीय शरद पवार ने 20 जुलाई 1974 को शेवगांव में आयोजित सभा में की।¹⁹

नेवासा तहसील के भूतपूर्व विधायक कॉमरेड वकीलराव लंघे की आगुआपनमें स्थापित समिति ने माननीय शरद पवार के सम्मुख बांध पीड़ितों को सीलिंग की सीमा तक जमीन उपलब्ध कराने की माँग की। शरद पवारजी ने अतिशीघ्र बांध पीड़ितों का पुनर्वास के संबंधी अधिनियम करने का विश्वास व्यक्त किया।²⁰

सन 1976 में महाराष्ट्र सरकार ने बांध पीड़ितों के 'पुनर्वास अधिनियम' को मंजूरी दी। इसके अनुसार

1. बांध पीड़ितों को सीलिंग सीमा के तहत सरकार की ओर जमीन प्रदान की जाएगी।
2. यदि किसानों को जमीन के बदले आर्थिक क्षतिपूर्ति की चाहत है तो उसे आर्थिक भुगतान दिया जाए।
3. ग्रामस्थल के गृह निर्माण के तहत किसान को उसके पारिवारिक सदस्य संख्या के मुताबिक भूखंड प्रदान किए जाएं। भूमिहीन किसान मजदूर व्यापारी अथवा उद्योजक को 186 से 280 चौरस मीटर के भूखंड देने का प्रावधान हो।

सन 1976 के अधिनियम को कानूनी दर्जा प्राप्त हुआ और पुनर्वास परियोजना के निर्वाह हेतु नेक प्रणाली तैयार करने की बात तय हो गई।²¹ मगर प्रावधान में कुछ समस्याएँ निर्माण हो गईं। बाढ़ पीड़ितों को जमीन देने का प्रावधान अधिनियम में करने पर भी सरकार पर इसका बंधन न था। पुनर्वास गाँव में वहाँ के बड़े जमींदार जमीन देने में आनाकानी कर रहे थे। इसलिए अनेक किसानों को आर्थिक रूप में सहायता देने का प्रयास रहा जिसे बांध पीड़ितों ने टुकराया। अतः गोदावरी बांध परिषद के नेताओं ने बांध पीड़ितों के सुशिक्षित युवकों को नौकरी में 10 प्रतिशत आरक्षण देने, बेघरों को 1500 रुपये में मकान देने, खेतीकार्य के लिए मुफ्त में बिजली, आंतरिक सड़क, सुजल एवं पाठशालाओं का इंतजाम करने की माँग पुनर्वास मंत्री प्रतापराव भोसले के सम्मुख रखी थी जिसपर यथायोग्य अमल करने का विश्वास परिषद के नेताओं को प्रतापराव भोसले ने दिया।²²

6. जायकवाड़ी बांध प्रथम के आंदोलन की फल निष्पत्ति:

सन 1976 के पुनर्वास अधिनियम के तहत कई बांध पीड़ितों का मूल गाँव के नजिक पुनर्वास किया गया। जायकवाड़ी बांध निर्माण में शेवगांव तथा नेवासा के जो गाँव डूब गए थे वहाँ के रास्ते, पाठशाला एवं अस्पतालकी 70 प्रतिशत तक की कार्यपूर्ति सन 1978 ई. तक पूरी की गई।²³ बांध पीड़ितों को सन 1979 तक मकान के लिए 94 लाख तथा जमीन खरीदी के लिए 4.8 करोड़ रुपये दिए गए। बांध पीड़ितों की संतानों के लिए सरकारी नौकरी में 10 प्रतिशत जगह आरक्षित की।²⁴ शेवगांव तहसील के बांध पीड़ितों को जिस गाँव में जमीन मिली, उन जमीनों के सिंचन की सुविधा हेतु जायकवाड़ी बांध योजना से पानी उठाकर ताजनापुर गाँव से लिफ्ट के माध्यम से कर देने की माँग की गई थी। सरकार ने 'ताजनापुर' लिफ्ट योजना को मंजूरी दी लेकिन यह योजना शुरू होने में विलंब हुआ।²⁵

1976 के पुनर्वास अधिनियम से बांध पीड़ित असंतुष्ट थे। जिन किसानों की जमीन बांध में गई उन किसानों की बहुत कम क्षतिपूर्ति होने का इल्जाम साम्यवादियों ने किया। कुछ किसानों ने कोर्ट कचहरी के जरिए यथा योग्य क्षतिपूर्ति कर ली थी। साथ ही कुछ किसानों को पुनर्वास के आहाते में जमीन प्राप्त नहीं हो सकी। उपरी दिक्कतों के अलावा 1976 में महाराष्ट्र सरकार ने पुनर्वास कानून के जरिए जायकवाड़ी बांध पीड़ितों के पुनर्वास करने का जो प्रयास किया, उससे बांध सरकार के प्रति का क्रोधभाव कम होने में मदद हो गई। बांध के प्रारूपण के साथ ही पुनर्वास प्रारूप तैयार हो जाना चाहिए। जमीन के बदले जमीन और मकान के बदले मकान देने के कानूनी अधिकार मिलने चाहिए। इस तरह की साम्यवादी नेताओं की दृढ़ता एवं तदसंबंधी के आंदोलन को अनुपम सफलता मिल गई। यह साम्यवादी दल को प्राप्त हुई सबसे बड़ी कामयाबी समझी जाती है।

निष्कर्ष:

1. जायकवाडी बांध परियोजना की कार्य गतिविधियों के स्पष्ट प्रारूपण को विशद न करके उसका ऐलानबांध पीड़ितों को धोखा देने के समान प्रतीत होता है।
2. साम्यवादियोंका अकालग्रस्त मराठवाड़ा के विकास के खातिर सरकारी योजनाओं के प्रति विरोध न था। बांध के जरिए एक प्रदेश के विकास के साथ-साथ वहां के अनगिनत लोगों का विस्थापनसाम्यवादियोंको नामंजूर था।
3. कोयना और वीर बांध योजना में पुनर्वासके दर्द को पूरी तरह मिटाया नहीं था। इसलिए 'पहले पुनर्वास फिर बांध योजना' इस खयाल को सम्मुख रखकर 'गोदावरी बांध परिषद' के माध्यम से बांध पीड़ितों का भव्य मोर्चा मार्क्सवादियों ने खड़ा करके लगभग दो शतक तक सरकार के साथ अथक संघर्ष करने का ऐलान ही उनके योगदान पर प्रकाश डालता है।
4. सन 1894 ई. के भूमिअधिग्रहण अधिनियम की तहत सरकार का बांध परियोजना ग्रस्त या पीड़ितों को मराठवाड़ा के विकास के नाम पर सितम करने का प्रयास शुरूसे देखा जाता है। साम्यवाद के दबाव तथा जन आंदोलन के परिणाम स्वरूप 1976 के पुनर्वास अधिनियम के प्रावधानों के अनुसार पीड़ितों को अपने गाँव के नजीक पुनर्वास की सुविधा देकर महाराष्ट्र सरकार ने लोगों केअसंतोष को कम जरूर किया है, इसमें कोई संदेह नहीं है।

संदर्भ सूची:

1. तुळपुळे, मालिनी, कॉमरेड वसंतराव तुळपुळे: कार्य व परिचय, शलाका प्रकाशन मुंबई 1979,पृ.85
2. पाक्षिक 'युगांतर', महाराष्ट्र राज्य कम्युनिस्ट पक्ष का मुखपत्र, दिनांक 25 जुलाई 1965,पृ.3.
3. राजदेव, त्रिंबक, महाराष्ट्र के विकास में कॉमरेड दत्ता देशमुख का कार्य(अप्रकाशित शोधप्रबंध),डॉ. बाबासाहेब आंबेडकर मराठवाडा विद्यापीठ,औरंगाबाद,2002,पृ. 213 और 214.
4. डीतौतं 'जंजम पतपहंजपवद ब्वउउपेपवद त्मचवतजए 1962ए च्त्पदजमक जंजीम ळवअमतदउमदज च्त्मेए छंहचनतए 1962ए चण116ण
5. तुळपुळे, वसंतराव, महाराष्ट्र राज्य धोरण व पुनर्वसन परिषद 26,27 जून 1965 अहवाल,कल्पना मुद्रणालय,पुणे, 1965, पृ. 14.
6. तैत्रव,पृ. 2
7. गवंडी, पुंडलिक, लाल सूर्य, अमोल प्रकाशन, नारायण पेठ पुणे,20 नवंबर 199, पृ. 139.
8. पक्षिक, 'युगांतर', महाराष्ट्र राज्य कम्युनिस्ट दल का एजेंडा (मुखपत्र). दि. 14/03/1965, पृ. 13.
9. कॉमरेड देशमुख, दत्ता, गोदावरी परियोजना और महाराष्ट्र शासन सिंचन आयोग, दैनिक केसरी, दिनांक 3 व 4 जून 1965(पुनर्मुद्रित).
10. पक्षिक, 'युगांतर', महाराष्ट्र राज्य कम्युनिस्ट दल का एजेंडा (मुखपत्र), दिनांक 25 जुलाई 1965,पृ. 13
11. कॉमरेड पवार, कृष्णा, साक्षात्कार, दिनांक 15 नोव्हेंबर 2015, भूतपूर्व तहसिल सचिव भाकप,शेवगाव जि. अहमदनगर.
12. लाड श्रीकांत (संपादक), भारतीय कम्युनिस्ट दल के 50 वर्ष, भारतीय कम्युनिस्ट दल प्रकाशन, मुंबई, जनवरी 1976, पृ. 56.
13. दैनिक नगर टाइम्स, वर्ष प्रथम, अंक 170, दिनांक 2 मे 1966, पृ.2.
14. पाक्षिक, 'युगांतर', महाराष्ट्र राज्य कम्युनिस्ट दल का मुखपत्र, दिनांक 12 जून पृ.1.
15. पाक्षिक, 'युगांतर', महाराष्ट्र राज्य कम्युनिस्ट दल का मुखपत्र,दिनांक 19 जून 1966 पृ. 3 व 8.

जायकवाडी बांध आंदोलन में जिला अहमदनगर के साम्यवादी दल का योगदान

★ प्रा.डॉ. विघाटे गणेश शंकर ★★ डॉ.राजाराम कानडे

सारांश:

जायकवाडी जलसिंचन परियोजना में सरकार की भूमिका और विस्थापित लोगों पर हुए सितम के कारण, विस्थापितों का पुनर्वास संबंधी प्रश्नों की ओर सरकार का नजरअंदाज की वजह से उभरा जन आंदोलन को सही अंजाम देने की भूमिका में अहमदनगर जिले के साम्यवादी दल के योगदान को उजागर करने के प्रयोजन में प्रस्तुत शोध आलेख पाठक, संशोधक को आंदोलन के प्रति सजग करेगा। इसमें जन आंदोलन के बढ़ते प्रभाव के कारण सरकार द्वारा पारित विभिन्न अधिनियम की जानकारी है। साथ ही आंदोलन कर्मियों का विश्वास कायम रखने के प्रयास में साम्यवादी अनुयायियों का अथक प्रयास ही मानवतावादी विचारधारा की तरफ पाठक को ले जाता है।

महत्त्वपूर्ण शब्द:

महाराष्ट्र राज्य सरकार तथा साम्यवादी भूमिका की फल निष्पत्ति.

उद्देश्य:

1. जायकवाडी जलसिंचन परियोजना निर्माण में सरकार की भूमिका पर प्रकाश डालना।
2. बांध निर्माण कार्य में पीड़ितों की मानसिकता को उजागर करना एवं जन आंदोलन के विषय पर प्रकाश डालना।
3. साम्यवादी विचारकों की भूमिका और उनका मानवतावादी प्रयास की दिशा पर प्रकाश डालना।
4. जायकवाडी बांध निर्माण एवं जन आंदोलन की शुरुआत और पुनर्वास संबंधी अधिनियम के प्रति वाचक कोसजग करना।
5. बांध पीड़ितों के आंदोलन की दिशा और फलनिष्पत्ति का अध्ययन करना।

प्रस्तावना:

महाराष्ट्र की मशहूर नदी गोदावरीके तट पे स्थित 'पैठण' के समीप स्थापितजायकवाडी बांध के कारण विस्थापित हुए किसान, खेती मजदूरों के आवास के प्रश्नों पर अहमदनगर के साम्यवादी विचार दलने बांध पीड़ितों के आंदोलन हेतु बिगुल बजाया जो अहमदनगर जिले के किसान आंदोलन एक यशस्वी आंदोलन के रूप में समझा जाता है। बेघर भूमिहीन किसान तथा मजदूरों की विपन्न अवस्था में वे बांध के वास्ते मृत्यु' को गले लगान सके, पुनर्वासके साथ बांध योजना इस तत्व के अनुसरण में अहमदनगर के साम्यवादी दल के अनुयायियों ने 'गोदावरी बांध परिषद' की सहयोग में राज्यव्यापी आंदोलन जारी रखने का ऐलान किया और उसे जिम्मेदारी के साथ निभाया।

1. जायकवाडी बांध योजना का ऐलान

तत्कालीन जलसंधारण मंत्री शंकरराव चौहान ने जनवरी 1965 में ख्यातनाम नदी गोदावरी एवं पैठण के पश्चिम दिशा में स्थित 'कावसन' गांव में जायकवाडी बांध निर्माण करने का ऐलान किया। जायकवाडी बांध की ऊंचाई 120 फीट और लंबाई 7मीलथी। इसकी बृहददीवारलगभग 120 फीट की थी। इस बांध से उपलब्ध पानी लगभग 25 मील दूर और 12 से लेकर 15 मील चौड़ाई के अहाते में रहनेवाला था।बांध का कुल खर्चा 70 करोड़ था। बांध की एक ओर 115 मील तथा दूसरी ओर 178 मील की दो नहरे निकालने का ऐलान किया गया।' सामान्यतः यह बांध मराठवाड़ा के अकाल को दूर करके वहां

★ इतिहास विभागाध्यक्ष,राधाबाई काळे महिला महाविद्यालय, अहमदनगर

★ ★ हिंदी विभागाध्यक्ष एस.एस.जी.एम.कॉलेज,कोपरगांव, जि. अहमदनगर

शैक्षिक, व्यवसायिक, औद्योगिक विकास की दृष्टि के तहत बांध निर्माण किया जा रहा था।¹ इस बांध परियोजना से मराठवाड़ा की 7.5 लाख एकड़ जमीन जलसिंचनमें आने वाली थी।² इसलिए जायकवाडी बांध परियोजना मराठवाड़ा के चहुँमुखी विकास की एक मौलिक चाबी प्रतीत हो रही थी।

2. जायकवाडी बांध पीड़ितों के सत्याग्रह आंदोलन की नींव

महाराष्ट्र के तत्कालीन मुख्यमंत्री यशवंतराव चौहान ने 7 दिसंबर 1960 में स.गो.बर्वे की अध्यक्षता में समिति गठित की थी।³ प्रस्तुत समिति ने पुनर्वास के बारे में निम्न सूचनाएं दी—बांध परियोजना में जिन किसानों की जमीन शासन ने अपने कब्जे में की हैं, उनके लिये पुनर्वास योजना तैयार करना और परियोजना के साथ ही मंजूर होना अनिवार्य है।⁴ गुल्हाटी समिति के सम्मुख महाराष्ट्र की ओर से महाराष्ट्र शासन ने अकाल से पीड़ितों को इस योजना में सबसे पहले हक देने का मुद्दा प्रस्तुत किया था। लेकिन जायकवाडी बांध के ऐलान में शासन ने इसके बारे में कोई भी प्रारूपण प्रस्तुत नहीं किया। अतः 1962 की बर्वे सिंचन समिति की सिफारिशों को रोकने की संभावनाएं किसानों में तीव्र होने लगी। इस बांध के कारण शेवगांव, नेवासा, पैठण तथा गंगापुर जैसे चार तहसीलों के 66 गांव, 7 लाख किंवटल से ज्यादा जवार फसल देने वाली 92 हजार एकड़ उपजाऊ जमीन और लगभग एक लाख से ज्यादा लोग बेघर होने वाले थे। इनमें से शेवगांव तहसील के 20 और नेवासा तहसील के 24 गांव बांध में डूबने वाले थे।⁵ स्वातंत्र्योत्तर महाराष्ट्र में वीर, पानशेत तथा कोयना इन बांध पीड़ितों के ढेर सारे प्रश्नों को सरकार ने अनदेखा किया था। इसलिए कई लोग दिशाहीन हो गए थे अतः 'वीर' बांध परियोजना परिषद के सामने भारतीय कम्युनिस्ट दल के कॉमरेड वसंतराव तुळपुळे ने 'पहले पुनर्वास फिर बांध' यह नारा देकर बांधों के आंदोलन का बिगुल बजाया था।⁶

बांध परियोजना निर्माण और उससे संबंधित प्रश्नों के कारण विपन्न किसानों ने नापसंदगी दिखाई। पैठण में आयोजित कांग्रेस की सभा में अहमदनगर के कांग्रेस अध्यक्ष घुले पाटील ने शंकरराव चव्हाण की निंदा की। उनकी राय द्रष्टव्य है, "जायकवाडी बांध परियोजना की जगह जब निश्चित की गई तब शंकर चव्हाण और बाळासाहेब भारदे ने बांध की जगह यदि बदलने का प्रस्ताव भी सामने आया तो वे उसका जमकर विरोध करते क्योंकि शेवगांव, नेवासा तथा पैठण इन तहसीलों में साम्यवादी दल का काफी प्रभाव था और उनका प्रभाव या असर कम करने हेतु उनकी धनयुक्त जमीन को जल परियोजना में डूबने पर उन्हें बेघर करने का एक सुअवसर प्राप्त हो रहा था। इसलिए सत्ताधारियों ने अपनी पूरी शक्ति इस कार्य में लगाई।⁷

साम्यवादियों ने 1 मार्च 1965 में शेवगांव तहसील के 'आगरनांदुर' में बांध पीड़ितों की एक सभा कॉमरेड नाना पाटील की अगुवाई में आयोजित की। इस परिषद में 'गोदावरी बांध परिषद' की स्थापना की गई। इस संगठन के सचिव कॉमरेड वसंतराव तुळपुळे, अध्यक्ष कॉमरेड विश्वनाथ कर्डिले थे। पुनर्वास प्रश्नके बारे में 'गोदावरी बांध परिषद' में कई मांगें स्वीकृत की गईं।

1. पुनर्वास का आलेखन तैयार करके उसे बांध परियोजना में स्थान मिलना चाहिए।
2. बांध में जिनकी जमीन जाने वाली है, उन्हें उतनी ही जमीन नहर पानी की मिलनी चाहिए।
3. जमीन का कब्जा लेते समय नई जमीन हक का ठहराव शीघ्र तैयार होना चाहिए।
4. पुनर्वास बांध योजना में गैर किसान को समाकर उन्हें उचित आर्थिक मदद करनी चाहिए।
5. बांध विकास में तबाह हो गई जमीन पर जितना भी कर्ज का बोझ हो उसे मिटाया जाए।
6. सरकार बांध पीड़ितों की संतानों को मुफ्त में शिक्षा देने का ऐलान करें।

सरकार ने उपर्युक्त बातों की ओर गौर करके उनपर यथाशीघ्र अमल करके उन्हें पूर्ण किया जाए।⁸ साथ इन मांगों की पूर्ति हेतु किसानों ने आंदोलन के लिए तैयार होने का नारा दिया।

3. जायकवाडी बांध और सत्याग्रह आंदोलन का प्रारंभ:

संगमनेरककॉमरेड दत्ता देशमुख ने जायकवाडी बांध पीड़ितों के असंतोष का अध्ययन करके 'गोदावरी परियोजना व महाराष्ट्र शासन' इस प्रकाशित निबंध में जायकवाडी बांध योजनाअशासकीय होने तथा गलत जगह पर निर्माण करने के प्रति मुहर लगाई।⁹ सरकार ने इस खयाल की ओर अनदेखा किया। इसलिए कॉमरेड विश्वनाथ पाटील कर्डिले एवं कॉमरेड एकनाथ भागवत केमोरचा में तत्कालीन मुख्यमंत्री वसंतराव नाईक बांध स्थल को देखने हेतु पधारे उस वक्त साम्यवादियों ने 2000 किसानों के मोर्चा में उन्हें आवेदन दिया।

महाराष्ट्र राज्य के सब बांध पीड़ितों की सभा का आयोजन दिनांक 26 तथा 27 जून 1965 को हुआ। जिसकी अध्यक्षता कॉमरेड डांगे ने की और यह सभा 'महाराष्ट्र राज्य बांध और पुनर्वास परिषद' तथा साम्यवादी दल के निर्देशन में हुई। इसमें काकासाहेब गाडगीळ ने जायकवाडी बांध योजनाका सबसे ज्यादा फायदा महाराष्ट्र के अलावा आंध्र प्रदेश को होने वाली बात कहकर इस योजना पर प्रश्नचिह्न लगाने का प्रयास किया। इसलिए गोदावरी घाटमें बन रहे महाराष्ट्र केबांधों का अधिक खर्चा उठाने संबंधी प्रस्ताव यदि आ भी जाता है तो उसे मंजूर करने का सवाल निर्माण न हो इस लिये तत्कालीन केंद्रीय जलसंधारन मंत्री के.एल.राव नेजायकवाडी बांध को अतिशीघ्र मंजूरी दी। परिणामतः गोदावरी का ज्यादातर पानी आंध्र प्रदेश को ही मिलने वाला है यह निश्चितहो गया।¹⁰

बाँध और पुनर्वास परिषदकेआदेश मुताबिक 29 जुलाई 1965 में मुंबई कोअहमदनगर जिले के हजारों बांध पीड़ित किसानों का विधानसभा पर मोरचानिकाला। उन्होंने सरकार को यह इशारा दिया कि पुनर्वास के प्रश्नों को कानून के तौर पर हक प्रदान नहीं किया तो प्रस्तुत बांध योजना को रोका जाएगा। महाराष्ट्र शासन ने इस बात की ओर अनदेखा करके जायकवाडी बांध परियोजना निर्माण हेतु भूमिपूजन समारोह को 18 अक्टूबर 1965 में प्रधानमंत्री लाल बहादुर शास्त्री के कर कमलों से निश्चित किया। साम्यवादी दल ने इस समारोह के खिलाफ बिगुल बजाया। पुलिसों की सजगता में भूमि पूजन के पहले कॉमरेड एकनाथ भागवत, कॉमरेड अचपळराव लांडेपाटील, कॉमरेड शशिकांत कुलकर्णी आदि साम्यवादी अनुयायियों को गिरफ्तार कर नासिक के हरसुल नामक कारागृह में बंद किया और भूमि पूजा समारोह संपन्न होने पर उन्हें रिहा किया।¹¹ इससे यह स्पष्ट होता है कि सरकार की ऐसी मनचाही भूमिका में कहीं ना कहीं उनकी तानाशाही भूमिका प्रतीत होती है। गोदावरी बांध परिषद द्वारा नियुक्त सभासद मंडल नेभुतपूर्व प्रधानमंत्री लाल बहादुर शास्त्री के सामने बांध पीड़ितों के प्रश्न प्रकट किए जिसे प्रधानमंत्री लाल बहादुर शास्त्री ने अपनी स्वीकृति दी। "जिन बांध पीड़ितों को जिस गांव में पुनर्वासके लिए जमीन मिलेगी वहाँ जलसिंचन तथा पीने के लिए यथा योग्य पानी की सुविधा मिले।" उन्होंने इसकी सूचना महाराष्ट्र शासन को दी।¹² इसके बावजूद महाराष्ट्र सरकार ने परियोजना पीड़ितों के लिए यथा योग्य सुविधाएं न देने के कारण 18 मार्च 1966 में हो गई महाराष्ट्र राज्य बांध परिषद की कार्यकारी मंडल की सभा में पुनर्वास के अधिनियम के लिए गोदावरी बांध परिषद ने सत्याग्रह की राह पर कूच करके गोदावरी बांध कार्य रोकने का निर्णय लिया।¹³

ऊपरी फैसले के मुताबिक 14 मई 1966 को कॉमरेड रामराव पाटील थोरात के अगुवाई में, 19 मई को एरंडगांव के सरपंच कॉमरेड चंद्रभान पाटील के अगुआपन में; 26 मई को नेवासा तहसील के वकीलराव लंघे, 2 जून 1966 को कॉमरेड विश्वनाथ पाटील कर्डिले के आगुआपन में सत्याग्रह किए जिसमें क्रमशः 29, 77, 130, 114 अनुयायी प्रतिभागी हुए थे और इन्हें कई दिनों का कारावास भी हुआ था।¹⁴ 9 जून को श्रमिक महिला परिषद की अध्यक्ष वत्सलाबाई भागवत, अंजनाबाई दादा पाटील, सीताबाई काशीनाथ कर्डिले और सत्यभामा विश्वनाथ पाटील के आगुआपन में 101 किसान महिला सत्याग्रही की टुकड़ी ने सत्याग्रह करके बांध का कारोबार पूर्ण रूप से बंद किया। हालाँकि क्रेन वाहक डोजर तथा रोडरोलर को अपने कब्जे में करने वाली 24 महिलाओं को पुलिस ने हिरासत में लिया था। शेष महिलाओं

ने पूरा दिन क्रेन वाहक के सम्मुख बैठकर अपना आंदोलन किया। शाम पाँच बजे आयोजित की गई सभा में अगले आंदोलन के स्वरूप की दिशा तय करने में अपने पारिवारिक सदस्यों को भी इस आंदोलन में प्रतिभागी करने का नारा दिया गया।¹⁵ महिलाओं के इसी प्रयास में आंदोलन को एक मौलिक दिशा मिल गई।

4. जायकवाडी बांध और पुनर्वास में सरकार की भूमिका:

महाराष्ट्र शासन ने 'जायकवाडी बांध परियोजना' के ऐलान के पश्चात बांध पीड़ितों के पुनर्वास संबंधी एकयोजनाबनाई। जिसके अनुसार सरकार ने 1884 के भूसंपादन अधिनियम के तहत 1000 रुपये की क्षतिपूर्ति की रकम देनी चाही। मंगर यह मदद विलंब से मिलने के कारण बांध पीड़ितों का असंतोष बढ़ गया। इसलिए सन 1965 में सरकार ने 'पुनर्वास मंडल' की स्थापना की। इसका कार्यक्षेत्र केवल बांध पीड़ितों को क्षतिपूर्ति के लिए आर्थिक बँटवारा ही थाना की पुनर्वास की कानूनी योजना बनाना। उसमें उन्होंने 1 एकड़ के लिए 1000 रुपये के बदले 2000 रुपये कर दिए थे फिर भी महंगाई के परिप्रेक्ष्य में यह रकम काफी न थी इसलिए आंदोलन जारी रहा।¹⁶

'महाराष्ट्र राज्य बांध एवं पुनर्वास परिषद' का दूसरा अधिवेशन अहमदनगर में 18 मार्च 1969 में कॉमरेड डांगे की अध्यक्षता में संपन्न हुआ। इस अधिवेशन के परिणाम स्वरूप सरकार ने किसानों की क्षतिपूर्ति की केवल नाममात्र रकम बढ़ाकर विद्रोही लोगों को खुश करने की कोशिश की। इसमें किसानों के जमीन का उचित साक्ष्यपत्र न देना, भ्रष्टाचार तथा किसानों के अज्ञान का नाजायद फायदा लेकर किसानों के कानूनी हक को नकारने कार्य प्रशासकीय अधिकारी कर रहे थे यह इल्जाम कॉमरेड डांगे ने किया। डांगे की राय से किसानों के लिए 'पुनर्वास कानून' ही एकमात्र राहत देने में सक्षम है। उसके लिए आवश्यक अधिनियम की आवश्यकता है और बांधपीड़ितों पर हो रहे सितम को रोकने हेतु उन्होंने एक कार्यक्रम सप्ताह का नारा दिया। इसके अनुसार 2 से लेकर 9 अप्रैल तक महाराष्ट्र में जहाँ कहीं पुनर्वास के प्रश्न हैं उन तहसिलों में सप्ताह में हर रोज सैकड़ों किसानों का जमघट तहसीलदार कार्यालय या कचहरी के सामने करने का ऐलान किया।¹⁷ यदि सरकार इसकी ओर अनदेखा करेगी तब महाराष्ट्र के प्रशासकीय अधिकारी तथा मंत्रीगण को रोकने की बात तय हो गई।

परिषद के आदेश के अनुसार शेवगांव में 9 अप्रैल को कॉमरेड विश्वनाथ कर्डिले के आगुआपन में पहले 98 और बाद में 68 किसानों ने 144 दफा खारिज करके कचहरी के सम्मुख सत्याग्रह किया। पी.बी. कडुपाटील की आगुआपन में राहुरी में 45 किसानों के सहयोग में सत्याग्रह किया। उन्हें 7 दिनों का कारावास मिला। जिन्हें कारावास मिला उनमें पुणे की कॉमरेड कमलाबाई भागवत, कॉमरेड विश्वनाथ कर्डिले, कॉमरेड बाबासाहेब नागवडे, कॉमरेड वकील राव लंधे, कॉमरेड पी.बी. कडु, कॉमरेड चंद्रभान थोरात आदि का समावेश था।¹⁸ इन्हें येरवड़ा कारागृह में भेज दिया गया। इस तरह क्षतिपूर्ति के प्रयास में सरकार की ओर से केवल नाममात्र प्रयास हुआ जिसका खंडन साम्यवाद के अनुयायियों ने बलपूर्वक करके आंदोलन को योग्य दिशा दी।

5. बांध पीड़ितों को जमीन और आर्थिक क्षतिपूर्ति करने का अधिनियम:

जायकवाडी बांध पीड़ितों के निरंतर आंदोलन के कारण महाराष्ट्र सरकार को इसकी ओर ध्यान आकृष्ट करना पड़ा। जायकवाडी बांध में भूमिहीन हुए किसानों, मजदूरों अथवा वंचितों को जमीन देने का फैसला लिया गया। नये पुनर्वास में पाठशाला, बिजली, पीने का पानी, अस्पताल आदि अत्यावश्यक सुविधाएँ नए गांव में स्थापित करने में सरकारके कटिबद्ध होने का ऐलान है। अगले छह माह में शेवगांव, नेवासा तहसील के बांध को 30 हजार एकड़ जमीन का बँटवारा किया जाएगा। इसकी घोषणा तत्कालीन राज्य पुनर्वासमंत्री माननीय शरद पवार ने 20 जुलाई 1974 को शेवगांव में आयोजित सभा में की।¹⁹

नेवासा तहसील के भूतपूर्व विधायक कॉमरेड वकीलराव लंघे की आगुआपनमें स्थापित समिति ने माननीय शरद पवार के सम्मुख बांध पीड़ितों को सीलिंग की सीमा तक जमीन उपलब्ध कराने की माँग की। शरद पवारजी ने अतिशीघ्र बांध पीड़ितों का पुनर्वास के संबंधी अधिनियम करने का विश्वास व्यक्त किया।²⁰

सन 1976 में महाराष्ट्र सरकार ने बांध पीड़ितों के 'पुनर्वास अधिनियम' को मंजूरी दी। इसके अनुसार

1. बांध पीड़ितों को सीलिंग सीमा के तहत सरकार की ओर जमीन प्रदान की जाएगी।
2. यदि किसानों को जमीन के बदले आर्थिक क्षतिपूर्ति की चाहत है तो उसे आर्थिक भुगतान दिया जाए।
3. ग्रामस्थल के गृह निर्माण के तहत किसान को उसके पारिवारिक सदस्य संख्या के मुताबिक भूखंड प्रदान किए जाएं। भूमिहीन किसान मजदूर व्यापारी अथवा उद्योजक को 186 से 280 चौरस मीटर के भूखंड देने का प्रावधान हो।

सन 1976 के अधिनियम को कानूनी दर्जा प्राप्त हुआ और पुनर्वास परियोजना के निर्वाह हेतु नेक प्रणाली तैयार करने की बात तय हो गई।²¹ मगर प्रावधान में कुछ समस्याएँ निर्माण हो गईं। बाढ़ पीड़ितों को जमीन देने का प्रावधान अधिनियम में करने पर भी सरकार पर इसका बंधन न था। पुनर्वास गाँव में वहाँ के बड़े जमींदार जमीन देने में आनाकानी कर रहे थे। इसलिए अनेक किसानों को आर्थिक रूप में सहायता देने का प्रयास रहा जिसे बांध पीड़ितों ने टुकराया। अतः गोदावरी बांध परिषद के नेताओं ने बांध पीड़ितों के सुशिक्षित युवकों को नौकरी में 10 प्रतिशत आरक्षण देने, बेघरों को 1500 रुपये में मकान देने, खेतीकार्य के लिए मुफ्त में बिजली, आंतरिक सड़क, सुजल एवं पाठशालाओं का इंतजाम करने की माँग पुनर्वास मंत्री प्रतापराव भोसले के सम्मुख रखी थी जिसपर यथायोग्य अमल करने का विश्वास परिषद के नेताओं को प्रतापराव भोसले ने दिया।²²

6. जायकवाड़ी बांध प्रथम के आंदोलन की फल निष्पत्ति:

सन 1976 के पुनर्वास अधिनियम के तहत कई बांध पीड़ितों का मूल गाँव के नजिक पुनर्वास किया गया। जायकवाड़ी बांध निर्माण में शेवगांव तथा नेवासा के जो गाँव डूब गए थे वहाँ के रास्ते, पाठशाला एवं अस्पताल की 70 प्रतिशत तक की कार्यपूर्ति सन 1978 ई. तक पूरी की गई।²³ बांध पीड़ितों को सन 1979 तक मकान के लिए 94 लाख तथा जमीन खरीदी के लिए 4.8 करोड़ रुपये दिए गए। बांध पीड़ितों की संतानों के लिए सरकारी नौकरी में 10 प्रतिशत जगह आरक्षित की।²⁴ शेवगांव तहसील के बांध पीड़ितों को जिस गाँव में जमीन मिली, उन जमीनों के सिंचन की सुविधा हेतु जायकवाड़ी बांध योजना से पानी उठाकर ताजनापुर गाँव से लिफ्ट के माध्यम से कर देने की माँग की गई थी। सरकार ने 'ताजनापुर' लिफ्ट योजना को मंजूरी दी लेकिन यह योजना शुरू होने में विलंब हुआ।²⁵

1976 के पुनर्वास अधिनियम से बांध पीड़ित असंतुष्ट थे। जिन किसानों की जमीन बांध में गई उन किसानों की बहुत कम क्षतिपूर्ति होने का इल्जाम साम्यवादियों ने किया। कुछ किसानों ने कोर्ट कचहरी के जरिए यथा योग्य क्षतिपूर्ति कर ली थी। साथ ही कुछ किसानों को पुनर्वास के आहाते में जमीन प्राप्त नहीं हो सकी। उपरी दिक्कतों के अलावा 1976 में महाराष्ट्र सरकार ने पुनर्वास कानून के जरिए जायकवाड़ी बांध पीड़ितों के पुनर्वास करने का जो प्रयास किया, उससे बांध सरकार के प्रति का क्रोधभाव कम होने में मदद हो गई। बांध के प्रारूपण के साथ ही पुनर्वास प्रारूप तैयार हो जाना चाहिए। जमीन के बदले जमीन और मकान के बदले मकान देने के कानूनी अधिकार मिलने चाहिए। इस तरह की साम्यवादी नेताओं की दृढ़ता एवं तदसंबंधी के आंदोलन को अनुपम सफलता मिल गई। यह साम्यवादी दल को प्राप्त हुई सबसे बड़ी कामयाबी समझी जाती है।

निष्कर्ष:

1. जायकवाडी बांध परियोजना की कार्य गतिविधियों के स्पष्ट प्रारूपण को विशद न करके उसका ऐलानबांध पीड़ितों को धोखा देने के समान प्रतीत होता है।
2. साम्यवादियोंका अकालग्रस्त मराठवाड़ा के विकास के खातिर सरकारी योजनाओं के प्रति विरोध न था। बांध के जरिए एक प्रदेश के विकास के साथ-साथ वहां के अनगिनत लोगों का विस्थापनसाम्यवादियोंको नामंजूर था।
3. कोयना और वीर बांध योजना में पुनर्वासके दर्द को पूरी तरह मिटाया नहीं था। इसलिए 'पहले पुनर्वास फिर बांध योजना' इस खयाल को सम्मुख रखकर 'गोदावरी बांध परिषद' के माध्यम से बांध पीड़ितों का भव्य मोर्चा मार्क्सवादियों ने खड़ा करके लगभग दो शतक तक सरकार के साथ अथक संघर्ष करने का ऐलान ही उनके योगदान पर प्रकाश डालता है।
4. सन 1894 ई. के भूमिअधिग्रहण अधिनियम की तहत सरकार का बांध परियोजना ग्रस्त या पीड़ितों को मराठवाड़ा के विकास के नाम पर सितम करने का प्रयास शुरूसे देखा जाता है। साम्यवाद के दबाव तथा जन आंदोलन के परिणाम स्वरूप 1976 के पुनर्वास अधिनियम के प्रावधानों के अनुसार पीड़ितों को अपने गाँव के नजीक पुनर्वास की सुविधा देकर महाराष्ट्र सरकार ने लोगों केअसंतोष को कम जरूर किया है, इसमें कोई संदेह नहीं है।

संदर्भ सूची:

1. तुळपुळे, मालिनी, कॉमरेड वसंतराव तुळपुळे: कार्य व परिचय, शलाका प्रकाशन मुंबई 1979,पृ.85
2. पाक्षिक 'युगांतर', महाराष्ट्र राज्य कम्युनिस्ट पक्ष का मुखपत्र, दिनांक 25 जुलाई 1965,पृ.3.
3. राजदेव, त्रिंबक, महाराष्ट्र के विकास में कॉमरेड दत्ता देशमुख का कार्य(अप्रकाशित शोधप्रबंध),डॉ. बाबासाहेब आंबेडकर मराठवाडा विद्यापीठ,औरंगाबाद,2002,पृ. 213 और 214.
4. डींतीतं 'जंजम प्ततपहंजपवद ब्वउउपेपवद त्मचवतजए 1962ए च्तपदजमक जंजीम ळवअमतदउमदज च्तमेए छंहचनतए 1962ए चण116ण
5. तुळपुळे, वसंतराव, महाराष्ट्र राज्य धोरण व पुनर्वसन परिषद 26,27 जून 1965 अहवाल,कल्पना मुद्रणालय,पुणे, 1965, पृ. 14.
6. तैत्रव,पृ. 2
7. गवंडी, पुंडलिक, लाल सूर्य, अमोल प्रकाशन, नारायण पेठ पुणे,20 नवंबर 199, पृ. 139.
8. पक्षिक, 'युगांतर', महाराष्ट्र राज्य कम्युनिस्ट दल का एजेंडा (मुखपत्र). दि. 14/03/1965, पृ. 13.
9. कॉमरेड देशमुख, दत्ता, गोदावरी परियोजना और महाराष्ट्र शासन सिंचन आयोग, दैनिक केसरी, दिनांक 3 व 4 जून 1965(पुनर्मुद्रित).
10. पक्षिक, 'युगांतर', महाराष्ट्र राज्य कम्युनिस्ट दल का एजेंडा (मुखपत्र), दिनांक 25 जुलाई 1965,पृ. 13
11. कॉमरेड पवार, कृष्णा, साक्षात्कार, दिनांक 15 नोव्हेंबर 2015, भूतपूर्व तहसिल सचिव भाकप,शेवगाव जि. अहमदनगर.
12. लाड श्रीकांत (संपादक), भारतीय कम्युनिस्ट दल के 50 वर्ष, भारतीय कम्युनिस्ट दल प्रकाशन, मुंबई, जनवरी 1976, पृ. 56.
13. दैनिक नगर टाइम्स, वर्ष प्रथम, अंक 170, दिनांक 2 मे 1966, पृ.2.
14. पाक्षिक, 'युगांतर', महाराष्ट्र राज्य कम्युनिस्ट दल का मुखपत्र, दिनांक 12 जून पृ.1.
15. पाक्षिक, 'युगांतर', महाराष्ट्र राज्य कम्युनिस्ट दल का मुखपत्र,दिनांक 19 जून 1966 पृ. 3 व 8.

५. अहमदनगर जिल्ह्यातील लाल निशाण गट व लालनिशाण पक्ष

प्रा. डॉ. विधाटे गणेश शंकर

इतिहास विभाग, राधाबाई काळे महिला महाविद्यालय, अहमदनगर, ता. जि. अहमदनगर.

महत्वाचे शब्द - कामगार किसान पक्ष, सिलींग, स्टेट फार्म कॉर्पोरेशन, खंडकरी, विडी सिंगार कायदा, जागला,

शोधनिबंधाचा उद्देश

१. लाल निशाण गटाच्या स्थापनेची कारणमीमांसा स्पष्ट करणे.
२. लाल निशाण गटाचे लाल निशाण पक्षात झालेल्या स्थित्यंतराचा आढावा घेणे.
३. कॉम्रेड दत्ता देशमुख यांच्या लाल निशाण पक्षातील योगदानाचा आढावा घेणे.
४. ट्रेड युनियन चळवळीतील लाल निशाण पक्षाच्या कामगिरीचा मागोवा घेणे.
५. शेतकरी व शेतमजुरांच्या चळवळीतील लाल निशाण पक्षाच्या कामगिरीचा मागोवा घेणे.
६. राजकीय पटलावरून लाल निशाण पक्षाच्या अस्ताची कारणमीमांसा स्पष्ट करणे व त्याचे डाव्या चळवळीवर झालेल्या परिणामांचा आढावा घेणे.

प्रस्तावना

अहमदनगर जिल्हा हा आशिया खंडात सहकार चळवळीचा पाया रचणारा महत्वाचा जिल्हा होय. हा जिल्हा स्वातंत्र्यपूर्व आणि स्वातंत्र्यानंतर १९८० च्या दशकापर्यंत डाव्या चळवळीचा जिल्हा म्हणून ओळखला जात होता. या डाव्या पक्षांमधील भारतीय कम्युनिस्ट पक्षाच्या खालोखाल लाल निशाण गट व लाल निशाण पक्षाने अहमदनगर जिल्ह्यातील वंचित वर्गाच्या उन्नतीसाठी केलेल्या विविध आंदोलनांमुळे त्याला जनसामान्यांचा चांगले समर्थन प्राप्त झाले होते. मार्क्सवाद-लेनिनवादाची तत्त्वे अंगीकारून या पक्षाने आपल्या पक्षाला बौद्धिकदृष्ट्या भारतीय कम्युनिस्ट पक्षाशी जोडून ठेवण्याचा प्रयत्न केला आहे. प्रस्तुत शोध निबंधात अहमदनगर जिल्ह्यातील कम्युनिस्ट पक्षाच्या समांतर लाल निशाण गट व लाल निशाण पक्षाने विविध चळवळींच्या संदर्भात केलेल्या कार्याचा आढावा घेण्यात आला आहे.

लाल निशाण गटाची स्थापना

१९५२ च्या निवडणुकीत डाव्या पक्षांना आलेल्या अपयशामुळे कामगार किसान पक्षातील कार्यकर्त्यांनी कामगार किसान पक्ष बरखास्त केला. पक्षाची ही पडझड पाहून कॅ. क्रांतिसिंह नाना पाटील यांनी कम्युनिस्ट पक्षात प्रवेश केला. उर्वरित कार्यकर्त्यांनी आपली भूमिका विशद करण्यासाठी 'लालनिशाण' साप्ताहिक काढले. पुढे १९५५ मध्ये कॅ. दत्ता देशमुख, कॅ. बापूसाहेब भापकर, कॅ. एस. के. लिमये, कॅ. यशवंत चव्हाण, कॅ. संतराम पाटील, कॅ. आबासाहेब काकडे, कॅ. नागनाथ नायकवाडी, कॅ. व्ही.एम. पाटील, भाई सथ्या यांनी लाल निशाण गटाची स्थापना केली. कम्युनिस्ट पक्षात सामील होण्याच्या धोरणामुळे लाल निशाण गटाने पक्ष स्थापन केला

नाही.^१ मुंबईसहित संयुक्त महाराष्ट्राच्या आंदोलनात लाल निशाण गटाने जिल्ह्यात इतर डाव्या पक्षांच्या मदतीने मोठी चळवळ उभारली. मुंबईसह संयुक्त महाराष्ट्राची एकमुखी केलेली मागणी डावलून १६ जानेवारी १९५६ रोजी मुंबई केंद्रशासित प्रदेश घोषित करण्याचा निर्णय पं. नेहरूंनी जाहीर करताच संयुक्त महाराष्ट्र समितीच्या आदेशावरून लाल निशाण गटाच्या का. बापूसाहेब भापकर यांनी जिल्हा लोकल बोर्डाचा व नगरपालिका सदस्यत्वाचा तर का. भास्करराव औटी यांनी राज्य विधानसभेचा राजीनामा दिला.^२ १९५७ च्या निवडणुकीच्या वेळी संयुक्त महाराष्ट्र समितीच्या तिकीटावर लाल निशाण गटाचे ८ आमदार निवडून आले. त्यात अहमदनगर जिल्ह्यातील ४ आमदारांचा समावेश होता. त्यामुळे अहमदनगर जिल्ह्यात लाल निशाण पक्षाला मानाचे स्थान प्राप्त झालेले दिसते.^३

लाल निशाण गट लाल निशाण पक्ष म्हणून संघटन व उद्दिष्ट

संयुक्त महाराष्ट्राच्या निर्मितीनंतर समिती मधील पक्षांमध्ये बेबनाव वाढू लागला. १९६२ साली संयुक्त महाराष्ट्र समितीत फाटाफुट झाली. काँग्रेसच्या बेरजेच्या राजकारणाला बळी पडून नगर जिल्ह्यातील डाव्या पक्षातील अनेक कार्यकर्ते काँग्रेस पक्षात सामील झाले. लाल निशाण गटाने कम्युनिस्ट पक्षात सामील होण्याचा निर्णय घेतला. परंतु १९६४ साली कम्युनिस्ट पक्षात फुट पडून कम्युनिस्ट चळवळीत विस्कळीतपणा आला. त्यामुळे लाल निशाण गटाने (दत्ता देशमुख गटाने) 'लाल निशाण' पक्ष म्हणून संघटित करण्याचा निर्णय १९६५ साली घेतला व पक्षाचे मुखपत्र म्हणून 'लालनिशाण' हे पाक्षिक सुरू केले. १९६२ च्या सार्वत्रिक निवडणुकीनंतर निवडणुकीचे स्वरूप पालटले. तात्त्विक मुद्यांवरून लढविल्या जाणाऱ्या निवडणुका धनशक्तीवर लढविल्या जाऊ लागल्या. त्यामुळे 'लालनिशाण पक्ष' असे नामाभिधान धारण करूनही निवडणुकांपासून लालनिशाण पक्ष दूरच राहिला. निवडणुकीमध्ये शक्ति व सामर्थ्य खर्ची न करण्याचे धोरण पक्षाने स्वीकारले व कष्टकरी समुदायाला जागृत व संघटित करण्याला प्राधान्य दिले.^४

लाल निशाण पक्षाचे अहमदनगर जिल्हा लोकल बोर्डातील कार्य

लालनिशाण पक्षाने शहरापासून ते गावपातळीपर्यंत कामगारांसाठीच्या संघटना बांधणीवर आपले लक्ष केंद्रित केले. १९५२-५३ साली नगर जिल्हा लोकल बोर्डात लाल निशाण गटाचे बहुमत होते. त्याचा संघटनात्मक बांधणीसाठी लाल निशाण गटाने उपयोग केला. लाल निशाणने लोकल बोर्डातर्फे टुप्काळी कामे केली. सार्वजनिक बांधकाम खाते, रस्त्यावरील मैल बिगार्यांना व पाटबंधारे कामगारांना अतिशय वेतन कमी होते. त्यांच्या सेवेची शाश्वती नव्हती. त्यांना नोकरीत कायम करावे, मासिक पगार द्यावा इत्यादी मागण्या लाल निशाण पक्षाने केल्या. सरकारने त्यासाठी कालेलकर यांचे अध्यक्षतेखाली समिती नेमली. या समितीवर कां. मधुकर कात्रे यांची निवड करण्यात आली. वरील खात्यातील हजारो कामगारांना कायम करणे, त्यांचे रोजंदारीचे दर व अन्य सेवाशर्ती लागू करणे या कमी त्यांनी अपार मेहनत घेतली. १९६७ साली सरकारने कालेलकर कमिशनच्या शिफारसी लागू केल्यामुळे हजारो कामगारांना त्याचा लाभ झालेला दिसतो. हे करत असतांना कामगारांचे जाणतेपण वाढविण्याचे काम पक्षाने केले. त्यामुळे नगर जिल्हा लोकल बोर्डाचा लौकिक वाढण्यास मदत झाली.^५ सरकारी नोकर संघटनेला राज्यव्यापी स्वरूप देण्यात अहमदनगरच्या लाल निशाण गटाच्या कां. दिनकरराव कलावडे यांचे महत्वाचे

योगदान होते. राज्य सरकारी कर्मचऱ्यांची पहिली परिषद एप्रिल १९६२ मध्ये लाल निशाण गटाने अहमदनगरला भरविली होती. कॅ. र. ग. कर्णिक हे राज्य कर्मचारी संघटनेचे सरचिटणीस होते. जिल्ह्यातील सरकारी-निमसरकारी, कामगार-कर्मचारी व शिक्षकांच्या एकजुटीच्या परिषदा १९७४ साला पासून लालनिशाण पक्षाने भरविण्यास सुरुवात केली होती. १९७७-७८ च्या १० लक्ष कामगार, कर्मचारी, शिक्षक, कोतवाल यांच्या ५४ दिवसांच्या ऐतिहासिक संपाचे नेतृत्व करणाऱ्या समन्वय समितीची पायाभरणी नगर जिल्ह्यातील या चळवळीने केलेली दिसते.^६

स्टेट फार्म कॉर्पोरेशनमधील लाल निशाण पक्षाचे योगदान

१९६२ साली महाराष्ट्र सरकारने सिर्लीगचा कायदा पास केला. सिर्लीगचा मुळ उद्देश बऱ्या जमीनदारांच्या जमिनी काढून घेऊन त्या भूमिहीन शेतकऱ्यांना वाटणे हा होता. ज्या शेतकऱ्यांनी अल्प खंडाने व दिर्घ मुदतीने आपल्या जमिनी साखर कंपनीला लागवडीसाठी दिल्या होत्या त्या जमिनी सिर्लीगच्या नावावर सरकारने साखर कंपन्यांकडून काढून घेतल्या व त्यांचे स्टेट फार्म कॉर्पोरेशन स्थापन केले. लाल निशाण गटाने स्टेट फार्म कॉर्पोरेशनच्या स्थापनेत महत्वाची भूमिका बजावलेली दिसते. कॅ. दत्ता देशमुख हे स्टेट फार्म कॉर्पोरेशनच्या संचालक मंडळाचे सभासद होते.^७ किसान सभा व कम्युनिस्ट चालवत असलेल्या खंडकरी शेतकऱ्यांचा लढा बागायतदारांचा असून कम्युनिस्ट बऱ्या बागायतदारांचे हित पाहत असल्याचा लालनिशाण पक्षाने आरोप केला. सरकारी शेती हे पुरोगामी पाऊल असून ते मोडण्याची भूमिका घेऊन किसान सभा व कम्युनिस्ट पक्ष खाजगी मालकीच्या शेतीचा पाठपुरावा करित आहेत. तसेच शेती महामंडळ मोडल्यामुळे महामंडळाकडील कामगार बेकार होणार आहेत. त्यामुळे काँग्रेस, समाजवादी व कम्युनिस्टांची ही भूमिका कामगार विरोधी असल्याचा ठपका ठेवून अहमदनगर जिल्हा लालनिशाण पक्षाने कम्युनिस्टांच्या अधिपत्याखालील खंडकरी शेतकऱ्यांच्या चळवळीला विरोध करण्याची भूमिका घेतली. त्यामुळे खंडकरी शेतकऱ्यांची चळवळ व स्टेट फार्मिंग कॉर्पोरेशन मोडीत काढण्याच्या प्रश्नावरून नगर जिल्ह्यात लाल निशाण विरुद्ध इतर पक्ष असा संघर्ष उभा राहिलेला दिसून येतो.^८

लाल निशाण पक्षाचे ट्रेड युनियन चळवळीमधील कार्य

संगमनेर व अकोले तालुक्यात का. रामभाऊ नागरे, कॅ. बी.डी. परब यांची लाल बावट्याची व साथी भास्करराव दुर्गे यांची समाजवाद्यांची अशा विडी कामगारांच्या दोन युनियन होत्या. या युनियनचे नेतृत्व करणारे पुढारी विडी कामगारांचे प्रश्न कोण अगोदर सोडवितो आहे, कामगारांना कोणी किती मजुरी व बोनस मिळवून दिला आहे याचाच पाढा वाचत असत. त्यामुळे एक प्रकारे विडी कामगारांच्या चळवळीत फुटीचे वातावरण तयार होवून कामगारांचे प्रश्न सुटण्यात अडचणी व अडथळे येऊ लागले. त्यामुळे विडी कामगार युनियनचे कामकाज एकजुटीने चालावे याकरिता लाल निशाण गटाच्या का. दत्ता देशमुख यांनी अकोले तालुक्यातील 'गणोरा' येथे परिषद घेऊन एकजुटीचा प्रयत्न केला. या परिषदेला का. क्रांतिसिंह नाना पाटील उपस्थित होते. का. दत्ता देशमुख हे 'विडी कामगारसमिती' युनियनचे अध्यक्षही होते.^९ संगमनेर, अकोले तालुक्यात विडी कामगारांची युनियन कम्युनिस्ट पक्षाच्या सहकार्याने उभी करण्यामध्ये लाल निशाण पक्षाच्या राधाकिसन सोनवणे, बाळा देशमुख, कॅ. मधुकर कात्रे, कॅ. काशीनाथ आळवणी यांनी भागीदारी केलेली दिसते. पुढे कम्युनिस्ट पक्षाच्या पुढार्यांनी १९६३ नंतर विडी कामगार युनियन मधून लाल निशाण पक्षाच्या पदाधिकऱ्यांची राजकीय कारणांसाठी हकालपट्टी केली. तरीही

पुढील ८ ते १० वर्षे नवीन संघटना न काढता लाल निशाणशी पक्षाला मानणार्या विडी कामगारांनी त्याच युनियन मध्ये रहावे, असे धोरण पक्षाने राबवले. पुढे १९६६ चा विडी सिंगार कायदा सन १९७१ मध्ये केंद्र सरकारने प्रत्यक्षात लागू केल्यावर संगमनेर, अकोले, सिन्नर भागातील कामगारांमध्ये मोठ्या अपेक्षा निर्माण झाल्या. मात्र तत्कालीन संघटना पुरेश्या कार्यक्षम नसल्याने कामगारांमध्ये नाराजी वाढली. तेव्हा सन १९७२ मध्ये कॅ. मधुकर कात्रे व कॅ. दत्ता देशमुख यांच्या मदतीने 'संगमनेर, अकोले, सिन्नर तालुका विडी कामगार समिती' या नावाने एक व्यासपीठ स्थापन करण्यात आले. १९६६ च्या विडी सिंगार विविध हक्क मिळवून घेण्यासाठी कामगारांचे अर्ज, तक्रारी भरून घेऊन कामगार खात्याकडे देण्याची मोहीम सुरु केली. मात्र अन्य संघटनांनी सरकारी पातळीवर याला आक्षेप घेतला. त्यामुळे कॅ. मधुकर कात्रे यांनी याच नावाने ट्रेड युनियन कायद्याखाली संघटनेची नोंदणी केली. सन १९७३ मध्ये ८०० सभासद संख्या असलेल्या ह्या युनियनची सभासद संख्या २००० सालापर्यंत ५००० च्या पुढे गेली. कॅ. दादाभाऊ देशमुख, कॅ. सुखदेव वर्णे, कॅ. वसंतराव मिस्त्री, कॅ. ता. गो. देशमुख, कॅ. गुलाबराव देशमुख आदी कार्यकर्त्यांनी कॅ. दत्ता देशमुख व कॅ. मधुकर कात्रे यांच्या मार्गदर्शनाखाली संगमनेर, अकोले, सिन्नर तालुका विडी कामगार युनियनचे कामकाज चालविले. मात्र जिल्ह्यातील लाल बावट्याच्या युनियनच्या तुलनेत या युनियनचे राजकीय व संघटनात्मक सामर्थ्य कमी असल्याचे दिसून येते.^{१०}

पश्चिम महाराष्ट्रात गावागावात 'जागल्याचे' काम करणारे ३५ हजार कोतवाल होते. त्यांना सरकारी नोकर म्हणून घ्यावे आणि पगारी नोकरदार म्हणून ठेवावे अशी मागणी नगर जिल्ह्यातील लाल निशाण पक्षाने केली. कोतवाल हा गावातील सर्वात तळाचा कामगार. त्याचीही राज्यव्यापी संघटना उभी करण्याचे काम लाल निशाण पक्षाने केले. पुढे ग्रामपंचायत, नगरपालिका कामगार, रेशन कार्डधारकांची संघटना उभारण्याचा प्रयत्न लाल निशाण पक्षाने केला.^{११}

नगर जिल्ह्यातील लाल निशाण पक्षाने साखर कामगार चळवळीत दिलेले योगदान हा त्यांच्या वाटचालीचा महत्त्वाचा टप्पा होय. १९५६ साली बेलवंडीच्या खाजगी साखर कारखान्यात लाल निशाण गटाच्या कॅ. रंगनाथ पंढरकर व कॅ. मधुकर कात्रे यांनी साखर कामगारांची व शेतीवरील कामगारांची नगर जिल्ह्यातील पहिली संघटना स्थापन केली.^{१२} राज्यातील साखर कामगार चळवळ ही बी.आय.आर. अॅक्ट या काळ्या कायद्याच्या जोखडात बांधली गेली होती. लाल निशाण पक्षाने नगर जिल्ह्यात संगमनेर, श्रीगोंदा, पारनेर, जगदंबा इत्यादी कारखान्यांमध्ये साखर कामगारांच्या प्रतिनिधिक संघटना उभारल्या होत्या. श्रीरामपूर, कोपरगाव भागात जुन्या संघटना होत्या. मात्र त्या संघटनांच्या कार्यक्षेत्रातील प्रवरा, टिळकनगर, हरेगाव, कोळपेवाडी, संजीवनी, लक्ष्मीवाडी, साखरवाडी इत्यादी कारखान्यांमधील कामगारांमध्ये व्यवस्थापनाकडून होणार्या पिळवणुकीविरुद्ध असंतोष होता. अशा वेळी लाल निशाण पक्षाचे पुढारी या कारखान्यांमधील कामगारांच्या मदतीला धावून जात असत. बी.आय.आर अॅक्टमधील काळ्या तरतुदींचा फायदा घेऊन कामगार वर्गावर मानसिक दबाव आणून युनियनचे प्रातिनिधिकत्व रद्द करणार्या व्यवस्थापनाला नमते घेण्यास लाल निशाण पक्षाच्या पुढार्यांनी यश प्राप्त केल्याचे दिसते.^{१३} १९८० साली महाराष्ट्रातील ऊस तोडणी आणि गाडीवान कामगारांचा पहिला यशस्वी संप लाल निशाण पक्षाच्या कॅ. मधुकर कात्रे यांनीच पुकारला होता. त्यातून साखर सम्राट व त्यांच्या इशार्यावर नाचणार्या राज्य

शासनाला पक्षाने वठणीवर आणले. कॅ. मधुकर कात्रे हे महाराष्ट्र राज्य साखर कामगार महासंघाचे सरचिटणीस होते. हा महासंघ पुढे साखर कामगारांची लढाऊ तुकडी म्हणून पुढे आला.^{१४}

१९५५ पासून नगर जिल्ह्यात शेतमजूर चळवळीची लाल निशाण गटाने उभारणी केली. कॅ. भास्करराव जाधव, कॅ. मधुकर कात्रे, कॅ. दत्ता देशमुख, कॅ. भि. र. बावके यांनी नगर जिल्ह्यात शेतमजुरांच्या अनेक संपात भागीदारी केली. ८ फेब्रुवारी १९७० रोजी श्रीरामपूर (जिल्हा अहमदनगर) येथे महाराष्ट्र राज्य भूमिहीन शेतमजूर व गरीब शेतकरी परिषद स्थापन करण्यात लाल निशाण, भाकप, माकप या पक्षांचा मोलाचा वाटा होता. कॅ. डांगे, कॅ. गोदावरी परुळेकर, कॅ. दत्ता देशमुख, साथी एस. एम. जोशी हे या परिषदेस उपस्थित होते. परिषदेत 'ज्याच्या हाताला नांगराचा घट्टा त्याच्या नावाने जमिनीचा पट्टा' असा जमिनविषयक ठराव पास करण्यात आला. १९७२-७३ च्या दुष्काळात दुष्काळी कामगारांच्या चळवळीने महाराष्ट्र ढवळून निघाला. १७ व १८ फेब्रुवारी १९७३ रोजी दहिवडी (जि. सातारा) येथे महाराष्ट्र राज्य भूमिहीन शेतमजूर व गरीब शेतकरी परिषदेचे अधिवेशन झाले. त्याचे अध्यक्ष कॅ. दत्ता देशमुख व प्रमुख पाहुणे प्रा. वि. म. दांडेकर व कॅ. एस.पी. मोहिते हे होते. कॅ. दत्ता देशमुख यांनी अध्यक्षपदावरून 'कफल्लक महाराष्ट्रीय कष्टकरी जनता आपल्या जुटीची मूठ वळून उभी राहिली आहे, या जनतेने स्वाभिमानाने आवाज काढला आहे की मला भीक नको, मला काम पाहिजे. मला केवळ पोटभरू काम नको. माझ्या भूमीला सुजला करणारे दुष्काळ निर्मूलनाचे काम पाहिजे' असा नियोजनपूर्वक श्रमशक्ती वापरून दुष्काळ निर्मूलनाचा विचार मांडला.^{१५} या परिषदेच्या माध्यमातून कॅ. दत्ता देशमुख व प्रा. वि. म. दांडेकर यांनी दुष्काळ निर्मूलन, पाणी प्रश्न आणि रोजगार यांची सांगड घालणारी प्रचंड चळवळ महाराष्ट्रात निर्माण केली. १६ मे १९७३ रोजी जिल्ह्यातील ३ लक्ष दुष्काळी कामगारांचा संप लाल निशाण पक्षाने संघटित केला. याच चळवळीतून रोजगार हमी कायदा निर्माण करणे महाराष्ट्र सरकारला भाग पडले.^{१६} १९७८ साली चळवळीला मदतीसाठी लाल निशाण पक्षाच्या कॅ. दत्ता देशमुख, कॅ. मधुकर कात्रे व कॅ. भास्करराव जाधव यांनी 'ग्रामीण श्रमिक' हे पाक्षिक वृत्तपत्र काढले.^{१७}

लाल निशाण पक्षातील वैचारिक मतभेद व पक्षात पडलेली फुट

भांडवलदारी सत्तेच्या विरोधात कामगार वर्गाच्या नेतृत्वाखाली जनतेची लोकशाही प्रस्थापित करणे हे लालनिशाण पक्षाचे धोरण होते. लालनिशाण पक्षातील कॅ. दत्ता देशमुख, कॅ. एस. के. लिमये, कॅ. संतराम पाटील यांना काँग्रेस पक्षातील रशिया, चीन बरोबर सहकार्य करू पाहणाऱ्या पं. नेहरू, इंदिरा गांधी, राजीव गांधी या पुरोगामी नेत्यांबद्दल आस्था वाढू लागली होती. काँग्रेसचे प्रतिगामी स्वरूप बदलून जनमाणसात तिला मूल्याधिष्ठित स्थान प्राप्त करून देण्याचा इंदिरा गांधी यांनी प्रयत्न केला होता. लालनिशाण पक्षाने इंदिरा गांधी आणि राजीव गांधी यांच्याशी देशातील खालावलेल्या राजकीय स्थितीवर चर्चा करतांना पुरोगामी म्हणविल्या जाणाऱ्या राजकीय पक्षांनी काँग्रेस विरोधासाठी अनेक राजकीय पक्षांशी युती करून प्रतिगामी व फुटीरतावादी शक्तींना मोकळी वाट करून दिल्याचा निष्कर्ष काढला. त्यांनी असे सूचित केली की, "कामगार कष्टकर्यांशी संबंध असलेल्या सर्व कम्युनिस्ट, समाजवादी, लोकशाहीवादी यांना धर्मांधांच्या विरोधात हाक देऊन देशव्यापी बांधणी करण्यासाठी एकजूट साधावी."^{१८} कॅ. दत्ता देशमुख व त्यांच्या सहकार्यांच्या या भूमिकेला पक्षातूनच विरोध होऊ

लागला व पक्षात दोन गट पडले. कॅ. भास्करराव जाधव, कॅ. कात्रे, कॅ. भोसले, कॅ. सुरेश गवळी यांनी लालनिशाण पक्ष (लेनिनवादी गट) या नावाने आपला वेगळा पक्ष स्थापन केला. या पक्षाने राजकीय निवडणुकांमध्ये कोणत्याही पक्षाचे समर्थन न करता अगर निवडणुकांमध्ये सहभागी न होता आपल्या पक्षाची चळवळ ट्रेड युनियन पुरतीच मर्यादित केली. कॅ. दत्ता देशमुख, कॅ. एस. के. लिमये, कॅ. संतराम पाटील यांच्या नेतृत्वाखालील लालनिशाण पक्षाचे ५ नोव्हेंबर १९८९ रोजी अधिवेशन भरले. त्यात कॅ. दत्ता देशमुख यांची लालनिशाण पक्षाच्या अध्यक्षपदी निवड करण्यात आली. कॅ. दत्ता देशमुख यांच्या लाल निशाण पक्षाने १९८९ व १९९१ मधील निवडणुकांमध्ये प्रतिगाम्यांचा पराभव करण्यासाठी काँग्रेस पक्षाला पाठिंबा दिला. कम्युनिस्ट पक्ष व इतर डावे पक्ष मात्र अलिप्त राहिल्याने जातीयवादी शक्तींना उधाण आलेले दिसते. नवजीवन संघटनेच्या स्थापनेपासून 'पक्ष अनेक असले तरी देशातील कामगारांची एकच एक संघटना असली पाहिजे, प्रत्येक थंड्यात एकच युनियन असली पाहिजे, पक्षवाचक युनियन बनता कामा नये किंवा फुटता कामा नये', अशी मूळच्या लालनिशाण पक्षाची भूमिका होती. मात्र आपल्या या घोषित भूमिकेनुसार लालनिशाण पक्षाचे धुरीणत्व व्यवहार करू शकले नाही. त्यामुळे लालनिशाण पक्षाची अहमदनगर जिल्ह्यातील राजकीय चळवळीची व ट्रेड युनियन चळवळीची मोठी हानी झाली.^{१९} कम्युनिस्ट पक्षाला उतरती कळा लागत असतांना लालनिशाण पक्षात पडलेल्या या फुटीमुळे अहमदनगर जिल्ह्यातील डाव्या पक्षांची चळवळ कमजोर झालेली दिसते.

निष्कर्ष

अहमदनगर जिल्हा हा जहाल डाव्या विचारांचा जिल्हा म्हणून ओळखला जात होता. १९५२ च्या निवडणुकीत आलेल्या अपयशाच्या पार्श्वभूमीवर लाल निशाण गट व पुढे लाल निशाण पक्षाची स्थापना झाली. संयुक्त महाराष्ट्र चळवळीच्या काळात संयुक्त महाराष्ट्र समितीच्या तिकिटावर या पक्षाने अहमदनगर जिल्ह्यात चार आमदार निवडून आणण्याची कामगिरी केली. लाल निशाण गट हा कम्युनिस्ट विचारांचा समर्थक असलेला पक्ष. मात्र संयुक्त महाराष्ट्राची निर्मितीमुळे समान कार्यक्रमाचा अभाव व १९६४ साली कम्युनिस्ट पक्षात पडलेल्या फुटीमुळे लाल निशाण गटाने कॉम्रेड दत्ता देशमुख यांच्या नेतृत्वाखाली लाल निशाण पक्ष म्हणून संघटीत होण्याचा निर्णय घेतला. निवडणुकीच्या राजकारणात न रमता आपले सामर्थ्य व मर्यादा याची जाणीव ठेवून या पक्षाने ट्रेड युनियन चळवळ, स्टेट फार्म कॉर्पोरेशन, कोतवालांचे प्रश्न, दुष्काळी कामांचे प्रश्न इत्यादी समस्यांवर आपले लक्ष केंद्रित केले. मात्र पुढे प्रतिगामी भांडवली, धर्मांध, फॅसिस्टविचारांच्या पक्षांना आवर घालण्यासाठी कॅ. दत्ता देशमुख, कॅ. एस. के. लिमये, कॅ. संतराम पाटील यांनी काँग्रेस पक्षाला सहकार्य करण्याची घेतलेली भूमिका लाल निशाण पक्षातील काही धुरिणांना न आवडल्याने लाल निशाण पक्षात फुट पडून अहमदनगर जिल्ह्यातील डाव्या विचारांच्या पक्षांची व चळवळीची मोठी हानी झाली. व पक्षाचे जिल्ह्याच्या राजकीय पटलावरील अस्तित्व कमी झालेले दिसते.

संदर्भसूची

१. शेवाळे विठ्ठल, संपादन, 'मी दत्ता दत्ता झालो त्याची गोष्ट', चि. स. लाटकर कल्पना मुद्रणालाय, सदाशिव पेठ, पुणे, ३०, पृ. क्र. ५०

२. भापकर रंगनाथ, 'क्रांतिगाथा-बापूसाहेब भापकर: जीवन व कार्य', गणराज प्रकाशन, अहमदनगर, प्रथमावृत्ती, ५ सप्टेंबर २०१४, पृ. क्र. ९१.
३. दैनिक सार्वमत, 'वर्धापन दिन विशेषांक-कर्तृत्वाचा ठेवा', दि. २६/०१/२०१३, पृ. क्र. २३.
४. शेवाळे विठ्ठल (संपा.), 'उज्ज्वल उद्यासाठी', (दिवंगत कॅ. दत्ता देशमुख विशेषांक) 'संघर्षयात्री', आनंद प्रिंटर्स, संगमनेर, त्रैमासिक नोव्हेंबर ते डिसेंबर २०१५, पृ. क्र. १५.
५. कॅ. मधुकर कात्रे यांच्या आठवणी व आत्मनिवेदन (राजकीय जडणघडण), कॅसेट क्रमांक ५, दि. २२/१०/२००६.
६. दैनिक लोकमत, 'नगर पंचशताब्दी विशेषांक', दि. ०२/०८/१९९०, पृ. क्र. १२९.
७. शेवाळे विठ्ठल, संपादन, 'मी दत्तूचा दत्ता झालो त्याची गोष्ट', उपरोक्त, पृ. क्र. १०५.
८. साप्ताहिक युगांतर, महाराष्ट्र राज्य कम्युनिस्ट पक्षाचे मुखपत्र, दि. ३०/०७/१९७२, पृ. क्र. ८.
९. शेवाळे विठ्ठल, संपादन, 'मी दत्तूचा दत्ता झालो त्याची गोष्ट', उपरोक्त, पृ. क्र. ६६-६७.
१०. बनसोड भीमराव, काकुस्ते सुभाष, वायकर आनंदराव आणि इतर, 'क्रांतीवेध- कॅ. मधुकर कात्रे स्मृतीग्रंथ', प्रकाशक, कॅ. मधुकर कात्रे स्मृतीग्रंथ संपादन समिती, श्रमिक, टिळक रोड, अहमदनगर, प्रथमावृत्ती १६ जानेवारी २०१०, पृ. क्र. ८१-८२.
११. शेवाळे विठ्ठल (संपा.), 'उज्ज्वल उद्यासाठी', (दिवंगत कॅ. दत्ता देशमुख विशेषांक) 'संघर्षयात्री', आनंद प्रिंटर्स, संगमनेर, त्रैमासिक नोव्हेंबर ते डिसेंबर २०१५, पृ. क्र. १६.
१२. कॅ. मधुकर कात्रे यांच्या आठवणी व आत्मनिवेदन (साखर कामगार युनियन), कॅसेट क्रमांक १, दि. २५/१०/२००६.
१३. बनसोड भीमराव, काकुस्ते सुभाष, वायकर आनंदराव आणि इतर, 'क्रांतीवेध- कॅ. मधुकर कात्रे स्मृतीग्रंथ', उपरोक्त, पृ. क्र. ८२-८३.
१४. किता, पृ. क्र. १६८.
१५. शेवाळे विठ्ठल (संपा.), 'उज्ज्वल उद्यासाठी', (दिवंगत कॅ. दत्ता देशमुख विशेषांक), उपरोक्त, पृ. क्र. १७-१८.
१६. लालनिशाण अंक, दि. २५ जून १९७५, पृ. क्र. ४.
१७. बनसोड भीमराव, काकुस्ते सुभाष, वायकर आनंदराव आणि इतर, 'क्रांतीवेध- कॅ. मधुकर कात्रे स्मृतीग्रंथ', उपरोक्त, पृ. क्र. १२५.
१८. उद्धत, शेवाळे विठ्ठल (संपा.), 'उज्ज्वल उद्यासाठी', (दिवंगत कॅ. दत्ता देशमुख विशेषांक), उपरोक्त, पृ. क्र. ४२.
१९. बनसोड भीमराव, काकुस्ते सुभाष, वायकर आनंदराव आणि इतर, 'क्रांतीवेध- कॅ. मधुकर कात्रे स्मृतीग्रंथ', उपरोक्त, पृ. क्र. ८८.

Personality Characteristics of Violent Young Adults in Romantic Relations

Anushka J.^{1*}, Ezaz S.²

ABSTRACT

The present study was intended to find out the levels of personality characteristics in among young adults in romantic relations. A sample of 222 young adults (N=116 Males and N=106 Females) were selected for the purposive sampling technique. Through the online survey two questionnaires were described to young adults aged between 18 to 25 years. NEOFFI, Paul T. Costa., et al, including 30 items was used to determine the personality characteristics. among young adults in romantic relations. CADRI, Wolfe et al.,2000 (Conflict in dating relationships) 46 item scale was to determine the effect of personality characteristics among young adults involved in dating relationships. Descriptive Statistics and Pearson Product moment correlation was done. According to Pearson product moment, it was found that there is no correlation between personality characteristics of violent young adults and their romantic relationship. The null hypothesis was accepted indicating that there is no significant relationship between personality characteristics of violent young adults and their romantic relationships.

Keywords: *Personality Characteristics, Romantic relationships, Young Adults*

Adolescence and young adulthood are identified by important changes in personality, changes in their behaviour and physical outfit and the creation of intimate relationships. We examined the role of personality traits which may affect to the violent behaviour of young adults and what are the types of personality traits which are effecting aggression and violence in the romantic relationships of young adults.

Overall, the current study provides important perception into the role of personality. The study of conflict in violent partner in relationship has supportably directed on violence carrying out on neurotism personality who does violence towards there partner, but current study of research suggests that, at least in minor couples, the difference between genders is shrinking or even reversing. The objective of this study is to analyze the personality traits of adolescents who are violent towards their partners. The main objectives of this research are to study the fact of aggressive behaviours against their partner of young adults according to gender of personality. To recognize the differential personality variables of male and female.

¹Research Scholar, Msc. Counselling Psychology, Karmaveer Bhaurao Patil College (Autonomous), Navi Mumbai, India

²Head of Dept. of Psychology, Karmaveer Bhaurao Patil College (Autonomous), Navi Mumbai, India

*Corresponding Author

Received: October 06, 2021; Revision Received: January 02, 2022; Accepted: February 19, 2022

Personality Characteristics of Violent Young Adults in Romantic Relations

To find which personality trait estimate violence against the partner male or female. Personality characteristics was measured by 60 item scale of NEOFFI-3 in which we included only two personality traits i.e., extroversion and neuroticism and violence of adolescence and young adults was measured by Conflict in adolescence dating relationship inventory. Result There is slightly relation between personality traits and violence behaviour in adolescence and young adults. Due to their personality traits adolescence are getting violent toward their romantic relationship. But in the current research it is proof that there is no relation between personality traits and violent behaviour in young adults.

Violent Behavior- The violent behavior of adolescents towards their romantic partners which involves action like verbal abuse, physical abuse, self-harm etc. are considered as violent behavior of adolescence. Violent behaviour is any behaviour by means of a man or woman that threatens or surely harms or injures the character or others or destroys assets. Violent behaviour frequently starts with verbal threats however over time escalates to involve physical harm. There are some things that can make someone much more likely to be violent. The three aggression types comprised reactive-expressive (i.e., verbal and physical aggression), reactive-inexpressive (e.g., hostility), and proactive-relational aggression (i.e., aggression that can break human relationships, for instance, by circulating malicious rumours).

Personality Traits- Personality traits are a characteristics/behavior of a person which is consistent and stable, the nature which is stable and constant is known as personality traits. personality developments mirror people's characteristic styles of thoughts, feelings, and behaviors. Character tendencies suggest consistency and balance someone who scores high on a selected trait like Extraversion is predicted to be sociable in exceptional situations and over time. Personality embraces moods, attitudes, and opinions and is most clearly expressed in interactions with other people.

METHODOLOGY

Purposive sampling method using descriptive statistics was used to determine the relationship between the personality characteristics among violent young adults and their romantic relationship. The key variable targeted in this investigation is; personality characteristics among violent young adults and their romantic relationship. The target population is; young adults in romantic relationships.

Objectives

- To understand the level of the personality characteristics among violent young adults and their romantic relationships.
- To understand the relationship of personality characteristics and violent young adults romantic relationships.

Hypothesis

1.	Null hypothesis	There is no relation between personality traits and violent behaviour of partner.
2.	Alternative -	There is relation between personality traits and violent behaviour of partner.

Personality Characteristics of Violent Young Adults in Romantic Relations

Research Design

The study has used correlation

To find out the relationship of personality characteristics and violent young adults romantic relationships.

Participants

The subject should be an adolescent or adult ie age 15-25 yrs. And should be involved in a romantic relationship. The collection of data was from 115 individuals by Judgmental/purposive sampling design. The research was online survey process in which they have to fill online questionnaires which were through Google form.

Data Collection Tools

- 60 items NEO FFI-3
- Conflict in dating relationships inventory scale.

Procedure

Adolescence and young adulthood are identified by important changes in personality, changes in their behaviour and physical outfit and the creation of intimate relationships. We examined the role of personality traits which may affect to the violent behaviour of young adults and what are the types of personality traits which are effecting aggression and violence in the romantic relationships of young adults. Data was collected from 115 college students and school going students (age 15 -25 yrs.) The method of data collection was online. And total 115 people responded to the survey.

RESULT

There is no significant relationship between personality characteristics and violent young adults romantic relationships.

The result shown accepts the null hypothesis and disproves the alternative hypothesis.

Descriptive Statistic

Table 1. Mean and Standard deviation of obtained sample

Descriptive Statistics			
	Mean	Std. Deviation	N
Neurotism	25.4696	6.03691	115
Extroversion	27.9130	6.78823	115
Partner	12.3652	10.37992	115

Table 2. Correlation between Personality Characteristic (Neuroticism and Extroversion) and partner (violent young adults in romantic relationship)

Correlations				
	Neurotic	Extroversion	partner	
Neurotism	Pearson Correlation	1	-.066	.332**
	Sig. (2-tailed)		.481	.000
	N	115	115	115
Extroversion	Pearson Correlation	-.066	1	-.012
	Sig. (2-tailed)	.481		.897
	N	115	115	115
Partner	Pearson Correlation	.332**	-.012	1
	Sig. (2-tailed)	.000	.897	
	N	115	115	115

** . Correlation is significant at the 0.01 level (2-tailed).

DISCUSSION

Personality characteristics of violent young adults in romantic relationship. The data was collected from 15 to 25 yrs age group students through online survey method. 115 participants were participated in this research, in which female- 58 and males-57 age group from 15 to 25 yrs. This research is based on personality traits and which personality trait affects for aggression in adolescence and young adults, there are total 5 personality traits i.e. Extroversion, neuroticism, conscientiousness, agreeableness and openness. In this trait I have chosen only 2 personality traits i.e., extroversion and neuroticism, which may affect the violent behaviour of young adults towards their partner. And as shown in the graph proves that people with extrovert personality are not involved in violent behaviour as compared to neuroticism people, so the result is slightly significant to the other results. So, the result proves that there is no relation between personality traits and violent behaviour towards their partner. The research is not link with other researchers and null hypothesis was proved that there is no relation between neurotic personality trait and their aggression towards partner. The correlation between neuroticism and extroversion was $-.066$, neuroticism and violent partners correlation was $.332^{**}$. The significance of the result was 0.01 so it proves that there is no relation between personality traits and violent young adults in relation.

CONCLUSION

The result shown in this survey rejects the alternative hypothesis and proves null hypothesis as, there is no relation between personality characteristics and violent behaviour in adolescence and young adults.

Implication

- According to the findings, it was seen that the null hypothesis is accepted
- The result concludes that there is no correlation between personality characteristics and violent young adults in romantic relationship.

Limitation

- The study was limited to 15 to 25 yrs. age group people and Geographical condition was also under control.
- Temperature is one of the limits because we can't control the temperature of the atmosphere.
- Lack of time.
- Geographical area is under limitation.

REFERENCES

- Christopher P. Barlett, Craig A. Anderson Iowa State University, Center for the Study of Violence, United States journal homepage: www.elsevier.com/locate/paid
- Danutamen Rode, Magdalena Rode, Maciej Januszek. Psychosocial characteristics of men and women as perpetrators of domestic violence (2015) University of Silesia University of Social Sciences and Humanities, Faculty in Katowice Polish Psychological Bulletin 2015, vol 46(1), 53-64
- Drahman, A., & Yusof, S. N. M. (2018). The Relationship Between Personality Traits and Marital Satisfaction on Quality of Marriage Among Married Couples in Selangor.
- Hellmuth, Julianne C., "Neuroticism, Marital Violence, and the Moderating Role of Stress and Behavioral Skills. "Master's Thesis, University of Tennessee, 2008. https://trace.tennessee.edu/utk_gradthes/380

Personality Characteristics of Violent Young Adults in Romantic Relations

- Irum Saeed Abbasi, Neelam Rattan, Tehmina Kousar & Fatma Khalifa Elsayed (2018): Neuroticism and Close Relationships: How Negative Affect is Linked with Relationship Disaffection in Couples, *The American Journal of Family Therapy*, DOI:10.1080/01926187.2018.1461030 <https://doi.org/10.1080/01926187.2018.1461030>
- Jaqueline Gomes CAVALCANTI1 Carlos Eduardo PIMENTEL <http://dx.doi.org/10.1590/1982-02752016000300008>
- Jasmina Kodzopeljic, Snezana Smederevac, Dusanka Mitrovic, Bojana Dinic and Petar <http://jiv.sagepub.com/content/29/4/736> *Journal of Interpersonal Violence* 2014, Vol. 29(4) 736–757
- Khaled Abd El Moeza, Mona Elsyeda, Ismail Yousefb, Amany Waheed Eldeenc, Wafa Ellithyb (2014) Psychosocial characteristic of female victims of domestic Violence. *Egyptian Journal of Psychiatry* 2014, 35(2):105–113
- Mokolapo Oluwatosin Tenibiaje, Dele Joseph Tenibiaje. Influence of Gender and Personality Characteristics on Violent Behaviour among Adolescents in Nigeria. *Asian Journal of Humanities and Social Studies* (ISSN: 2321 – 2799) www.ajouronline.com.

Acknowledgement

The author(s) appreciates all those who participated in the study and helped to facilitate the research process.

Conflict of Interest

The author(s) declared no conflict of interest.

How to cite this article: Anushka, J. & Ezaz, S.(2022). Personality Characteristics of Violent Young Adults in Romantic Relations. *International Journal of Indian Psychology*, 10(1), 001-005. DIP:18.01.001.20221001, DOI:10.25215/1001.001

10. Impact of COVID- 19 on Online Education in India

Prof. Sunil Shripat Deokar

Head, Dept. of English, R. B. Narayanrao Borawake College, Shrirampur, Ahmednagar.

Prof. Tarhal Anandrao Tarhal

Department of Economics, Rajarshri Chattrapati Shahu College, Kolhapur.

Abstract

The COVID-19 pandemic has affected human race globally upon social, economic, health and educational sectors. A global emergency resulted in measures to be implemented, of which included lockdown, social distancing, mask and sanitation. This study aims to understand the impact of lockdown on online education during the COVID-19 pandemic. Traditional face-to-face teaching has been replaced with online teaching and learning to acquire new skills through digital platforms. It has also affected mental health in students and learners. This study will support provided educational institutions to accept a 'new normal' culture. This review will make us understand the importance of regular class room teaching and introduction to a new life concept of online education. Corona virus introduced a new life concept called online teaching after March 2020. Though there were many online apps, but very few were familiar but pandemic made familiar every student know the word Google meet, Google Classroom, Zoom meet, Teams. This online education system made the students to learn more technically but away from their physical mode of learning.

Key Words: Covid-19, online education, tradition, teaching, technology.

Introduction

The findings reveal that almost all schools and colleges have switched to some form of online teaching since the beginning of the COVID-19 crisis, and believe that school practices will not be the same when they reopen, with more online teaching. For many teachers and students, it was first experience with online teaching, which has been both positive and challenging. Psychologists say this online education system made both the Students and Teachers to be more stressful than the classroom teaching. Each teacher must prepare in a different way keeping away the traditional modes of teaching. Adaption of different styles in day

to day teaching must be innovative in every day class as there is fear of losing jobs in private schools and colleges. Wide spread job and income loss puts a lot of pressure on the teachers to lack concentration on the teaching methodologies to reflect in their teaching style. Layoffs, cut down in salary for a parent, makes him to not paying fees for their ward, this in turn outbreaks in job insecurity to teachers or paying low salary to them. When there is a lay off Teacher-student ratio differs and a teacher cannot concentrate a crowd more then what was actually assigned. This results in imparting poor education due to the pandemic situation. The current data according to UNO says more than 90% of the students around the world are learning from home, due to school closure. This online method also has caused various health defects among students reports WHO. This pandemic situation has affected almost all the sectors but what is the remedy to overcome the situation faced by the students in their routine learning.

Opportunities of Online Teaching

“Difficulties in your life do not come to destroy you. But it helps you realize your hidden potential and power. Let difficulties know that you are too difficult”. - *Dr. A.P.J.Abdul kalam.*

In the period of crises, this lockdown has given a good opportunity for learners for acquiring new skills through digital devices, media and other latest technologies to improve their talents. Technology has reached ‘its digital heights’ in the area of networking. For example, earlier and even in present situation some social media platforms like Facebook, Twitter, Skype, MySpace flourish rapidly with wide alternatives. Amidst the networking development witnessed in the above said social Medias, professional networking sites have recently emerged in the business world mainly, in this pandemic period of Covid-19. Many websites, weblogs and apps entered the market place and enriched equally in education. World Wide Web creates liveliness, instructiveness, voluntary participation for collaborative learning and sharing, effective interactions pursuits in interesting webs. Some of the platforms like LinkedIn, Zoom Info, Google meet, Microsoft Team with Sharp point tool, Google Duo, Cisco WebEx, IBM Blue pages, Google Classroom etc., are effective online tool in any organizations. Similarly, proper training is very essential to acquire these skills.

Technology Assisted Online Learning

In pandemic, our traditional classrooms are replaced in to computerized platforms which can create a positive atmosphere to the learners. Audio-visual aids and media are used in teaching and learning process now. It develops study skills also .Audio- visual aids can easily

provide positive impact for the learners to learn and recognize their learning objectives. The internet keeps learning resources by providing end number of resources to the learners from all over the world. The technology takes the role of a facilitator now. Technology develops creative power of the students. Students are enthusiastically performed their roles with practical skills and motivated games. A student can receive both information and enjoyment during this pandemic. PowerPoint presentations magnify the teaching by providing and supporting the students with different study materials. It helps a teacher to organize and re-organize the learning materials efficiently. Teacher can merge the text items, graphics and sounds. It becomes an additional source of learning material for them. Technology becomes an integral part of online classroom. The technical communication in the teaching and learning process combines sounds and visuals. This is the dynamic aspect of the technology. Computers, TV channels, cables, Whatsapp and YouTube are examples of our technology.

Obligatory mode of Online Learning

All the stakeholders, without acquiring online skills in the lockdown are illiterate. E-learning is the demand of the era. Students and teachers are in the learning stage with the new gadgets. Not only students and teachers, even parents need to learn the new technology, because children below 12 years need parental assistance. Teachers across the nation are struggling to find ways to continue teaching their students in a situation where physical contact is no longer possible. Again, class and social division play a important role in determining how successful teachers are in teaching school children during the pandemic. This prevailing situation is fulfilled through, online classes conducted by educational institutions through digital platforms encouraging their studies.

Segregation of Rural and Urban in Online Teaching

Data showing the Pandemic affecting students' online education Teachers at the urban private schools are experts and have access to the internet at home, as well as the other digital infrastructure required to share course material. Some of these schools may even have experimented e-learning facilities like online homework submission before the crisis. These teachers will be able to provide an adequate e-learning experience for their pupils, ensuring continuity. This, unfortunately, is not the case when it comes to the vast majority of teachers in the rural area. We see, one in five primary school teaching positions is vacant today. Many times, many schools in rural India were run by just a single teacher. Some teachers cope in this

new world, but the majority of the teachers will need to upgrade not only their technical skills but also their teaching resources, in most cases; it will just not be feasible. Online learning is a burden to parents. This system has forced the guardians to give the electronic gadgets in their kid's hands. At one time, the kids were restricted, now they are forced to do what they were advised not to. This makes many parents adverse supporters of schooling in the best of times. It's not understandable how parents in rural areas are reacting to this lockdown situation. Passive learners Change in education system where a country like India was not prepared made great impact in adapting the system. Right from curriculum to managing the students without a classroom was a great challenge. The design of the system mainly focused in avoiding passive learning, a risk that was expected. Lack of concentration and rushing of portions within a short span of time and the method of taking up exams made a great change in the student community. It is realized that online learning is dull and if it continues more passive learners will be created. Students should be given moral classes to overcome stress. Parents should also be given special advises to juggle between household work and their own work from home during children's online education

Online Education Advantages

Blended Learning Higher education system will now move to blended learning where taking classes will be combined with face to face delivery along with an online model. This requires teachers to be more tech savvy and they should go through training to upgrade themselves according to the changes that is required to teach the students. Blending technology brings improvement in the quality of education by preparing better learning material. As blended learning becomes the new method, preparation of quality concepts to have a transparent education system. Teamwork Online teaching also gives opportunities for collaborative strengthening. Teachers from various education institutions can share their method and learn from others methodologies, thus developing an easy arena to avoid passive learning and get benefits from all kinds of resources available. Nothing has changed in this sector for almost last two centuries maybe this was just the wake-up call that was needed. It is not period to wait and let the situation pass, but to rise and re-frame the education sector to benefit all the components.

Conclusion

The sudden change globally has made us to learn many new things. It has changed our life style in all ways to which we are adapting. Covid-19 situation has altered the life for all of us.

Let's take only the positive heights, ignore negative thoughts and comments and learn to live with whatever the situation with a balanced mind and soul to support and nurture the young minds, because they are representing our future.

References

1. <https://link.springer.com/article/10.1007/s40031-021-00581-x>
2. <https://www.schooleducationgateway.eu/en/pub/viewpoints/surveys/survey-on-online-teaching.htm>
3. Meenakshi Raman and Prakash Singh. Business Communication. Oxford Higher Education, 2006. Print
4. <https://statustown.com/quote/235/>
5. https://52.198.147.142/jobsearch/1003/list?income_ll=&dispatchfromymd=2021B&clickfrom=conditions tag

प्रा. वाय.बी. लबडे

ग्रंथपाल

महाराजा जिवाजीराव शिंदे महाविद्यालय, श्रीगोंदा

प्रा. सी.के. खैरनार

ग्रंथपाल

राधाबाई काळे महिला महाविद्यालय, अहमदनगर

सांगणे :-

पर्यावरणीयदृष्ट्या हरित आणि टिकाऊ ग्रंथालयांची व्याख्या, ग्रंथालय इमारतीचे बांधकाम करताना राष्ट्रीय आणि आंतरराष्ट्रीय माणक वाचा वापर, आंतरराष्ट्रीय ग्रंथालय संघाचे योगदान, हरित ग्रंथालयासाठी ग्रंथपालांची भूमिका आणि भागताली काही हरित ग्रंथालयांची माहिती या लेखात दिलेली आहे. तसेच ग्रंथालयांनी पर्यावरणीयदृष्ट्या पूरक वातावरण तयार करून हरित ग्रंथालयासाठी दिशादर्शक म्हणून काम करणे ही काळाची गरज आहे.

शोपसंज्ञा :- हरित ग्रंथालये, आंतरराष्ट्रीय प्रमाणक, राष्ट्रीय प्रमाणक, अंतरराष्ट्रीय ग्रंथालय संघाचे योगदान

प्रस्तावना :-

रोजच्या हवामानात होत असलेला बदल, जागतिक तापमान वाढ यामुळे पर्यावरणाचा न्हास होत आहे, त्याचे परिणाम आपण उपभोगत आहोत. पर्यावरणाला पूरक असे वातावरण तयार करण्यासाठी अनेक क्षेत्रात बदल होताना दिसत आहे, त्यास ग्रंथालये सुद्धा अपवाद नाहीत. १९९० पासून हरित ग्रंथालये चळवळ सुरु झालेली असून मागील काही काळापासून ही संकल्पना जोर धरू लागली आहे. हरित ग्रंथालये ही संकल्पना या संकल्पनेमध्ये नैसर्गिक सूर्यप्रकाशाचा वापर करून, तसेच नैसर्गिक व मोकळी हवा येईल अशा प्रकारे तयार करण्यात आलेले आहेत. सर्व वयोगटासाठी ग्रंथालये ही शिकण्याची केंद्रे आहेत. यामध्ये ग्रंथालये ही केवळ ज्ञानाची भांडारे नसून पर्यावरणासंबंधी जागरूकता वाढविण्यासाठी महत्वाची मदत करतात, तसेच मानवी आरोग्यावर कोणताही परिणाम होणार नाही याची दक्षता हरित ग्रंथालये घेतात. मानवी आरोग्याचा विचार करत असतांना वेगवेगळ्या मानसिक बदलावर ग्रंथालयातील हरित वातावरण सकारात्मक परिणाम करण्यास मदत करते.

व्याख्या :-

ऑनलाईन डिक्शनरी ऑफ लायब्ररी अँड इन्फॉर्मेशन सायन्स च्या व्याख्येनुसार,

नैसर्गिक वातावरणावर नकारात्मक प्रभाव कमी करण्यासाठी आणि अंतर्गत वातावरणाची गुणवत्ता टिकविण्यासाठी ग्रंथालयाचे स्वच्छ निश्चित करणे, बांधकामासाठी लागणारे नैसर्गिक साहित्य आणि जैव वर्गीकरण करण्यायोग्य उत्पादनाचा वापर, पाणी, ऊर्जा, कागद या संसाधनाचे संरक्षण करणे इ.चा विचार करून आणि लीड (LEED - Leadership in Energy and Environmental Design) आणि (USGBC- United States Green Building Council) यांच्या माणकानुसार बांधकाम करणे. युनाइटेड स्टेट्स ग्रीन बिल्डिंग कौन्सिल (USGBC) ची स्थापना १९९३ मध्ये ना नफा ना तोटा या तत्वावर व्यक्तिगत सदस्यशासाठी झाली. त्यांनी लीड (LEED - Leadership in Energy and Environmental Design) ची स्थापना केली. या संस्थेद्वारे संपूर्ण जगामध्ये हरित इमारतीची तपासणी करून चार प्रकारची प्रमाणपत्र (Certified Silver, Gold, Platinum) दिले जातात. हरित इमारतीसाठी आंतरराष्ट्रीय माणक

लीड प्रमाणकाद्वारे हरित इमारत तयार करताना पुढील प्रकारचे मुद्दे विचारात घ्यावेत असे सुचविले आहे.

- **स्थाननिश्चिती (Location) :-** ग्रंथालयाची इमारत बांधत असताना लीड ने अनेक प्रकारची मार्गदर्शक तत्वे दिलेली आहेत. ग्रंथालयाचे स्थान हे गजबजलेल्या ठिकाणी लोकवस्तीत असावे, रस्त्याच्या दोन्ही बाजूने झाडे लावलेली असावेत, गाडी पार्किंग करण्याची सोय असावी. ग्रंथालयाच्या सभोवती हिरवीगार झाडी असावी, बाहेर झाडांच्या खाली असे कट्टे तयार करावेत की तेथे बसून वाचनाचा आस्वाद घेता यावा.
- **पाणी (Water) :-** ग्रंथालयामध्ये पाण्याचे योग्य प्रकारे व्यवस्थापन करण्यात यावे. पावसाचे पाणी जमिनीमध्ये मुरविण्यासाठी वॉटर हार्वेस्टिंग करावे, तसेच शुद्ध पिण्याच्या पाण्याची सोय करण्यात यावी, त्यासाठी वॉटर कूलर बसवून घ्यावेत. संडास आणि बॉशरूम साठी योग्य प्रमाणात पाण्याचा वापर करावा.



विलास उत्तम एलके

शारीरिक शिक्षण संचालक
राधाबाई काळे महिला
महाविद्यालय, अहमदनगर
vilashandball@gmail.com

डॉ. शरद आहेर

प्रोफेसर
चंद्रशेखर आगाशे शारीरिक
शिक्षण महाविद्यालय, पुणे
Sharadaher3@gmail.com

One Day International E - Conference On Covid-19 Pandemic: Challenges, Opportunities & Solutions in Front of Higher Education

on 21st August, 2021 @

S.K. College Akola, AS College Kurha, S.K. Maha Dahihanda & PEFI, New Delhi.

पुणे जिल्ह्यातील प्राथमिक शालेय शारीरिक शिक्षण शिक्षकांच्या अध्यापन संसाधन गरजांचे विश्लेषण

ABSTRACT

शारीरिक हालचालींच्या माध्यमातून दिले जाणारे शिक्षण म्हणजे शारीरिक शिक्षण होय. प्रस्तावित अभ्यासातून संशोधकाने पुणे जिल्ह्यातील प्राथमिक शालेय शारीरिक शिक्षण शिक्षकांच्या अध्यापन संसाधन गरजांच्या विश्लेषणाचा अभ्यास केला आहे. संशोधनासाठी पुणे जिल्ह्यातील महाराष्ट्र राज्य प्राथमिक शिक्षण अभ्यासक्रमानुसार चालणाऱ्या शाळेतील इयत्ता ५ वी ला शारीरिक शिक्षण अध्यापन करणाऱ्या ५० शारीरिक शिक्षण शिक्षकांची सहेतुक न्यादर्श पद्धतीने निवड केली. टेलिफोनिक मुलाखत या संशोधन साधनाचा वापर करून माहिती गोळा करण्यात आली. प्रस्तुत संशोधनाच्या निष्कर्षावरून असे समजले की, शारीरिक शिक्षण शिक्षकांना स्नायूंचा दमदारपणा, दिशाभिमुखता, स्थानांतरणीय हालचाल कौशल्य, उभे राहून योगासने, मनोरंजात्मक खेळ, एरोबिक्स आणि कबड्डी या शारीरिक शिक्षण घटकांवर शारीरिक शिक्षण अध्यापन संसाधन (व्हिडिओ) जास्त आवश्यक आहे. महत्वाच्या संज्ञा - शारीरिक शिक्षण, शारीरिक शिक्षण अध्यापन घटक.

प्रस्तावना

शालेय जीवनात विद्यार्थ्यांना अनेक शैक्षणिक विषयांचे अध्यापन केले जाते. त्यामध्ये विविध भाषा, विज्ञान, गणित,, समाजशास्त्र आणि इतर विषयांचा समावेश असतो. प्रत्येक विषयाचे अध्यापन करण्यासाठी स्वतंत्र शिक्षकाची नेमणूक केलेली असते. विषयांचे अध्यापन त्या त्या विषयानुसार अध्यापन कौशल्य वापरून केले जाते. शाळेमध्ये शैक्षणिक विषयांबरोबर विद्यार्थ्यांच्या कलागुणांना वाव मिळण्यासाठी संगीत, चित्रकला आणि शारीरिक शिक्षण हे विषय असतात. शारीरिक शिक्षण आता फक्त स्नायू संस्थेचा विकास किंवा बालसंवर्धन करावयाचे इतकेच ध्येय नसून शरीर, मन व बुद्धी यांच्या माध्यमातून बोधात्मक, भावनात्मक, क्रिया कौशल्यात्मक व सामाजिक क्षेत्रांद्वारे सर्वांगीण विकास घडविणे हे देखील आहे. शारीरिक हालचालींच्या माध्यमातून दिले जाणारे शिक्षण म्हणजे शारीरिक शिक्षण होय. शरीर क्रियांमधून शरीर मजबूत करणे, शरीर निकोप ठेवणे, नागरिकत्वाच्या गुणांचा विकास करणे, आत्मसंरक्षणास, राष्ट्रसेवेस व संरक्षणास शरीर लायक करणे इत्यादी शारीरिक शिक्षणाची काही प्रमुख उद्दीष्ट्ये आहेत. शारीरिक शिक्षण कार्यक्रम विद्यार्थ्यांना विकासात्मकरीत्या योग्य उपक्रमात सहभागी होण्यास अनुमती देतो, सहकारी वर्तन अधिक मजबूत आणि विकसित करणे

आणि विद्यार्थ्यांना जीवनभर सुदृढता लक्ष्य स्थापित करण्यासाठी शिकवतो. नॅशनल असोसिएशन फॉर स्पोर्ट अँड फिजिकल एज्युकेशन यांच्या मते शारीरिकदृष्ट्या सुशिक्षित व्यक्ती हा शारीरिकदृष्ट्या तंदुरुस्त, नियमितपणे शारीरिक हालचालींमध्ये सहभागी होणारा, शारीरिक उपक्रमांच्या सहभागाचे फायदे व परिणाम माहिती असणारा, शारीरिक उपक्रमांचे मुली व आरोग्यपूर्ण जीवनशैलीत त्यांचे योगदान असणारा आणि विविध शारीरिक उपक्रम करण्यासाठी आवश्यक कौशल्य शिकलेला असणारा असतो. शालेय जीवनात शारीरिक शिक्षण हे एक प्रकारचे मनोरंजन आणि स्वास्थ्य गाठण्यासाठी शारीरिक शिक्षणातील हालचाली, चिंता आणि मुलांना येणारी काळजी दूर करण्यासाठी असते. शारीरिक शिक्षणामध्ये विद्यार्थ्यांना विविध प्रकारचे खेळ, मनोरंजनात्मक उपक्रम, शारीरिक उपक्रम आणि आरोग्य शिक्षणाचे अध्यापन केले जाते. शारीरिक शिक्षणाची सुरुवात हि शालेय जीवनातच चांगली झाली तर पुढे जाऊन त्याचा चांगला फायदा होतो. जर शालेय जीवनात शारीरिक शिक्षणाचे अध्यापन चांगले झाले तर भविष्यात सुदृढ नागरिक तयार होतील. खेळामध्ये उच्च कार्यमान करावयाचे असेल तर प्राथमिक हालचाली व सुदृढता चांगली असणे आवश्यक असते. शालेय अभ्यासक्रमात शारीरिक शिक्षण हा एक अविभाज्य घटक आहे त्याचे अध्यापन योग्य पद्धतीने झाल्यास विद्यार्थी सर्वोत्तमरी परिपूर्ण म्हणून गणला जातो.

विविध उपक्रम व खेळातून मनोरंजनास संधी देणे, नियमित व्यायामाचे महत्त्व पटवणे व प्रवृत्त करणे, शारीरिक सुदृढता विकसित करणे व टिकवणे, कारक व क्रीडा कौशल्यांचे उपयोजन करण्याची जाणीव निर्माण करणे. क्रीडाकौशल्य विकसित करण्यासाठी आंतरिक उर्जा वापरण्याची जाणीव निर्माण करणे, संघशक्तीचे महत्त्व जाणून उपयोजनास संधी देणे, एकाग्रता व मानसिक शांतता मिळवण्यासाठी योगाभ्यासाद्वारे संधी देणे, समूह सहभाग व स्पर्धामधून जीवनकौशल्ये विकसित करणे, खिलाडूवृत्ती जोपासणे, पारंपारिक खेळांद्वारे संस्कृती व मुल्यांची जोपासना करणे आणि राष्ट्रीय भावना निर्माण करणे व जोपासणे. महाराष्ट्र राज्य प्राथमिक शिक्षण अभ्यासक्रमानुसार शालेय शारीरिक शिक्षणामध्ये मुलभूत हालचालींचे विकसन, मुलभूत हालचालींचे खेळामधून विकसन, प्रास्ताविक हालचाली व व्यायाम, पूरक व्यायाम, सूर्यनमस्कार, तालबद्ध व्यायाम (लेझीम, एरोबिक्स) ए.बी.सी.ड्रिल, जिम्नॅस्टिक्स मधील व्यायाम, मानवी मनोरे, स्वसंरक्षण, गतिरोध मालिका, पोषक व्यायाम, कवायत संचलन, लघुखेळ व शर्यती, पूरक खेळ, परिवर्तीत खेळ, विविध स्पर्धा व कुलपद्धती, मनोरंजन खेळ आणि योग परिचय या (उपक्रम) गोष्टींचा समावेश होतो.

शारीरिक शिक्षण अध्यापन हे प्रभावी असेल तर विद्यार्थ्यांचे जास्तीत जास्त अध्ययन होते. शारीरिक शिक्षण अध्यापनात विद्यार्थ्यांच्या वयायोग्य शारीरिक उपक्रम व शारीरिक हालचाली घेतल्या जातात. प्राथमिक शालेय शारीरिक शिक्षण अध्यापन करतांना शारीरिक शिक्षण शिक्षकांस शारीरिक शिक्षण अध्यापन घटकांची निवड कशी करावी व कशा प्रकारे अध्यापन करावे हे गरजेचे असते. शारीरिक शिक्षण शिक्षकांस शाळेमध्ये विविध प्रकारे शारीरिक शिक्षण अध्यापन घटकांची आवश्यकता असते. त्यासाठी शारीरिक शिक्षकांना विविध अध्यापन घटकांवर संसाधनांची (व्हिडिओची) आवश्यकता असते. मराठी मध्ये कोणत्याही प्रकारचे शारीरिक शिक्षण अध्यापन संसाधन (व्हिडिओ) उपलब्ध नाहीत. त्यामुळे महाराष्ट्र राज्य प्राथमिक शिक्षण अभ्यासक्रमानुसार चालणाऱ्या शाळेतील शारीरिक शिक्षकांना कोणत्या शारीरिक शिक्षण घटकांवर संसाधनांची (व्हिडिओची) आवश्यकता असते हे पाहणे गरजेचे ठरेल. म्हणून संशोधकाने पुणे जिल्ह्यातील प्राथमिक शालेय शारीरिक शिक्षण शिक्षकांच्या अध्यापन संसाधन गरजांच्या विश्लेषणाचा अभ्यास ही समस्या निवडलेली आहे.

संशोधन उद्दीष्ट्ये

पुणे जिल्ह्यातील महाराष्ट्र राज्य प्राथमिक शिक्षण अभ्यासक्रमानुसार चालणाऱ्या शाळेच्या शारीरिक शिक्षण शिक्षकांच्या अध्यापन संसाधन गरजांचे विश्लेषण करणे.

संशोधन कार्यपद्धती

प्रस्तुत संशोधनासाठी पुणे जिल्ह्यातील महाराष्ट्र राज्य प्राथमिक शिक्षण अभ्यासक्रमानुसार चालणाऱ्या शाळेतील इयत्ता ५ वी ला

शारीरिक शिक्षण अध्यापन करणाऱ्या ५० शारीरिक शिक्षण शिक्षकांची सहेतुक न्यादर्श पद्धतीने निवड केली. संशोधनात पुणे जिल्ह्यातील महाराष्ट्र राज्य प्राथमिक शिक्षण अभ्यासक्रमानुसार चालणाऱ्या शाळेच्या शारीरिक शिक्षण शिक्षकांच्या अध्यापन गरजांचा अभ्यास करण्यात येणार असल्याने शारीरिक शिक्षण शिक्षकांच्या अध्यापन गरजांची माहिती मिळविण्यासाठी टेलिफोनिक मुलाखत या संशोधन साधनाचा वापर करण्यात आला.

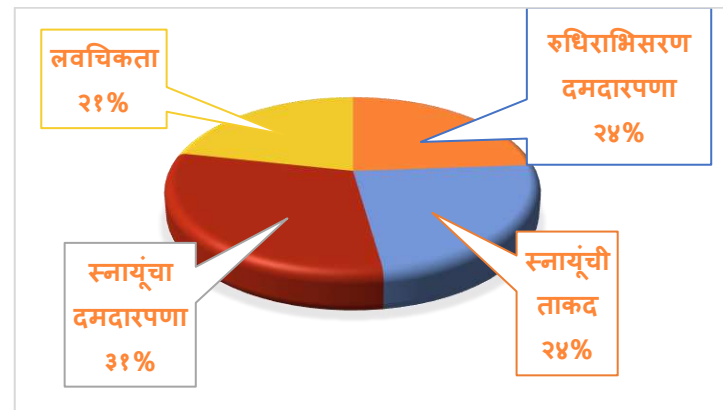
विश्लेषण आणि अर्थनिर्वचन

संशोधनात पुणे जिल्ह्यातील महाराष्ट्र राज्य प्राथमिक शिक्षण अभ्यासक्रमानुसार चालणाऱ्या शाळेच्या शारीरिक शिक्षण शिक्षकांच्या अध्यापन गरजांची माहिती मिळविण्यासाठी टेलिफोनिक मुलाखत या संशोधन साधनाचा वापर करण्यात आला आहे. मिळालेल्या माहितीचे विश्लेषण पुढीलप्रमाणे केले आहे.

कोष्टक क्र. १

आपणास कोणत्या आरोग्याधीष्ठीत शारीरिक सुदृढता घटकांवर शारीरिक शिक्षण अध्यापन संसाधन (व्हिडिओ) आवश्यक आहे.

	रुधिराभिसरण दमदारपणा	स्नायूंची ताकद	स्नायूंचा दमदारपणा	लवचिकता
मिळालेली एकूण मते	२१	२१	२७	१९



आकृती क्र.१: आरोग्याधीष्ठीत शारीरिक सुदृढता घटकांसंबंधी शारीरिक शिक्षण शिक्षकांच्या अध्यापन संसाधन (व्हिडिओ) गरजांचे विश्लेषण अर्थनिर्वचन

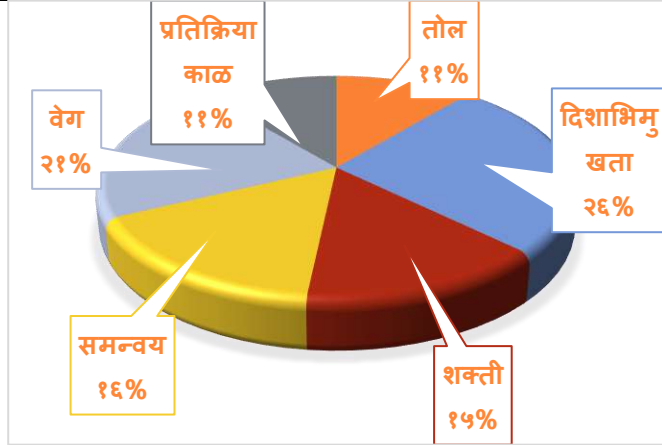
आकृती क्र.१ प्रस्तुत संशोधनामध्ये शारीरिक शिक्षण शिक्षकांच्या अध्यापन गरजांची माहिती मिळविण्यासाठी टेलिफोनिक मुलाखत या संशोधन साधनाचा वापर करण्यात आला. मिळालेल्या माहितीच्या विश्लेषणावरून आरोग्याधीष्ठीत शारीरिक सुदृढता घटकांसंबंधी ३१% शारीरिक शिक्षण शिक्षकांना असे वाटते की, स्नायूंचा दमदारपणा या घटकावर शारीरिक शिक्षण संसाधन

(व्हिडिओ) आवश्यक आहे. २४% शारीरिक शिक्षण शिक्षकांना असे वाटते की, स्नायूंची ताकद या घटकावर शारीरिक शिक्षण संसाधन (व्हिडिओ) आवश्यक आहे. २४% शारीरिक शिक्षण शिक्षकांना असे वाटते की, रुधिराभिसरण दमदारपणा या घटकावर शारीरिक शिक्षण संसाधन (व्हिडिओ) आवश्यक आहे. २१% शारीरिक शिक्षण शिक्षकांना असे वाटते की, लवचिकता या घटकावर शारीरिक शिक्षण संसाधन (व्हिडिओ) आवश्यक आहे. स्नायूंचा दमदारपणा या घटकावर शारीरिक शिक्षण शिक्षकांना शारीरिक शिक्षण अध्यापन संसाधनाची (व्हिडिओ) जास्त आवश्यकता आहे.

कोष्टक क्र. २

आपणास कोणत्या कौशल्याधीष्ठीत शारीरिक सुदृढता घटकांवर शारीरिक शिक्षण अध्यापन संसाधन (व्हिडिओ) आवश्यक आहे.

	लवचिकता	तोल	दिशाभिमुखता	शक्ती	समन्वय	वेग	प्रतिक्रिया काळ
मिळालेली एकूण मते	१९	१३	३१	१७	१९	२५	१३



आकृती क्र.२: कौशल्याधीष्ठीत शारीरिक सुदृढता घटकांसंबंधी शारीरिक शिक्षण शिक्षकांच्या अध्यापन संसाधन (व्हिडिओ) गरजांचे विश्लेषण

अर्थनिर्वचन

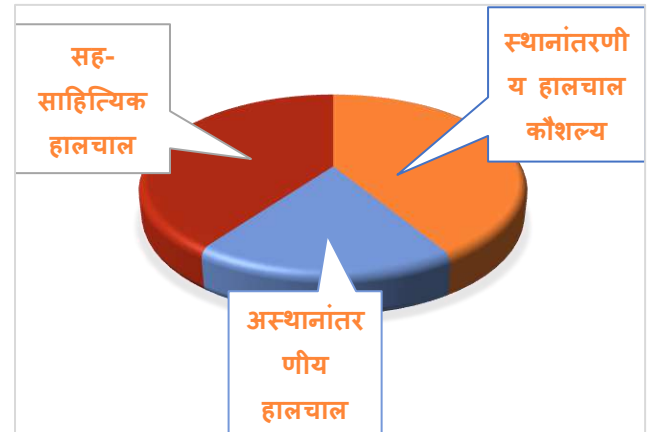
आकृती क्र.२ प्रस्तुत संशोधनामध्ये शारीरिक शिक्षण शिक्षकांच्या अध्यापन गरजांची माहिती मिळविण्यासाठी टेलिफोनिक मुलाखत या संशोधन साधनाचा वापर करण्यात आला. मिळालेल्या माहितीच्या विश्लेषणावरून कौशल्याधीष्ठीत शारीरिक सुदृढता घटकांसंबंधी २६% शारीरिक शिक्षण शिक्षकांना असे वाटते की, दिशाभिमुखता या घटकावर शारीरिक शिक्षण संसाधन (व्हिडिओ) आवश्यक आहे. २१% शारीरिक शिक्षण शिक्षकांना असे वाटते की, वेग या घटकावर शारीरिक शिक्षण संसाधन (व्हिडिओ)

आवश्यक आहे. १६% शारीरिक शिक्षण शिक्षकांना असे वाटते की, समन्वय या घटकावर शारीरिक शिक्षण संसाधन (व्हिडिओ) आवश्यक आहे. १५% शारीरिक शिक्षण शिक्षकांना असे वाटते की, शक्ती या घटकावर शारीरिक शिक्षण संसाधन (व्हिडिओ) आवश्यक आहे. ११% शारीरिक शिक्षण शिक्षकांना असे वाटते की, प्रतिक्रिया काळ या घटकावर शारीरिक शिक्षण संसाधन (व्हिडिओ) आवश्यक आहे. ११% शारीरिक शिक्षण शिक्षकांना असे वाटते की, तोल या घटकावर शारीरिक शिक्षण संसाधन (व्हिडिओ) आवश्यक आहे. दिशाभिमुखता या घटकावर शारीरिक शिक्षण शिक्षकांना शारीरिक शिक्षण अध्यापन संसाधनाची (व्हिडिओ) जास्त आवश्यकता आहे.

कोष्टक क्र. ३

आपणास कोणत्या मूलभूत हालचाल कौशल्यावर शारीरिक शिक्षण अध्यापन संसाधन (व्हिडिओ) आवश्यक आहे.

	स्थानांतरणीय हालचाल कौशल्य	अस्थानांतरणीय हालचाल कौशल्य	सह-साहित्यिक हालचाल कौशल्य
मिळालेली एकूण मते	३१	१४	३०



आकृती क्र.३: मूलभूत हालचाल कौशल्य घटकांसंबंधी शारीरिक शिक्षण शिक्षकांच्या अध्यापन संसाधन (व्हिडिओ) गरजांचे विश्लेषण

अर्थनिर्वचन

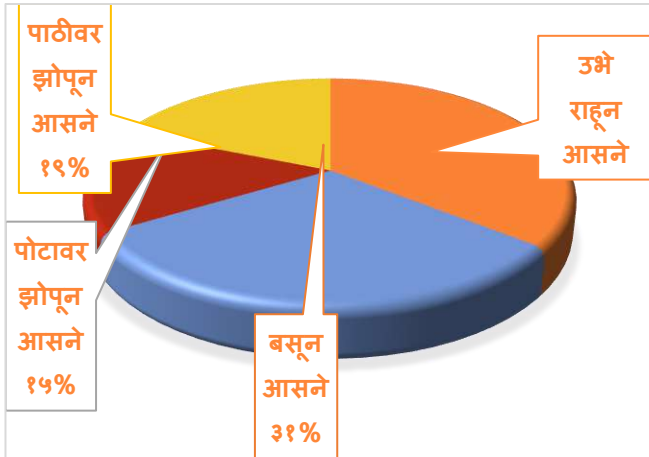
आकृती क्र.३ प्रस्तुत संशोधनामध्ये शारीरिक शिक्षण शिक्षकांच्या अध्यापन गरजांची माहिती मिळविण्यासाठी टेलिफोनिक मुलाखत या संशोधन साधनाचा वापर करण्यात आला. मिळालेल्या माहितीच्या विश्लेषणावरून मूलभूत हालचाल कौशल्य घटकांसंबंधी ४१% शारीरिक शिक्षण शिक्षकांना असे वाटते की, स्थानांतरणीय हालचाल कौशल्य या घटकावर शारीरिक शिक्षण संसाधन (व्हिडिओ) आवश्यक आहे. ४०% शारीरिक शिक्षण शिक्षकांना असे वाटते की, सह-साहित्यिक हालचाल कौशल्य या

घटकावर शारीरिक शिक्षण संसाधन (व्हिडिओ) आवश्यक आहे. १९% शारीरिक शिक्षण शिक्षकांना असे वाटते की, अस्थानांतरणीय हालचाल कौशल्य या घटकावर शारीरिक शिक्षण संसाधन (व्हिडिओ) आवश्यक आहे. स्थानांतरणीय हालचाल कौशल्य या घटकावर शारीरिक शिक्षण शिक्षकांना शारीरिक शिक्षण अध्यापन संसाधनाची (व्हिडिओ) जास्त आवश्यकता आहे.

कोष्टक क्र. ४

आपणास कोणत्या योगासनावर शारीरिक शिक्षण अध्यापन संसाधन (व्हिडिओ) आवश्यक आहे.

	उभे राहून आसने	बसून आसने	पोटावर झोपून आसने	पाठीवर झोपून आसने
मिळालेली एकूण मते	३६	३१	१५	१९



आकृती क्र.४: योगासन घटकांसंबंधी शारीरिक शिक्षण शिक्षकांच्या अध्यापन संसाधन (व्हिडिओ) गरजांचे विश्लेषण अर्थनिर्वचन

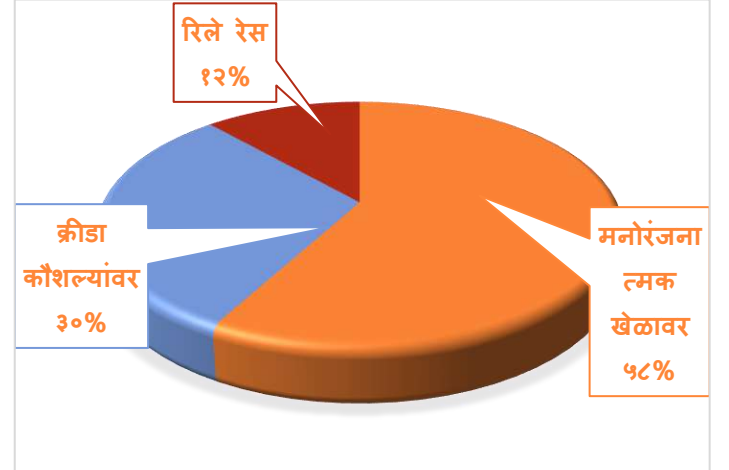
आकृती क्र.४ प्रस्तुत संशोधनामध्ये शारीरिक शिक्षण शिक्षकांच्या अध्यापन गरजांची माहिती मिळविण्यासाठी टेलिफोनिक मुलाखत या संशोधन साधनाचा वापर करण्यात आला. मिळालेल्या माहितीच्या विश्लेषणावरून योगासन घटकांसंबंधी ३५% शारीरिक शिक्षण शिक्षकांना असे वाटते की, उभे राहून योगासन या घटकावर शारीरिक शिक्षण संसाधन (व्हिडिओ) आवश्यक आहे. ३१% शारीरिक शिक्षण शिक्षकांना असे वाटते की, बसून योगासन या घटकावर शारीरिक शिक्षण संसाधन (व्हिडिओ) आवश्यक आहे. १९% शारीरिक शिक्षण शिक्षकांना असे वाटते की, पाठीवर झोपून योगासन या घटकावर शारीरिक शिक्षण संसाधन (व्हिडिओ) आवश्यक आहे. १५% शारीरिक शिक्षण शिक्षकांना असे वाटते की, पोटावर झोपून योगासन या घटकावर शारीरिक शिक्षण संसाधन (व्हिडिओ) आवश्यक आहे. उभे राहून योगासन या घटकावर शारीरिक शिक्षण शिक्षकांना शारीरिक

शिक्षण अध्यापन संसाधनाची (व्हिडिओ) जास्त आवश्यकता आहे.

कोष्टक क्र. ५

आपणास कोणत्या घटकावर शारीरिक शिक्षण अध्यापन संसाधन (व्हिडिओ) आवश्यक आहे.

	मनोरंजनात्मक खेळावर	क्रीडा कौशल्यांवर	रिले रेस
मिळालेली एकूण मते	४०	२१	८



आकृती क्र.५: शारीरिक शिक्षण शिक्षकांच्या अध्यापन संसाधन (व्हिडिओ) गरजांचे विश्लेषण

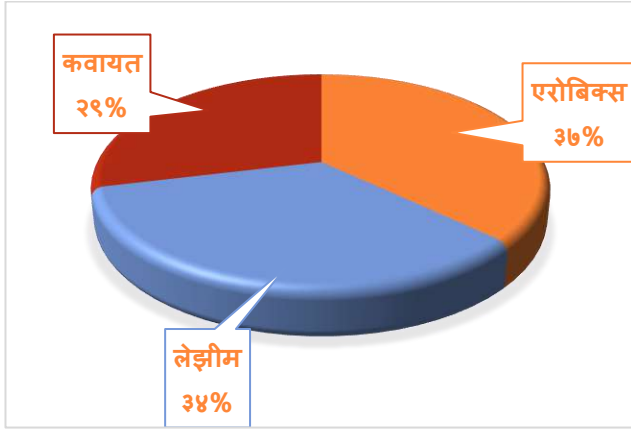
अर्थनिर्वचन

आकृती क्र.५ प्रस्तुत संशोधनामध्ये शारीरिक शिक्षण शिक्षकांच्या अध्यापन गरजांची माहिती मिळविण्यासाठी टेलिफोनिक मुलाखत या संशोधन साधनाचा वापर करण्यात आला. मिळालेल्या माहितीच्या विश्लेषणावरून ५८% शारीरिक शिक्षण शिक्षकांना असे वाटते की, मनोरंजनात्मक खेळ या घटकावर शारीरिक शिक्षण संसाधन (व्हिडिओ) आवश्यक आहे. ३०% शारीरिक शिक्षण शिक्षकांना असे वाटते की, क्रीडा कौशल्य या घटकावर शारीरिक शिक्षण संसाधन (व्हिडिओ) आवश्यक आहे. १२% शारीरिक शिक्षण शिक्षकांना असे वाटते की, रिले रेस या घटकावर शारीरिक शिक्षण संसाधन (व्हिडिओ) आवश्यक आहे. मनोरंजनात्मक खेळ या घटकावर शारीरिक शिक्षण शिक्षकांना शारीरिक शिक्षण अध्यापन संसाधनाची (व्हिडिओ) जास्त आवश्यकता आहे.

कोष्टक क्र. ६

आपणास कोणत्या तालबद्ध घटकावर शारीरिक शिक्षण अध्यापन संसाधन (व्हिडिओ) आवश्यक आहे.

	एरोबिक्स	लेडीम	कवायत
मिळालेली एकूण मते	२७	२५	२१



आकृती क्र.६: तालबद्ध घटकांसंबंधी शिक्षकांच्या अध्यापन संसाधन (व्हिडिओ) गरजांचे विश्लेषण

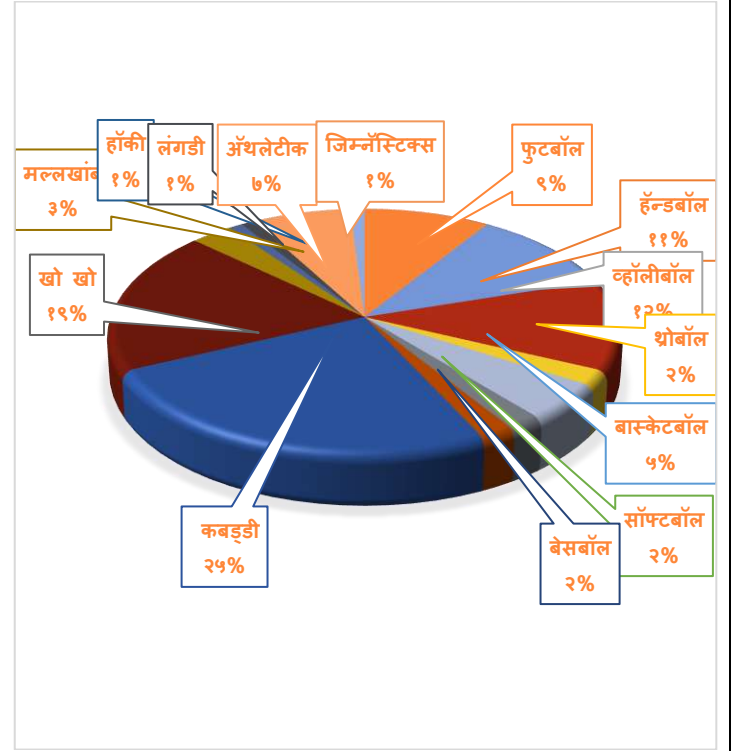
अर्थनिर्वचन

आकृती क्र.६ प्रस्तुत संशोधनामध्ये शारीरिक शिक्षण शिक्षकांच्या अध्यापन गरजांची माहिती मिळविण्यासाठी टेलिफोनिक मुलाखत या संशोधन साधनाचा वापर करण्यात आला. मिळालेल्या माहितीच्या विश्लेषणावरून तालबद्ध घटकांसंबंधी ३६% शारीरिक शिक्षण शिक्षकांना असे वाटते की, एरोबिक्स या घटकावर शारीरिक शिक्षण संसाधन (व्हिडिओ) आवश्यक आहे. ३४% शारीरिक शिक्षण शिक्षकांना असे वाटते की, लेझीम या घटकावर शारीरिक शिक्षण संसाधन (व्हिडिओ) आवश्यक आहे. २९% शारीरिक शिक्षण शिक्षकांना असे वाटते की, कवायत या घटकावर शारीरिक शिक्षण संसाधन (व्हिडिओ) आवश्यक आहे. एरोबिक्स या घटकावर शारीरिक शिक्षण शिक्षकांना शारीरिक शिक्षण अध्यापन संसाधनाची (व्हिडिओ) जास्त आवश्यकता आहे.

कोष्टक क्र. ७

आपणास कोणत्या खेळावर शारीरिक शिक्षण अध्यापन संसाधन आवश्यक आहे.

	मिळालेली एकूण मते
फुटबॉल	९
हॅन्डबॉल	११
व्हॉलीबॉल	१२
थोबॉल	२
बास्केटबॉल	५
सॉफ्टबॉल	२
बेसबॉल	२
कबड्डी	२५
खो खो	१९
मल्लखांब	३
हॉकी	१
लंगडी	१
अॅथलेटिक	७
जिम्नॅस्टिक्स	१



आकृती क्र.७: खेळ घटकांसंबंधी शिक्षकांच्या अध्यापन संसाधन (व्हिडिओ) गरजांचे विश्लेषण

अर्थनिर्वचन

आकृती क्र.७ प्रस्तुत संशोधनामध्ये शारीरिक शिक्षण शिक्षकांच्या अध्यापन गरजांची माहिती मिळविण्यासाठी टेलिफोनिक मुलाखत या संशोधन साधनाचा वापर करण्यात आला. मिळालेल्या माहितीच्या विश्लेषणावरून खेळ घटकांसंबंधी २५% शारीरिक शिक्षण शिक्षकांना असे वाटते की, कबड्डी या घटकावर शारीरिक शिक्षण संसाधन (व्हिडिओ) आवश्यक आहे. १९% शारीरिक शिक्षण शिक्षकांना असे वाटते की, खोखो या घटकावर शारीरिक शिक्षण संसाधन (व्हिडिओ) आवश्यक आहे. १२% शारीरिक शिक्षण शिक्षकांना असे वाटते की, व्हॉलीबॉल या घटकावर शारीरिक शिक्षण संसाधन (व्हिडिओ) आवश्यक आहे. ११% शारीरिक शिक्षण शिक्षकांना असे वाटते की, हॅन्डबॉल या घटकावर शारीरिक शिक्षण संसाधन (व्हिडिओ) आवश्यक आहे. ९% शारीरिक शिक्षण शिक्षकांना असे वाटते की, फुटबॉल या घटकावर शारीरिक शिक्षण संसाधन (व्हिडिओ) आवश्यक आहे. ७% शारीरिक शिक्षण शिक्षकांना असे वाटते की, अॅथलेटिक या घटकावर शारीरिक शिक्षण संसाधन (व्हिडिओ) आवश्यक आहे. ५% शारीरिक शिक्षण शिक्षकांना असे वाटते की, बास्केटबॉल या घटकावर शारीरिक शिक्षण संसाधन (व्हिडिओ) आवश्यक आहे. ३% शारीरिक शिक्षण शिक्षकांना असे वाटते की, मल्लखांब या घटकावर शारीरिक शिक्षण संसाधन (व्हिडिओ) आवश्यक आहे. २% शारीरिक शिक्षण शिक्षकांना असे वाटते की, थोबॉल या घटकावर शारीरिक शिक्षण संसाधन (व्हिडिओ) आवश्यक आहे. २% शारीरिक शिक्षण शिक्षकांना असे वाटते की, सॉफ्टबॉल या

घटकावर शारीरिक शिक्षण संसाधन (व्हिडिओ) आवश्यक आहे. २% शारीरिक शिक्षण शिक्षकांना असे वाटते की, बेसबॉल या घटकावर शारीरिक शिक्षण संसाधन (व्हिडिओ) आवश्यक आहे. १% शारीरिक शिक्षण शिक्षकांना असे वाटते की, हॉकी या घटकावर शारीरिक शिक्षण संसाधन (व्हिडिओ) आवश्यक आहे. १% शारीरिक शिक्षण शिक्षकांना असे वाटते की, लंगडी या घटकावर शारीरिक शिक्षण संसाधन (व्हिडिओ) आवश्यक आहे. १% शारीरिक शिक्षण शिक्षकांना असे वाटते की, जिम्नॅस्टिक्स या घटकावर शारीरिक शिक्षण संसाधन (व्हिडिओ) आवश्यक आहे. कबड्डी या घटकावर शारीरिक शिक्षण शिक्षकांना शारीरिक शिक्षण अध्यापन संसाधनाची (व्हिडिओ) जास्त आवश्यकता आहे.

निष्कर्ष

पुणे जिल्ह्यातील महाराष्ट्र राज्य प्राथमिक शिक्षण अभ्यासक्रमानुसार चालणाऱ्या शाळेच्या शारीरिक शिक्षण शिक्षकांच्या अध्यापन गरजांचा अभ्यास करण्यात आला. शारीरिक शिक्षण शिक्षकांना स्नायूंचा दमदारपणा, दिशाभिमुखता, स्थानांतरणीय हालचाल कौशल्य, उभे राहून योगासने, मनोरंजात्मक खेळ, एरोबिक्स आणि कबड्डी या शारीरिक शिक्षण घटकांवर शारीरिक शिक्षण अध्यापन संसाधन (व्हिडिओ) जास्त आवश्यक आहे.

संदर्भ

1. Burke, S., & Snyder, S. (2008). Youtube: An Innovative Learning Resource for College Health Education Courses. *International Electronics Journal of Health Education*, 11, 39-46.
2. Fevre, D. (2003). Designing for Teacher learning: Video-based curriculum design. *Using video in teacher education*, 235-258.
3. Godbout, P., Brunelle, J., & Tousignant, M. (1983). Academic learning time in elementary and secondary physical education classes. *Research Quarterly in Exercise and Sport*, 54(1), 11-19.

4. Hastie, P.A., & Saunders, J.E. (1991). Effect of class size and equipment availability on student involvement in physical education. *The Journal of Experimental Education*, 59 (3), 212-224.
5. Locke, L.F., & Lambdin, D. (2003). *Putting Research to Work in Elementary Physical Education*. Human Kinetic, Champaign.
6. McKenzie, T., Sallis, F., & Rosengard, P. (2009). Beyond the stucco tower: Design, development, and dissemination of the SPARK physical education programs. *Quest* 61(1), 114-127.
7. National Association for Sports and Physical education. Retrieved from <https://www.ericdigests.org/1997-4/physical.htm>
8. Placek, J., Silverman, S.S., Dadds, P., & Rife, F. (1982). Academic learning time (ALT-PE) in a traditional elementary physical education setting: A descriptive analysis. *Journal of Classroom Interaction*, 41-47.
9. Rink, J.E. (1985). *Teaching Physical Education for Learning*. St.Louis, Missouri: Times Mirror / Mosby College Publishing.
10. Silverman, S.J., & Ennis, C.D. (2003). Student Learning in Physical Education Applying Research to enhance Instruction. U.S.A: Human Kinetics, Champaign, IL.
11. कांगणे, सो., आहरे, श., & महाडिक, श्री.(२०१३).शारीरिक शिक्षण सेट/नेट (द्वितीय आवृत्ती) अभ्युदय प्रगती, १३१२, शिवाजीनगर, पुणे.
12. नॅगी. श., & बिबर, हे. (२०१७). गुणात्मक संशोधनाची कार्यपद्धती, सेज पब्लिकेशन, नवी दिल्ली.
13. महाराष्ट्र राज्य पाठ्यपुस्तक निर्मिती व अभ्यासक्रम संशोधन मंडळ (२०१५). शारीरिक शिक्षण हस्तपुस्तिका – इयत्ता पाचवी (प्रथमावृत्ती), पुणे.

COMPARISON OF PHYSICAL ACTIVITY LEVEL AMONG STUDENTS FROM DIFFERENT COURSES

Dr. Yogesh Bodke

Assistant Professor, CACPE, Pune.

Mr. Vilas Elke

Director of Physical Education, Radhabai Kale Mahila Mahavidyalaya, Ahmednagar.

Abstract

The purpose of this study was to study the physical activity level of the students from different courses run by the college in order to plan further fitness activity for them. This study was carried out by descriptive survey method. Total 180 students from Science, Commerce, Arts and BBA courses were selected by random sampling technique. Physical Activity Level was decided by asking the students to fill up Physical Activity Index Questionnaire. Data was collected through google form. Questionnaire was sent to 60 students from each course randomly and first 45 responses were considered for the study. Based on the total points of the questions, students were categorized as Sedentary, Low Active, Moderate Active and High Active. Students from all different course differ in the Physical Activity. Students of BA course seems more active than all other courses. BBA students were more sedentary compare to all other courses.

Keywords: Physical Activity, Fitness, Sedentary, Active.

Physical activity is defined by the World Health Organization as any physiological movement that needs energy expenditure and is performed by skeletal muscles. Physical exercise encompasses all forms of movement, whether it is done for fun, to go to and from locations, or as part of one's job. Physical activity, both moderate and intense, is beneficial to one's health. (*Physical Activity*, 2020)

According to WHO Recommended Activity Level for the age group of 18 years to 65 years is at least 150–300 minutes of moderate-intensity aerobic physical activity per week. 2 or More days must be given for muscle-strengthening activities at moderate or greater intensity. All adults and older individuals should try to perform more than the recommended amounts of moderate- to vigorous-intensity physical activity to help decrease the negative effects of excessive levels of sedentary behavior on health. (*Physical Activity*, 2020)

Exercise has been shown to assist with depression in a number of studies. Exercise can help filter out unpleasant thoughts and divert attention away from daily problems. Exercising with others allows to make more social connections. Increased exercise can help feel better and sleep better. (*Physical Activity - It's Important - Better Health Channel*, 2018)

During various Batchelor's courses, students have to undergo different course work and accordingly their study time differs. Many students find themselves in new routine that do not normally include physical activity. College's PE faculty always take initiative to keep the students fit and help them to maintain their fitness level. If faculty wants to decide the physical activity program for students, he must first understand the physical activity level of the students.

The purpose of this study was to study the physical activity level of the students from different courses run by the college in order to plan further fitness activity for them.

Method:

This study was carried out by descriptive survey method (Gay, 2000). Total 180 students from Ahmednagar city from Science, Commerce, Arts and BBA courses were selected by random sampling technique (Best, 2010) (45 from each course).

Physical Activity Level was decided by asking the students to fill up Physical Activity Index Questionnaire. Data was collected through google form. Questionnaire was sent to 60 students from each course randomly and first 45 responses were considered for the study. Based on the total points of the questions, students were categorized as Sedentary, Low Active, Moderate Active and High Active.

Statistical Analysis:

Table No 1 Courses wise Cross Tabulation of Physical Activity

		Science	Commerce	Arts	BBA	Total
PA	Sedentary	21	18	3	39	81
	Low Active	3	6	21	3	33
	Moderate Active	18	18	21	0	57
	High Active	3	3	0	3	9
Total		45	45	45	45	45

Table 1 shows that there were total 81 students were having sedentary activity. (Science 21, Commerce 18, Arts 3 and BBA 39), 33 students were low Active (Science 3, Commerce 6, Arts 21 and BBA 3), 57 students were Moderately active (Science 18, Commerce 18, Arts 21 and BBA 0) and only 9 students were highly active.

Table 2 Chi-Square Tests

	Value	df	Asymp. Sig. (2-sided)
Pearson Chi-Square	81.754 ^a	9	.000

Above table shows that Pearson chi square value is 81.75 which is significant at 0.05 level of significance.

Conclusions:

Students from all different course differ in the Physical Activity. Students of BA course seems more active than all other courses. BBA students were more sedentary compare to all other courses.

Overall students are following sedentary lifestyle more than active lifestyle.

Discussion:

Students need to follow well designed physical activity program in order to make them more active and help them to keep more fit, energetic, stress free and follow active lifestyle.

References

Best, J. (2010). Educational Research (10th ed.). Pearson.

Gay, L. (2000). Educational Research (6th ed.). Pearson.

Physical activity. (2020, November 26). <https://www.who.int/news-room/fact-sheets/detail/physical-activity>

Physical activity—It's important—Better Health Channel. (2018). <https://www.betterhealth.vic.gov.au/health/healthyliving/physical-activity-its-important>

16	प्रा.डॉ. अशोक कानडे	सिंधू संस्कृती: समृद्ध कलेचा प्राचीन वारसा	74
17	अमित कवठाळे	सामाजिक संशोधनात सर्वेक्षण पद्धतीचे महत्व	76
18	डॉ.लोखंडे. बी.बी.	नवीन शैक्षणिक धोरण उच्चशिक्षणासाठी सुसंगत	80
19	डॉ. बाळासाहेब निर्मळ	भारतीय रोजगार निर्मितीत सार्वजनिक उपक्रमांचे योगदान	82
20	डॉ.बब्रुवान मोरे	महान समाज सुधारक महात्मा बसवेश्वरांचे कार्य	87
21	डॉ. रायठक दिपमाला	कौटुंबिक, औद्योगिक समस्या	91
22	डॉ. सांगळे भगवान	ग्रामीण विकास प्रशासनाचे पर्यावरण	94
23	प्रा.डॉ. सवाई एम.के.	डॉ. बाबासाहेब आंबेडकर यांची सामाजिक विचार व कार्य	99
24	सौ. सुनिता रंगारी	मराठी काव्यातून उमटलेली शेतकरी समस्या : एक वेध	101
25	डॉ. मुक्ता सोमवंशी	स्वच्छ भारत अभियान - एक चिकित्सक अभ्यास	106
26	प्रा.शिवकुमार उस्तुर्गे	स्त्री-भ्रण हत्या : एक सामाजिक समस्या	110
27	प्रा.अरूणा वाळके	महाविद्यालयीन विद्यार्थ्यांमध्ये मोबाईलचा वापर : एक अभ्यास संदर्भ : श्री पं.पा. महाविद्यालय, सिरसाळा	113
28	प्राचार्य पुष्पा तायडे	बहुराष्ट्रीय कंपन्यांचा भारतीय अर्थ व्यवस्थेवर प्रभाव	116
29	डॉ.एन.एन. कुंभारीकर	सुशासन : एक आदर्श प्रशासकीय व्यवस्था	124
30	डॉ.दाडगे सुरेखा	नवीन कृषी कायदे: आपेक्षा आणि फायदे व तोटे	126
31	डॉ. बा. आ. साबळे प्रा. वि. भ. काळे	अहमदनगर जिल्ह्यातील असंघटित क्षेत्रावर कोविड-१९ चा झालेला आर्थिक व सामाजिक परिणाम.	129

अहमदनगरजिल्ह्यातील असंघटित क्षेत्रावर कोविड-१९ चा झालेला आर्थिकव सामाजिक परिणाम.

डॉ. बा. आ. साबळे

सहा. प्राध्यापक तथा संशोधक मार्गदर्शक

श्री पंडितगुरु पाडीकर महाविद्यालय सिरसाळा ता. परळी वै. जि. बीड

प्रा. वि. भ. काळे

राधाबाई काळे महिला महाविद्यालय, अहमदनगर

प्रस्तावना :-

कोविड-१९ विषाणूच्या संक्रमणामुळे निर्माण झालेले संकट भारतातील असंघटित क्षेत्रामध्येकाम करणाऱ्या 42कोटी कामगारांना गरिबीच्या खोल गर्तेत लोटून गेला याचा गंभीर परिणाम भारतीय अर्थव्यवस्थेवर झाला. कोविड-१९चा प्रादुर्भाव रोखण्यासाठी केंद्र सरकारने मार्च 2020 ला संपूर्ण देशामध्ये लॉकडाऊन घोषित केलं त्यामुळे या असंघटित कामगारांच्या रोजगारावर आणि मिळकतीवर नकारात्मक परिणाम झाला . सध्या निर्माण झालेली संकटाची स्थिती हाताळण्यासाठी पुरेशी तयारी नसलेल्या देशात भारताचा समावेश असल्याची जाणीव आपल्याला वेळोवेळी होताना दिसून येते .कोविड-१९ चा विषाणू रोखण्यासाठी करण्यात आलेल्या उपाय योजनांचा फटका भारतातील असंघटित क्षेत्रातील कोट्यावधी कामगारांना बसलेला आहे. लॉकडाऊन सारख्या उपाय योजनांमुळे फटका बसलेल्या असंघटित क्षेत्रातील कामगारांची संख्या नायजेरिया , भारत आणि ब्राझील या देशां मध्ये सर्वाधिक आहे . भारतात एकूण कामगार लोकसंख्या पैकी 92% लोक असंघटित क्षेत्रात काम करतात त्यामुळे सध्याच्या संकट काळात असंघटित क्षेत्रातील सुमारे 42कोटी कामगारांवर दारिद्र्य आलेल आहे . त्यामुळे शहरांमध्ये स्थायिक झाले त्या कामगारांवर या लॉकडाऊनच्या स्थितीत ग्रामीण भागाकडे परत येण्याची वेळ आली . नैसर्गिक आपत्ती ,सक्तीचे विस्थापन, विविध संघर्ष आदींचा सामना करणाऱ्या देशांमध्ये सध्याच्या जागतिक साथीच्या रोगांमुळे अतिरिक्त भर पडली.कोविड-१९ शी सामना करण्यासाठी असंघटित क्षेत्रातील कामगार सक्षम नाही त तसेचया वर्गाला उपलब्ध असलेल्या मूलभूत सोयीसुविधा विशेषत आरोग्य आणि स्वच्छता मर्यादित आहे त. त्यांना चांगले काम , सामाजिक संरक्षण, आर्थिक संरक्षण , कामाच्या ठिकाणी सुरक्षा या बाबींपासून वंचित राहावे लागते . कोविड-१९मुळे जागतिक स्तरावर 2008-09 पेक्षाही मोठे आर्थिक संकट निर्माण झाले ले आहे. राहण्याच्या सोयी सुविधा , अन्न सेवा, उत्पादन रिटेल, व्यापार आणि प्रशासकीय कामकाजात या क्षेत्रांना खूप मोठ्या प्रमाणात धोका निर्माण झाला. जागतिक पातळीवर खूप मोठी बेरोजगारीची लाट निर्माण झाली.

कोविड-१९ मुळे असंघटित कामगारांवर उपासमारीची वेळ आली. जगाचा पोशिंदा असलेला शेतकऱ्यांच्या फळ बागाला लॉकडाऊन मुळे बाजार मिळाला नसल्याने कवडीमोल भावात फळ पिक विकावे लागले. बिगारी कामगार, भाजीपाला विक्रेते यांचे हातावर पोट असल्यामुळे त्यांना खूप मोठ्या प्रमाणात सामाजिक-आर्थिक त्रास

सहन करावा लागतो. बांधकाम कामगार व घर काम करणाऱ्या स्त्रियांचे काम बंद झाले त्यामुळे त्यांच्या आर्थिक स्थितीवर वाईट परिणाम होऊन हलाखीची परिस्थिती निर्माण झालेली आहे . जगभरात ज्या काही मूठभर देशांच्या अर्थव्यवस्था झपाट्याने विकसित होत आहेत त्यात भारताचा वरचा क्रमांक लागतो . त्यामुळे भारताचे आर्थिक भवितव्य उज्वल असल्याचा विद्यमान सरकारला जबरदस्त अभिमान वाटत असला तरी वस्तुस्थिती नेमकी याच्या उलट आहे कारण भारतीय अर्थव्यवस्थेत असंघटित कामगारांचे प्रमाण हे 92 % आहे याच कामगारांची आर्थिक स्थिती सध्या कोविड-१९मुळे बिकट झालेली आहे . असंघटित क्षेत्रातील 42 कोटी कामगारांचे देशाच्या GDP मध्ये 50% योगदान देतात. काम बंद हाती पैसा नाही. पैसा नाही तर घर गाढा कसा हाकायचा. सतत दुष्काळाशी करावा लागत असलेला सामना आणि आर्थिक परिस्थिती बेताची गावाकडे कामधंदा मिळना या ना त्या कारणामुळे ग्रामीण भागातील असंख्य नागरिक रोजीरोटीच्या निमित्ताने मोठ्या शहरांकडे जातात हे लोक कंत्राटी किंवा हंगामी काम करतात कंत्राटदाराच्या मनात आले तर त्यांना काम मिळते परिणामी घरातील चूल पेटत असते तर हजारोंच्या संख्येने नाक्यावरील कामगारांना रोज कामाचा शोध घ्यावा लागतो ही वस्तुस्थिती आहे. यातच चीनमध्ये सुरु झालेला कोविड-१९चा प्रसार संपूर्ण जगभर झाला. आपल्या देशातही कोविड-१९चा फैलाव झाला व तो रोखण्यासाठी लॉकडाउन करावे लागले अत्यावश्यक सेवा वगळता सर्वच लॉकडाउन करण्यात आले.

कोविड-१९ संकल्पना :-

17 नोव्हेंबर 2019 मध्ये चीनच्या हुबेई प्रांताची राजधानी वूहान मध्ये या नवीन आजाराची पहिली ओळख करण्यात आली होती आणि त्या नंतर जागतिक स्तरावर या आजाराचा प्रसार झाला व त्याने जागतिक महामारीचे रूप धारण केले महाराष्ट्रातील कोरोना विषाणू उद्रेकातील पहिल्या रुग्णाची नोंद 9 मार्च 2020 रोजी पुण्यात झाली. हा विषाणू प्रामुख्याने जवळच्या संपर्कादरम्यान, खोकल्यामुळे, शिंकण्याने किंवा बोलताना नकळत बाहेर पडणाऱ्या थुंकीच्या तुषारांमुळे लोकांमध्ये पसरतो. हे विषाणू 72 तासापर्यंत दुषित पृष्ठभागावर जिवंत राहू शकतात. या रोगाच्या निदानाची मानक पद्धत म्हणजे नाकातून घेतलेल्या नमुन्यांची रिअल टाईम रिव्हर्स ट्रान्सक्रिप्शनपॉलीमरेज चेन रिएक्शन (RRT-PCR) नावाची तपासणी होय. जागतिक आरोग्य संघटनेने हा कोरोनाव्हायरस हा रोग 2019 (कोविड-१९) चा उद्रेक हा सार्वजनिक आरोग्यासाठी आंतरराष्ट्रीय आणीबाणी असल्याचे सांगत या उद्रेकाला जागतिक महामारी म्हणून जाहीर केले. कोविड-१९ हे नाव टेड्रोस अँडम हॅनोम गेब्रेयेसोस यांनी घोषित केले. इंटरनॅशनल कमिटी ऑफ टोक्सोनॉमीऑफ व्हायरस यांनी SARS-CoV-2 हे नाव दिले.

कोविड-१९ चे लक्षण :-

सर्दी, ताप, कोरडा खोकला, दम लागणे, श्वास घेण्यात अडचण, घसा खवखवणे, मळमळ, अतिसार, वास किंवा चव जाणे, अंगदुखी, डोकेदुखी.

संशोधन विषयाचे महत्त्व व आवश्यकता :-

कोविड-१९ चे अर्थव्यवस्थेत अर्थव्यवस्थेवर झालेले परिणाम :-

आज कोरोना मुळे संपूर्ण जग अडचणीत आले. बहुतांश देशांचे आर्थिक व्यवहार ठप्प झालेले दिसून येत आहेत. यामुळे देशांतर्गत उत्पादन सेवा आणि उद्योग बंद करण्यात आले. या कामात आरोग्य सेवेवर मोठा निधी खर्च होत आहे या कामात निधी कमी पडला तर इतर विकासकामांना कात्री लावून तो निधी आरोग्य व इतर अत्यावश्यक सेवेवर खर्च करण्यात येईल यात काही शंका नाही. 2020-21 या आर्थिक वर्षामध्ये प्रत्यक्ष कर संकलनात 1.44 लाख कोटी रुपयांची तुट पडली. या शिवाय GST कर संकलना मध्ये मोठी तुट दिसून येतेय मार्च 2020 या महिन्याचे नियोजित कर संकलन 1.25 लाख कोटी होते परंतु प्रत्यक्षात 0.98 लाख कोटी कर संकलन झाले. फेब्रुवारी 2020 अखेर पर्यंत जाहीर केलेल्या आकडेवारीनुसार वित्तीय तूट 3% वरून 5% पर्यंत वाढली. यामुळे अंदाजित उत्पन्न आणि प्रत्यक्ष मिळालेले उत्पन्न यामध्ये मोठी तफावत दिसून येते. जागतिक मंदीमुळे जागतिक बँक व इतर वित्तीय संस्था यांच्याकडून कर्ज घेण्यावर काही मर्यादा येणार आहेत देशातील टाळेबंदी मुळे विविध उद्योग मोठ्या प्रमाणावर बाधित झाले आहेत यामध्ये प्रामुख्याने बांधकाम व्यवसाय, पर्यटन उद्योग, वाहन उद्योग, वित्तीय संस्था, हॉटेल उद्योग, वाहतूक उद्योग, माहिती तंत्रज्ञान क्षेत्र आणि या सर्व व्यवसायात वर अवलंबून असणारे इतर छोटे मोठे उद्योग व सेवा क्षेत्र मोठ्या प्रमाणावर बाधित झालेले आहे यामुळे असंघटित कामगारांचे रोजगार जाऊन त्यांच्यावर खूप मोठे आर्थिक संकट निर्माण झाले. भारतामध्ये दर तीन महिन्यांनी GDP मधील वाढ किंवा घटीचे आकडे प्रकाशित होत असतात. ही पद्धत 1996 पासून आज पर्यंत सुरू आहे 2020-21 च्या पहिल्या तिमाहीत (एप्रिल-जून) भारतीय GDP मध्ये 23.9% घट नोंदवली गेली. जगामध्ये भारताचा GDP सर्वात जास्त घसरला आहे. भारताच्या GDP ची जगातील इतर देशांच्या GDP शी तुलना केली असता भारत -23.9% युके -20.4% फ्रान्स -13.8% इटली -12.4% कॅनडा -12% जर्मनी -10.1% युएस -9.5% जपान -7.6% भारताचा GDP चा घसरण दर जास्त आढळून येईल.

कोविड-१९ एक गंभीर समस्या :-

कोरोना विषाणूचा वेगाने फैलाव झाल्याने अवघ्या जगावर त्याचे परिणाम जाणवले. कोविड-१९ ही जागतिक महामारी घोषित झाली. अजूनही संपूर्ण जगामध्ये लसीकरण होणे आणि ही स्थिती बदलण्यासाठी लस किती उपयुक्त आहे हे ठरविणे बाकी आहे. विषाणूचा प्रसार होत असल्याने राज्य सरकारांनी मुक्तसंचारावर लावलेल्या निर्बंधांमुळे सर्वात मोठा परिणाम सेवा क्षेत्रावर झाला लोकांना कामाच्या ठिकाणी सार्वजनिक वाहनातून जाता येत नसल्याने बेरोजगारी वृद्धी झाली. भारतातील बहुसंख्य रोजगार असंघटित क्षेत्रात असल्यामुळे कामाच्या अभावाने लाखो स्थलांतरित मजूर यांना त्यांच्या मूळ गावी परतावे लागले या धोरणामुळे अनेक कंपन्यांना त्यांच्या कामकाजात मोठा बदल करावा लागला. कोरोनाच्या उद्रेकामुळे सोशल डिस्टेंसिंग च्या नियमाने वर्क फ्रॉम होम चा प्रसार झाला. कोविड-१९ चा उद्रेक झाल्याने सरकारी आणि मध्यवर्ती बँकांनी जागतिक मंदीच्या काळापेक्षाही मोठ्या प्रमाणात प्रोत्साहनपर आर्थिक पॅकेज जाहीर करावी लागली. महाराष्ट्रातील महा विकास आघाडी शासनाने लॉकडाऊन मुळे बाधित होणाऱ्या कामगारांसाठी आर्थिक पॅकेज जाहीर केले केंद्र शासनाने ही याच धर्तीवर आर्थिक पॅकेज जाहीर करावे अशी मागणी समाज माध्यमावर होताना दिसून येत आहे. राज्यात निर्बंध सुरू करण्यात आले, राज्यातील उद्योग व दुकाने यांचे काम बंद झाल्याकारणाने राज्यातील असंघटित क्षेत्रातील कामगारांचे उत्पन्न बंद होणार असल्याने या घटकावर

या काळात कसे जगायचे असा प्रश्न आहे राज्य शासनाने आर्थिक पॅकेज जाहीर केले परंतु नोंद कामगारांना हे आर्थिक सहाय्य देण्यात येईल ही अट अन्यायकारक आहे त्यामुळे बहुसंख्य कामगारांना या आर्थिक पॅकेजचा लाभ मिळणार नाही म्हणून शासनाने कामगारांची नोंद असण्याची अट रद्द करून सर्व असंघटित कामगारांना आर्थिक पॅकेज द्यावे. भर उन्हाळ्याच्या दिवसांमध्ये कुंभार व्यवसाय आर्थिक अडचणीत असलेला आपल्याला पाहायला मिळेल. या कुंभार व्यवसाय करण्याची नोंद सरकार दरबारी नसते मग यांना आर्थिक मदत कशी मिळेल हे महाराष्ट्र सरकार ने नियोजन करायला पाहिजे.

जनसामान्यांचे जनजीवन विस्कळीत :-

कोरोना विषाणूच्या संसर्गामुळे आपल्यापैकी अनेकांच्या जीवाला घोर लावला आहे इतकंच नाही तर या जागतिक साथीचा लोकांच्या मन स्वास्थ्यावर विपरीत परिणाम झालेला आहे आणि हे आरोग्यआरोग्य संकट निघून गेल्यावरही त्यांना मानसिक समस्यांचा सामना करावा लागेल भारतीय अर्थव्यवस्थेतील 92% कामगार असंघटित क्षेत्रांमध्ये कार्य करतात पण या कोरोना साथीमुळे या असंघटित कामगारबेरोजगार होऊन त्यांच्यावर उपासमारीची वेळ आली आहे.

अनाथांचा उदरनिर्वाहाचा प्रश्न :-

कोरोना काळात जन्मापासून अनाथ असणारी आणि कोरोना मुळे ज्यांच्या पालकांचे निधन झाले अश्या मुलांचा उदरनिर्वाहाचा प्रश्न ऐरणीवर आला आहे. या मुलांपैकी अनेकांसमोर दोन वेळचे जेवण मिळवणे हेच आयुष्याचे ध्येय बनले. अनाथालयाचे य छत्र सुटल्यानंतर अनेक मुले एकत्र येऊन भाड्याच्या खोलीत राहत मात्र रोजगारच नसल्याने भाडे भरण्याची ऐपत नसलेल्या तरुणांना नैराश्याने घेरले आहे टाळेबंदी च्या काळात प्रचंड हाल झाले असे संशोधन करत्याच्या लक्षात आले म्हणून यावर संशोधन होणे संशोधन करत्याला आवश्यक वाटले.

संशोधनाचे उद्दिष्टे :-

1. कोविडचा असंघटित क्षेत्रावर होणाऱ्या परिणामांचा अभ्यास करणे १९-
2. कोविड.चा भारतीय अर्थव्यवस्थेवर झालेल्या परिणामाचा उपाययोजनात्मक अभ्यास करणे १९-

ग्रहीतके :-

1. कोविड चा १९-भारतीय अर्थव्यवस्थेवर अनुकूल व प्रतिकूल परिणाम होत आहे.
2. कोविड.मुळे असंघटित क्षेत्रावर प्रतिकूल परिणाम होत आहेत १९-

असंघटित क्षेत्राची कोविड-१९ काळातील परिस्थिती :-

दिवसेंदिवस वाढती बेरोजगारी :-

अहमदनगर जिल्ह्यात बेरोजगारी ही मोठ्या प्रमाणात वाढलेली असताना कोविड-१९मुळे कंपन्यांना टाळेबंदी लागली या टाळेबंदी मुळे हंगामी रोजगार आणि कंत्राटी कामगार यांना कोणी वाली राहिलेला नाही. या स्थितीत या कामगारावर अति दारिद्र्य आलेले असताना त्यातून घरभाडे जेवणाचा खर्च देखील हे लोक करू शकत नाहीत

सरकारची तुटपुंजी मदत किती दिवस चालणार छोटी छोटी हॉटेल्स, खाद्यपदार्थांच्या गाड्या, छोट्या चहाच्या टपऱ्या, यात काम करणारे लोक आर्थिक अडचणीत आले त्यातच अहमदनगर जिल्हा हा राज्याच्या मध्यभागी येतो त्यामुळे बाहेरून आलेले मजुरांची संख्या येथे जास्त आहे लॉकडाऊन च्या काळात या मजुरांना परत गावी जाण्यासाठी देखील पैसे राहिलेली नव्हते. अहमदनगर शहरांमध्ये घर काम करणाऱ्या स्त्रियांचे प्रमाण जास्त आहे कोरोना व्हायच्या भीतीपोटी या महिलांचे काम गेले आणि लोकांच्या घरात स्वयंपाकाचे काम करणाऱ्या या स्त्रियांची घरची चूल पेटणे बंद झाली. भाजीविक्रेते बिगारी कामगार यांचे हातावरचे पोट काम मिळणे बंद झाल्याने तर या लोकांना दोन वेळचे जेवण मिळणे कठीण झाले किती हि दारिद्र्याची अवस्था.

अहमदनगर जिल्ह्यातील शेती क्षेत्रावर झालेला परिणाम :-

भारत हा कृषिप्रधान देश. देशात 65% रोजगार हा शेती क्षेत्रातून प्राप्त होतो ह्या क्षेत्राचा 2020-21 या आर्थिक वर्षाच्या पहिल्या तिमाहीत जी डी पी मधील वाढ 3.4% नोंदवली गेली जेव्हा भारताचा जीडीपी 23.9% होता. तरीपण लॉकडाऊन मुळे अहमदनगर जिल्ह्यातील फळबाग शेतकऱ्यांवर वाईट वेळ आली त्यांच्या फळांना या लॉकडाऊन मध्ये वेळीच बाजार मिळाला नाही म्हणून सर्व फळबागा ग्राहकाविना ओस पडून होत्या.

अहमदनगर जिल्ह्यातील कोविड-१९ चा व्यवसाय क्षेत्रावर झालेला परिणाम:-

भारत सरकार ने 24मार्च 2020 रोजीच्या सायंकाळी 21 दिवसांचा लॉकडाऊन घोषित केला आणि 138 कोटी लोकसंख्या स्वतःच्या घरांमध्ये कैद झाली. त्यात लहान व्यावसायिकांचे कंबरडे मोडले. वडापाव गाडी चालवणारे व्यावसायिक, चहाची टपरी वाले, लहान लहान हॉटेल, सगळे बंद पडले ज्यांनी नवीन उद्योग, व्यवसाय सुरु केला त्याचा पैसा डब्यात गेला. काही नव-उद्योजकंवर तर आत्महत्या करण्याची वेळ आली या कोविड-१९ने कित्येक व्यावसायिकांचे जीव घेतले. त्यामुळे या क्षेत्रात काम करणार्यांचा रोजगार गेला परिणाम यांची आर्थिक व सामाजिक परिस्थिती हलाखीची बनली.

स्थलांतरित कामगारांची परिस्थिती :-

केंद्रसरकारने लॉकडाऊन ची प्रक्रिया सुरु केली तेव्हा लोकांना वाटले हे फक्त थोडा काळाकरिता राहिल पण सरकारने ही प्रक्रिया पुढे तशीच सुरु ठेवली प्रथम 25 मार्च 2020 ते 14 एप्रिल 2020 हे लॉकडाऊन 21 दिवसांचे, 15 एप्रिल 2020 ते 3 मे 2020 हे लॉकडाऊन 19 दिवस, 4 मे 2020 ते 17 मे 2020 हे लॉकडाऊन 14 दिवस, 18 मे 2020 ते 31 मे 2020 हे लॉकडाऊन 14 दिवस असे 68 दिवस ही प्रक्रिया चालली या कालावधीत जे स्थलांतरित कामगार आहेत त्यांच्या जवळील पैसे संपले त्यांचे खायचे हाल व्हायला लागल्यामुळे ते परत त्यांच्या घराकडे निघाले. परत जाण्यासाठी वाहने नव्हती म्हणून त्यांना पायी-पायी, सायकल ने जावेलागले. वाटेत खाण्यापिण्यासाठी त्यांना बऱ्याच अडचणींना सामोरे जावे लागले. बरेच कामगार परराज्यातून आलेले होते बऱ्याच कामगारांचा मे महिन्यातील कडक उन्हात उपासमारीने आणि चालून-चालून मृत्यू झाला. त्यात शासनाचा गलथान कारभार या लोकांच्या जीवावर आला. लाल फितीचा प्रक्रिया पूर्ण व्हायला काही दिवसांचा काळ लोटला कामगारांचे हाल व्हायला लागले बऱ्याच ठिकाणी निदर्शने गोंधळ पाहायला मिळालालाखो कामगार प्रामुख्याने बांधकाम क्षेत्र, हॉटेल, वडापावच्या गाड्या, चहाच्या टपऱ्या, बिगारी काम करणारे आहेत यांची मुळातच आर्थिक परिस्थिती ही दारिद्र्याची आहे.

कोविड-१९ चे सामाजिक व आर्थिकपरिणाम :-**सामाजिक,अनुकूल परिणाम:-**

1. सार्वजनिक वाहतूक बंद,खाजगी वाहतूक बंद असल्यामुळे हवेचा दर्जा सुधारलेला आहे ,
2. कारखाने बंद जल पर्यटन बंद असल्यामुळे पाण्याचा दर्जा सुधारला पिण्यासाठी स्वच्छ पाणी उपलब्ध , झालेले आहे
3. लोकांना कोरोनाव्हायरस मुळे आरोग्याचे काळजी घेण्याची सवय लागली उदा , साबणाने हात धुणे . तो ,खोकताना ,सॅनिटायझर चा वापर करणे सार्वजनिक ठिकाणी नथुंकणे शिंकताना ंडाला रुमाल लावने.
4. मानवतेच्या दृष्टिकोनातून समाजातील लोक एकमेकांची मदत करण्यासाठी समोर आले
5. या दगदगीच्या जीवनात माणूस कुटुंबापासून व नातेवाईकांपासून दुरावत होता या महासाथीतील लॉकडाऊन मध्ये कुटुंबासोबत व नातेवाईकांसोबत वेळ घालवला त्यामुळे नात्यांमध्ये गोडवा निर्माण झाला.
6. लोकांना वर्क फ्रॉम होम मुळे तंत्रज्ञानाचा वापर करावा लागेला त्यामुळे तांत्रिक ज्ञानमध्ये वाढ झाली.

प्रतिकूल परिणाम :-

1. कोरोनाव्हायरस अकाली निधनामुळे कुटुंबाच्या कुटुंब उध्वस्त झाले.
2. समाजामध्येवाईट प्रवृत्ती मध्ये वाढ झालीउदा.चोरी करणे .
3. भीतीयुक्त वातावरणामुळे तनावजन्य परिस्थितीत वाढ झाली.
4. जीवनचक्र कोलमडले.
5. शाळा.प्रशासकीय कार्यालय बंद असल्यामुळे समाजजीवन विस्कळीत झाले ,कॉलेज,

आर्थिक परिणाम ,अनुकूल परिणाम :-

1. या कोविड.साथी मध्ये लोकांना बचतीचे महत्व समजले१९-
2. सरकारला अशा महासाथीच्या विरुद्ध लढण्यासाठी अगोदर कोणकोणती अतिरिक्त काळजी घ्यावी लागते याबद्दल ज्ञान प्राप्त झाले आरोग्य , अतिरिक्त ऑक्सिजनचा साठा , अतिरिक्त हॉस्पिटलची निर्मिती .उदा . अतिरिक्त राखीव निधी ,कर्मचाऱ्यांना प्रशिक्षण
3. पी केअर फंड मध्ये सर्व देशातील लोकांनी आर्थिक मदत केली तेव्हा द .एम .ेशाची एकात्मता दिसून आली.
4. कोविड.मुळे सरकारला अर्थव्यवस्थेतील कमजोर बाजू निदर्शनास आली १९-

प्रतिकूल परिणाम :-

1. बेरोजगारीत वाढ.
2. समाजाचा आर्थिक गणित बिघडले.
3. दारिद्र्या मध्ये वाढ झाली.

निष्कर्ष :-

1. कडक निर्बंध लावल्यामुळे गरीब कामगारांचे मोठ्या प्रमाणावर आर्थिक स्थिती खालावली आहे
2. पैसे नसल्यामुळे व मालकांनी घर भाड्याचा तगादा लावल्यामुळे हे लोक पुन्हा त्यांच्या मूळ गावी स्थलांतरित करित आहे
3. बस रेल्वे सेवा बंद असल्याने किंवा त्यांचे भाडे द्यायला तेवढे पैसे नसल्याने हे लोक पायी प्रवास करत , आहेत
4. आर्थिक स्थिती खालावल्यामुळे कामगारांना दोन वेळचे जेवण व्यवस्थित मिळत नसल्याने त्यांच्या आरोग्यावरही परिणाम होत आहे
5. मजूर बऱ्यापैकी वेगवेगळ्या ठिकाणावरून कामानिमित्त येथे आले असल्याने त्यांना स्थानिकरेशन दुकानातून धान्य मिळत नाही
6. भत्ता जेवणाची जबाबदारी घ्यायला तयार , वेतन मिळत नाही मालक वर्ग या कामगारांची राहण्याची , नसल्याचे दिसून येत आहे
7. गरीब लोकांसाठी असलेल्या शिवभोजन थाळी ची संख्या कमी असल्याने सर्व कामगारा पर्यंत हि योजना पोहोचत नाही तसेच या ठिकाणी मोठ्या प्रमाणावर गर्दी होऊन लांबच लांब रांगा लागत आहेत.
8. लोकांच्या समस्या सोडविण्यासाठी सरकार कडून कोणत्याही प्रकारची हेल्पलाइन सुविधा निर्माण करण्यात आली नाही.
9. स्वयंसेवी संस्था म्हणावे इतका या लोकांसाठी पुढाकार घेत नाही

उपायोजना :-

1. सरकारने शिवभोजन थाळी सारख्या योजना राबूउन थाळी च्या संख्येमध्ये वाढ करावी
2. स्वयंसेवी संस्था पुढे येऊन ह्या लोकांना कपडे, औषध या गोष्टीची मदत केली पाहिजे-अन्न .
3. सरकारनेया लोकांना आर्थिक भत्ता देउन मदत करावी.
4. ह्या लोकांच्या कर्जाचे हप्ते वसुलीवर काही कालावधीसाठी बंदी घालवी.
5. हे लोक ज्या घरात राहत आहे त्या घर मालकांनी घर भाडे वसुली काही काळ थांबवण्याचे आदेश सरकारने द्यावेत.
6. वेगाने लसीकरण करून आणि कडक निर्बंध लाऊन व्यवसाय करण्यास परवानगी देता येईल का याबाबत तपासणी करावी.
7. स्वस्त धान्य दुकानातून ह्या लोकांना कुटुंबाला पुरेल एवढे धान्य मिळावे आधार कार्ड रेशन कार्ड या बाबत काही प्रमाणात सूट द्यावी.
8. लोकांनी सतत हात धुण्याची सवय लाऊन आरोग्याची पुरेशी काळजी घ्यावी याबाबत सामाजसेवकानी प्रबोधन करावे.

9. लोकांच्या अडचणी सोडविण्यासाठी हेल्पलाइन नंबर सुविधा सुरू कराव्यात
10. विधवा ज्येष्ठ व्यक्ती अपंग यासारख्या व्यक्तींना मदत करावी
11. देवस्थानांनी या लोकांसाठी अन्नछत्र व आरोग्यविषयक सुविधा उपलब्ध करून द्यायला पाहिजे
12. जे लोक त्यांच्या मूळ गावी परतु इच्छितात त्यांच्या जाण्याची सुविधा सरकारने करून द्यायला पाहिजे

संदर्भसूची :-

01. डॉ.श्र,आगलावे प्रदीप .ी साईनाथ प्रकाशन.सहावी आवृत्ती ,नागपूर ,
02. www.esakal.com
03. www.orfonline.org
04. www.who.int
05. www.livescience.com
06. www.bbc.com
07. www.lokmat.com
08. mr.wikipedia.org
09. maharashtratimes.com
10. pib.gov.in



ANALYSIS OF THE TEACHING RESOURCE NEEDS OF PHYSICAL EDUCATION TEACHERS

Mr. Vilas Uttam Elke Director of Physical Education, Radhabai Kale Mahila
Mahavidyalaya, Ahmednagar.

Dr. Sharad Aher Professor, CACPE, Pune.

Abstract

The purpose of this study was to analyze the teaching resource (Video) needs of the primary school physical education teachers. This study was carried out by descriptive survey method. Total 184 primary school physical education teachers from Maharashtra state were selected by random sampling technique. Teaching resources needs were decided by asking the physical education teachers to fill up Need Analysis Questionnaire. Data was collected through google form. Questionnaire was sent to 184 primary school physical education teachers from Maharashtra state randomly and their responses were considered for the study. Based on the questionnaire, physical education teachers responses were categorized as Health Related Physical Fitness Components, Skill Related Physical Fitness Components, Fundamental Movement Skills, Yoga Asana, Rhythmic Components and Sports. Different responses received from Physical education teachers. Primary School Physical education teacher needs more physical education teaching resources (video) on the physical education components such as Cardiovascular Endurance, Co-ordination, Manipulative Movement Skills, Standing Yoga Asanas, Sports Skills, Aerobics and Athletics.

Keywords: Physical education, Teaching Resource.

Introduction

Physical Education is "education through the physical". It aims to develop students' physical competence and knowledge of movement and safety, and their ability to use these to perform in a wide range of activities associated with the development of an active and healthy lifestyle. It also develops students' confidence and generic skills, especially those of collaboration, communication, creativity, critical thinking and aesthetic appreciation. These, together with the nurturing of positive values and attitudes in PE, provide a good foundation for students' lifelong and life-wide learning. (Physical Education, 2020)

If physical education teaching is effective then students get maximum learning. Physical education involves Physical Fitness, Rhythmic activities, Physical activities and Physical movements of students. While teaching to elementary school, physical education teachers need to know how to choose and teach physical education teaching elements. Physical education teachers need physical education teaching elements in different ways in school. For this, primary school physical education teachers need resources (video) on various physical education teaching elements. There are no physical education teaching resources (videos) more available in Maharashtra. Therefore, it will be important for the physical education teachers of the primary schools running in Maharashtra to see on which physical education components resources (videos) are required. The purpose of this study was to analyze the teaching resource (Video) needs of the primary school physical education teachers.

Method:

This study was carried out by descriptive survey method (Gay, 2000). Total 184 primary school physical education teachers who teach physical education to class 5th in a school from Maharashtra state were selected by random sampling technique. (Best, 2010)

Teaching resources needs were decided by asking the physical education teachers to fill up Need Analysis Questionnaire. Data was collected through google form. Questionnaire was sent to 184 primary school physical education teachers from Maharashtra state randomly and their responses were considered for the study. Based on the questionnaire, physical education teachers responses were categorized as Health Related Physical Fitness Components, Skill Related Physical Fitness Components, Fundamental Movement Skills, Yoga Asana, Rhythmic Components and Sports. Different responses received from Physical education teachers.

Statistical Analysis:

Table No. 1 You need a physical education teaching resource (Video) on which of the following health-related physical fitness components.

	Frequency	Percentage
Cardiovascular Endurance	119	26.86
Muscular Strength	107	24.15
Muscular Endurance	104	23.48
Flexibility	113	25.51
Total	443	100

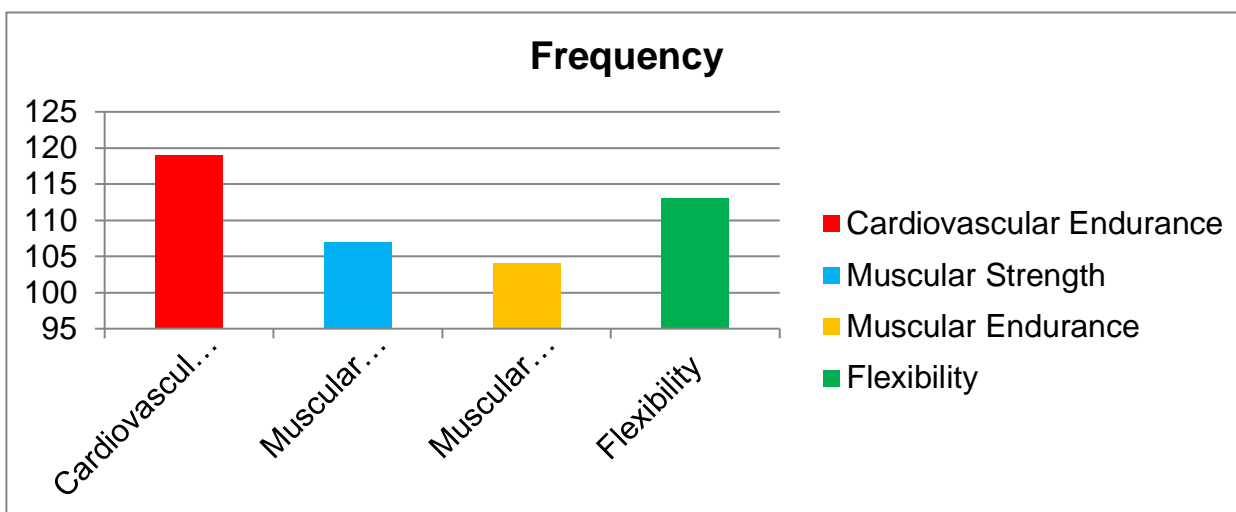


Table no.1 shows that, In this study there were 184 physical education teachers selected for this study, many physical education teachers chose one, two and more options to determine which teaching resource component is needed for teaching. Frequency of 443 responses given by 184 physical education teachers. Responses of physical education teachers need of teaching resources (Video) on Health Related Physical Fitness components (Cardiovascular Endurance 119, Muscular Strength 107, Muscular Endurance 104, and Flexibility 113).

Table No. 2 You need a physical education teaching resources (video) on which of the following skill related physical fitness components.

	Frequency	Percentage
Balance	84	14.02
Agility	94	15.69
Power	93	15.53
Co-ordination	121	20.20

Speed	105	17.53
Reaction Time	102	17.03
Total	599	100

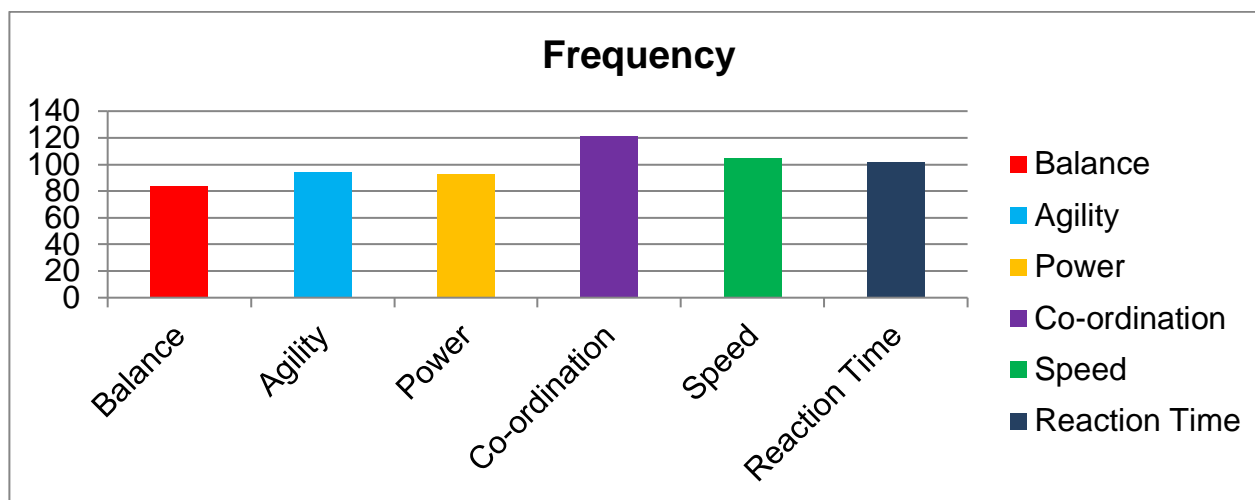


Table no.2 shows that, In this study there were 184 physical education teachers selected for this study, many physical education teachers chose one, two and more options to determine which teaching resource component is needed for teaching. Frequency of 599 responses given by 184 physical education teachers. Responses of physical education teachers need of teaching resources (Video) on Skill Related Physical Fitness Components (Balance 84, Agility 94, Power 93, Co-ordination 121, Speed 105, and Reaction Time 102).

Table No. 3 You need a physical education teaching resource (Video) on which of the following Fundamental Movement Skills.

	Frequency	Percentage
Locomotor Movement Skills	112	35.00
Non locomotor Movement Skills	85	26.56
Manipulative Movement Skills	123	38.44
Total	320	100

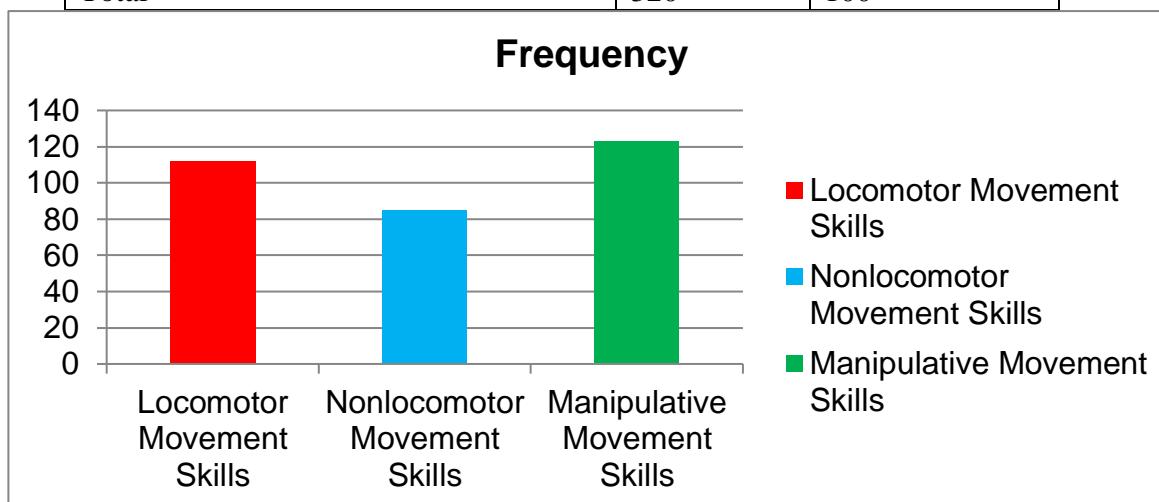


Table no.3 shows that, In this study there were 184 physical education teachers selected for this study, many physical education teachers chose one, two and more options to determine which

teaching resource component is needed for teaching. Frequency of 320 responses given by 184 physical education teachers. Responses of physical education teachers need of teaching resources (Video) on Fundamental Movement Skills (Locomotor Movement Skills 112, Non locomotor Movement Skills 85, and Manipulative Movement Skills 123).

Table No. 4 You need a physical education teaching resources (Video) on which of the following yoga asanas.

	Frequency	Percentage
Standing Posture Asanas	120	28.92
Sitting Posture Asanas	104	25.06
Prone Posture Asanas	94	22.65
Supine Posture Asanas	97	23.37
Total	415	100

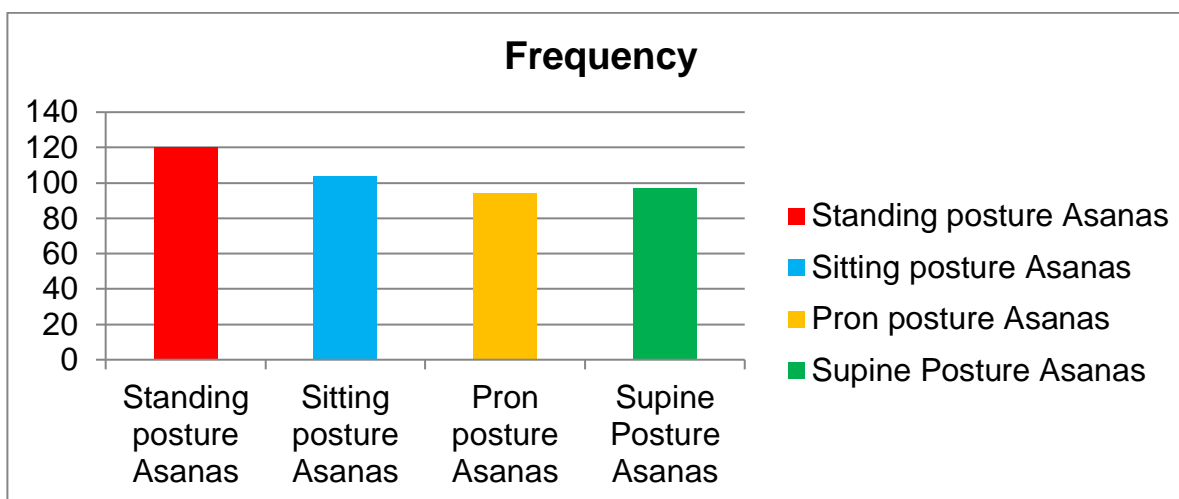


Table no.4 shows that, In this study there were 184 physical education teachers selected for this study, many physical education teachers chose one, two and more options to determine which teaching resource component is needed for teaching. Frequency of 415 responses given by 184 physical education teachers. Responses of physical education teachers need of teaching resources (Video) on Yoga Asanas (Standing posture Asanas 120, Sitting posture Asanas 104, Prone posture Asanas 94, and Supine Posture Asanas 97)

Table No. 5 You need a physical education teaching resource (video) on which of the following components.

	Frequency	Percentage
Recreational Games	85	29.51
Sports Skills	148	51.39
Relay Race	55	19.10
Total	288	100

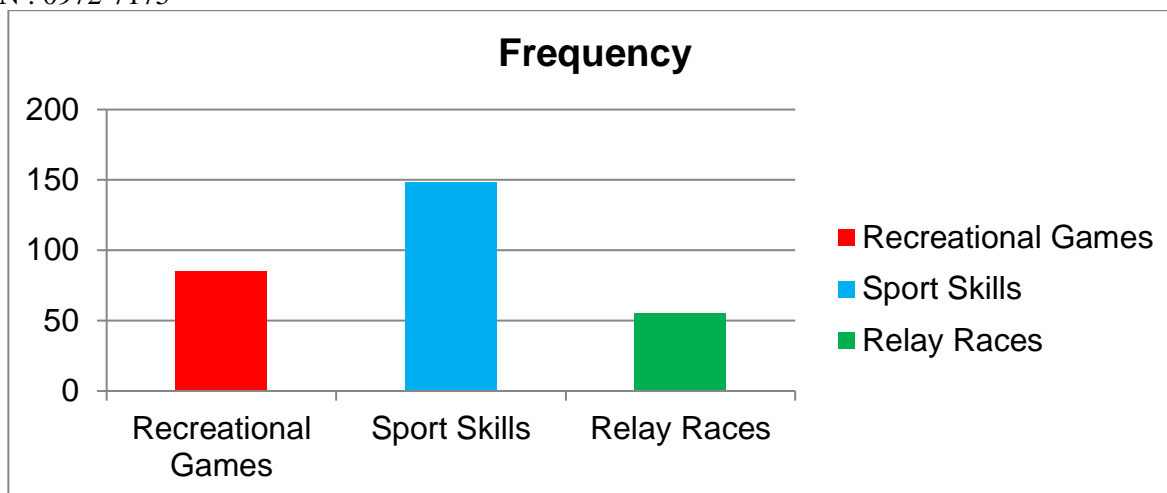


Table no.5 shows that, In this study there were 184 physical education teachers selected for this study, many physical education teachers chose one, two and more options to determine which teaching resource component is needed for teaching. Frequency of 288 responses given by 184 physical education teachers. Responses of physical education teachers need of teaching resources (Video) on Components of Recreational Games 85, Sports Skills 148, and Relay Races 55.

Table No. 6 You need a physical education teaching resource (video) on which of the rhythmic components.

	Frequency	Percentage
Aerobics	127	39.08
Lezim	103	31.69
Mass PT (Light Apparatus)	95	29.23
Total	325	100

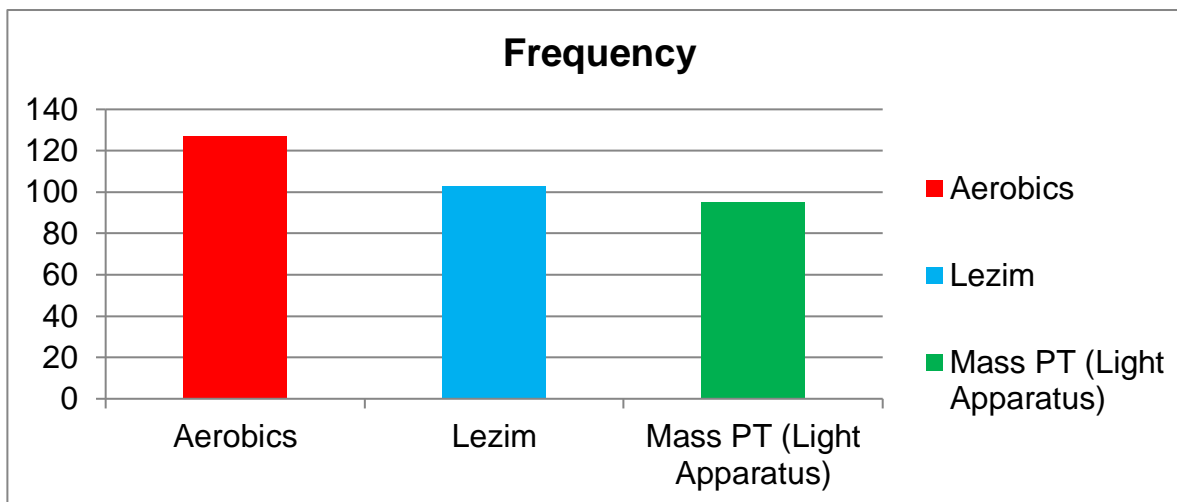


Table no.6 shows that, In this study there were 184 physical education teachers selected for this study, many physical education teachers chose one, two and more options to determine which teaching resource component is needed for teaching. Frequency of 325 responses given by 184 physical education teachers. Responses of physical education teachers need of teaching resources (Video) on Rhythmic Components. (Aerobics 127, Lezim 103, and Mass PT 95)

Table No. 7 You need a physical education teaching resource (video) on which Sports?

	Frequency	Percentage
Cricket	11	5.64
Athletics	43	22.05
Volleyball	18	9.23
Handball	14	7.18
Fencing	1	0.51
Hockey	5	2.56
Kho-Kho	18	9.23
Baseball/ Softball	9	4.62
Kabaddi	21	10.77
Basketball	15	7.69
Badminton	3	1.54
Football	21	10.77
Mallakhamb	2	1.03
Yoga	4	2.05
Karate/ Taekwondo	7	3.59
Skating	3	1.54
Total	195	100

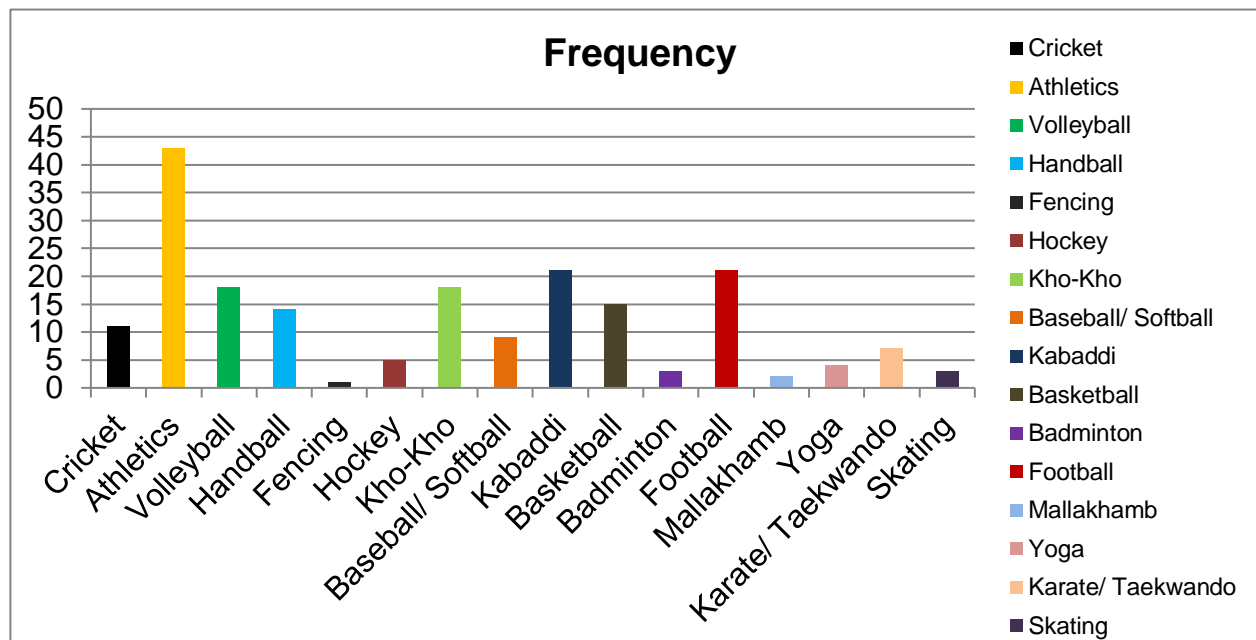


Table no. 7 shows that, In this study there were 184 physical education teachers selected for this study, many physical education teachers chose one, two and more options to determine which teaching resource component is needed for teaching. Frequency of 195 responses given by 184 physical education teachers. Responses of physical education teachers need of teaching resources (Video) on Sports. (Cricket 11, Athletics 43, Volleyball 18, Handball 14, Fencing 1, Hockey 5, Kho-Kho 18, Baseball/Softball 9, Kabaddi 21, Basketball 15, Badminton 3, Football 21, Mallakhamb 2, Yoga 4, Karate/Taekwondo 7, and Skating 3).

Discussion:

Primary school physical education teacher’s needs physical education teaching resources for
 Vol.: XXII, No.: 1, 2021

effective physical education teaching in school. Physical Education teaching resources helps to develop their knowledge regarding physical education and get idea for teaching physical education. Effective Physical Education classes help student to develop skills, maintain physical fitness, and learn about personal health and wellness.

Conclusions:

Different responses received from Physical education teachers. Primary School Physical education teacher needs more physical education teaching resources (video) on the physical education components such as Cardiovascular Endurance, Co-ordination, Manipulative Movement Skills, Standing Yoga Asanas, Sports Skills, Aerobics and Athletics.

References

Best, J. (2010). Educational Research (10th ed.). Pearson.

Gay, L. (2000). Educational Research (6th ed.). Pearson.

Physical education. (2020). <https://www.edb.gov.hk/en/curriculum-development/kla/physical-education/index.html>

Kangane, S., Aher, S., & Mahadik, S. (2013). Physical Education Set / Net (2nd Edition) Abhuday Pragati, 1312, Shivajinagar, Pune.

Maharashtra State Textbook Production and Curriculum Research Board (2015). Physical Education Handbook - Class V (First Edition), Pune.